LIME TREATMENT TO IMPROVE FRICTIONAL RESISTANCE AND STABILITY OF STIFF CLAY SLOPES

BY

MOHAMMAD MORIDZADEH

DISSERTATION

Submitted in partial fulfilment of the requirements
for the degree of Doctor of Philosophy in Civil Engineering
in the Graduate College of the
University of Illinois at Urbana-Champaign, 2019

Urbana, Illinois

Doctoral Committee:

Professor Gholamreza Mesri, Chair
Professor Timothy D. Stark
Professor Emeritus James H. Long
Professor Emeritus Gabriel Fernandez

ABSTRACT

Landslides occurring around the world are often associated with substantial damage to human life, infrastructures, and private properties, thus affecting the economy. Introducing lime, cement or other stabilizers to the potential shear zone or along the pre-existing slip surface of reactivated landslides is an alternative to increase the stability and reduce the rate of movement. The effectiveness of lime treatment of soils has been commonly evaluated in terms of increased unconfined compressive strength; however, if the objective of lime treatment is to improve long-term stability of first-time or reactivated landslides in stiff clays and shales, permanent changes in the size and shape of clay particles must be realized to increase drained frictional resistance.

Lime improvement of frictional resistance was examined using samples of Chicago clay from Chicago, Brenna clay from North Dakota, and Beaumont clay from Harris County Flood Control District (HCFCD), Texas. Chicago clay is known as an illitic clay, whereas Brenna and Beaumont clays are montmorillonitic clays. There are similarities between reaction of clay with lime and that with cement. Understanding clay-lime reactions would help in comprehending pozzolanic reactions occurring when cement or other additives are added to clay. Immediately after introduction of hydrated lime, pH increased to a range of 12.2 to 12.7; within hours, however, pH began to decrease. Whereas there was a large increase in plastic limit, the liquid limit response to lime treatment was dependent on the effective confining pressure. Lime treatment increased substantially peak, post-peak and residual friction angles. A major increase in the secant peak friction angle of lime-treated clays occurred in the first week of treatment. The peak strength continued to increase after the first week of treatment, yet with a reduced rate.

As shearing continues along the shear plane to large strains, the shearing resistance decreases to post-peak and ultimately to residual strength. The secant residual friction angle of lime-treated clay increased within the first few days of treatment and remained relatively constant as curing time increased. Residual strength is controlled by aggregation which takes place at early stages of treatment and remains constant, whereas the peak (intact) shear strength is controlled by both aggregation and inter-aggregate bonds, with latter improving with time.

No major improvement in residual strength was observed for Lower Brenna and Beaumont clays treated with 3% lime. For lime contents above 3%, the secant residual friction angle of Lower Brenna clay increased substantially, suggesting the aggregation of clay particles. The bonds survived at this stage are the intra-cluster bonds. As lime content increased to 7%, the secant residual friction angle continued to increase. For lime contents above 7%, the secant residual friction angle increased but at a decreasing rate. In a similar way, a major aggregation occurred for Beaumont clay treated with 5% lime content. As lime content increased to 7%, the secant residual friction angle continued to increase at a lower rate. As the lime content increased above 7%, the secant residual friction angle remained constant or slightly decreased.

Brenna clay contains a small amount of sulfate in its composition, which in reaction with lime produces ettringite; needle-shaped products observed in SEM images. Ettringite formed over time caused the plasticity of the treated Lower Brenna clay to increase when cured under unconfined condition.

Two methods were proposed to introduce lime or cement to the potential shear zone of a first-time or reactivated slope to enhance the stability and impede the movement of reactivated slopes. A retractable mixing tool was designed to effectively target and treat a shear zone. The mixing tool is extended when reaching the treatment depth and it is retracted after mixing process is complete. The second proposed method is to use horizontal directional drilling technique. This method is employed to mix lime or cement with soil along a shear zone. The mixing tool is advanced along the shear zone to near the slope toe, then treating the shear zone when it is withdrawn.

The stability of Red River slopes in Grand Forks, North Dakota, CUP O'Hare reservoir slopes in Chicago, Illinois, and the slope failures in drainage channels in Harris County, Texas, was evaluated pre- and post-lime treatment using the shear strength envelopes determined from the laboratory tests. Five slides along Red River (i.e. 27th Avenue, Alpha Avenue, Riverside Drive, Water Tank, Reeves Drive) were analyzed. The factors of safety calculated for the slopes before treatment showed that they were marginally stable with the factors of safety in the range of 1-1.1.

The factors of safety increased significantly subsequent to treatment of ten percent of the slip surface with 7% lime. The analysis of the lower and upper slopes of CUP O'Hare following

treatment with 3% lime showed a major increase in the stability of the slopes. It was recommended that 7 ft (2.1 m) of soil on the lower slope be replaced with 3% lime-treated Chicago clay. Additionally, lime treatment of thirty percent of the upper slope was proposed. The stability of the upper and lower slopes was improved following treatment.

Three slope failures in Harris County Flood Control District were analyzed, including Greens Bayou, Berry Bayou, and Carpenters Bayou, and the effect of lime treatment on stability of the slopes were investigated. Three channel slope failures at Greens Bayou (i.e. Middle slope, North slope and South slope) were analyzed. The slope stability analyses performed for post-treatment condition showed satisfactory factors of safety.

This thesis is dedicated to my family.

ACKNOWLEDGEMENTS

This study was carried out under the direct supervision of Professor Gholamreza Mesri to whom I am in debt for all he taught me in geotechnical engineering and life to develop a career path. I would like to extend my gratitude to him for all the time and effort he put into this research and for being patient and accommodating.

I also wish to thank the doctoral committee members professors Timothy D. Stark, James H. Long, and Gabriel Fernandez for their contributions. My sincere appreciation goes to my colleagues in Stantec Dr. Mohammad Djavid, Jason Hedien, Tom Andrews, Chris Ottsen, Manoshree Sundaram, John Hynes and Abid Mirza for being cooperative during the ups and downs.

The assistance provided by Timothy J. Prunkard and the staff at the Machine Shop to repair and maintain the facilities at the Soil Mechanics Laboratory is gratefully acknowledged. My appreciation is extended to the undergraduate and graduate students contributing to the testing program at the Soil Mechanics Laboratory at different stages of the study including Thierno Kane, Emily Roen, Pouyan Assem, Lan Jiang, Li Lanting, Hamed Keshmiri, Cai Wang, Sebastian Lopez, Ana Maria Alzate, and Xichen Xu. The SEM and EDS tests were performed at the Material Research Laboratory. I would like to also thank the CEE staff Joyce Snider for her help in setting things up and friendliness.

I deeply appreciate my wife, Dr. Mehrnoush Gorjian, for being supportive when I had to put extra hours into my study. I am grateful to my parents, Mohammadreza and Mehri, my sister, Maryam, and my brother Masih for all their support and love.

TABLE OF CONTENTS

CHAPTER 1: INTRODUCTION 1

CHAPTER 2: LITERATURE ON PROPERTIES OF LIME OR CEMENT TREATED SOIL ... 3

CHAPTER 3: MATERIAL AND TESTING PROCEDURE 42

CHAPTER 4: PEAK AND POST-PEAK SHEAR STRENGTH..... 68

CHAPTER 5: RESIDUAL SHEAR STRENGTH 148

CHAPTER 6: ATTERBERG LIMITS AND PH MEASUREMENTS..... 229

CHAPTER 7: CLAY-LIME REACTION MANIFEST..... 248

CHAPTER 8: LIME TREATMENT TO INCREASE THE STABILITY OF SLOPES 299

CHAPTER 9: SUMMARY AND CONCLUSION 368

REFERENCES 374

CHAPTER 1

INTRODUCTION

Landslides are responsible for significant loss of life and property around the world. A landslide is remediated by a reduction in the driving forces or by an increase in the available resisting forces or both simultaneously. The cantilever piles and gravity retaining structures physically add resistance to sliding. It has been preferable, in the last several decades, to use non-structural remediation methods such as drainage, slope geometry modification, and some novel methods such as lime/cement stabilization or soil nailing, as the cost is considerably lower compared with structural solutions. Furthermore, structural solutions such as retaining walls involve opening slopes during construction and having steep temporary cuts susceptible to failure. In contrast, soil strength improvement by soil drainage or lime treatment does not need to open or change the original geometry of the slope.

The remedial methods are selected upon understanding of the landslide mechanism, extent of the landslide, geology and hydrology of the site, characteristics of the slope material, depth to the slip surface, and cost. A geotechnical investigation program plays a crucial role in identifying the factors involved in the selection of remedial methods. Inclinometers are typically used to identify the slip surface geometry and slope movement.

Excavation/backfilling is one of the methods used to remediate small landslides. Drainage treatments (e.g. horizontal drains) increase resisting forces by increasing the effective stress on the slip surface. Introducing lime or cement to the shear zone along the pre-existing slip surface could be an alternative for increasing the frictional resistance of the soil. Lime treatment can be used together with horizontal drains to improve the factor of safety and minimize the movement of a landslide.

The effectiveness of lime treatment of soils has been commonly evaluated in terms of improved workability and increased undrained unconfined stiffness and compressive strength, in connection to road and airfield construction (Bell 1996). Soil improvement is expected to result

from the flocculation of clay minerals and cementing action of lime-soil chemical reactions. On the other hand, if the objective of lime treatment is to improve long-term stability of first-time or reactivated landslides in stiff clays and clay shales, permanent changes in the size and shape of clay particles must be realized to increase drained frictional resistance. Lime-soil reactions that may produce less platy and larger soil particles begin and continue with time under the highly alkaline pH environment. In this study, measurements of pH as an indicator of chemical environment, SEM images as a direct measure of particle size, shape and arrangement, Atterberg plastic limit and liquid limit as indirect measures of changes in particle size and shape, and fully softened friction angle and residual friction angle, are used to examine possible mechanisms of lime-soil reactions. The main variables, in addition to soil mineralogy, are soil water content, lime content, and duration of lime-soil reactions. Drained direct shear tests are used for the measurement of fully softened and residual shear strength.

CHAPTER 2

LITERATURE ON PROPERTIES OF LIME OR CEMENT TREATED SOIL

There are similarities between soil reaction with lime and with cement. When cement is added to the soil, in addition to the primary cementitious products resulting from the pozzolans in cement, hydrated lime is formed. The secondary reactions responsible for the long-term strength improvement are due to soil reacting with hydrated lime. Therefore, it is necessary to comprehend soil-lime reactions to understand the basics of pozzolanic reactions. A review of experimental and theoretical studies on the behavior of lime and cement treated soils is presented in this chapter. The fundamental characteristics and stabilization mechanism of treated soils are discussed and the factors influencing the behavior are presented. The limitations of available studies are further reviewed. Although the main goal of this study is to investigate the long-term strength improvement, it is decisive to grasp it in connection to changes in microstructure and Atterberg limits as indirect measures of change in particle size and shape. Moreover, the behavior of treated soil under one dimensial or isotropic compression particularly beyond the yield stress (apparent pre-consolidation pressure) where the cementation bonds collapse can be used as an indication of permanent change in microfabric of stabilized soils. The results of tests conducted on remolded treated soil are another way to investigate this phenomenon. These are discussed in the following sections. The properties of the soils presented in this chapter including Atterberg limits, clay size fraction and dominant clay minerals are illustrated in Table 2.1.

2.1 MICROSTRUCTURAL CHARACTERISTICS AND MINERALOGY

Microstructure of lime treated clay is decisive in understanding the behavior of treated soil. As it was mentioned earlier, there are similarities in the products of lime and cement stabilized clays. Therefore, a review of both lime and cement reactions is expected to shed light on stabilization mechanism. Cement has various components such as calcium, alumina and silica, whereas hydrated lime only constitutes of $Ca(OH)_2$. The silica and alumina required for lime reaction are provided by soil.

Table 2.1: Properties of soils in the literature

Soil	Liquid limit, w_l (%)	Plastic limit, w_p (%)	Plasticity index, I_p (%)	Clay fraction, CF (%)	Initial water content, w_0 (%)	Unified classification	Dominant clay minerals	Remarks	References
Massachusetts clay (M-21)	21	15	6	15	15	CL-ML	Illite	-	Wissa et al., 1965
Vicksburg Buckshot clay (VBC)	65	28	37	30	30	CH	Illite (50%); montmorillonite (50%)	-	Wissa et al., 1965
Ariake clay	120	57	63	55	180	CH	Smectite	-	Horpibulsuk et al., 2004
Buckingham	53	23	30	42	37	CH	Illite; Vermiculite;	Contains 0.2% organic matter	Locat et al., 1990
Soft Bangkok clay	104	41	63	70	76-88	CH	Montmorillonite (60%); kaolinite (25%); illite (15%)	-	Uddin et al., 1997; Balasubramaniam et al., 1989
Local clay from the coast of Madras, India	85	32	53	-	-	CH	Montmorillonite; kaolinite; chloride	Contains 0.2% sulfate, 1.8% chloride, and 1.4% organic matter	Narasimha Rao and Rajasekaran, 1996
Black Cotton Indian	81	33	48	35	81	CH	Montmorillonite	-	Sivapullaiah et al., 2000a, 2000b
Red Earth	49	27	22	35	49	CH	Kaolinite	-	Sivapullaiah et al., 2006
Kaolin from Indonesia	77	40	37	47	40-100	MH	Kaolinite	-	Banks et al, 2001; Lee and Lee, 2002
Aberdeen	54	43	11	-	27	ML	-	-	Muhunthan and Sariosseiri, 2008
Palouse	33	20	13	-	17	ML-CL	-	-	Muhunthan and Sariosseiri, 2008

Table 2.1: *(cont'd)*

Soil	Liquid limit, w_l (%)	Plastic limit, w_p (%)	Plasticity index, I_p (%)	Clay fraction, CF (%)	Initial water content, w_0 (%)	Unified classification	Dominant clay minerals	Remarks	References
Loftabro	66	23	43	72	89	CH	Illite	Contains 0.18% sulphide.	Ahnberg et al., 1995; Ahnberg, 1996; Ahnberg et al., 2003; Ahnberg, 2007
Linkoping	70	24	46	63	78	CH	Illite	Contains 0.05% sulphide.	Ahnberg et al., 1995; Ahnberg, 1996; Ahnberg et al., 2003; Ahnberg, 2007
Singapore Marine clay	88	38	50	68	50-133	CH	Kaolinite (60-70%); smectite and mica (30-40%)	-	Wang et al., 1999; Kamruzzaman, 2002, Kamruzzaman et al., 2009; Chew et al., 2004; Xiao, 2009
Hong Kong Marine clay	62	30	32	30	60-100	CH	Illite	-	Yin and Lai, 1998
Black Soil	73	36	37	60	70	CH	Kaolinite	-	Azman et al., 1995

According to Lea (1956), the main components of Portland cement which contribute to strength increase are tricalcium silicate (C_3S), dicalcium silicate (C_2S), tricalcium aluminate (C_3A) and tetracalcium alumino-ferrite (C_4AF). In these chemical formulations, C, S, A and F stand for CaO, SiO_2, Al_2O_3 and Fe_2O_3, respectively. Schaefer et al. (1997) and Saitoh et al. (1985) outlined the mechanism of soil-cement reaction as follows. When cement is added to wet soil, the pore water in soil reacts with cement and produces primary cementitious products such as hydrated calcium silicates (C_2SH_x, $C_3S_2H_x$, also known as hydrated gel), hydrated aluminates (C_3AH_x, C_4AH_x) and hydrated lime $Ca(OH)_2$. The hydrated lime is deposited as a separate crystalline solid phase. The dissociation of hydrated lime increases the concentration of Ca^{2+} and OH^- which accounts for the rise in pH of the pore water. The strongly alkaline condition promotes dissolution of silica (SiO_2) and alumina (Al_2O_3) of soil. Calcium ions resulting from the dissociated lime react with the silica and alumina of the clay minerals and form insoluble hardening compounds known as pozzolanic products or secondary cementitious products if the binding agent is cement. In lime reaction, the pozzolanic products reported by various researches are CSH, CAH and CASH. In cement reaction, however, primary cementitious product known as hydrated gel ($C_3S_2H_x$) has also been observed by researchers, which is believed to contribute to increased strength of the treated soil (Saitoh et al., 1985). It has been suggested that cement slurry surrounds clusters of clay particles upon addition of cement. The primary hydration reactions contribute to hardening of cement body between the clay clusters and the pozzolanic reactions takes place inside the clay clusters resulting in hardened clay bodies (Saitoh et al., 1985).

The Ca^{2+} concentration on the particle surface of a local clay from the coast of Madras, India (Table 2.1) measured by Narasimha Rao and Rajasekaran (1996) shows that the concentration of Ca^{2+} increases in a few days (in less than 1 week) after treatment and it stabilizes afterwards. The increased Ca^{2+} concentration along with increased pH of the pore fluid are conducive to pozzolanic reactions. The pozzolanic products are expected to form within 7 to 15 days of treatment. Rajasekaran and Narasimha Rao (1998) identified various cementitious products such as CSH, CAH and CASH using X-ray Diffraction (XRD) analysis.

The Scanning Electron Microscopy (SEM) images of lime-treated clay cured for a short time show floccules with a porous nature and cementitious products coating the clay particles and

floccules. The edges of the clay particles are ragged once attacked by lime. An open microfabric with higher porosity has been observed by several researches due to the formation of larger aggregates (Eades and Grim, 1960; Croft, 1964; Narasimha Rao and Rajasekaran, 1996; Rajasekaran et al., 1997a; Rajasekaran and Narasimha Rao 1998). As the curing time prolongs, more cementitious products are formed by pozzolanic reactions coating the aggregates and filling the voids between the floccules. These products develop a network contributing to strength increase in the long term (Choquette et al., 1987). The voids between the aggregates are gradually filled by the new products causing a change in pore size distribution as the curing time increases.

The studies by Locat et al. (1990) on the microstructure of remolded Buckingham soil (Table 2.1) show an open microfabric with individual particles and aggregates. The SEM images on the soil treated by 4% quicklime show early stage (10 days) products in the form of floccules and large lumps. As pozzolanic reactions continue over time, these lumps are cemented together by the subsequent cementitious products. The SEM images taken at longer curing period of 100 days show a network of cementitious products as being responsible for long term strength development. The SEM images and Energy Dispersive Spectroscopy (EDS) analyses verify the formation of platy CASH and reticular CSH. These sheet-like and reticular products have previously been observed by other researchers (e.g., Diamond et al., 1964; Kawamura and Diamond, 1975, Choquette et al., 1987).

Chew et al. (2004), Kamruzzaman (2002) and Kamruzzaman et al. (2009) studied microstructure of Singapore marine clay before and after addition of cement using SEM and XRD analyses. They found that the remolded untreated clay exhibited a microfabric with platy clay particles in a dispersed arrangement. The analyses were then performed on the microstructure of 10% to 50% cement-treated marine clay specimens after 28 days. The SEM images of the 10% cement content show an open fabric with some signs of reticulation. As the cement content increased to 30-50%, the formation of individual large clusters is more evident. In this case, the fabric becomes less platy and the degree of reticulation increases. At 50% cement content, fine network of reticulation was observed in the SEM images. The increased reticulation was believed to be attributed to CSH formation which is reticular in nature (Locat et al., 1990).

Choquette et al. (1987) noted that particles were agglomerated, and the flaky texture completely disappeared for the four Quebec soils treated with 4% lime after 100 days of curing. The XRD results confirmed the decrease in clay minerals due to the attack by the lime in alkaline environment (Eades and Grim, 1960) and formation of new products. The decrease in the phyllosilicates has also been observed by Diamond et al. (1964) and Quigley and Di Nardo (1982). Locat et al. (1990) believed that the silicates and aluminates from the kaolinite go into the solution and react with the Ca^{2+} ions adsorbed on the surface of illite particles to form CSH and CASH. These cementitious products are responsible for cementation of the flocculated clay particles, and form clay-cement clusters, similar to that reported by Rao and Rajasekaran (1996). The early flocculation caused by ion exchange is followed by the formation of pozzolanic products enhancing cementation bonds between the aggregates (Locat et al., 1990; Chew et al., 2004). In summary, Locat et al. (1990) believed that both consumption of kaolinite and formation of the cementitious products between the flocculated particles contribute to a more open structure with higher strength. According to Eades ad Grim (1960), kaolinite is more reactive to cement than illite. Once the cementitious products resulting from consumption of kaolinite is formed around the illite clusters, illite particles become encapsulated and protected from further attack by lime.

Bergado et al. (1996) reported that the rate of increase in strength of treated soil decreases with increase of clay fraction, plasticity index, and in general, activity of the soil. Bell (1993) also found that as the clay content increases, due to increase in specific surface area of the soil a greater quantity of stabilizing agent is required to increase the strength.

A study by Choquette et al. (1987) on 18 different soils from Quebec shows that the initial controlling factors in stabilization are grain size and associated specific surface area. Once pozzolanic reactions are developed, mineralogy is the most influencing parameter in strength increase (Choquette et al., 1987). Locat et al. (1990), in a study of 4 different soils from Quebec, noted that at 10% lime content and 300 days curing time, strength values for all soils merged, indicating a more uniform strength development with time.

A minimum amount of water is required to ensure thorough mixing of soil and lime, and also provide enough water for hydration and pozzolanic reactions. The higher the water content, the easier the mixing and the better the lime distribution. However, higher water contents mean

lower lime concentrations. The slower strength development is due to more cementitious products required to be formed between more distant soil particles (Locat et al., 1990). Several researchers have reported that the strength of treated soil decreases with the increase of initial water content (Porbaha et al., 2000; Miura et al., 2001; Chew et al., 1997; Nagaraj et al., 1996). Locat et al. (1990) studied four sensitive clays with low plasticity from Quebec. They noted that even at a water content above liquid limit, significant strength can be obtained if enough lime and time are provided. The mixing water content ranged from 5% above plastic limit to twice the liquid limit. Although the optimum lime content obtained from the Eades and Grim (1966) was calculated about 4%, they noted increased strength even up to 10% lime content. Even 0.5% lime was enough to saturate the pore water. In most cases of treated soils with 4% lime, undissolved lime was left after 300 days. For all soils, the lower the water content, the higher the initial shear strength. The rapid increase in strength within the first 50 to 100 days slowed down or levelled off afterwards. Eades and Grim (1966) found that at very low or very high water contents, the trend of strength change is similar for all soils. It is at the liquid limit that the strength-time curve is mostly influenced by the nature of the soil. They observed that the unconfined compressive strength of all stabilized soils approached the same value with time and this is more evident for higher lime content of 10%. The effect of water content diminished at high lime contents and long curing periods.

As shown in Figures 2.1 and 2.2, two different stabilization mechanisms for low and high water contents were proposed by Locat et al. (1990) based on what had previously been proposed by Ingles and Metcalf (1973) and later modified by Perret et al. (1977) and Choquette (1988). The proposed model shows the formation of cementitious products creating bridges between or coating soil particles. Locat et al. (1990) implied that a high water content mix may perform better in the long term because the reactants can move easily within the matrix. In Phase I, cementitious reactions are active, but they do not improve the mechanical behavior of the soil. During phase II, bridges between particles are developed, thus the mechanical behavior of soil begins to improve rapidly. Low water content silty soils may exhibit two phases of strength increase (Perret, 1977), as shown in Figure 2.2. The rate of strength increase reduces or levels off in Phase III due to absence of lime, incapability of lime to move within the matrix or lime not contributing to strength increase as the treated soil is already a rigid structure.

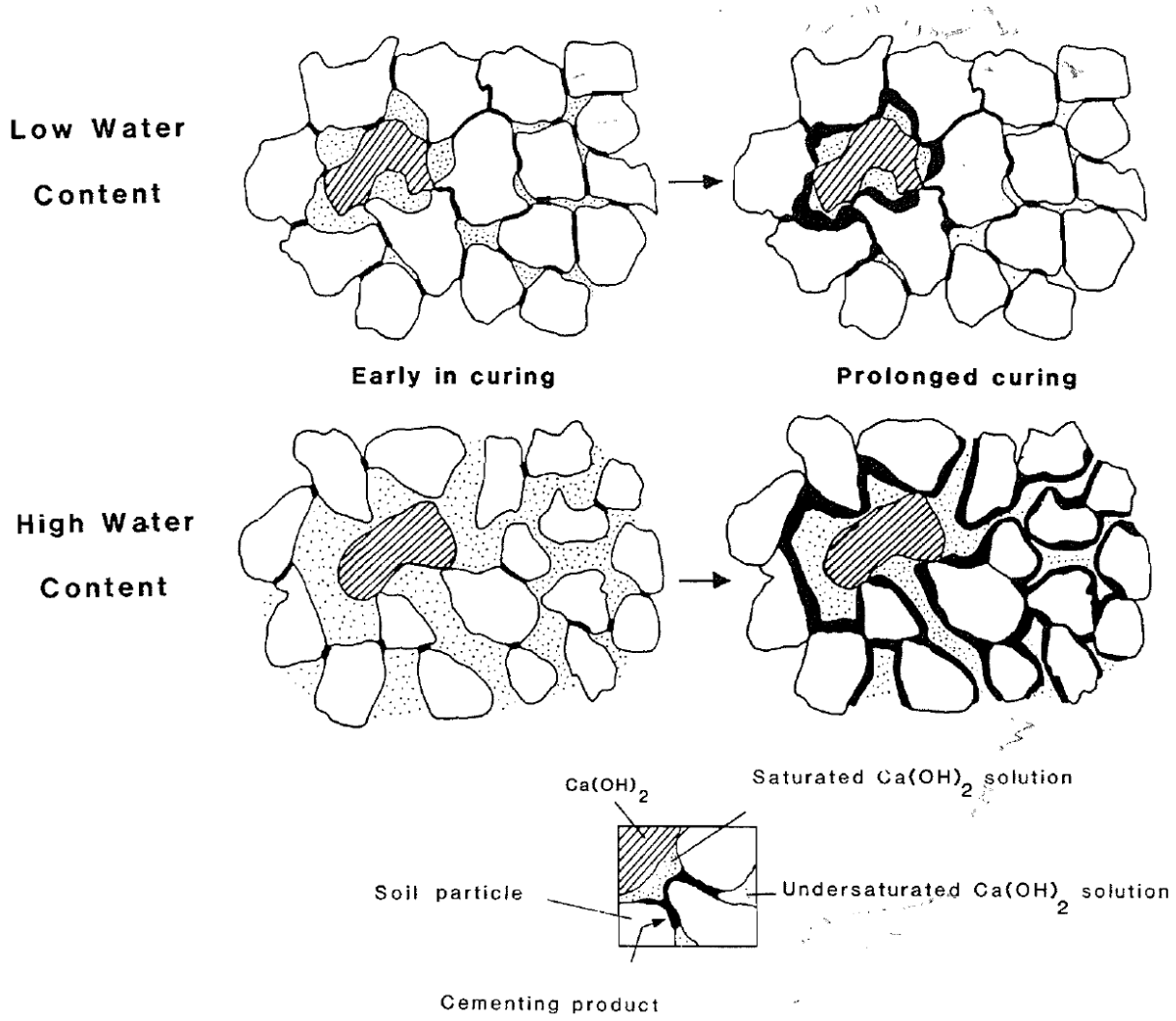

Figure 2.1: Conceptual model for lime stabilization of sensitive clays (Ingles and Metcalf, 1973)

The specimens in Locat et al. (1990) were mixed with lime and then for water contents below the liquid limit, they were compacted into cylinders. The specimens with water contents near or above the liquid limit, were poured into cylenderical plastic bottles of size similar to that of the compacted specimens. After designated curing periods, the specimens were subject to unconfined compressive tests. The conceptual models proposed by Locat et al. (1990) show that soils stabilized, with low water content exhibit a significant shear strength likely due to successful compaction. Diamond and Kinter (1965) suggest that the rapid improvement in strength is due to immediate but limited reactions and formation of pozzolanic products at the point of contact

between the edges and faces of clay particles. The cementitious products in high water content stabilized soils need more time to bridge between the soil particles (Phase II) but low- and high-water-content soils reach the same ultimate shear strength.

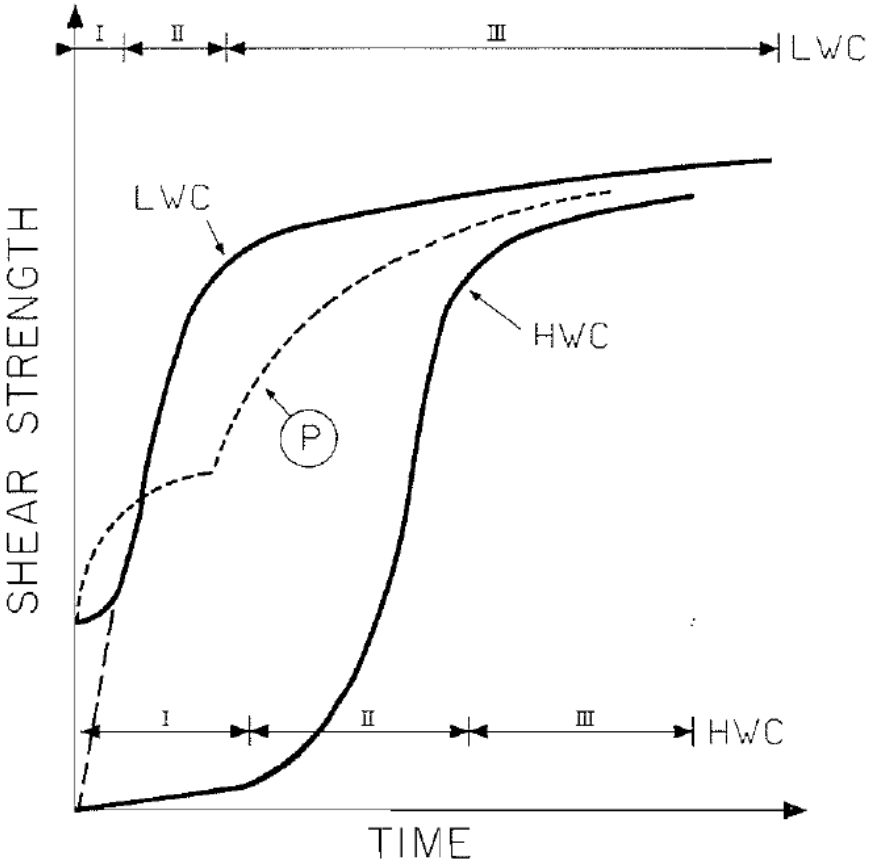

Figure 2.2: Conceptual model for shear strength development in high and low water content lime-stabilized clayey soils; P refers to the model for silty soils (Perret et al., 1977 and Locat et al., 1990)

2.2 ATTERBERG LIMITS

Research has shown that addition of lime to soils results in reduction of the plasticity index (PI) (Al-Khashab and Al-Hayalee, 2008a, 2008b; Lasledj and Al-Mukhtar, 2008). Usually an immediate increase in the plastic limit (w_p) is observed on the addition of lime (Hausmann 1990). Xiao (2009) also found that the specific volume, volume containing unit volume of solids, ($1+e=V/V_s$) of the remolded treated samples increased with cement content. Hence more water was needed to bring the soil to the same consistency as cement content increased. The rapid

increase of plastic limit has been attributed to flocculation of the clay particles (Hilt and Davidson, 1960). The increase in plastic limit could be explained as a result of water entrapped in the clay particle floccules and aggregates. The observed increase in plastic limit may be also explained as a result of increased water retention capacity in the micropores of the newly formed cementitious products and minerals as pointed out by Locat et al. (1996). There is an analogy between the structure of lime-treated clays and the diatomaceous Mexico City clay (Mesri et al., 1975).

The increase in plastic limit varies directly with the amount of lime or cement added, up to some limiting lime content; further increments of lime usually bring little or no additional increase or even result in a decrease in the plastic limit (Bell, 1996). In the method suggested by Eades and Grim (1966) to determine the optimum percentage of lime, a minimum pH of 12.4 is necessary to activate the pozzolanic reactions. The alkaline environment is responsible for the slow dissolution of the aluminosilicate constituents of clay, which react with lime producing hydrated cementitious products that bond adjacent soil particles together (Ingles and Metcalf, 1973; Little, 1995; Bell, 1996). According to Ingles (1987), a good rule of thumb in practice is to allow 1% by weight of lime for each 10% of clay size fraction in the soil. Exact prescriptions, however, can be made after tests. Because it is exceptional for the clay content of a natural soil to exceed 80%, it is normally not necessary to add more than 8% lime. The "lime fixation" term was first introduced by Hilt and Davidson (1960) and is defined as the amount of lime held by soil which is not available for pozzolanic reactions. They noted that the plastic limit increases up to a lime content known as lime fixation capacity (about 1% to 3%) and remains constant for the lime contents beyond that specific lime content. The lime fixation capacity of a soil is also the percentage of lime at which strength just begins to increase. It is noted that unconfined compressive strength was used in their study which may not necessarily reflect the change in size and shape of the particles. Later, Bell (1996) found that the minimum lime percentage is normally between 1% and 3% lime by weight depending on the amount and type of clay minerals in soil, and further additions of lime do not induce changes in the plastic limit but increase the strength.

Lasledj and Al-Mukhtar (2008) found that addition of 2% lime increased the plastic limit and decreased the liquid limit only by small amounts. Addition of 4% lime, however, increased the plastic limit and reduced the liquid limit significantly. Further increments of lime above 6% brought little increase in plastic limit and gradual decrease in liquid limit. Thus, the plasticity index

suffered a significant reduction between 2% and 6% and a slight reduction up to 10% addition of lime. The point of inflection on the plot of w_p with lime content at about 6% lime was termed as "lime fixation point" (Hilt and Davidson, 1960; Eades and Grim, 1966). It is noted that the clay used in their study was a bentonitic clay of high plasticity consisting of smectite with sodium ions as exchangeable cations which explains the high lime fixation capacity. Lee and Lee (2002) found that 2% cement reduced the plasticity index of kaolin by mainly increasing the plastic limit and addition of more than 2% cement did not reduce further the plasticity index of the treated kaolin.

Because the liquid limit (w_l) of a clay is far more sensitive to the kind of cation present than is the plastic limit (w_p), it is more difficult to summarize the effect of lime or cement on the liquid limit (w_l). Some researchers have observed a decrease in the liquid limit after addition of lime or cement (Huat et al., 2005; Al-Khashab and Al-Hayalee, 2008a, 2008b; Lasledj and Al-Mukhtar, 2008). Chin (2006) and Chew et al. (2004) found that the liquid limit of cement treated soil increased with cement content. Even when the w_l increases due to the addition of lime, the increase is not usually as great as the accompanying increase in w_p. Thus, the separate effects on w_l and w_p usually combine to yield a rather sharp decrease in I_p (Clare and Cruchley, 1957). Plasticity index may decrease to such an extent that the treated soil becomes non-plastic (Little et al. 1982).

Uddin et al. (1997) found that the plasticity index of cement-treated clay reduces by increasing of cement content and curing time. The decrease in the plasticity index resulted from an increase in plastic limit and constant to slight decrease in liquid limit. Sivapullaiah et al. (2000a) found that the liquid limit of Black Cotton Indian soil decreases immediately after addition of lime up to 6% and stabilized as lime content further increased. The liquid limit increased generally as the curing time increased to 7 days. The liquid limit corresponding to the 7-day curing time showed an increase up to 6% lime followed by a drop as lime content increased to 12%. The plastic limit increased immediately after addition of lime even as low as 2%, then it remained constant for higher lime contents. The plastic limit increased continuously with curing time. For the 7-day cured soil, the plastic limit increased for lime content up to 4% and remained constant as further lime was added. Immediately after addition of lime, the plasticity index decreased up to 4% lime and then stabilized. The liquid limit increased as the curing time extended to 7 days; however, it remained below that of the untreated soil. Sivapullaiah et al. (2000a) proposed that the immediate

reduction in the liquid limit was due to the reduction of double layer water resulting from calcium ion concentration on the surface of clay particles (cation exchange). The increase in liquid limit with curing time was explained by the change in clay fabric. The pH measurements showed an increase to slightly above 12 for up to 4% lime and remained constant for higher lime contents.

Chew et al. (2004) found that the liquid limit of Singapore marine clay treated with cement decreased with curing time but remained significantly greater than that of the untreated clay. The liquid limit of the treated clay increased for up to 10% cement followed by a slight decrease for higher cement content. The plastic limit increased continuously with the cement content and curing time; however, the increase was more pronounced up to 10% cement content. Chew et al. (2004) attributed this to the aggregation and cementation of clay particles, turning them into clusters of larger size as explained by Locat et al. (1990). The changes in the liquid and plastic limits are such that the plasticity index decreases with cement content and curing time.

2.3 PORE SIZE DISTRIBUTION

Pore size measurements of cement-treated Singapore marine clay by Chew et al. (2004) showed that the pore size increases significantly after treatment, and it increases with cement content. A slight decrease in pore size was observed with curing time in some cases; however, it was still larger than that of the untreated soil. It was believed that kaolinite dissolution, flocculation and formation of clay-cement clusters contribute to a more open structure. The reduction in pore size with curing time confirms the formation of cementitious products around the flocculated clay-cement clusters. Also, the Kamruzzaman et al. (2009) studies show that the treated soil has larger pore sizes than untreated soil for the same pore volume due to formation of clay-cement clusters, and thus larger voids.

The process of coating of aggregates and filling of the large pore space by CSH (Chew et al., 2004) and ettringite (Du et al., 2014) forms a porous space inside each aggregate, contributing to greater pore size distribution. The ettringite formation is discussed later. The water trapped in the pores inside the aggregates explains the higher plastic limit observed in treated soils.

Pore size distribution is in consistent correlation with permeability. The conceptual model of lime stabilization shown in Figure 2.1 can explain the reduction in permeability after an initial

increase due to flocculation and aggregation. The permeability is expected to decrease with time as reaction products gradually fill the pore space (Locat et al., 1990). This is in agreement with the mercury porosimetry measurements (Delage and Lefebvre, 1984) for four sensitive clays of Quebec with different mineralogy (Choquette at al., 1987; Choquette, 1988). The Mercury porosimetry tests showed that lime stabilization changed the pore size distribution by lowering the number of large pores to smaller size pores. The partitioning of the larger pores was done by the new cementitious products. Moreover, these products with reticular texture have a network with very small pores, contributing to the increase in the number of smaller pores (Choquette et al., 1987).

2.4 PH MEASURMENT

An increase of pH to above 12.4 upon addition of lime has been widely reported by researchers (e.g. Eades and Grim, 1966, Sivapullaiah et al., 2000a; Chew et al., 2004). The increase in pH upon addition of lime was discussed to some extend in previous sections. An elevated pH above 12.4 can be a sign of available lime and ongoing pozzolanic reactions. However, availability of both lime and clay participating in reactions is necessary. Chew et al. (2004) found that the pH of 7-day cured cement-treated Singapore marine clay increased sharply to just above 12 for cement content up to 10%, after which it remained more or less the same. For cement content up to 10%, the pH reduced with time but remained significantly above that of the untreated clay. For higher cement contents, the PH remained above 12 after 28 days curing period. Chew et al. (2004) recognized the exhaustion of clay participating in the reactions to be the reason for pH stabilization at high cement contents.

2.5 STRAIN SOFTENING BEHAVIOR

Treated soils when subjected to shearing display a substantial peak followed by strain softening. This section aims to elaborate on the strain softening behavior of soils to allow defining the peak and post-peak strengths of treated soils. Strain softening and strain localization in stiff clays has previously been studied (e.g. Viggiani et al., 1993; Georgiannou and Burland, 2001; Leroueil and Hight, 2003). Viggiani et al. (1993) noted that strain softening is due to strain

localization and takes place at maximum stress ratio (q/p'). Strain localization is a progressive phenomenon leading to formation of a shear band.

Brittleness is defined for strain softening behavior to quantify the reduction in shear strength as strain increases. Most natural soils including stiff clays and shales displays this behavior, i.e. a drop in shear strength following peak strength (Bishop, 1967, 1971). Structured soft clays display a brittle behavior when bonds between particles break due to shearing (Leroueil and Hight, 2003). Degree of brittleness controls progressive failure and post-failure phenomena and hence has practical implications. The brittleness index (I_B) was defined by Bishop (1967) for drained condition as follows:

$$I_B = \frac{\tau_P - \tau_u}{\tau_p}$$

Where τ_p and τ_u are the peak and minimum post-peak strengths under the same effective stress condition. However, the brittleness index is not the only factor determining the susceptibility of a soil to progressive failure. The rate of strength reduction, and thus the energy necessary to drop from peak to post-peak conditions are other important factors. Hence, a generalized brittleness index (I_{GB}) was defined by D'Elia et al. (1998) as follows:

$$I_{GB} = \frac{\tau_P - \tau_{mob}}{\tau_p}$$

where τ_{mob} is the mobilized shear stress at a particular strain level. Thus I_{GB} varies with strain level from zero at the peak to a value equal to I_B at large strains. Leroueil and Hight (2003) noted that the generalized brittleness index proposed by D'Elia et al. (1998) is associated with a given stress path and is not an intrinsic characteristic of a soil.

Progressive failure of slopes in overconsolidated clays and shales showing strain softening behavior was first investigated by Skempton (1964) and Bjerrum (1967). Dam et al. (1997) noted the differences between stress-strain behavior of a lightly cemented natural clay and that of a remolded specimen of the same clay measured by Direct Shear Tests (DST). Direct shear test was recommended by Taylor (1948) as one of the best procedures to study the progressive deformation behavior. Dam et al. (1997) studied fifteen sensitive marine clays from Japan, Southeast Asia,

Scotland, Norway and Canada, with the plasticity index in the range of 18-152% and overconsolidation ratio in the natural state in the range of 1-4.6. It was concluded that the structure developed with time in naturally structured clays makes the stress-strain behavior quite different than that of remolded specimens. However, a similar post-peak shear strength at large strains was measured for natural and destructured specimens, as shown in Figure 2.3. Remolded specimens prepared with a overconsolidation ratio comparable to that for the naturally structured clay also showed a different stress-strain behavior.

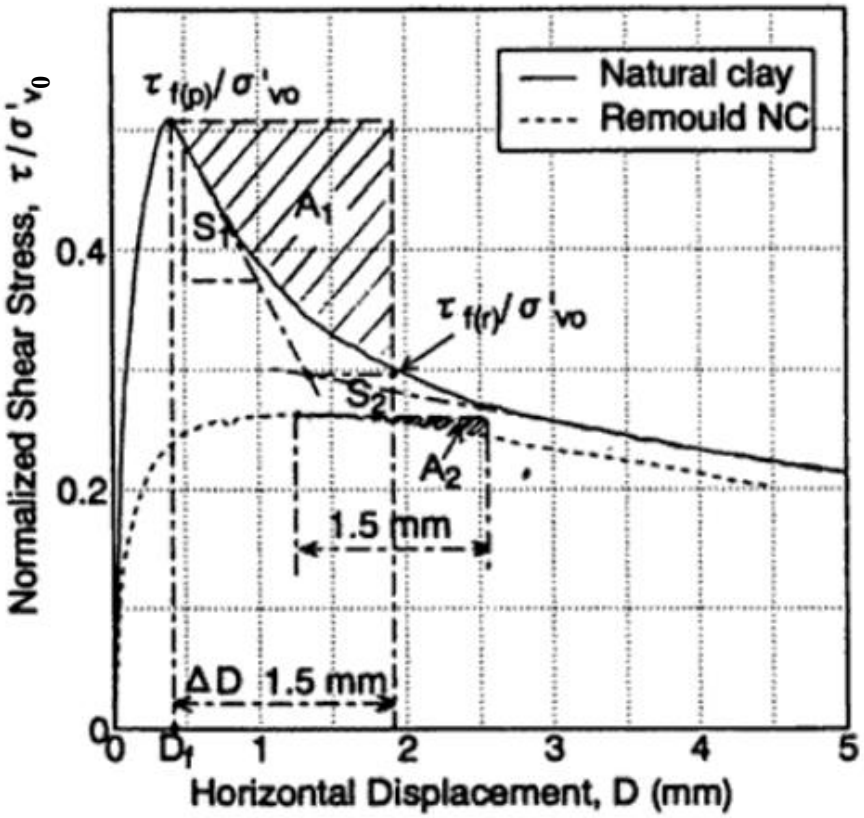

Figure 2.3: Stress-displacement curves of natural and normally consolidated remolded specimens obtained from DST (Dam et al., 1997)

Triaxial tests performed by Xiao (2009) showed that the shear strains are concentrated in the shear band. The microstructure study on the samples revealed that destruction of bonds within and among aggregates occurred within the slip plane is much more than that of outside the slip

plane. Chin (2006) confirmed that a distinct shear plane is apparent in the treated samples where it experiences larger shear strains and explains the significant drop in the strength.

Georgiannou and Burland (2001) stated that rapid strength drop to a relatively constant post-peak value is a result of microstructure changes due to the breaking of inter-particle bonds. The strain localization around the peak strength is responsible for the brittle behavior. Thereafter, slip plane forms and rigid body sliding takes place along the slip plane.

The soil softening in treated soils as well as natural structured soils are further discussed in post-peak strength section.

2.6 YIELDING OF TREATED SOIL

The yield stress of cement-treated clay, where the breakage of inter-aggregate bonds occurs, is characterized by a drop in stiffness during loading (Cotecchia and Chandler, 2000; Chin, 2006). Drained triaxial compression tests conducted on cement-treated Singapore marine clay by chin (2006) showed a stiff response up to peak strength followed by strain softening and volumetric dilation for the samples sheared at confining pressures much lower than their isotropic preconsolidation stress, σ_{PI} (Terzaghi et al., 1996). For this case, large aggregated particles were still observed within the shear zone. The samples sheared at higher effective confining pressures under drained condition reached the peak strength at a higher strain level. The specimens subjected to high effective confining pressures before shearing experienced strain hardening and volumetric contraction before reaching the peak strength. An examination of the shear plane revealed signs of very sever clay aggregate crushing; the higher the effective confining pressure, the greater the severity of the aggregate crushing.

Although some researchers have reported two yield points for naturally cemented soils (e.g., Jardine et al., 1991; Jardine, 1992; Vaughan, 1988; Bressani, 1990), it appears that there is a well-defined yield point for strongly cemented soils such as artificially treated soils, where the elastic behavior is followed by a significant drop in stiffness (Malandraki and Toll, 1996). It appears that the yield point defined by various methods lead to the same value, representing the breakage of cementation bonds. For example, the first yield point defined by Vaughan (1988) and Bressani (1990), the yield point defined by Coop and Atkinson (1993) and Cuccovillo and Coop

(1997) and the second yield point defined by Jardine (1992), Smith et al. (1992) and Malandraki and Toll (1996) coincide in the case of strongly cemented soils. The primary yielding defined by Rotta et al. (2003) is also expected to lead to the same yield stress.

Xiao (2009) used the Coop and Atkinson (1993) method to determine the yield stress, i.e., the end of linear part on the plot of deviatoric stress-strain and mean effective stress-volumetric strain. This is also consistent with the method utilized by Rotta et al. (2003). Xiao (2009) collected the yield stresses determined from isotropic compression, K_0 compression and CID triaxial tests under various confining pressures and found a relatively consistent yield locus for cement treated Bangkok clay.

2.7 COMPRESSION CHARACTERISTICS OF TREATED SOILS

Characteristics of treated soils under compression have been studied by a limited number of investigators through laterally constrained or isotropic compression tests (e.g. Kamruzzaman, 2002; Kamruzzaman et al., 2009; Xiao, 2009). The tests by Xiao (2009) showed a decrease in initial void ratio with an increase in cement content, curing stress (stress under which specimens are cured), and curing time. The initial void ratio decreased with a decrease in water content at which the specimens were cured.

The yield stress of intact specimens of soils treated with lime or cement is a function of lime or cement content, curing time and curing stress. Another way of investigation of the fabric change of treated soil is to break the bonds and structure of treated soil and remolding the destructed treated samples. However, the degree of destruction depends on the severity of destruction and remolding. Hence a complete breakage of bonds is not guaranteed. The treated samples destructed by remolding did not exhibit the high cementation-induced yield stress observed for intact treated samples (Xiao, 2009). This is an indication of destruction of inter-particle cementation bonds.

In general, it appears that lime/cement treatment produces aggregates and bonds connecting the aggregates together (inter-aggregate bonds). When subjected to isotropic compression, treated specimens exhibit the behavior of an overconsolidated clay with a significant yield stress. Inter-aggregate bonds begin to break down at yield stress. The post-yield compression

curve corresponds to a close packed arrangement of aggregates. As stress increases above the yield stress, some damage to the aggregates is expected. The sharp breaking point observed in the e-logp curves of the treated intact specimens indicates the breakage of the inter-aggregate bonds. A muted breaking point in the e-logp curves of treated destructed specimens is observed, implying the damage to the aggregates.

2.8 SHEAR STRENGTH PARAMETERS

The increase in shear strength of treated clay is partially due to ion exchange, as multivalent ions from stabilizers (e.g. Ca^{2+}) replace monovalent ions (e.g. Na^{+} and K^{+}) as stated by several investigators (Herzog and Mitchell, 1963; Mitchell, 1976, Broms, 1986). However, strength improvement has been observed in some soils with calcium already in exchange sites, when stabilized with lime (Diamond and Kinter, 1965).

The shear strength of soil-lime mixtures has been measured in the laboratory using various tests, including unconfined compression, triaxial compression, indirect tensile (diametral compression), CBR and California R-value. The most common method of strength measurement has been the unconfined compression test (Little 1999). However, there is limited data available on the long-term shear strength of lime-treated soils. It has been previously interpreted that lime stabilization is a cementation process that significantly increases shear strength (Lade and Overton, 1989; Locat et al., 1990, 1996; Narasimha Rao and Rajasekaran, 1996; Wissa et al., 1965; Clough et al., 1981; Uddin et al., 1997; Kasama et al., 2000; Horpibulsuk et al., 2004). The stress-strain behavior of treated clays has been investigated under triaxial condition by a number of researchers (e.g. Endo, 1976; Tatsuoka and Kobayashi, 1983; Uddin et al., 1997; Yu et al., 1997; Yin and Lai, 1998; Miura et al., 2001; Kamruzzaman, 2002; Horpibulsuk et al., 2004; Chin, 2006; Chiu et al., 2008).

Three different conditions are generally recognized for drained shear strength of stiff clays: (1) peak or intact strength of overconsolidated clays reflecting bonding between particles or aggregates; (2) fully softened strength where the volume change becomes constant; and (3) residual strength where the particles are oriented along the direction of shearing to the maximum extent possible for the effective normal stress condition (Skempton 1964; Mesri and Cepeda-Diaz,

1986; Terzaghi et al., 1996; Mesri and Shahien, 2003). The fully softened strength has been also referred to as critical state strength of remolded clays (Leroueil and Hight, 2003). According to Skempton (1970), softening process reduces the clay strength to the critical state strength. In critical state, there is no further strength reduction due to water content or void ratio increase. However, additional shear displacements can reduce the strength further by orienting the particles along the direction of shearing.

The stress-strain behavior of treated soils shows a significant peak, particularly at low confining stresses, followed by strain softening to a post-peak strength. The peak strength is influenced by the cementation structure of the soil while the post-peak strength is the state at which the cementation bonds are being broken.

Highly overconsolidated clays subjected to shearing exhibit a well-defined shear zone followed by a rigid-body sliding (Viggiani et al., 1993; Tillard-Ngan et al., 1993; Desrues et al., 1996). The behavior of treated clays under shearing appears to be similar to the behavior observed in highly overconsolidated clays showing a distinct shear surface.

Determination of unstructured state for treated clay is not as easy as that for natural structured soils (Chin, 2006). It was found to be difficult to fully break the structure of treated soil even after long hours of remolding process. Chin (2006) realized that the particle size distribution keeps becoming finer by remolding. Cementation in naturally cemented soils is a slow process and forms at interparticle contacts of sediments consolidated for a long period of time. In contrast, as speculated by Chew et al. (2004), when lime or cement is added to soil, reaction in early stages produces pouros clusters due to flocculation of the clay particles. The following cementitious bonds form on surface of these porous grains. The SEM study by Chin (2006) showed that yielding is associated with breaking the bonds between these grains. In other words, the grains themselves remain intact during yielding. Collapse of the individual grains take place within the shear zone after a significant strain softening (Chin, 2006). The degree of grain breakup depends on the effective normal stress as well. At high normal stresses, the grains experience a greater degree of crushing. This is similar to what is observed in cohesionless soils and the decrease in the friction angle with normal stress.

When the treated soil is compressed to a consolidation pressure equal to the apparent pre-consolidation (yield) stress, the cementation bonds between the soil-cement grains collapse and large inter-grain voids reduce but the small intra-grain (within individual grains) voids still remain (kamruzzaman et al., 2009). A significantly greater consolidation pressure far beyond the yield stress is required to break the intra-grain bonds and further reduce void ratio. This was observed in SEM images and pore size distribution curves for treated Singapore clay under yield stress of 1,600 kPa and a higher pressure of 6,400 kPa (kamruzzaman et al., 2009). The particle size distribution showed that the particle size of treated clay is greater than that of untreated clay even at the higher consolidation pressure of 6,400 kPa, confirming that some grains survived despite some particle damage. The magnitude of the stress at which a complete destruction of cementation bonds occurs, depends on the cement content and curing time (kamruzzaman et al., 2009). The compression tests revealed that the samples still exhibited some cementation effects during shearing, suggesting that the soil-cement grains were not completely broken down during isotropic consolidation.

The particle size analysis of the samples taken from the shear zone of CIU tests indicated the crushing of inter-grain bonds and some intra-grain bonds. The particle size of treated soil within the shear zone was measured to be larger than that of untreated soil. The breaking of large grains was observed outside of the shear zone but some reticulated grains were still noted (kamruzzaman et al., 2009).

Kamruzzaman et al., (2009) proposed that the principal effect of cement was to reduce the initial void ratio of compacted soil and to introduce a well-defined yield point (apparent preconsolidation stress) into the stress-strain behavior of treated soil in compression and shearing. At confining pressures below the yield stress, the destruction of cementation bonds only took place during shearing followed by strain softening behavior. At higher confining stresses well above the yield stress, the sample still appeared to show some cementation effect during shearing despite the destruction of the cementation bonds. Kamruzzaman et al., (2009) concluded that a complete destruction of cementation bonds only occurs along the shear plane.

2.8.1 Intact samples of treated soil

The isotropically consolidated undrained (CIU) triaxial compression tests conducted by Uddin et al. (1997) showed that the intact cement treated samples exhibit a behavior similar to overconsolidated clays which becomes more significant as the cement content increases. Triaxial compression tests on treated specimens under a confining stress lower than the yield stress show stiff behavior with a significant peak strength in the axial strain range of 1-3% (Endo, 1976; Uddin et al., 1997, Chin, 2006; Xiao, 2009). The CIU triaxial compression tests conducted by Porbaha et al. (2000) on 5% cement treated marine clay also show a well-defined peak at strain level of less than 5% before reaching the post peak strength. As confining stress increases, the specimen undergoes significant strain hardening before reaching the peak strength (Kamruzzaman, 2002). The stress-strain relationship of treated soil changes from strain softening to strain hardening at confining pressures above the yield stress (Tatsuoka and Kobayashi, 1983; Yu et al. 1997; Uddin et al. 1997; Chin, 2006).

In the tests performed by Chin (2006) and Xiao (2009), the destruction occurred in two stages as follows. The first stage is associated with aggregate crushing and void closure. The second stage is the strain softening phase where the slip plane forms and soil undergoes significant particle crushing.

As effective confining pressure increases, the volumetric response changes from dilation to contraction in drained compression triaxial tests on treated soil (Chin, 2006). Kamruzzaman (2002) noted the change in the behavior for undrained tests on treated soil under various effective confining pressures. As effective confining pressure increased, the behavior type changed from that of an overconsolidated soil and negative pore water pressure to that of a normally consolidated soil and positive pore water pressure.

Although the peak strength is not the focus of present investigation because it is not a measure of permanent long-term improvement, it is briefly reviewed herein. It is generally understood that the peak strength increases with an increase of cement content, curing stress and curing period or decrease in water content (Xiao, 2009).

Uddin et al. (1997) found that the Bangkok clay samples treated with higher cement content showed a greater strain softening behavior at low confining pressures. However, treatment effect on the peak strength tends to vanish by increasing confining pressures due to breakdown of cementation bonds and reduction of overconsolidation ratio of the treated soil, defined in terms of yield tress and consolidation pressure. The behavior of treated soil at low confining pressures is mostly controlled by cementation bonds, whereas the frictional component becomes more dominant as confining pressure increases (Azman et al., 1995). The post-peak strength of the treated soil measured by Uddin et al. (1997) shows values slightly above the Critical State Line (CSL) of the untreated soil. Chin (2006) used the term "post-rupture" strength after Burland (1990), referring to a reasonably constant strength after the peak strength and found that the friction angle of the treated soil after experiencing high degree of cluster breakup is near or greater than the friction abgle of the untreated soil. Chew et al. (2004) noted that cementation products covered the soil particles and reduced their surface activity.

The rate of increase in strength of treated soil with curing time decreases with increase of clay fraction, plasticity index and in general activity of the soil (Bergado et al., 1996). As the clay content increases, greater quantity of stabilizing agent is required to increase the strength due to increase in specific surface area of the soil (Bell, 1993).

Broms (1986) suggested that the shear strength parameters (c' and ϕ') of treated clay improved as a result of the following. Hydrated cement particles surround clay particles and form a skeleton which increases the frictional component of the shear strength by increasing the particle interlocking. Moreover, the cohesion component and inter-particle bond strength was found to increase due to cementation products formed by pozzolanic reactions.

Uddin et al. (1997) reported that the failure strain decreased with an increase of cement content and curing time at low confining pressures. However, the stress-strain curves at greater confining pressures were similar to those of normally consolidated behavior with greater failure strain. It was found that the failure strain reduced significantly with an increase of cement content up to a certain cement content; however, the reduction rate in failure strain decreases thereafter.

Yin and Lai (1998) found that the failure strain also depended on the initial water content. At high cement content with water content of more that liquid limit, the treated clay showed a ductile behavior. The CIU triaxial compression tests conducted by Yin and Lai (1998) on cement treated Hong Kong marine deposits (Table 2.1) under various confining pressures and initial water contents showed that the stress-strain behavior type of treated soil changed to that of overconsolidated soil under the same confining pressure as the cement content increased and initial water content remained constant. The samples with the same cement content under the same confining pressure but having lower initial water content showed more improvement. The cohesion intercept (c') of treated soil increased with increase of cement content and reduction of initial water content. The friction angle (ϕ'), however, decreased with the increase of cement content and reduction of initial water content. They concluded that as cement content increases the failure criterion become closer to von Mises criterion (independent of confining pressures) rather than Mohr Coulomb criterion. This could be an indication of high nonlinearity of shear strength envelope for treated clays.

Similarly, Kamruzzaman (2002) found that the treated marine clay has a brittle behavior with a distinct yield stress. The distinct yield stress was believed to be due to the destruction of the cementation bonds. Once the confining pressure increases above the yield stress, the treated soil shows a normally consolidated behavior due to deconstruction of cementitious bonds. Porbaha et al. (2000) and Azman et al. (1995) also investigated the confining pressure effect on the behavior of treated soils. They concluded that the stress-strain behavior of treated soil at a confining pressure equal to the yield stress of the treated clay is no longer brittle. As the confining pressure increases above the yield stress, progressive breaking of the cementation bonds occurs. The cement treated clay tested by Uddin et al. (1997) at low confining pressure, i.e. in the range of 50 to 100 kPa showed small positive shear-induced pore pressure and then dropped to negative values. At higher confining pressures, however, shear-induced pore pressure was positive. The pore water pressure increased to a maximum value and then dropped to a lower value. For the same confining pressure but higher cement content, the treated clay showed a peak positive pore water pressure occurring at a lower strain.

Azman et al. (1995) studied the cement content and consolidation pressure effect on the shear strength parameters of the Black Soil in Malaysia (Table 2.1). Azman et al. (1995) found

that the shear strength parameters do not change significantly with the confining pressure at cement contents up to 2%. For the cement contents more than 2%, they classified the failure pattern based on the range of confining pressure, as shown in Figure 2.4. They found that the failure pattern at high confining pressures is frictional where the failure envelope is parallel to the failure envelope of the untreated soil. At low confining pressures, they found that cementation is responsible for the great increase in strength of treated soil compared to that of untreated soil. At medium confining pressures, they suggested that the failure is dominated by a combination of cementation and friction. The results indicate a great degree of nonlinearity in peak strength envelope.

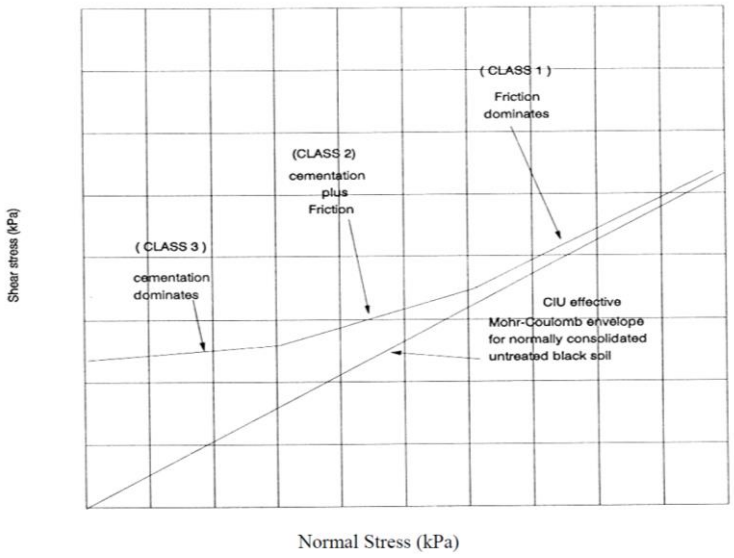

Figure 2.4: Effective shear envelope of cemented treated clay (Azman et al., 1995)

Kamruzzaman et al. (2009) noted that the peak deviatoric stress for a given cement content is almost constant for a range of consolidation pressures below yield stress, indicating a high degree of nonlinearity in the failure envelope. This was found for the samples cured for 7 and 28 days. Cement Deep Mixing (CDM) Association of Japan (1994) has presented peak and post-peak strengths of a cement treated soil over a range of confining pressures. The post-peak data show a linear shear strength envelope; however, the peak strength data show a highly nonlinear shear strength envelope.

As discussed earlier in lime fixation capacity definition, a minimum cement content is required to increase the strength of a clay (Hilt and Davidson, 1960; Kamruzzaman 1998; Uddin et al. 1997). Overall, it has been found that the strength of treated clay increases with the increase of cement content (Chew et al., 1997; Uddin et al. 1997). According to Uddin et al. 1997, however, the rate of increase of strength reduces beyond a certain cement content. Uddin et al. (1997) and Horpibulsuk et al. (2004) found that cohesion and friction angle increased for treated Bangkok clay with an increase in cement content (up to 15%) and curing time of 28 days. The shear strength may become constant and eventually decrease with increasing lime or cement content beyond an optimum value.

Several researchers have reported an increase in strength of treated clay with curing time particularly for the peak strength (Kawasaki et al. 1981; Nagaraj et al. 1997; Uddin et al. 1997). The pozzolanic reactions may continue for months or years leading to strength increase if free lime or cement is available (Bergado et al. 1996). The rate of increase is rapid at early stages of curing and decreases afterwards (Porbaha et al., 2000). Sivapullaiah et al. (2000b) and Sivapullaiah et al. (2006) found a significant increase in the peak strength of lime treated Black Cotton soil (Table 2.1) and Red Earth clay (Table 2.1), respectively, as the curing period increased. Uddin et al. (1997) noted that the clay samples with the same cement content but cured for a longer period showed a greater peak followed by greater strain softening behavior. The samples cured for a longer period showed greater negative shear-induced porewater pressure. It was found that the effect of curing period on the peak strength is larger at higher cement contents (Kamruzzaman et al., 2009). Wissa et al. (1965) found the same behavior for the peak strength; however, the curing period did not influence the post-peak strength. The treated soils had the same post-peak strength independently of curing time.

Wissa et al. (1965) performed undrained triaxial compression tests with pore water pressure measurements on two clays treated by lime or cement. The increase in the effective stress strength parameters was greater for the high plasticity Vicksburg Buckshot clay (VBC) than for the low plasticity Massachusetts clay (M-21). They considered two components of the shear resistance of treated soils, i.e. a cohesive resistance independent of the normal stress, and a friction resistance proportional to the normal effective stress. The effective cohesion was found to increase as a function of soil type, type and amount of cementing agent and curing period. The effective friction

angle was found to be a function of only type of soil and type and amount of cementing agent, independent of curing time. Furthermore, they used the large strain (post-peak) strength where the cementation between aggregates is destroyed in the shear zone and cohesive resistance is zero, as an indication of improvement in the frictional resistance of treated soils. It was noted that 5% lime increased the post-peak friction angle of M-21 from 30.5 to 35 degrees and that of VBC from 20 to 30.5 degrees. Hence aggregation can substantially increase the frictional resistance of particularly high plasticity clays probably due to formation of large strongly cemented aggregates of soil particles.

Ahnberg et al. (2003) and Ahnberg (2007) found that lime did not have much effect on shear strength of Linkoping clay and the difference between 1 day and 1 year strength was very small. However, cement-stabilized Linkoping clay showed a considerably higher strength. Addition of lime to Loftabro clay with the similar plasticity as Linkoping clay but different mineralogical composition and origin increased the effective stress strength parameters. The strength of lime treated Loftabro clay kept increasing with curing time up to 365 days (limit of the curing time used in the tests). It was also shown that the long-term increase in strength of lime stabilized Loftabro clay was larger than cement stabilized Loftbro. Cement also increased the effective stress strength parameters corresponding to peak strength of Loftabro clay up to a curing period of 28 days; but no further increase was observed after 28 days. In general, the cement stabilized samples showed more brittle behavior than lime stabilized samples. It was found that lime stabilization was more sensitive to the mineralogical composition of the soil. This may be explained as the source of pozzolans required for reactions. In case of lime, pozzolans are provided by the clay minerals.

Horpibulsuk et al. (2004) showed that the peak shear strength of cement-treated Ariake clay kept increasing for cement contents of up to 18%; however, the post-peak strength did not change once more than 6% cement was added. Balasubramaniam et al. (1989) also found that the peak strength parameters of soft Bangkok clay increased with lime content up to 7.5%. Addition of more than 7.5% lime had a small effect on the shear strength and addition of 15% lime decreased the shear strength. Addition of 2.5% lime did not improve the post-peak strength but 5% lime increased the post-peak strength for consolidation pressures up to 200 kPa. Under 400 kPa consolidation pressure, although the stress-strain curve shows a significant peak, it drops to a post-

peak strength lower than the fully softened strength of the untreated soil. Ahnberg (2007) found that more than 3% lime caused only little additional improvement to the post-peak shear strength of Loftabro clay cured for 28 days.

Chin (2006) found that the post-peak friction angle decreases with an increase in effective stress. It was suggested that the reduction is due to increasing disaggregation at the shear plane as the normal stress increases. The samples cured under pressure showed higher isotropic yield stress and peak strength . The increase in the strength was attributed to the void ratio reduction when the samples were cured under pressure. The liquid limit and compressibility of the samples decreased with an increase in the stresses under which the samples were cured.

Some researchers have correlated the strength gain of treated soils with the reduction in the initial void ratio of the compacted soil (Chin, 2006; Kamruzzaman et al., 2009). The void ratio decreases with cement content and curing time due to the reduction in water content resulting from hydration reactions and formation of pozzolanic products (Kamruzzaman et al., 2009).

Figures 2.5 and 2.6 show the secant friction angle, respectively, corresponding to peak and post-peak shear strength of clays treated with lime or cement (Wissa et al., 1965; Horpibulsuk et al., 2004; Balasubramaniam et al., 1989; Sivapullaiah et al., 2006; Banks et al., 2001; Lee and Lee, 2002; Muhunthan and Sariosseiri, 2008; Ahnberg, 2007). The peak and post-peak strengths of treated clays reported in the literature were used to calculate the secant friction angle as a function of effective normal stress. The liquid limit, plasticity index, and clay size fraction of the untreated clays in Figures 2.5 and 2.6 are in the range of 20 to 120%, 6 to 63%, and 15 to 70% (Table 2.1), respectively, and the curing periods are in the range of 1 to 400 days. The peak shear strengths of the treated clays in Figure 2.5 occurred at axial strains of less than 2%. In some cases where small amount of lime or cement was used, the strain corresponding to the peak shear strength reached up to 4%. The axial strain level corresponding to the post-peak shear strength is 10% or more.

Figures 2.5 and 2.6 show that in the most of cases a lime or cement content of 5% to 7% provides the maximum peak and post-peak shear strength increase. The effect of treatment on the secant peak and post-peak friction angles decreases at higher normal stresses, suggesting a highly nonlinear shear envelope particularly for the peak strength.

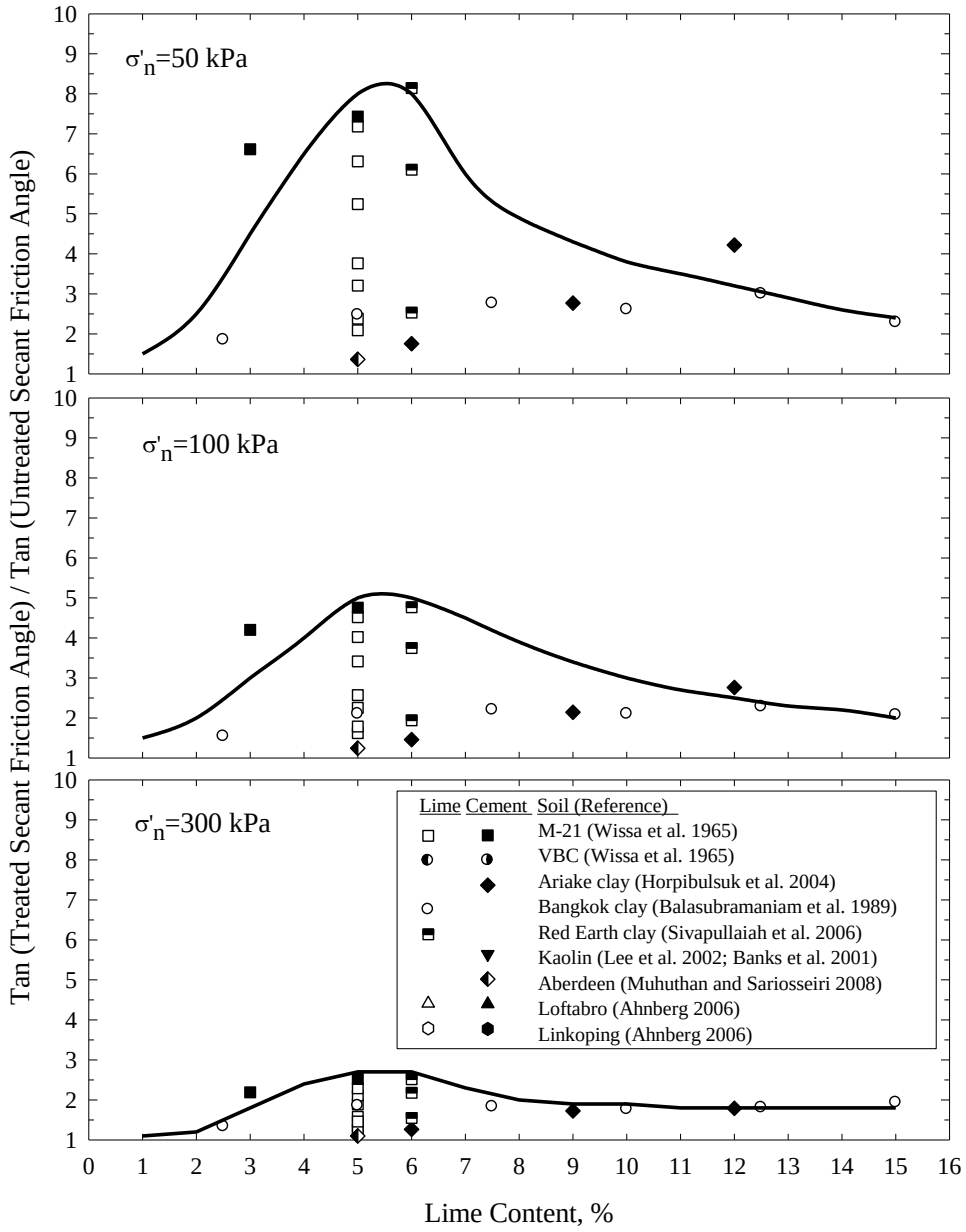

Figure 2.5: Secant peak friction angle of treated clays referenced to that of untreated clays

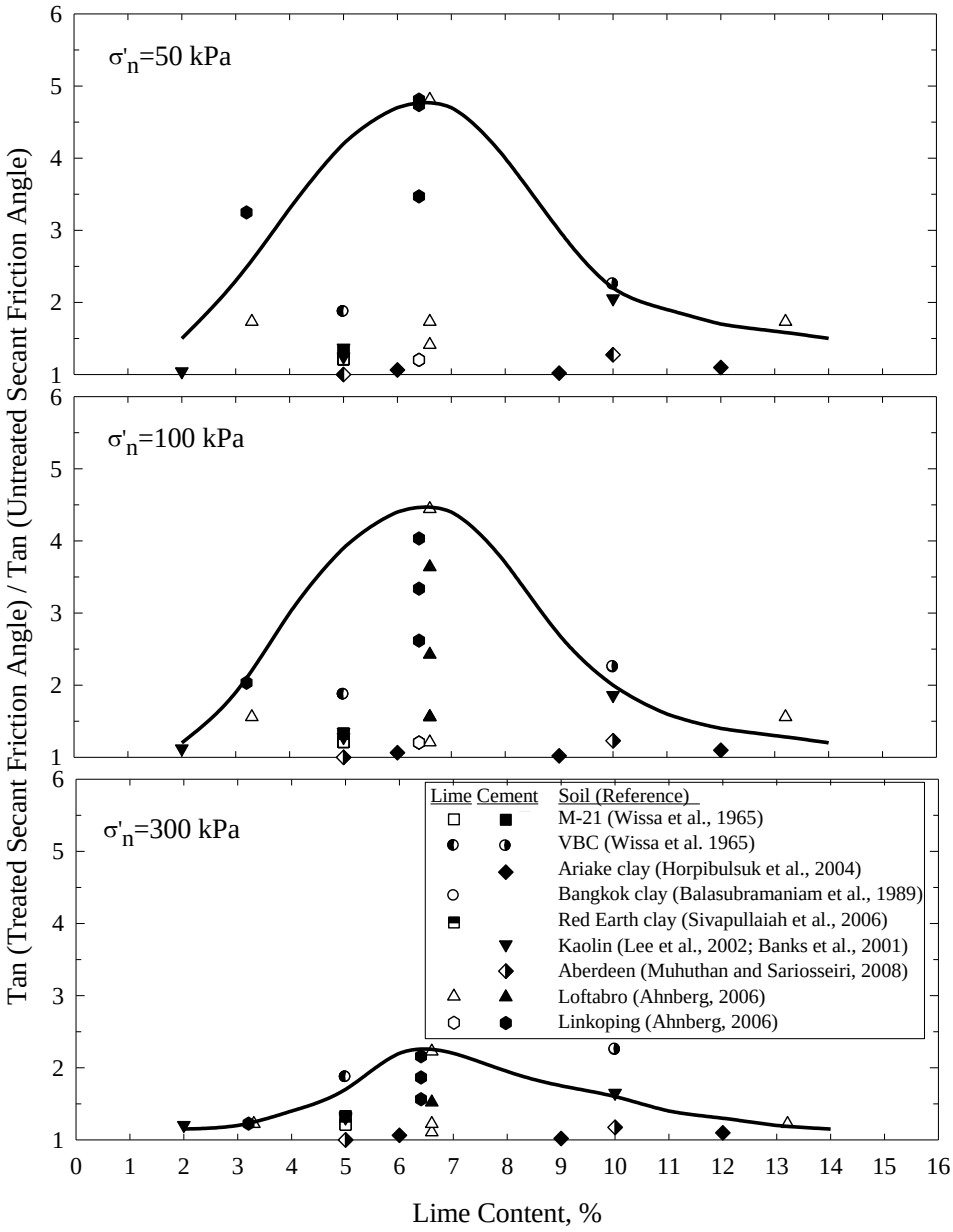

Figure 2.6: Secant post-peak friction angle of treated clays referenced to that of untreated clays

The data presented in the literature suggest that a minimum amount of lime is required to initiate the pozzolanic reactions and increase the shear strength of soil. By adding more lime than a specific percentage which depends on the soil mineralogy, the peak strength increases but the post peak strength remains constant or may even decrease. For example, in the case of Singapore marine clay, the peak strength keeps increasing for lime contents up to 50%; however, most of the

improvement in the post-peak or remolded strength occurs after addition of 10-20% lime (Kamruzzaman, 2002, Xiao, 2009). The lime contents for treatment of Singapore clay is considered to be higher than what is typically used to treat soils, which may be due to high water content of soft Singapore clay.

2.8.2 Remolded samples

The secant fully softened friction angle of the untreated Singapore marine clay was reported to be 23 degrees. The CIU tests by Xiao (2009) confirmed this value after about 13% strain. The CIU triaxial compression tests were later performed by Xiao (2009) on remolded cement-treated marine clay with the following range of properties:

- Cement content of 10% to 50%
- Water content of 100% to 167%
- Confining effective stress of 100 kPa to 1,250 kPa
- Curing period of 7 and 28 days
- Curing Stress (before remolding) of 0 (atmospheric) to 250 kPa

Below is a summary of the findings:

- The tests did not show the peak and strain-softening behavior observed in the intact cement treated specimens. In some cases, a slight peak was observed at about 6% to 12% axial strain. The maximum friction angle of remolded specimens was considered as the fully softened friction angle.
- Curing stress, water content and curing period did not have any major effect on the strength of the remolded treated soil.
- The peak friction angle of the remolded treated soil was found to depend mostly on the cement content. For 10%, 20%, 30%, and 50% cement contents, the peak friction angles were measured 37, 41, 42 and 43, respectively.

The fully softened friction angle measured by various types of tests and specimens are as follows:

- Post-peak strength in CIU triaxial tests on intact specimens under low confining stress: ϕ'=39 to 46 degrees.
- Peak strength in CIU triaxial tests on remolded specimens: ϕ'=37 to 43 degrees.
- Post-peak strength in CID triaxial tests on intact samples under high confining stress: ϕ'=19.5 to 24.5 degrees. In this case, major particle breakup was observed in SEM images.

The post-peak strength in intact samples seems to be reasonably close to the peak strength of remolded treated samples, as realized by several researchers (e.g. Cuccovillo and Coop, 1999; Chin, 2006; Xiao, 2009). The low friction angles in the CID tests was interpreted according to the fact that the friction angle decreases with an increase in the confining pressure due to more severe particle crushing occurring within the shear zone (Chin, 2006; Xiao, 2009).

Many researchers found it very difficult to determine an intrinsic strength for treated soil, reflecting only size and shape of particles as it depends on how intense the treated soil can be remolded to break as many bonds as possible. Chin (2006) used the wet remolding approach while Xiao (2009) dried the treated soil and then pounded and ground it into powder to break the bonds. However, it seems that the residual strength measured in precut samples presented in present study can be a reliable indicator for the unstructured state.

The triaxial tests performed by Xiao (2009) under confining presses as high as 2,500 kPa (well above the yield stress), where a major destruction of the inter-particle bonds is expected, showed a friction angle greater than that of untreated soil. This along with the post-peak strength of intact samples and peak strength of remolded treated samples discussed above confirm that the treated soil in destructed state displays improved frictional behavior.

2.9 LIME-SOIL REACTION INHIBITORS

Porbaha et al. (2000) suggested that special considerations are required for the soil with high organic or sault (sulfate) content as it may disrupt the hydration reactions. An organic content of 2% is considered high and influences the reactions (Locat et al., 1984; Choquette et al., 1987). Le Roux (1969) and Le Roux and Toubeau (1987) identified chlorite, carbonates, and sulfates as reaction inhibitors. One of the soils studied by Locat et al. (1999) having the highest carbonate, organic matter and chlorite contents showed the lowest strength development among the four soils. Thompson (1966) has shown that soils with chloritic minerals are less reactive than soils with higher smectite, kaolinite or illite content. Du et al. (2014) reported an interruption in formation of CSH and ettringite in zinc-contaminated clay, which leads to formation of other products filling the pore space but not contribute to the strength.

2.10 EFFECT OF SULFATE ON LIME TREATMENT OF SOIL

Observation of needle-shaped crystals in the SEM images of treated Brenna clay along with detection of a small amount of sulfate in the composition of Brenna clay determined from EDS analysis, was the motive for study of sulfate effect on lime treatment of soils.

Sulfate can exist either in the clay composition or in additives used to stabilize clays. It is very likely for marine clays to include sulfate either naturally or through contaminated industrial waste (Rajasekaran, 1994). Gypsum (calcium sulfate) is quite common in marine clays (Kawasaki, 1988). Sulfate of sodium, calcium and potassium are common in soils of certain regions with limited precipitation (Grim, 1968; Wild et al., 1999). Both beneficial and detrimental effects of sulfate on lime or cement treated soils have been reported by researchers (Mehra et al., 1955; Lambe et al., 1960; Ladd et al., 1960; Sherwood, 1962, 1982).

Sulfate has been recognized by some researchers to have harmful effects on the strength of cement-stabilized soils by swelling and disintegration of the soil structure due to ettringite formation (Mehra et al., 1955; Cordon, 1962; Mitchell, 1986a, 1986b). Sulfate has two major effects on lime-treated clays. It increases the PH of the soil due to formation of NaOH, which enhances the dissolution of silica and alumina of the clay minerals. Thus, lime reactivity is expected to be enhanced in presence of sulfate. However, sulfate reacts with lime to form $CaSO_4$

and reduces the amount of lime available for the pozzolanic reactions. This can explain the reduced strength with time of lime treated clay in the presence of sulfate. The strength also reduces due to decrease in cementation ability as a result of sulfate adsorption on the surface of CSH (Mehta, 1983).

Studies have shown formation of expansive minerals such as ettringite and thaumasite in the presence of sulfate (Mitchel, 1986a; Hunter, 1988; Rajasekaran, 1994). The reactions leading to formation of these products are as follows (Hunter, 1988):

$$6Ca^{2+} + 2Al(OH)_4^- + 4(OH)^- + 3(SO_4)^{2-} + 26H_2O \rightarrow Ca_6[Al(OH)_6]_2 \cdot (SO_4)_3 \cdot 26H_2O \text{ (ettringite)}$$

$$Ca_6[Al(OH)_6]2 \cdot (SO_4)_3 \cdot 26H_2O + 2H_2SiO_4^{2-} + 2CO_3^{2-} + O_2 \rightarrow Ca_6[Si(OH)_6]_2 \cdot (SO_4)_2 \cdot (CO_3)_2.24H_2O \text{ (thaumasite)} + 2Al(OH)_4^- + (SO_4)^{2-} + 4OH^- + 2H_2O$$

As these products form, pH drops as a result of the reduction of available lime (Mitchell, 1986a). Ettringite formation is a complex phenomenon and limited information is available on how it affects engineering properties of lime-treated clays. Study of ettringite and its effect on long-term behavior of treated soils is deemed necessary for successful treatment of marine clays and to the use of proper corrective measurements. The silica required for thaumasite formation is mostly supplied by decomposition of CSH formed by pozzolanic reactions in lime-stabilized soils, unreacted calcium silicate in cement-stabilized soils, or by dissolved silica from clay particles (Crammond, 1985; Kohler et al., 2006).

Experimental studies have shown that soils containing about 1,000 to 10,000 ppm (0.1 to 1%) sulfate may lead to ettringite formation once treated with calcium-based stabilizers such as lime or cement (Hunter 1988; Mitchell and Dermatas 1992; Puppala et al. 2002; Little et al. 2005; Little 2006). A threshold value of 2,000 ppm (0.2%) has been suggested for soluble sulfate, below which no significant problems are expected in stabilized soils due to expansive minerals (Petry and Little, 1992). Hunter (1988) found that if the clay percentage is more than 10% and soluble

sulfate exceeds 1% (10,000 ppm), lime addition induces the formation of expansive products. As indicated by Mitchell and Dermatas (1992) and Snedker (1996), a low sulfate content of 0.3% is sufficient to induce swelling. A sulfate content as little as 0.05% can induce favorable conditions for ettringite formation (Raja, 1990; Rajasekaran et al., 1997b, Rajasekaran, 2005). In general, it has been reported that 0.01% to 0.5% sulfate can cause low to moderate swelling and heave, 0.5% to 1.2% can cause moderate to serious heave, and severe heave is expected for more than 1.2% sulfate content (Raja, 1990; Petry, 1994; McCallister and Tidwell, 1997). The ettringite formation is an expansive process (Hunter, 1988; Mitchell and Dermatas, 1992) causing a reduction of strength of treated soil (Sherwood, 1993). Sherwood (1993) noted 24% and 67% strength loss in lime-treated London clay with 0.25% and 2% sulfate content, respectively. Sivapullaiah et al. (2000b) noted that despite an early increase in the strength of treated soil, the sulfate effect becomes more pronounced as the curing time increases. Sridhran et al. (1995) also noted that the sodium sulfate in soil turns lime into insoluble gypsum and sodium hydroxide and thus reduces the lime available for pozzolanic reactions. The reduction in strength may be owing to alteration of pozzolanic reactions. Rajasekaran and Narasimha Rao (2000) observed a significant shear strength reduction after the addition of sodium sulfate to lime-treated clay. They attributed it to the detrimental effect of sodium sulfate as a monovalent cation stabilizer and also to the formation of ettringite. The ettringite mineral has a needle-shaped structure with lengths ranging from a few microns to as high as 200 microns (Moore and Taylor, 1970; Dermatas, 1995; Moon et al., 2007) and in the presence of water is believed to weaken the treated soil system (Mitchell, 1986a; Hunter, 1988). Ettringite has also been known by many researchers to be the product of sulfate attack on concrete (Irassar et al., 1996; Collepardi, 2003).

In the presence of water, needle-shaped crystals of ettringite formed under unconfined condition hydrate significantly, showing a high liquid limit, whereas the needle-shaped crystals forms under confining pressure have a major role in reinforcing soil structure and contributing to shear strength.

The tubular structure of ettringite consists of column and channels (Moore and Taylor, 1970), in which water (if available) can be held causing swelling of ettringite. The other product of sulfate attack, i.e. thaumasite, has similar structure but lower swelling characteristics (Crammond, 2003). Thaumasite results in loss of bonding and strength (Crammond, 2003).

Sherwood (1962) observed cracking and swelling in 10% lime-treated clay subject to sodium sulfate or magnesium sulfate solutions due to ettringite formation. Mitchell (1986b) reported expansion and disintegration after a few years of lime-treated sulfate-bearing clay used in road construction. Sivapullaiah et al. (2000b) noted an interruption of CSH formation in the lime-treated Black Cotton soil in the presence of sulfate. In this case, ettringite and thaumasite were formed instead of calcium silicate hydrate. The reactions leading to formation of ettringite and thaumasite in presence of calcium cations and sulfate ions have been presented in Hunter (1988). As indicated by Mitchell and Dermatos (1990), the reaction mechanism and products are altered in presence of sulfate. Calcium sulpho-aluminate phase ettringite ($C_3A.3CS.H_{32}$) is formed in this case. The metastable phase ($C_3A.CS.H_{12}$) may also be formed at low sulfate concentrations.

Despite the negative effect of sulfate on lime or cement treated clay, there are some researchers who have reported an improvement to the strength due to the formation of ettringite (Kozan, 1960; Lambe et al., 1960; Mehta, 1983; Kamon and Nontananandh, 1991). Kozan (1960) and Lambe et al. (1960) found that small sodium sulfate contents increased the strength of some cement-treated soils. Beneficial effects of needle-shaped ettringite in intercrossing soil particles, filling large inter-particle voids, thus removing water trapped in the voids, resulting in a denser microfabric and greater strength, have been recognized by some researchers (e.g. Mehta 1983; Kawamura et al., 1986; Kamon and Nontananandh, 1991). It was found that after consumption of sulfate in the alternation reactions, normal lime-soil reactions may continue. It has been found that the natural sulfate-bearing clay (natural sulfate content of less than 1%) shows strength improvement by addition of lime as cementitious products are formed with time.

In contrast to the general understanding of ettringite formation in concrete, i.e. fast and solely dependent on sulfate content, the process is more complicated in soils. The sulfate content is one among several contributing factors. Ettringite formation is gradual due to slow release of alumina from soil minerals (Dermatas et al. 2005; Taylor et al. 2001; Little et al. 2005, Ouhadi and Yong, 2008). The sulfate effect on treated soils depends on soil type including mineralogical composition specially clay mineral content (available alumina and silica), water content, lime content, sulfate content including sulfate cation rank in lyotropic series, pH and temperature (Sherwood, 1982; Mitchel and Dermatas, 1992, Dermatas 1995, Little and Graves,1995, Littleton, 1995; Rollings et al., 1999; Rajasekaran, 2005; Little et al., 2005 and 2010). Due to the less rigid

and more open structure of stabilized soils compared to concrete, the ettringite reactants can move more easily through the structure and form additional ettringite (Hunter, 1988).

Little et al. (2010) noted that it is unlikely to dissolve all the sulfate available in the soil, even with using a high amount of initial mixing water, due to low solubility of gypsum. The solubility of gypsum, the most common sulfate-bearing mineral in soils, is rather small, i.e., 2.58 g/L (Burkart et al., 1999). The water content used in mixing process of soil is usually too low to dissolve all of the sulfates present in the soil (Little et al., 2010). In a soil with water content of 25% containing 0.167% sulfate and 5% lime, only about 0.036% of sulfate (1/5 of available sulfate) will be dissolved, and thus available for ettringite formation (Little et al., 2010). The higher the water content is used during mixing, the more the amount of ettringite is expected to form. It is thus recommended to use as much water as practical and extend the mixing process as long as possible to ensure a uniform distribution of ettringite nucleation sites, and minimize subsequent ettringite formation in the presence of external water (e.g. rainfall). The fairly low water content range which is typically used in soil treatment with calcium-based stabilizers together with relatively high void ratios of compacted soil matrix, are expected to accommodate a uniform distribution of ettringite crystals (Little and Graves, 1995; Dermatas, 1995; Little et al., 2005). Some of the water is consumed by the pozzolanic reactions during lime stabilization and may not be available for ettringite formation (Little et al., 2010). However, the other sulfate saults with higher solubility such as sodium sulfate may lead to greater amounts and more rapid ettringite formation. Studies by Little et al. (2010) are mostly focused on expedition of ettringite formation by using as much water as possible and prolonged uniform mixing to ensure that most of the ettringite is formed before the soil compaction. However, as the purpose of lime stabilization is to improve soil and complete the process in the minimum possible time, the use of high water content and prolonged mixing do not seem to be favorable in field (Jefferis, 2011). Little et al. (2010) did not address the influence of ettringite formation on drained strength of soil. Whether or not the formation of ettringite disrupts the stabilization process depend on whether the ettringite grows within open voids or within a dense matrix leading to swelling (Little et al., 2010). The expansion process may open up the soil structure and attract more water into the newly created voids leading to strength reduction (Jefferis, 2011).

Stanley et al. (2012) observed the formation of thaumasite in the soft silty Melbourne clay consisting of illite and kaolinite minerals, 3% pyrite (source of sulfate) and 4% organic matter treated with lime. Thaumasite was detected after 1 month of curing. It was further found that thaumasite can be formed at the expense of decomposition of cementitious products (e.g. CSH) as curing time increases to 3-6 months. Although more thaumasite was detected at 3 months than 1 month, the strength increased with curing time up to 3 months. This was believed to be due to formation of more pozzolanic products suppressing the detrimental effect of thaumasite. However, the strength dropped to some extent at 6 months of curing likely due to the gradual slowing of pozzolanic reactions and increasing influence of thaumasite.

The negative charge and high surface area of ettringite crystals attract large amounts of water causing inter-particle repulsion and expansion in absence of strong bonding among ettringite crystals (Mehta, 1973a). This is similar to the mechanism of attraction of water molecules occurring in expansive clays. It has been suggested that external water is the dominant factor in detrimental reactions (Little et al., 2010). Water (rain) introduced into the soil system following soil stabilization can move any unreacted lime as well as other reagents including sulfate to nucleation sites formed during early stages of stabilization due to limited availability of sulfate and aluminum, leading to formation of additional ettringite (Hunter, 1988; Burkart et al, 1999, Little et al., 2010).

Vichan et al. (2013) studied the properties of soft high plasticity Bangkok clay containing a small natural amount of sulphur (1.2%) in the form of gypsum, treated by calcium carbide, which contains mainly $Ca(OH)_2$. Furthermore, less than 1% of sulphur was found in the composition of the calcium carbide. This much sulphur was enough to react with $Ca(OH)_2$ and form ettringite, (so-called sulpho-pozzolanic reaction product) and amorphous calcium silicate hydrate, which were detectable in the XRD and SEM results. The SEM images of 90-days specimens illustrated that the stabilized clay particles were coated with small rectangular or fibrous CASH crystals. When the curing time increased to 150 days, the larger aggregated crystals of CASH, and also what was believed to be gismondine were noted. Vichan et al. (2013) believed that gismondine was the main cementitious product contributing to the long-term strength gain. For greater lime contents, supplementary cementitious products (CASH) were formed by pozzolanic reactions,

leading to the subsequent filling of pores and to a greater strength. Therefore, a small amount of sulphur did not have detrimental effects.

The SEM images on 12% cement treated kaolin after 28 days of curing show reticulate CSH, needle-shaped ettringite and a gel-type CSH coating the surface of the aggregates (Du et al., 2014). The flocculated fabric and fine network of reticulation was observed in the stabilized soil. It is noted that the cement used in their study carried about 4% (of cement weight) sulfate, which is believed to be the source of ettringite formation.

Crystallization inhibitors have long been used in concrete to minimize the product formed by sulfate attack. The same techniques have been proposed by researchers to be applied to the soil stabilized by calcium-based binders (lime or cement). Harris et al. (2014) suggested using phosphate compound to avoid ettringite formation responsible for the heave caused by sulfate. Harris et al. (2014) were successful in changing the hydration products and stopping ettringite formation; however, the effectiveness of the new alternative products was not investigated.

Rajasekaran (2005) studied the properties of lime treated soft marine clay from the east coast of India. Quick lime mixed with sodium sulfate or calcium sulfate in a 1:1 ratio was used to treat the soil. It was found that sodium sulfate has detrimental effects on the properties of lime-treated clay, whereas calcium sulfate (gypsum) improved the properties. The SEM images of lime-sodium sulfate-treated soil after 45 days of curing revealed the needle-shaped ettringite crystals. Lime-sodium sulfate-treated soil shows more signs of ettringite formation compared to lime-calcium sulfate-treated soil (Rajasekaran, 2005). Larger aggregates were observed in case of calcium sulfate. Kinuthia et al. (1999) studied the effect of various sulfate cations such as Na^+, K^+, Ca^{2+} and Mg^{2+} on lime-treated kaolinite clay. Kinuthia et al. (1999) found that Ca^{2+} and Mg^{2+} have beneficial effects, whereas the monovalent sulfate cations have detrimental effects on lime-treated soil. The addition of calcium or magnesium sulfates lowered the liquid limit and plasticity index of lime-treated kaolinite. For sodium and potassium sulfates, despite an initial decrease in the liquid limit and plasticity index, they increased with time.

There have been numerous studies raising concern on adverse effect of sulfate on lime-treated soils due to the heave-induced damage to lightly loaded structures (Rajasekaran and Narasimha Rao, 2005). However, this may not be a factor if soil is not free to expand.

Clay-size fraction and type of clay minerals present in soil determine the aluminum available to dissolve at high pH and form ettringite (Mitchel and Dermatas, 1992; Dermatas, 1995; Petry and Little, 1992; Herbert et al., 2009). Tsatsos and Dermatas (1998) evaluated the formation of ettringite in lime-treated kaolinite and montmorillonite minerals in the presence of sulfate. They noted significant swelling in the lime-sulfate-treated kaolinite due to high amount of alumina available for ettringite formation. On the contrary, minimal swelling was noted in the case of montmorillonite due to lower release of alumina (lower Al/Si ratio). The higher release of silica in montmorillonite promoted CSH formation, so the hydration products were different than the ettringite alone observed in treated kaolinite. This is consistent with the findings by Dermatas (1995) and Little et al. (2010) that the availability of alumina bearing clay minerals is a key factor in the rate of ettringite formation. Furthermore, the study by Little et al. (2010) shows that the ettringite concentration during initial curing periods (i.e. the first week) is mostly controlled by kaolinite and the steady increase in the ettringite concentration is due to alumina released from both kaolinite and montmorillonite. Alternatively, the release of soluble silica from clay minerals or additives can react with available lime and restrict lime-sulfate-aluminum reaction to produce ettringite (Tasong et al., 1999).

CHAPTER 3

MATERIAL AND TESTING PROCEDURE

The properties of each clay and the binder used in this study are presented in this chapter. This is followed by the apparatuses and experimental procedure for the tests carried out as part of this study. The variables under investigation and properties of each specimen are presented at the end of this chapter.

3.1 CHARACTERIZATION OF UNTREATED CLAYS

3.1.1 Brenna formation

The highly plastic lacustrine clays of Lake Agassiz lead to slope instability along the banks of the Red River that separates Grand Forks, North Dakota from East Grand Forks, Minnesota, as it flows north to Lake Winnipeg in Manitoba, Canada (Mesri and Huvaj, 2004). The clays of the Red River slopes are the glacio-lacustrine deposits of glacial Lake Agassiz that is believed to have existed from 13,000 to 8,500 years before present, during the Late Wisconsin Glacial Episode of the Pleistocene Epoch (Quigley 1980).

The Brenna Formation, which is characterized as a uniform, soft to firm, dark grey, glacio-lacustrine clay with little or no visible stratification, is full of slickensided surfaces. The major source of sediment for the Brenna Formation is the highly plastic montmorillonitic Pierre Shale bedrock (Quigley, 1968; Baracos 1977). The clay size fraction of Brenna Formation ranges from 60 to 95% (Arndt 1977). This unit is divided into Lower Brenna and Upper Brenna members. The natural water content, plastic limit and liquid limit of Lower Brenna are in the range of 42 to 69%, 20 to 40%, and 62 to 103%, respectively, and the corresponding range for Upper Brenna are 60 to 85%, 27 to 38%, and 107 to 154%, respectively. Samples of both Lower Brenna and Upper Brenna were used in the present investigation.

3.1.2 Beaumont formation

One of the main sources of slope instability in Harris County Flood Control District (HCFCD), Texas is the Beaumont clay. This Clay formation was built up during the early Wisconsin stage of Pleistocene epoch from multiple episodes of flood-plain deposition, desiccation, and weathering, associated with sea-level fluctuations coincidental with glacial cycling (Al-Layla 1970). Subsequently, there was a substantial drop in sea level and Beaumont clay was subjected to prolonged desiccation during Late Wisconsin Ice Age. Therefore, the Beaumont clay formation was preconsolidated by desiccation 70 to 100 thousand years before present and displays overconsolidation ratios in the range of 4 to 6 (Al-Layla, 1970; Maher and O'Neill, 1983).

The clay is reddish-brown and highly plastic. In general, the Beaumont clay formation consists of poorly-bedded, plastic clay inter-bedded with silt and sand lentils, and has some more or less continuous layers of sand (Sellards et al. 1932).

Typical samples of Beaumont clay are composed of 23-47% calcium montmorillonite and 28-55% illite; the remaining minerals being kaolinite and finely ground quartz. Beaumont clay contains a network of closely spaced (2 to 4 mm spacing) fissures and slickensides (Al-Layla 1970). The plastic limit and liquid limit and of Beaumont clay are in the range of 19 to 45% and 37 to 112%, respectively. The natural water content is generally at or a few percentage points above the plastic limit. An undisturbed wrapped sample had a natural water content of 21%. The clay fraction of Beaumont clay varies between 69 and 88%.

3.1.3 Chicago clay formation

The Chicago clay was deposited during the glacial epoch. The clay consists of a series of several ground moraines or till sheets lying one on another. Thus, it possesses a degree of stratification. Each till sheet represents the clay deposited upon the pre-existing surface by the advancing glacier plus that deposited from the melting ice as the glacial front receded. The clay is found in gray, bluish gray and blue color. The natural water content, plastic limit and liquid limit of Chicago clay are in the range of 15 to 25%, 12 to 21%, and 22 to 42%, respectively. The clay size fraction is in the range of 32-36%. The dominant clay mineral in Chicago clay is illite. Typical

samples of Chicago clay are composed of 40% illite, 5% montmorillonite and the remaining are non-clay minerals.

The index properties of the clay samples used in this study are summarized in Table 3.1. The Chicago Blue clay is classified as low plasticity silty clay (CL), whereas and the Brenna and Beaumont clays are classified as high plasticity clay (CH) according to the Unified Soil Classification System. The soils have been selected to investigate the lime treatment of low and high plasticity clays.

Table 3.1: Properties of soils utilized in laboratory tests

	Chicago clay	Upper Brenna clay	Beaumont clay	Lower Brenna clay
Plastic limit, w_p (%)	20	33	23	40
Liquid limit, w_l (%)	38	117	62	87
Plasticity index, I_p (%)	18	84	39	47
Optimum water content, w_{opt} (%)	14.5	23	19	30
Clay fraction, CF (%)	32	70-95	70-80	87
pH	7.9	7.4	8.3	7.5
Unified classification	CL	CH	CH	CH

3.2 BINDER PROPERTIES

Dry hydrated lime [$Ca(OH)_2$] was used as the stabilizing binder. It is 98% extra pure calcium hydroxide, supplied by ACROS Organics. The remaining 2% in the composition includes other alkli salts. The solubility of this product in water is 1.65 g/L (20°C).

3.3 SAMPLE PREPARATION AND TESTING PROCEDURE

3.3.1 Direct shear tests

Drained direct shear tests on lime-treated clay were performed using reconstituted specimens. Drained multiple reversal direct shear tests on precut specimens were used to measure

residual shear strength, and drained direct shear tests on uncut reconstituted specimens were used to measure peak and post-peak shear strengths. One of the two Wykeham Farrance direct shear apparatuses utilized in the present study is shown in Figure 3.1.

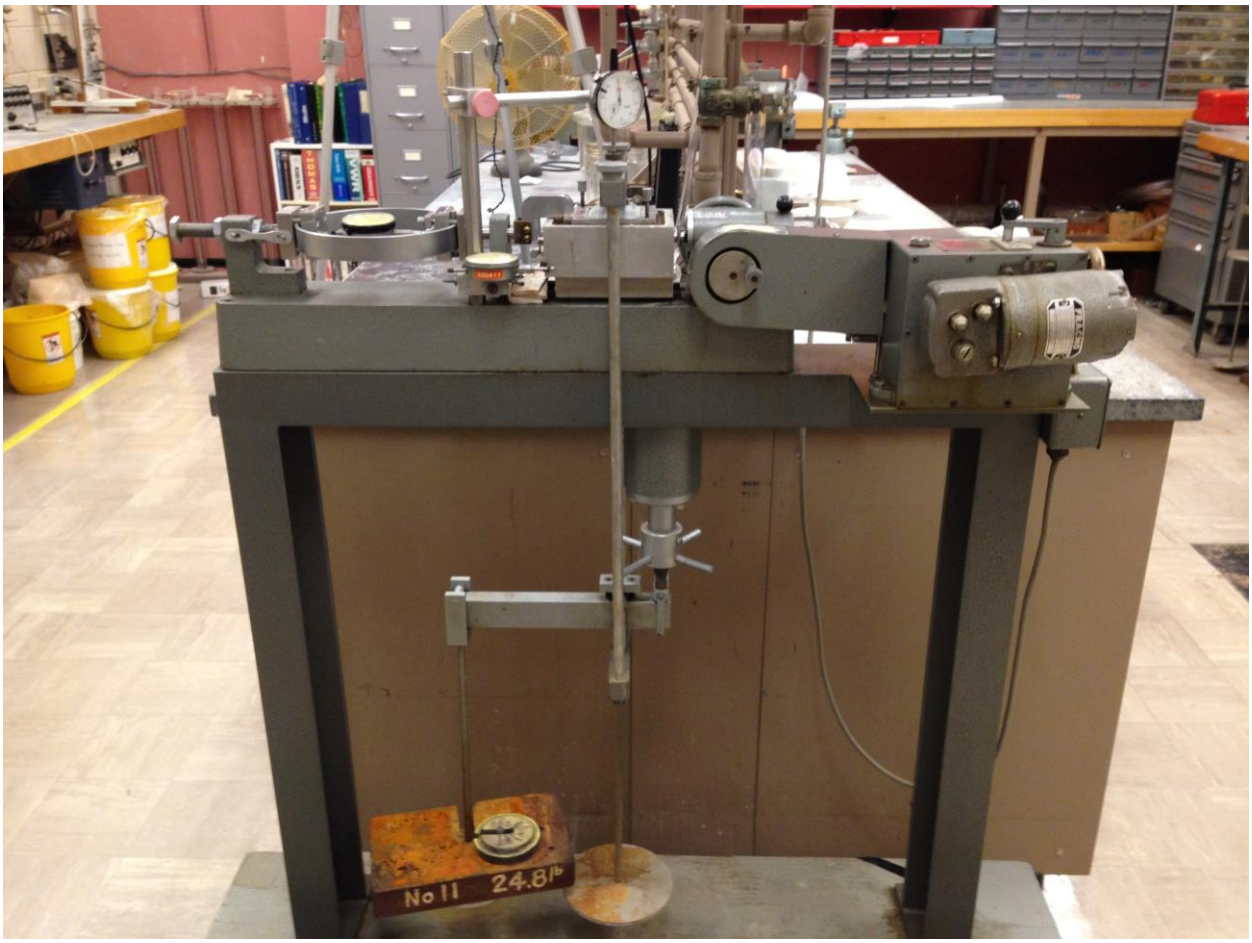

Figure 3.1: Direct shear aparatus

Air dry clay was pulverized until all of a representative sample passed the no. 40 US standard sieve. The pulverized clay was thoroughly mixed with dry hydrated lime and was rehydrated using distilled water. Enough water was added to ensure proper mixing. This much water often brought the samples to just about liquid limit. After the mixing process was completed, the clay was spread on a glass plate to reduce its water content. The clay was then placed by remolding into the shear box in a water content range between plastic limit and liquid limit, closer to liquid limit to ensure that the sample was saturated and had enough water for future hydration.

The direct shear specimens remained saturated by adding water to the shear box every day. The specimens were subjected to a total normal stress of 50 kPa immediately after preparation. The samples were consolidated in stages to the final normal load by doubling the normal pressure each time. In most cases, it took one to two days to complete the primary consolidation under each load. An attempt was made to reach the final normal stress as soon as possible, so most of curing took place under the normal stress at which the samples was subsequently sheared. For comparison, a few samples of Brenna clay and Chicago clay were cured unconfined under atmospheric pressure. After the desired curing period, these samples were then placed by remolding into the shear box, consolidated in stages and sheared. A number of the direct shear tests on treated Chicago clay were performed on specimens compacted at optimum water content. These specimens were compacted directly into the shear box and cured under pressure. The specimens prepared by the aforementioned procedures are used to measure peak and post-peak strengths and are referred to as "intact" specimens. A detailed description of samples is presented later in this chapter.

In the case of precut specimens, the two halves of the precut specimen were formed by remolding or compaction and separately consolidated inside the top and bottom halves of the shear box using the procedure described by Mesri and Cepeda-Diaz (1986) and Mesri and Huvaj-Sarihan (2012). Another way to prepare precut samples is to cut an intact sample after the peak and post-peak strengths were measured. The slip surface during shear remained within the gap between the halves due to low compressibility of treated soil, in the range of normal stresses at which the samples were sheared. This was examined after each test to ensure that the shearing took place along the precut surface. The specimens prepared in two separate halves or by cutting an intact sample, are called "precut" samples. Two precut specimens of Brenna clay and Beaumont clay are shown in Figure 3.2.

In general, Lime content as a percent of dry weight of clay ranges from 0 to 15%; water content is in the range of 15 to 274%; normal stress ranges from 20 to 450 kPa; curing time ranges from 1 to 49 days for intact specimens and from 3 to 206 days for precut specimens. In a few direct shear tests, dry hydrated lime was sprinkled on the exposed shear surface or on the top and bottom, of the direct shear specimen to examine lime diffusion. A shear displacement rate of 0.2 mm/hr was used for the drained shear condition.

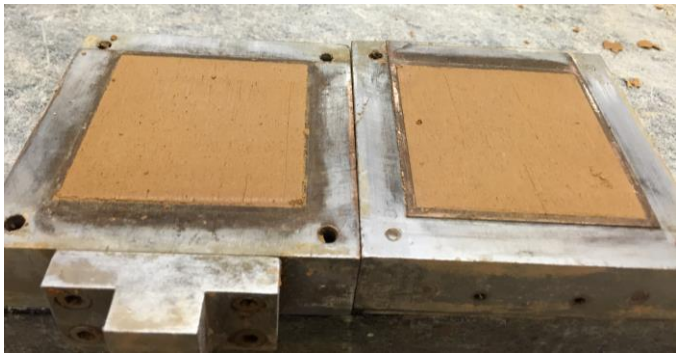

(a)

(b)

Figure 3.2: Precut specimens before shear of: (a) Beaumont clay; (b) Brenna clay

The following convention was utilized to facilitate identification of the characteristics of the direct shear test specimens:

For intact specimens

[name of clay]-[type of specimen]-[lime content]-[initial water content]-[Maximum effective curing stress]-[curing time]-[effective normal stress]

CH, UB, LB and BE are used as abbreviations for Chicago, Upper Brenna, Lower Brenna and Beaumont clay, respectively. For majority of the samples, curing occurred under confining pressure (effective vertical stress). For the curing periods of more than 7 days, most of curing occurred under the final effective normal stress at which the sample was sheared. The precut specimens were cured under one effective normal stress and sheared under a range of effective normal stresses. Therefore, the curing stress is not necessarily the same as the effective normal

stress at shearing. There are two different stresses included in the name of the precut samples: $[\sigma_n]_{cur}$ is the initial curing stress and the second stress, σ_n, is the normal stress at which the sample was sheared. In some cases, the shearing of a precut sample was halted and resumed after a longer curing period. It is noted that the pozzolanic reaction is an ongoing process and it is influenced by the loading history under which the sample has been cured. Hence it is valuable to know the loading and curing history of the tested samples. The loading history and characteristics of the samples including the curing periods under various normal stresses are shown in Tables 3.2-3.8.

For example, "LB-LC10-W70-7d-200kPa-I" refers to an intact sample of Lower Brenna clay with 10% lime and 70% initial water content, cured for 7 days, and cured and sheared at normal stress of 200 kPa. Similarly, "BE-LC10-W62-P_{cu} 100kPa-30d-200kPa-P" refers to a precut sample of Beaumont clay with 10% lime and 62% initial water content, cured for 30 days under 100 kPa normal stress, and sheared at 200 kPa normal stress. The name of each sample only provides its general characteristics. Refer to Tables 3.2-3.4 for detailed information on the intact samples. The precut samples properties are summarized in Tables 3.5-3.8.

3.3.2 Atterberg limit tests

The Casagrande apparatus and thread-rolling procedure (ASTM D4318-10) were used as the standard methods to determine liquid and plastic limits, respectively. About 300 g of soil was mixed with lime in dry condition and distilled water was added to bring the water content of the mixture to liquidity index of about 1.5. After the sample was cured unconfined for the desired period of time, it was spread on a glass plate and mixed periodically to prevent non-uniform drying. The number of blows for the groove to close was recorded each time. A minimum of 4 points between 15 and 35 were used to determine the liquid limit in the Casagrande method. The process of drying was continued toward plastic limit measurement (rolling thread). At least 3 samples were taken to determine plastic limit in the standard thread-rolling procedure.

For a number of direct shear test specimens, liquid limit and plastic limit were determined at the end of the direct shear test using the specimen. These samples were cured under confining pressure. The specimens were air dried, crushed and pulverized at the end of the direct shear test. The same aforementioned procedure was used to determine the Atterberg limits.

All index tests and direct shear tests reported here were performed at laboratory temperature of 20 ± 2°C. For both the characterization tests and molding specimens for the drained direct shear tests, distilled water was used.

3.3.3 pH measurement

The pH of the treated clay was measured as an indicator of lime availability and continuation of pozzolanic reactions. The pH measurements were performed using the HI1292D, a pH probe supplied by Hanna Instruments, as shown in Figure 3.3. The probe has a glass body filled with electrolyte connected to Hanna's HI99121 pH meter for direct pH measurement. The probe has a conic pH sensing tip with an integrated amplifier and built-in temperature sensor for automatically temperature compensated pH readings. The probe has been designed specifically for pH measurement in soils. The probe was calibrated periodically in the course of the study using the buffers provided by the manufacturer.

Representative samples of various lime contents were prepared as described for the Atterberg limit tests and stored in the humidity room. At designated curing periods, pH of the samples was measured to determine the variation of pH with time. In addition, the pH measurements were conducted on the direct shear test specimens at the end of the tests. The direct shear specimens were air dried and pulverized after being dismantled and mixed with water to measure the pH.

Figure 3.3: pH meter (HI99121, Hanna Instrument)

3.3.4 Scanning Electron Microscopy (SEM) and Energy Dispersive Spectroscopy (EDS)

The Scannig Electron Microscope (SEM) has extensive applications in soils. The SEM with high magnification was used to assess the change in size and shape of clay particles and new products formed by pozzolanic reactions. The JEOL JSM-6060LV scanning electron microscope (Figure 3.4) in the Materials Research Laboratory (MRL) of the University of Illinois at Urbana-Champaign was utilized to take the SEM images.

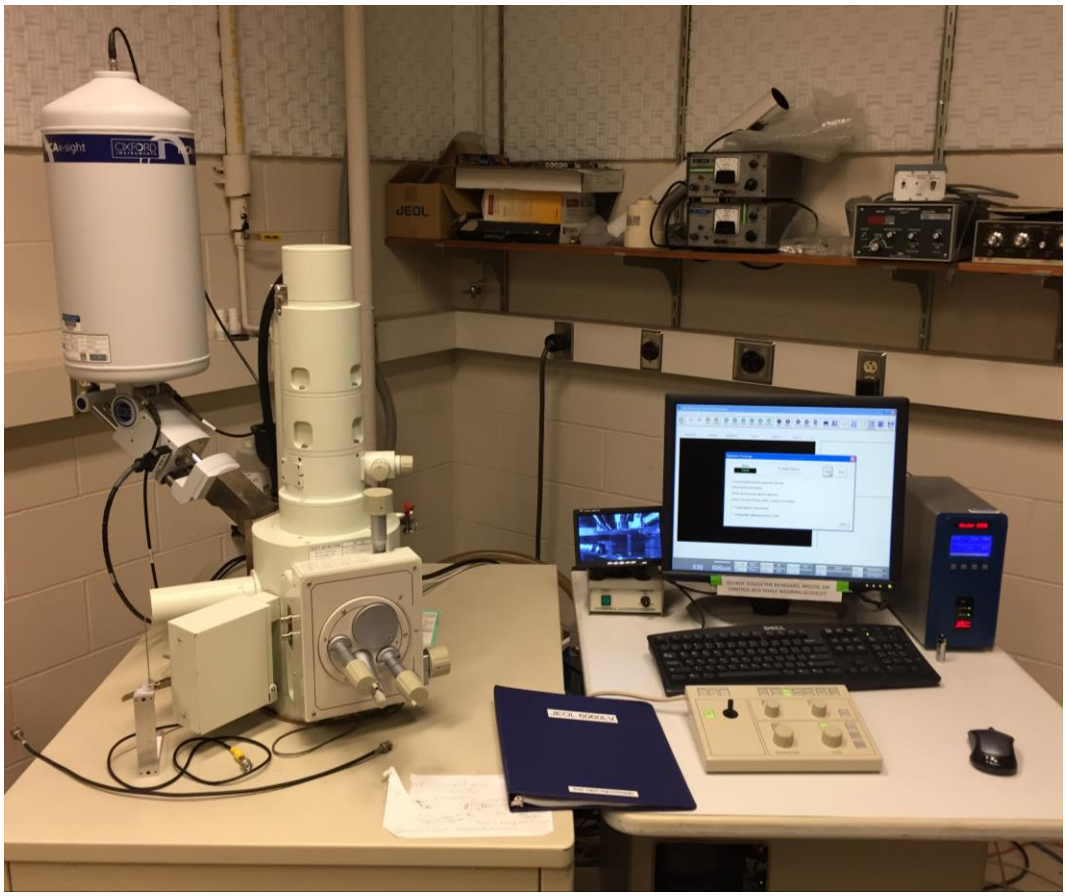

Figure 3.4: Scanning Electron Microscope (JEOL JSM-6060LV)

The apparatus is a high-performance microscope with a magnification of up to 300,000. The specimen chamber can accommodate a specimen of up to 5 inches in diameter. The chamber space can be used to examine four (4) samples simultaneously, as shown in Figure 3.5. However, it is preferred to keep the size of each sample below half an inch in diameter. It takes a significant

amount of time for the apparatus to apply vacuum to the chamber in the case of larger samples and it often fails to maintain the vacuum.

Figure 3.5: Specimen chamber in Scanning Electron Microscope

A sample examined by SEM is struck on the surface by a large number of electrons. If these electrons are not removed, the sample may be damaged by heating and an area with a high electric charge may form. This is called “charging” and affects the quality of SEM images. Therefore, samples are often coated with a very thin layer of conductive material to prevent charging. The Emscope SC500 Sputter Coater in the MRL was utilized to spray a very thin layer

(about 10 nm) of gold-palladium in a vacuum to the surface of the samples. A diffuse cloud is observed around the samples when being coated, as shown in Figure 3.6.

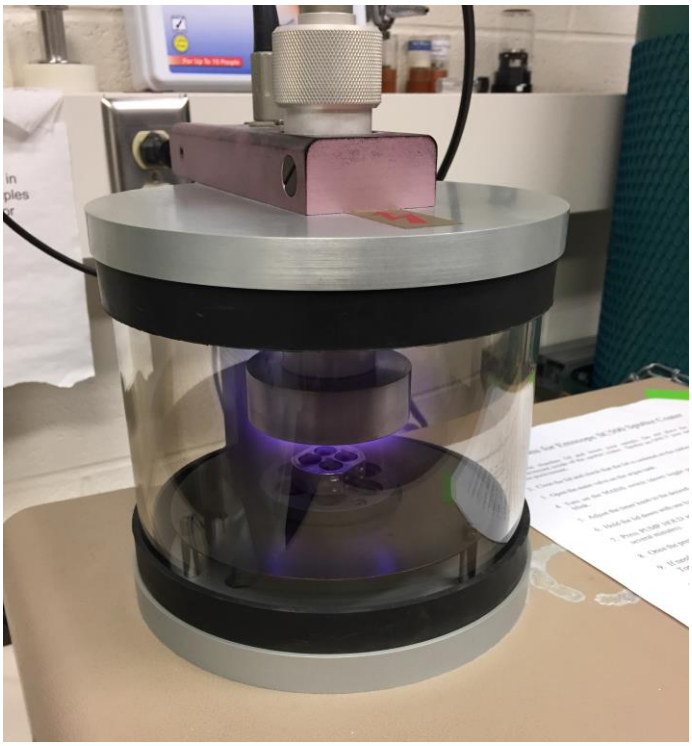

Figure 3.6: Emscope SC500 Sputter Coater

The apparatus is connected to an Energy Dispersive X-ray Spectroscopy (EDS) elemental analysis system to detect various elements of the samples. The system is capable of detecting the elements of the areas focused by the SEM. The EDS analyzer connected to the scanning electron microscope is shown in Figure 3.7.

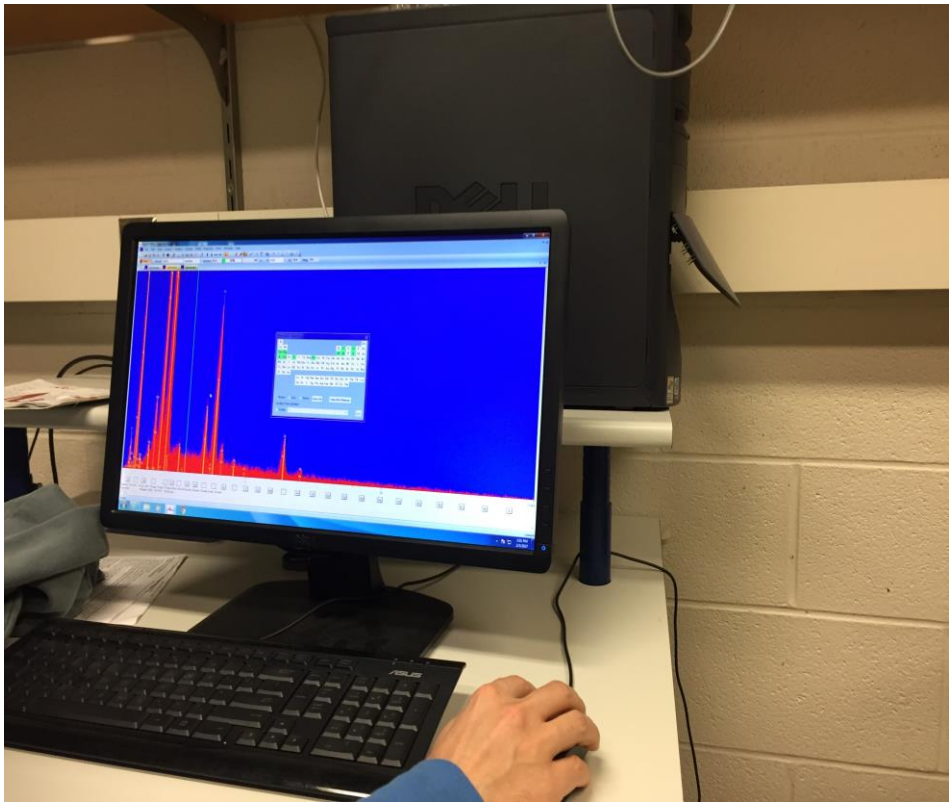

Figure 3.7: Energy Dispersive Spectroscopy (EDS) analyzer

The SEM was performed on selected direct shear specimens. After competition of the direct shear tests, the specimens were dismantled and were broken in small pieces. The specimen was left at room temperature to air dry. One representative piece of the specimen preferably from the shear surface was chosen for SEM examination. The SEM operated at 10 kV and the images were taken with a magnification ranging from 2,000 to 25,000.

Table 3.2: Intact Chicago (CH) clay samples

Sample No.	Lime Content, LC (%)	Initial Water Content, w (%)	Curing Time Before Shearing (days)							Normal Stress (kPa)	Designated Name
			Curing Normal Stress (kPa)						Total		
			Atm.	50	100	200	300	400			
1	0	15	-	-	-	-	-	-	-	50	CH-R-0-15-0-0-50
2	0	15	-	-	-	-	-	-	-	100	CH-R-0-15-0-0-100
3	0	15	-	-	-	-	-	-	-	300	CH-R-0-15-0-0-300
4	1	15	0	2	5	-	-	-	7	100	CH-I-1-15-100-7-100
5	2	15	0	2	5	-	-	-	7	100	CH-I-2-15-100-7-100
6	3	48	0	7	-	-	-	-	7	50	CH-I-3-48-50-7-50
7	3	15	0	2	5	-	-	-	7	100	CH-I-3-15-100-7-100
8	3	47	0	2	2	-	3	-	7	300	CH-I-3-47-300-7-300
9	3	15	0	28	-	-	-	-	28	50	CH-I-3-15-50-28-50
10	3	15	0	2	26	-	-	-	28	100	CH-I-3-15-100-28-100
11	3	15	0	2	1	-	25	-	28	300	CH-I-3-15-300-28-300
12	5	36	0	2	2	-	3	-	7	300	CH-I-5-36-300-7-300
13	5	15	0	2	26	-	-	-	28	100	CH-I-5-15-100-28-100
14	5	40	0	41	-	-	-	-	41	50	CH-I-5-40-50-41-50
15	5	60	56	-	-	-	-	-	56	100	CH-I-5-60-0-56-100
16	10	15	0	2	5	-	-	-	7	100	CH-I-10-15-100-7-100
17	10	50	0	2	2	-	3	-	7	300	CH-I-10-50-300-7-300
18	10	15	-	2	26	-	-	-	28	100	CH-I-10-15-100-28-100
19	10	50	0	2	2	-	31		35	300	CH-I-10-50-300-35-300

Table 3.3: Intact Lower Brenna (LB) clay samples

Sample No.	Lime Content, LC (%)	Initial Water Content, w (%)	Curing Time Before Shearing (days)							Normal Stress (kPa)	Designated Name
			Curing Normal Stress (kPa)						Total		
			Atm.	50	100	200	300	400			
20	0	70	-	-	-	-	-	-	-	50	LB-R-0-70-0-0-50
21	0	70	-	-	-	-	-	-	-	100	LB-R-0-70-0-0-100
22	0	70	-	-	-	-	-	-	-	200	LB-R-0-70-0-0-200
23	3	42	0	2	5	-	-	-	7	100	LB-I-3-42-100-7-100
24	3	72	0	3	1	3			7	200	LB-I-3-72-200-7-200
25	5	71	0	7	-	-	-	-	7	50	LB-I-5-71-50-7-50
26	5	70	0	2	5	-	-	-	7	100	LB-I-5-70-100-7-100
27	5	73	0	2	2	3	-	-	7	200	LB-I-5-73-200-7-200
28	5	53	0	14	-	-	-	-	14	50	LB-I-5-53-50-14-50
29	5	53	0	3	3	8	-	-	14	200	LB-I-5-53-200-14-200
30	7	70	0	7	-	-	-	-	7	50	LB-I-7-70-50-7-50
31	7	70	0	2	5	-	-	-	7	100	LB-I-7-70-100-7-100
32	7	71	0	2	2	3	-	-	7	200	LB-I-7-71-200-7-200
33	7	63	0	14	-	-	-	-	14	50	LB-I-7-63-50-14-50
34	7	73	0	2	12	-	-	-	14	100	LB-I-7-73-100-14-100
35	7	63	0	3	3	8	-	-	14	200	LB-I-7-63-200-14-200
36	7	62	0	35	-	-	-	-	35	50	LB-I-7-62-50-35-50
37	7	73	0	3	32	-	-	-	35	100	LB-I-7-73-100-35-100
38	7	62	0	3	3	29	-	-	35	200	LB-I-7-62-200-35-200
39	7	67	0	3	3	3	-	26	35	400	LB-I-7-67-400-35-400
40	10	42	0	7	-	-	-	-	7	50	LB-I-10-42-50-7-50
41	10	42	0	2	5	-	-	-	7	100	LB-I-10-42-100-7-100
42	10	42	0	2	2	3			7	200	LB-I-10-42-200-7-200
43	10	65	0	2	33	-	-	-	35	100	LB-I-10-65-100-35-100
44	10	64	0	2	2	45			49	200	LB-I-10-64-200-49-200
45	15	64	0	3	5	27			35	200	LB-I-15-64-200-35-200

Table 3.4: Intact Beaumont (BE) clay samples

Sample No.	Lime Content, LC (%)	Initial Water Content, w (%)	Curing Time Before Shearing (days)							Normal Stress (kPa)	Designated Name
			Curing Normal Stress (kPa)						Total		
			Atm.	50	100	200	300	400			
46	0	63	-	-	-	-	-	-	-	50	BE-I-0-63-0-0-50
47	0	61	-	-	-	-	-	-	-	100	BE-I-0-61-0-0-100
48	0	63	-	-	-	-	-	-	-	200	BE-I-0-63-0-0-200
49	1	64	0	7	-	-	-	-	7	50	BE-I-1-64-50-7-50
50	1	64	0	3	4	-	-	-	7	100	BE-I-1-64-100-7-100
51	3	23	0	2	5	-	-	-	7	100	BE-I-3-23-100-7-100
52	3	62	0	2	5	-	-	-	7	100	BE-I-3-62-100-7-100
53	5	63	0	0	1	-	-	-	1	100	BE-I-5-63-100-1-100
54	5	54	0	7	-	-	-	-	7	50	BE-I-5-54-50-7-50
55	5	23	0	2	5	-	-	-	7	100	BE-I-5-23-100-7-100
56	5	65	0	2	2	3	-	-	7	200	BE-I-5-65-200-7-200
57	5	63	0	2	12	-	-	-	14	100	BE-I-5-63-100-14-100
58	5	59	0	2	33	-	-	-	35	100	BE-I-5-59-100-35-100
59	7	52	0	7	-	-	-	-	7	50	BE-I-7-52-50-7-50
60	7	52	0	2	5	-	-	-	7	100	BE-I-7-52-100-7-100
61	7	68	0	2	2	3	-	-	7	200	BE-I-7-68-200-7-200
62	10	55	0	7	-	-	-	-	7	50	BE-I-10-55-50-7-50
63	10	55	0	2	5	-	-	-	7	100	BE-I-10-55-100-7-100
64	10	60	0	2	2	3			7	200	BE-I-10-60-200-7-200
65	10	51	0	14	-	-	-	-	14	50	BE-I-10-51-50-14-50
66	10	51	0	2	12	-	-	-	14	100	BE-I-10-51-100-14-100
67	10	51	0	3	2	2	-	4	14	100	BE-I-10-51-600-14-100
68	10	54	0	3	1	10	-	-	14	200	BE-I-10-54-200-14-200
69	10	64	0	35	-	-	-	-	35	50	BE-I-10-64-50-35-50
70	10	66	0	3	32	-	-	-	35	100	BE-I-10-66-100-35-100
71	10	64	0	3	8	24	-	-	35	200	BE-I-10-64-200-35-200
72	15	67	0	3	5	27	-	-	35	200	BE-I-15-67-200-35-200

Table 3.5: Precut Chicago (CH) clay samples

Specimen No.	LC (%)	Initial w (%)	Curing Time Before Shearing (days)							During Shear		Total Curing Time (days)	Designated Name
			Curing Normal Stress (kPa)						Total	Normal Stress (kPa)	Curing Time (days)		
			Atm.	50	100	200	300	400					
73a	0	15	0	-	-	-	-	-	-	50	-	-	CH-P-0-15-0-0-50
73b										100	-	-	CH-P-0-15-0-0-100
73c										300	-	-	CH-P-0-15-0-0-300
74	1	15	0	2	5	-	-	-	7	100	2	9	CH-P-1-15-100-9-100
75	2	15	0	2	5	-	-	-	7	100	2	9	CH-P-2-15-100-9-100
76	3	15	0	2	5	-	-	-	7	100	2	9	CH-P-3-15-100-9-100
77	3	47	0	2	5	-	-	-	7	300	7	14	CH-P-3-47-100-14-300
										300	20	34	CH-P-3-47-100-34-300
78	3	15	0	28	-	-	-	-	28	50	4	32	CH-P-3-15-50-32-50
										50	42	74	CH-P-3-15-50-74-50
79	3	15	0	2	1	-	25	-	28	300	2	30	CH-P-3-15-300-30-300
										300	22	52	CH-P-3-15-300-52-300
80	3	15	0	2	26	-	-	-	28	100	2	30	CH-P-3-15-100-30-100
81	3	15	0	28	-	-	-	-	28	50	62	90	CH-P-3-15-50-90-50
										100	10	100	CH-P-3-15-50-100-100
										200	20	120	CH-P-3-15-50-120-200
82	5	15	0	2	26	-	-	-	28	100	2	30	CH-P-5-15-100-30-100
83	5	60	56	-	-	-	-	-	56	100	33	89	CH-P-5-60-0-89-100
										300	25	114	CH-P-5-60-0-114-300
										100	8	122	CH-P-5-60-0-122-100
84	5	40	0	41	-	-	-	-	41	50	23	64	CH-P-5-40-50-64-50
										100	46	110	CH-P-5-40-50-110-100
										200	10	120	CH-P-5-40-50-120-200
										400	2	122	CH-P-5-40-50-122-400
										400	45	167	CH-P-5-40-50-167-400
85	10	15	0	2	5	-	-	-	7	100	2	9	CH-P-10-15-100-9-100
86	10	15	0	2	26	-	-	-	28	100	2	30	CH-P-10-15-100-30-100
87	10	40	0	2	2	-	24	-	28	300	6	34	CH-P-10-40-300-34-300
										100	4	38	CH-P-10-40-300-38-100
										50	2	40	CH-P-10-40-300-40-50
88	10	40	180	-	-	-	-	-	180	100	13	193	CH-P-10-40-0-193-100

Table 3.6: Precut Lower Brenna (LB) clay samples

Specimen No.	LC (%)	Initial w (%)	Curing Time Before Shearing (days)							During Shear		Total Curing Time (days)	Designated Name
			Curing Normal Stress (kPa)						Total	Normal Stress (kPa)	Curing Time (days)		
			Atm.	50	100	200	300	400					
89	0	42	0	-	-	-	-	-	-	50	-	-	LB-P-0-42-0-0-50
										100	-	-	LB-P-0-42-0-0-100
										300	-	-	LB-P-0-42-0-0-300
90	3	42	0	2	5	-	-	-	7	100	9	16	LB-P-3-42-100-16-100
										50	2	18	LB-P-3-42-100-18-50
										20	3	21	LB-P-3-42-100-21-20
										100	8	29	LB-P-3-42-100-29-100
										200	4	33	LB-P-3-42-100-33-200
91	5	70	0	2	2	3	-	-	7	200	2	9	LB-P-5-70-200-9-200
										200	2	11	LB-P-5-70-200-11-200
										100	2	13	LB-P-5-70-200-13-100
										50	2	15	LB-P-5-70-200-15-50
										300	2	17	LB-P-5-70-200-17-300
										400	2	19	LB-P-5-70-200-19-400
92	5	70	0	2	5	-	-	-	7	100	3	10	LB-P-5-70-100-10-100
										100	29	39	LB-P-5-70-100-39-100
										50	2	41	LB-P-5-70-100-41-50
										300	2	43	LB-P-5-70-100-43-300
										100	60	103	LB-P-5-70-100-103-100
										50	4	107	LB-P-5-70-100-107-50
										300	5	112	LB-P-5-70-100-112-300
93	5	100	7	-	-	-	-	-	7	50	33	40	LB-P-5-100-0-40-50
										100	12	52	LB-P-5-100-0-52-100
										200	16	68	LB-P-5-100-0-68-200
94	5	100	120	-	-	-	-	-	120	50	33	153	LB-P-5-100-0-153-50
95	5	100	140	-	-	-	-	-	140	50	6	146	LB-P-5-100-0-146-50
										200	14	160	LB-P-5-100-0-160-200
										300	12	172	LB-P-5-100-0-172-300
										100	6	178	LB-P-5-100-0-178-100
										400	9	187	LB-P-5-100-0-187-400

Table 3.6: (cont'd)

Specimen No.	LC (%)	Initial w (%)	Curing Time Before Shearing (days)							During Shear		Total Curing Time (days)	Designated Name
			Curing Normal Stress (kPa)						Total	Normal Stress (kPa)	Curing Time (days)		
			Atm.	50	100	200	300	400					
96	7	70	0	7					7	50	12	19	LB-P-7-70-50-19-50
										20	3	22	LB-P-7-70-50-22-20
										100	4	26	LB-P-7-70-50-26-100
										200	13	39	LB-P-7-70-50-39-200
										50	11	50	LB-P-7-70-50-50-50
										20	5	55	LB-P-7-70-50-55-20
97	7	70	0	2	5	-	-	-	7	100	12	19	LB-P-7-70-100-19-100
										50	3	22	LB-P-7-70-100-22-50
										20	4	26	LB-P-7-70-100-26-20
										200	13	39	LB-P-7-70-100-39-200
98	7	70	0	2	2	3	-	-	7	200	2	9	LB-P-7-70-200-9-200
										200	2	11	LB-P-7-70-200-11-200
										100	2	13	LB-P-7-70-200-13-100
										50	2	15	LB-P-7-70-200-15-50
										300	2	17	LB-P-7-70-200-17-300
										400	2	19	LB-P-7-70-200-19-400
99	7	67	0	3	4	84	-	-	91	200	3	94	LB-P-7-67-200-94-200
										100	2	96	LB-P-7-67-200-96-100
										50	2	98	LB-P-7-67-200-98-50
										300	6	104	LB-P-7-67-200-104-300
100	10	42	0	7	-	-	-	-	7	50	25	32	LB-P-10-42-50-32-50
										20	5	37	LB-P-10-42-50-37-20
										100	2	39	LB-P-10-42-50-39-100
										200	6	45	LB-P-10-42-50-45-200
101	10	42	0	2	5	-	-	-	7	100	9	16	LB-P-10-42-100-16-100
										50	2	18	LB-P-10-42-100-18-50
										20	3	21	LB-P-10-42-100-21-20
										100	7	28	LB-P-10-42-100-28-100
										200	4	32	LB-P-10-42-100-32-200

Table 3.6: (cont'd)

Specimen No.	LC (%)	Initial w (%)	Curing Time Before Shearing (days)							During Shear		Total Curing Time (days)	Designated Name
			Curing Normal Stress (kPa)						Total	Normal Stress (kPa)	Curing Time (days)		
			Atm.	50	100	200	300	400					
102	10	42	0	2	2	3	-	-	7	200	20	27	LB-P-10-42-200-27-200
										100	10	37	LB-P-10-42-200-37-100
										50	2	39	LB-P-10-42-200-39-50
103	10	70	0	36	-	-	-	-	36	50	38	74	LB-P-10-70-50-74-50
										100	6	80	LB-P-10-70-50-80-100
										200	6	86	LB-P-10-70-50-86-200
										400	40	126	LB-P-10-70-50-126-400
										800	41	167	LB-P-10-70-50-167-800
										400	7	174	LB-P-10-70-50-174-400
104	10	70	0	2	2	45	-	-	49	200	6	55	LB-P-10-70-200-55-200
										100	4	59	LB-P-10-70-200-59-100
										50	3	62	LB-P-10-70-200-62-50
										400	4	66	LB-P-10-70-200-66-400
105	10	100	180	-	-	-	-	-	180	100	30	210	LB-P-10-100-0-210-100
										50	12	222	LB-P-10-100-0-222-50
										200	12	234	LB-P-10-100-0-234-200
										300	30	264	LB-P-10-100-0-264-300
106	15	64	0	3	5	27	-	-	35	50	11	46	LB-P-15-64-200-46-50
										100	3	49	LB-P-15-64-200-49-100
										200	5	54	LB-P-15-64-200-54-200
										400	9	63	LB-P-15-64-200-63-400

Table 3.7: Precut Beaumont (BE) clay samples

Specimen No.	LC (%)	Initial w (%)	Curing Time Before Shearing (days)							During Shear		Total Curing Time (days)	Designated Name
			Curing Normal Stress (kPa)						Total	Normal Stress (kPa)	Curing Time (days)		
			Atm.	50	100	200	300	400					
107	0	52	0						-	50	-	-	BE-P-0-52-0-0-50
										100	-	-	BE-P-0-52-0-0-100
										300	-	-	BE-P-0-52-0-0-300
108	1	62	0	7	-	-	-	-	7	50	16	23	BE-P-1-62-50-23-50
										50	2	25	BE-P-1-62-50-25-50
										50	2	27	BE-P-1-62-50-27-50
										20	2	29	BE-P-1-62-50-29-20
										100	2	31	BE-P-1-62-50-31-100
										150	2	33	BE-P-1-62-50-33-150
										200	2	35	BE-P-1-62-50-35-200
										50	2	37	BE-P-1-62-50-37-50
109	1	62	0	3	4	-	-	-	7	100	18	25	BE-P-1-62-100-25-100
										100	2	27	BE-P-1-62-100-27-100
										50	2	29	BE-P-1-62-100-29-50
										20	2	31	BE-P-1-62-100-31-20
										150	2	33	BE-P-1-62-100-33-150
										200	2	35	BE-P-1-62-100-35-200
										300	2	37	BE-P-1-62-100-37-300
										100	2	39	BE-P-1-62-100-39-100
110	3	23	0	2	5	-	-	-	7	100	18	25	BE-P-3-23-100-25-100
										50	8	33	BE-P-3-23-100-33-50
										200	13	46	BE-P-3-23-100-46-200
										300	7	53	BE-P-3-23-100-53-300
111	3	62	0	2	5	-	-	-	7	100	15	22	BE-P-3-62-100-22-100
										100	3	25	BE-P-3-62-100-25-100
										50	8	33	BE-P-3-62-100-33-50
										200	4	37	BE-P-3-62-100-37-200
										200	9	46	BE-P-3-62-100-46-200
										300	7	53	BE-P-3-62-100-53-300

Table 3.7: (cont'd)

Specimen No.	LC (%)	Initial w (%)	Curing Time Before Shearing (days)							During Shear		Total Curing Time (days)	Designated Name
			Curing Normal Stress (kPa)						Total	Normal Stress (kPa)	Curing Time (days)		
			Atm.	50	100	200	300	400					
112	5	62	0	0	1		-	-	1	100	2	3	BE-P-5-62-100-3-100
										100	2	5	BE-P-5-62-100-5-100
										200	2	7	BE-P-5-62-100-7-200
113	5	62	0	7	-	-	-	-	7	50	2	9	BE-P-5-62-50-9-50
										100	2	11	BE-P-5-62-50-11-100
										200	2	13	BE-P-5-62-50-13-200
114	5	23	0	2	5	-	-	-	7	100	3	10	BE-P-5-23-100-10-100
										100	29	39	BE-P-5-23-100-39-100
										50	2	41	BE-P-5-23-100-41-50
										300	2	43	BE-P-5-23-100-43-300
										100	60	103	BE-P-5-23-100-103-100
										50		107	BE-P-5-23-100-107-50
										300	10	113	BE-P-5-23-100-113-300
115	5	62	0	2	5	-	-	-	7	100	13	20	BE-P-5-62-100-20-100
										50	12	32	BE-P-5-62-100-32-50
										300	14	46	BE-P-5-62-100-46-300
										300	20	66	BE-P-5-62-100-66-300
										100	26	72	BE-P-5-62-100-72-100
										50	7	79	BE-P-5-62-100-79-50
116	5	62	0	2	2	3	-	-	7	200	2	9	BE-P-5-62-200-9-200
										200	2	11	BE-P-5-62-200-11-200
										100	2	13	BE-P-5-62-200-13-100
										50	2	15	BE-P-5-62-200-15-50
										300	2	17	BE-P-5-62-200-17-300
										400	2	19	BE-P-5-62-200-19-400
117	5	52	0	2	2	4	-	4	14	100	128	142	BE-P-5-52-600-142-100
										50	4	146	BE-P-5-52-600-146-50
										200	2	148	BE-P-5-52-600-148-200
										100	27	175	BE-P-5-52-600-175-100
										50	2	177	BE-P-5-52-600-177-50
										200	5	182	BE-P-5-52-600-182-200

Table 3.7: (cont'd)

Specimen No.	LC (%)	Initial w (%)	Curing Time Before Shearing (days)							During Shear		Total Curing Time (days)	Designated Name
			Curing Normal Stress (kPa)						Total	Normal Stress (kPa)	Curing Time (days)		
			Atm.	50	100	200	300	400					
118	5	62	0	2	33	-	-	-	35	100	4	39	BE-P-5-62-100-39-100
										100	2	41	BE-P-5-62-100-41-100
										50	2	43	BE-P-5-62-100-43-50
										200	2	45	BE-P-5-62-100-45-200
										300	2	47	BE-P-5-62-100-47-300
119	7	52	0	7	-	-	-	-	7	50	7	14	BE-P-7-52-50-14-50
										20	2	16	BE-P-7-52-50-16-20
										100	2	18	BE-P-7-52-50-18-100
										200	5	23	BE-P-7-52-50-23-200
										200	2	25	BE-P-7-52-50-25-200
										100	2	27	BE-P-7-52-50-27-100
120	7	52	0	2	5	-	-	-	7	100	7	14	BE-P-7-52-100-14-100
										50	2	16	BE-P-7-52-100-16-50
										20	2	18	BE-P-7-52-100-18-20
										200	5	23	BE-P-7-52-100-23-200
121	7	52	0	0.2	0.3	0.5	-	1	7	100	3	10	BE-P-7-52-2,700-10-100
										50	2	12	BE-P-7-52-2,700-12-50
										300	2	14	BE-P-7-52-2,700-14-300
										100	10	24	BE-P-7-52-2,700-24-100
										50	3	27	BE-P-7-52-2,700-27-50
										100	39	66	BE-P-7-52-2,700-66-100
										50	2	68	BE-P-7-52-2,700-68-50
										100	41	109	BE-P-7-52-2,700-109-100
										50	11	120	BE-P-7-52-2,700-120-50
										300	5	125	BE-P-7-52-2,700-125-300
										50	7	132	BE-P-7-52-2,700-132-50
										100	7	139	BE-P-7-52-2,700-139-100
										300	5	144	BE-P-7-52-2,700-144-300

Table 3.7: (cont'd)

Specimen No.	LC (%)	Initial w (%)	Curing Time Before Shearing (days)							During Shear		Total Curing Time (days)	Designated Name
			Curing Normal Stress (kPa)						Total	Normal Stress (kPa)	Curing Time (days)		
			Atm.	50	100	200	300	400					
122	10	52	0	7	-	-	-	-	7	50	8	15	BE-P-10-52-50-15-50
										20	2	17	BE-P-10-52-50-17-20
										100	4	21	BE-P-10-52-50-21-100
										200	2	23	BE-P-10-52-50-23-200
123	10	52	0	2	5	-	-	-	7	100	8	15	BE-P-10-52-100-15-100
										50	2	17	BE-P-10-52-100-17-50
										20	4	21	BE-P-10-52-100-21-20
										200	2	23	BE-P-10-52-100-23-200
124	10	62	0	2	2	3	-	-	7	200	2	9	BE-P-10-62-200-9-200
										200	2	11	BE-P-10-62-200-11-200
										100	2	13	BE-P-10-62-200-13-100
										50	2	15	BE-P-10-62-200-15-50
										300	2	17	BE-P-10-62-200-17-300
										400	2	19	BE-P-10-62-200-19-400
125	10	51	0	14	-	-	-	-	14	50	9	23	BE-P-10-51-50-23-50
										20	5	28	BE-P-10-51-50-28-20
										100	2	30	BE-P-10-51-50-30-100
										200	6	36	BE-P-10-51-50-36-200
										100	11	47	BE-P-10-51-50-47-100
										50	3	50	BE-P-10-51-50-50-50
										200	5	55	BE-P-10-51-50-55-200
126	10	51	0	2	12	-	-	-	14	100	12	26	BE-P-10-51-100-26-100
										20	4	30	BE-P-10-51-100-30-20
										200	7	37	BE-P-10-51-100-37-200
										50	13	50	BE-P-10-51-100-50-50
										200	2	52	BE-P-10-51-100-52-200

Table 3.7: (cont'd)

Specimen No.	LC (%)	Initial w (%)	Curing Time Before Shearing (days)							During Shear		Total Curing Time (days)	Designated Name
			Curing Normal Stress (kPa)						Total	Normal Stress (kPa)	Curing Time (days)		
			Atm.	50	100	200	300	400					
127	10	64	0	35	-		-	-	35	50	29	64	BE-P-10-64-50-64-50
										100	3	67	BE-P-10-64-50-67-100
										200	5	72	BE-P-10-64-50-72-200
										400	4	76	BE-P-10-64-50-76-400
										100	12	88	BE-P-10-64-50-88-100
128	10	62	0	3	32	-	-	-	35	100	4	39	BE-P-10-62-100-39-100
										100	2	41	BE-P-10-62-100-41-100
										50	2	43	BE-P-10-62-100-43-50
										200	2	45	BE-P-10-62-100-45-200
										300	2	47	BE-P-10-62-100-47-300
129	10	64	0	3	8	24	-	-	35	50	29	64	BE-P-10-64-200-64-50
										100	3	67	BE-P-10-64-200-67-100
										200	5	72	BE-P-10-64-200-72-200
										400	4	76	BE-P-10-64-200-76-400
										100	12	88	BE-P-10-64-200-88-100
130	10	51	0	3	2	2	-	4	14	100	9	23	BE-P-10-51-600-23-100
										50	4	27	BE-P-10-51-600-27-50
										300	4	31	BE-P-10-51-600-31-300
										100	33	64	BE-P-10-51-600-64-100
										50	12	76	BE-P-10-51-600-76-50
										300	2	78	BE-P-10-51-600-78-300
										100	45	123	BE-P-10-51-600-123-100
										50	9	132	BE-P-10-51-600-132-50
										300	4	136	BE-P-10-51-600-136-300
										100	23	159	BE-P-10-51-600-159-100
										50	5	164	BE-P-10-51-600-164-50
										200	2	166	BE-P-10-51-600-166-200
										100	33	199	BE-P-10-51-600-199-100
										50	2	201	BE-P-10-51-600-201-50
										200	5	206	BE-P-10-51-600-206-200

Table 3.7: (cont'd)

Specimen No.	LC (%)	Initial w (%)	Curing Time Before Shearing (days)							During Shear		Total Curing Time (days)	Designated Name
			Curing Normal Stress (kPa)						Total	Normal Stress (kPa)	Curing Time (days)		
			Atm.	50	100	200	300	400					
131	15	67	0	3	5	27	-	-	35	50	11	46	BE-P-10-64-200-46-50
										100	3	49	BE-P-10-64-200-49-100
										200	5	54	BE-P-10-64-200-54-200
										400	9	63	BE-P-10-64-200-63-400

Table 3.8: Precut Upper Brenna (UB) clay samples

Specimen No.	LC (%)	Initial w (%)	Curing Time Before Shearing (days)							During Shear		Total Curing Time (days)	Designated Name
			Curing Normal Stress (kPa)						Total	Normal Stress (kPa)	Curing Time (days)		
			Atm.	50	100	200	300	400					
132	0	67	-	-	-	-	-	-	-	100	-	-	UB-P-0-67-0-0-100
										300	-	-	UB-P-0-67-0-0-300
133	3	74	5	-	-	-	-	-	5	300	2	7	UB-P-3-74-0-7-300
134	3	98	7	-	-	-	-	-	7	100	4	11	UB-P-3-98-0-11-100
										300	2	13	UB-P-3-98-0-13-300
135	3	74	52	-	-	-	-	-	52	300	2	54	UB-P-3-74-0-54-300
136	4	74	1	-	-	-	-	-	1	100	0	1	UB-P-4-74-0-1-100
137	5	109	7	-	-	-	-	-	7	100	4	11	UB-P-5-109-0-11-100
										300	2	13	UB-P-5-109-0-13-300
138	5	274	38	-	-	-	-	-	38	300	2	40	UB-P-5-274-0-40-300
139	5	274	54	-	-	-	-	-	54	100	2	56	UB-P-5-274-0-56-100
										300	2	58	UB-P-5-274-0-58-300
140	6.6	75	0	1	1	-	-	-	2	100	1	3	UB-P-6.6-75-100-3-100
										300	2	5	UB-P-6.6-75-100-5-300
141	6.6	97	0	2	4	-	-	-	6	100	2	8	UB-P-6.6-97-100-8-100
142	6.6	75	0	1	11	-	-	-	12	100	2	14	UB-P-6.6-75-100-14-100
										300	2	16	UB-P-6.6-75-100-16-300
143	6.6	64	0	2	22	-	-	-	24	100	2	26	UB-P-6.6-64-100-26-100
144	6.6	77	0	2	22	-	-	-	24	300	2	26	UB-P-6.6-77-100-26-300
145	8	74	0	0	0.4	-	-	-	0.4	100	0	0.4	UB-P-8-74-100-0.4-100

CHAPTER 4

PEAK AND POST-PEAK SHEAR STRENGTH

In this chapter, first the behavior of an overconsolidated clay is reviewed to help in understanding the response of lime treated clays to shearing. The results of laboratory tests including Atterberg limits, drained direct shear, pH measurements, and SEM/EDS are presented. The direct shear test results on intact specimens are used to determine peak and post-peak strengths, and precut specimens are used to determine residual strength of lime treated clays. The post-peak shear strength refers to several strains, including one corresponding to the minimum strength reached at the end of shearing on an intact specimen. The post-peak strength is reached at shear displacements in the range of 7-8 mm. The shear strain is calculated as the ratio of the shear displacement to the initial height of the specimen, which is 25.4 mm. The shear strain at the end of the shearing of an intact sample is in the range of 28-31%.

Atterberg limits test results are interpreted to better understand the change in clay particles due to lime treatment. The effects of lime content, curing period and effective normal stress on shear strength are further investigated. The clay-lime reaction process and reaction phases are manifested by the interpretation of the test results.

4.1 STRESS-STRAIN AND VOLUME-CHANGE RELATIONSHIP

According to the similarities between the behavior of lime treated clays and overconsolidated clays, it is beneficial to review the behavior in shear of an overconsolidated clay. A typical shear stress-displacement curve of an intact sample of an overconsolidated clay, subjected to drained direct shear or torsional shear is illustrated in Figure 4.1.

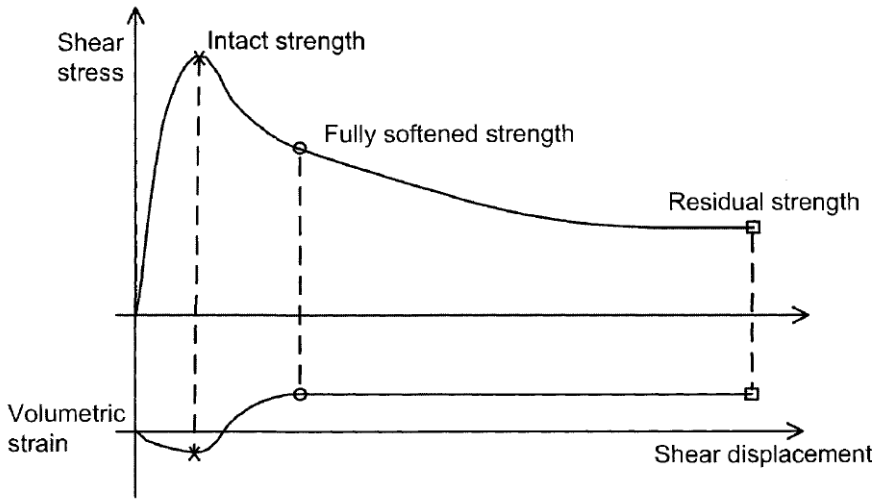

Figure 4.1: Schematic shear stress-displacement and volumetric strain-displacement curves for an intact sample of an overconsolidated clay

The relationships shown in Figure 4.1 may be obtained from a drained multiple reversal direct shear test on an intact sample of an overconsolidated clay. As the shear displacement continues, the shear stress increases to a peak value while the specimen experiences a volume decrease due to closing of existing fissures. The peak (intact) strength is usually reached at small shear displacements. After the peak, the specimen softens by opening of fissures and swelling; therefore, there is a drop in the shear stress. The fully softened strength is reached at the end of softening where the swelling is complete and volume increase levels off.

In a multiple reversal direct shear test, the specimen is subjected to a large shearing displacement in the order of several centimeters by reversing the direction of shearing. By continuing the shearing, the shear resistance continues to decrease to a state called residual condition at which the clay particles are orientated along the shear surface to the maximum extent possible for the particular effective normal stress (Mesri and Shahien, 2003). The Intact, fully softened, and residual shear strengths of London clay with overconsolidation pressure (σ'_p) of 4,100 kPa and plasticity index (I_p) of 50-60% are shown in Figure 4.2.

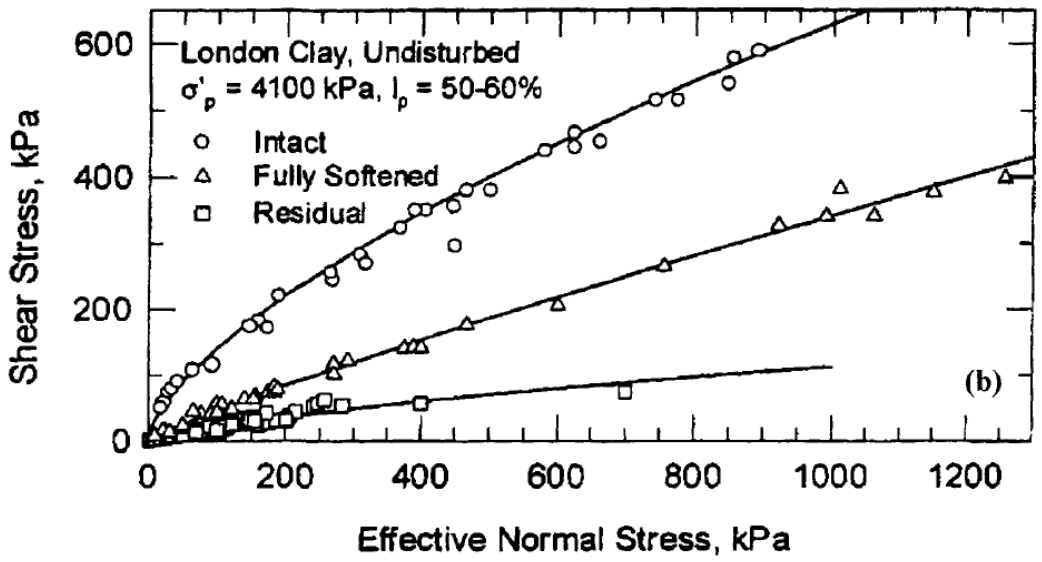

Figure 4.2: Intact, fully softened, and residual shear strength of London clay (Mesri and Shahien, 2003)

Shear stress-shear displacement and vertical deformation-shear displacement curves for untreated and treated Chicago clay with lime contents in the range of 1-10% and various curing periods are shown in Figures 4.3-4.12. The tests were performed under normal stresses in the range of 50-300 kPa. Except for one of the specimens, i.e., Specimen 15, the rest of the specimens were cured under confined condition. The specimen cured under unconfined condition, Figure 4.10, did not exhibit a significant peak as observed for the test carried out on a similar specimen but cured under confined condition, Figure 4.11.

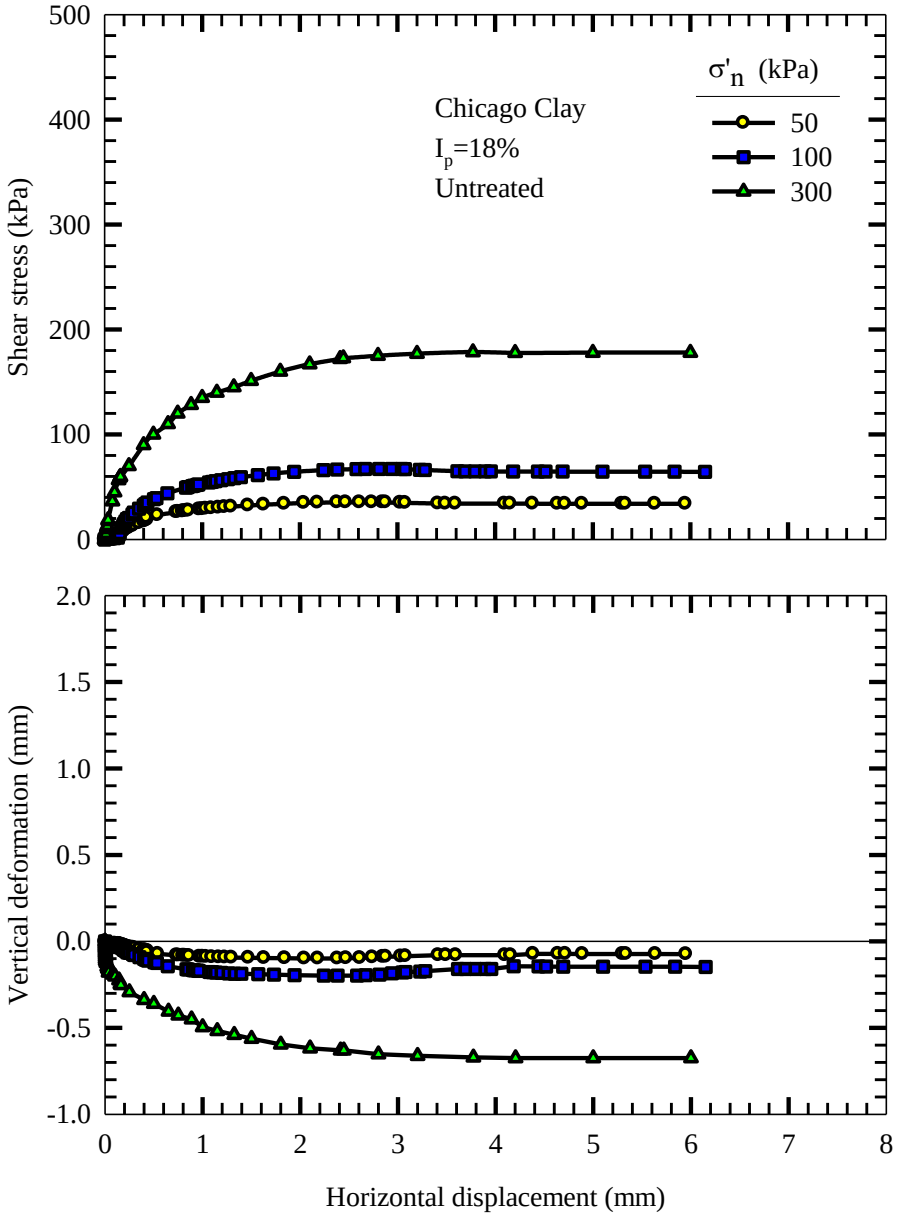

Figure 4.3: Shear stress-shear displacement and vertical displacement-shear displacement curves for untreated reconstituted Chicago clay (Specimen 1-3)

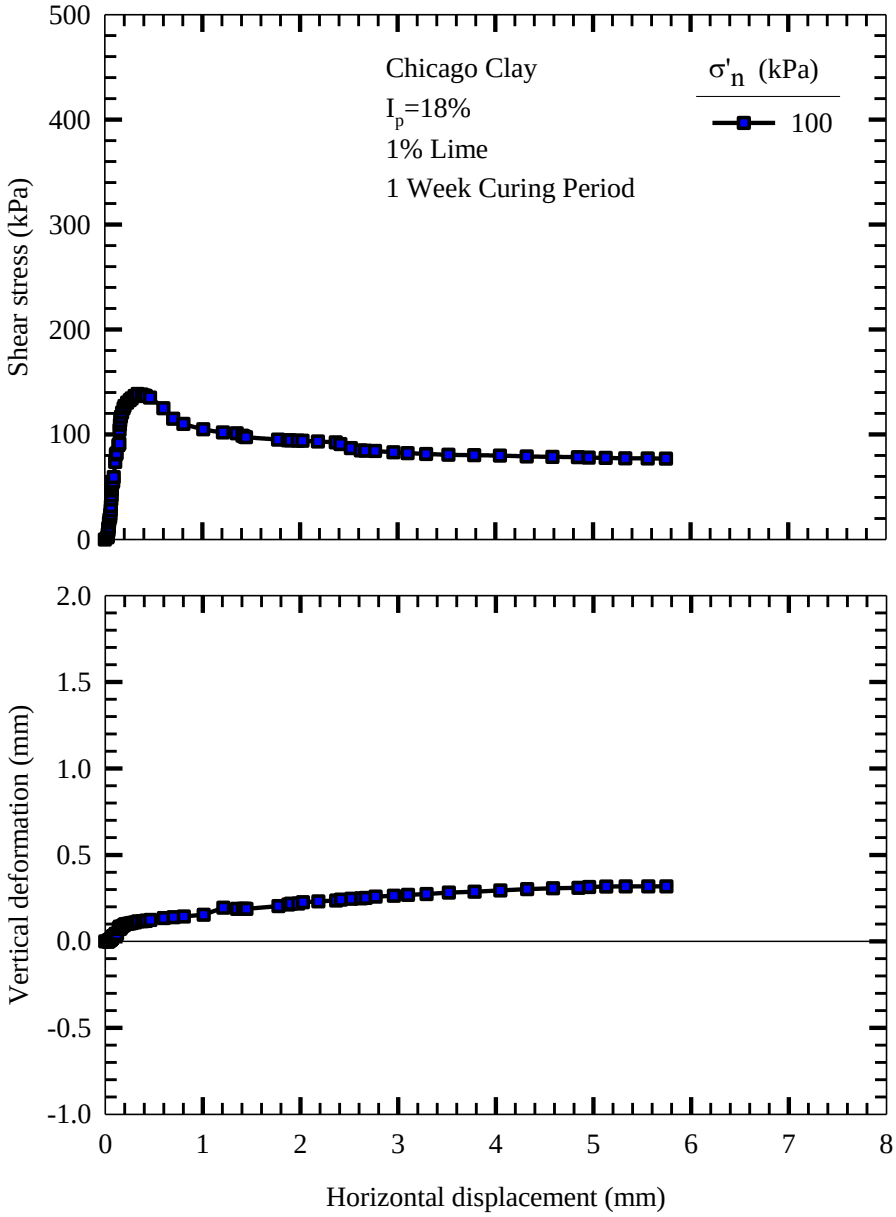

Figure 4.4: Shear stress-shear displacement and vertical displacement-shear displacement curves for Chicago clay tretaed with 1% lime, cured for 7 days (Specimen 4)

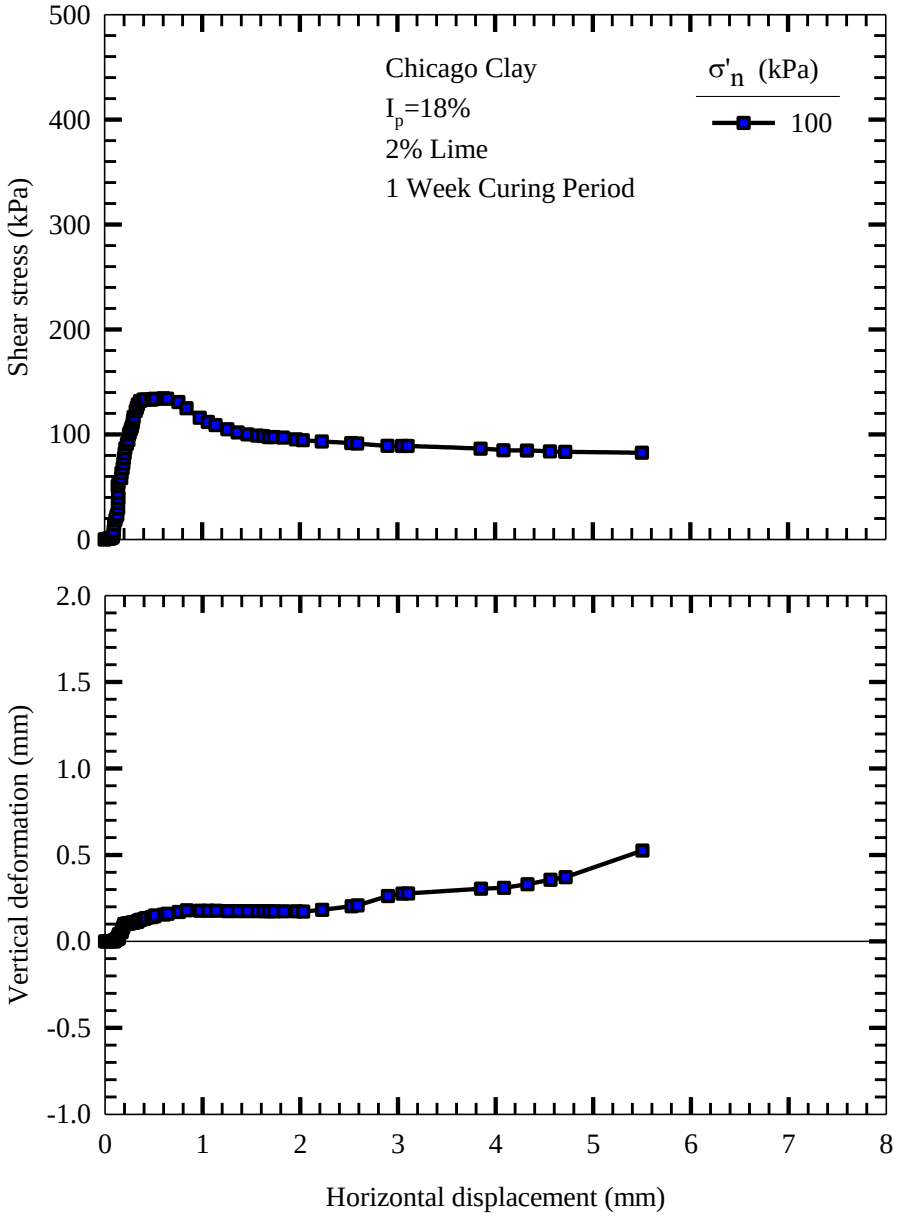

Figure 4.5: Shear stress-shear displacement and vertical displacement-shear displacement curves for Chicago clay tretaed with 2% lime, cured for 7 days (Specimen 5)

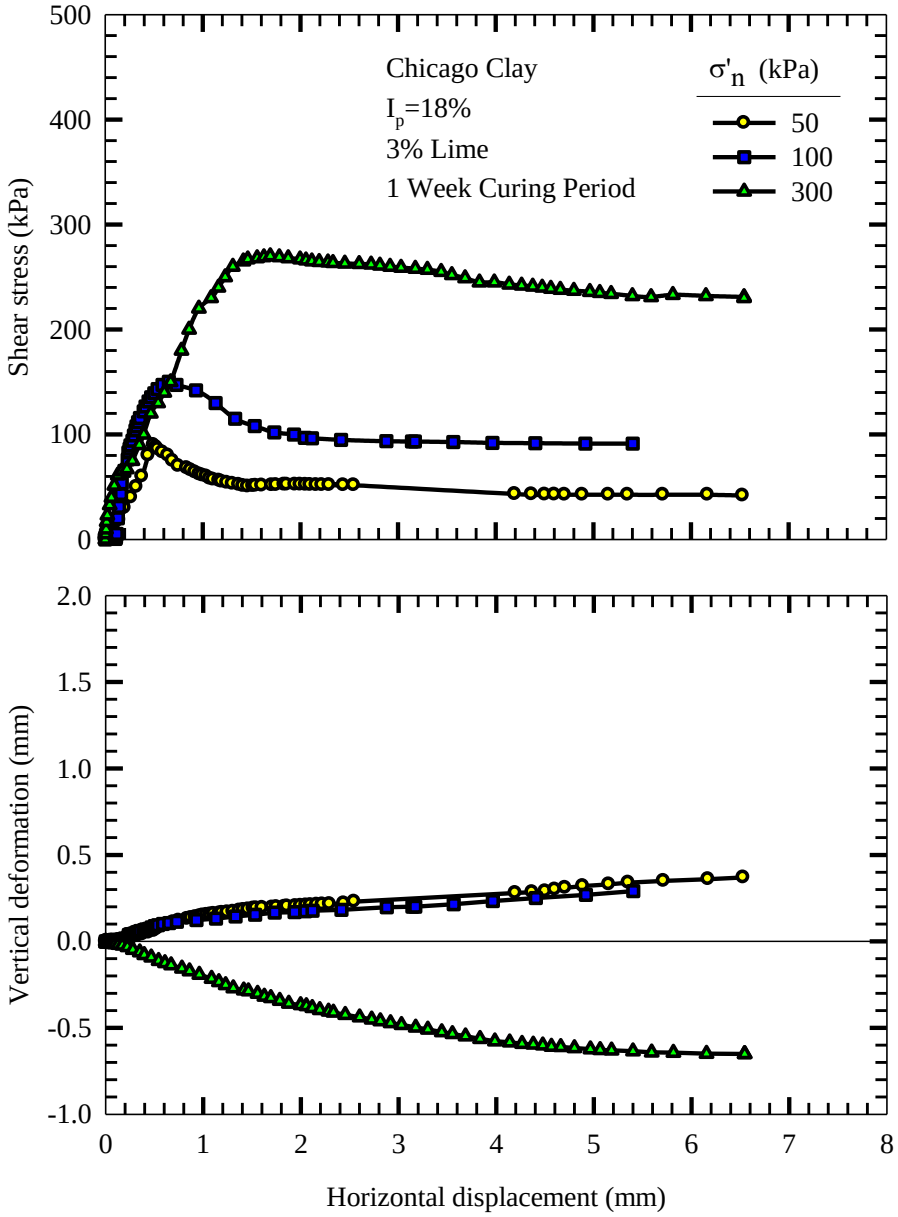

Figure 4.6: Shear stress-shear displacement and vertical displacement-shear displacement curves for Chicago clay tretaed with 3% lime, cured for 7 days (Specimens 6-8)

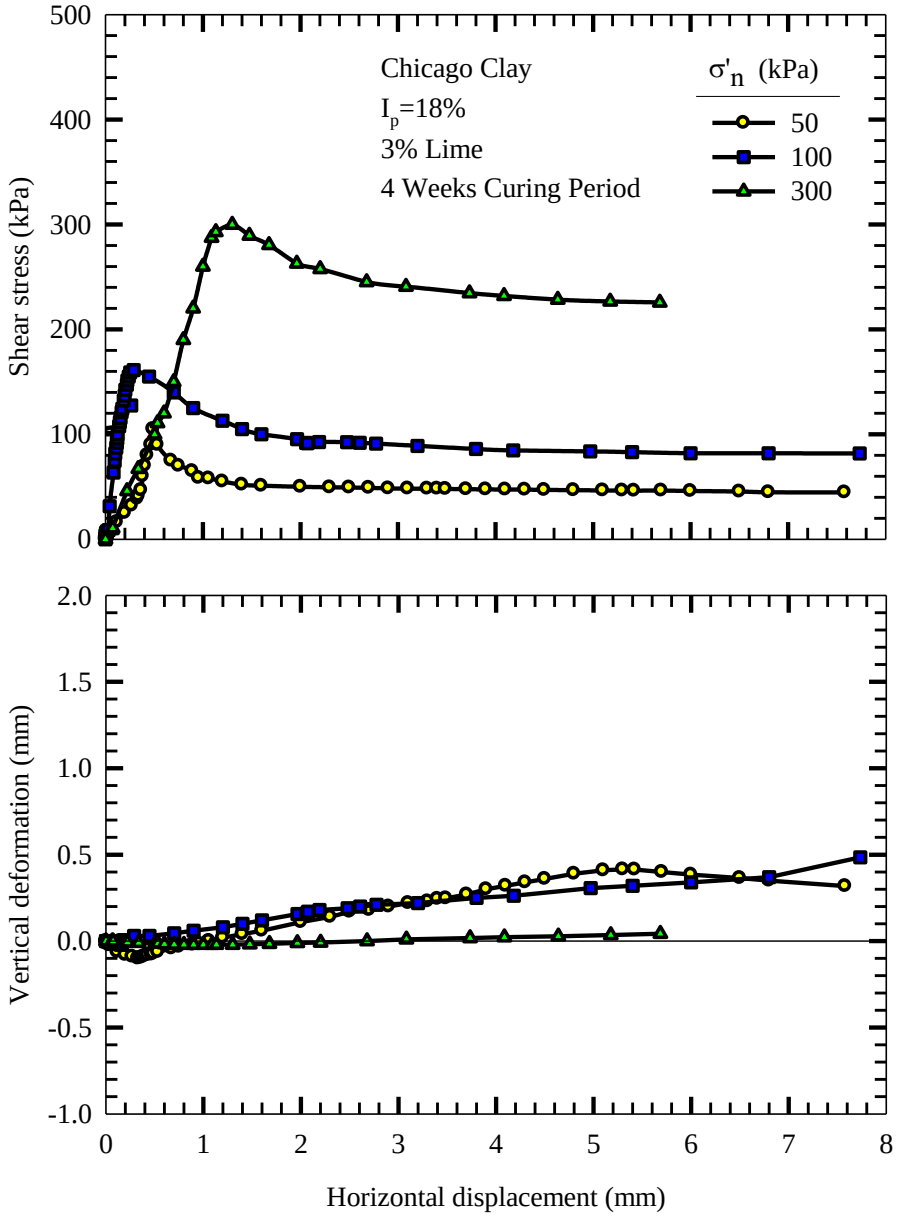

Figure 4.7: Shear stress-shear displacement and vertical displacement-shear displacement curves for Chicago clay tretaed with 3% lime, cured for 28 days (Specimens 9-11)

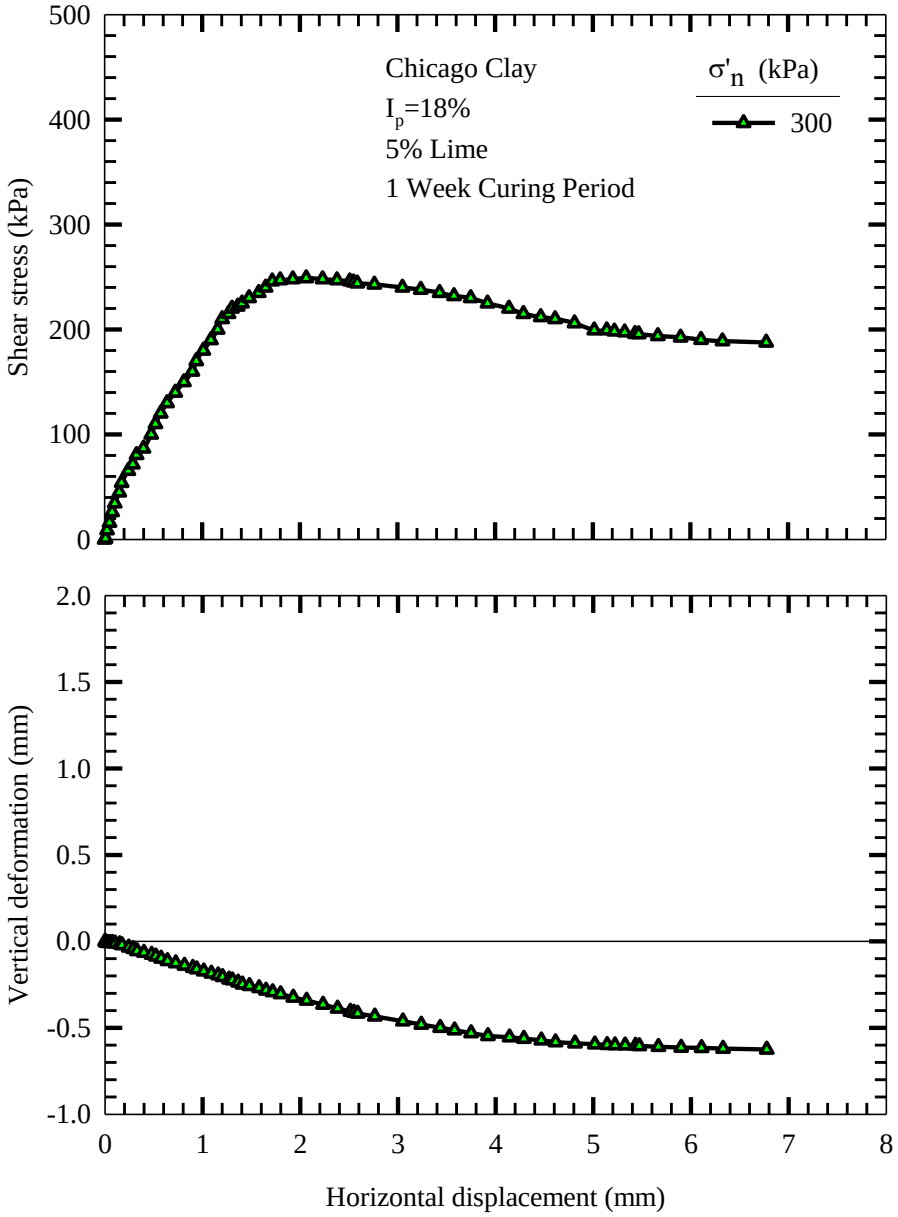

Figure 4.8: Shear stress-shear displacement and vertical displacement-shear displacement curves for Chicago clay tretaed with 3% lime, cured for 28 days (Specimen 12)

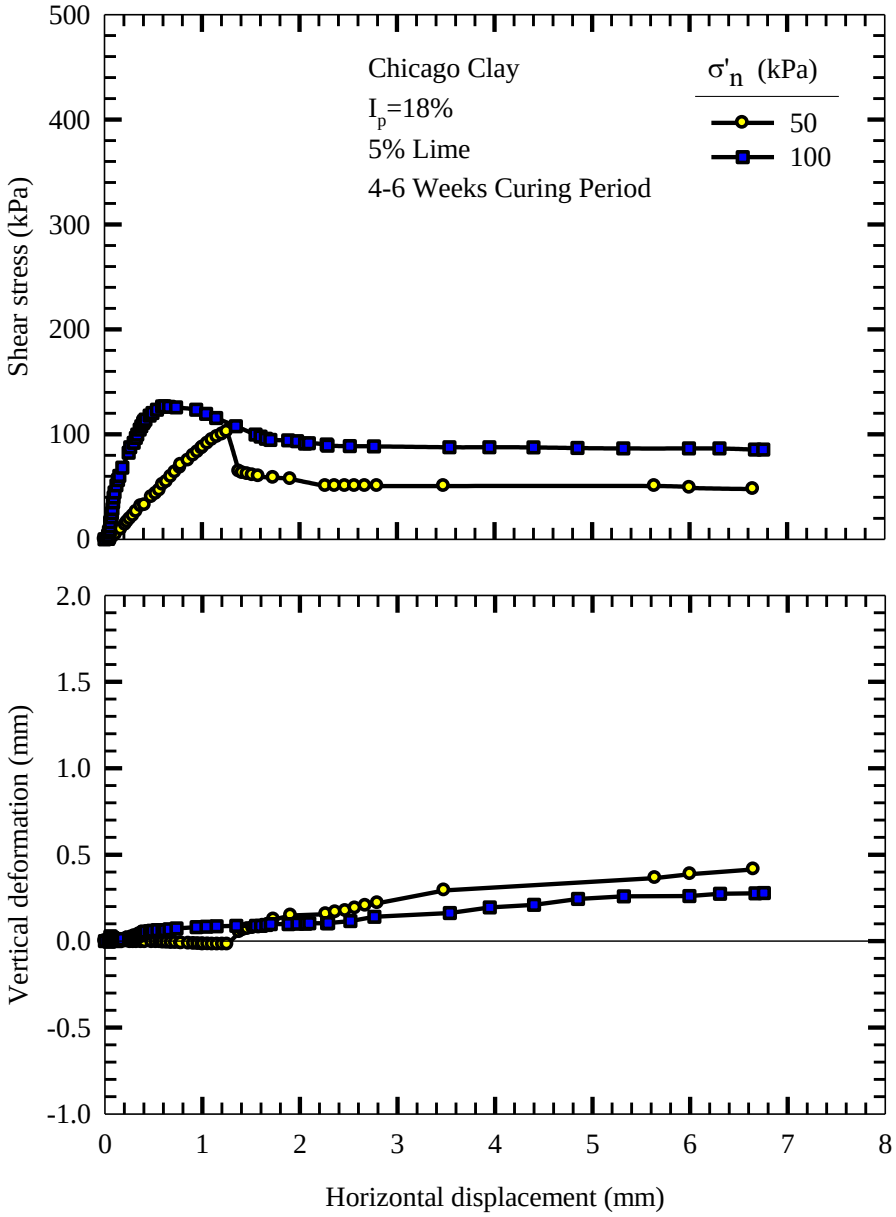

Figure 4.9: Shear stress-shear displacement and vertical displacement-shear displacement curves for Chicago clay tretaed with 5% lime, cured for 28-41 days (Specimens 13&14)

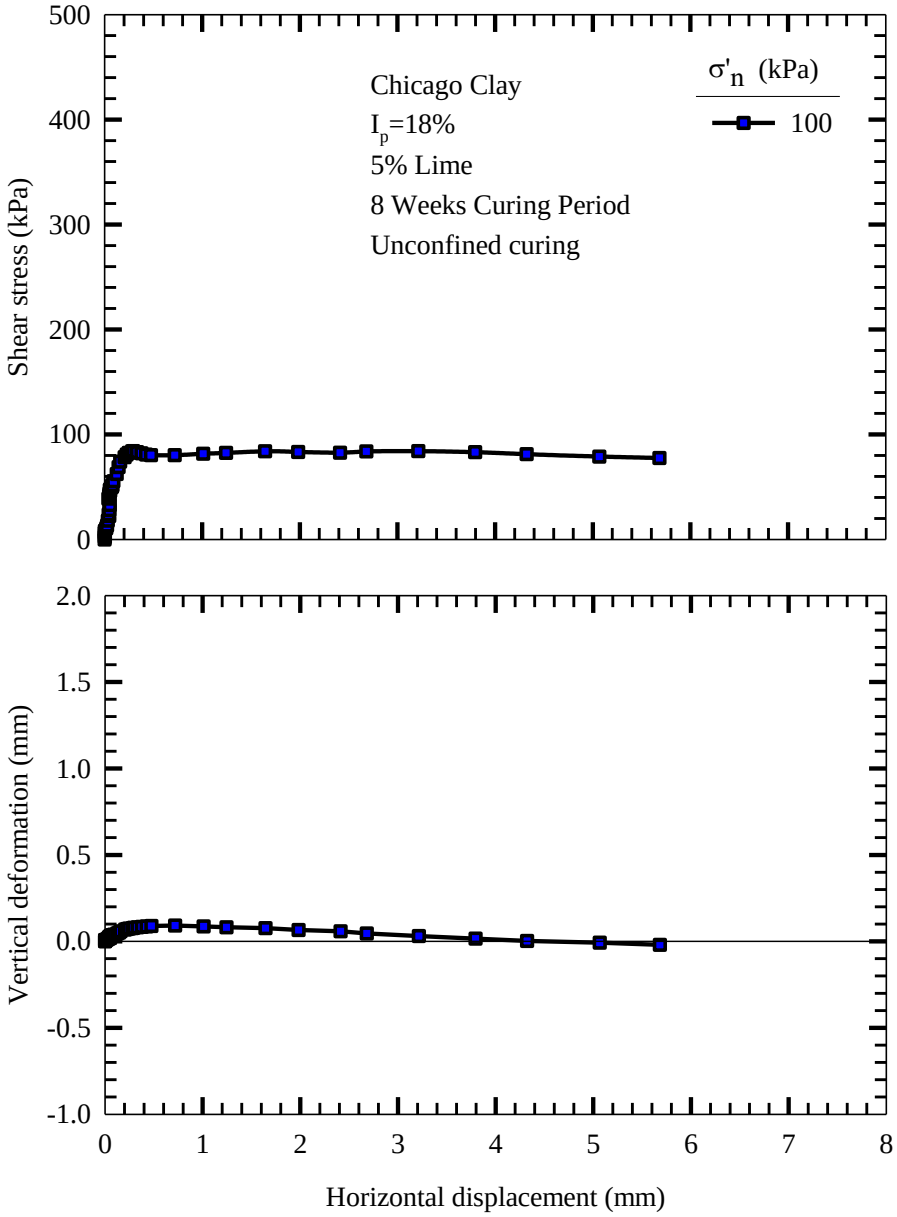

Figure 4.10: Shear stress-shear displacement and vertical displacement-shear displacement curves for Chicago clay tretaed with 5% lime, cured for 56 days under uncnfined condition (Specimen15)

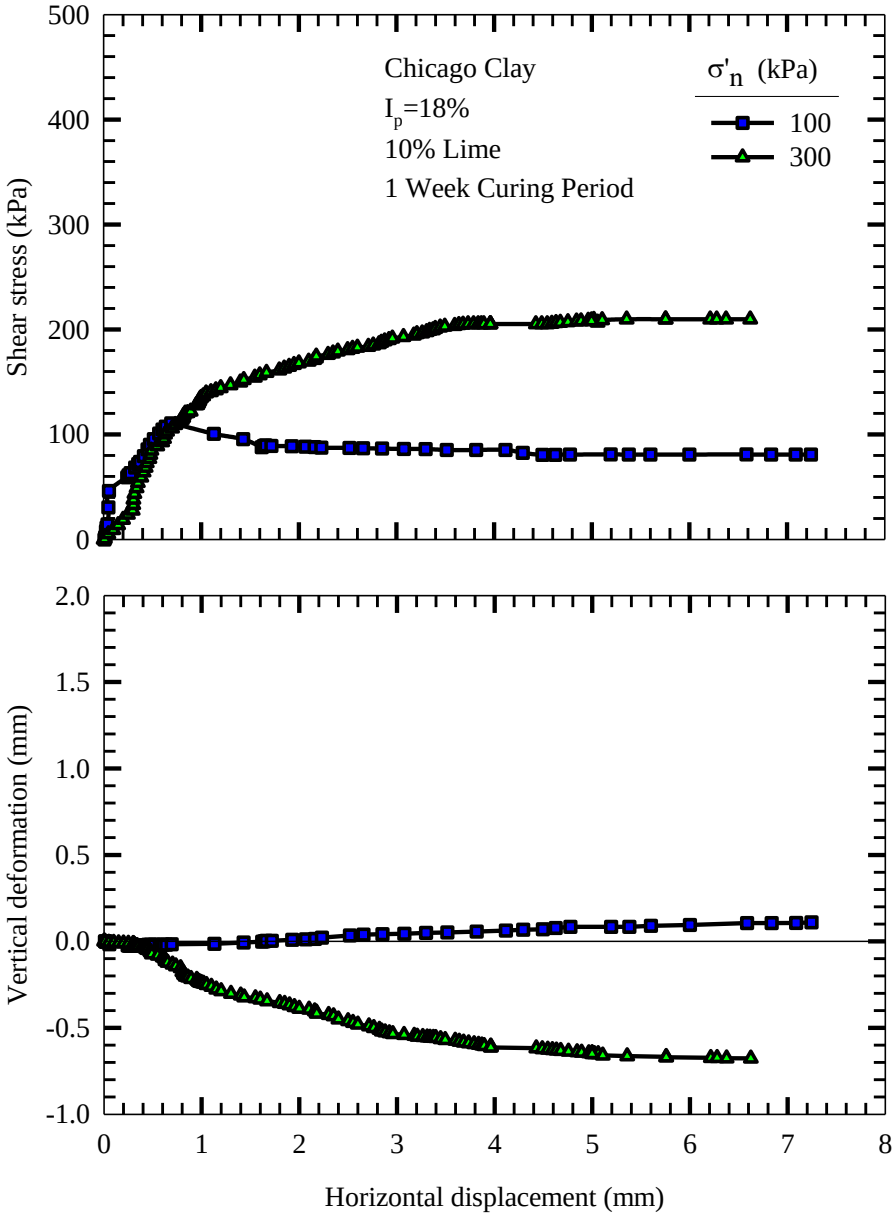

Figure 4.11: Shear stress-shear displacement and vertical displacement-shear displacement curves for Chicago clay tretaed with 10% lime, cured for 7 days (Specimens 16&17)

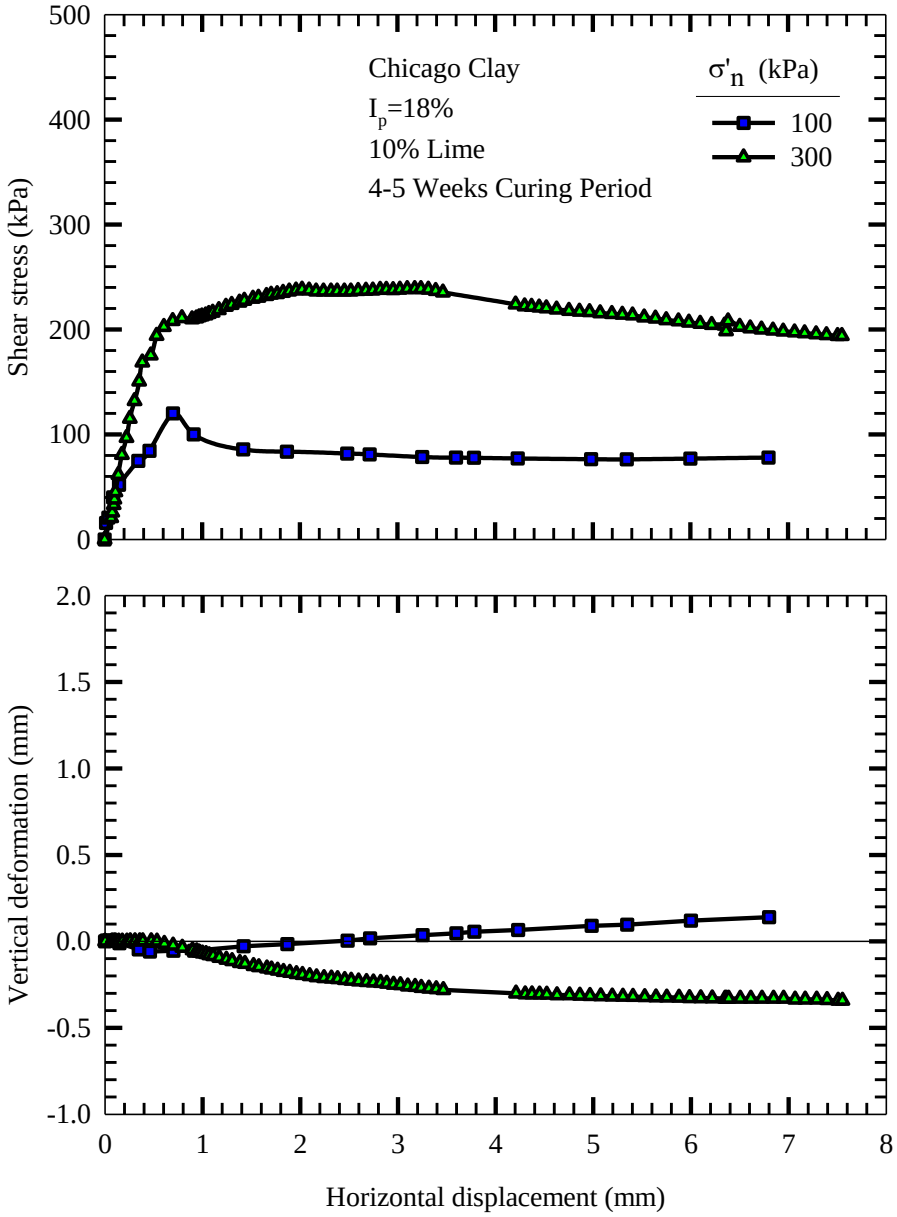

Figure 4.12: Shear stress-shear displacement and vertical displacement-shear displacement curves for Chicago clay tretaed with 10% lime, cured for 28-35 days (Specimens 18&19)

Shear stress-shear displacement and vertical deformation-shear displacement curves for untreated and treated Lower Brenna clay with lime contents of 3-15% and cured for 1-5 weeks under normal pressures in the range of 50-400 kPa are shown in Figures 4.13-4.22. The shear stress-displacement curves show a significant peak followed by strain softening. The curing stress for these tests is equal to the effective vertical stress at shearing. For example, the specimen treated with 7% lime and cured for 35 days, Figure 4.19, shows that higher effective confining pressures contribute to higher peak strengths, including the effect of curing stress on the peak strength. The stress-strain and volume-change behavior of a lime treated clay is qualitatively similar to that of an overconsolidated clay. This is best shown in Figure 4.19 for 7% lime treated specimen. The shear stress reaches a peak value and then drops to a post-peak value. The brittle nature of the failure, as indicated by a sharp peak in the stress –strain curve, is associated with the formation of a distinct slip plane. The peak strength increases with an increase in lime content up to 7%. Lime contents greater than 7% leads to a slight decrease in peak strength. The peak strength also increases with an increase in curing time. The dilatant response decreases as the effective normal stress increases; however, 7% lime treated specimen, cured for 5 weeks still displays a dilatant behavior under an effective normal stress of 400 kPa, Figure 4.19.

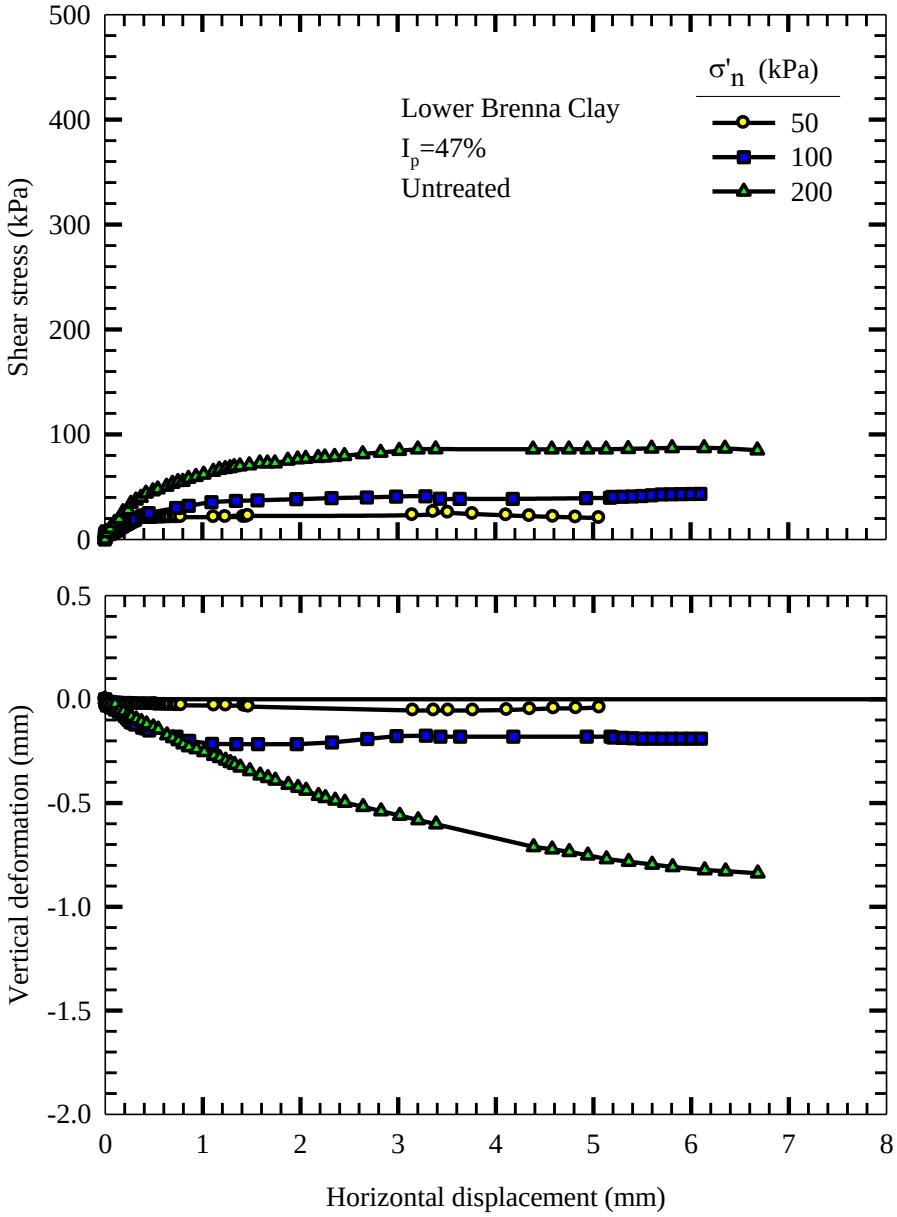

Figure 4.13: Shear stress-shear displacement and vertical displacement-shear displacement curves for untreated reconstituted Lower Brenna clay (Specimens 20-22)

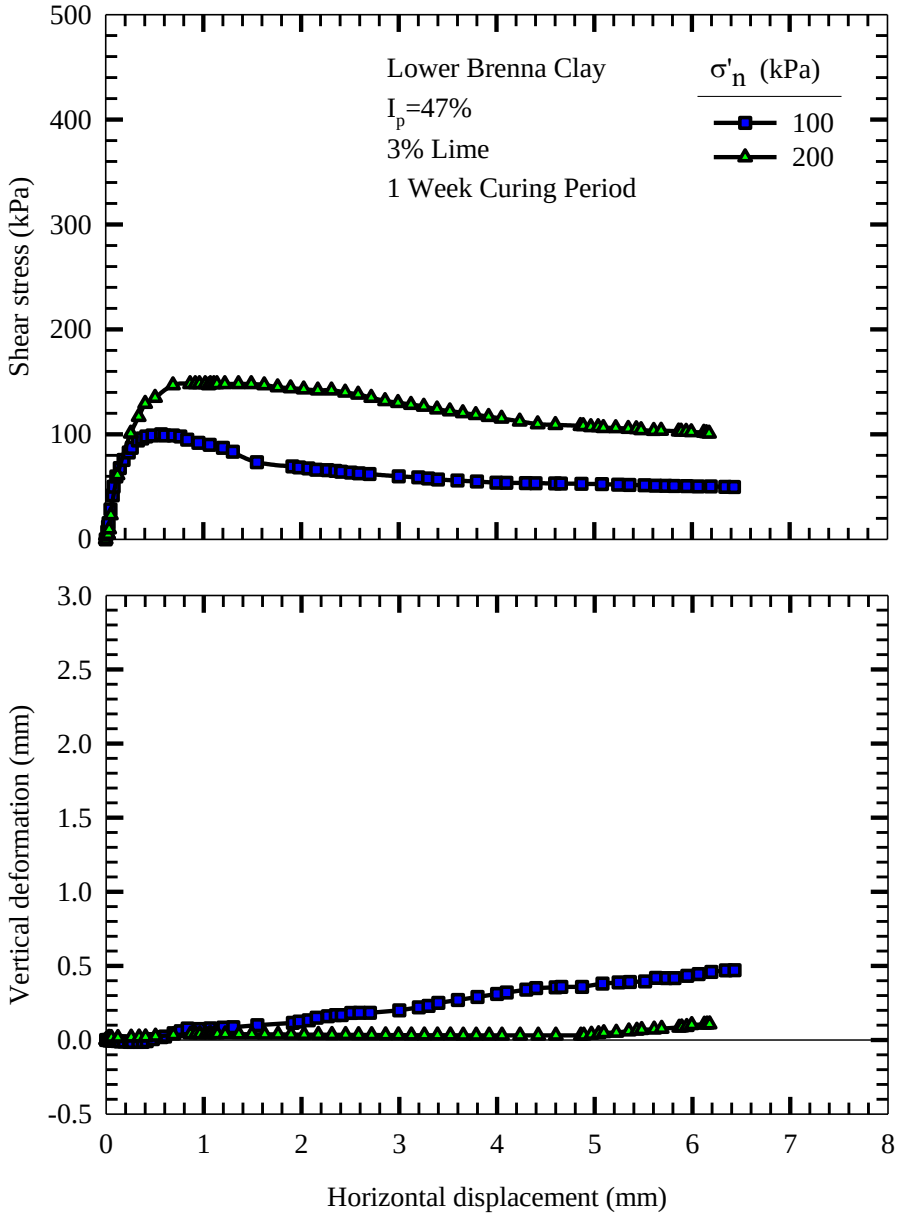

Figure 4.14: Shear stress-shear displacement and vertical displacement-shear displacement curves for Lower Brenna clay tretaed with 3% lime, cured for 7 days (Specimens 23&24)

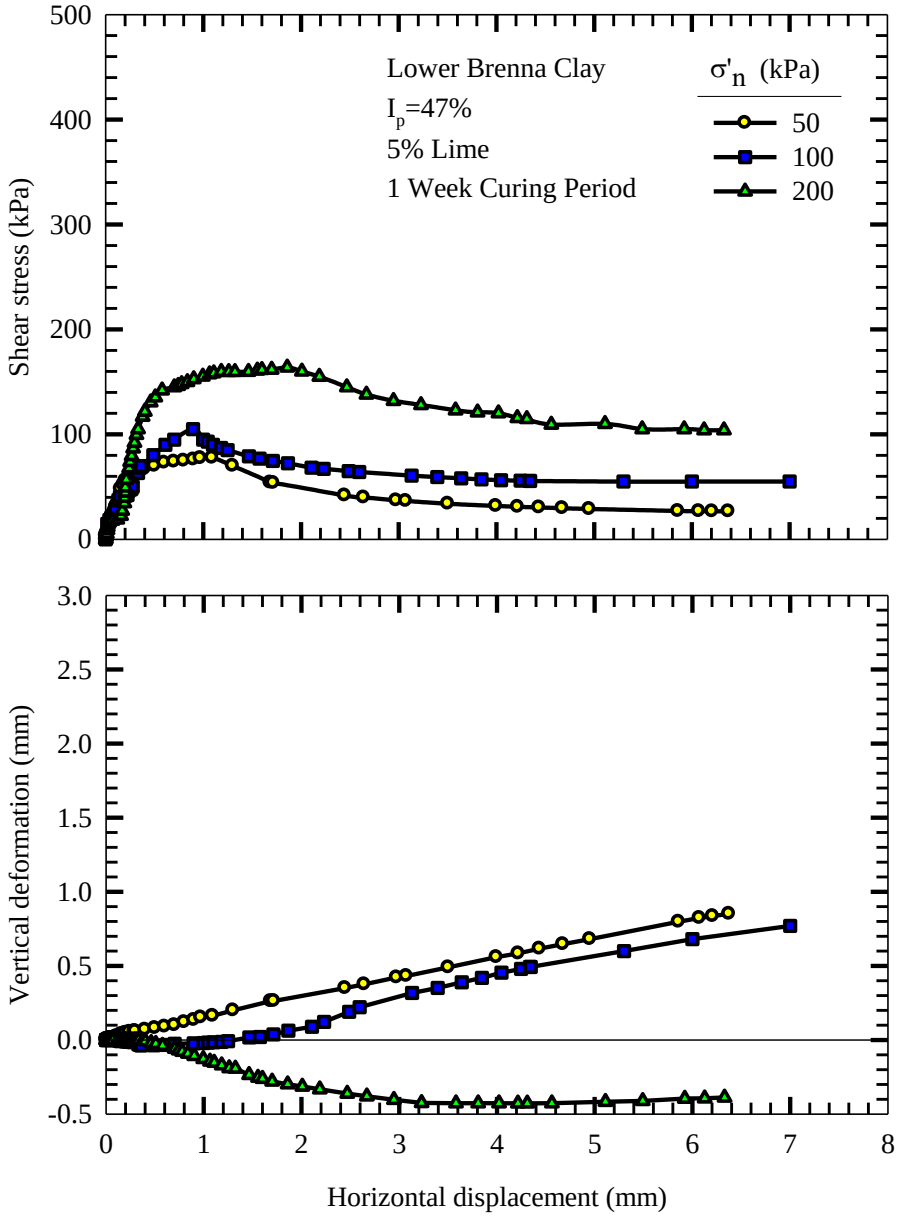

Figure 4.15: Shear stress-shear displacement and vertical displacement-shear displacement curves for Lower Brenna clay tretaed with 5% lime, cured for 7 days (Specimens 25-27)

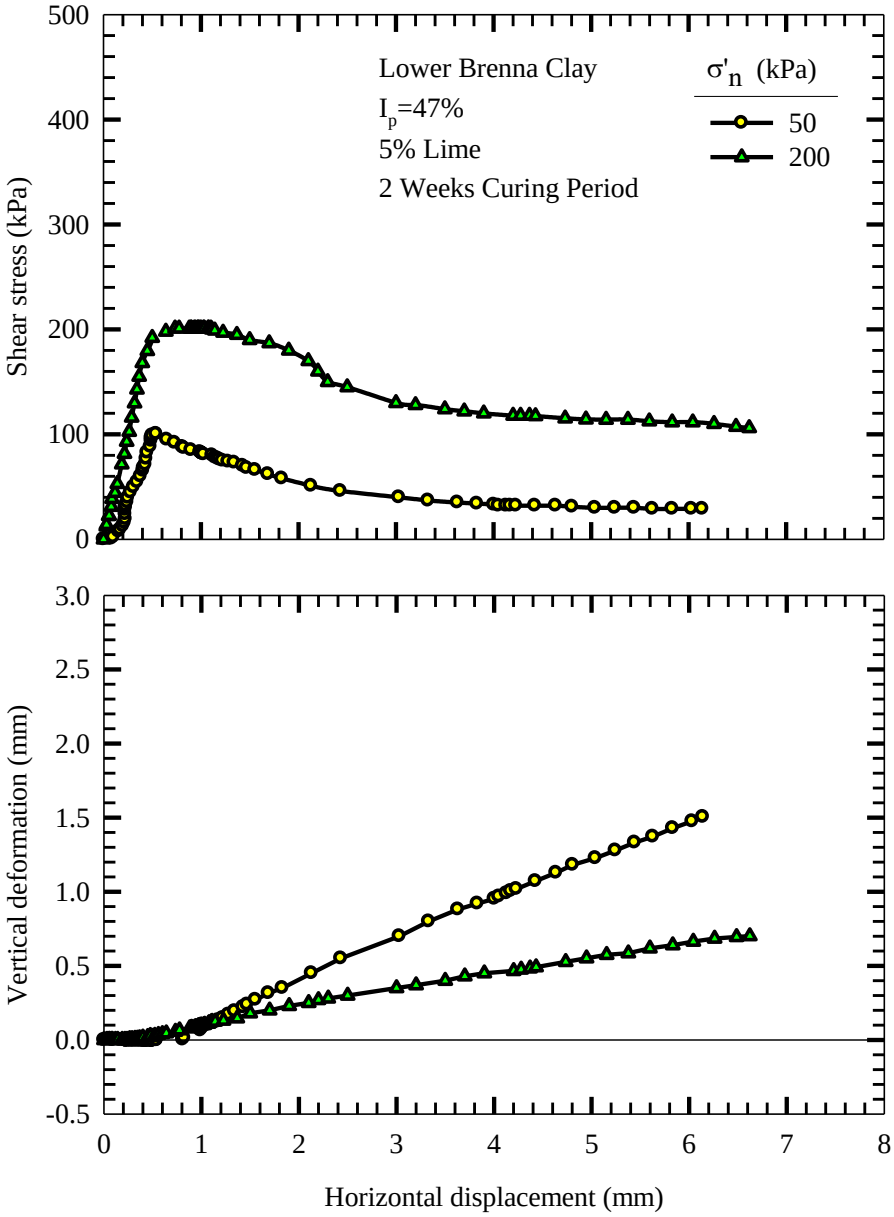

Figure 4.16: Shear stress-shear displacement and vertical displacement-shear displacement curves for Lower Brenna clay tretaed with 5% lime, cured for 14 days (Specimens 28&29)

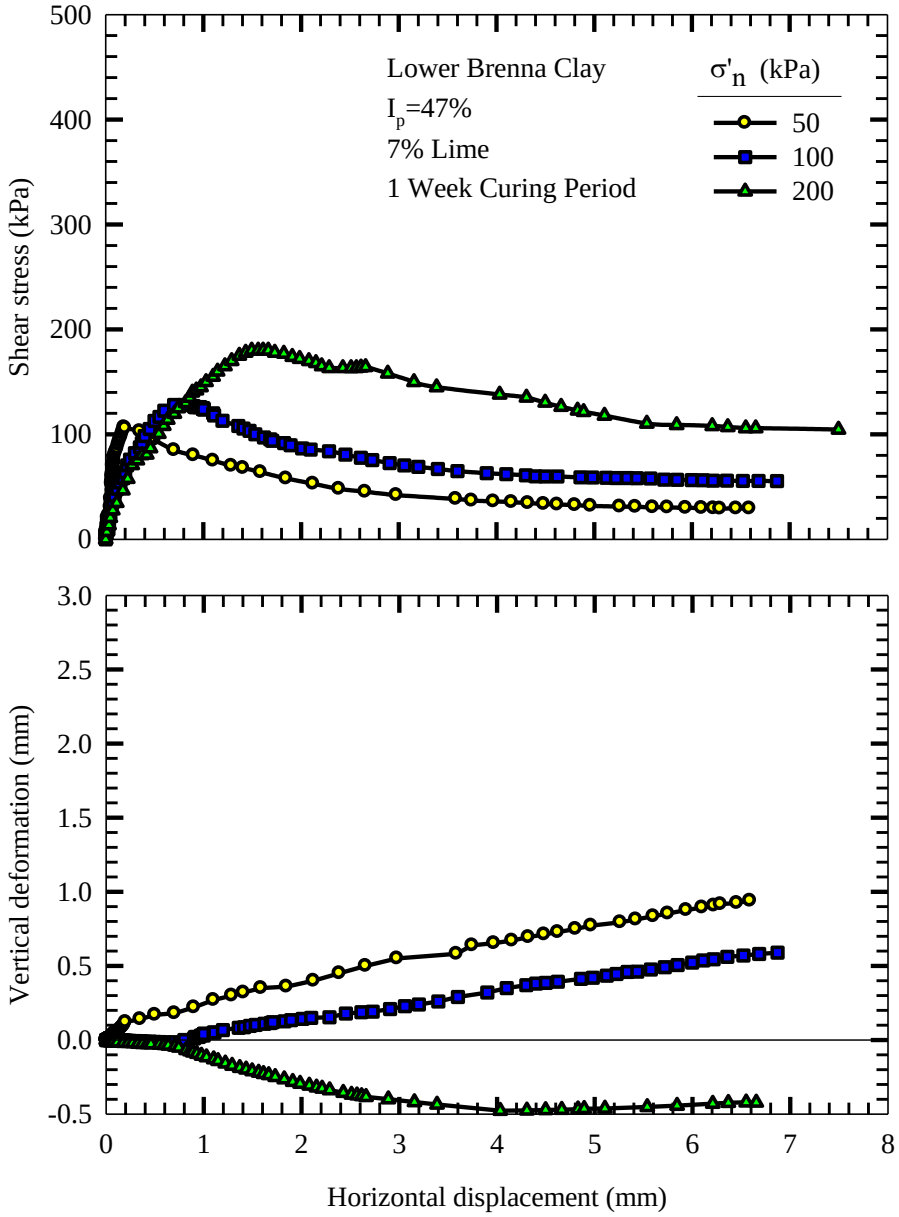

Figure 4.17: Shear stress-shear displacement and vertical displacement-shear displacement curves for Lower Brenna clay tretaed with 7% lime, cured for 7 days (Specimens 30-32)

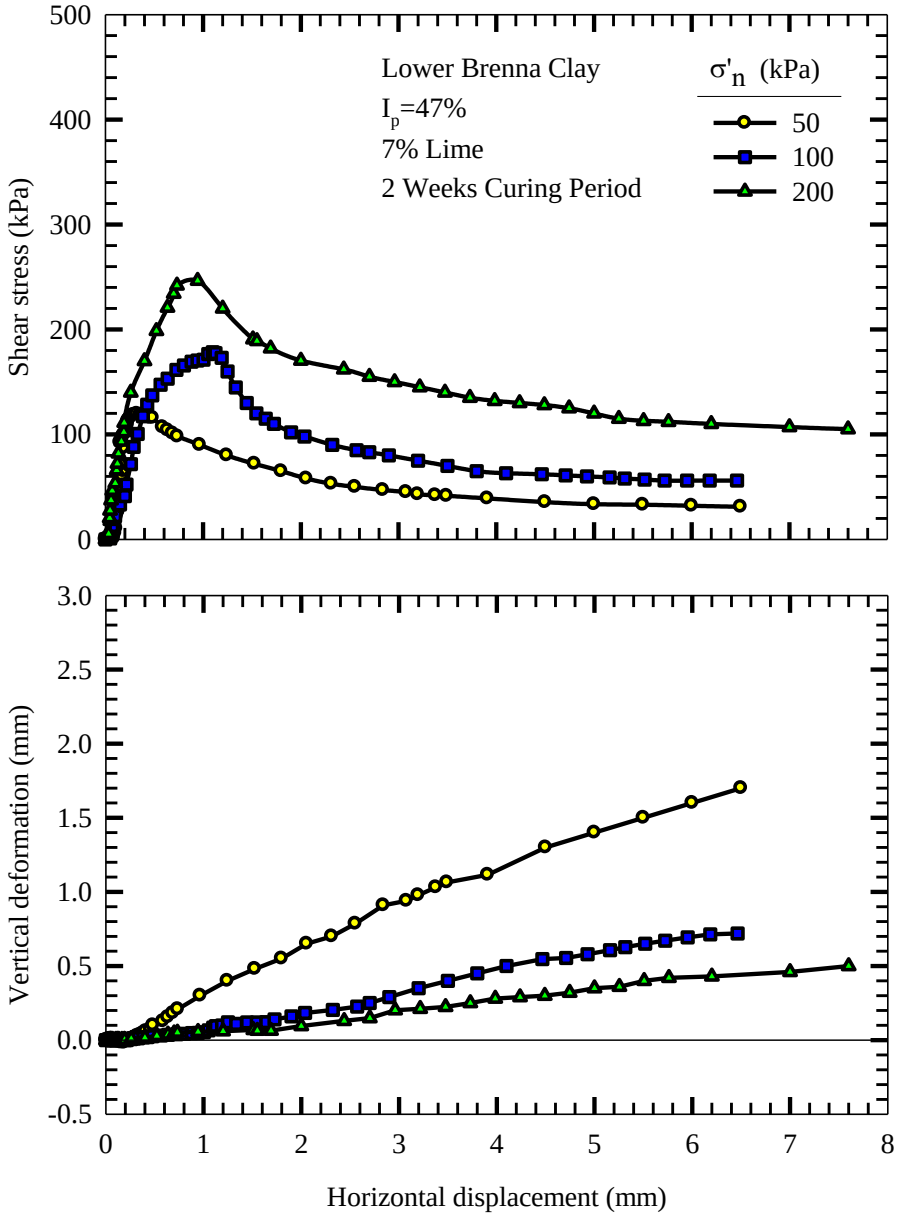

Figure 4.18: Shear stress-shear displacement and vertical displacement-shear displacement curves for Lower Brenna clay tretaed with 7% lime, cured for 14 days (Specimens 33-35)

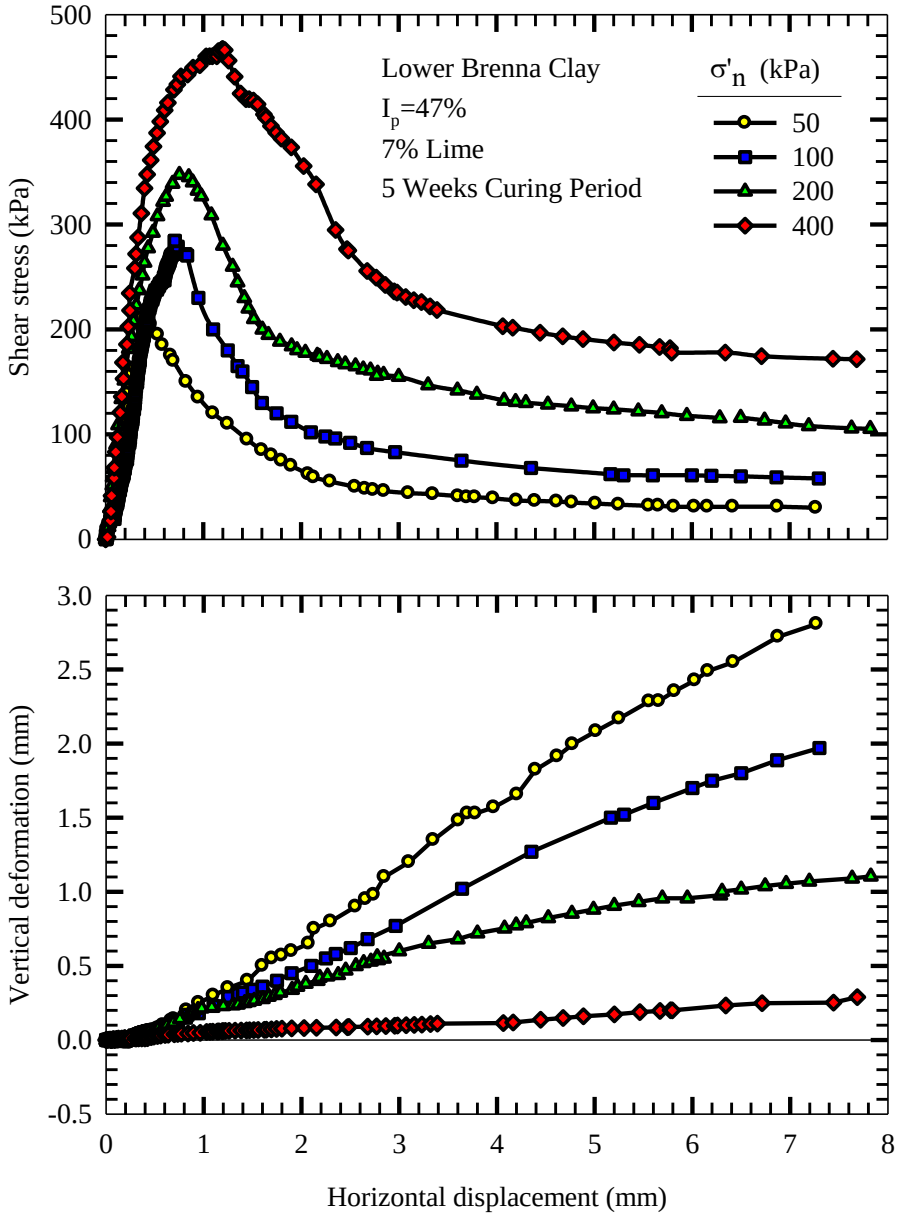

Figure 4.19: Shear stress-shear displacement and vertical displacement-shear displacement curves for Lower Brenna clay tretaed with 7% lime cured for 35 days (Specimens 36-39), $[\sigma'_n]_{cur}=\sigma'_n$

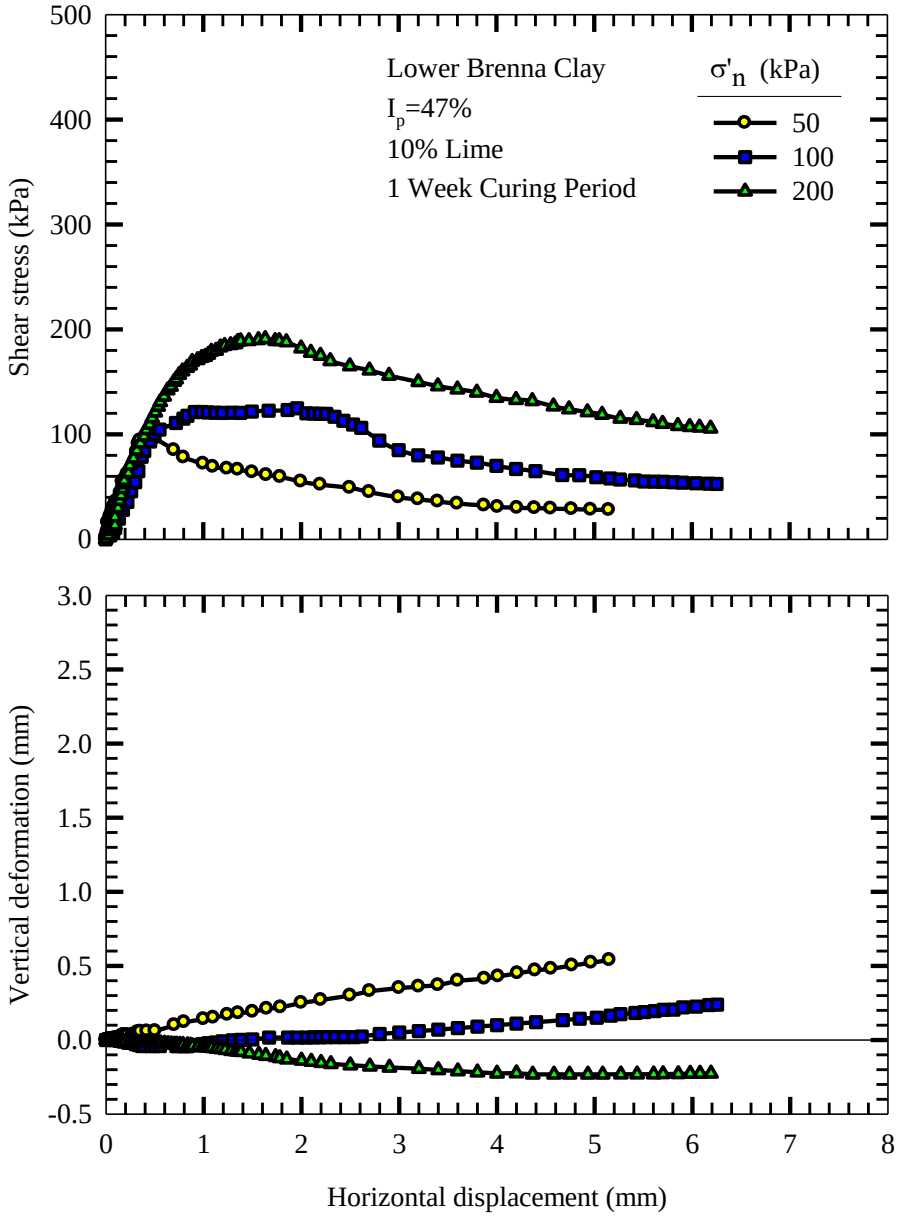

Figure 4.20: Shear stress-shear displacement and vertical displacement-shear displacement curves for Lower Brenna clay tretaed with 10% lime cured for 7 days (Specimens 40-42)

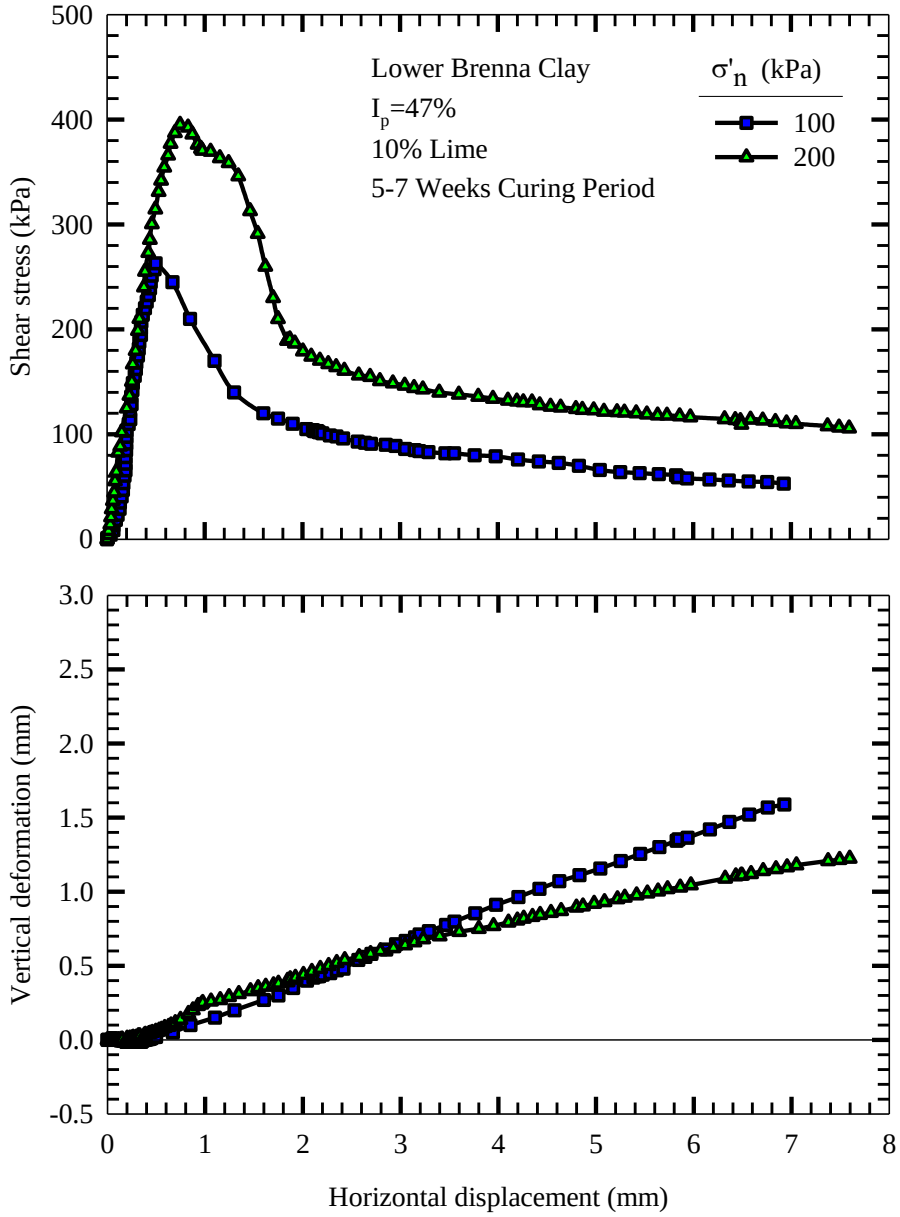

Figure 4.21: Shear stress-shear displacement and vertical displacement-shear displacement curves for Lower Brenna clay tretaed with 10% lime cured for 35-49 days (Specimens 43&44)

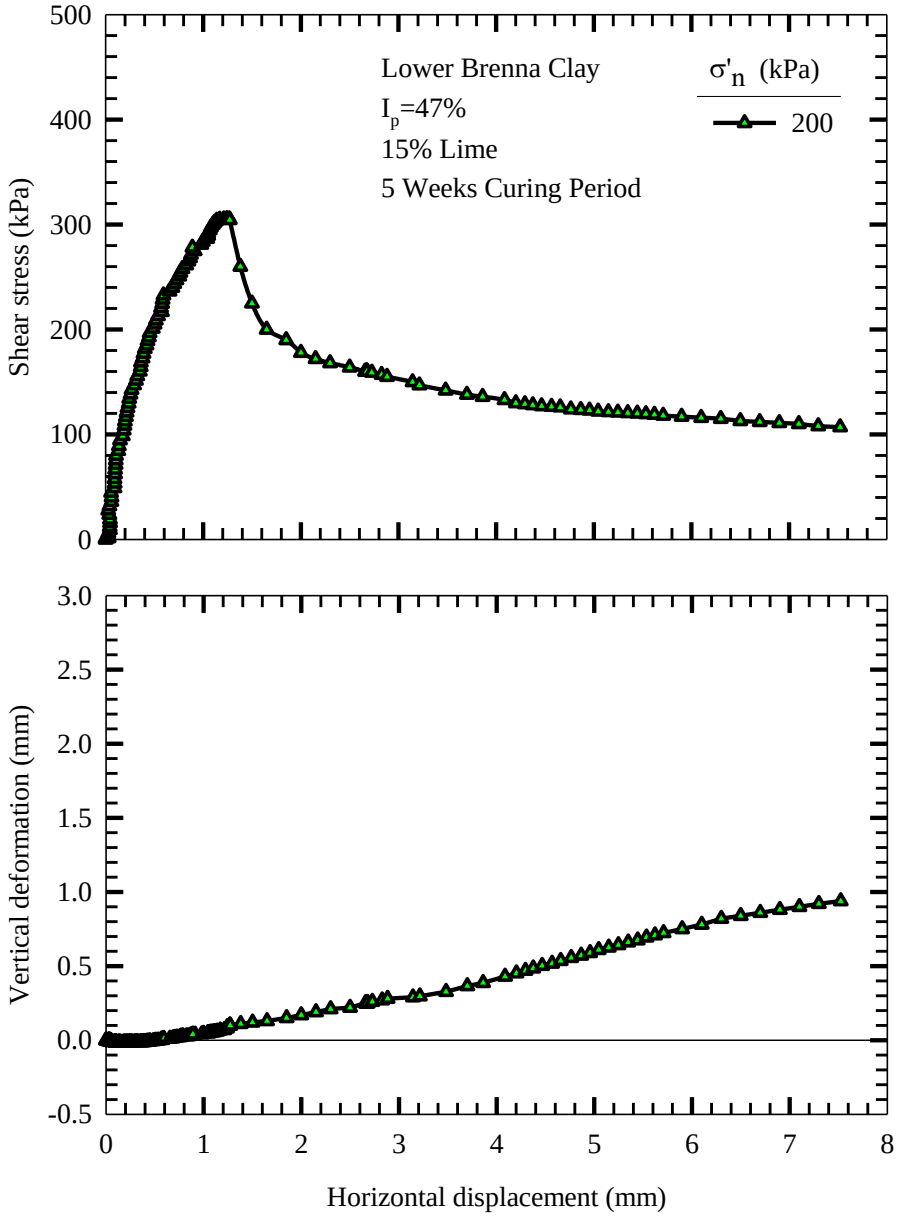

Figure 4.22: Shear stress-shear displacement and vertical displacement-shear displacement curves for Lower Brenna clay tretaed with 15% lime cured for 35 days (Specimen 45)

Shear stress-shear displacement and vertical deformation-shear displacement curves for untreated and treated Beaumont clay with lime contents of 1-15% and cured for 1-35 weeks under normal pressures in the range of 50-300 kPa are shown in Figures 4.23-4.34. The behavior of treated Beaumont clay is similar to that of treated Lower Brenna clay. The shear strength of Beaumont clay increases by addition of 1% lime; however, it does not show a sharp peak as observed in specimens treated with 3% lime content or higher, Figure 4.24. Two specimens treated with 3% lime but prepared with different initial water contents of 23% or 62% show similar peak and post-peak strength values. These samples were immediately placed and cured under 100 kPa normal pressure. This range of initial water content did not have an effect on the strength of treated clay once it was cured under confined condition. Use of very high water contents which is only possible when clay is cured under unconfined condition decreases the peak strength of treated clay.

Figure 4.26 shows the results of a Beaumont clay specimen treated with 5% lime and cured for 1 day. The specimen shows a higher strength compared to untreated clay with a slight peak at high strains. The volumetric response is still contractive. The specimen begins to pick some strength but there is no major peak strength in the first day of curing. As lime content and curing time increase, a major peak and dilative volume response during shearing are observed.

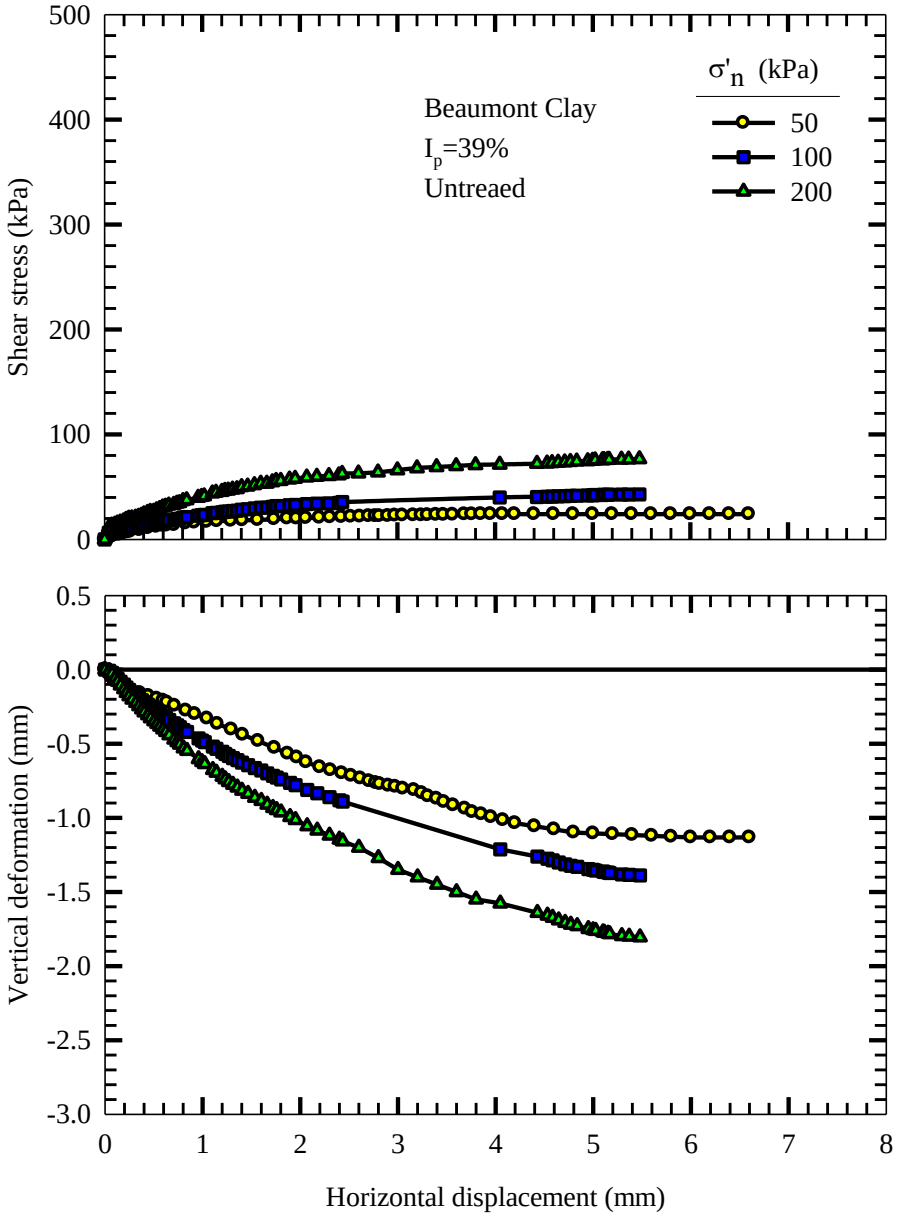

Figure 4.23: Shear stress-shear displacement and vertical displacement-shear displacement curves for untreated Beaumont clay (Specimens 46-48)

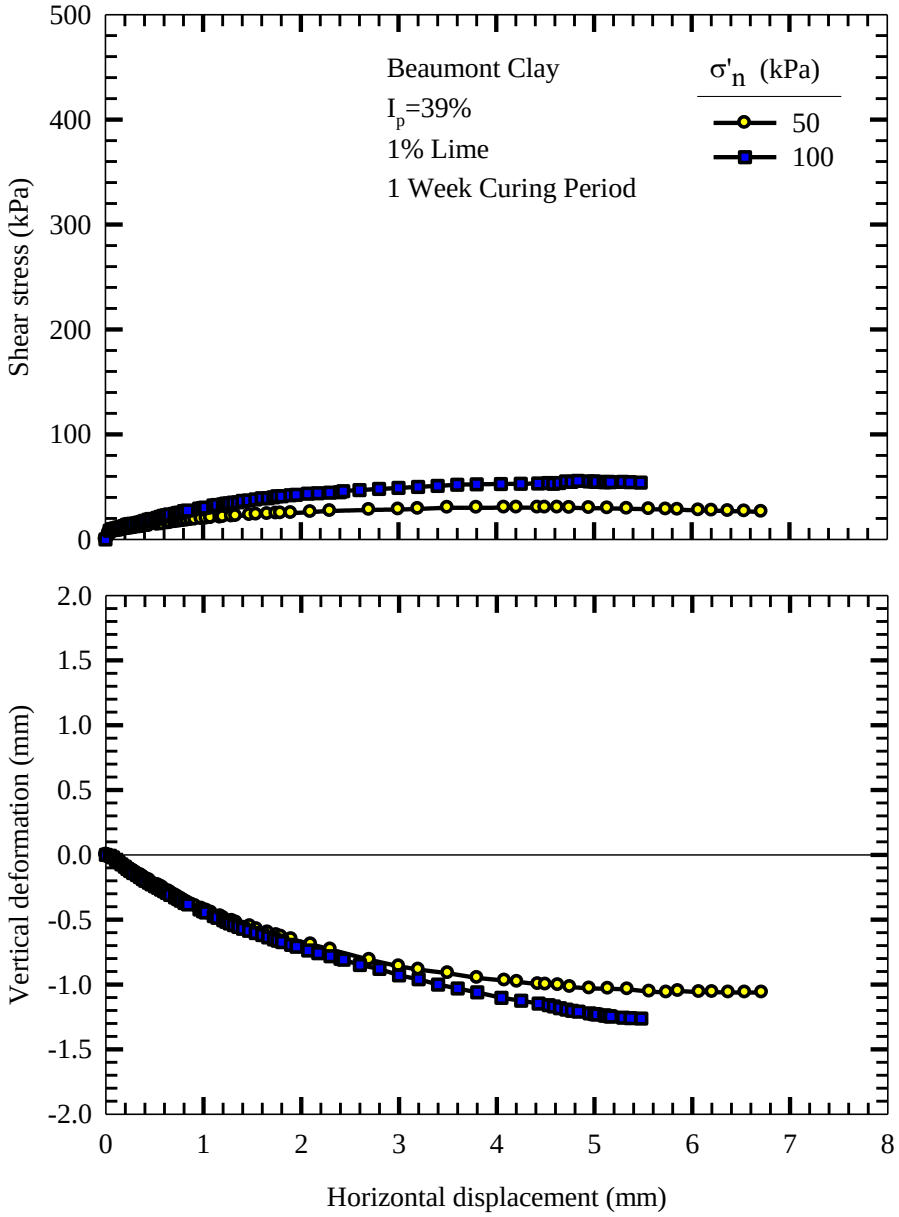

Figure 4.24: Shear stress-shear displacement and vertical displacement-shear displacement curves for Beaumont clay tretaed with 1% lime cured for 7 days (Specimen 49&50)

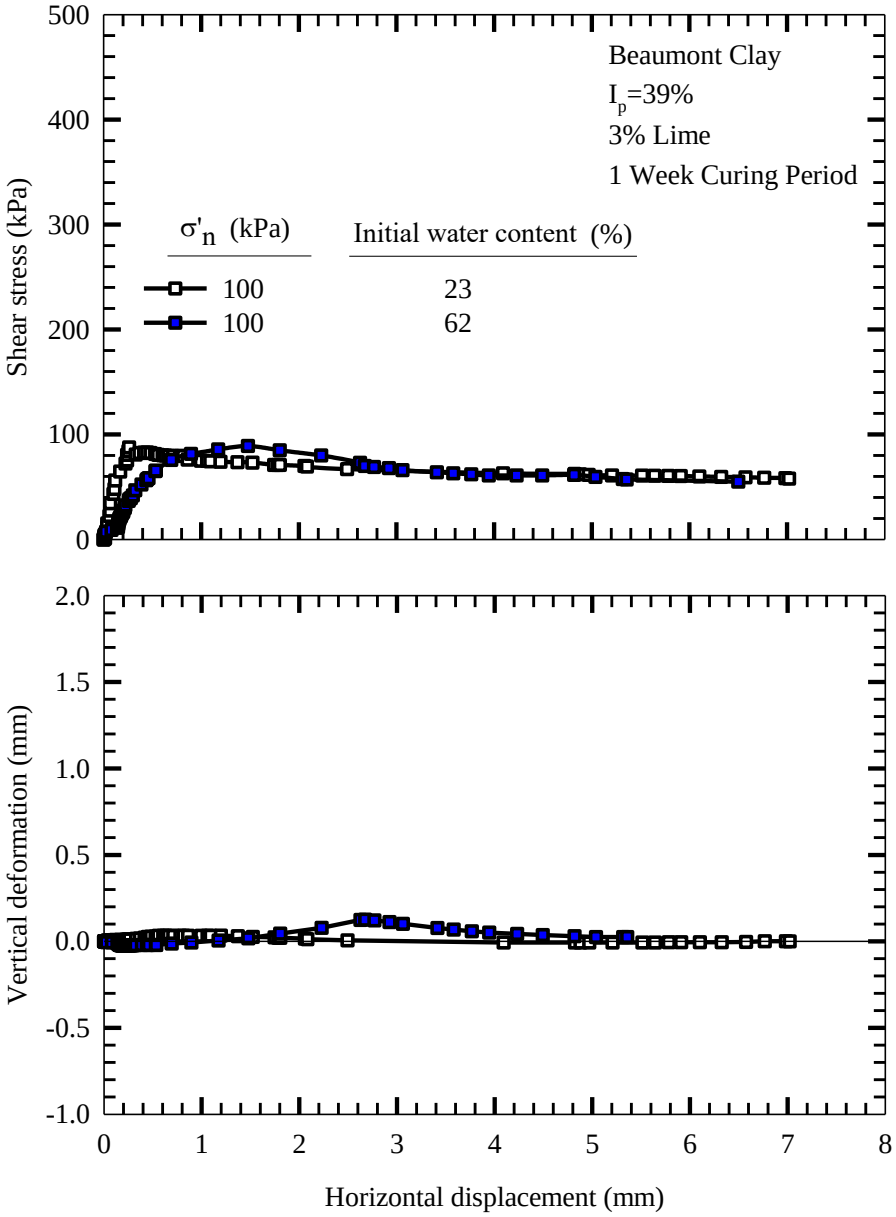

Figure 4.25: Shear stress-shear displacement and vertical displacement-shear displacement curves for Beaumont clay tretaed with 3% lime cured for 7 days (Specimens 51&52)

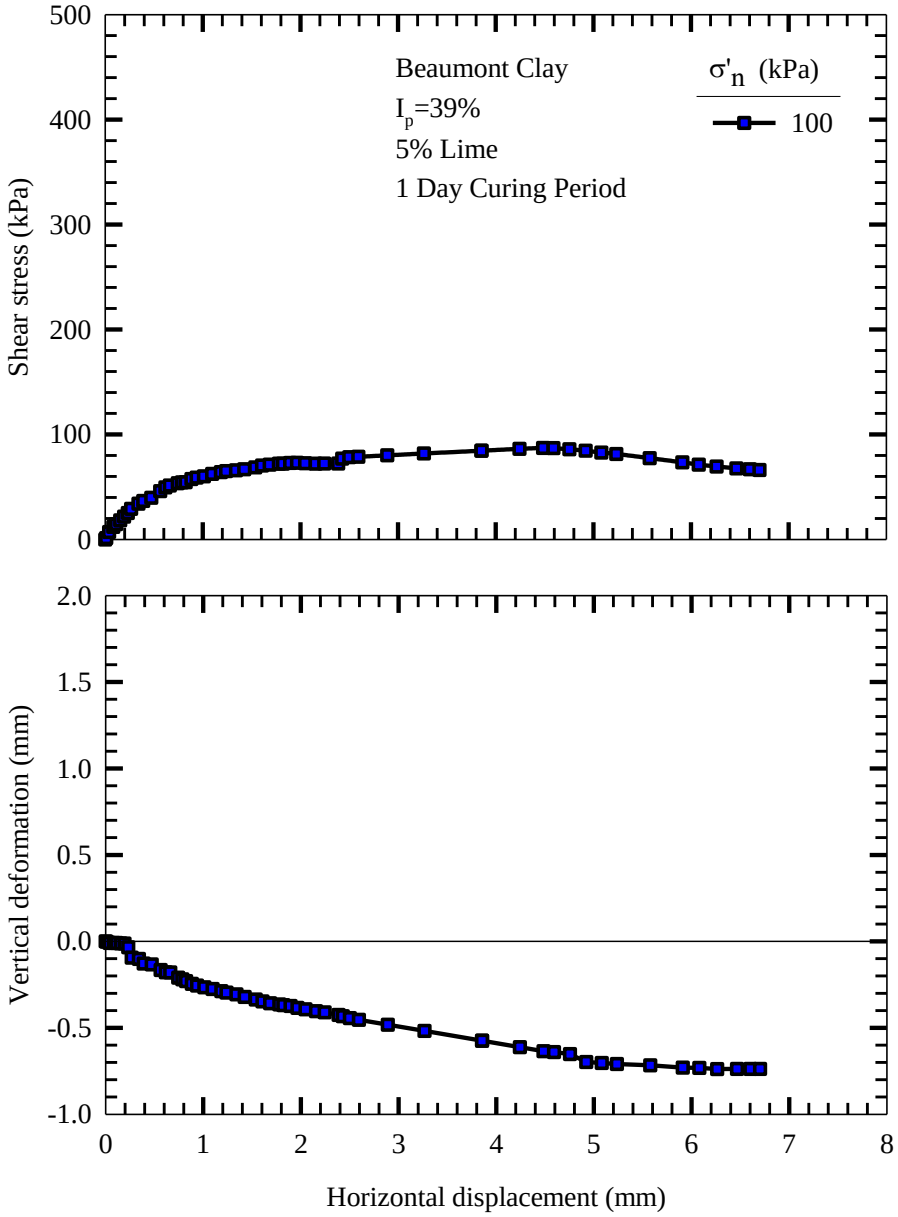

Figure 4.26: Shear stress-shear displacement and vertical displacement-shear displacement curves for Beaumont clay tretaed with 5% lime cured for 1 day (Specimen 53)

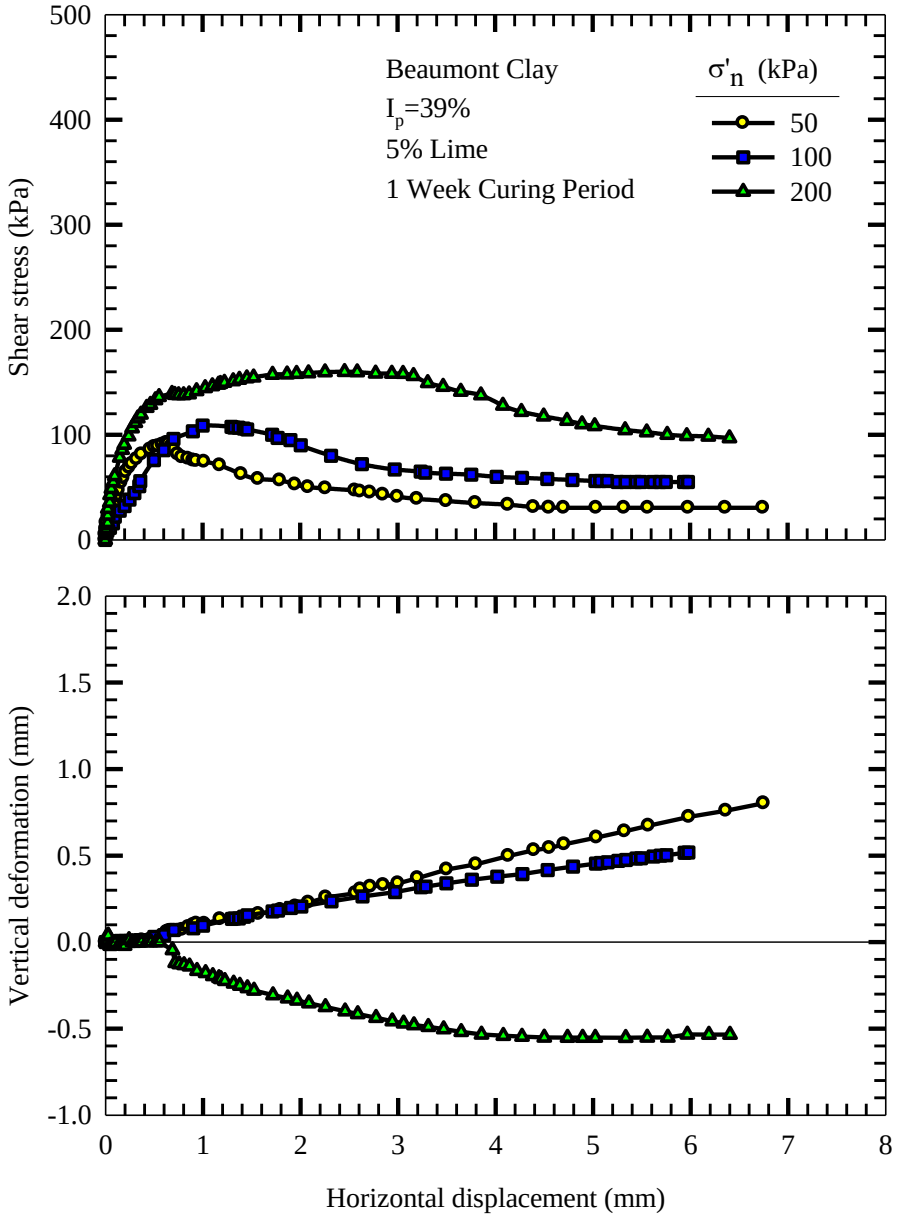

Figure 4.27: Shear stress-shear displacement and vertical displacement-shear displacement curves for Beaumont clay tretaed with 5% lime cured for 7 days (Specimens 54-56)

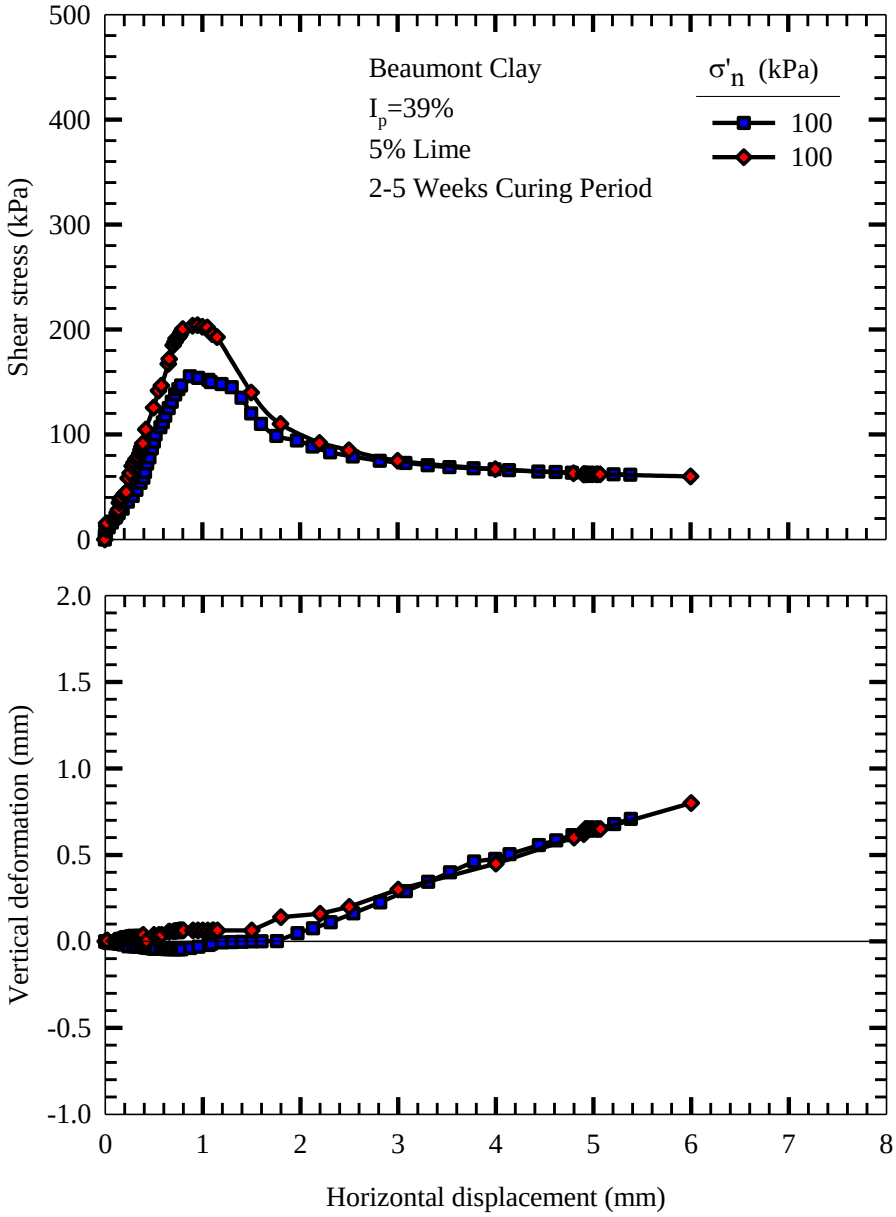

Figure 4.28: Shear stress-shear displacement and vertical displacement-shear displacement curves for Beaumont clay tretaed with 5% lime cured for 14-35 days (Specimens 57&58)

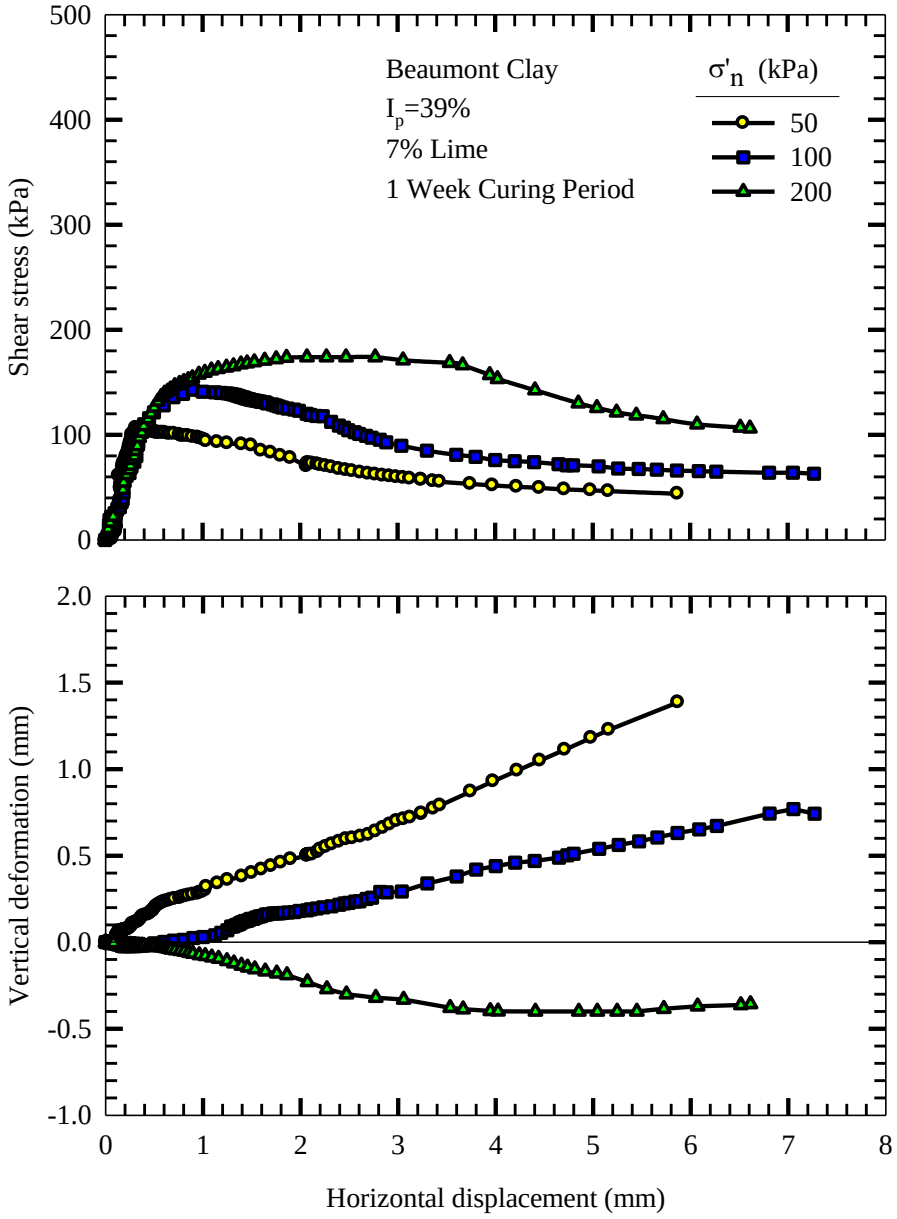

Figure 4.29: Shear stress-shear displacement and vertical displacement-shear displacement curves for Beaumont clay tretaed with 7% lime cured for 7 days (Specimens 59-61)

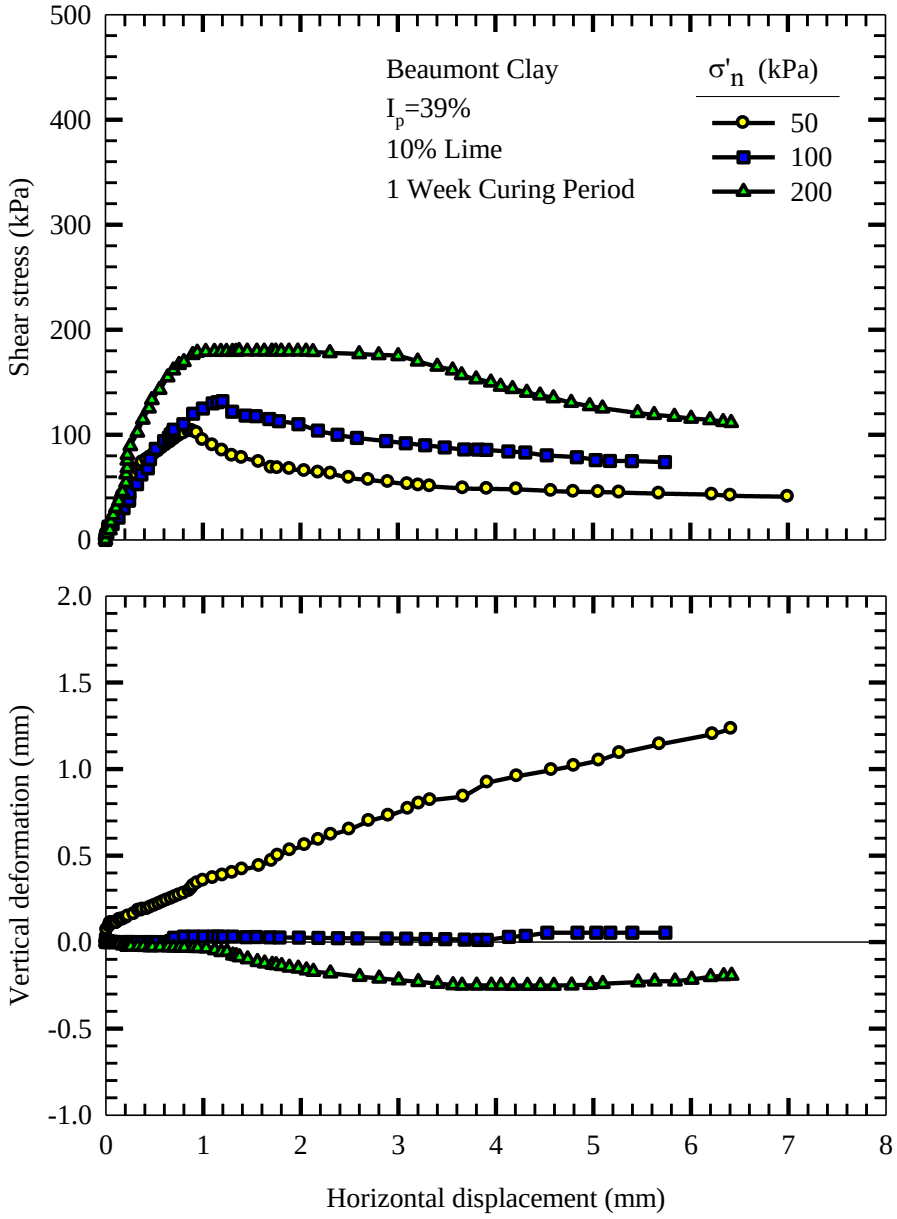

Figure 4.30: Shear stress-shear displacement and vertical displacement-shear displacement curves for Beaumont clay tretaed with 10% lime cured for 7 days (Specimens 62-64)

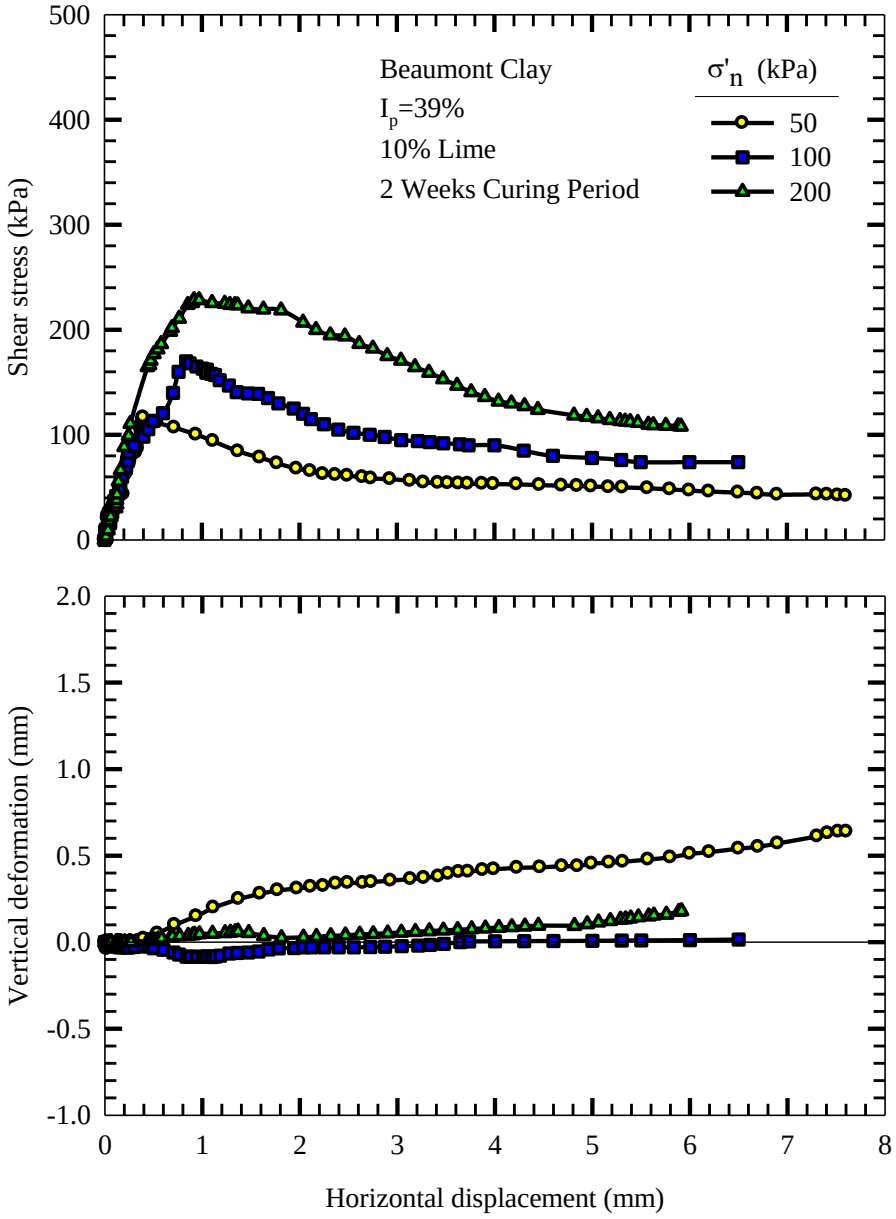

Figure 4.31: Shear stress-shear displacement and vertical displacement-shear displacement curves for Beaumont clay tretaed with 10% lime cured for 14 days (Specimens 65, 66&68)

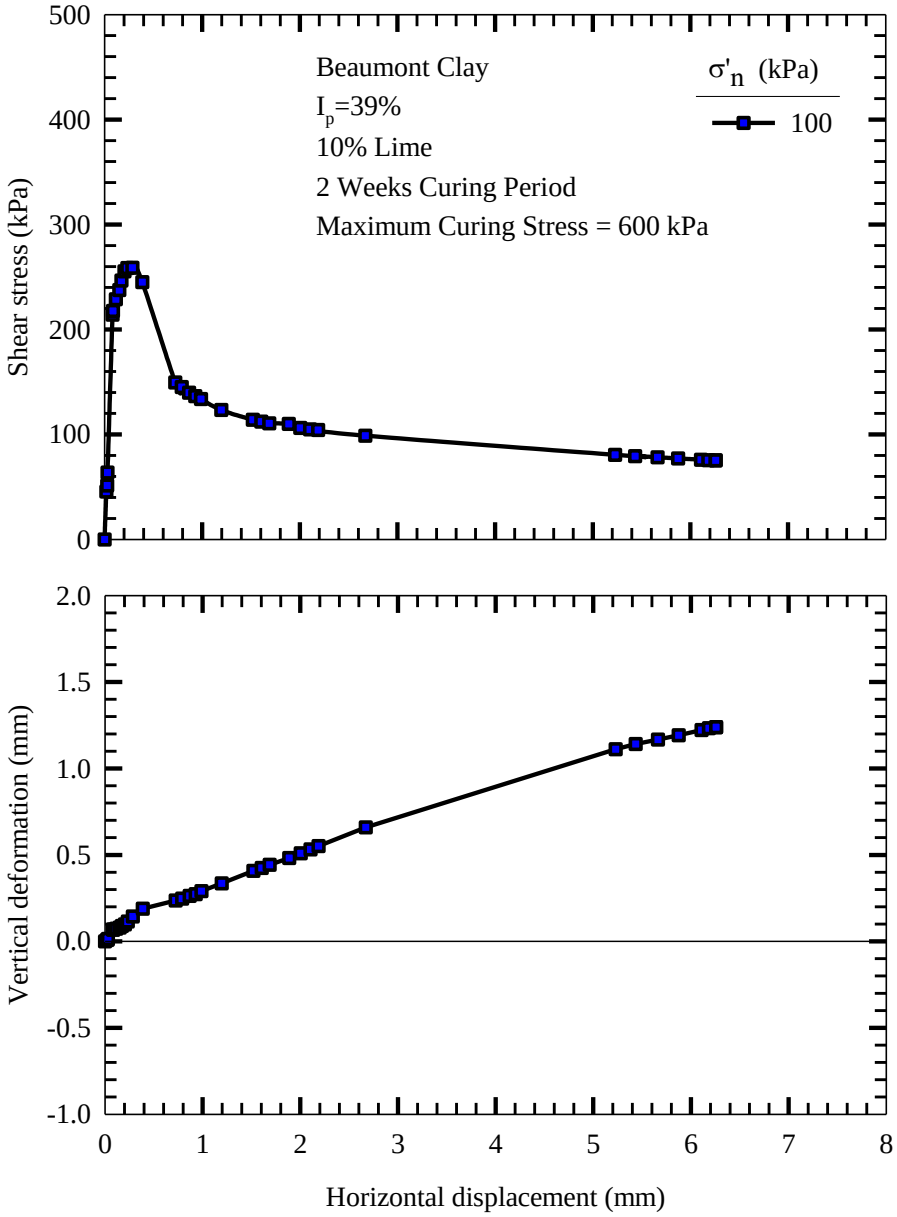

Figure 4.32: Shear stress-shear displacement and vertical displacement-shear displacement curves for Beaumont clay tretaed with 10% lime cured for 14 days (Specimen 67)

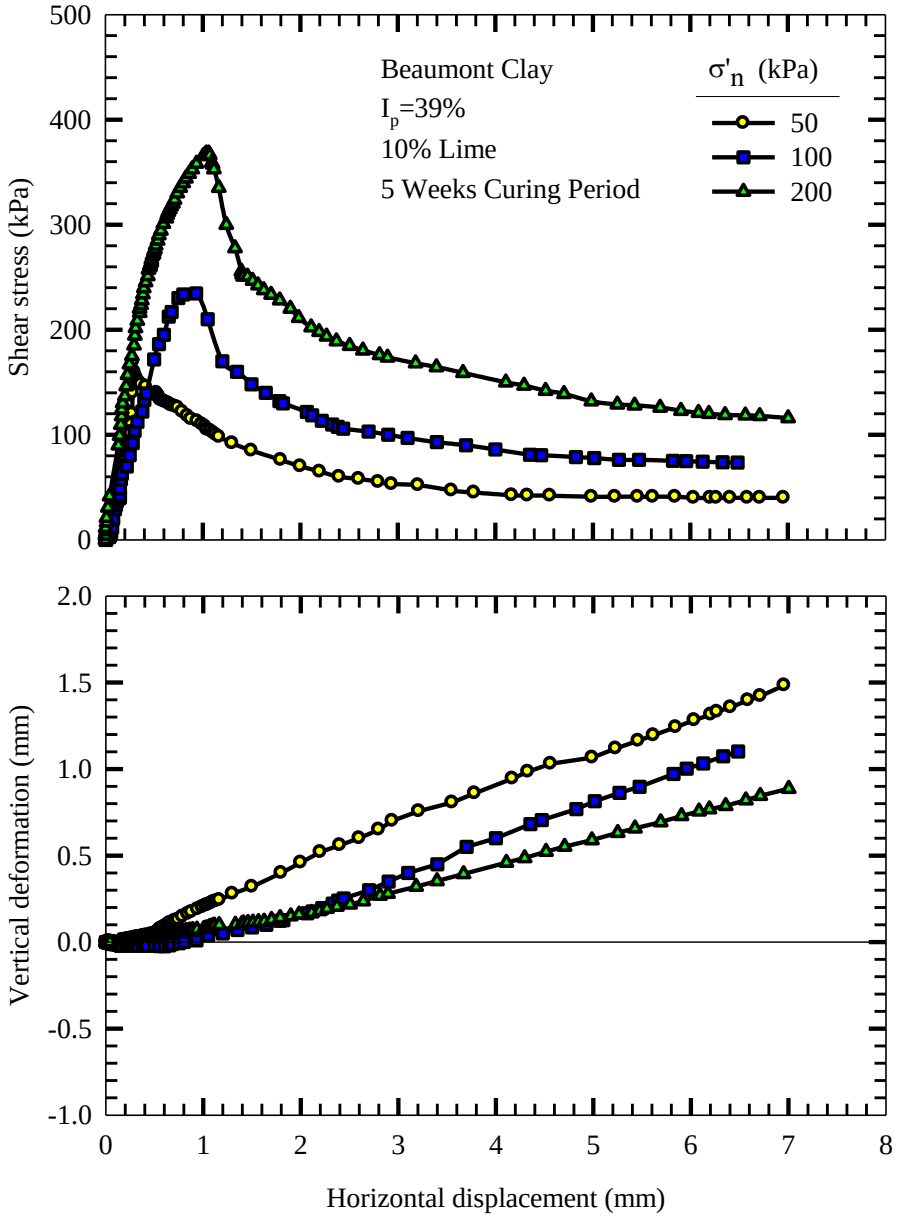

Figure 4.33: Shear stress-shear displacement and vertical displacement-shear displacement curves for Beaumont clay tretaed with 10% lime cured for 35 days (Specimens 69-71)

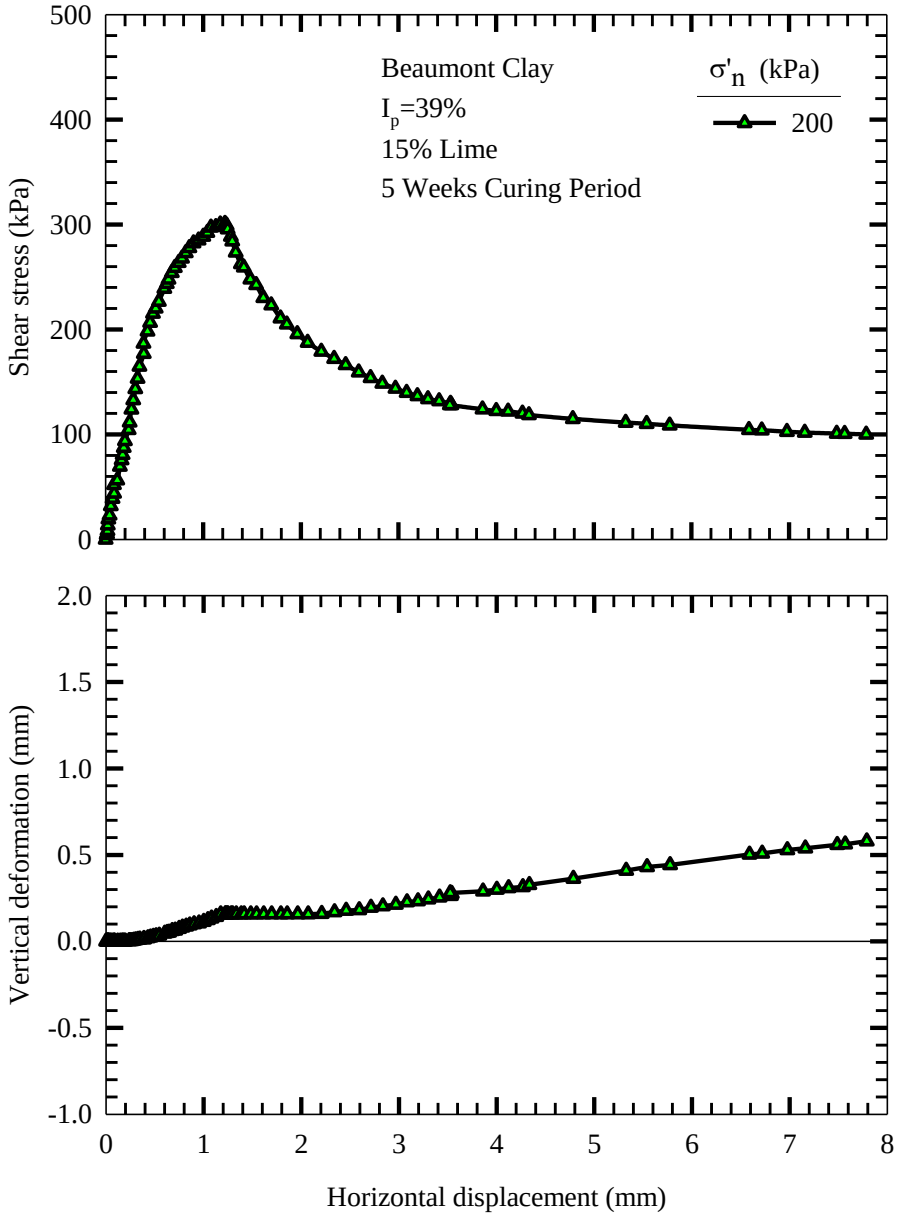

Figure 4.34: Shear stress-shear displacement and vertical displacement-shear displacement curves for Beaumont clay tretaed with 10% lime cured for 14 days (Specimen 72)

For an overconsolidated clay, the decrease in the shear stress after the peak reduces as the effective confining pressure increases, meaning that the behavior becomes less brittle. Only a small decrease in shear stress is observed after the peak when an overconsolidated clay is consolidated to a confining pressure exceeding the preconsolidation pressure. For a treated clay, there is an apparent preconsolidation pressure which increases with the confining pressure at which the treated clay has been cured (curing stress). As shown in Figure 4.19, a significant drop in the shear stress is still observed after the peak as the confining pressure increases. However, if the effective confining stress at which the specimen is sheared increases beyond the apparent preconsolidation stress (which is a function of the curing stress), it is expected that the specimen response becomes ductile.

The behavior of treated clays resembles that of highly overconsolidated clays resembles in that dilatancy is likely to begin past the peak shear stress. The dilatant behavior of treated clays at the peak is due to the breaking of cementitious bonds between floccules and formation of a distinct slip plane along which the treated clay has an opportunity to swell and soften.

The behavior of treated clays differs from that of overconsolidated clays in that in overconsolidated clays a volume reduction occurs before the peak, whereas in treated clays no volume change takes place before the peak. The volume reduction before the peak in overconsolidated clays is due to closing of existing fissures, while lime treated clays do not contain fissures. In some cases, little volume increase is observed before the peak strength of treated clays due to breakage of some of the bonds.

Another difference between the behaviors of overconsolidated and lime treated clays is that in overconsolidated clays shear stress drops to a value, known as fully softened strength, at which volume increase levels off, whereas in treated clays volume increase continues and barely levels off particularly at low effective confining pressures. For lime treated clays, the best approach is to define the shear strength as a function of shear strain. The same approach has been previously utilized for sensitive clays, where volume increase during shearing does not level off (Lefebvre, 1981).

4.2 PEAK SHEAR STRENGTH ENVELOPES

The peak shear strength envelopes of Chicago clay are shown in Figures 4.35-4.37 for lime contents of 3, 5, and 10%, respectively. The peak strength increases considerably after 1 week of curing, but there is only a slight increase as curing time increases from 1 to 4-6 weeks. Figures 4.38 and 4.39 show the shear strength envelopes of Chicago clay treated by various lime contents for curing periods of 1 and 4-6 weeks, respectively. Lime contents higher than 3% decrease shear strength of treated Chicago clay.

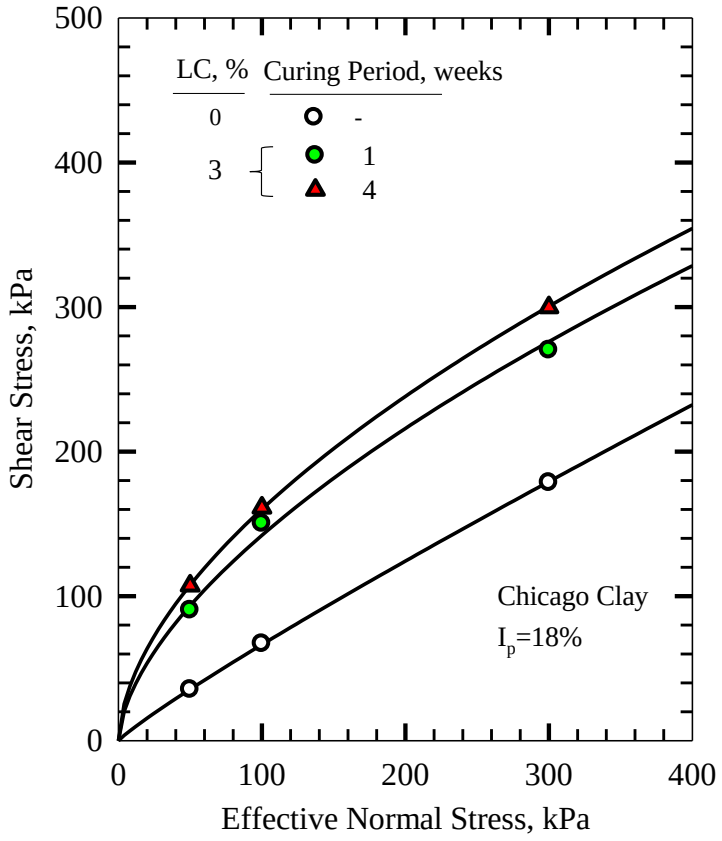

Figure 4.35: Peak shear strength envelopes for Chicago clay tretaed with 3% lime

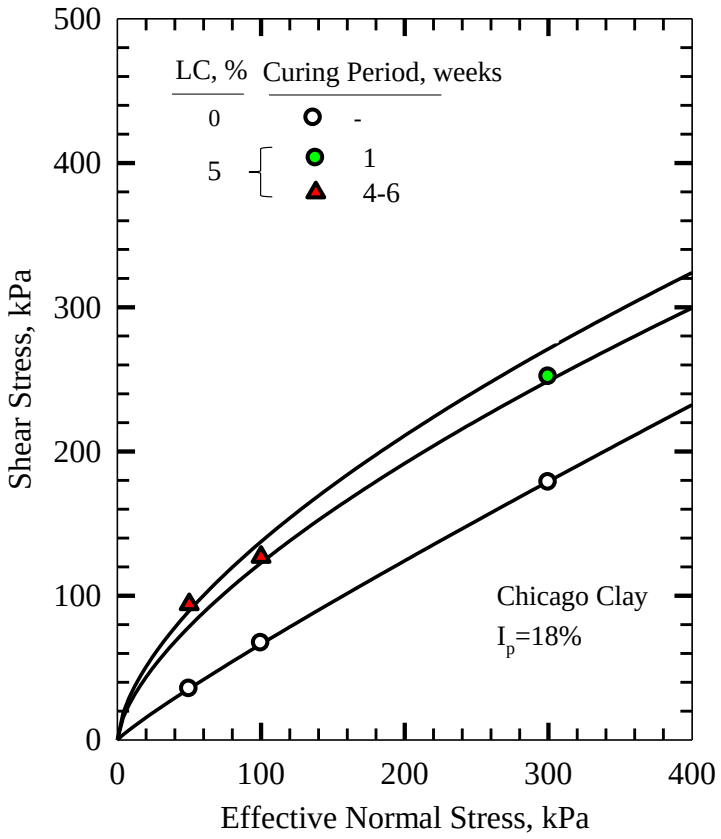

Figure 4.36: Peak shear strength envelopes for Chicago clay tretaed with 5% lime

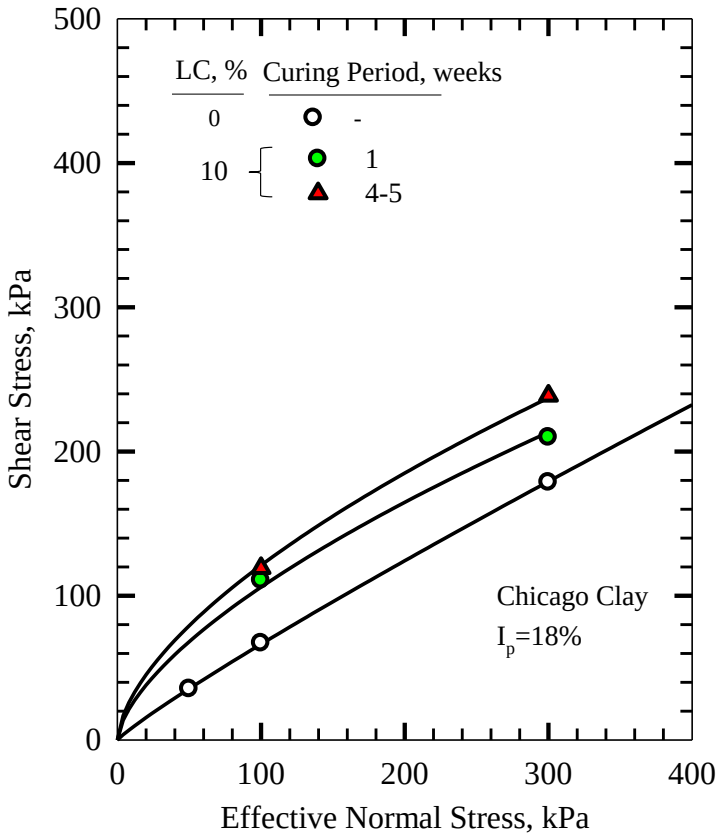

Figure 4.37: Peak shear strength envelopes for Chicago clay tretaed with 10% lime

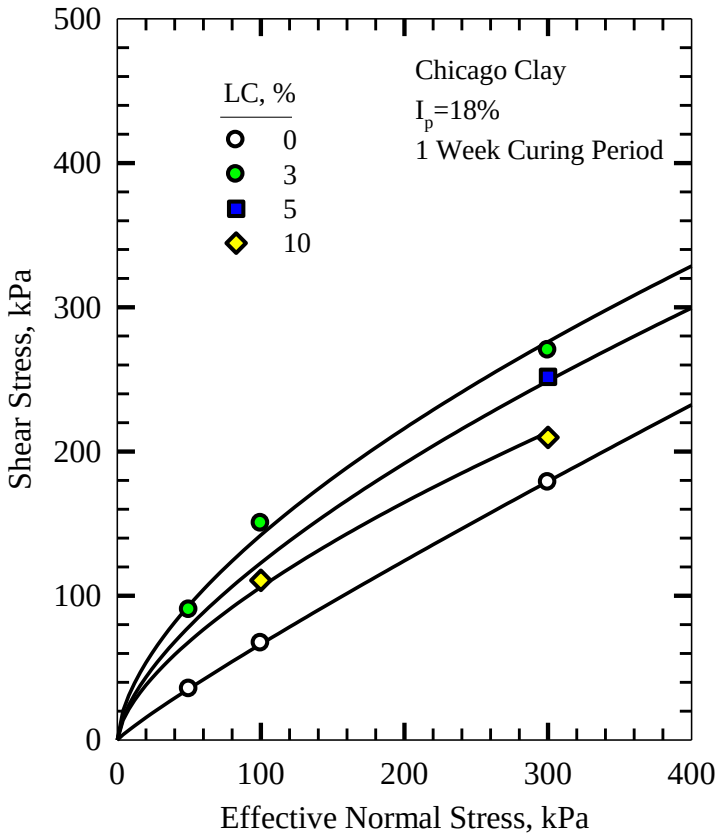

Figure 4.38: Peak shear strength envelopes for Chicago clay tretaed with various lime contents and cured for 7 days

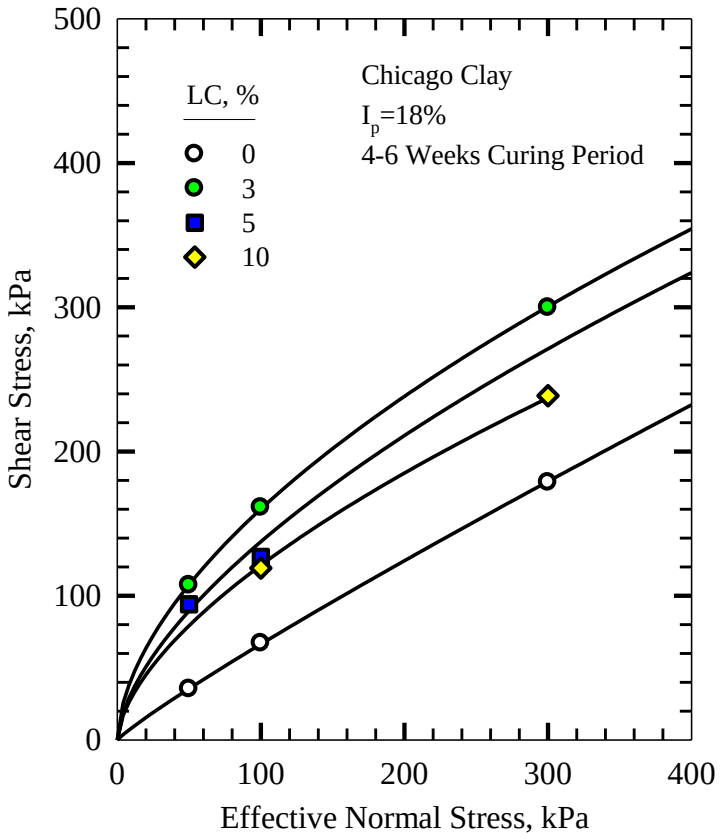

Figure 4.39: Peak shear strength envelopes for Chicago clay tretaed with various lime contents, and cured for 28-42 days

The peak shear strength envelopes of Lower Brenna clay are shown in Figures 4.40-4.43 for lime contents of 3, 5 and 10%, respectively. The peak shear strength increases with curing time for each lime content. The shear strength envelopes of Lower Brenna clay treated by various lime contents for curing periods of 1, 2 and 5 weeks are shown in Figures 4.44-4.46, respectively. Lime contents higher than 7% do not lead to an additional increase in the shear strength.

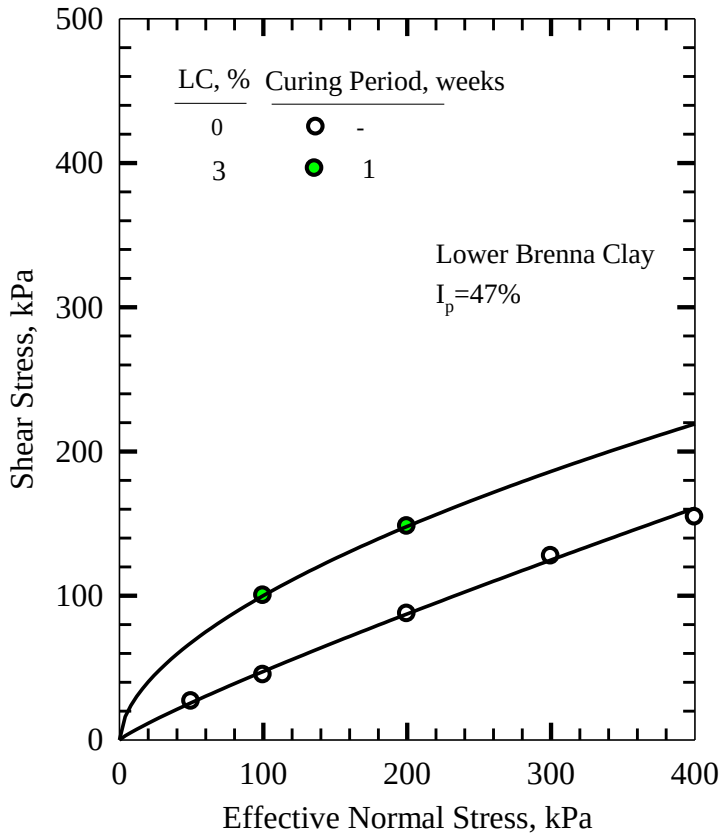

Figure 4.40: Peak shear strength envelopes for Lower Brenna clay tretaed with 3% lime and cured for 7 days

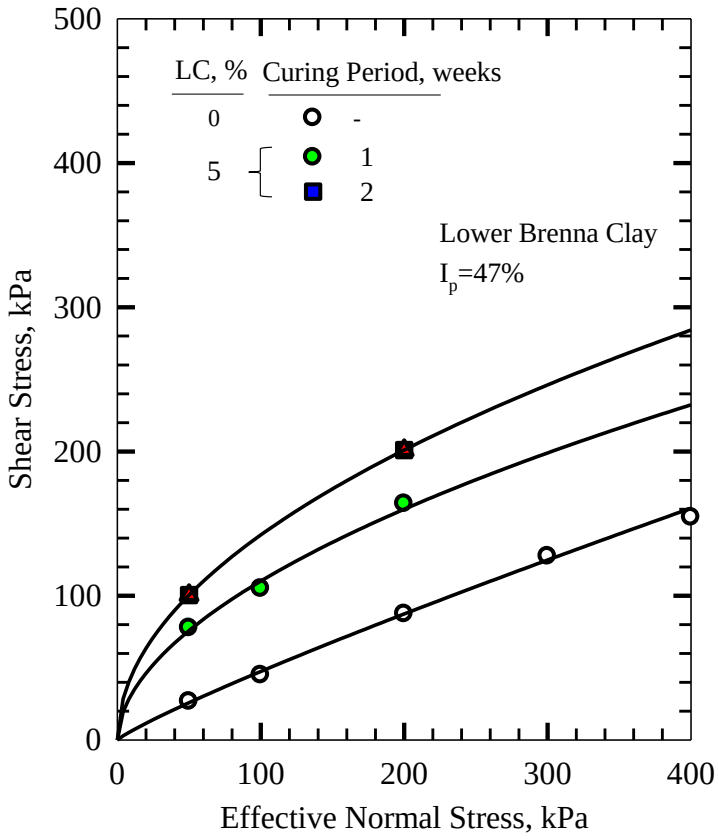

Figure 4.41: Peak shear strength envelopes for Lower Brenna clay tretaed with 5% lime

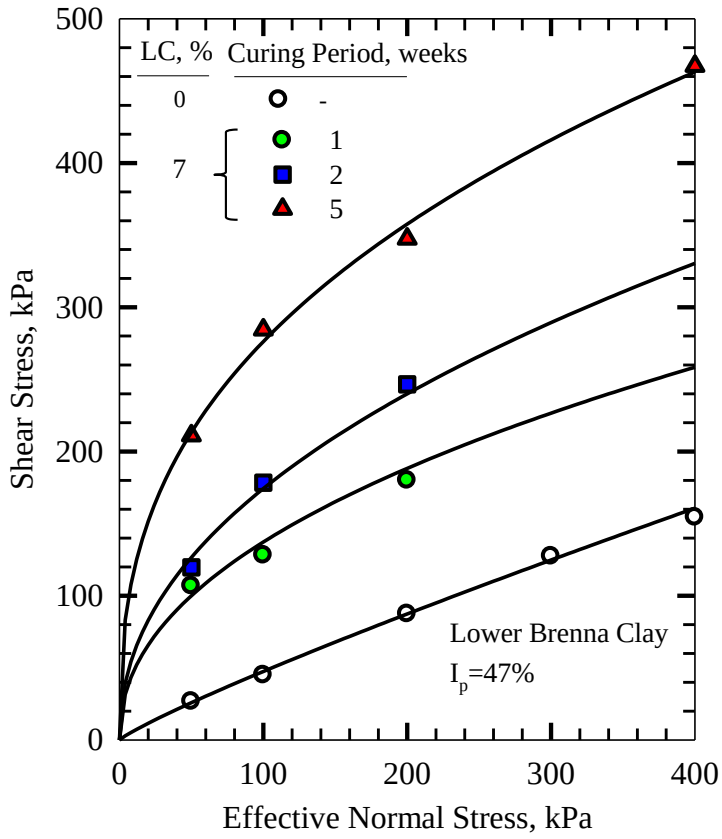

Figure 4.42: Peak shear strength envelopes for Lower Brenna clay tretaed with 7% lime

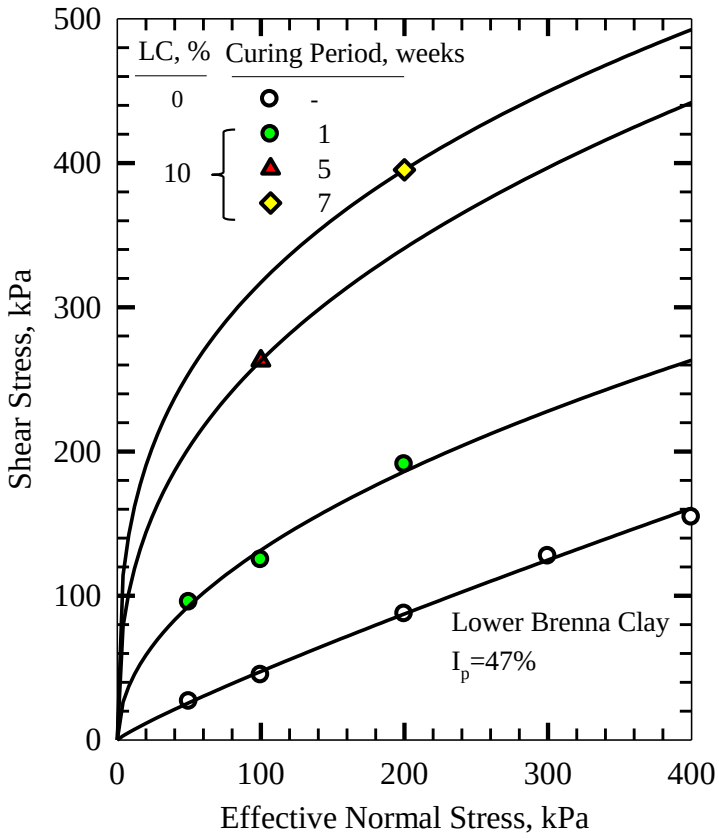

Figure 4.43: Peak shear strength envelopes for Lower Brenna clay tretaed with 10% lime

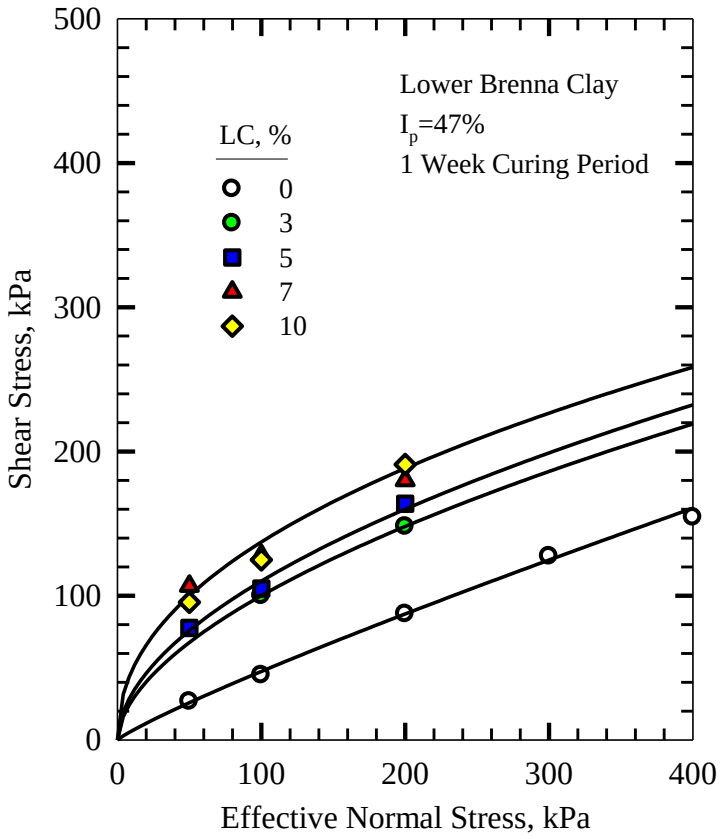

Figure 4.44: Peak shear strength envelopes for Lower Brenna clay with vaious lime contents and cured for 7 days

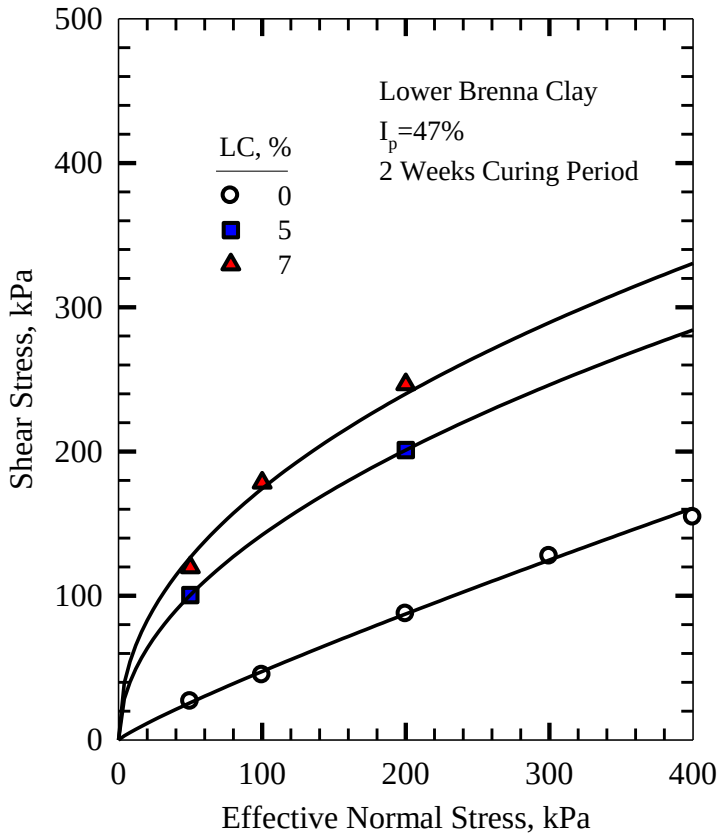

Figure 4.45: Peak shear strength envelopes for Lower Brenna clay with vaious lime contents and cured for 14 days

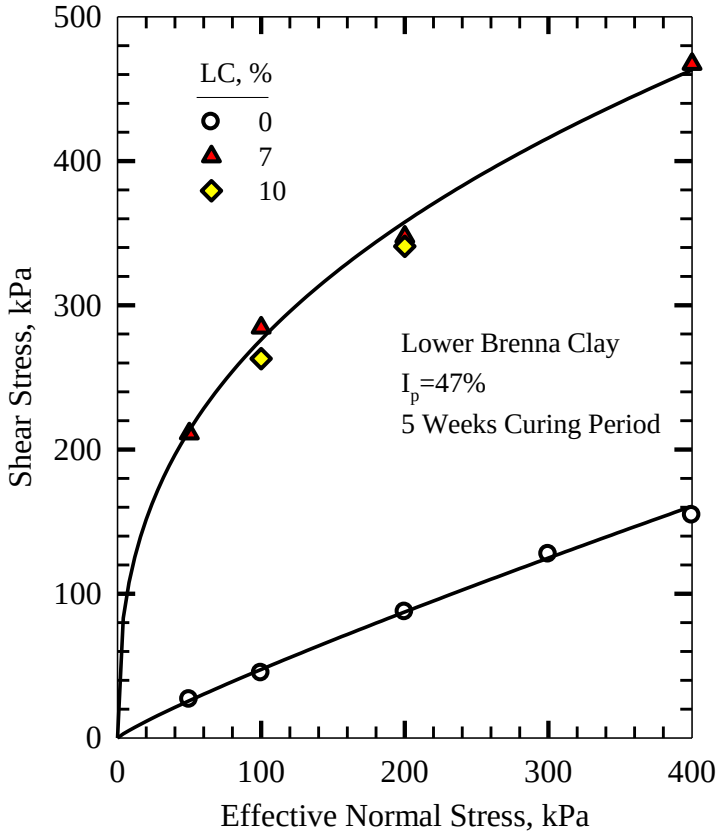

Figure 4.46: Peak shear strength envelopes for Lower Brenna clay with vaious lime contents and cured for 35 days

The peak shear strength envelopes of Beaumont clay are shown in Figures 4.47-4.51 for lime contents of 1, 3, 5, 7 and 10%, respectively. The shear strength envelopes of the specimens treated by various lime contents are shown in Figures 4.52-4.54 for curing periods of 1, 2 and 5 weeks, respectively. No Major improvement was observed by addition of 1% lime. Lime contents higher than 7% do not appear to further increase the shear strength of treated clay.

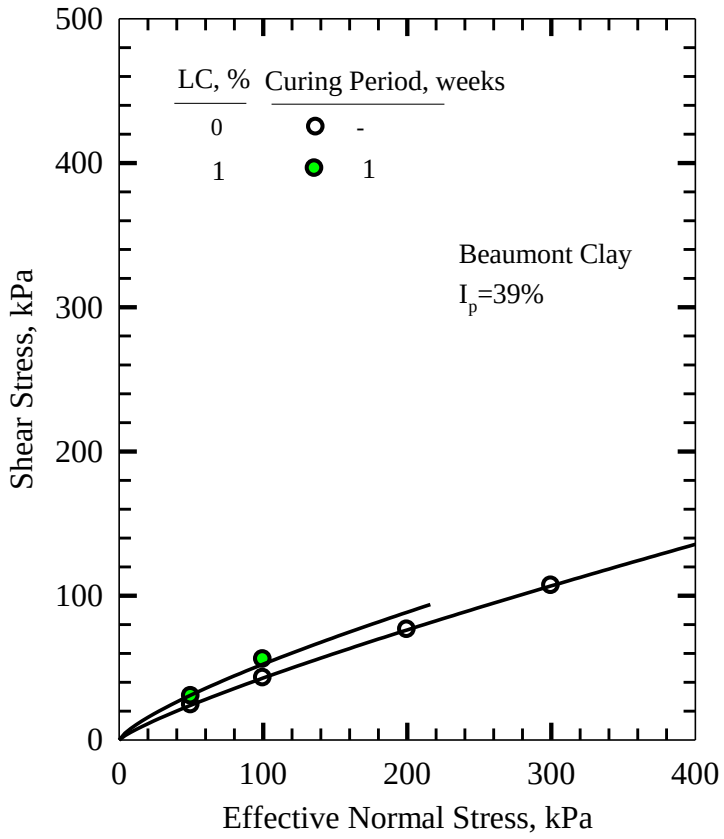

Figure 4.47: Peak shear strength envelopes for Beaumont clay tretaed with 1% lime

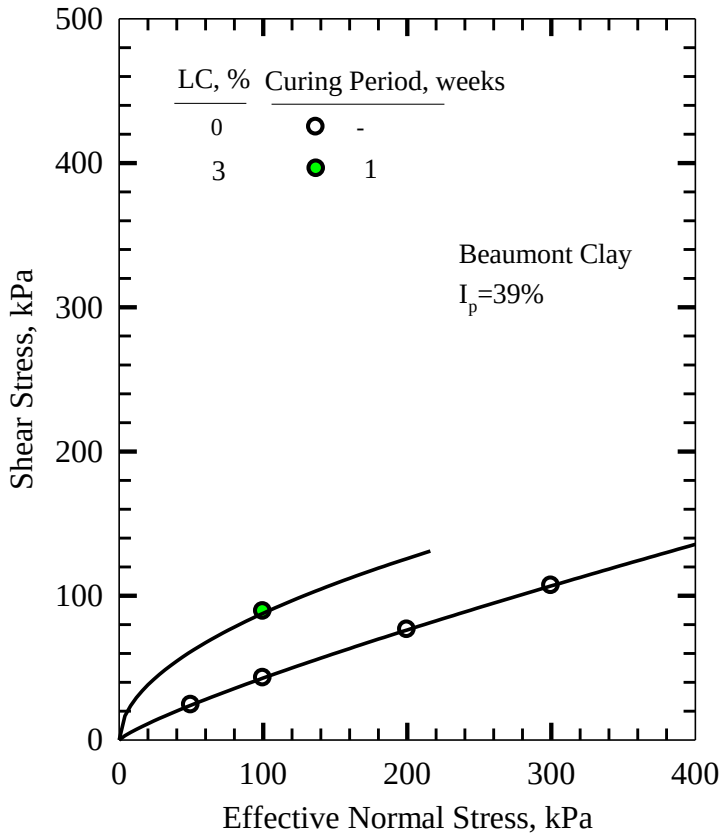

Figure 4.48: Peak shear strength envelopes for Beaumont clay tretaed with 3% lime

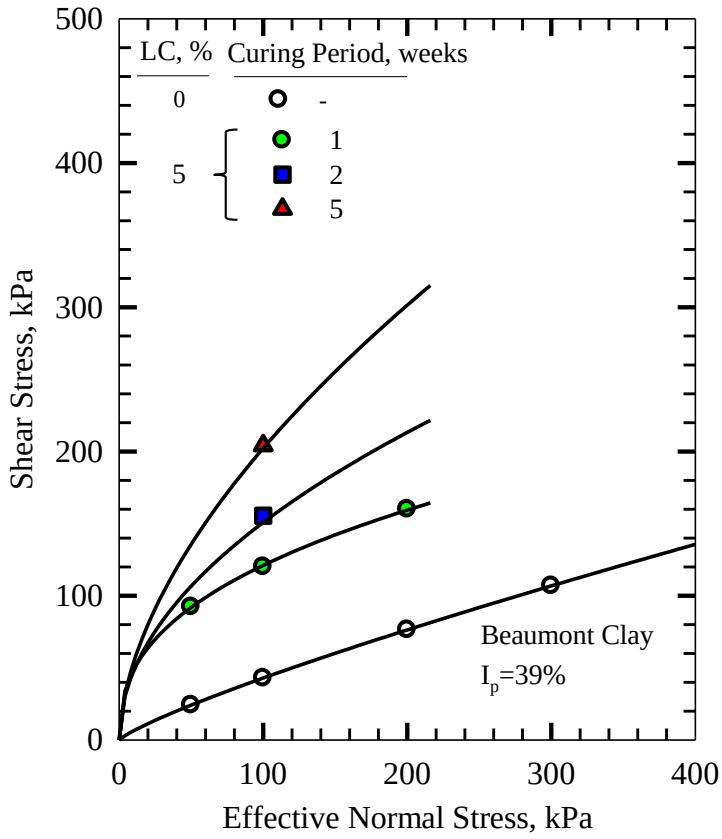

Figure 4.49: Peak shear strength envelopes for Beaumont clay tretaed with 5% lime

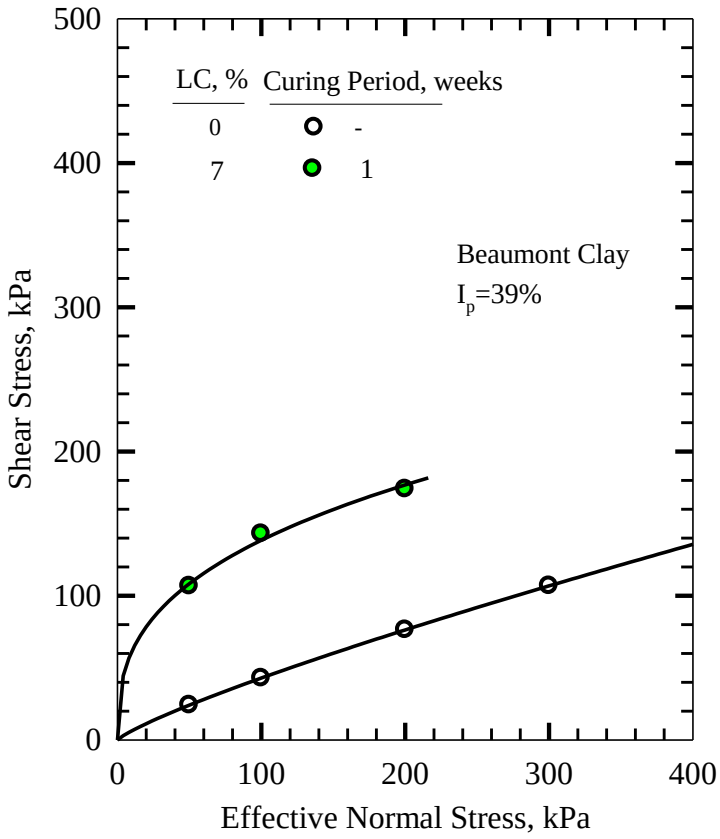

Figure 4.50: Peak shear strength envelopes for Beaumont clay tretaed with 7% lime

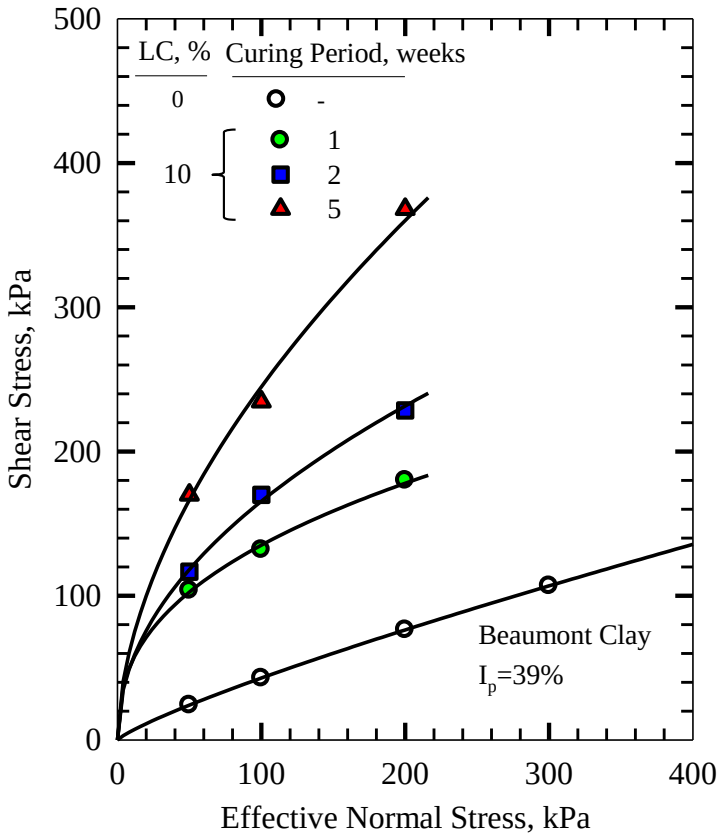

Figure 4.51: Peak shear strength envelopes for Beaumont clay tretaed with 10% lime

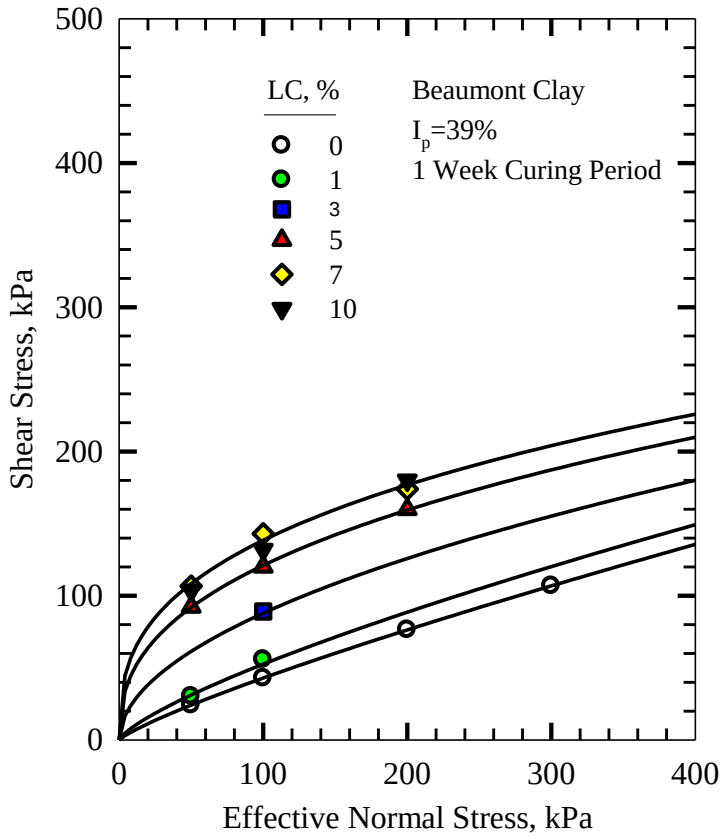

Figure 4.52: Peak shear strength envelopes for Beaumont clay with vaious lime contents and cured for 7 days

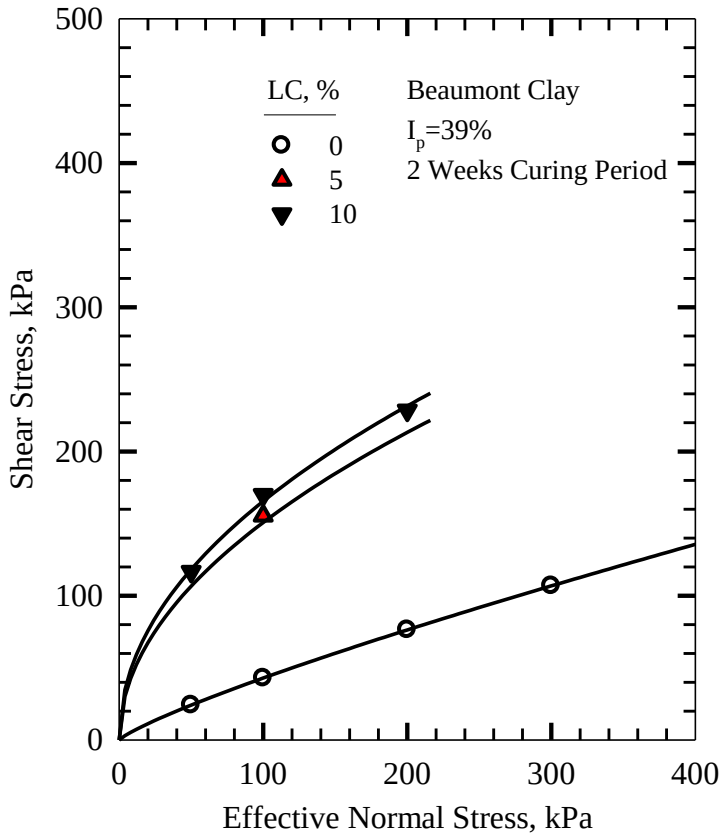

Figure 4.53: Peak shear strength envelopes for Beaumont clay with vaious lime contents and cured for 14 days

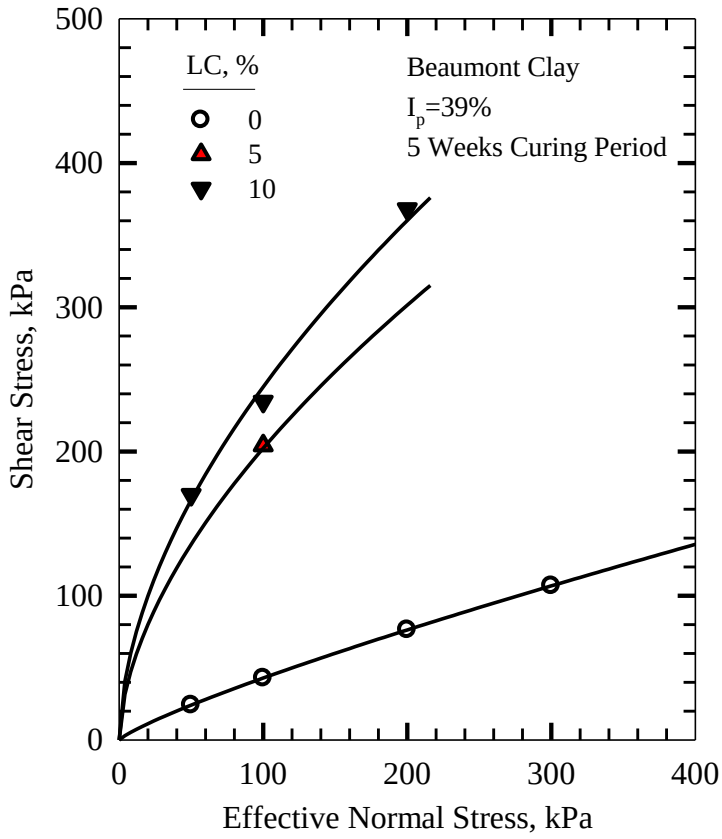

Figure 4.54: Peak shear strength envelopes for Beaumont clay with vaious lime contents and cured for 35 days

The peak (intact) strength envelope of treated Chicago, Lower Brenna and Beaumont clays displays a pronounced curvature due to a decrease in dilatant response of cemented soil structure as effective normal stress increases. Cementitious bonds formed within and in between clay floccules and lower tendency of treated clays to dilate at high effective normal stresses are responsible for high degree of nonlinearity of the shear strength envelope.

4.3 PEAK SHEAR STRENGTH WITH CURING TIME

The peak shear strength of treated clays increases with curing time as cementitious products crystalize and harden. The increase in secant peak friction angle of Chicago clay with curing time for lime contents of 3% is shown in Figure 4.55. No major increase in secant peak friction angle was observed between 1 and 4 weeks of curing.

The increase in secant peak friction angle of Lower Brenna clay with curing time for lime contents of 5%, 7% and 10% is shown in Figures 4.56-4.58, respectively. The data are for curing periods up to 35 days and effective normal stresses of 50, 100 and 200 kPa. There is a major increase in the secant peak friction angle in the first week of treatment, particularly at low effective normal stresses. The increase in the peak strength continues after the first week of treatment, though with a reduced rate. The significant improvement in the peak strength during the first week of curing is due to the formation of cementitious bonding products under elevated pH condition. As time passes, these products harden and increase the peak strength.

The increase in the peak strength of Beaumont clay is shown in Figures 4.59 and 4.60 for lime contents of 5% and 10%, respectively, for curing periods up to 35 days and effective normal stresses of 50, 100 and 200 kPa. A major improvement takes place during the first week. This is more pronounced for low effective normal stresses. The peak strength continues to increase with curing time but at a relatively lower rate compared to the initial rate during the first week.

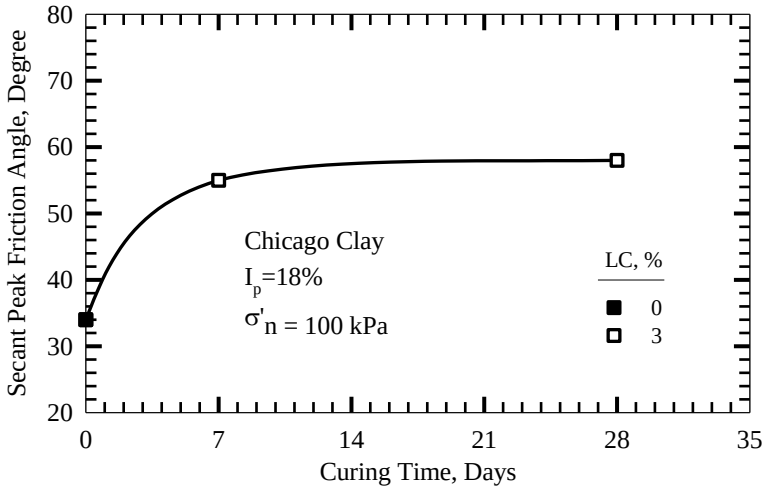

Figure 4.55: Secant peak friction angle plotted against time for Chicago clay tretaed with 3% lime

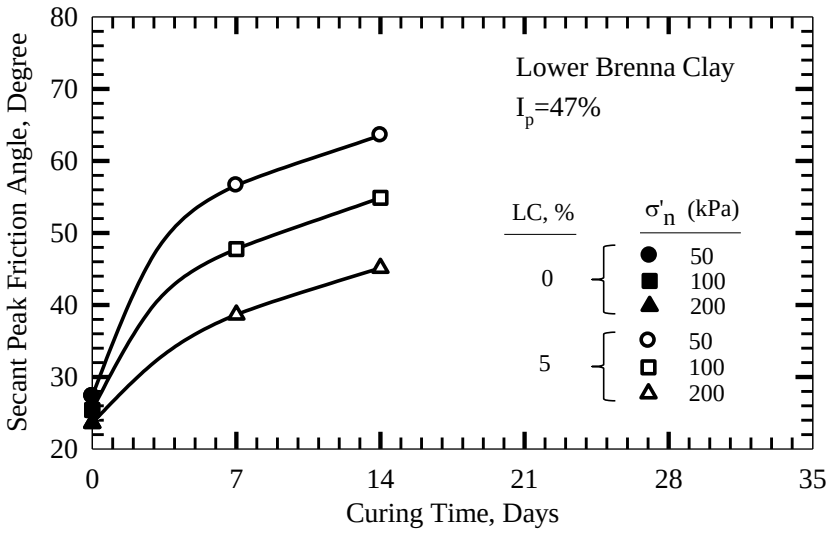

Figure 4.56: Secant peak friction angle plotted against time for Lower Brenna clay tretaed with 5% lime

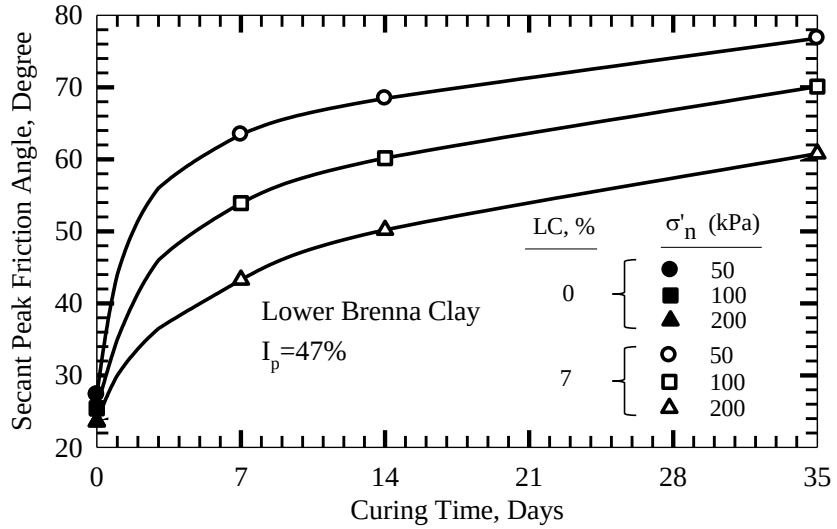

Figure 4.57: Secant peak friction angle plotted against time for Lower Brenna clay tretaed with 7% lime

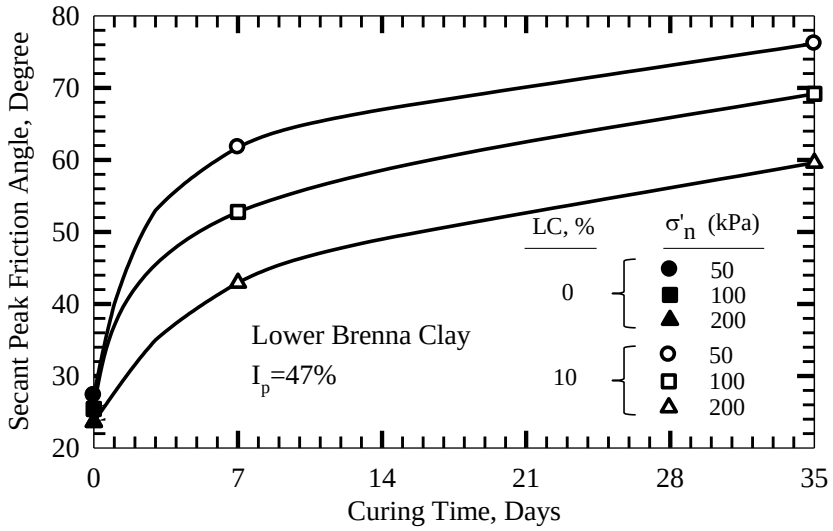

Figure 4.58: Secant peak friction angle plotted against time for Lower Brenna clay tretaed with 10% lime

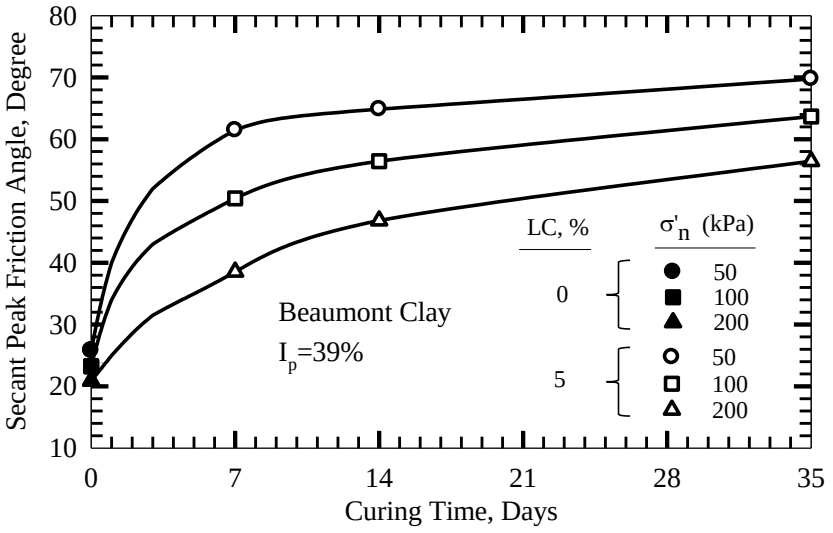

Figure 4.59: Secant peak friction angle plotted against time for Beaumont clay tretaed with 5% lime

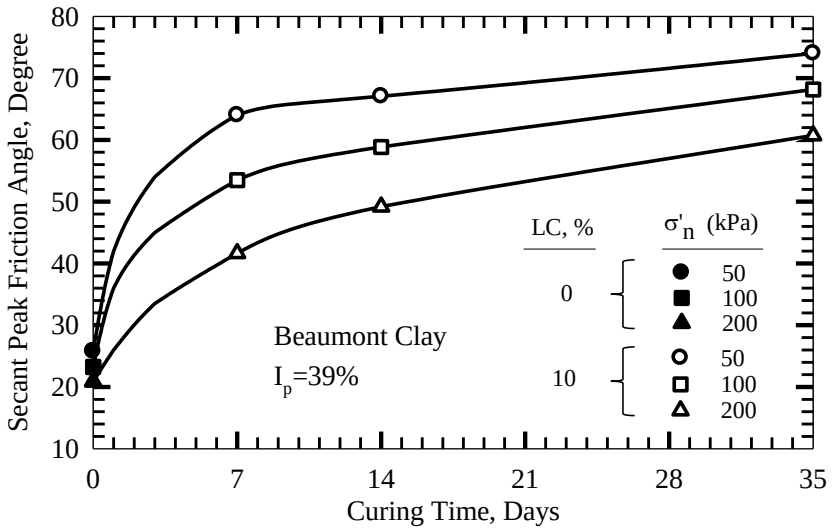

Figure 4.60: Secant peak friction angle plotted against time for Beaumont clay tretaed with 10% lime

4.4 SECANT PEAK FICTION ANGLE-LIME CONTENT RELATIONSHIP

The secant peak friction angle of Chicago clay plotted against lime content is shown in Figures 4.61 and 4.62 for curing periods of 1 and 4-6 weeks. A lime content of 1-3% causes the most improvement in the secant peak friction angle. Curing time does not cause a major increase in the secant peak friction angle of Chicago clay as shown in Figure 4.63.

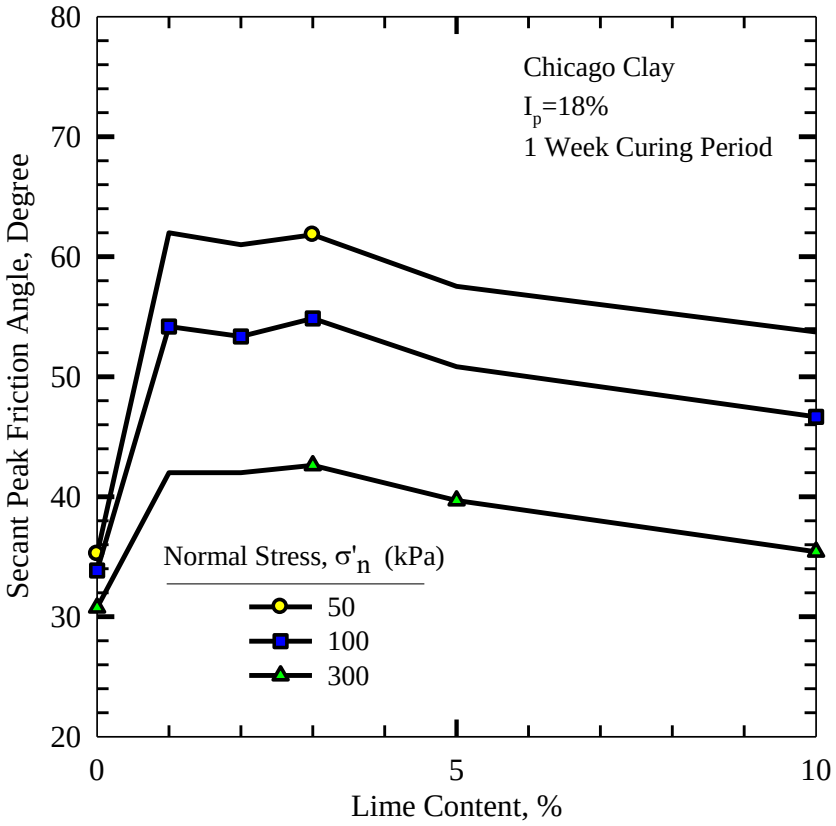

Figure 4.61: Secant peak friction angle plotted against lime content for Chicago clay cured for 7 days

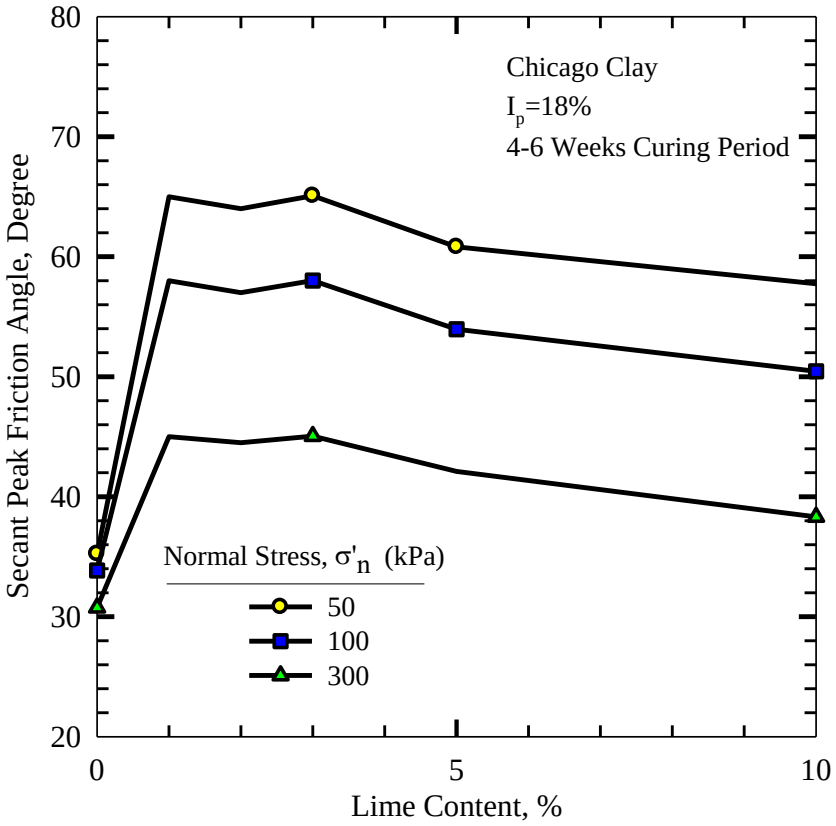

Figure 4.62: Secant peak friction angle plotted against lime content for Chicago clay cured for 28-42 days

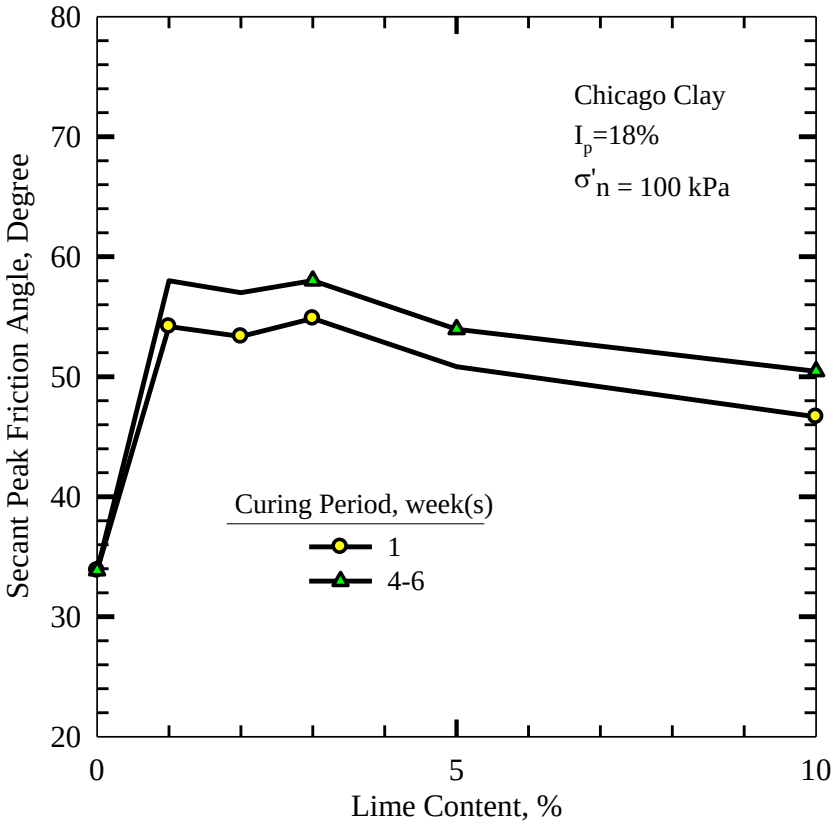

Figure 4.63: Secant peak friction angle plotted against lime content for Chicago clay with various curing periods

The secant peak friction angles plotted against lime content are shown in Figures 4.64-4.66 for Lower Brenna clay cured for 7 , 14 and 35 days, respectively. The lime content ranges from 1% to 15%. The figures show the influence of a range of effective normal stresses, i.e. 50, 100 and 200 kPa on the secant peak friction angle. The peak shear strength increases with lime content for the values up to 7%, above which the peak strength remains constant or slightly decreases as lime content further increases. Figure 4.67 presents the secant peak friction angle plotted against lime content for Lower Brenna clay cured for 7, 14 and 35 days for an effective normal stress of 200 kPa.

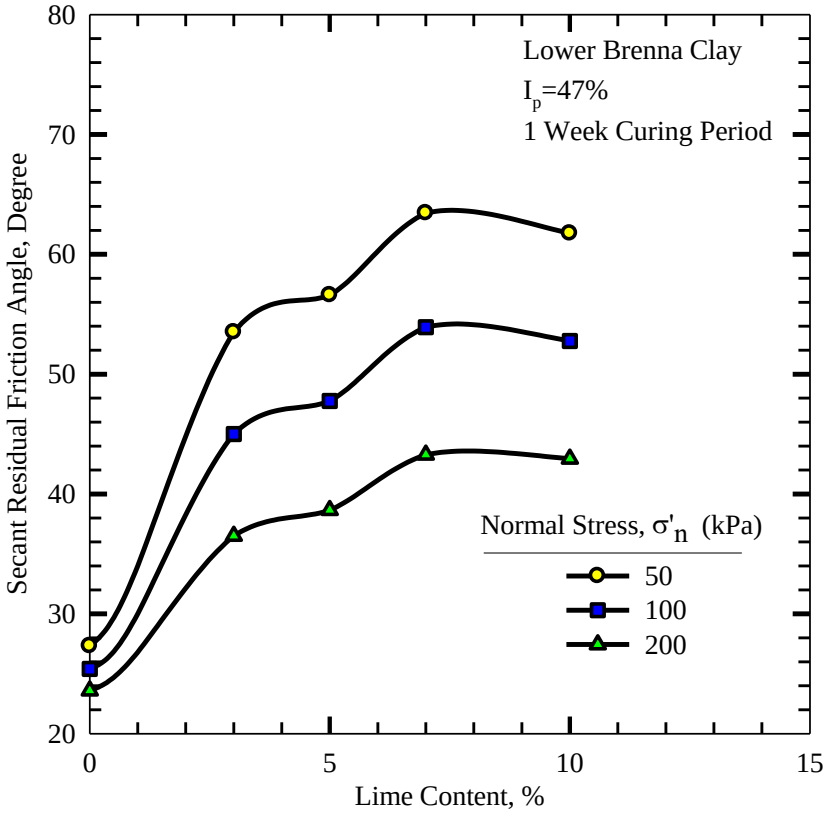

Figure 4.64: Secant peak friction angle plotted against lime content for Lower Brenna clay cured for 7 days

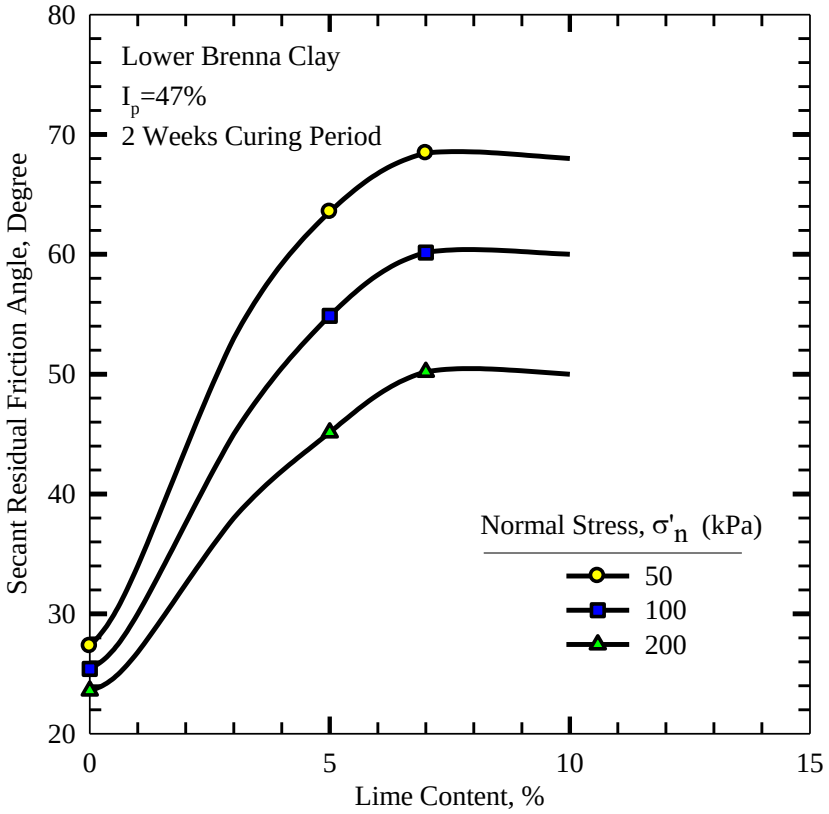

Figure 4.65: Secant peak friction angle plotted against lime content for Lower Brenna clay cured for 14 days

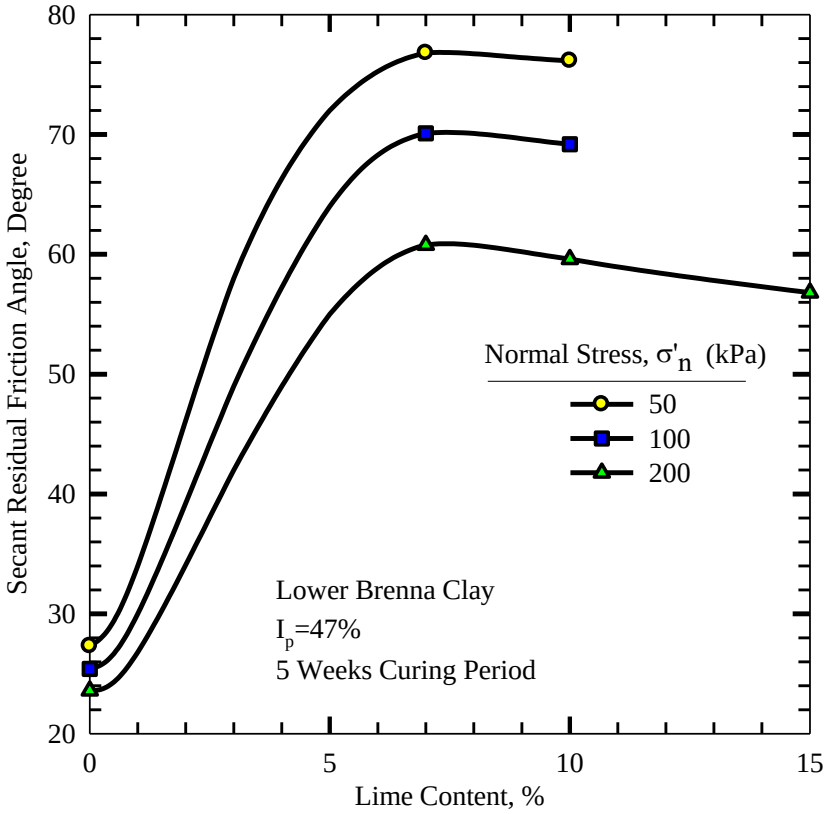

Figure 4.66: Secant peak friction angle plotted against lime content for Lower Brenna clay cured for 35 days

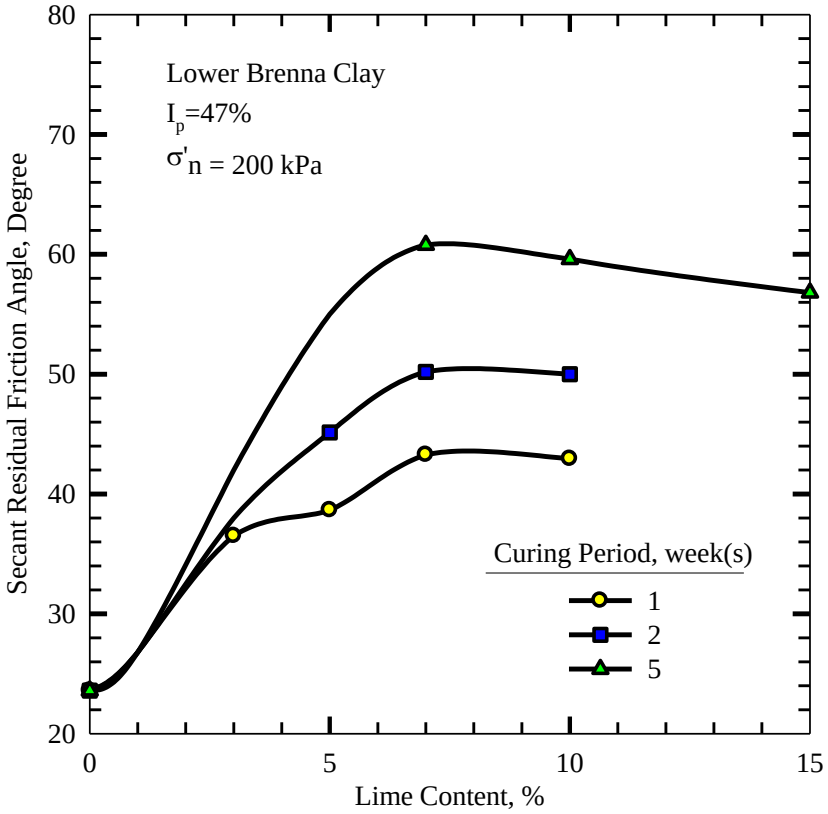

Figure 4.67: Secant peak friction angle plotted against lime content for Lower Brenna clay with various curing periods

The secant peak friction angle of Beaumont clay cured for 7 , 14 and 35 days is plotted against lime content ranging from 1% to 15% in Figures 4.68-4.70, respectively. The peak strength reaches a maximum at 7% lime content and then remains constant or slightly decreases with an increase in lime content. Figure 4.71 presents the secant peak friction angle plotted against lime content for Beaumont clay cured for 7, 14 and 35 days for an effective normal stress of 200 kPa.

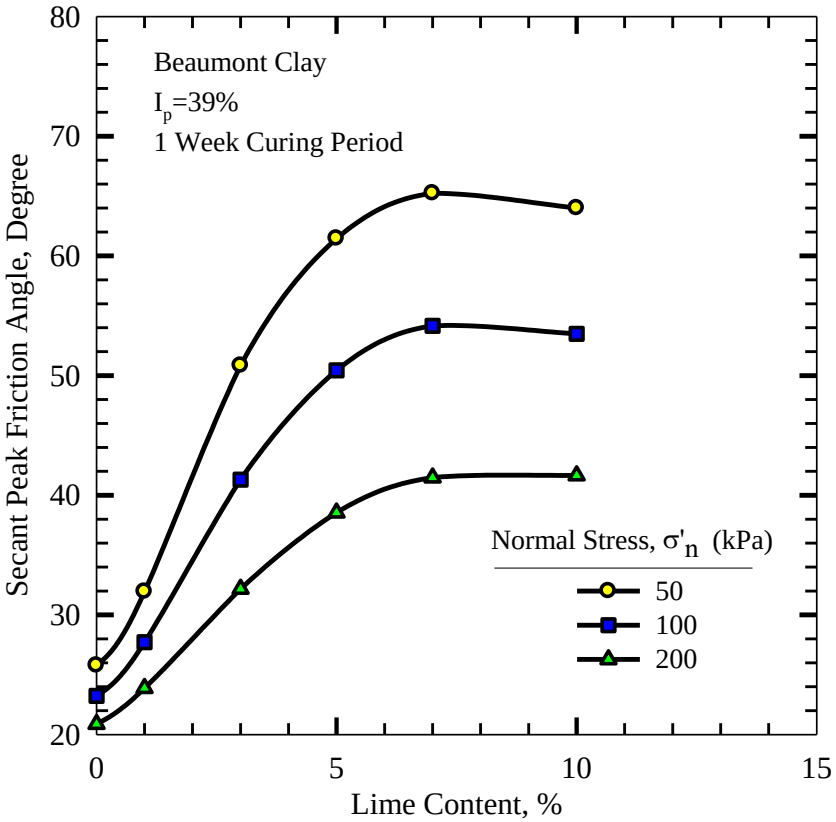

Figure 4.68: Secant peak friction angle plotted against lime content for Beaumont clay cured for 7 days

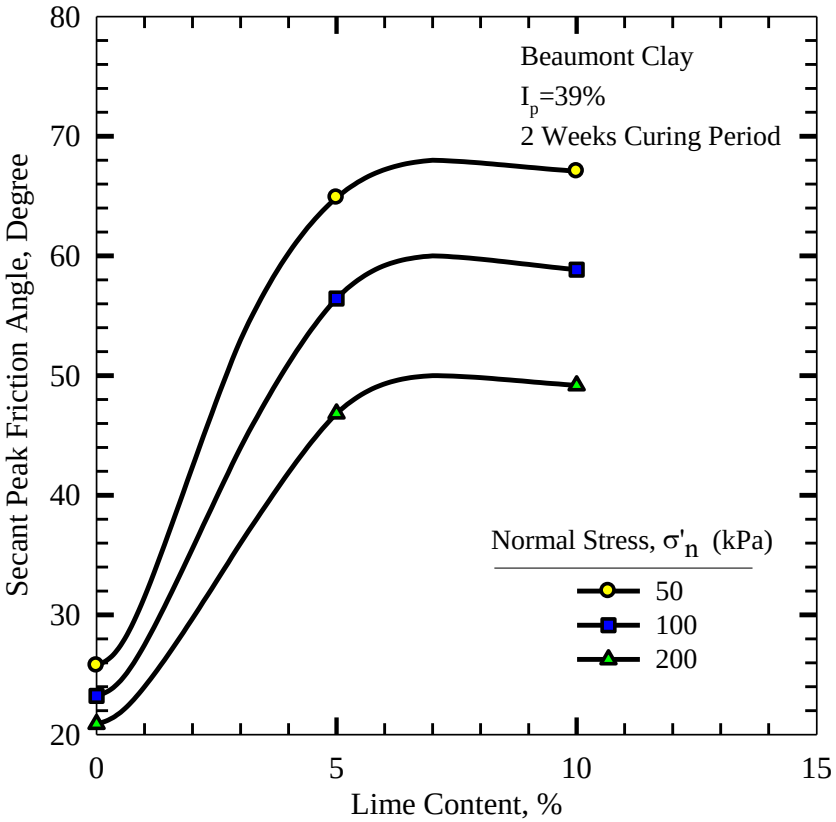

Figure 4.69: Secant peak friction angle plotted against lime content for Beaumont clay cured for 14 days

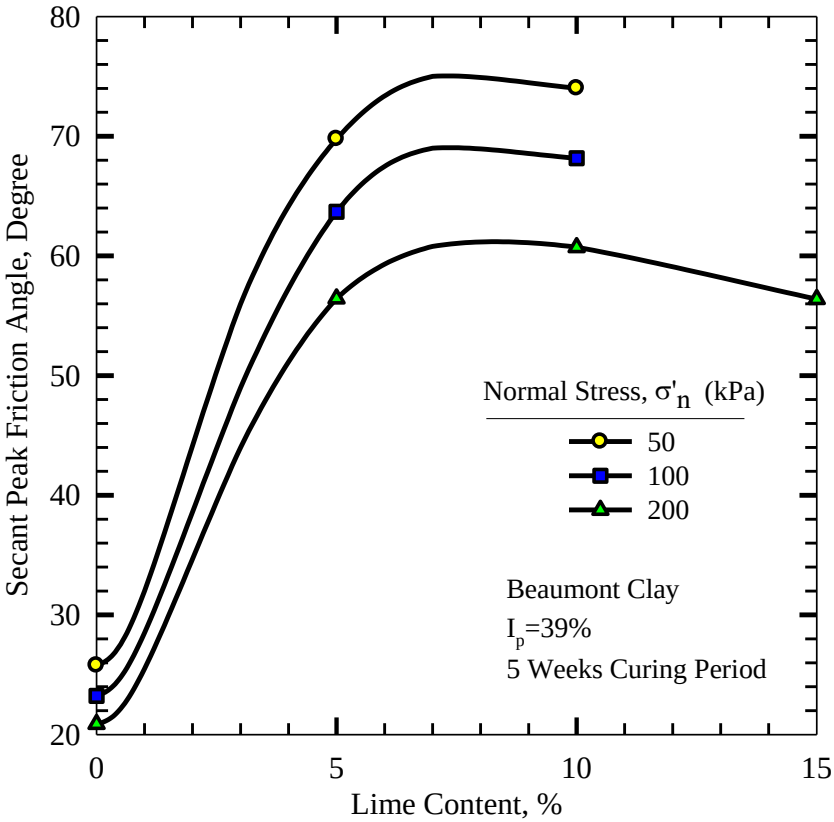

Figure 4.70: Secant peak friction angle plotted against lime content for Beaumont clay cured for 35 days

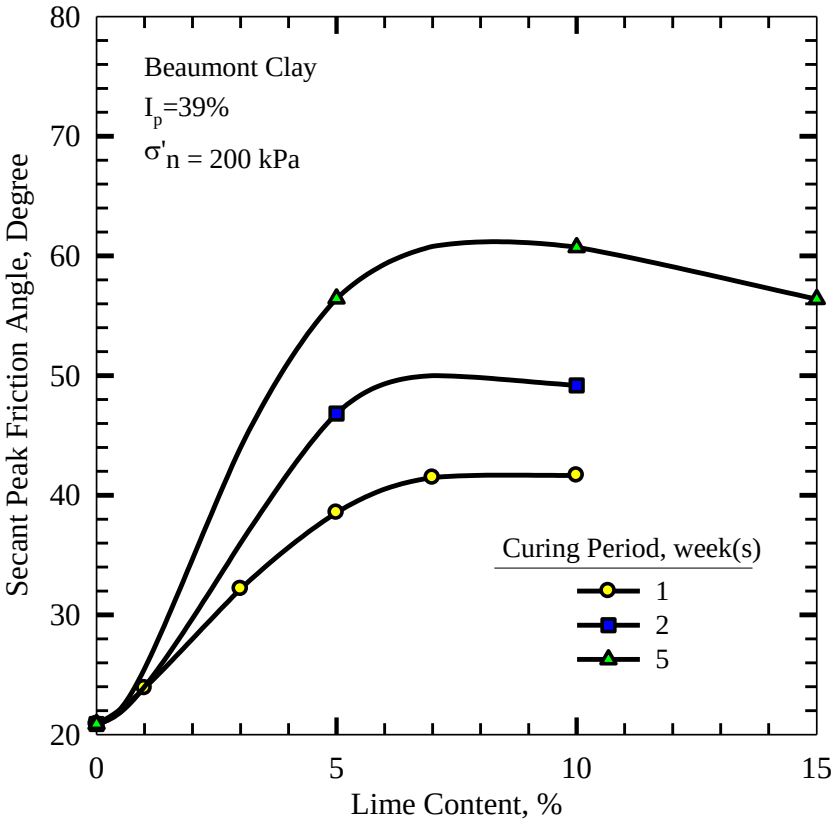

Figure 4.71: Secant peak friction angle plotted against lime content for Beaumont clay with various curing periods

4.5 POST-PEAK SHEAR STRENGTH

Clay minerals in some overconsolidated clays are in aggregated condition. Aggregation decreases the plateyness of the clay particles, hence decreasing the ability of particles to hold water and increasing the potential for inter-particle contact. For naturally aggregated clays, the shearing process toward fully softened and residual condition disaggregates the clay particles.

In treated clays, if shearing displacement continues beyond the peak strength, inter-cluster bonds begin to break, causing partial disaggregation. As shear shearing continues, more bonds break and secant friction angle drops to post-peak value. The partial disaggregation is caused by the breakage of bonds between clusters and floccules. However, intra-cluster bonds and aggregation within the floccules survive the shearing, except at very high normal stresses.

The post-peak secant friction angle of treated Chicago clay, Lower Brenna clay and Beaumont clay as a function of shear strain is shown in Figures 4.72-4.74, respectively. The secant friction angle at lowest shear strains correspond to the peak strength. Figure 4.72 shows the test results for Chicago clay treated with 3% lime, cured for 4 weeks and sheared at effective normal tresses . As shear strain increases, the secant friction angle drops sharply and levels off at a shear strain of 15%. The minimum post-peak secant friction angle of treated Chicago clay remains higher than that of untreated clay due to aggregation. However, the difference between the minimum post peak secant friction amgle of treated clay and that of untreated clay decreases as effective normal stress increased as a result of disaggregation of clay particle.

Figure 4.73 shows the secant friction angle as a function of the shear strain for Lower Brenna clay treated width 7% lime and cured for 35 day at effective normal stresses in the range of 50-400 kPa. As shearing continues to larger strains, the secant friction angle decreases and approaches that of untreated clay. At high effective vertical stresses, the friction angle of treated clay drops to that of the untreated clay at large strains, suggesting that the slip plane passes through clay particles or the aggregated particles entirely disaggregate within the shear zone. At low effective normal stresses, the friction angle drops to a value at large strains which is higher than that of the untreated clay, implying that some of the inter-cluster bonds survive and a full breakage does not occur.

Figure 4.74 shows the secant friction angle as a function of the shear strain for Beaumont clay treated width 10% lime and cured for 35 day at effective normal stresses in the range of 50-200 kPa. The post-peak secant friction angle is more or less constant for shear strains greater than 20%. The minimum post-peak secant friction angle of treated Beaumont clay for effective normal stresses of 50-200 kPa is higher than that of untreated clay due to aggregation of clay particles.

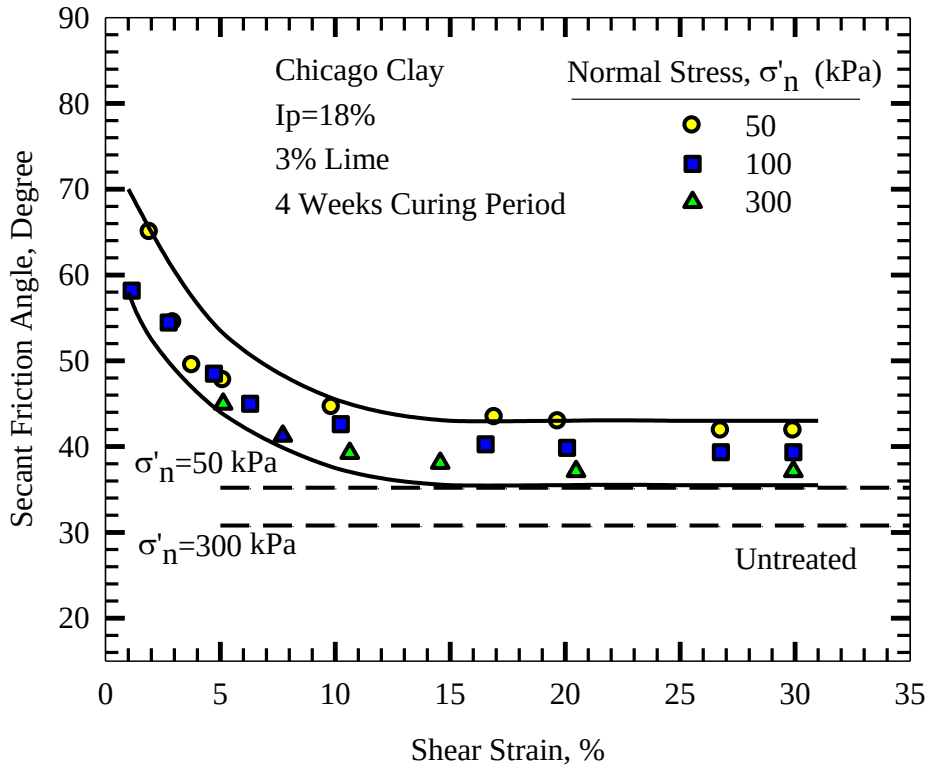

Figure 4.72: Secant fiction angle-shear strain relationship for Chicago clay tretaed with 3% lime, cured for 28 days

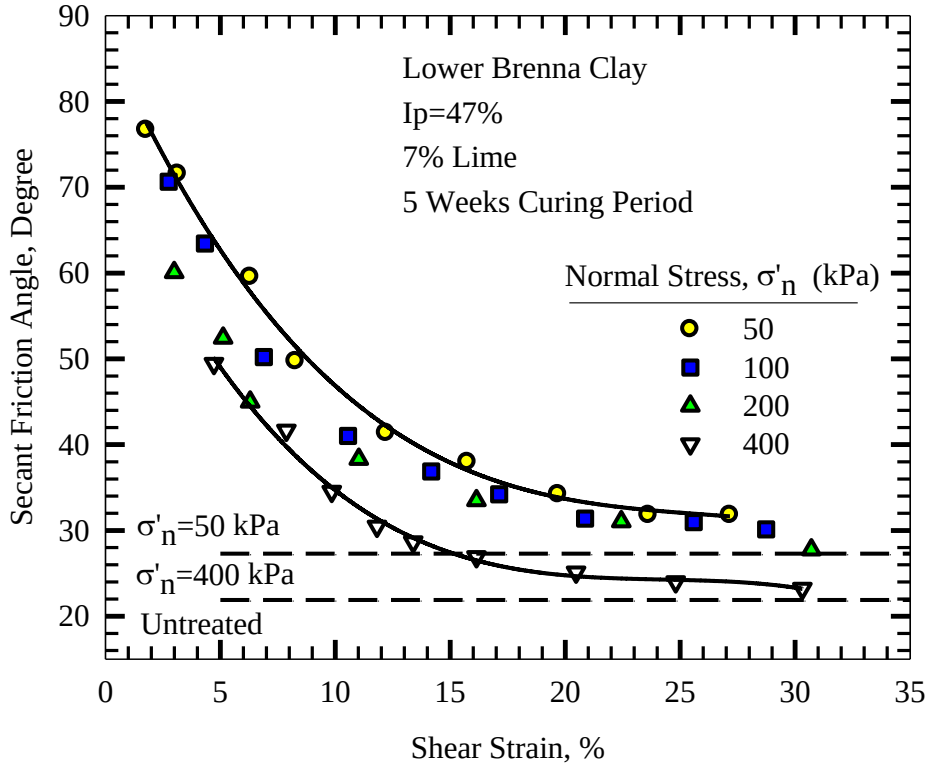

Figure 4.73: Secant fiction angle-shear strain relationship for Lower Brenna clay tretaed with 7% lime, cured for 35 days

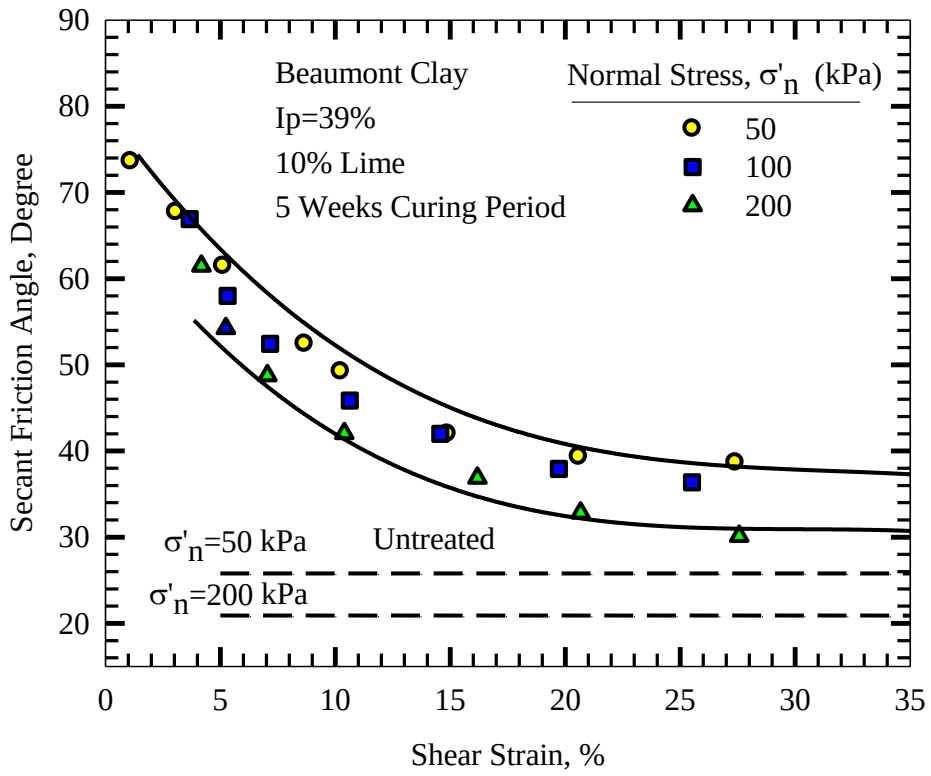

Figure 4.74: Secant fiction angle-shear strain relationship for Beaumont clay tretaed with 10% lime, cured for 35 days

4.6 SHEAR STRENGTH AND EFFECTIVE NORMAL STRESS RELATIONSHIP

For untreated overconsolidated clays, the relationship between shear strength and effective normal stress, for intact, fully softened, and residual conditions, is curved, and there is no shear strength at zero effective normal stress (Mesri and Shahien, 2003). A convenient method to describe the nonlinear shear strength envelopes is to employ secant friction angles that are functions of the effective normal stress:

$$s(i)=\sigma'_n \tan\left[\phi'_i\right]_s \quad (4.1)$$

$$s(fs)=\sigma'_n \tan\left[\phi'_{fs}\right]_s \quad (4.2)$$

$$s(i)=\sigma'_n \tan\left[\phi'_r\right]_s \quad (4.3)$$

where the secant friction angles $[\phi'_i]_s$, $[\phi'_{fs}]_s$, and $[\phi'_r]_s$ are functions of the effective normal stress, σ'_n.

The empirical equations proposed by Mesri and Abdel-Ghaffar (1993) and rewritten by Mesri and Shahien (2003) are used to define the curvature of the shear strength envelopes.

The intact strength envelope is expressed as:

$$s(i)=\sigma'_n \tan\left[\phi'_{fs}\right]_s^p \left[\frac{\sigma'_p}{\sigma'_n}\right]^{1-m_i} \quad (4.4)$$

Where $[\phi'_{fs}]_s^p$=secant fully softened friction angle at $\sigma'_n=\sigma'_p$, and σ'_p=preconsolidation pressure. This equation together with ($[\phi'_{fs}]_s^p$,m_i) defines the intact shear strength versus effective normal stress curves.

Similar empirical equations define nonlinear fully softened and residual shear strength envelopes:

$$s(fs)=\sigma'_n \tan\left[\phi'_{fs}\right]_s^{100} \left[\frac{100}{\sigma'_n}\right]^{1-m_{fs}} \quad (4.5)$$

$$s(r)=\sigma'_n \tan\left[\phi'_{r}\right]_s^{100} \left[\frac{100}{\sigma'_n}\right]^{1-m_r} \quad (4.6)$$

where $[\phi'_{fs}]_s^{100}$ and $[\phi'_r]_s^{100}$ = secant fully softened and secant residual friction angles at σ'_n=100 kPa. The curvature of the fully softened and residual shear strength envelopes is defined by m_{fs} and m_r, which depend on the plasticity index. The curvature of fully softened and residual shear strength envelopes is due to increased reorientation of plate-shaped particles to face to face interaction with an increase in effective normal stress.

For lime-treated clays, as shearing displacement continues beyond the peak strength, the inter-cluster bonds begin to break. As shearing continues, more bonds break, resulting in a decrease in nonlinearity of the shear strength envelope at large shear strains. Figures 4.75-4.77 show the decrease in the nonlinearity (m) of the shear strength envelope with shear strain for treated Chicago

clay, Lower Brenna clay and Beaumont clay, respectively. For Chicago clay treated with 3% lime and cured for 28 days, the nonlinearity of shear strength envelope increased from, m_i=0.57, for peak shear strength to 0.94 at a shear strain of 5% and remained near 0.90 for shear strains in the range of 10-30%, as shown in Figure 4.75. For Lower Brenna clay treated with 7% lime and cured for 35 days, the peak strength exhibits a highly curved envelope, m_i=0.37. The m value, however, increases to 0.8 at a shear strain of 10% and remains more or less constant for higher strains in the range up to 30%, as shown in Figure 4.76. The nonlinearity of shear strength envelope of Beaumont clay treated with 10% lime and cured for 35 days increased from 0.56 for peak shear strength to 0.8 at a shear strain of 5% and remained more or less in the same range for higher shear strains up to 30%, as shown in Figure 4.77.

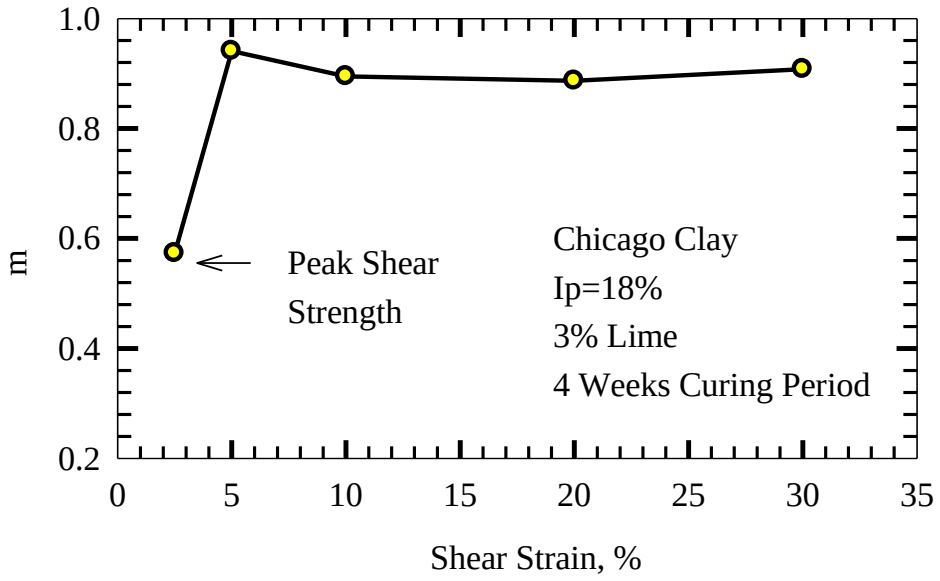

Figure 4.75: Nonlinearity, m, of shear stremgth envelope with shear strain for Chicao clay treated with 3% lime, cured for 28 days

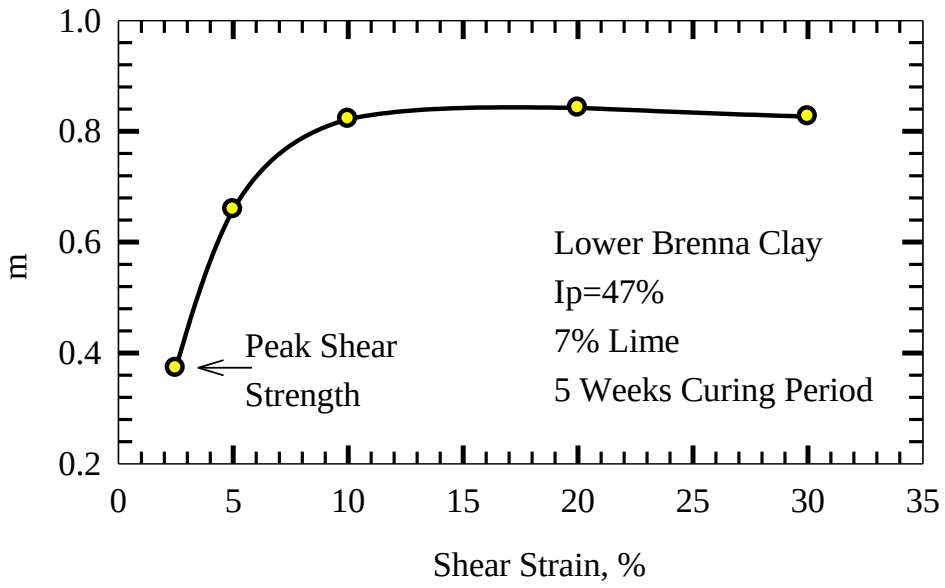

Figure 4.76: Nonlinearity, m, of shear stremgth envelope with shear strain for Lower Brenna clay treated with 7% lime, cured for 35 days

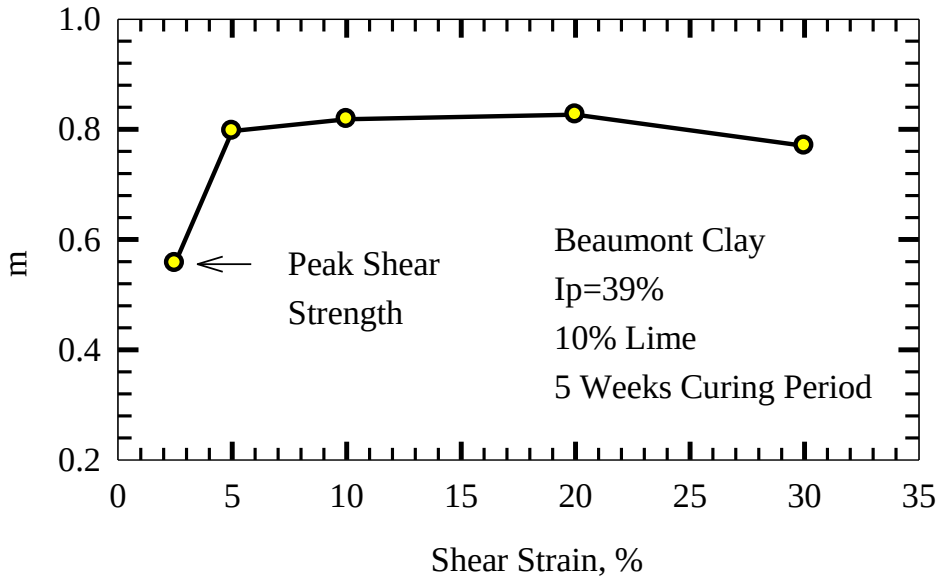

Figure 4.77: Nonlinearity, m, of shear stremgth envelope with shear strain for Beaumont clay treated with 10% lime, cured for 35 days

CHAPTER 5

RESIDUAL SHEAR STRENGTH

When a global instability develops in the field, the peak shear strengths of the treated and untreated zones are not mobilized at the same time. The axial strain at the peak shear strength of the treated zone is small compared to the failure strain of the untreated clay. When the peak strength of the untreated clay is reached, the shear strength of the treated zone has already decreased to the post-peak shear strength. The peak strength of treated clay is typically reached at axial strains of 1% to 2% while some organic soils and highly plastic untreated clays may experience 10% to 20% strain before reaching peak strength (Ahnberg 1996). The strain incompatibility between treated and untreated zones of a first-time landslide can be taken into account by assuming a high failure strain and reducing the strength of the treated clay to post-peak shear strength for portions of the slip surface which are in fully softened condition. The strain incompatibility between treated and untreated zones of a reactivated landslide or portions of the slip surface in a first-time landslide which are in residual condition can be taken into account by assuming the residual condition for both treated and untreated clays.

If shearing of stiff clays and clay shales continues to very large strains, the shearing resistance drops to a value, known as residual strength. The large relative displacement aligns platy clay particles in the shear zone parallel to the shear direction to the maximum extent possible for the effective normal stress and reduces the resistance to a minimum value. The residual strength of an overconsolidated clay is the least uncertain strength parameter (Morgenstern, 1977) and directly reflects the size and shape of the particles (Mesri and Cepeda-Diaz, 1986). Furthermore, the residual shear strength is independent of stress history (Skempton, 1964; Bishop et al., 1971). The residual friction angle which is a function of effective normal stress (Mesri and Huvaj-Sarihan, 2012) is not influenced by the method of specimen preparation. The residual strength measured in the lab using an undisturbed overconsolidated sample, remolded sample, and precut sample should all be the same and in good agreement with the mobilized friction angle back-calculated from

reactivated landslides (Skempton, 1964, 1985; Chandler, 1984; Mesri and Shahien, 2003; Mesri and Huvaj-Sarihan, 2012).

As the sample is sheared to large displacements to reach the residual condition, a perfectly smooth shear surface may not always be possible for shales containing lithorelicts. Leroueil and Hight (2003) pointed out that the residual strength envelope of a natural (structured) soil may then be above that of the same constituted soil. It is noted that multiple reversal direct shear test on pre-cut specimens prepared by the procedure described in Mesri and Cepeda-Diaz (1986) and Mesri and Huvaj-Sarihan (2012) is the best available method to measure the residual strength. The minimum frictional strength of clay particles oriented parallel to the shearing surface to the maximum extent possible is measured by this approach.

5.1 SHEAR STRESS-SHEAR DISPLACEMENT AND VOLUME-CHANGE CURVES

Shear stress-shear displacement and vertical deformation-shear displacement curves for precut specimens of Chicago clay with lime contents in the range of 0-10% (Specimens 73-88) are shown in Figures 5.1-5.18. Measurement of residual strength involves shearing precut specimens multiple times, hence curing time varies during a test.

Shear stress-shear displacement and vertical deformation-shear displacement curves for precut specimens of Lower Brenna clay with lime contents in the range of 0-15% (Specimens 89-106) are shown in Figures 5.19-5.36.

Shear stress-shear displacement and vertical deformation-shear displacement curves for precut specimens of Beaumont clay with lime contents in the range of 0-15% (Specimens 107-131) are shown in Figures 5.37-5.61.

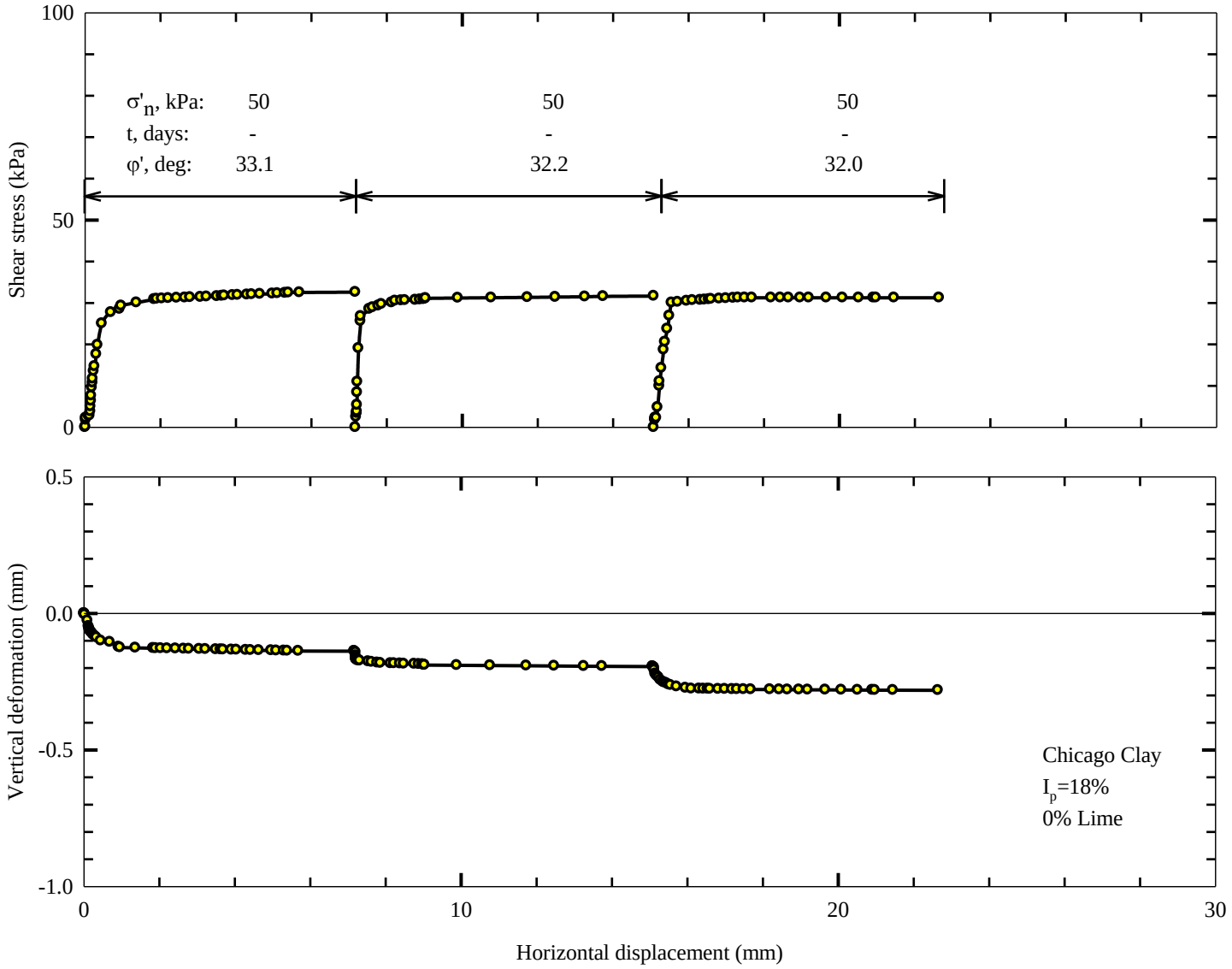

Figure 5.1: Shear stress-shear displacement and vertical displacement-shear displacement curves for pre-cut untreated Specimen 73a (precut)

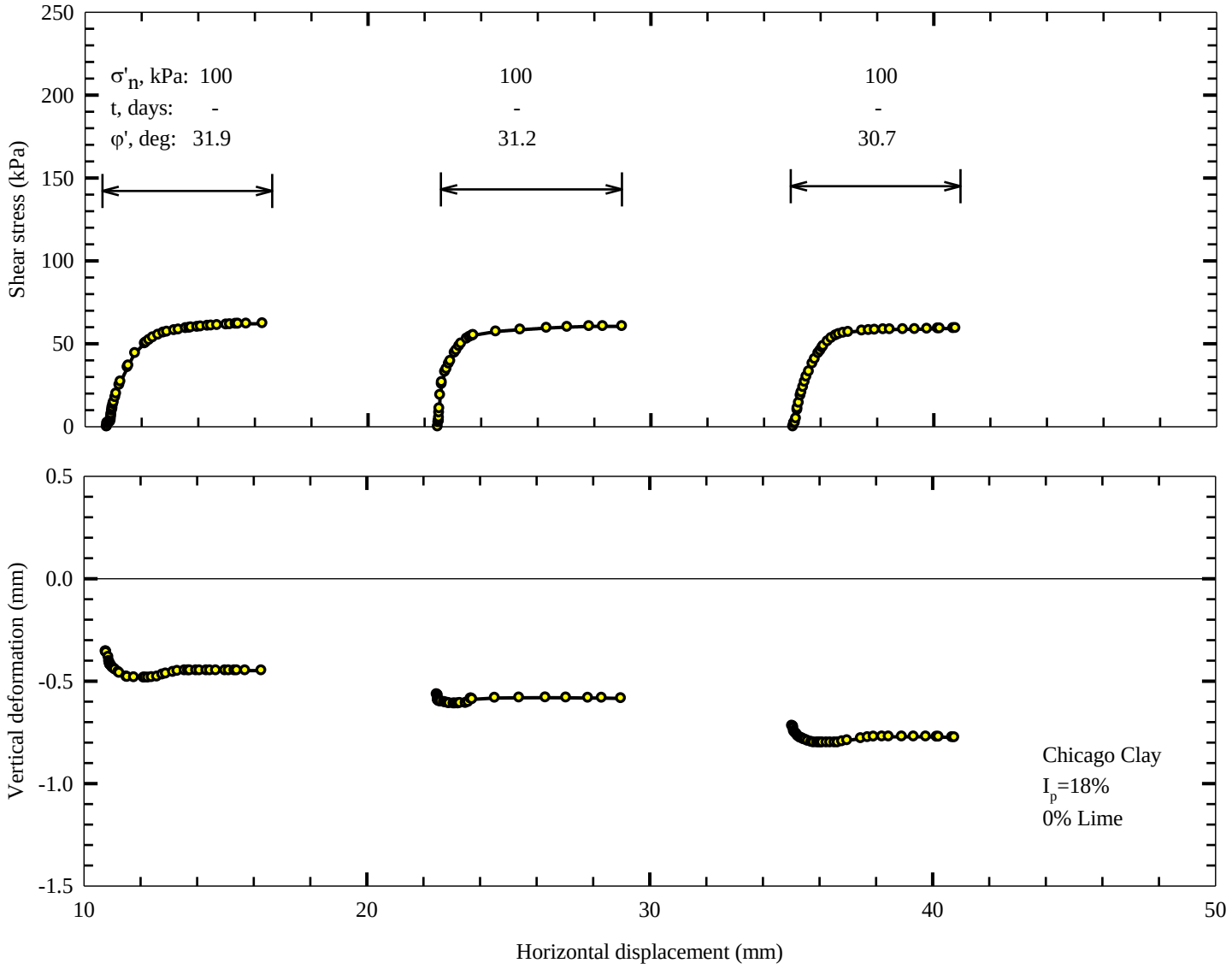

Figure 5.2: Shear stress-shear displacement and vertical displacement-shear displacement curves for Specimen 73b (after an intact specimen was cut); reverse not shown due to proving ring inaccuracy

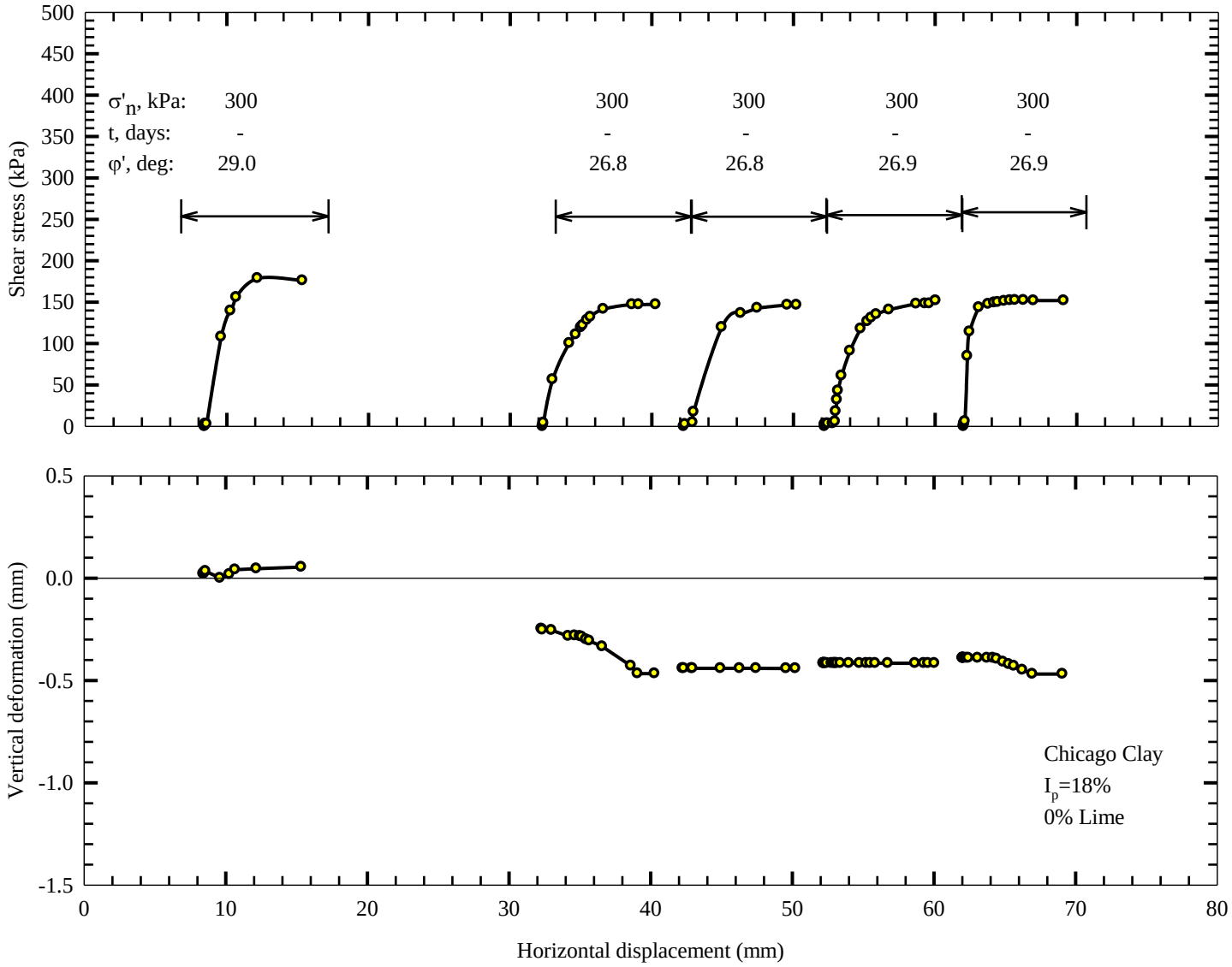

Figure 5.3: Shear stress-shear displacement and vertical displacement-shear displacement curves for Specimen 73c (after an intact specimen was cut); one reverse and one forward not shown due to proving ring malfunction

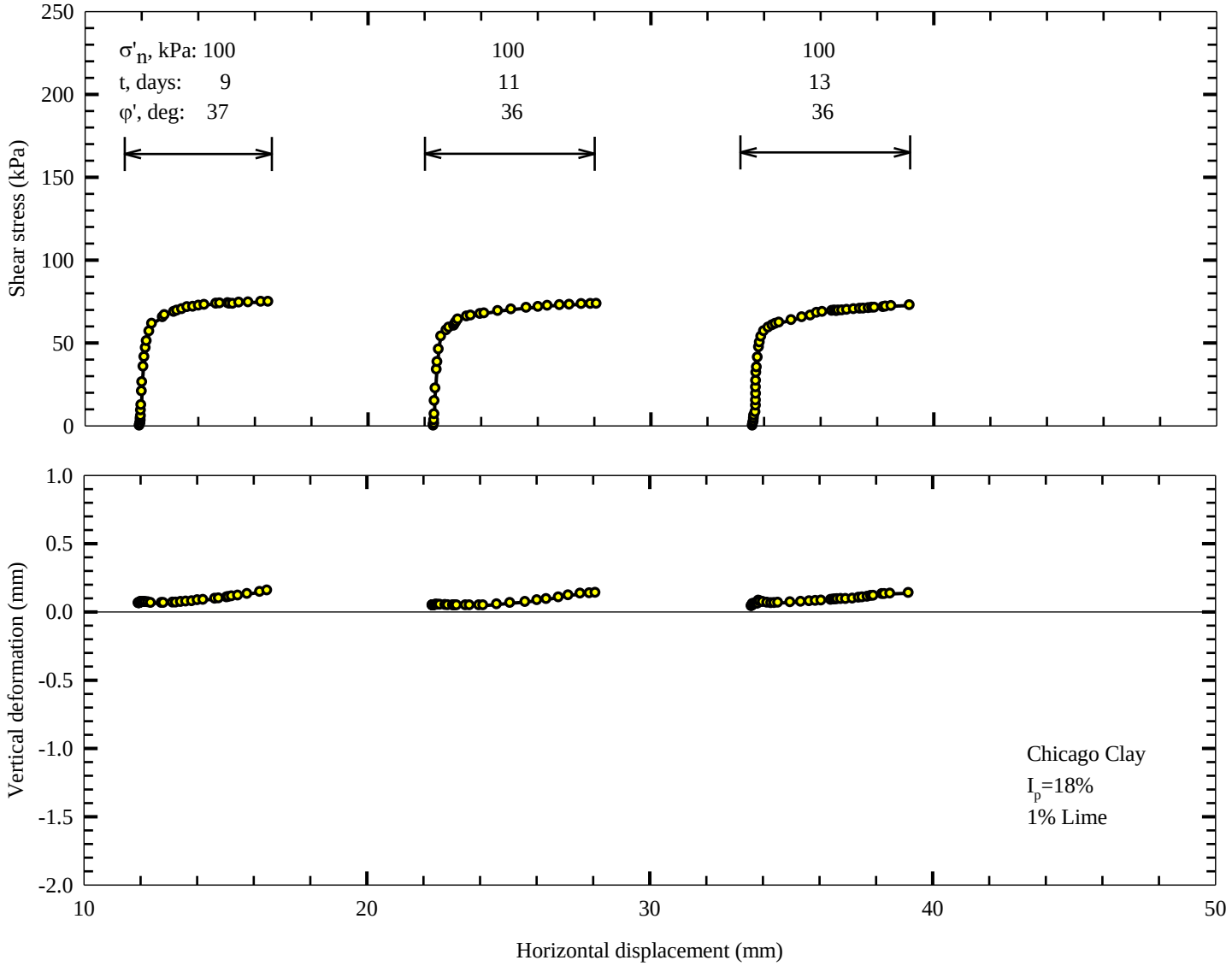

Figure 5.4: Shear stress-shear displacement and vertical displacement-shear displacement curves for Specimen 74 (after an intact specimen was cut); reverse not shown due to proving ring inaccuracy

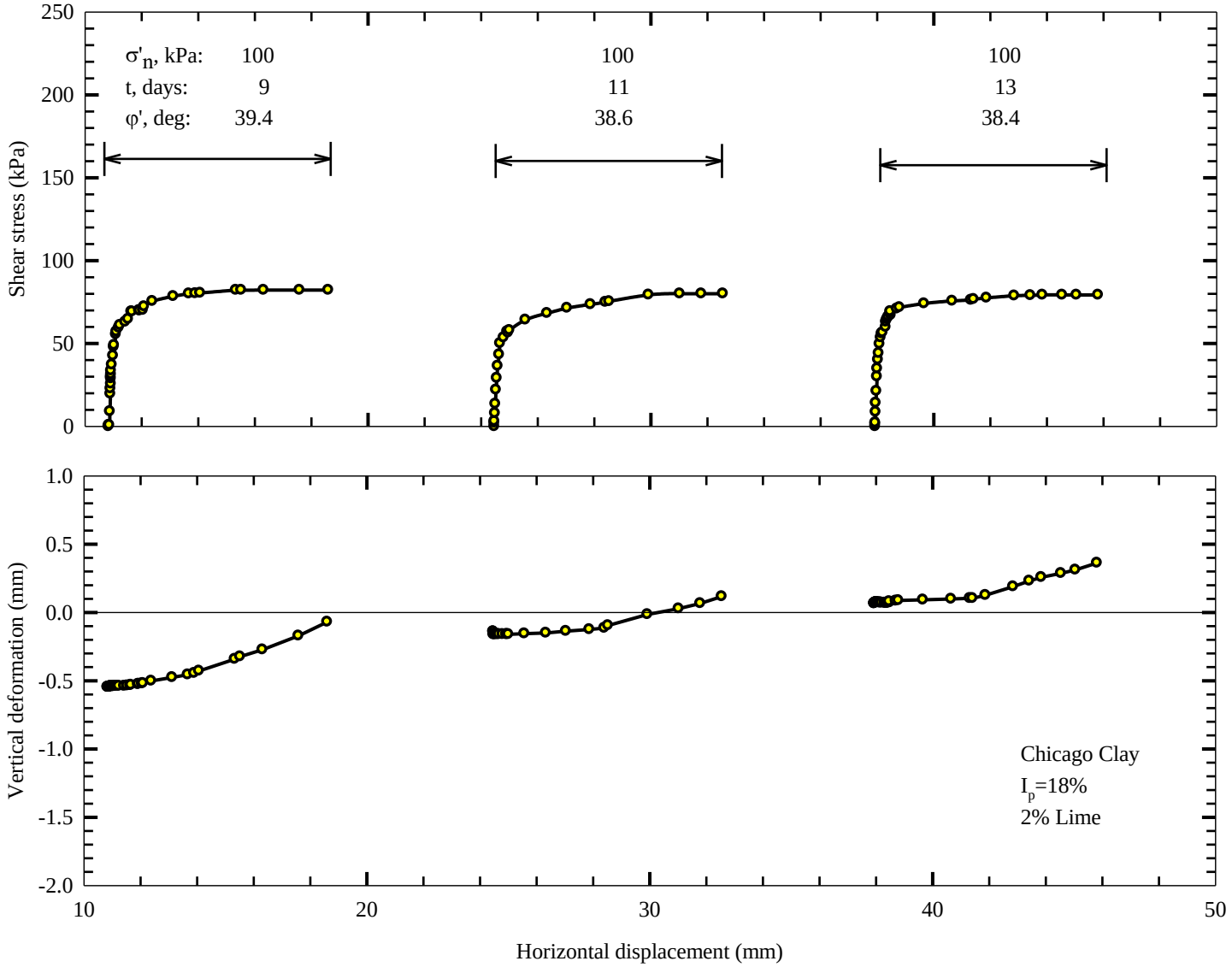

Figure 5.5: Shear stress-shear displacement and vertical displacement-shear displacement curves for Specimen 75 (after an intact specimen was cut); reverse not shown due to proving ring inaccuracy

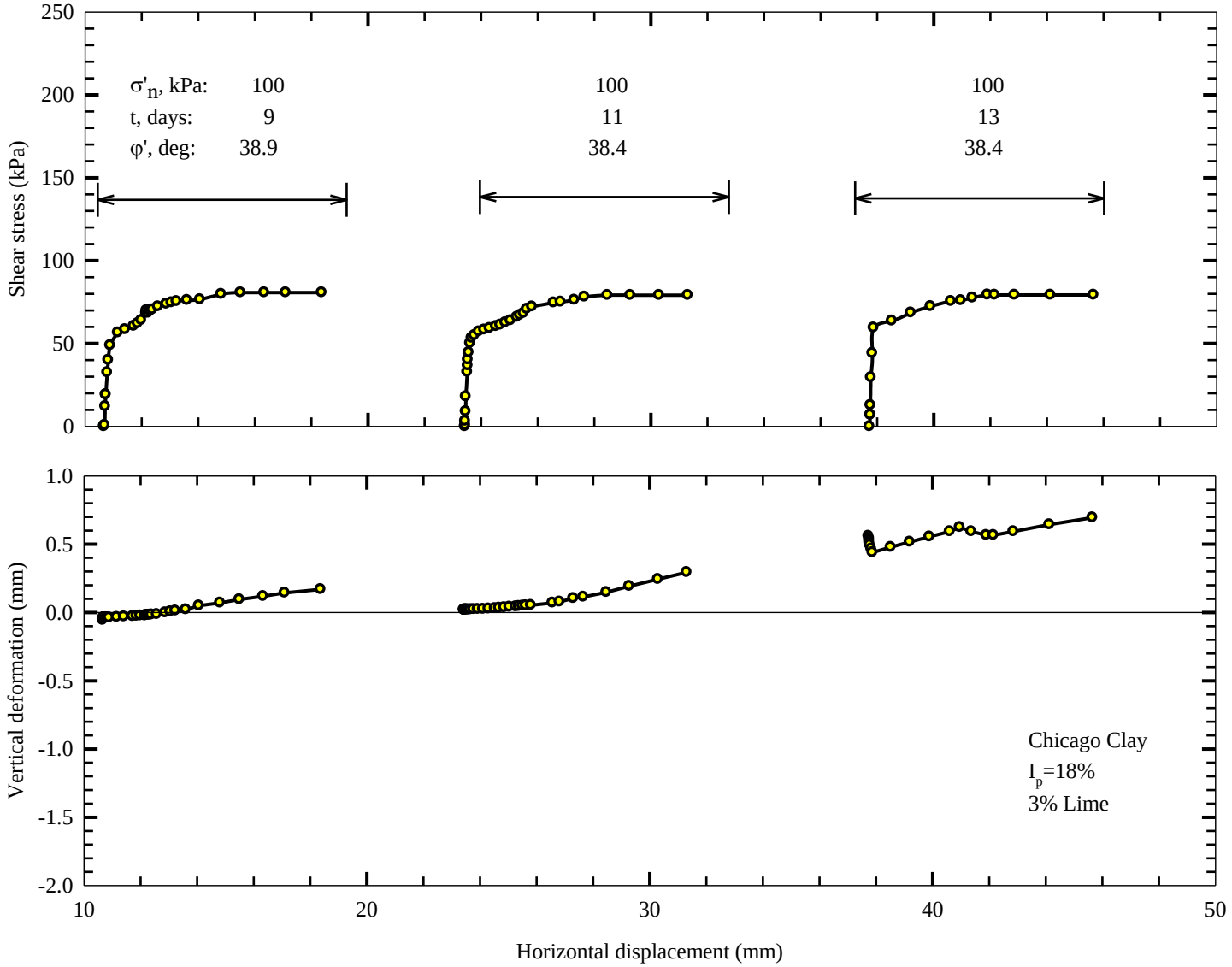

Figure 5.6: Shear stress-shear displacement and vertical displacement-shear displacement curves for Specimen 76 (after an intact specimen was cut); reverse not shown due to proving ring inaccuracy

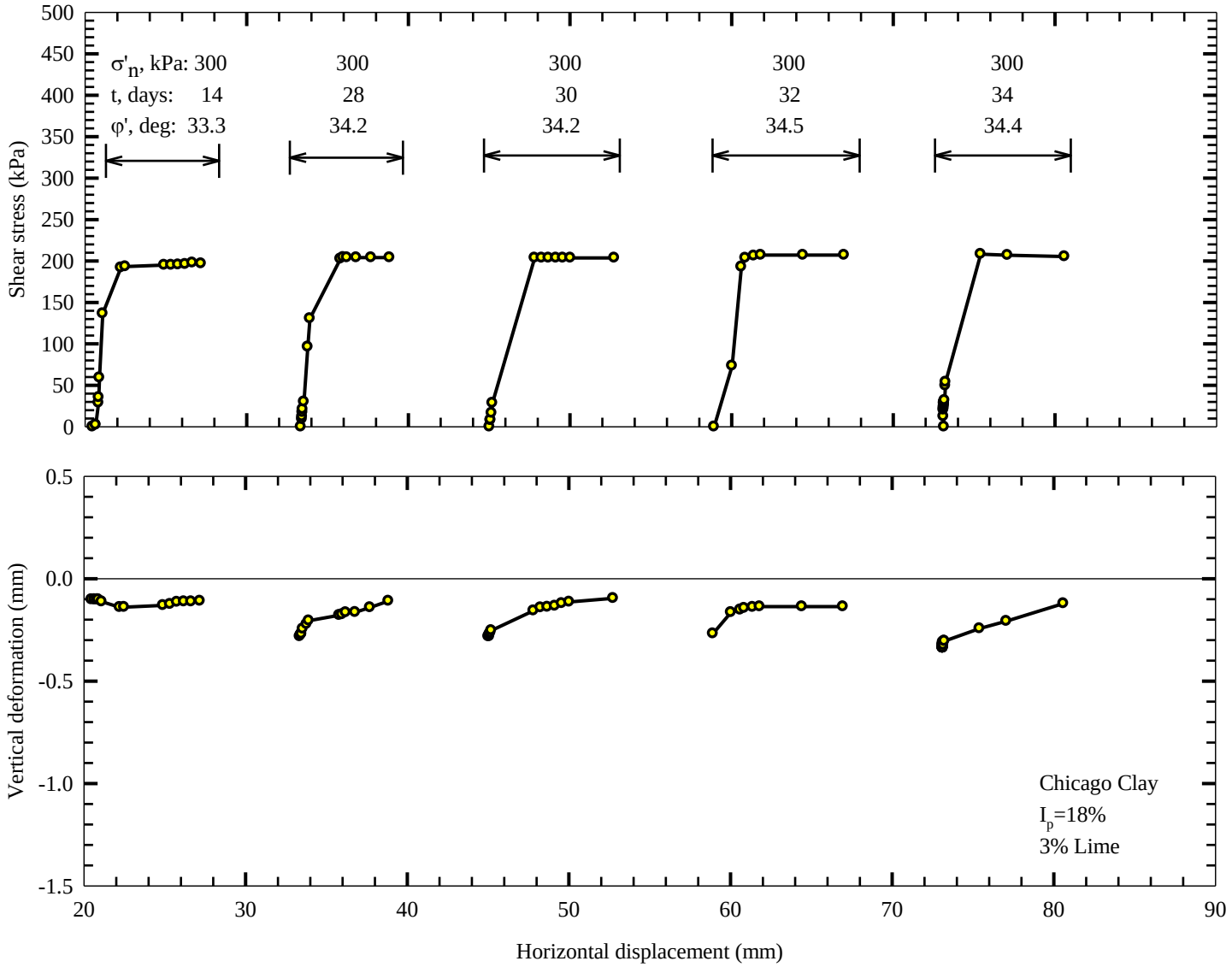

Figure 5.7: Shear stress-shear displacement and vertical displacement-shear displacement curves for Specimen 77 (after an intact specimen was cut); reverse not shown due to proving ring inaccuracy

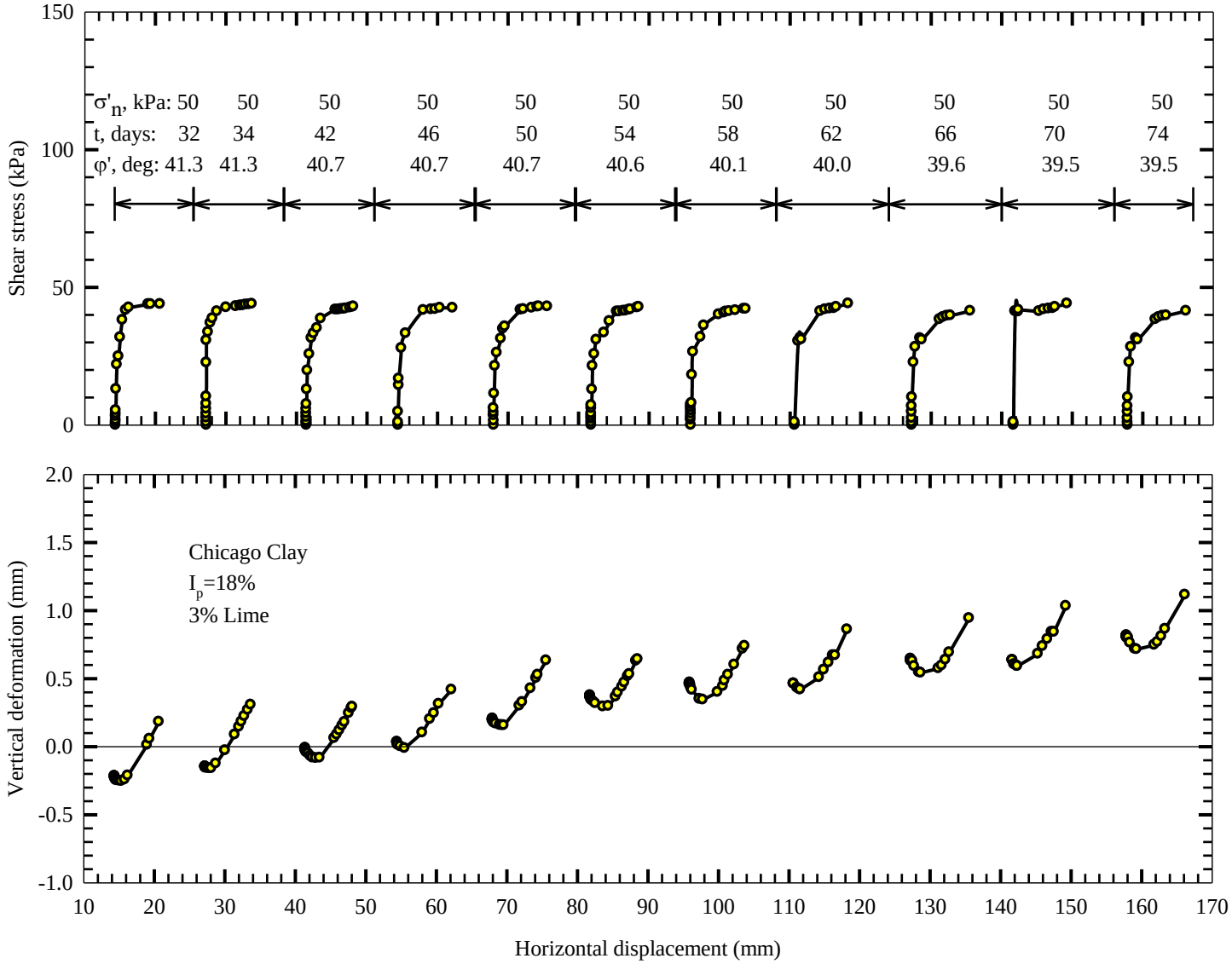

Figure 5.8: Shear stress-shear displacement and vertical displacement-shear displacement curves for Specimen 78 (after an intact specimen was cut); reverse not shown due to proving ring inaccuracy

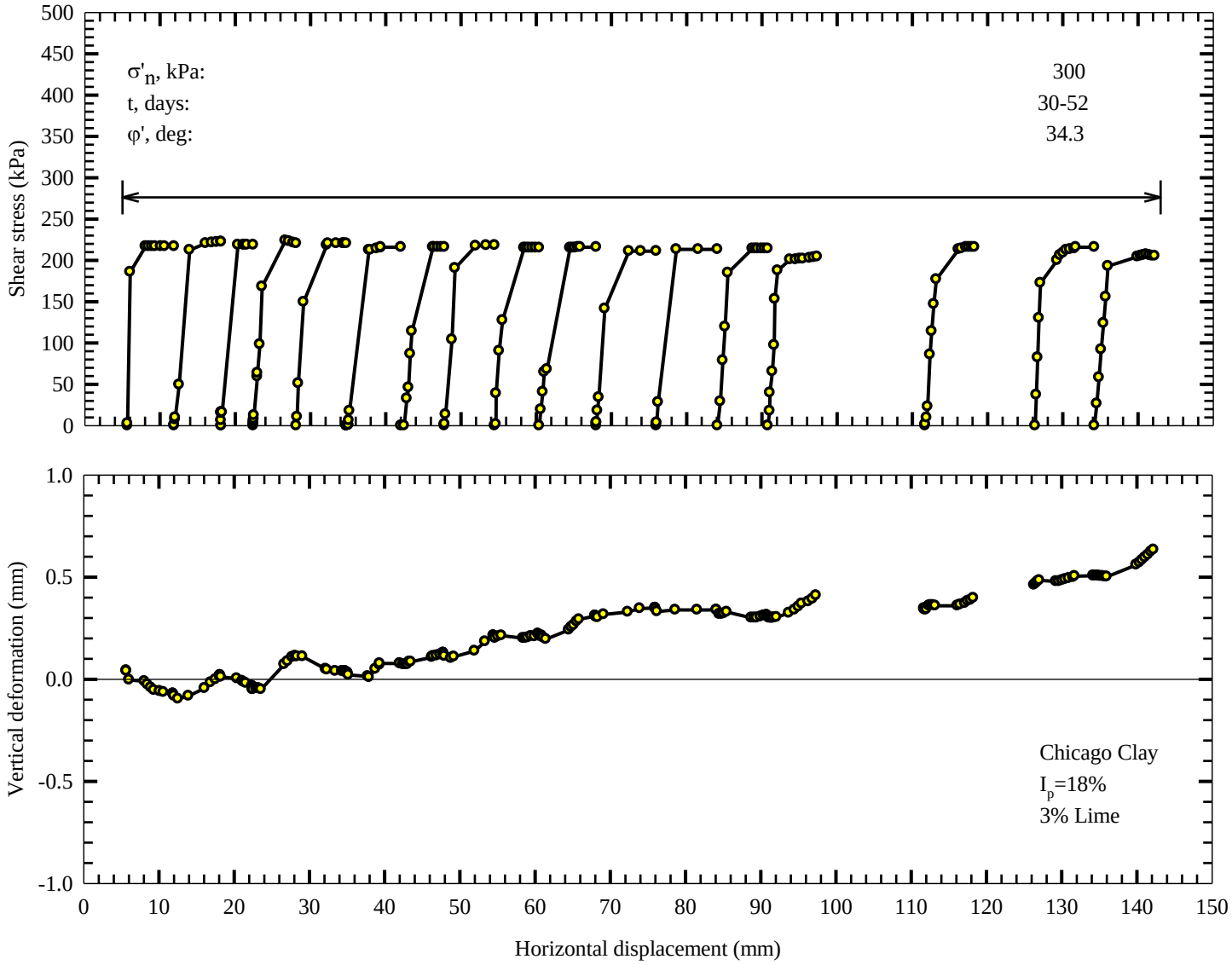

Figure 5.9: Shear stress-shear displacement and vertical displacement-shear displacement curves for Specimen 79 (after an intact specimen was cut); two forwards and one reverse not shown due to proving ring malfunction

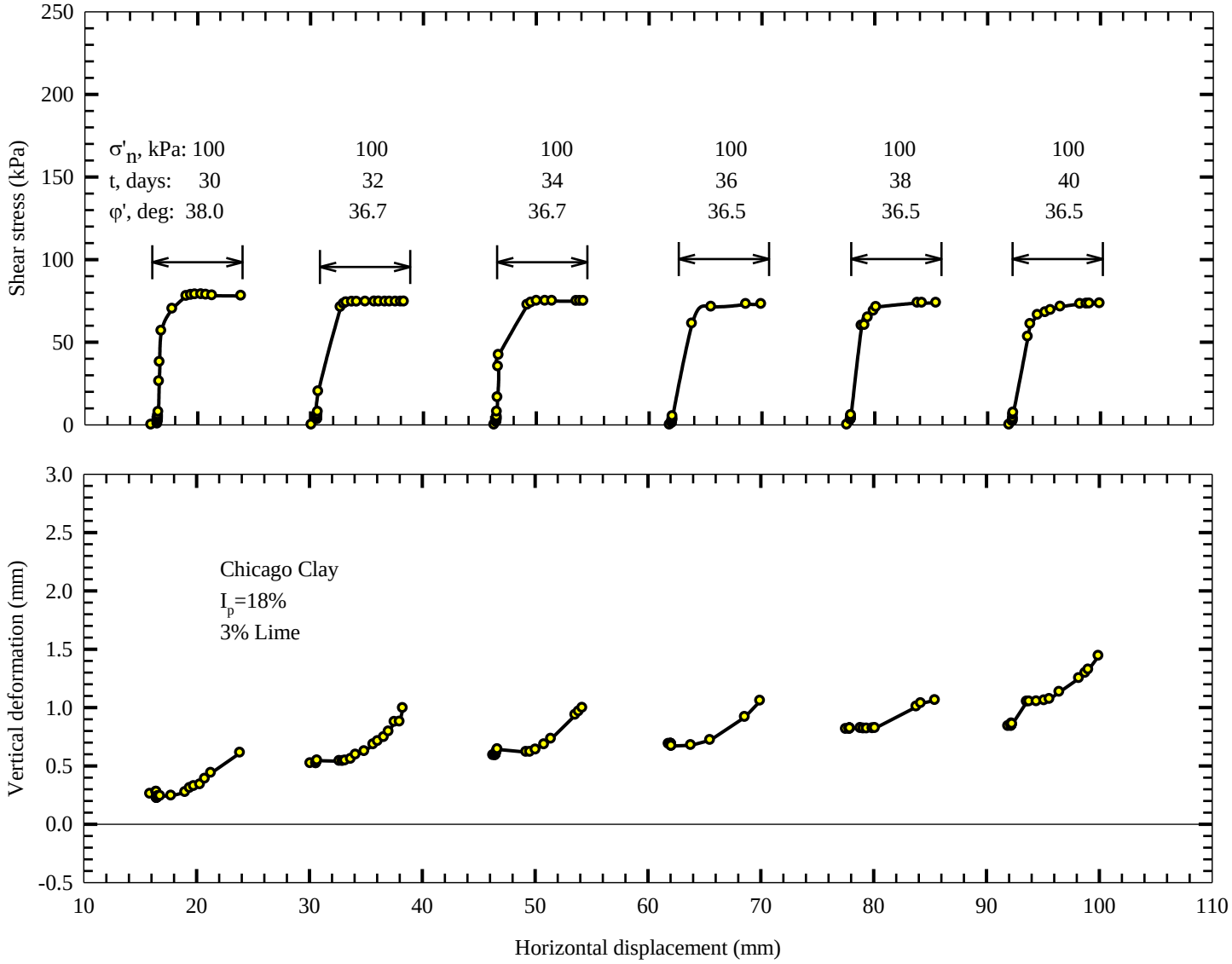

Figure 5.10: Shear stress-shear displacement and vertical displacement-shear displacement curves for Specimen 80 (after an intact specimen was cut); reverse not shown due to proving ring inaccuracy

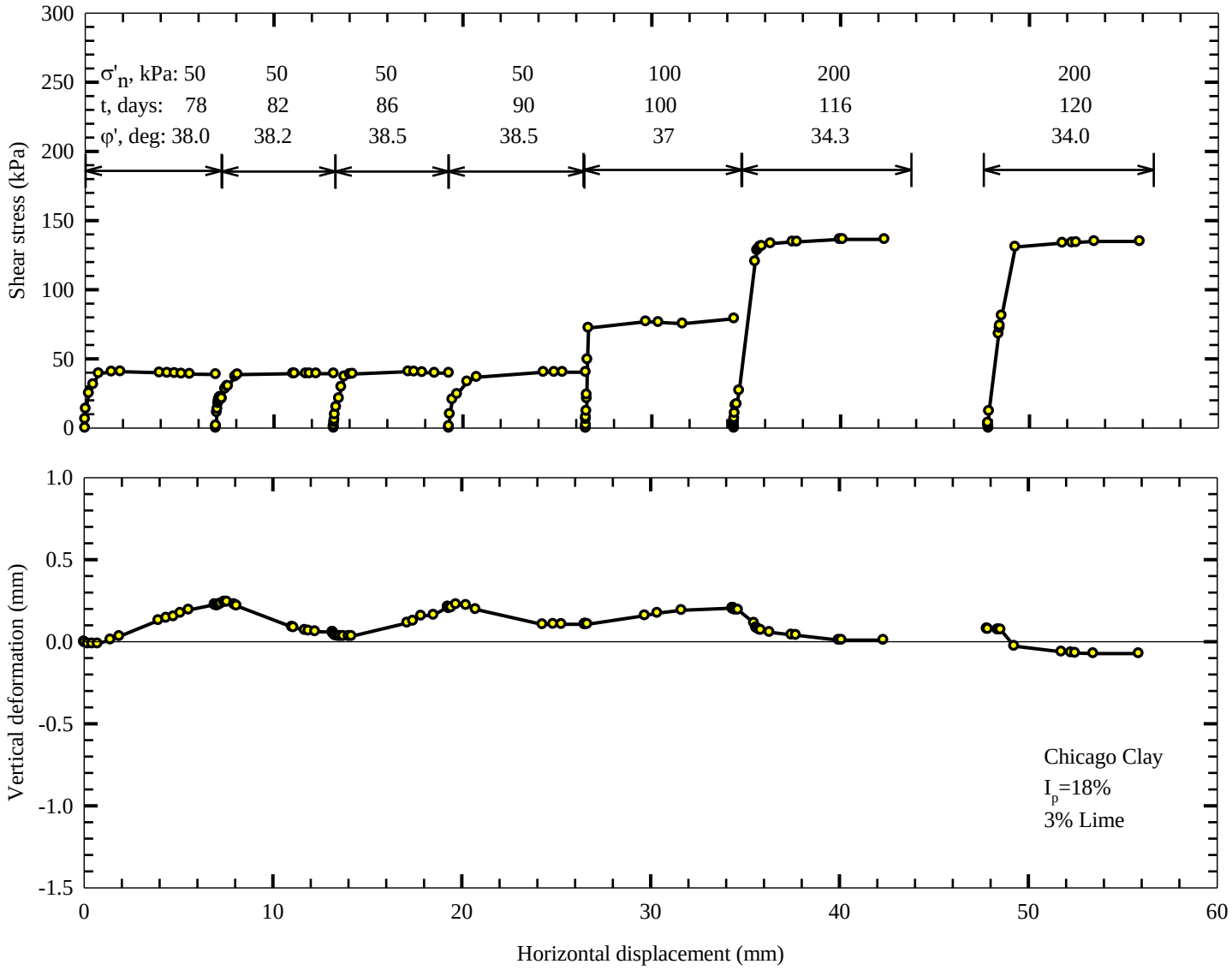

Figure 5.11: Shear stress-shear displacement and vertical displacement-shear displacement curves for Specimen 81 (precut); one forwar not shown due to proving ring malfunction

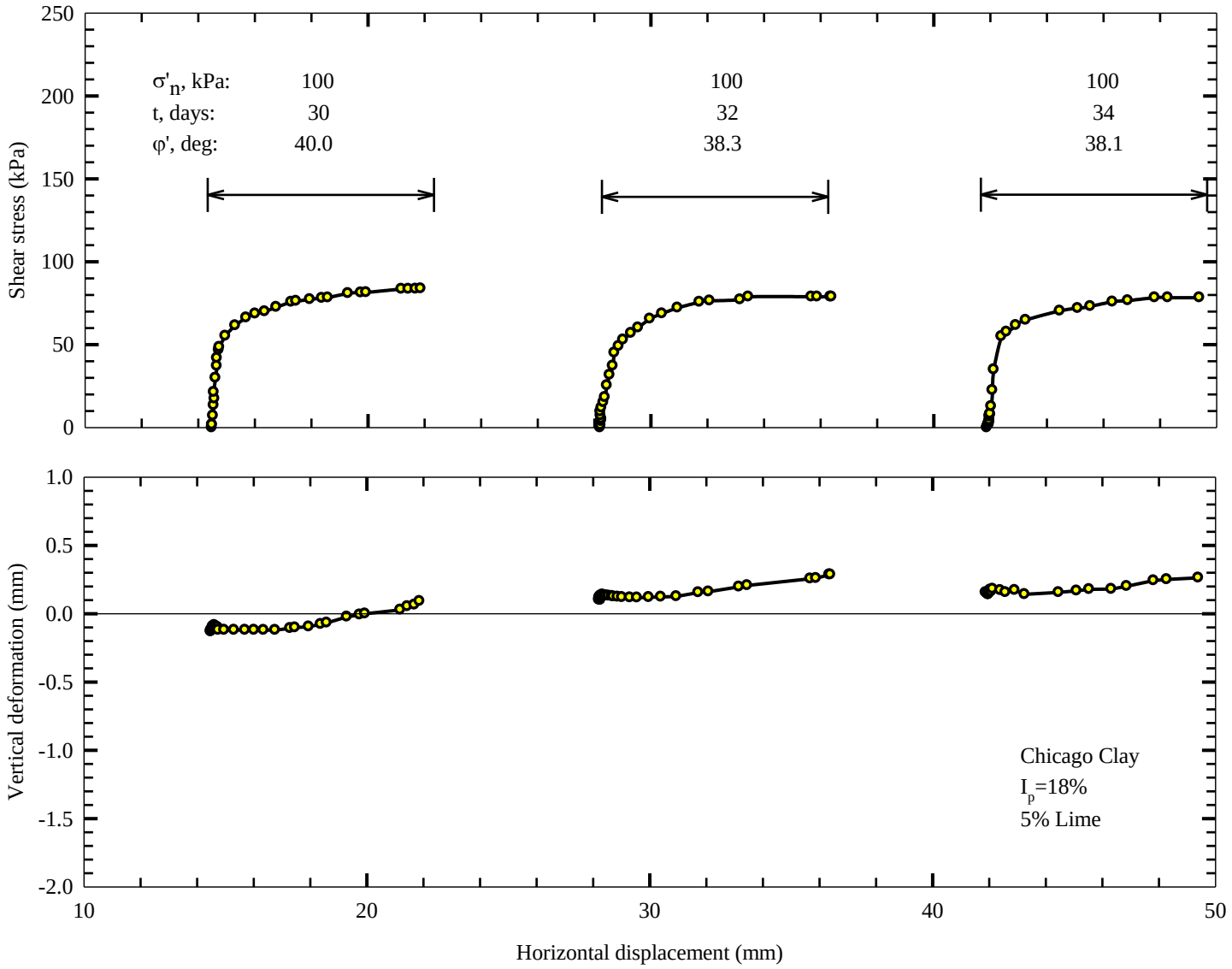

Figure 5.12: Shear stress-shear displacement and vertical displacement-shear displacement curves for Specimen 82 (after an intact specimen was cut); reverse not shown due to proving ring inaccuracy

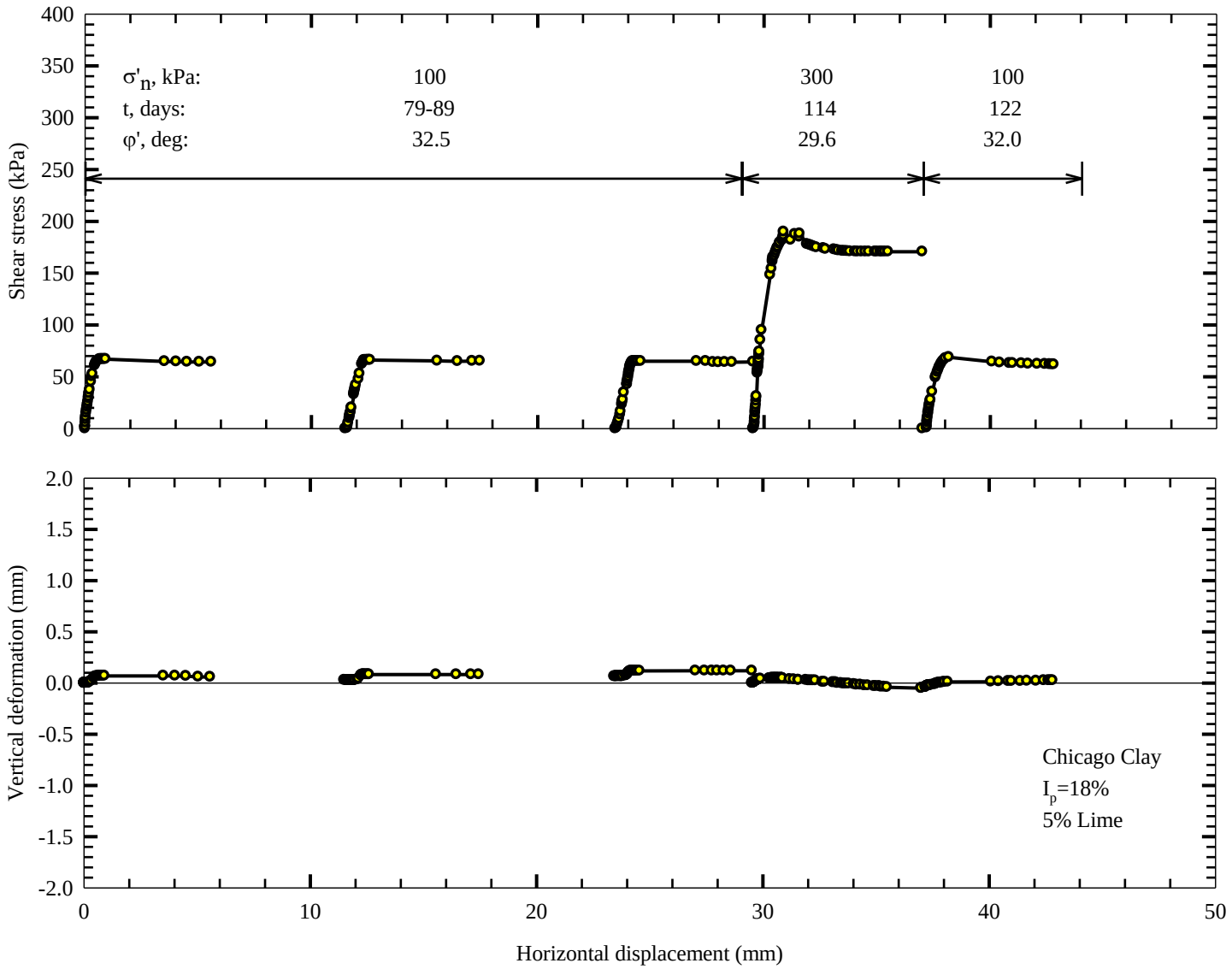

Figure 5.13: Shear stress-shear displacement and vertical displacement-shear displacement curves for Specimen 83 (precut); two reverses not shown due to proving ring inaccuracy

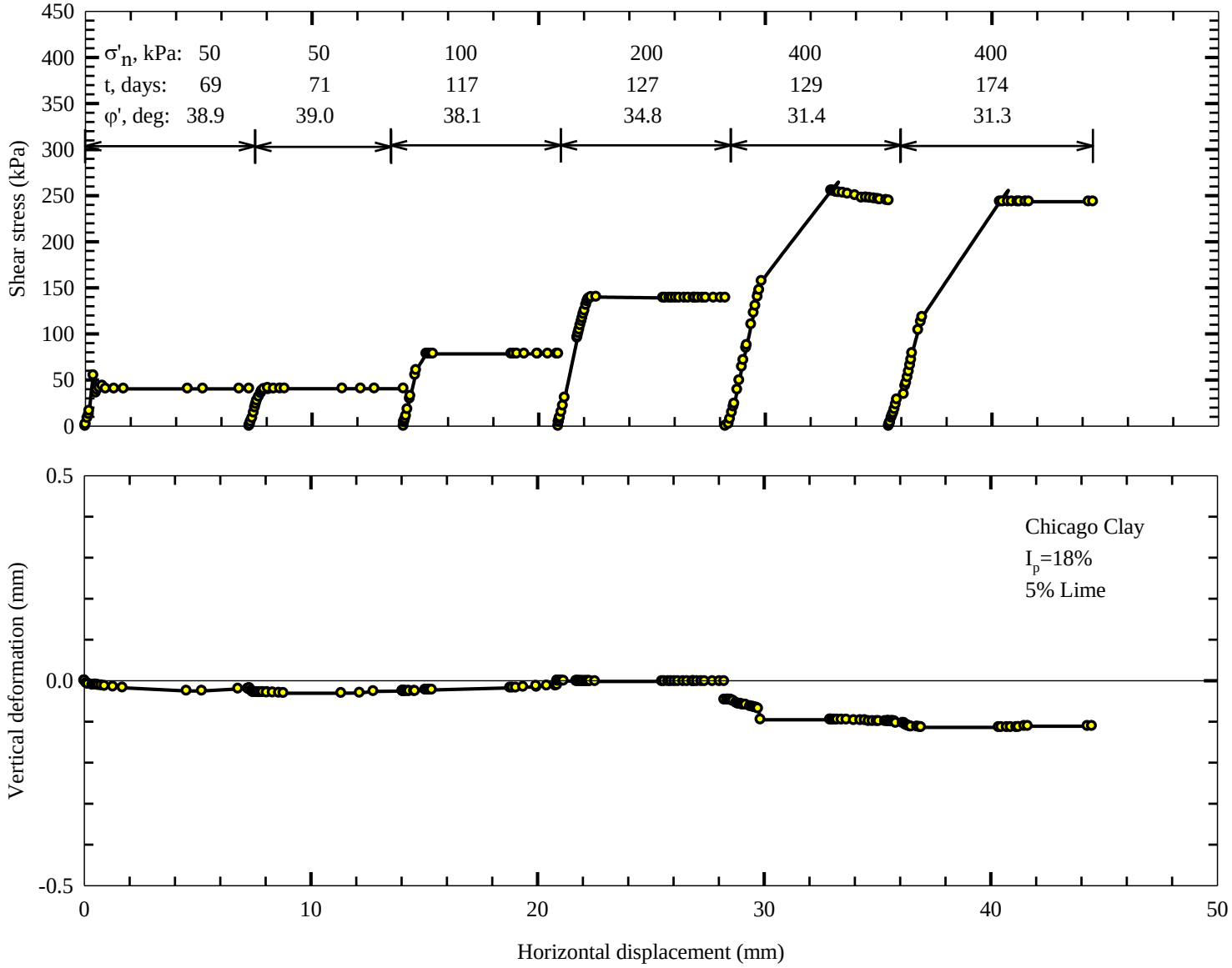

Figure 5.14: Shear stress-shear displacement and vertical displacement-shear displacement curves for Specimen 84 (precut)

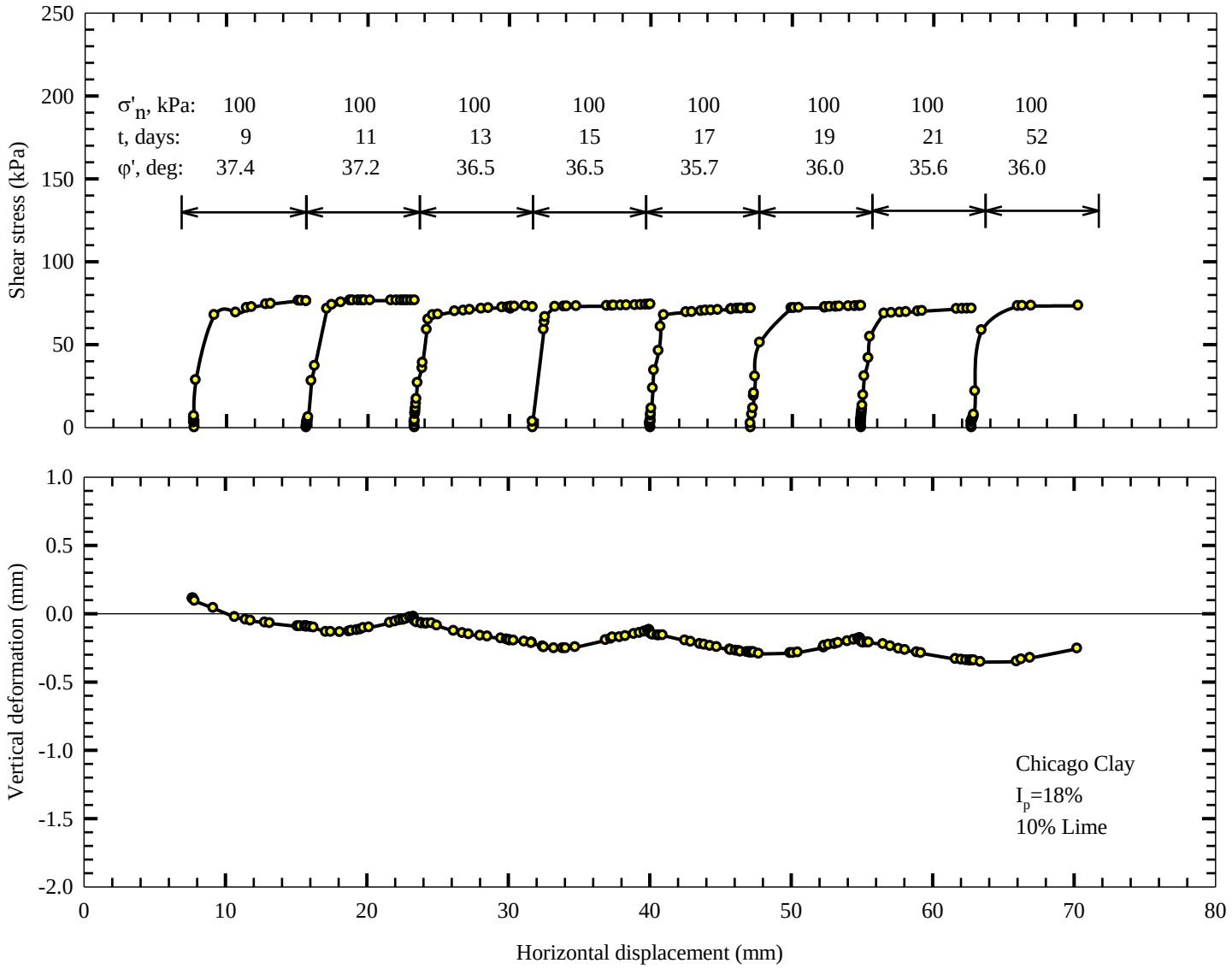

Figure 5.15: Shear stress-shear displacement and vertical displacement-shear displacement curves for Specimen 85 (after an intact specimen was cut)

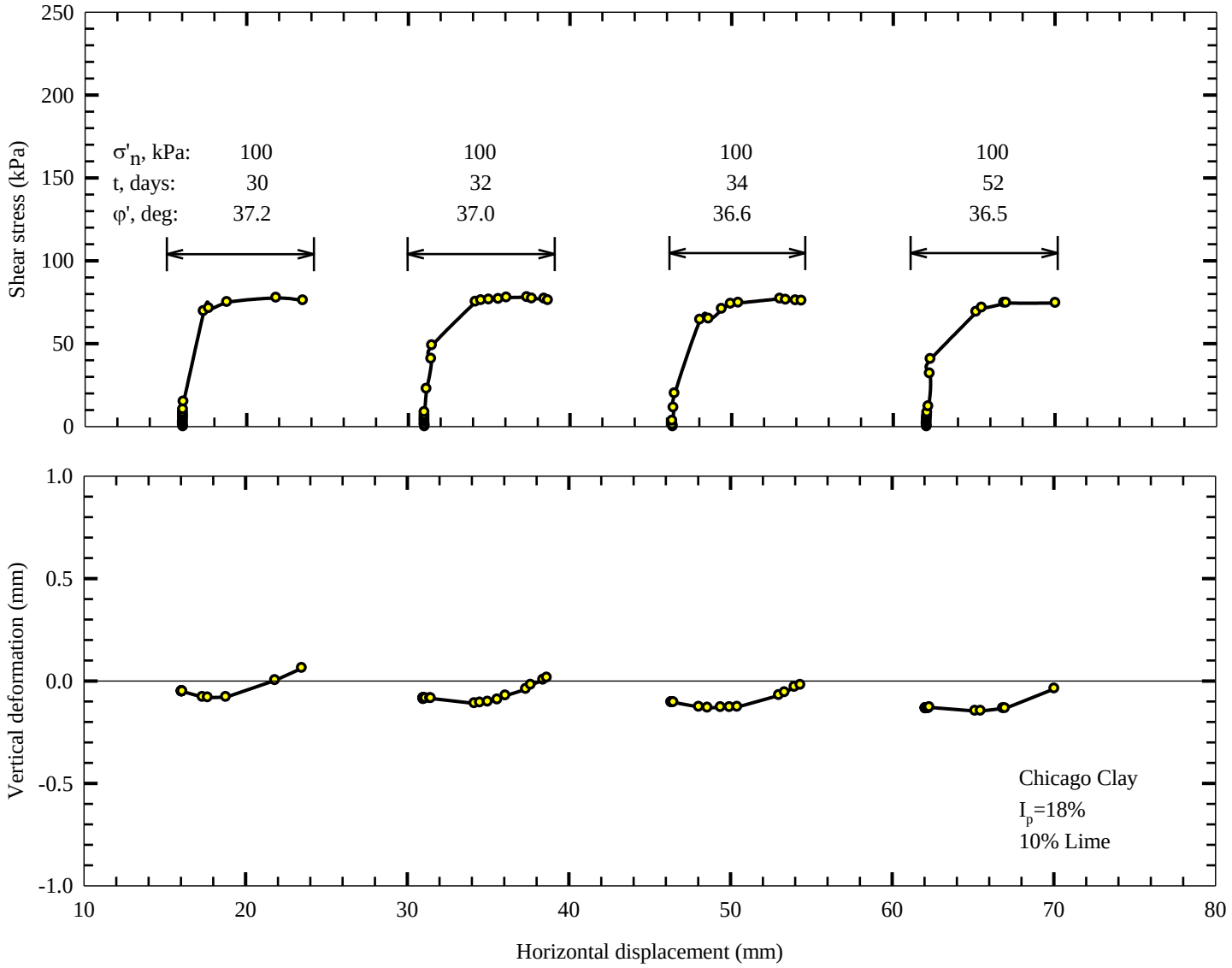

Figure 5.16: Shear stress-shear displacement and vertical displacement-shear displacement curves for Specimen 86 (after an intact specimen was cut); reverse not shown due to proving ring inaccuracy

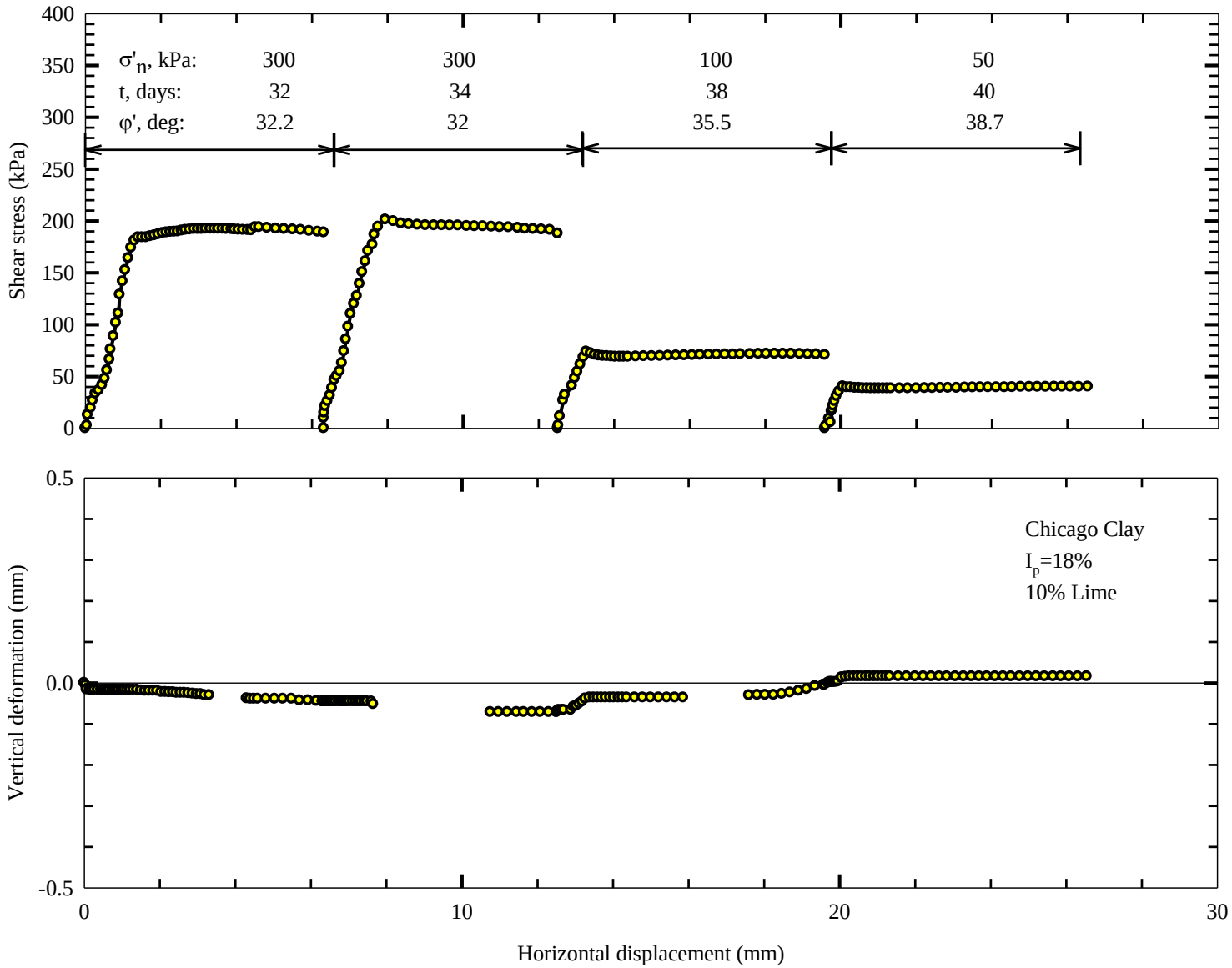

Figure 5.17: Shear stress-shear displacement and vertical displacement-shear displacement curves for Specimen 87 (precut)

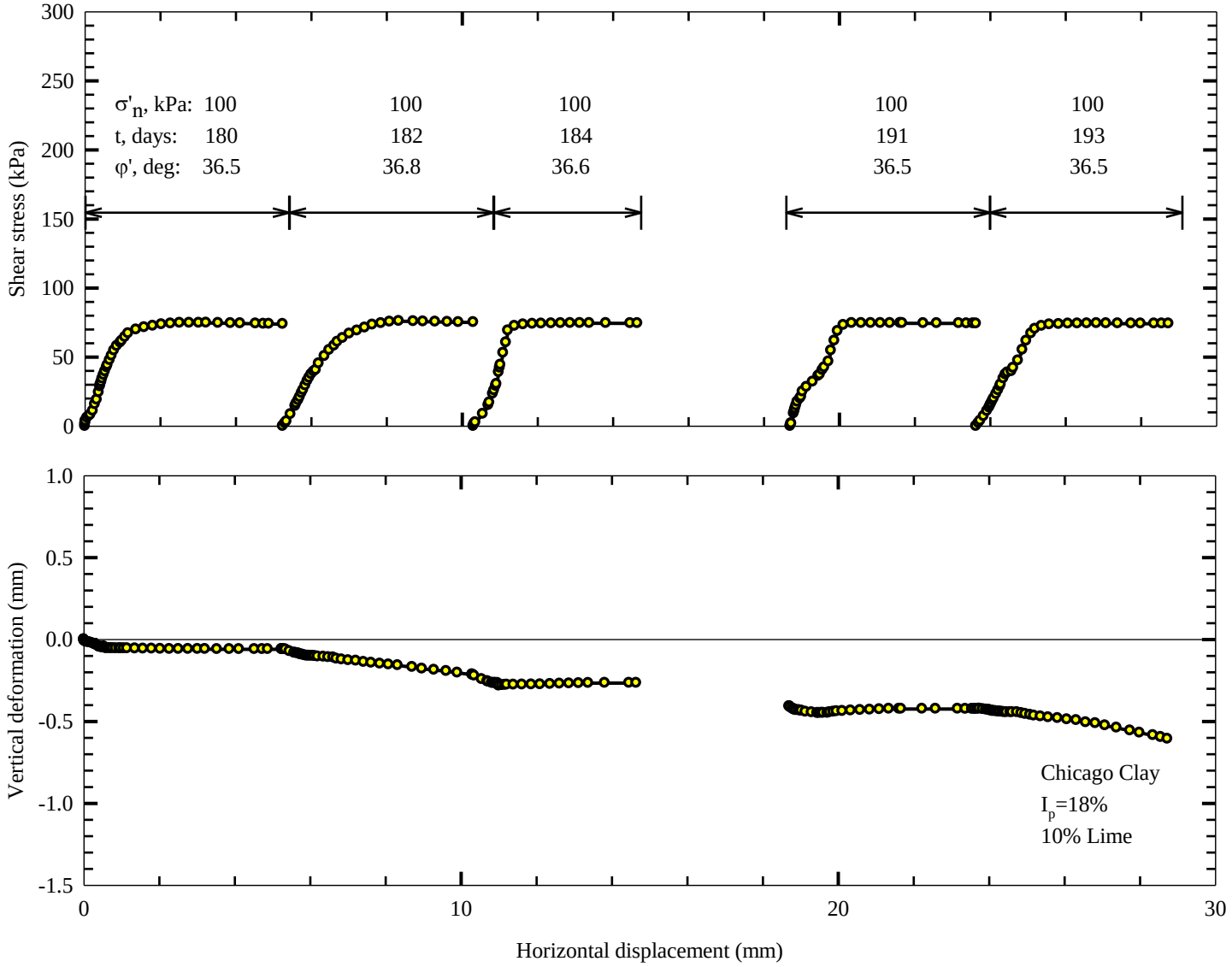

Figure 5.18: Shear stress-shear displacement and vertical displacement-shear displacement curves for Specimen 88 (precut); one reverse not shown due to proving ring malfunction

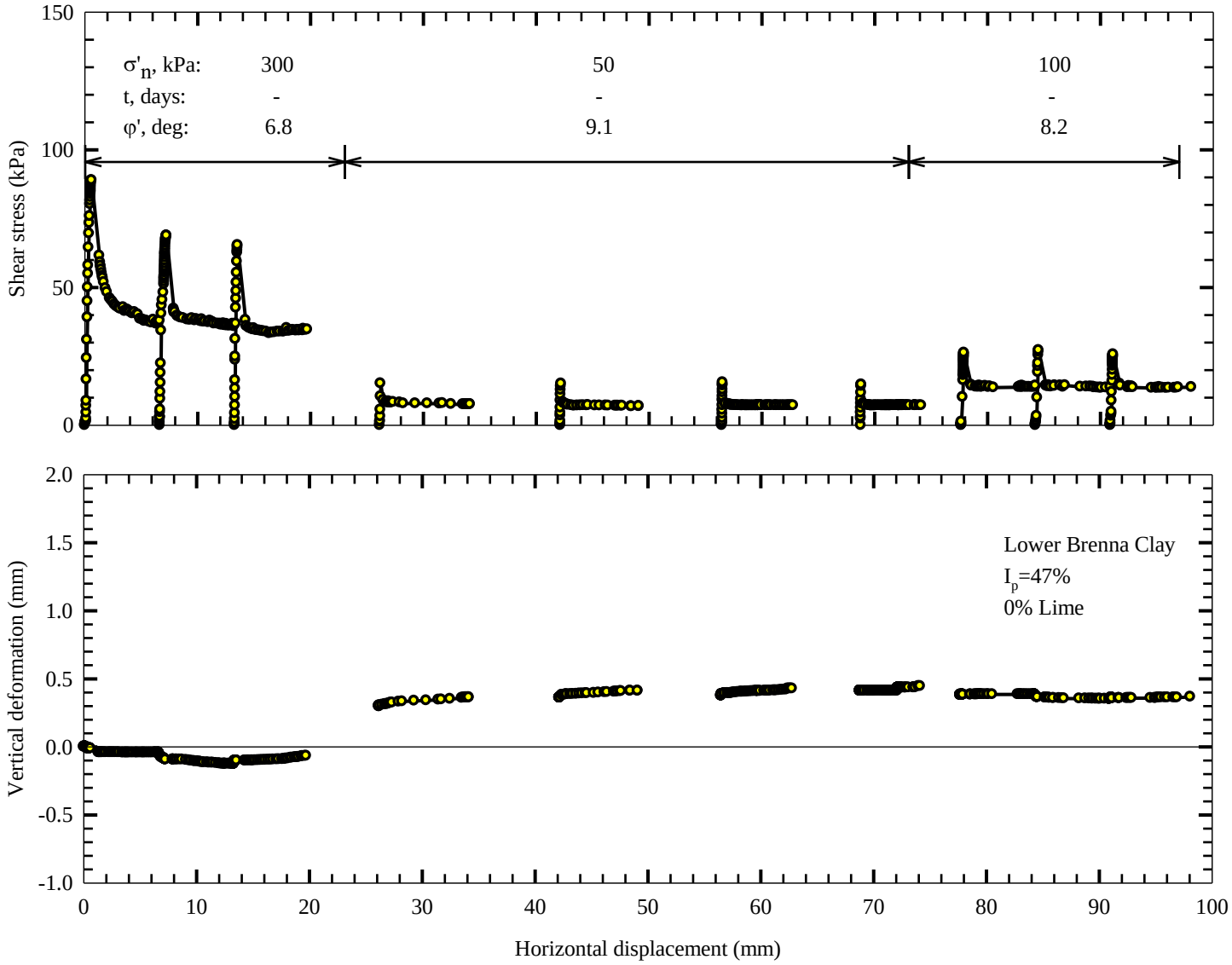

Figure 5.19: Shear stress-shear displacement and vertical displacement-shear displacement curves for Specimen 89 (precut); five reverses not shown due to proving ring malfunction or inaccuracy

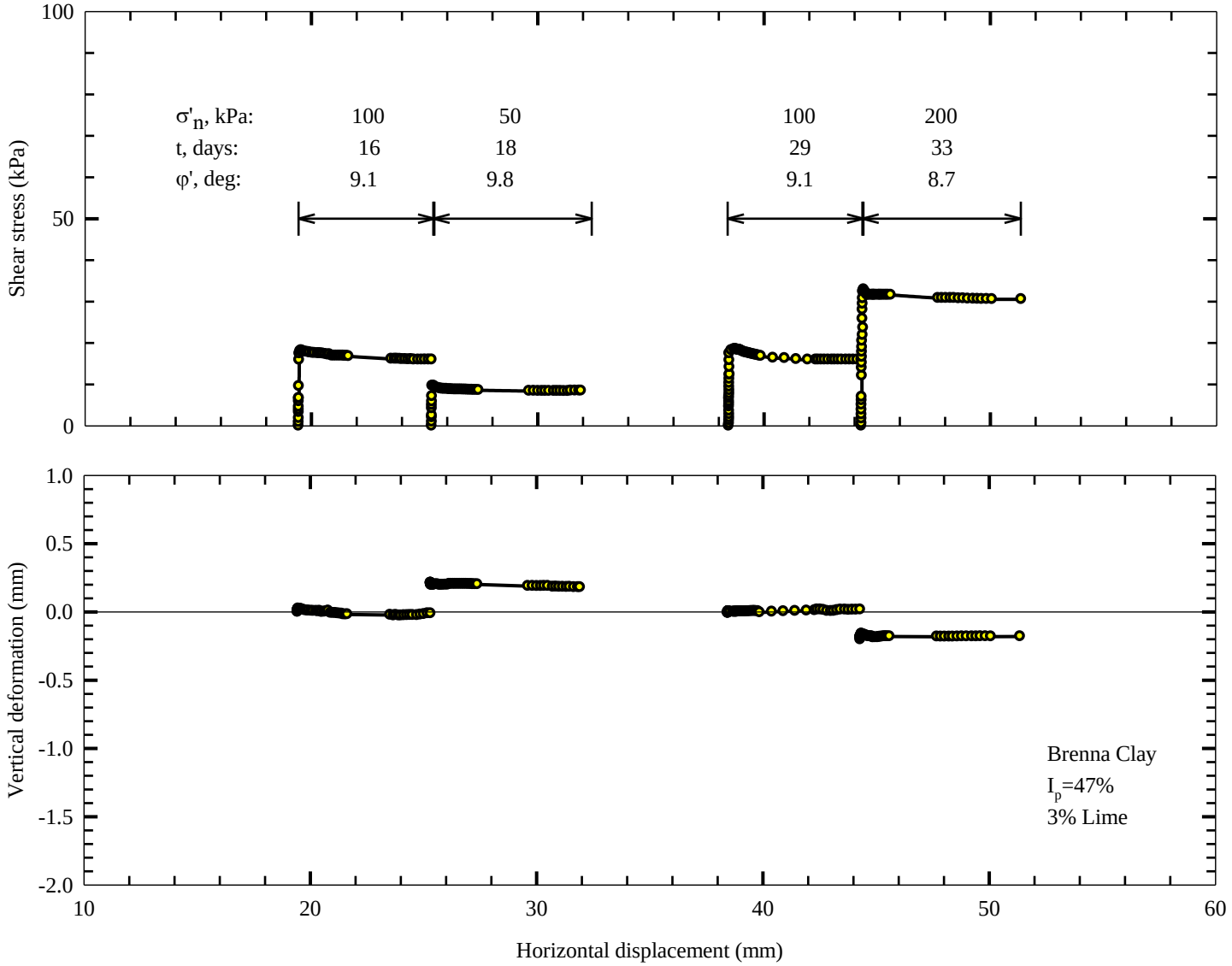

Figure 5.20: Shear stress-shear displacement and vertical displacement-shear displacement curves for Specimen 90 (after an intact specimen was cut); manually reversed; one forward not due to proving ring malfunction

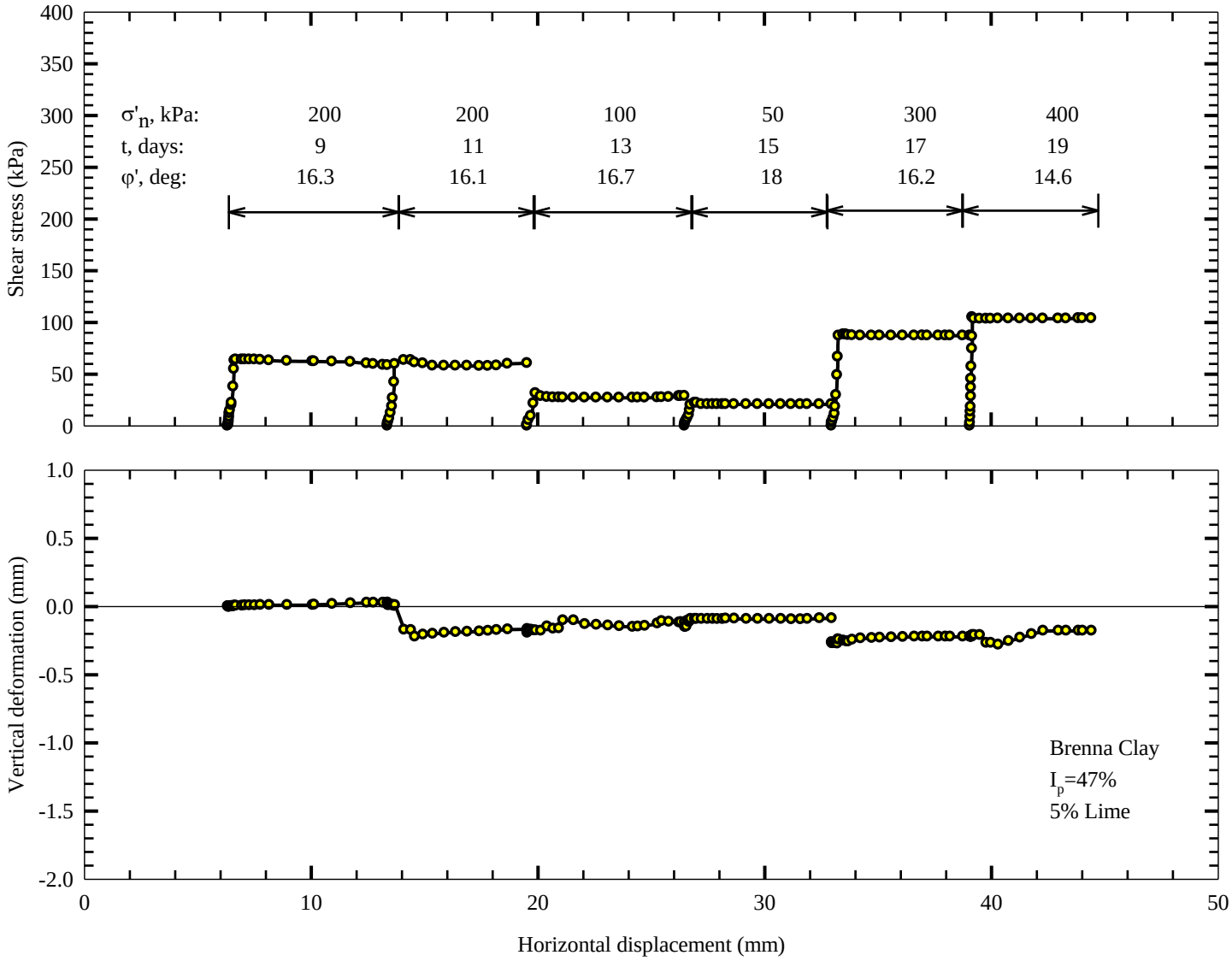

Figure 5.21: Shear stress-shear displacement and vertical displacement-shear displacement curves for Specimen 91 (after an intact specimen was cut)

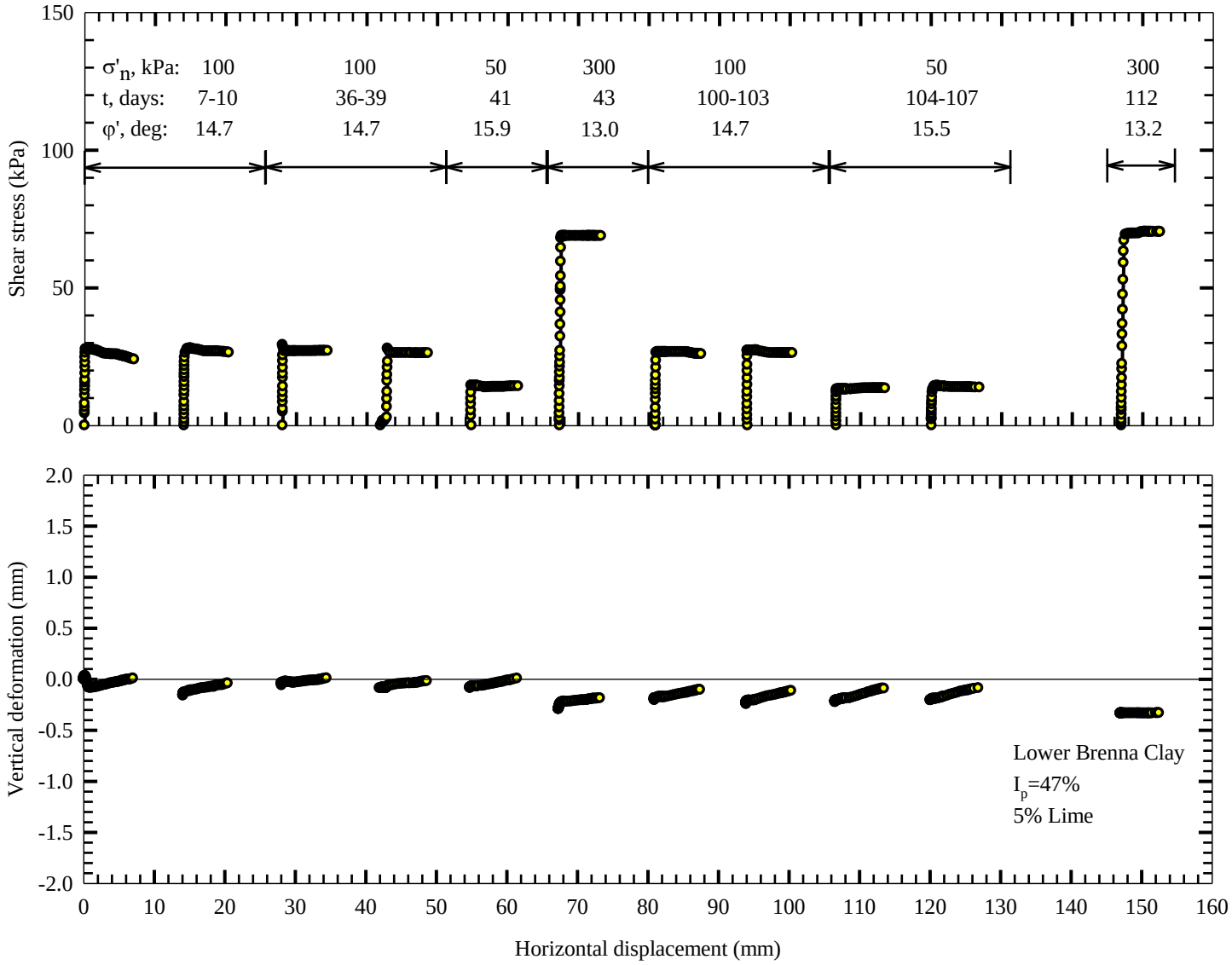

Figure 5.22: Shear stress-shear displacement and vertical displacement-shear displacement curves for Specimen 92 (precut); reverses and one forward not shown due to proving ring inaccuracy and malfunction

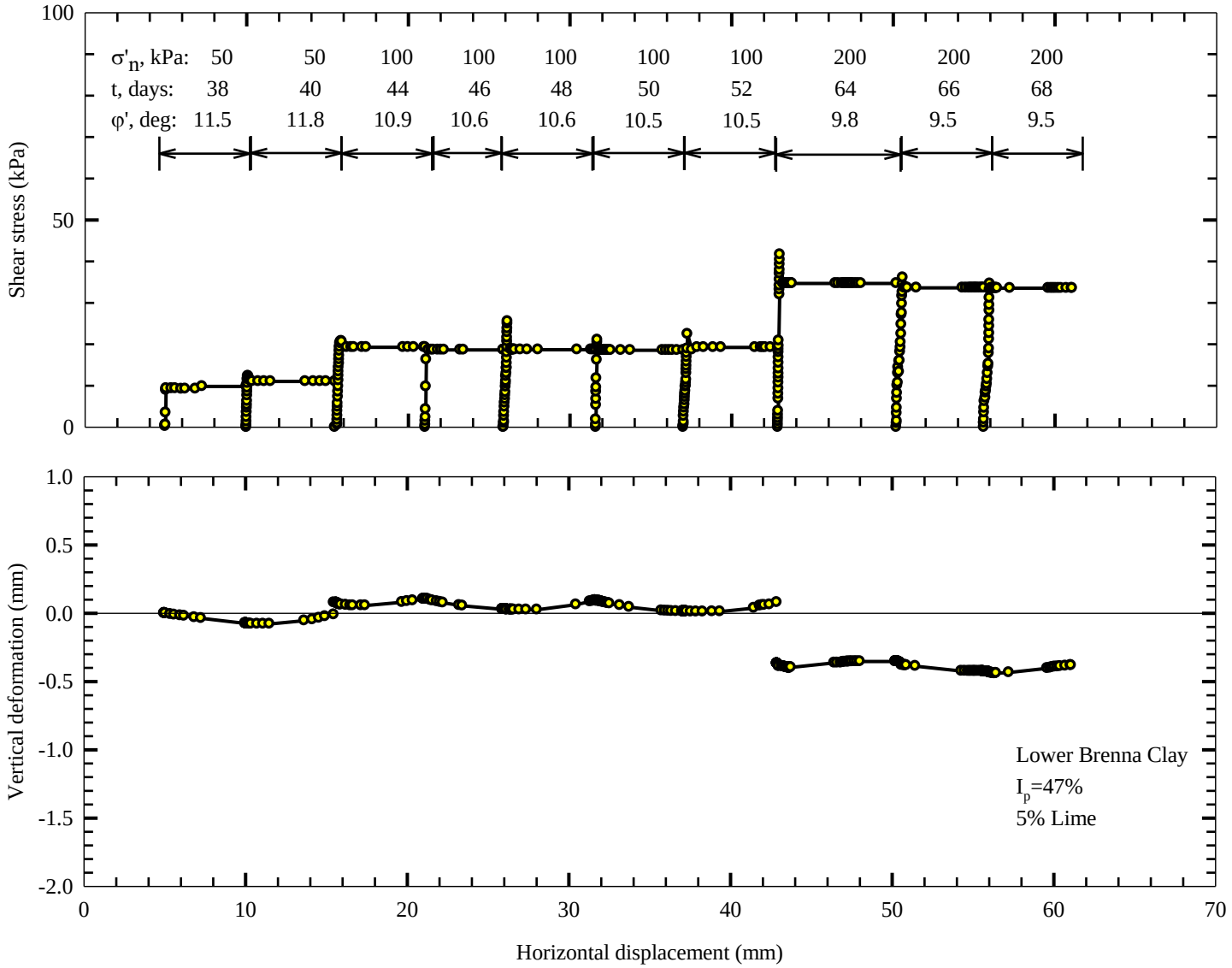

Figure 5.23: Shear stress-shear displacement and vertical displacement-shear displacement curves for Specimen 93 (after an intact specimen was cut)

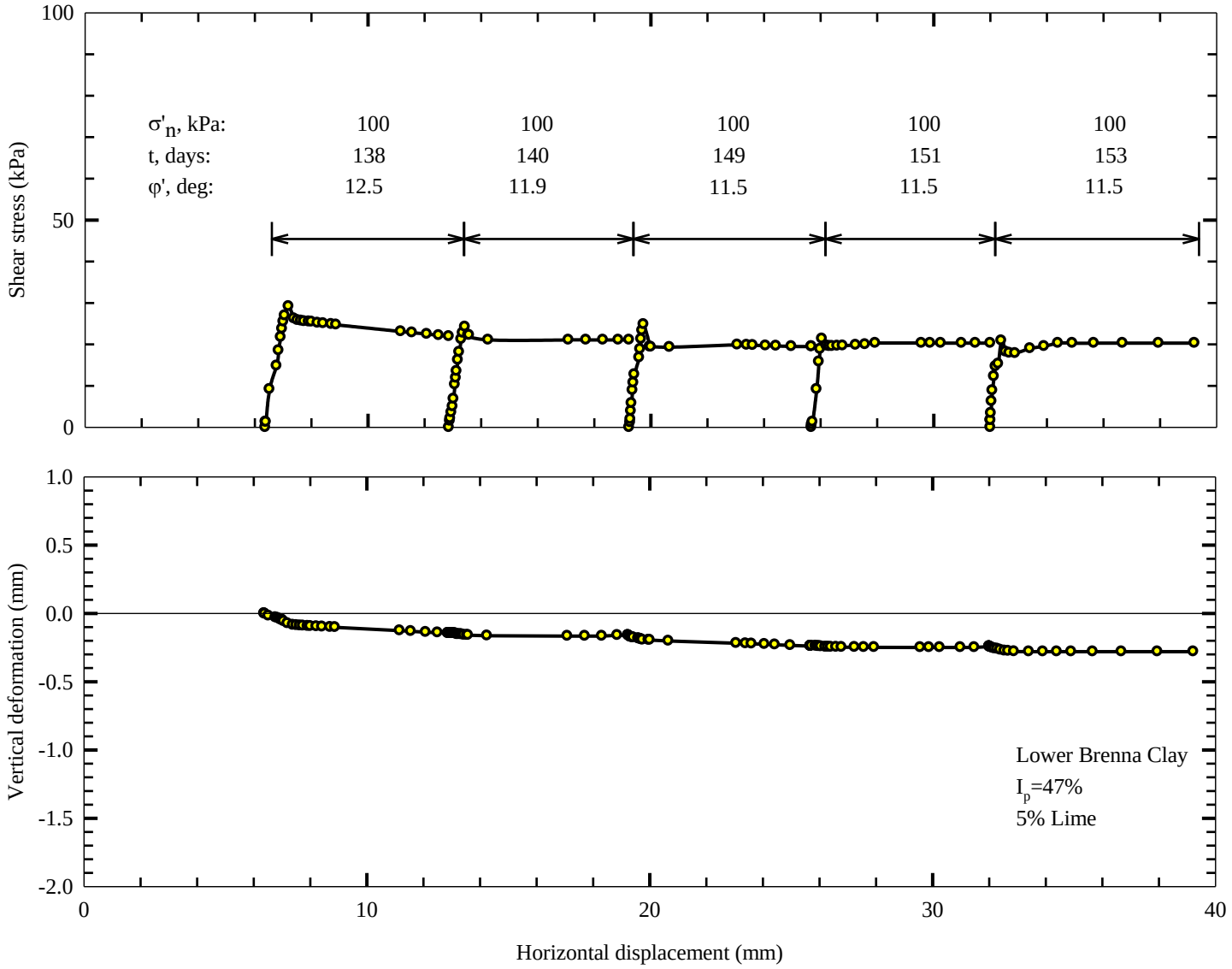

Figure 5.24: Shear stress-shear displacement and vertical displacement-shear displacement curves for Specimen 94 (after an intact specimen was cut)

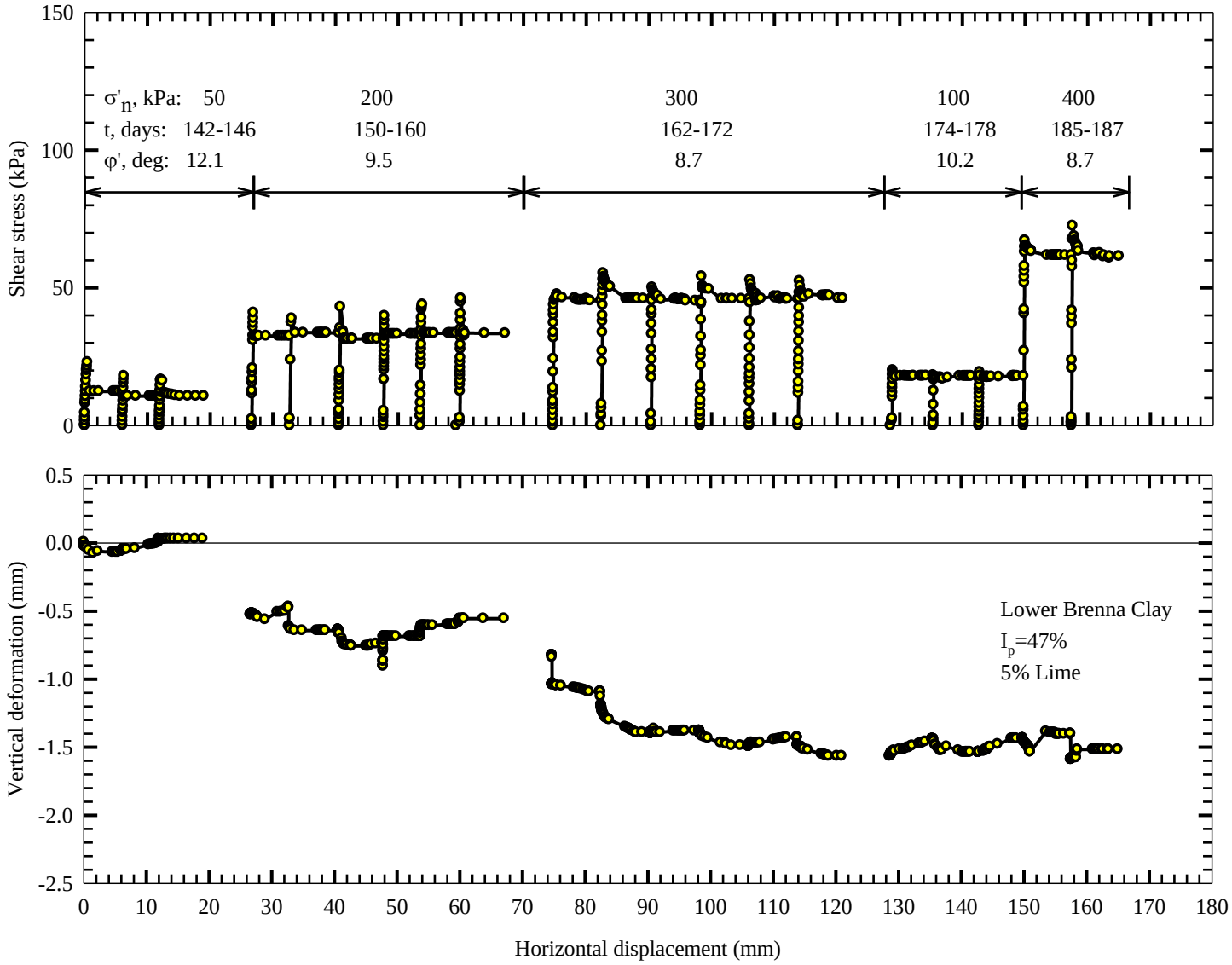

Figure 5.25: Shear stress-shear displacement and vertical displacement-shear displacement curves for Specimen 95 (precut); two forwards and one reverse not shown due to proving ring malfunction

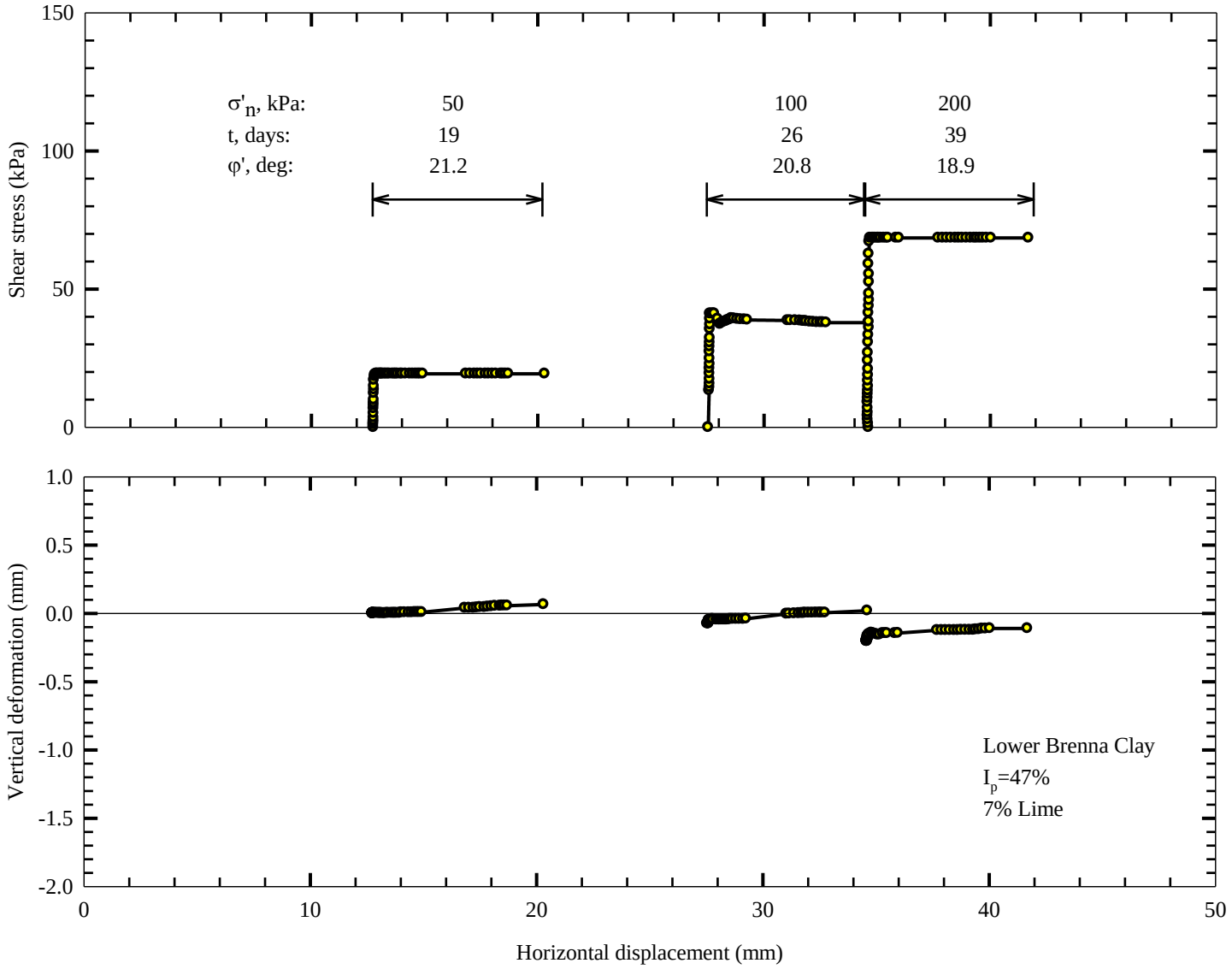

Figure 5.26: Shear stress-shear displacement and vertical displacement-shear displacement curves for Specimen 96 (after an intact specimen was cut); manaully reversed; one forward under low effective normel stresses not shown due to rotation of top half

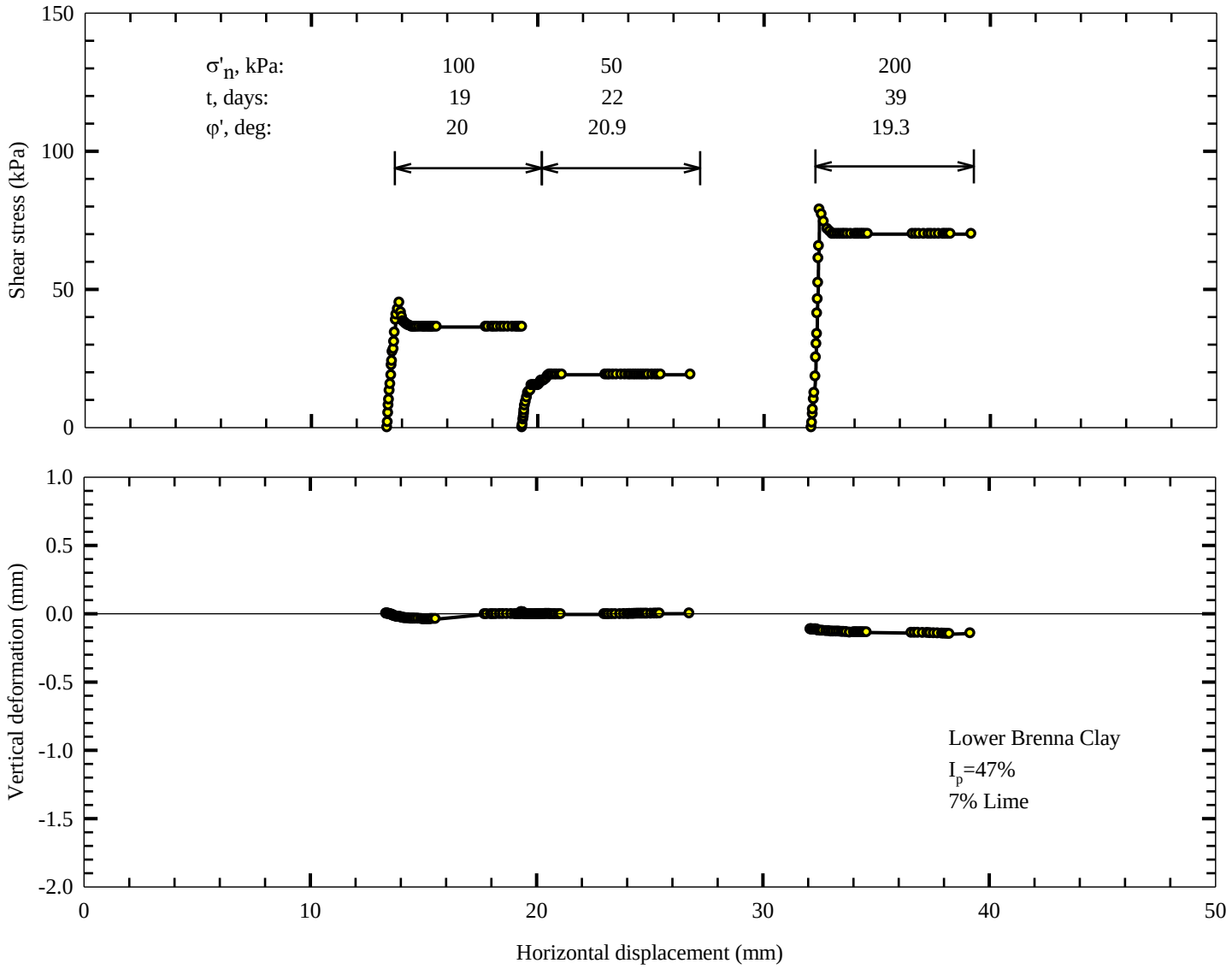

Figure 5.27: Shear stress-shear displacement and vertical displacement-shear displacement curves for Specimen 97 (after an intact specimen was cut); manaully reversed; one forward under low effective normel stresses not shown due to rotation of top half

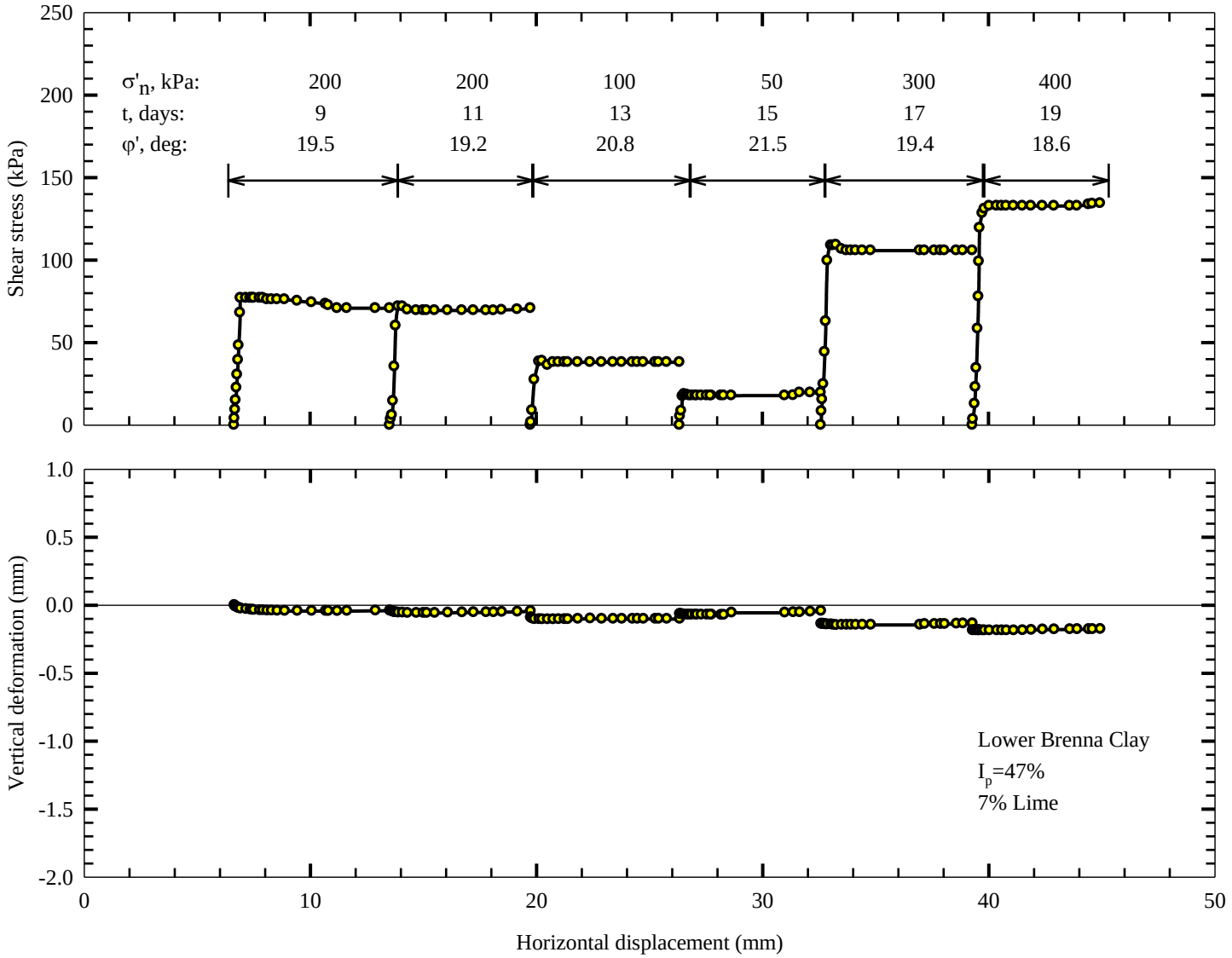

Figure 5.28: Shear stress-shear displacement and vertical displacement-shear displacement curves for Specimen 98 (after an intact specimen was cut); manually reversed

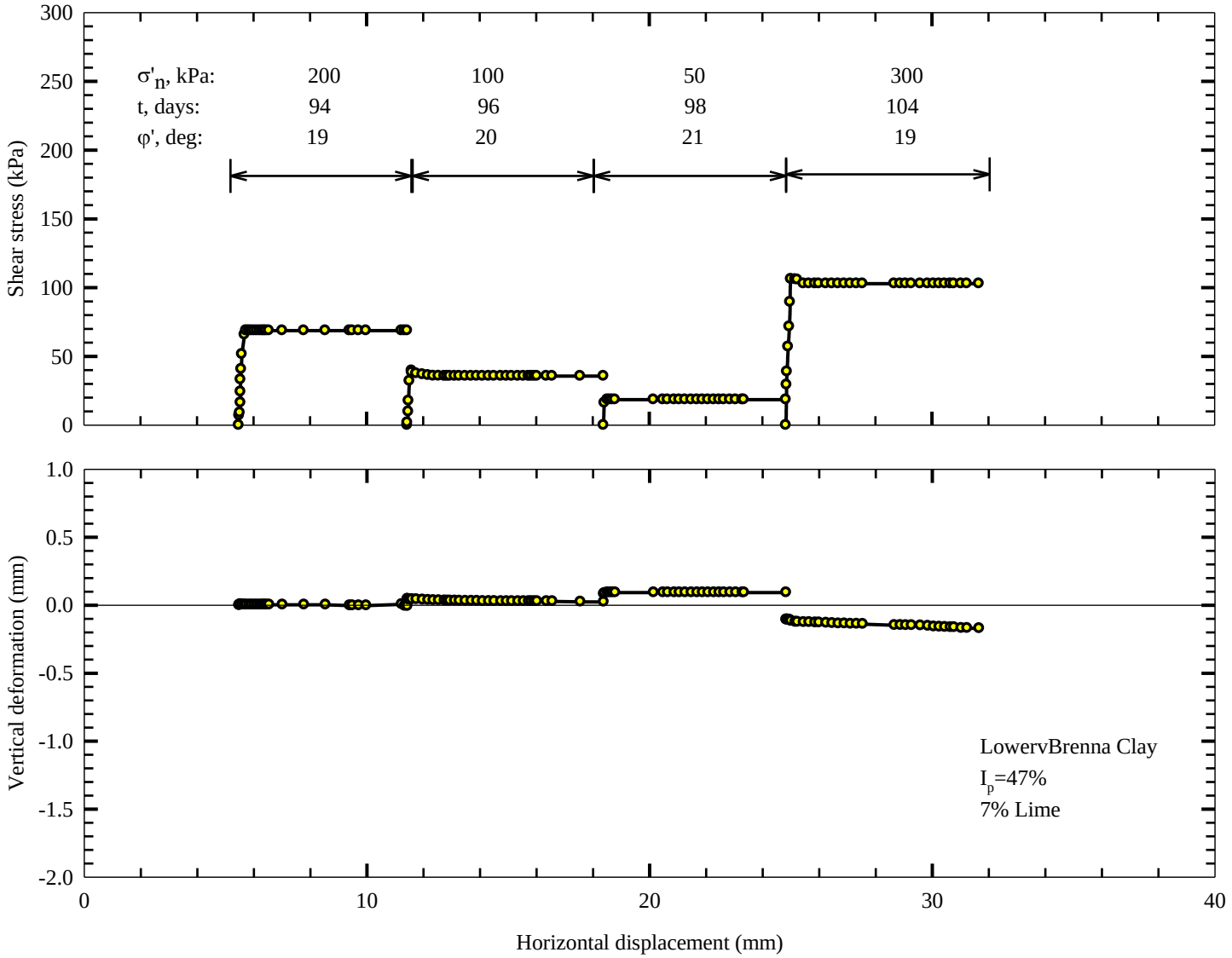

Figure 5.29: Shear stress-shear displacement and vertical displacement-shear displacement curves for Specimen 99 (after an intact specimen was cut); manually reversed

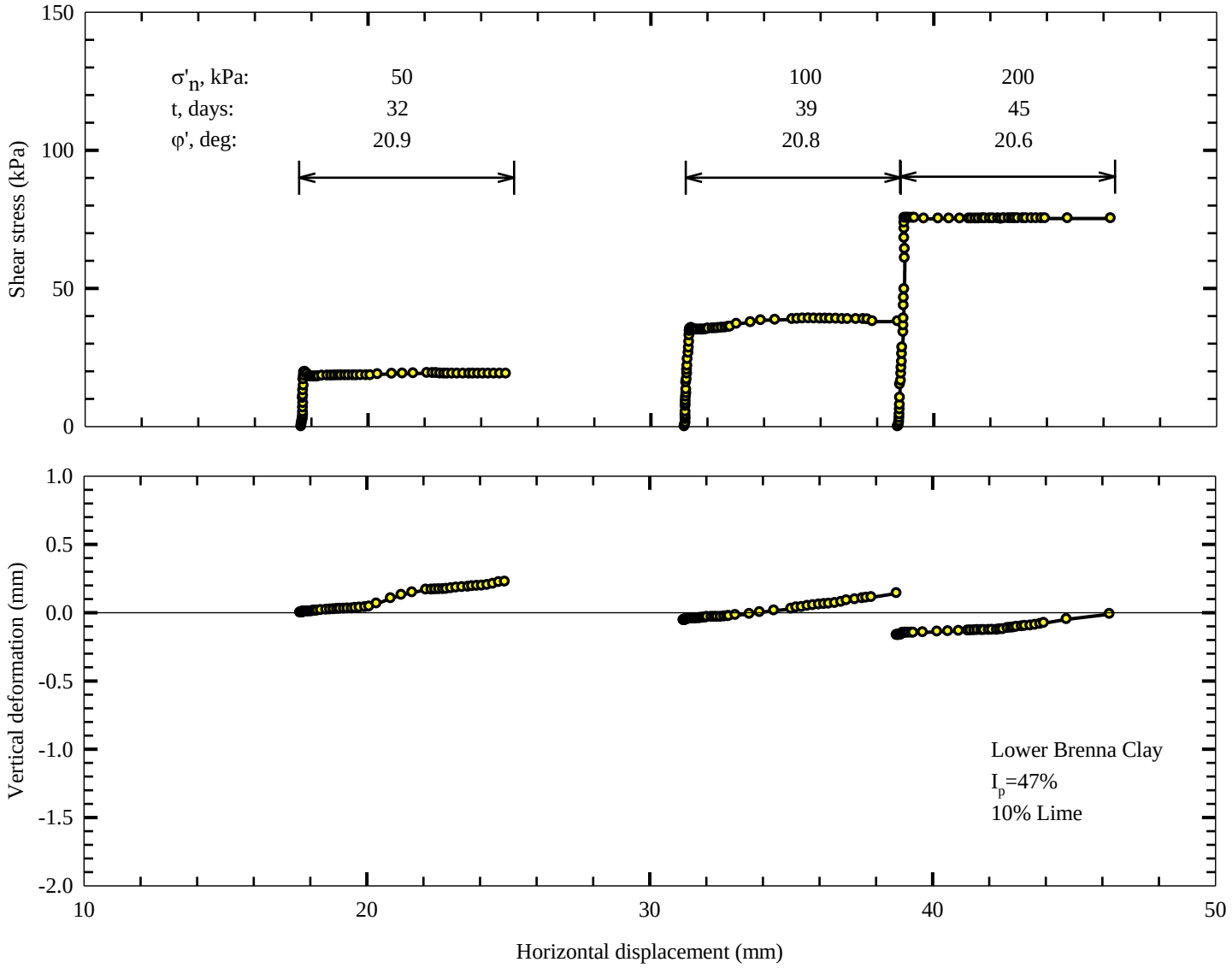

Figure 5.30: Shear stress-shear displacement and vertical displacement-shear displacement curves for Specimen 100 (after an intact specimen was cut); manually reversed; one forward under low effective normel stresses not shown due to rotation of top half

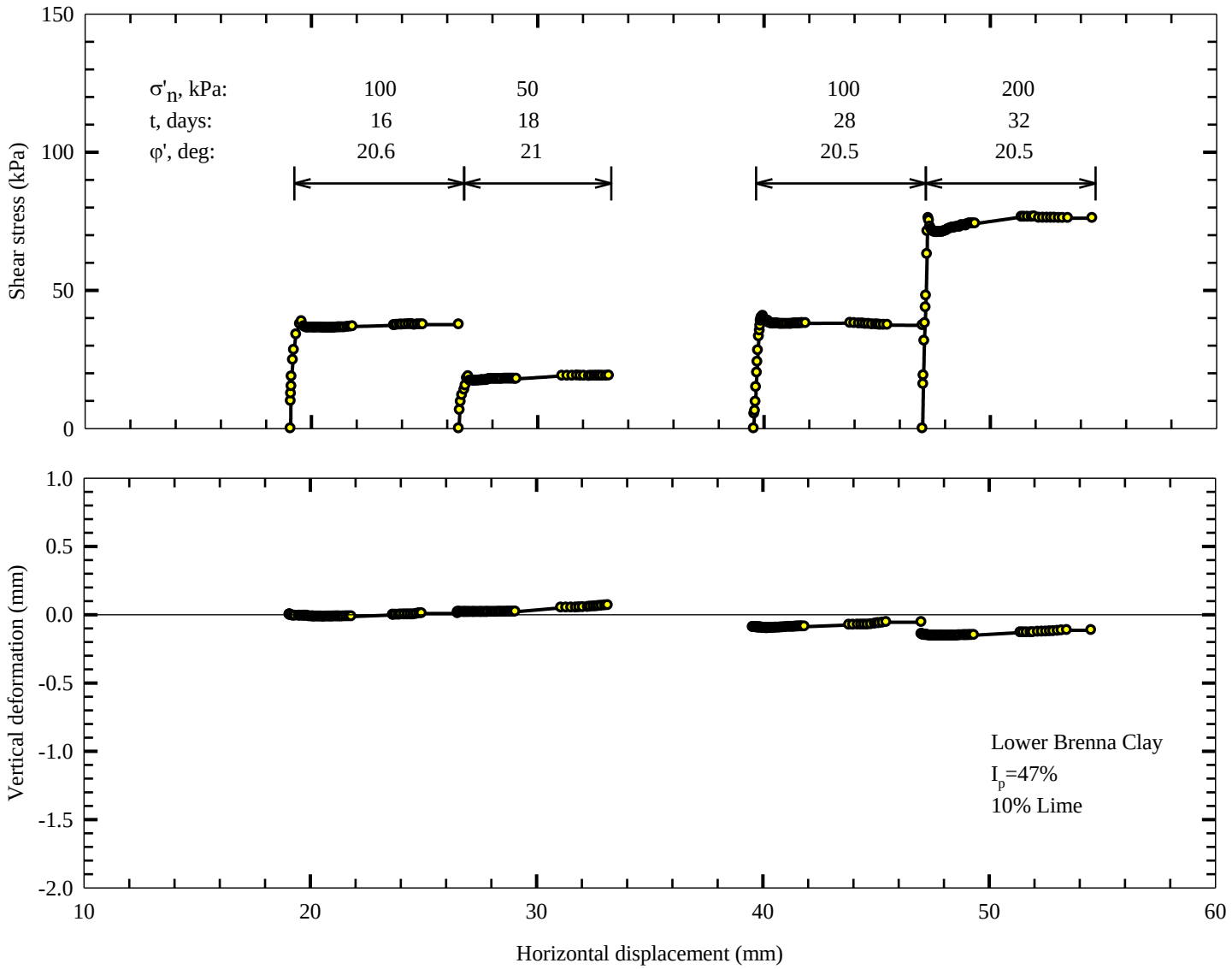

Figure 5.31: Shear stress-shear displacement and vertical displacement-shear displacement curves for Specimen 101 (after an intact specimen was cut); manually reversed; one forward under low effective normel stresses not shown due to rotation of top half

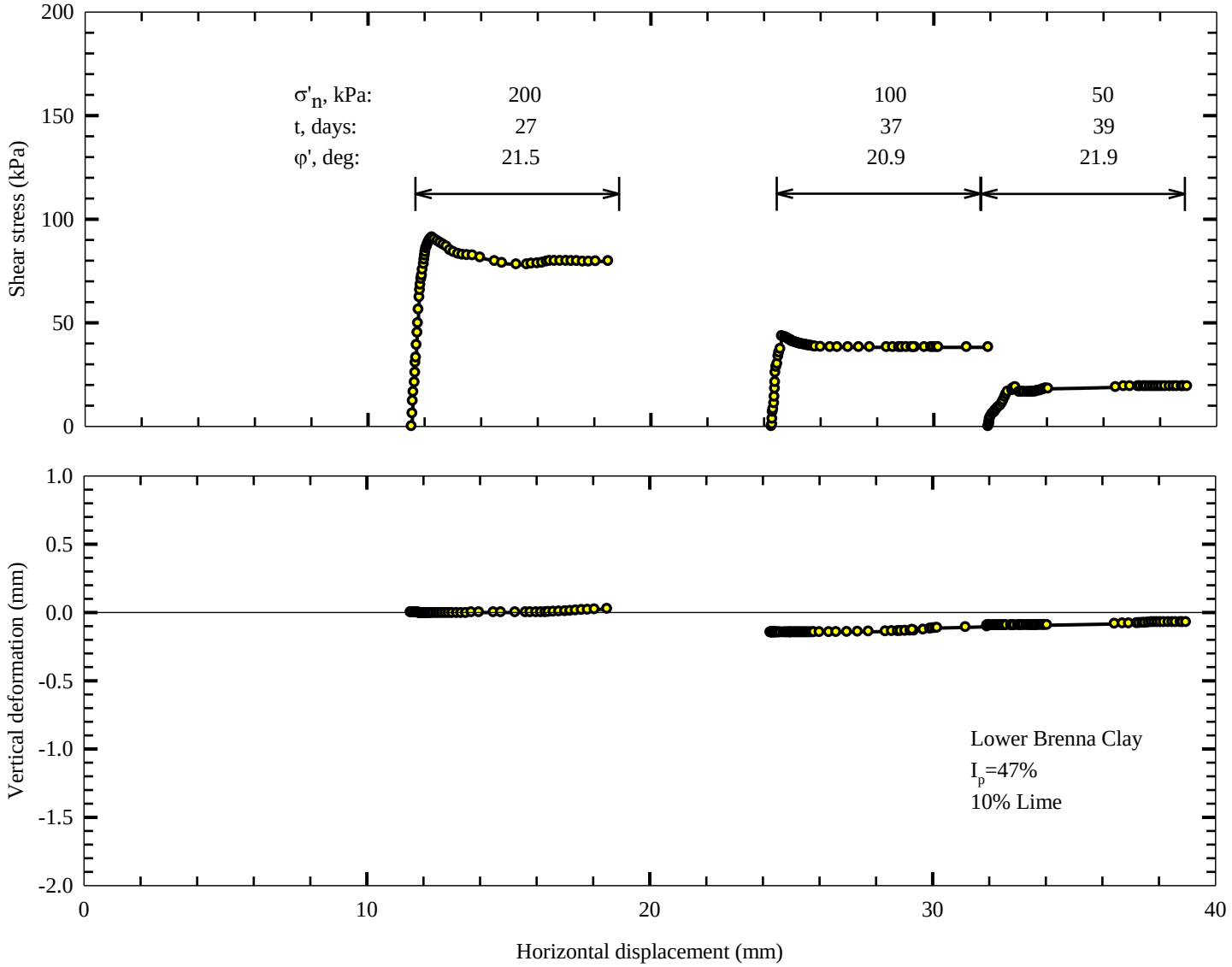

Figure 5.32: Shear stress-shear displacement and vertical displacement-shear displacement curves for Specimen 102 (after an intact specimen was cut); manually reversed; one forward under low effective normel stresses not shown due to rotation of top half

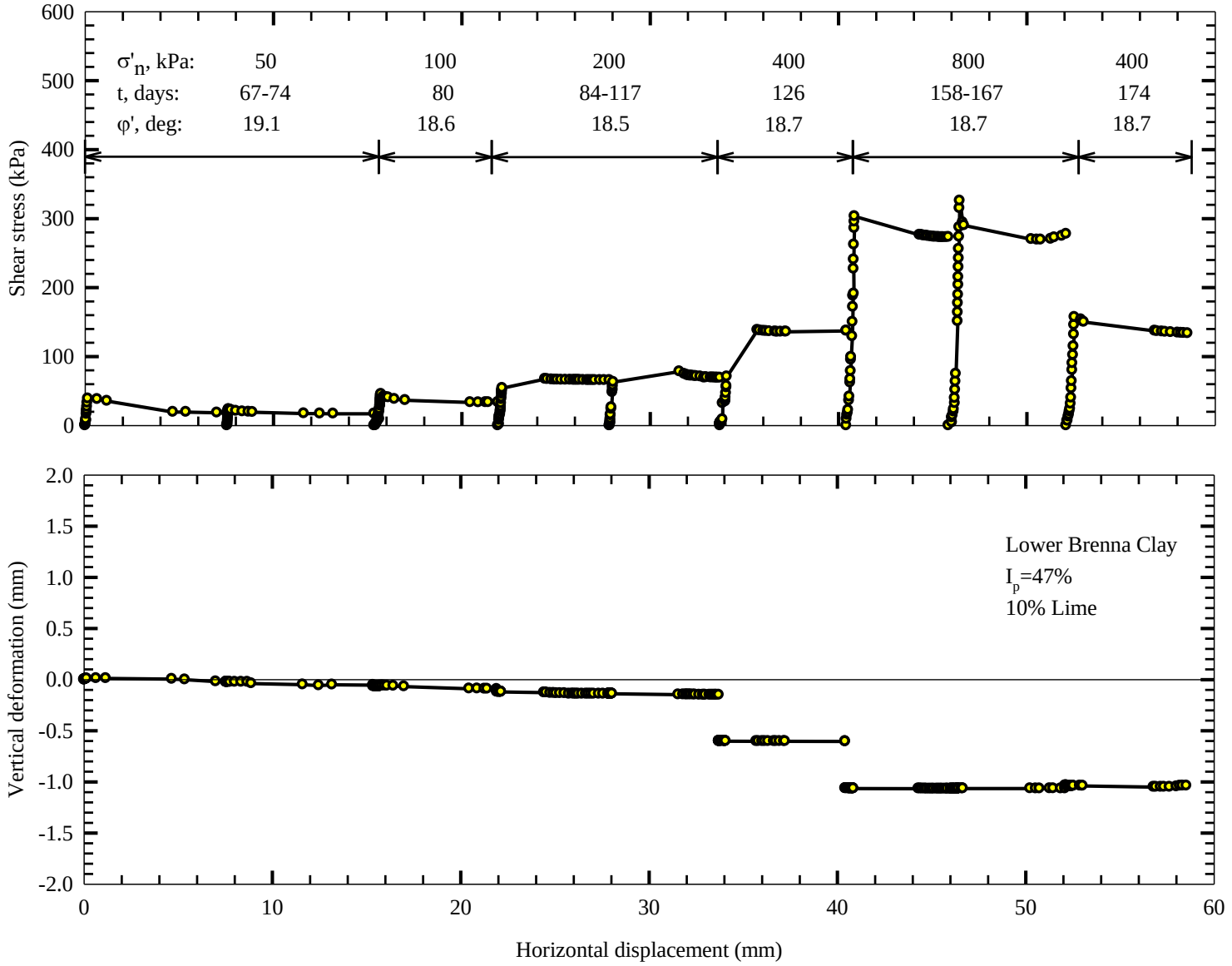

Figure 5.33: Shear stress-shear displacement and vertical displacement-shear displacement curves for Specimen 103 (precut)

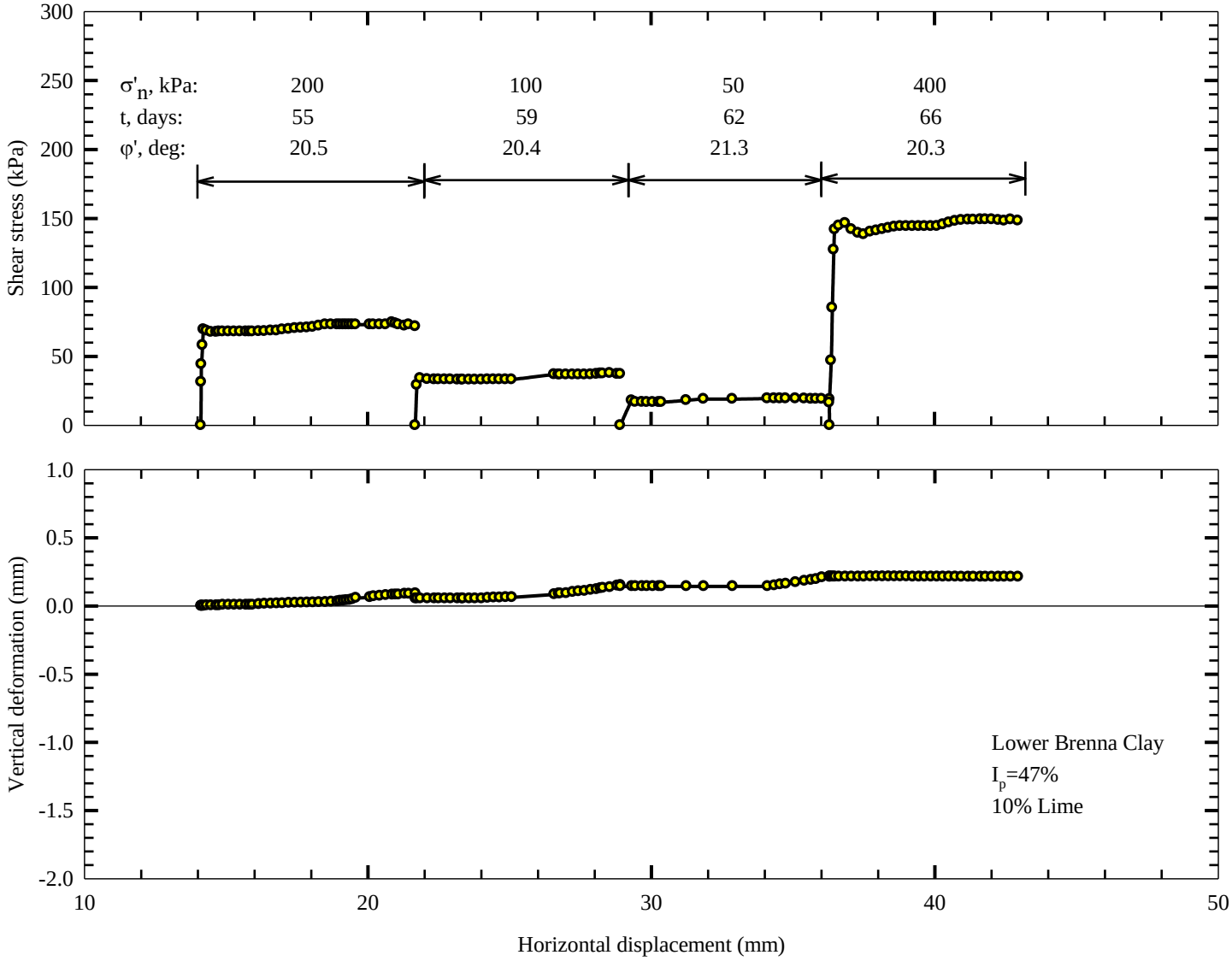

Figure 5.34: Shear stress-shear displacement and vertical displacement-shear displacement curves for Specimen 104 (after an intact specimen was cut); manually reversed; one forward under low effective normel stresses not shown due to rotation of top half

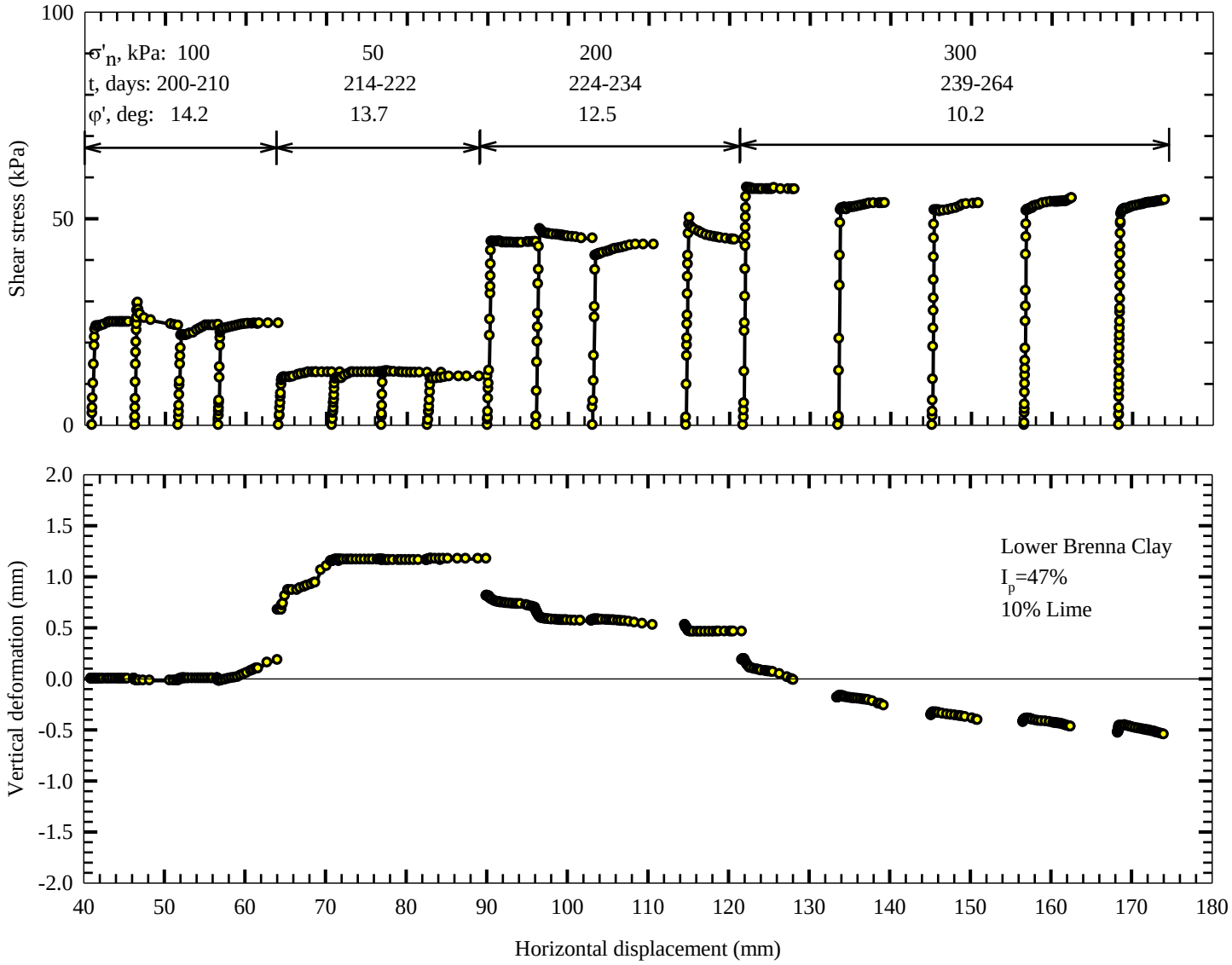

Figure 5.35: Shear stress-shear displacement and vertical displacement-shear displacement curves for Specimen 105 (after an intact specimen was sheared multiple times and cut)

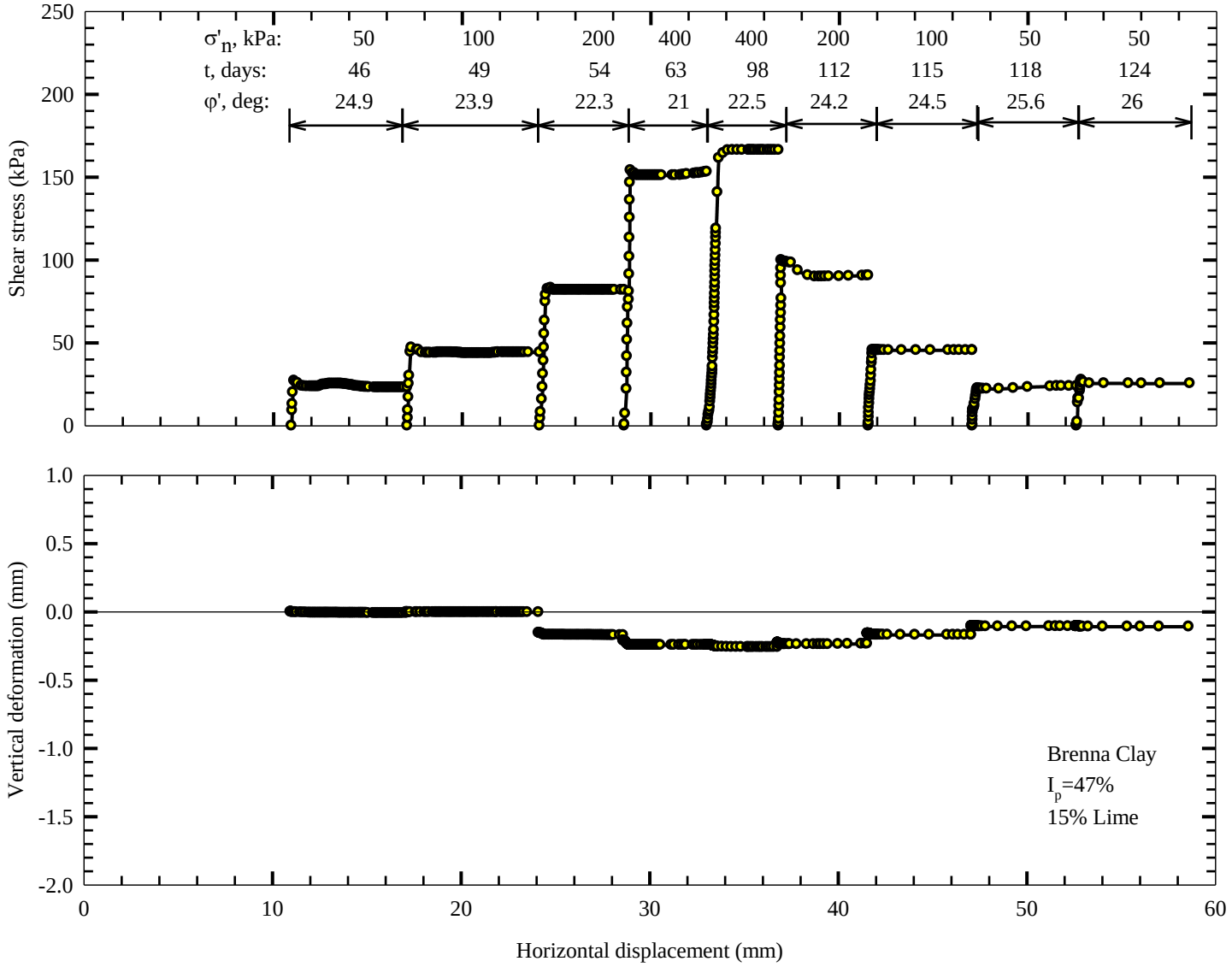

Figure 5.36: Shear stress-shear displacement and vertical displacement-shear displacement curves for Specimen 106 (after an intact specimen was cut); manually reversed

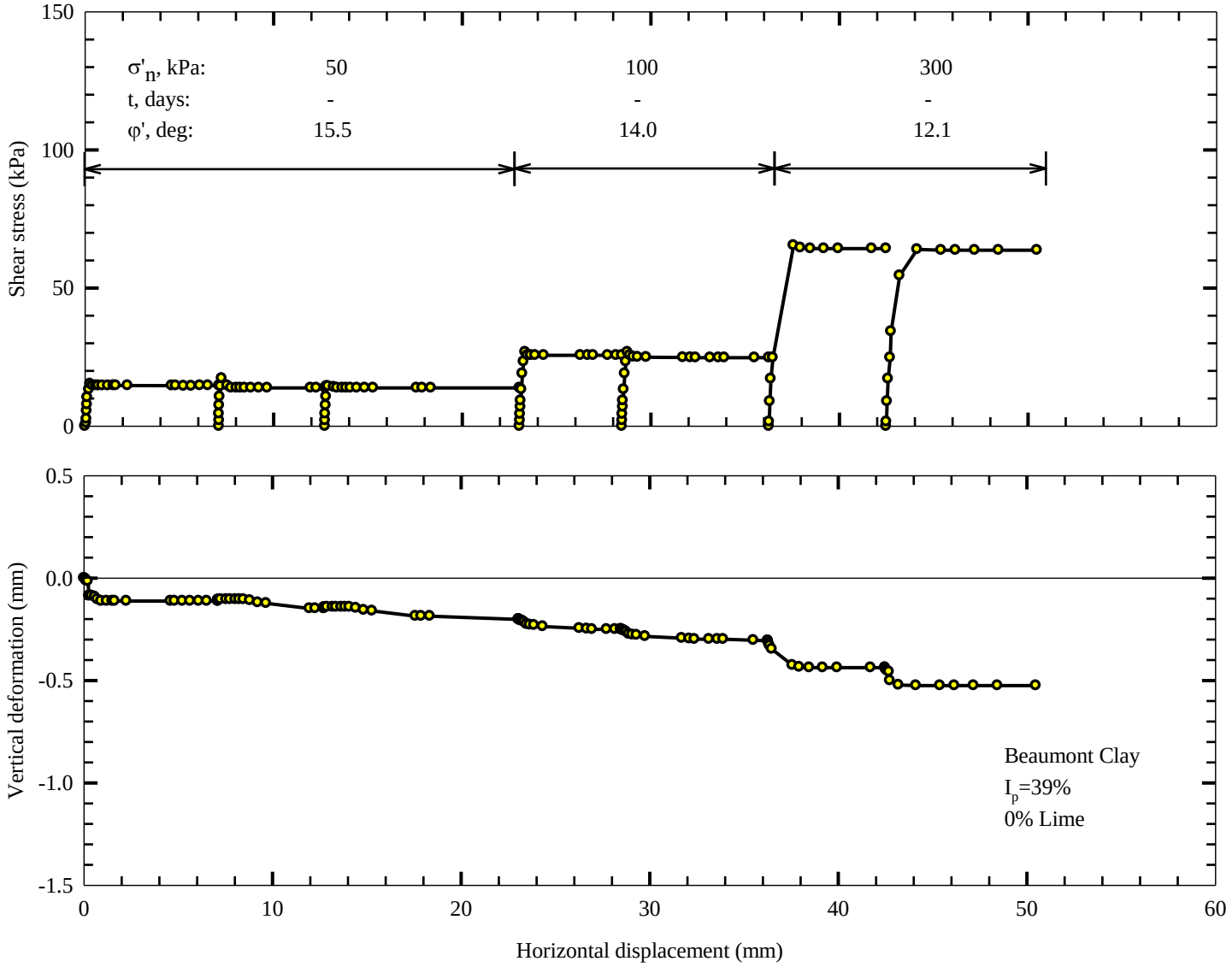

Figure 5.37: Shear stress-shear displacement and vertical displacement-shear displacement curves for Specimen 107 (precut), manually reversed

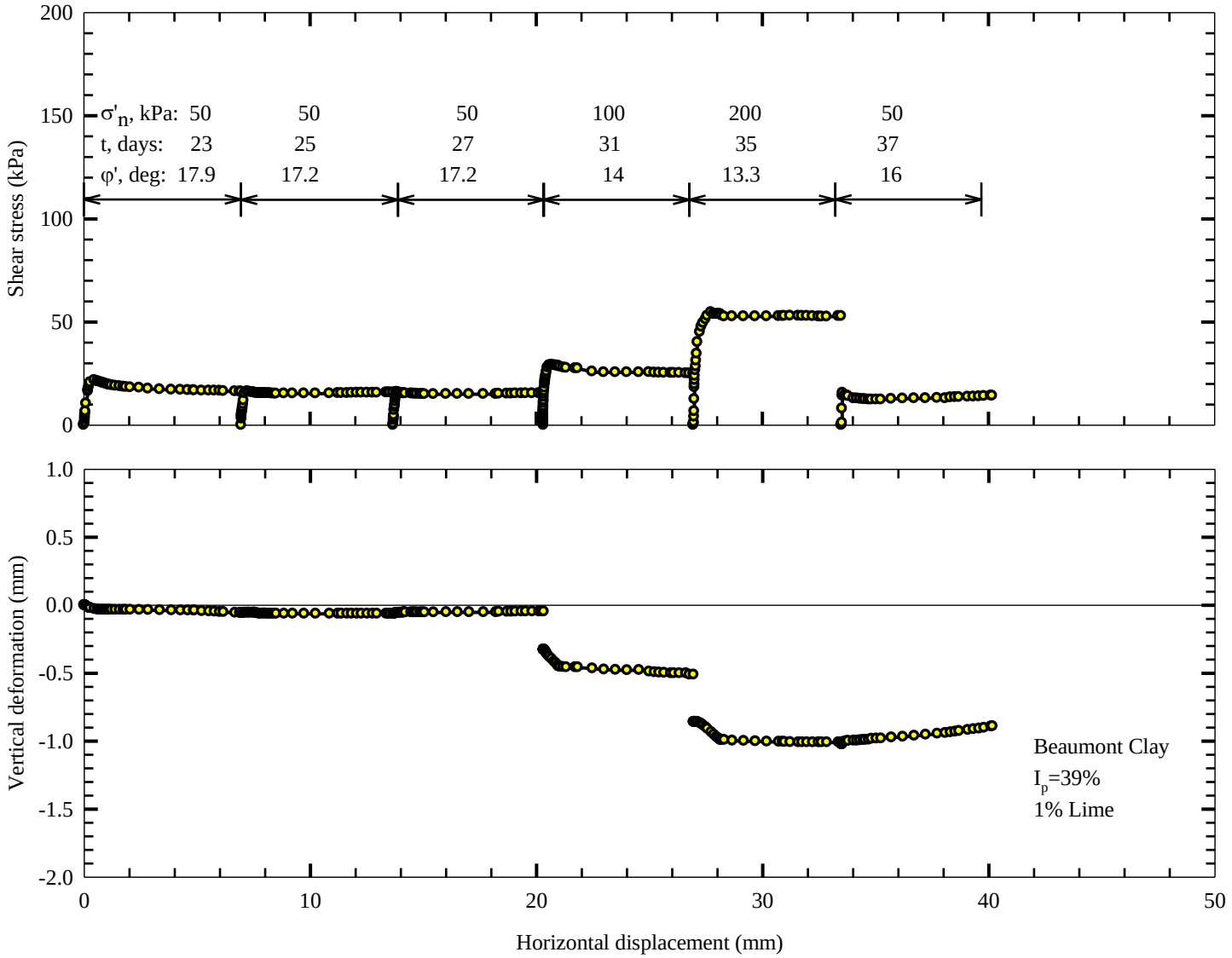

Figure 5.38: Shear stress-shear displacement and vertical displacement-shear displacement curves for Specimen 108 (after an intact specimen was cut); manually reversed

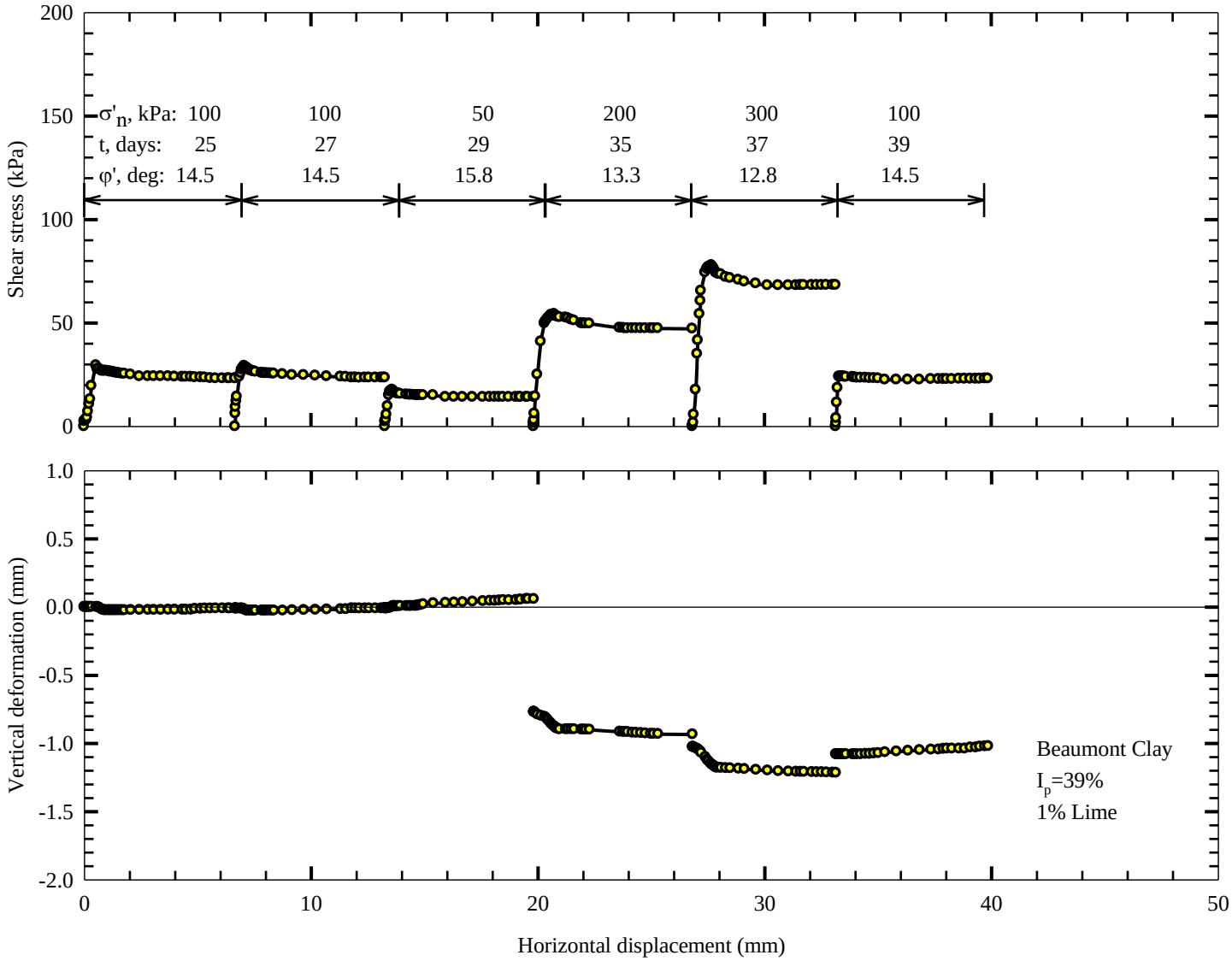

Figure 5.39: Shear stress-shear displacement and vertical displacement-shear displacement curves for Specimen 109 (after an intact specimen was cut); manually reversed

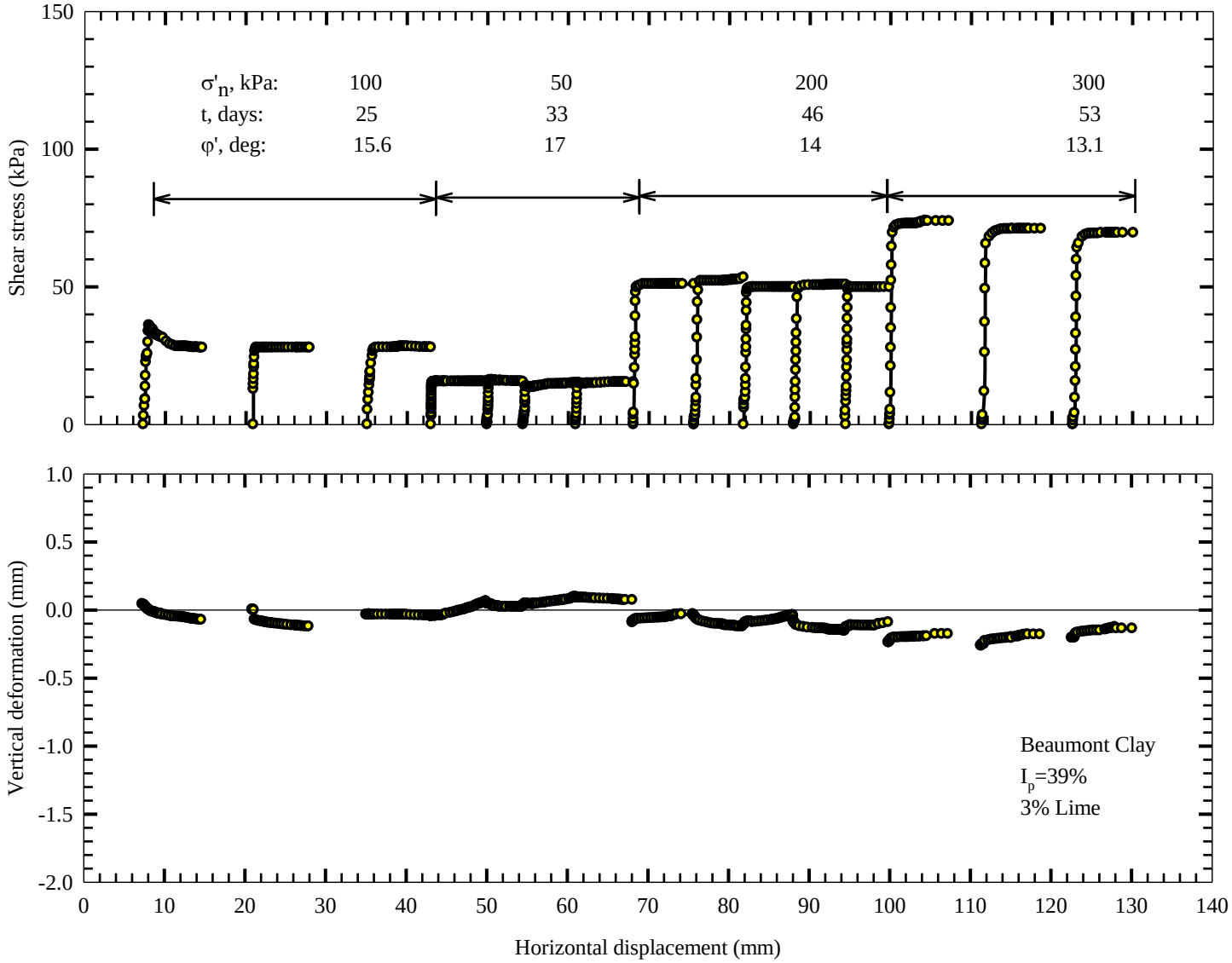

Figure 5.40: Shear stress-shear displacement and vertical displacement-shear displacement curves for Specimen 110 (after an intact specimen was cut); two forwards at 100 kPa not included due to proving ring inacuracy; manually reversed at 200 kPa and 300 kPa

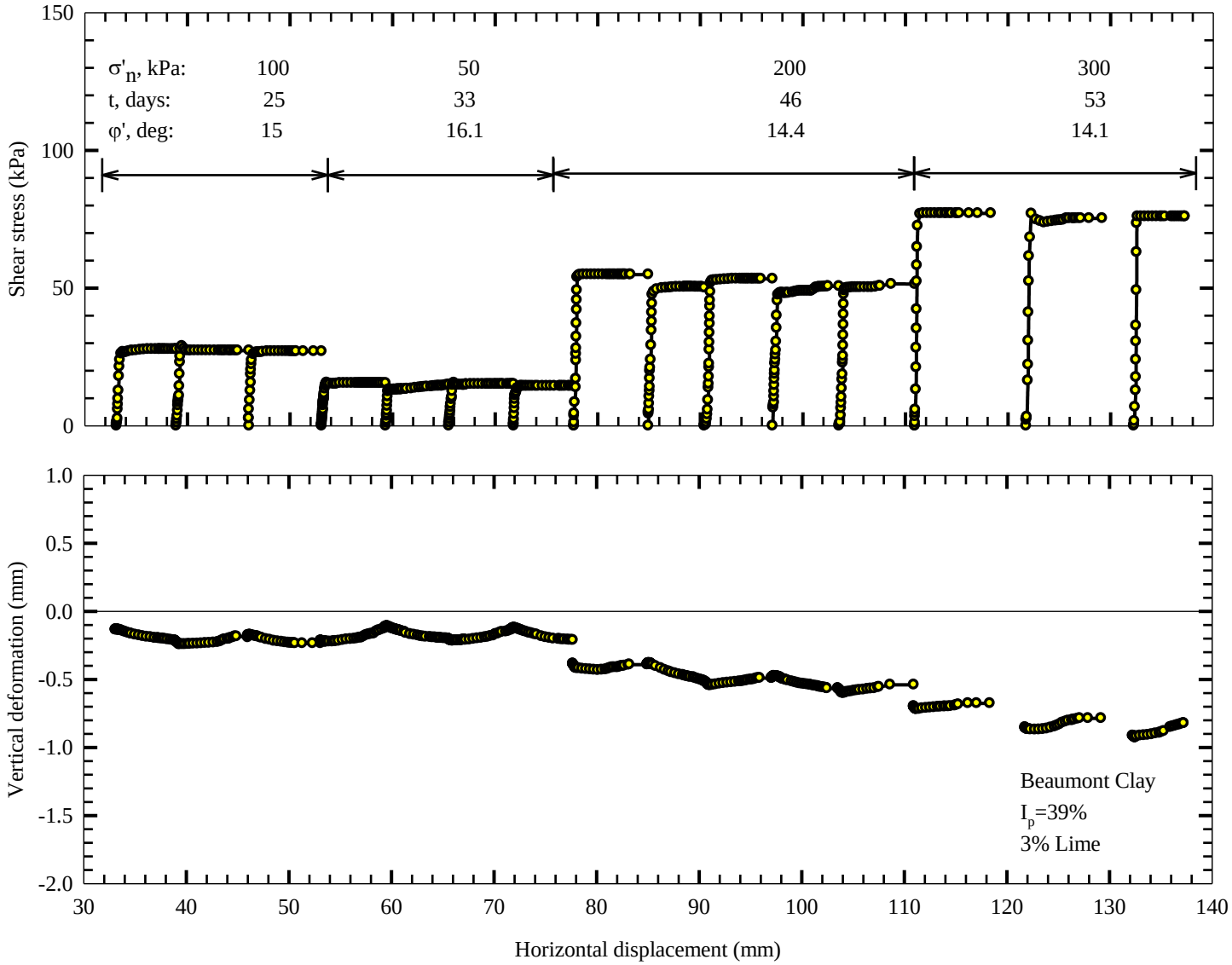

Figure 5.41: Shear stress-shear displacement and vertical displacement-shear displacement curves for Specimen 111 (after an intact specimen was sheared multiple times and cut); two reverses perfomed manually

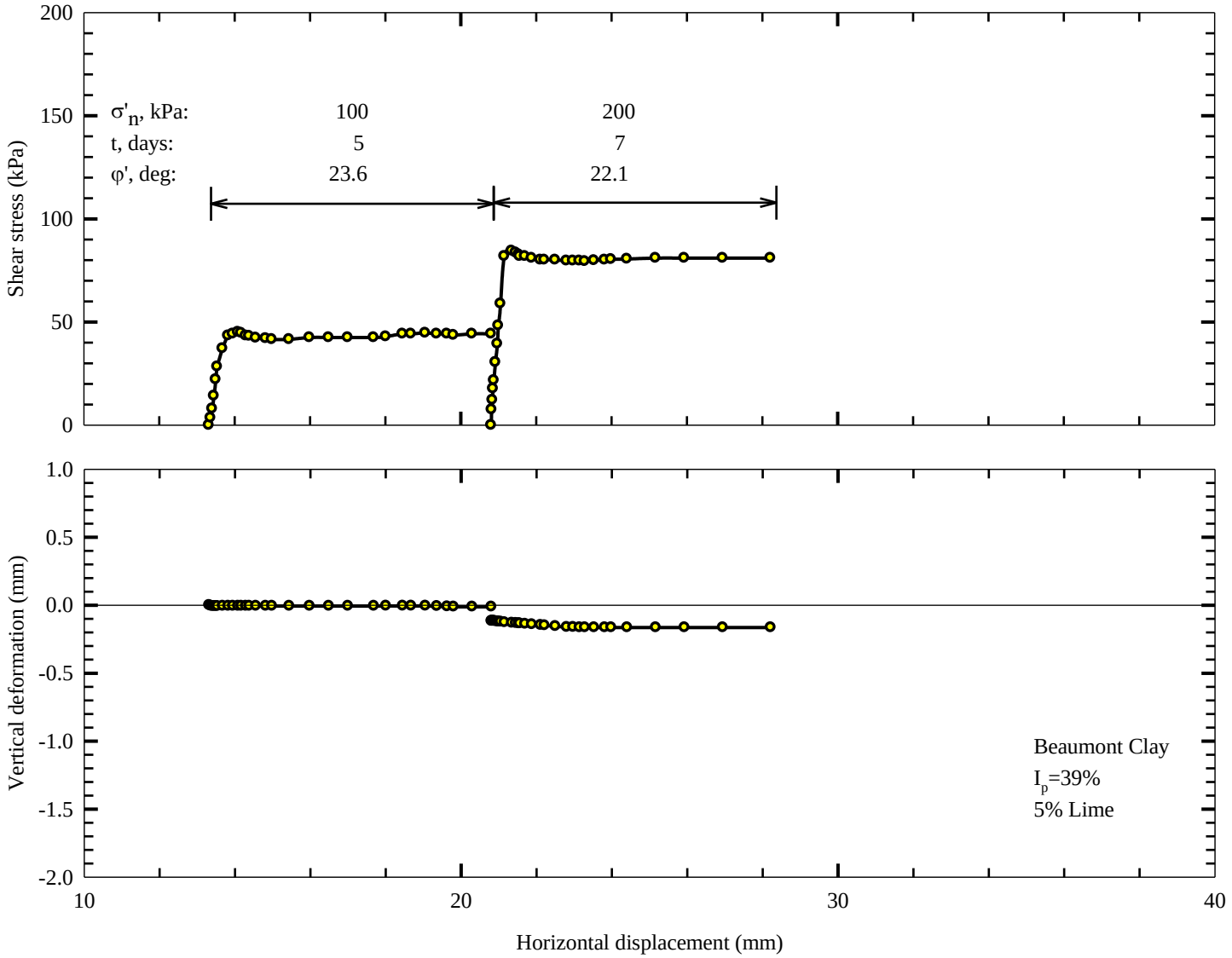

Figure 5.42: Shear stress-shear displacement and vertical displacement-shear displacement curves for Specimen 112 (after an intact specimen was cut); manually reversed

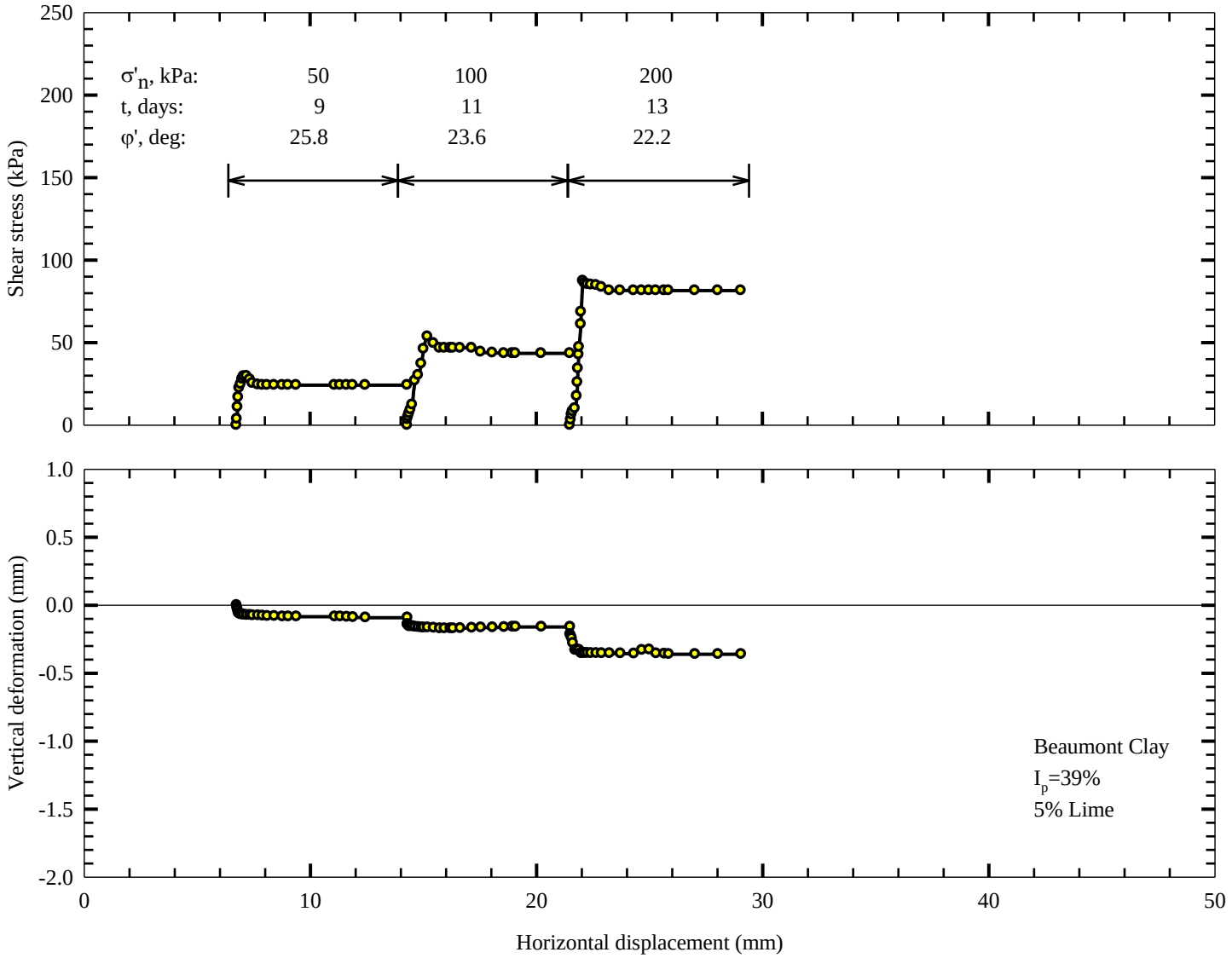

Figure 5.43: Shear stress-shear displacement and vertical displacement-shear displacement curves for Specimen 113 (after an intact specimen was cut); manually reversed

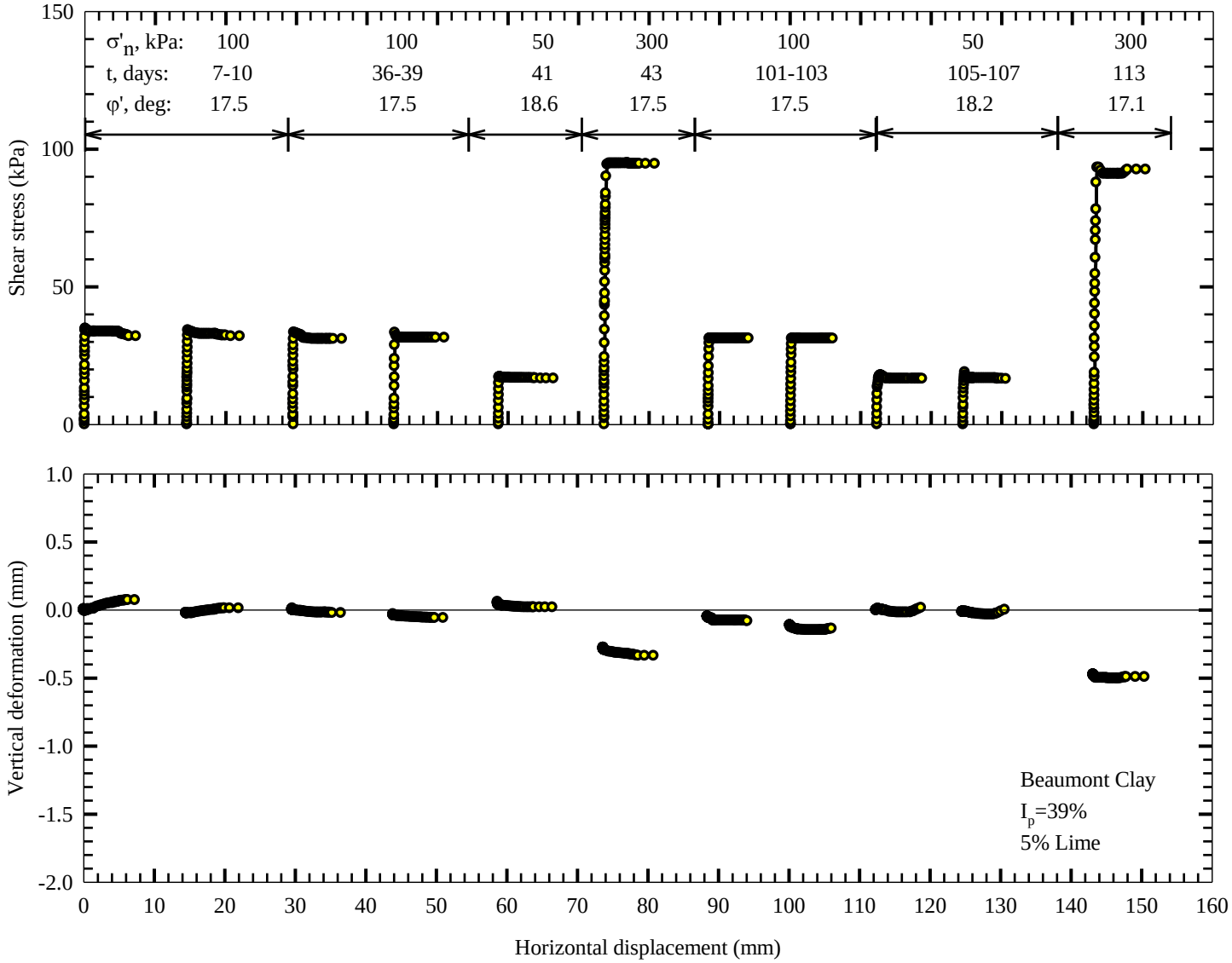

Figure 5.44: Shear stress-shear displacement and vertical displacement-shear displacement curves for Specimen 114 (precut), Reverse not included due to proving ring inacuracy

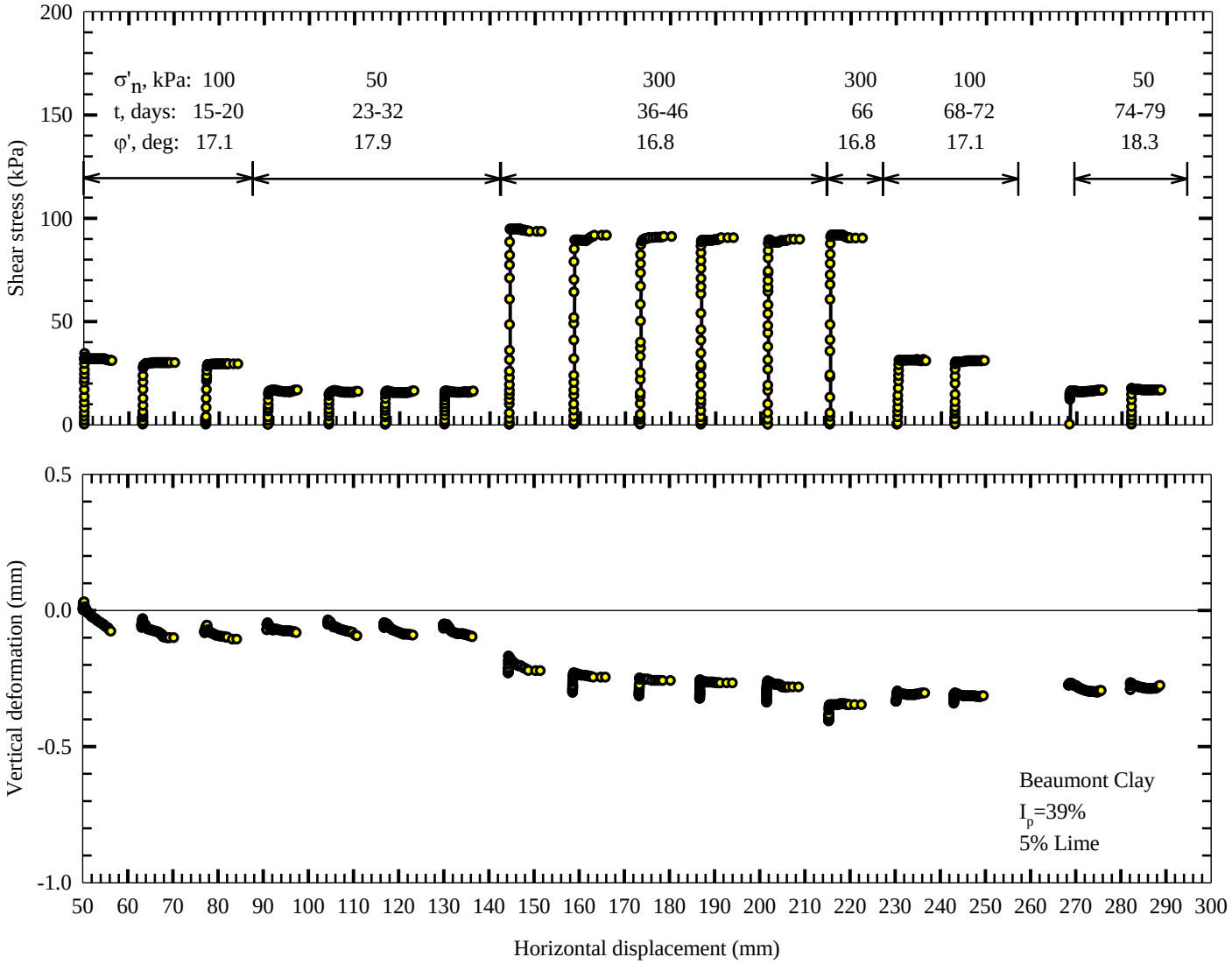

Figure 5.45: Shear stress-shear displacement and vertical displacement-shear displacement curves for Specimen 115 (after an intact specimen was sheared multiple times and cut); reverse not included due to proving ring inaccuracy; one forward at low effective nornal stress not included due to rotation of top half

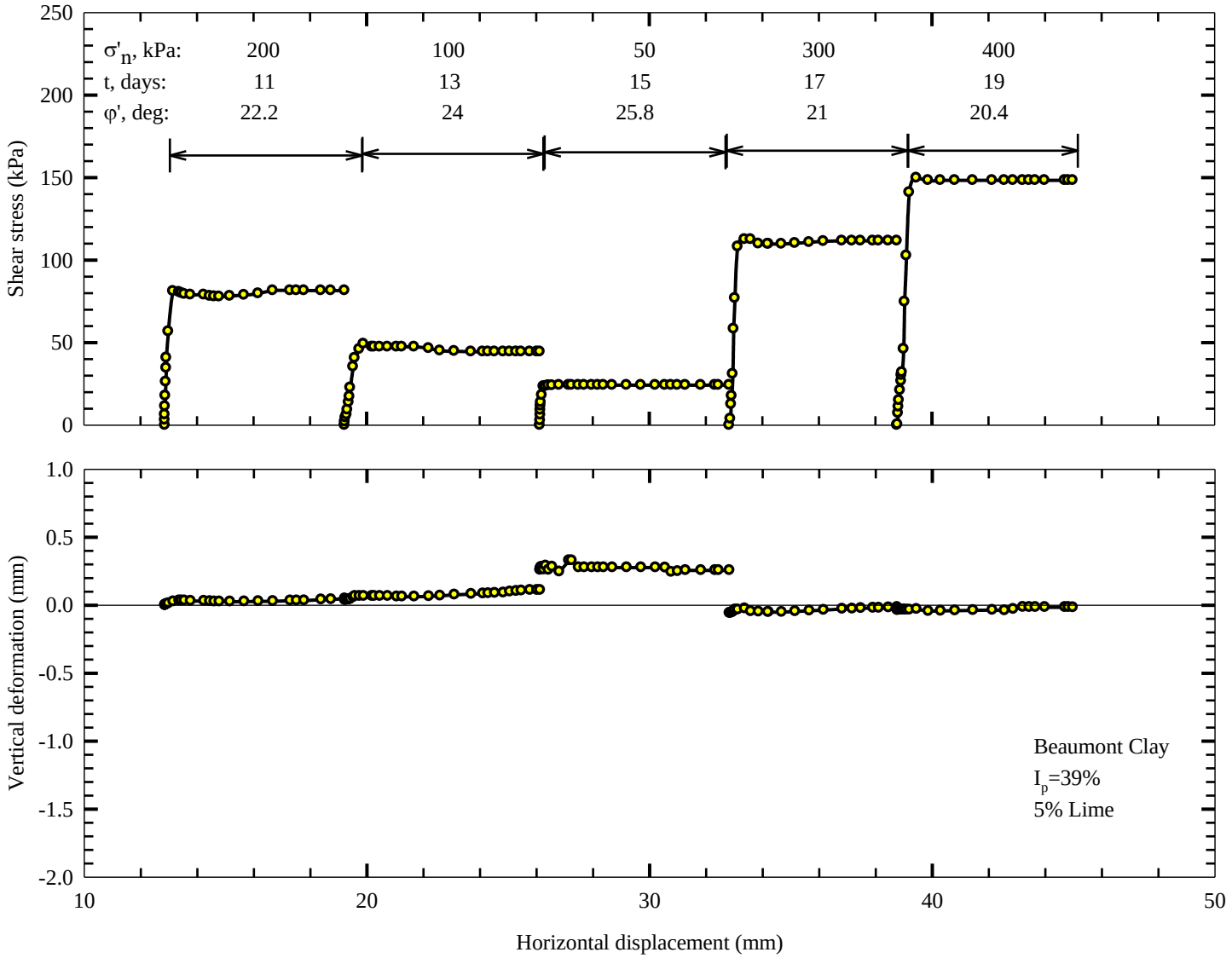

Figure 5.46: Shear stress-shear displacement and vertical displacement-shear displacement curves for Specimen 116 (after an intact specimen was cut); manually reversed

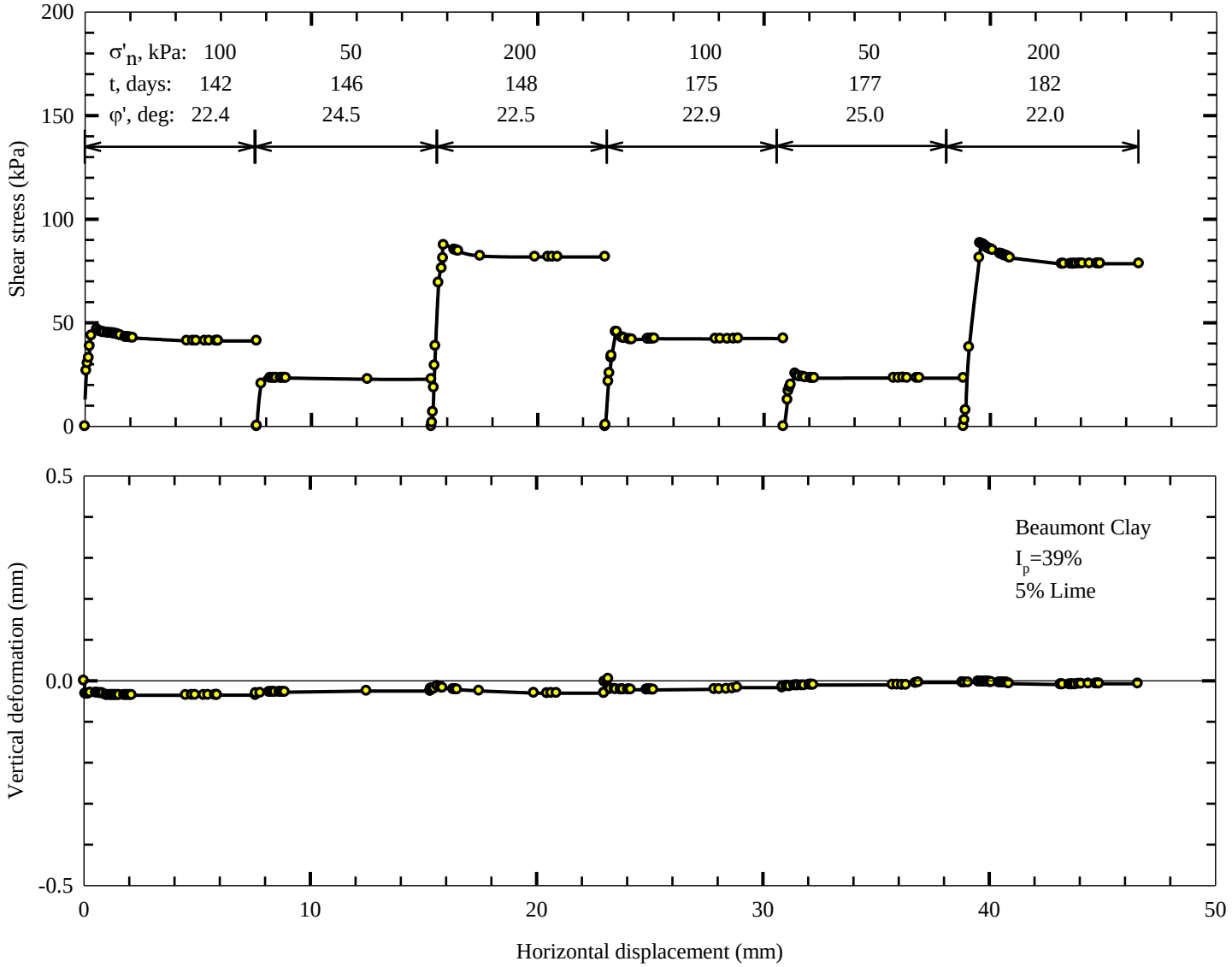

Figure 5.47: Shear stress-shear displacement and vertical displacement-shear displacement curves for Specimen 117 (precut); manually reversed

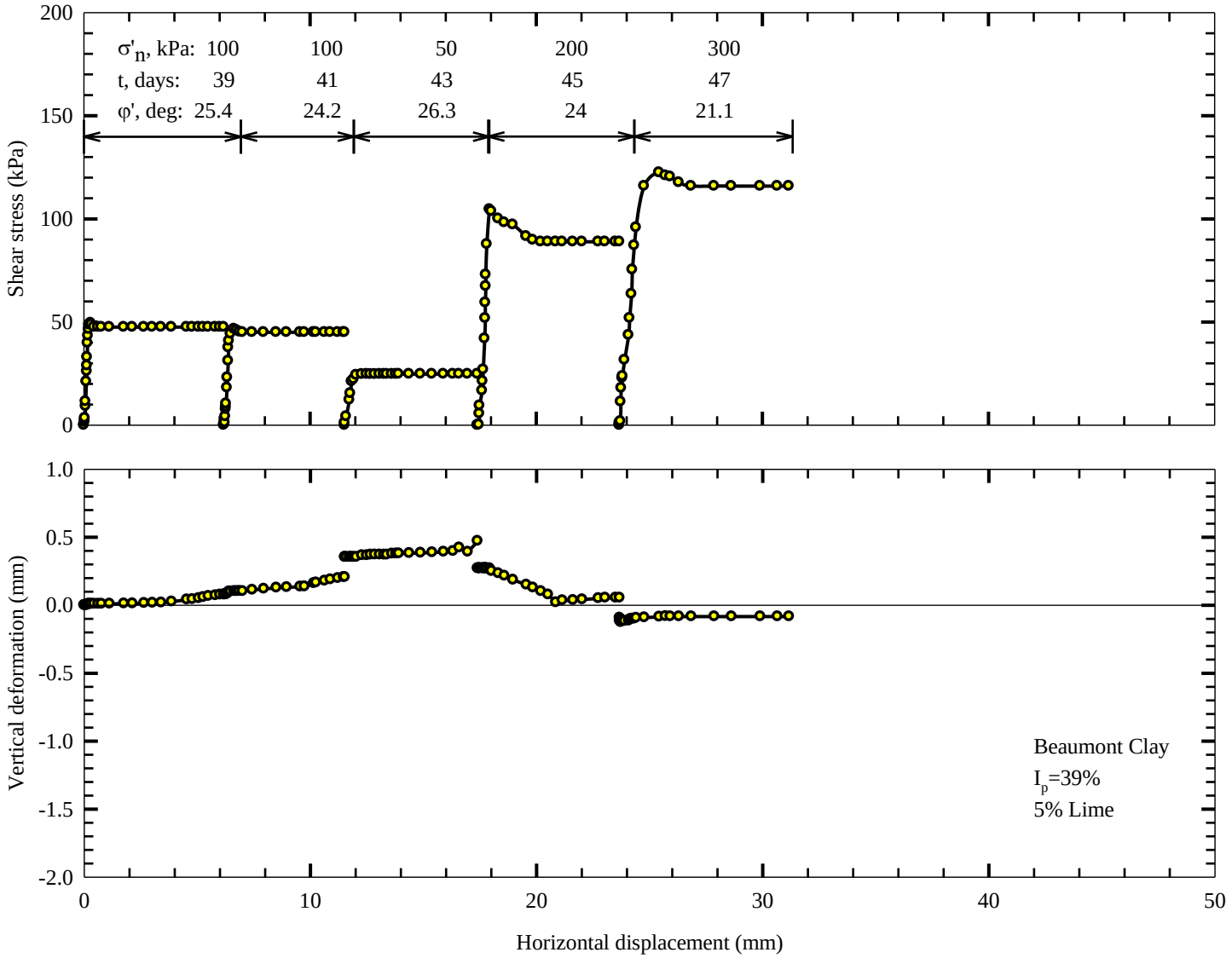

Figure 5.48: Shear stress-shear displacement and vertical displacement-shear displacement curves for Specimen 118 (precut); manually reversed

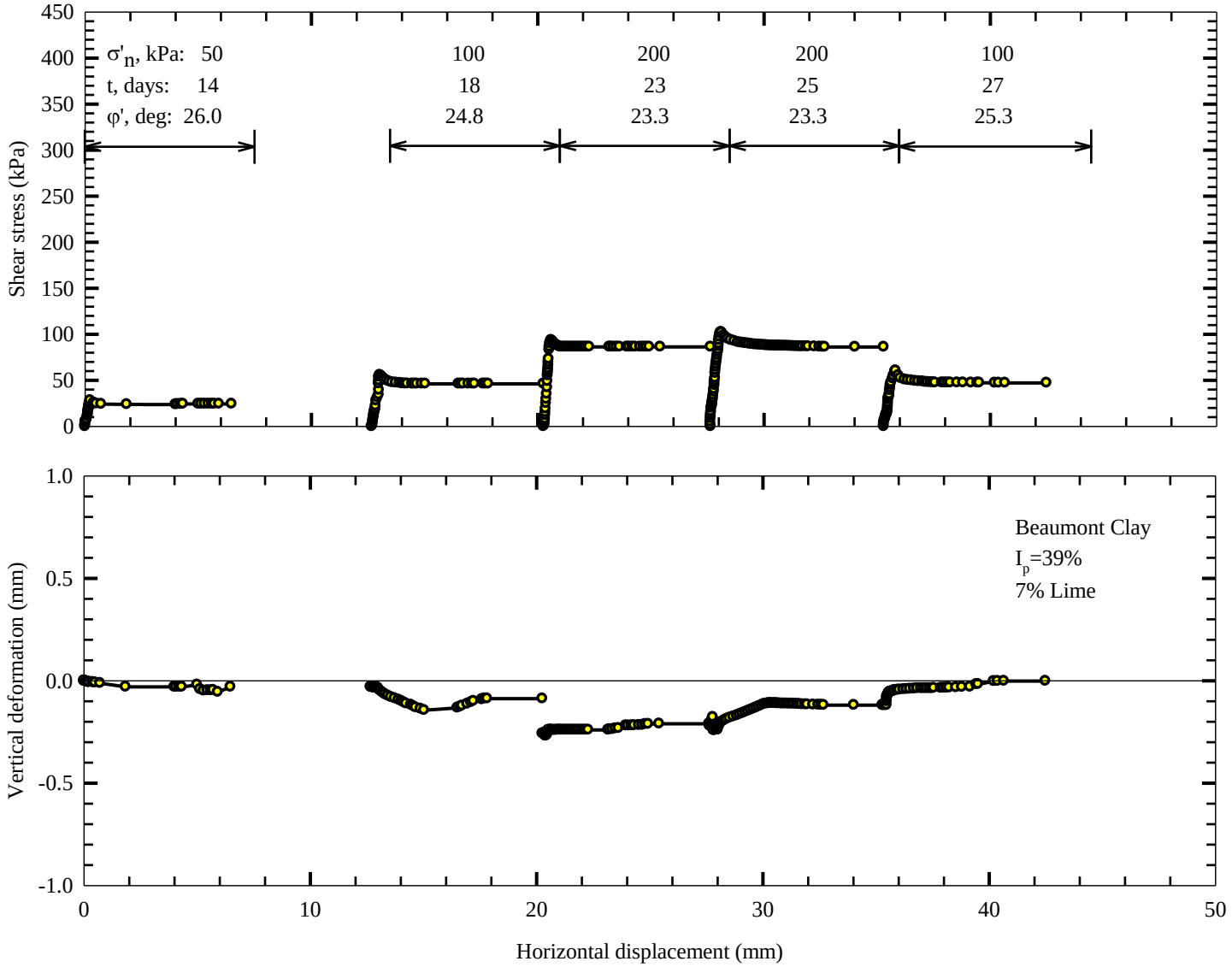

Figure 5.49: Shear stress-shear displacement and vertical displacement-shear displacement curves for Specimen 119 (precut); manually reversed; one forward under low effective normal stress not shown due to rotation of top half

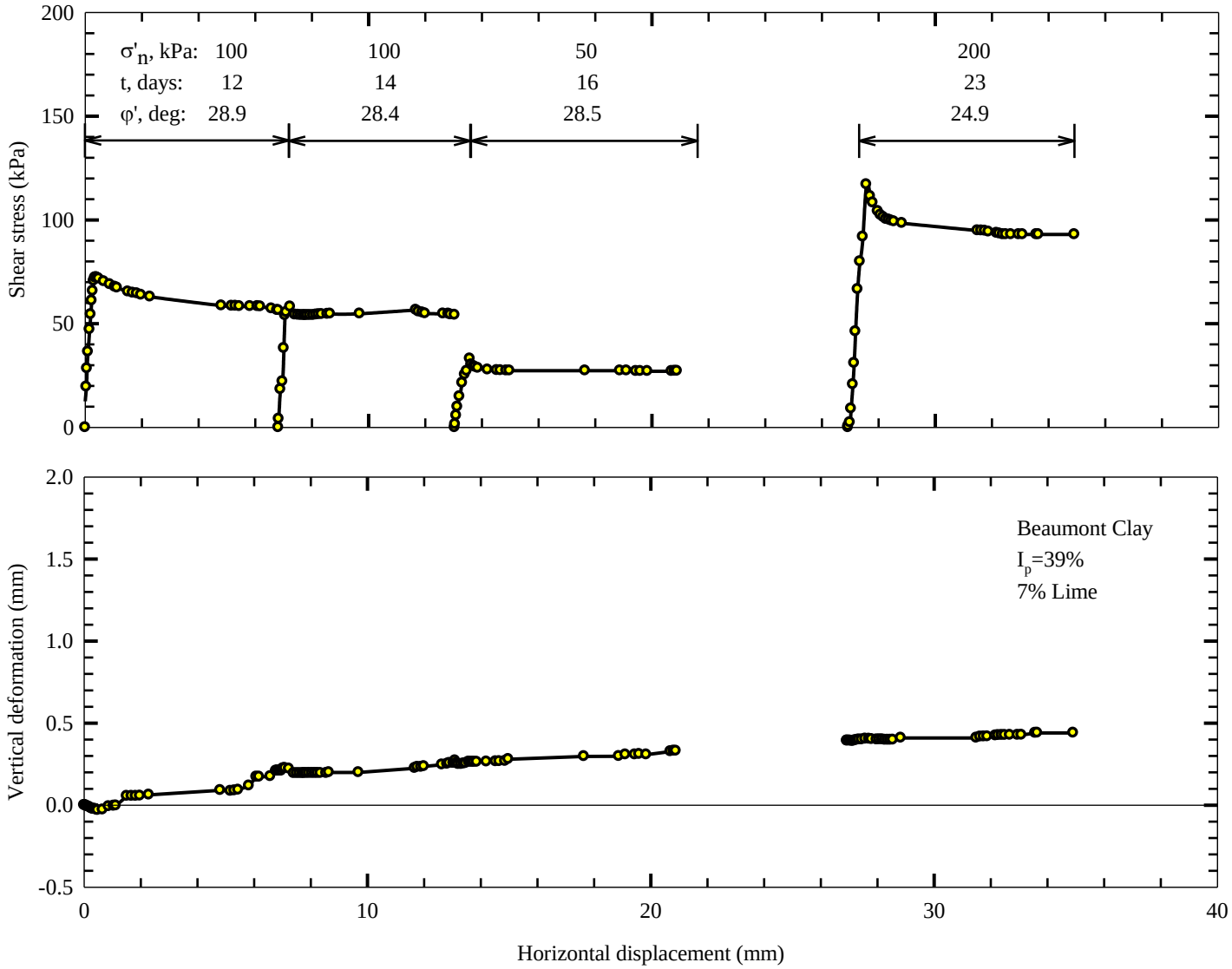

Figure 5.50: Shear stress-shear displacement and vertical displacement-shear displacement curves for Specimen 120 (precut); manually reversed; one forward under low effective normal stress not shown due to rotation of top half

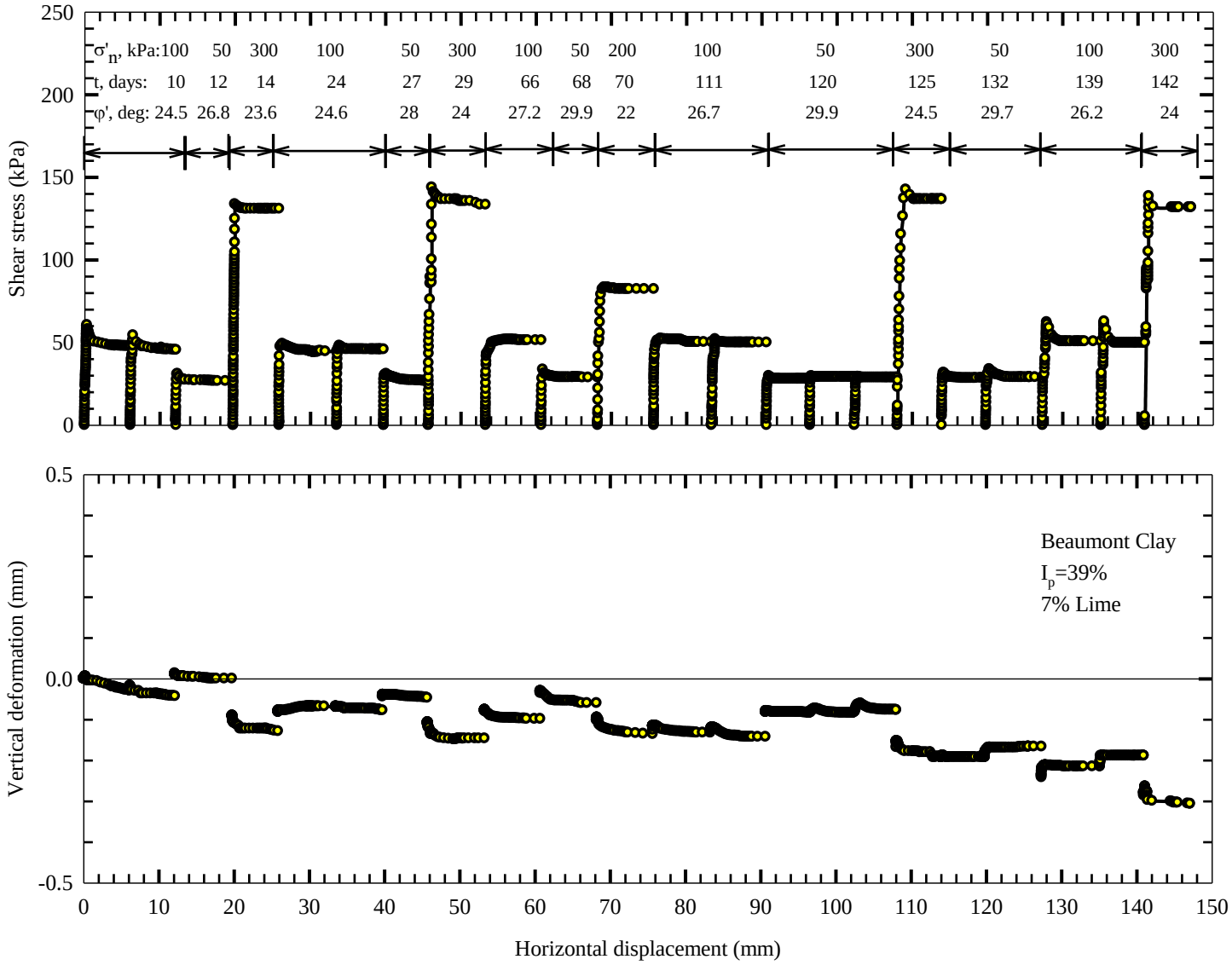

Figure 5.51: Shear stress-shear displacement and vertical displacement-shear displacement curves for Specimen 121(precut); manually reversed

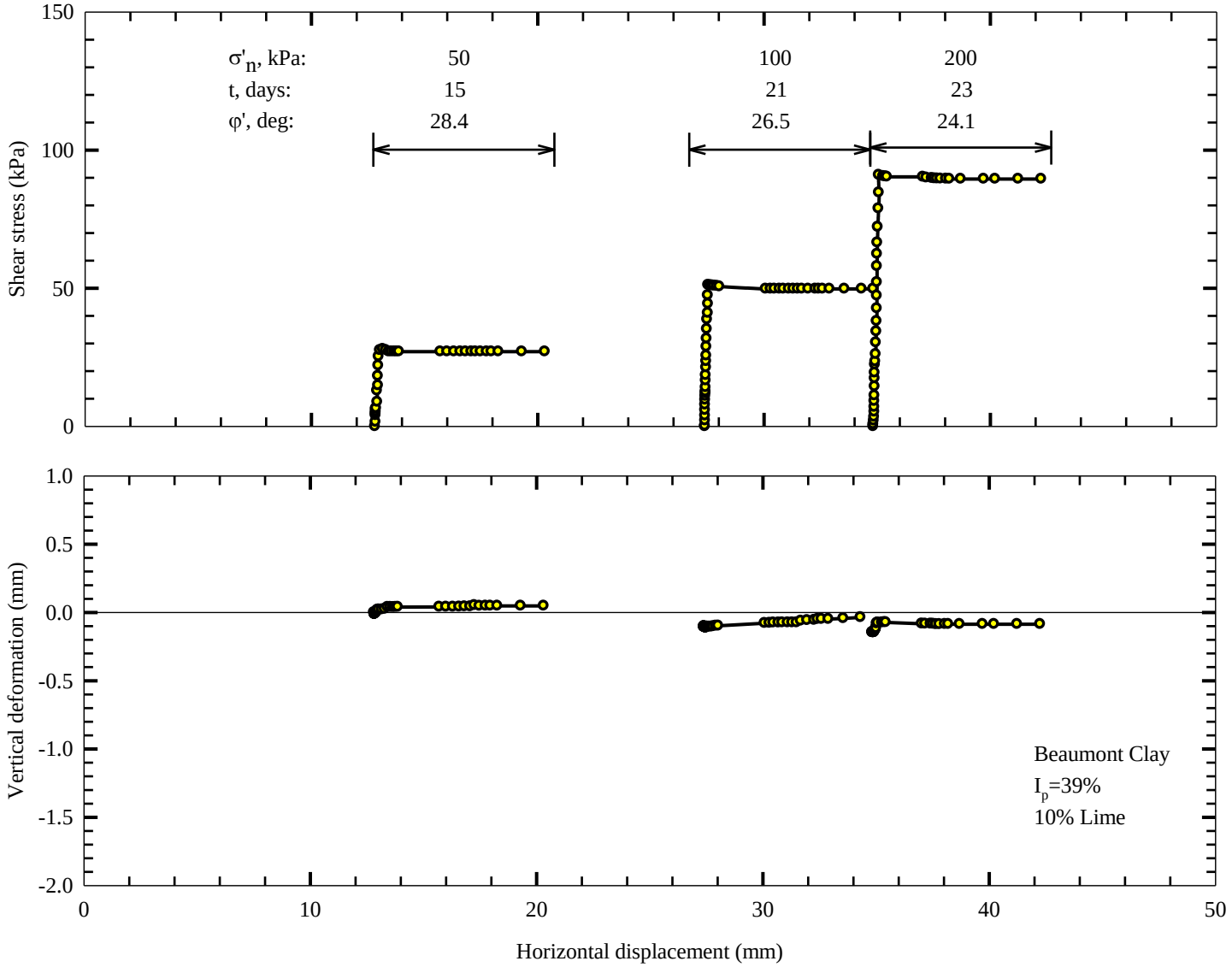

Figure 5.52: Shear stress-shear displacement and vertical displacement-shear displacement curves for Specimen 122 (an intact specimen was cut); manually reversed; one forward under low effective normal stress not shown due to rotation of top half

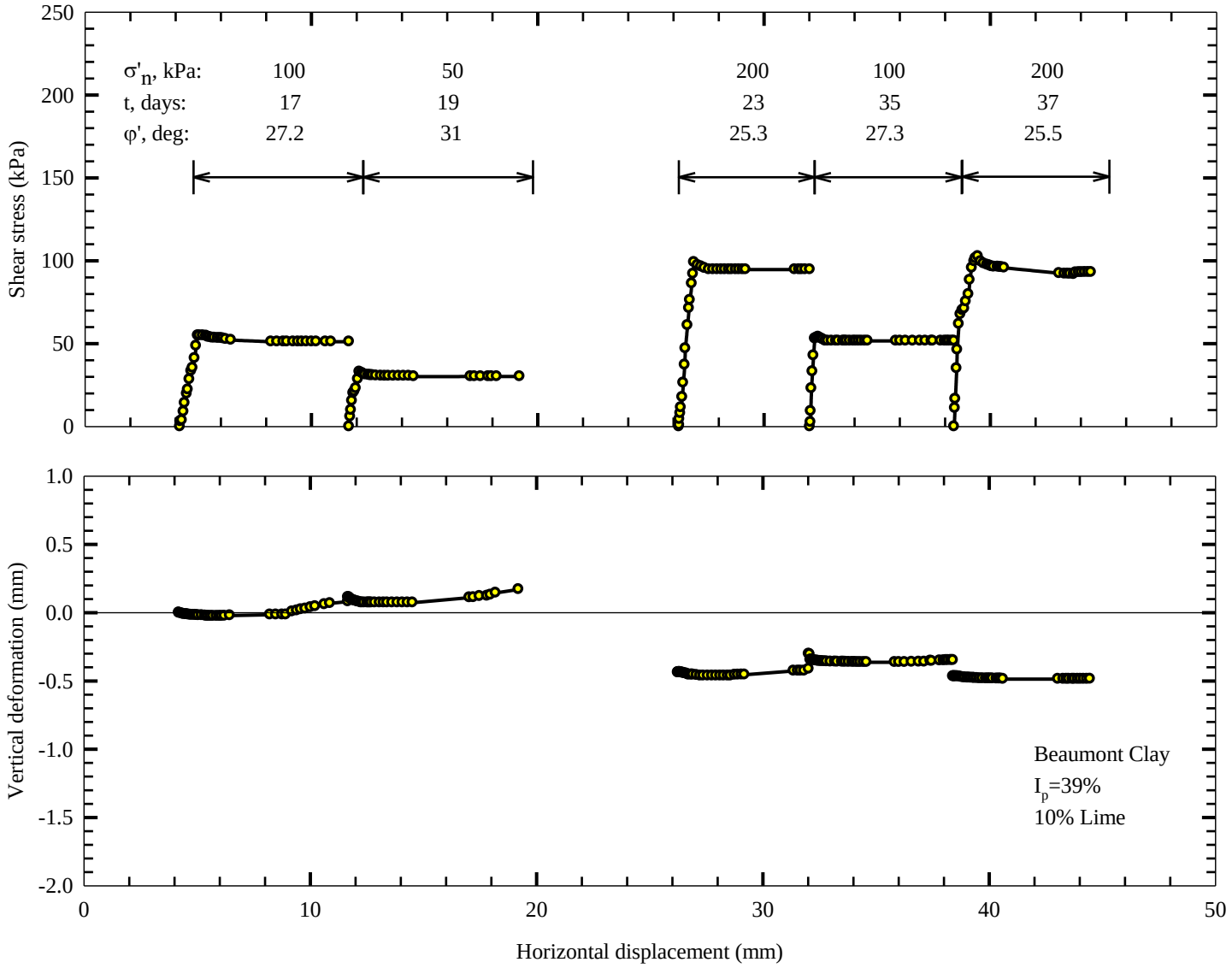

Figure 5.53: Shear stress-shear displacement and vertical displacement-shear displacement curves for Specimen 123 (an intact specimen was cut); manually reversed; one forward under low effective normal stress not shown due to rotation of top half

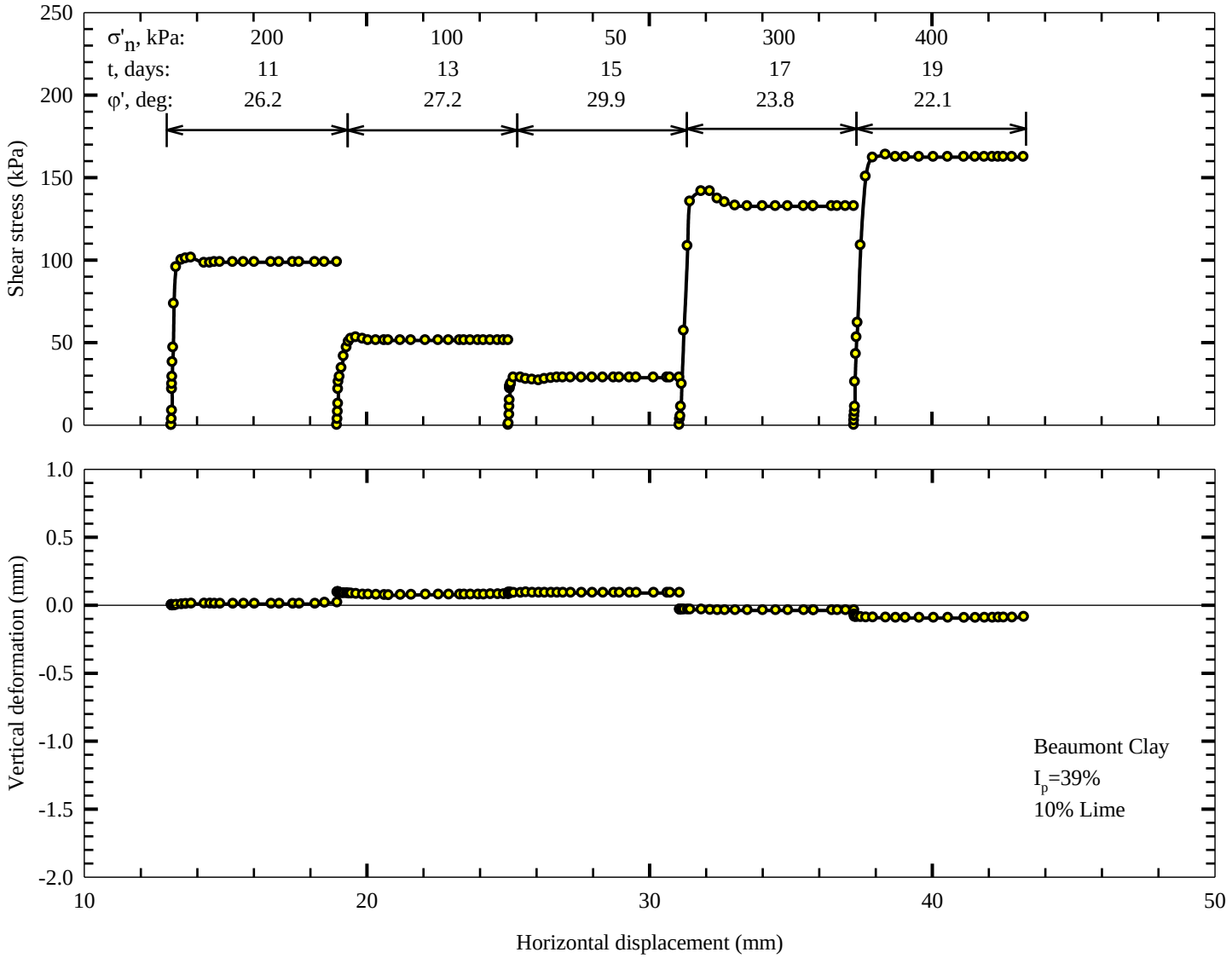

Figure 5.54: Shear stress-shear displacement and vertical displacement-shear displacement curves for Specimen 124 (an intact specimen was cut); manually reversed

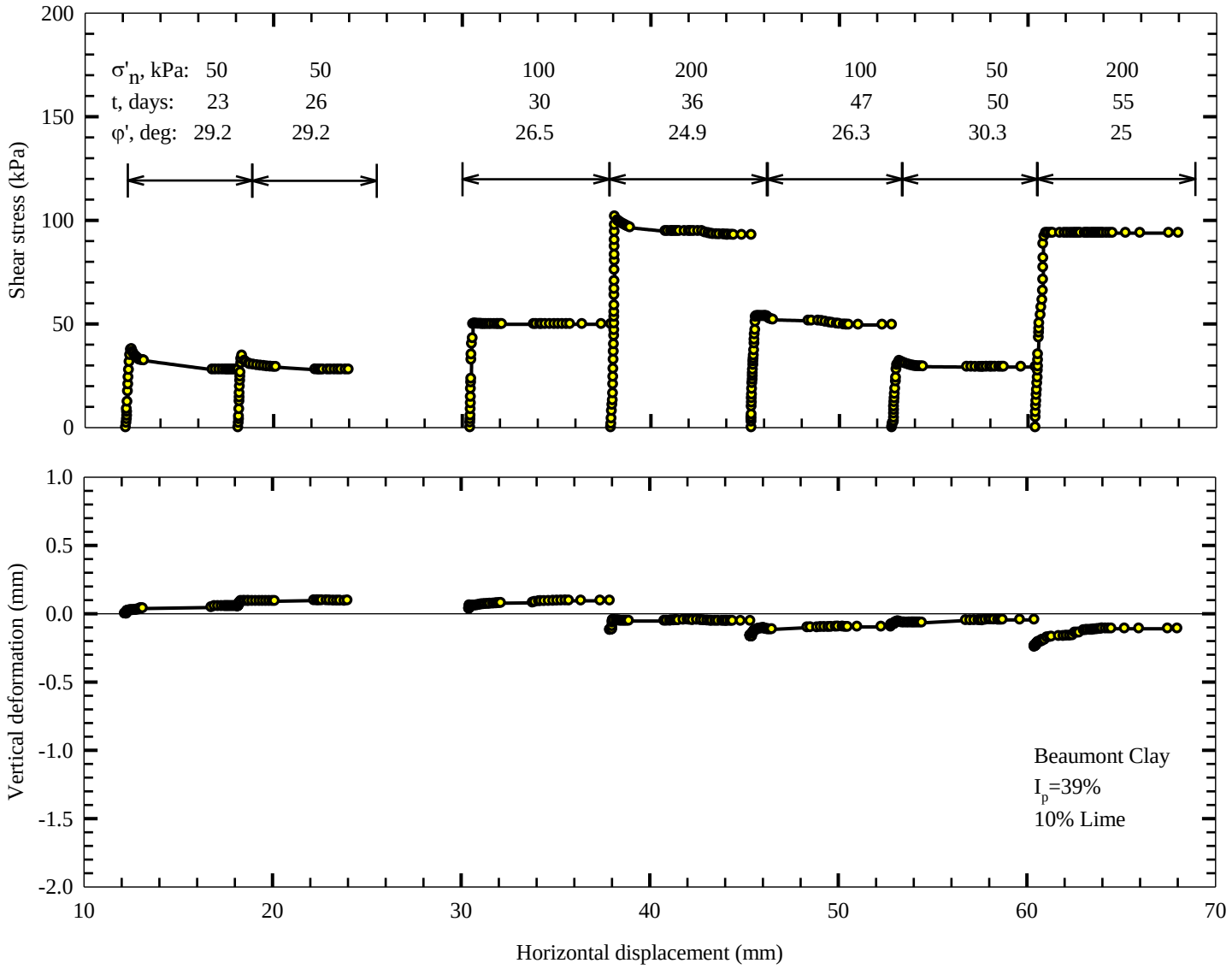

Figure 5.55: Shear stress-shear displacement and vertical displacement-shear displacement curves for Specimen 125 (an intact specimen was cut); manually reversed; one forward under low effective normal stress not shown due to rotation of top half

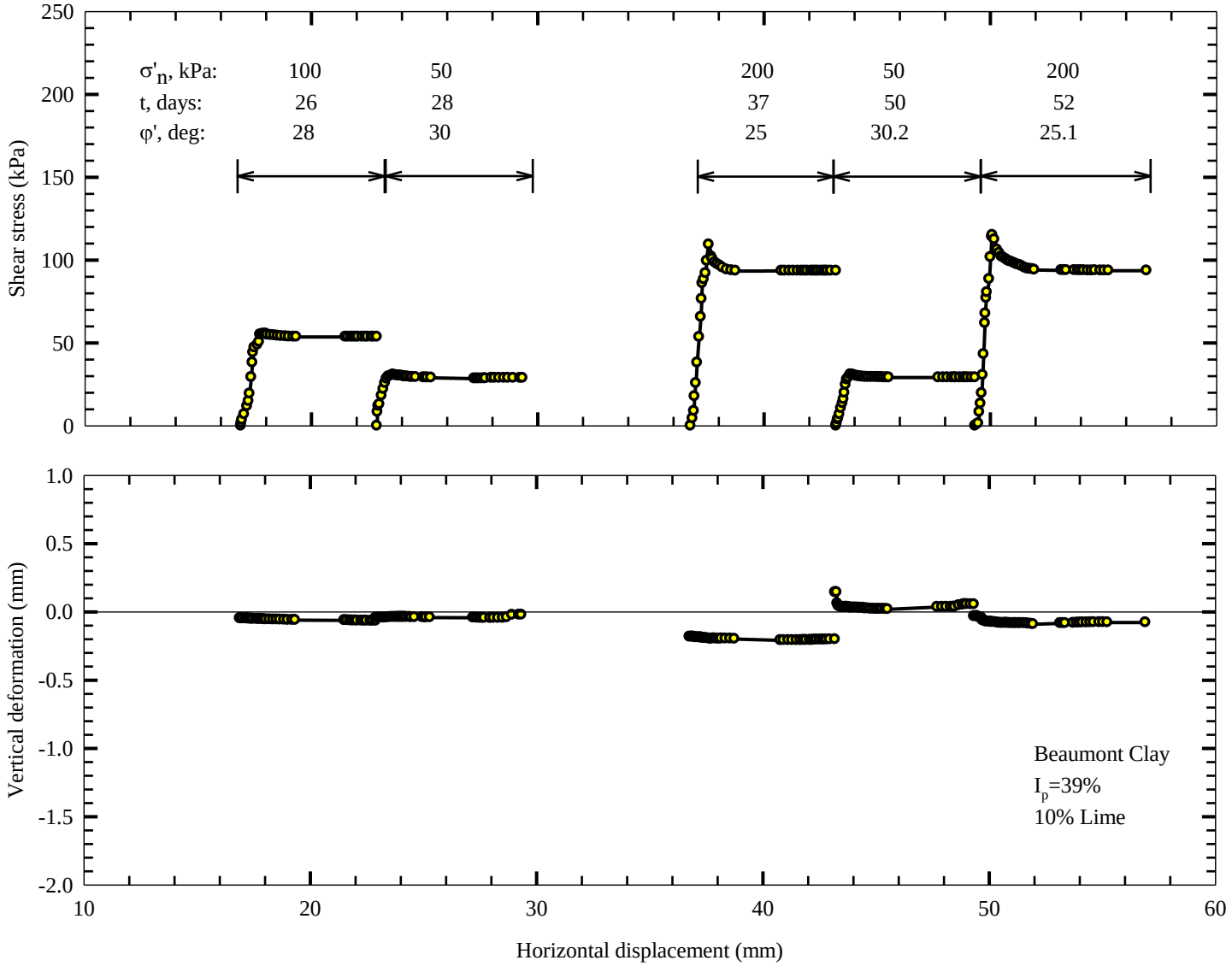

Figure 5.56: Shear stress-shear displacement and vertical displacement-shear displacement curves for Specimen 126 (an intact specimen was cut); manually reversed; one forward under low effective normal stress not shown due to rotation of top half

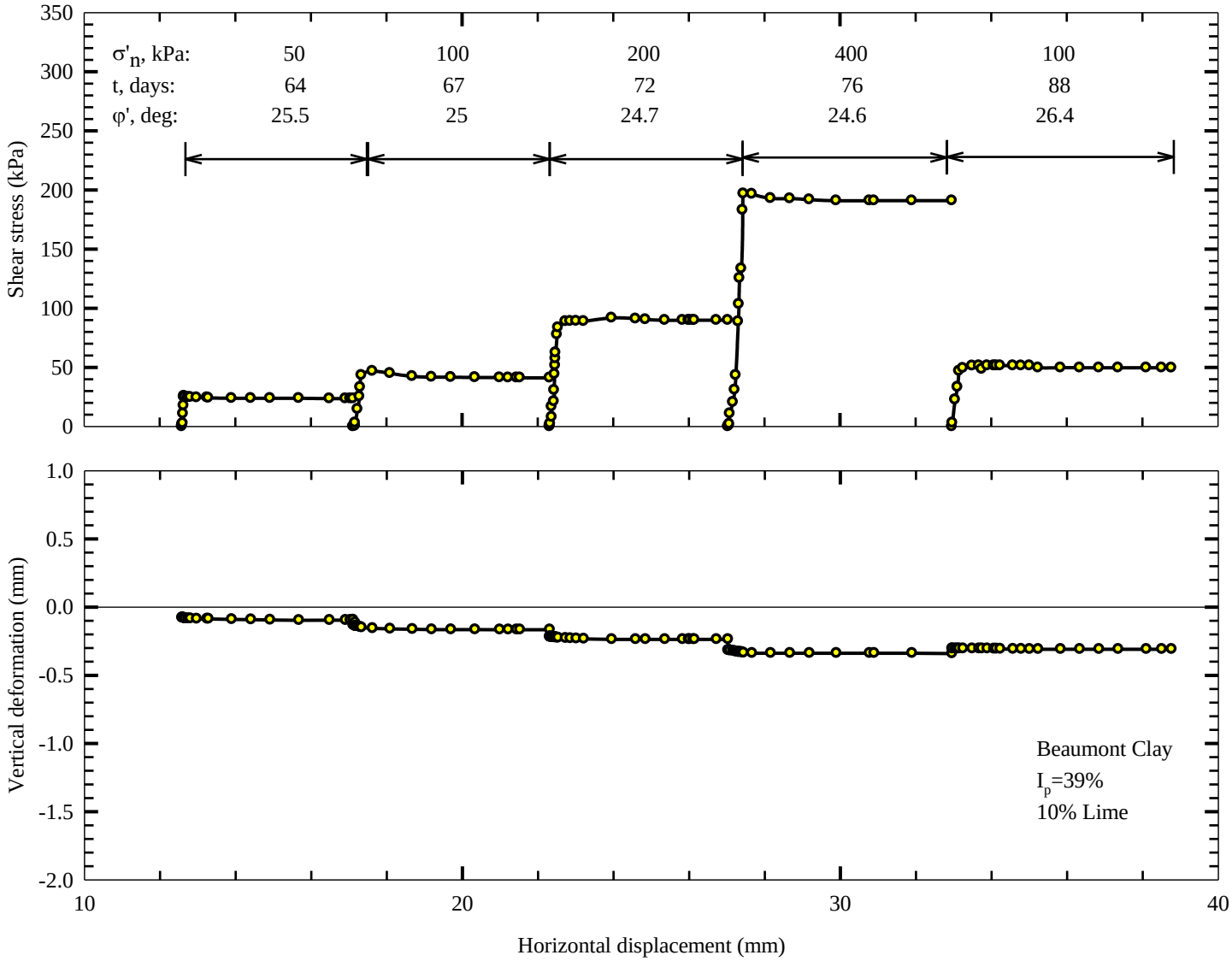

Figure 5.57: Shear stress-shear displacement and vertical displacement-shear displacement curves for Specimen 127 (an intact specimen was cut); manually reversed

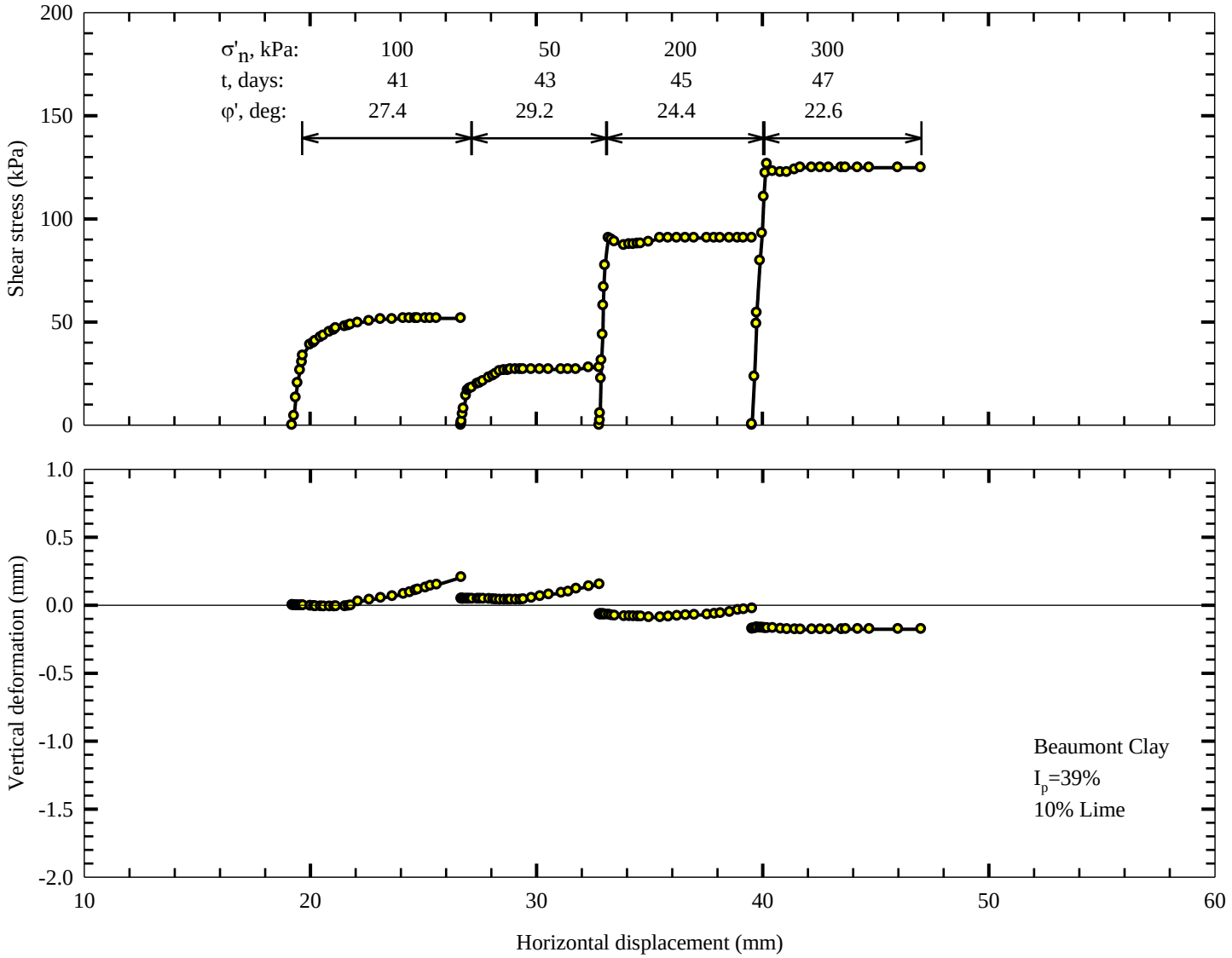

Figure 5.58: Shear stress-shear displacement and vertical displacement-shear displacement curves for Specimen 128 (an intact specimen was cut); manually reversed

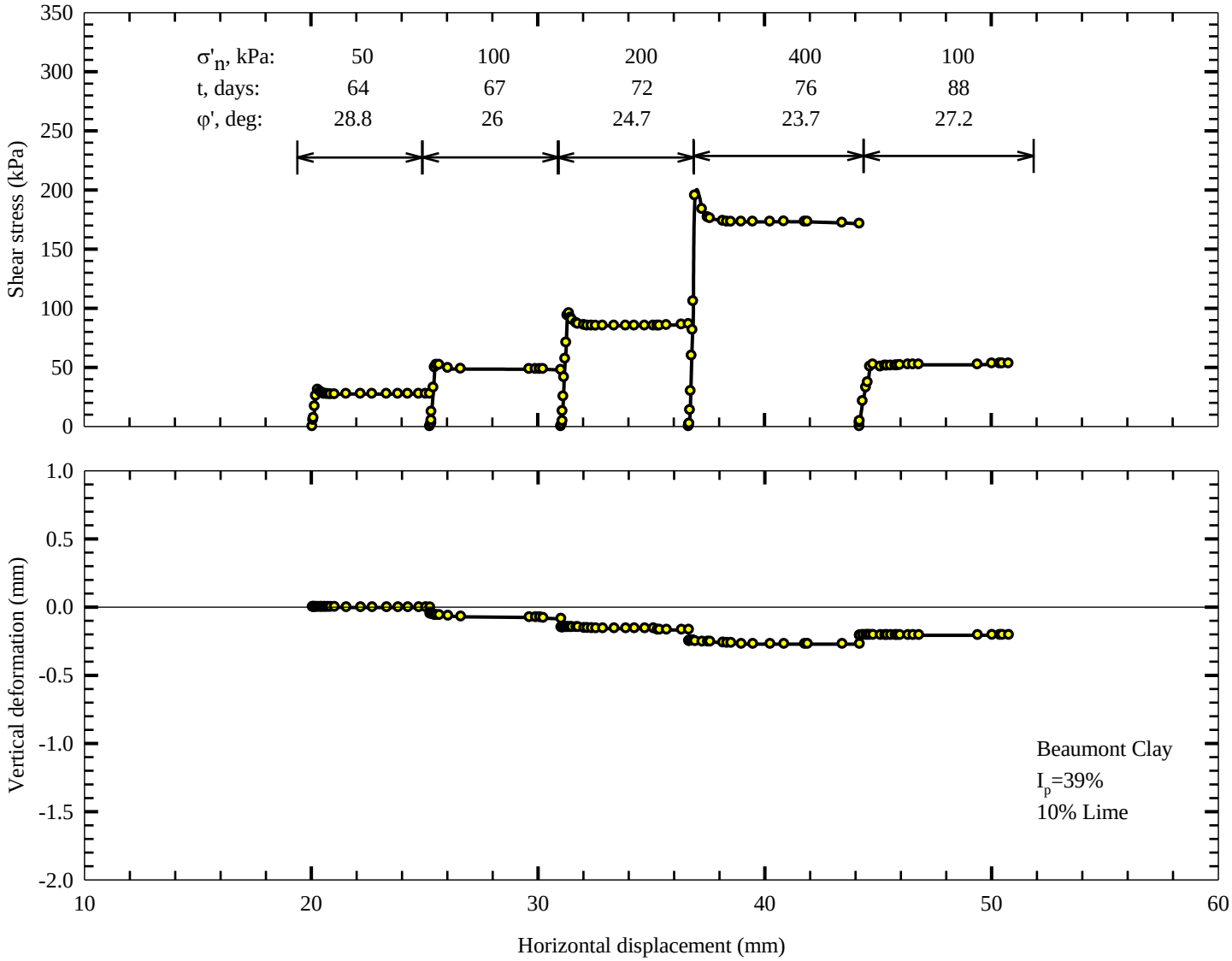

Figure 5.59: Shear stress-shear displacement and vertical displacement-shear displacement curves for Specimen 129 (an intact specimen was cut); manually reversed

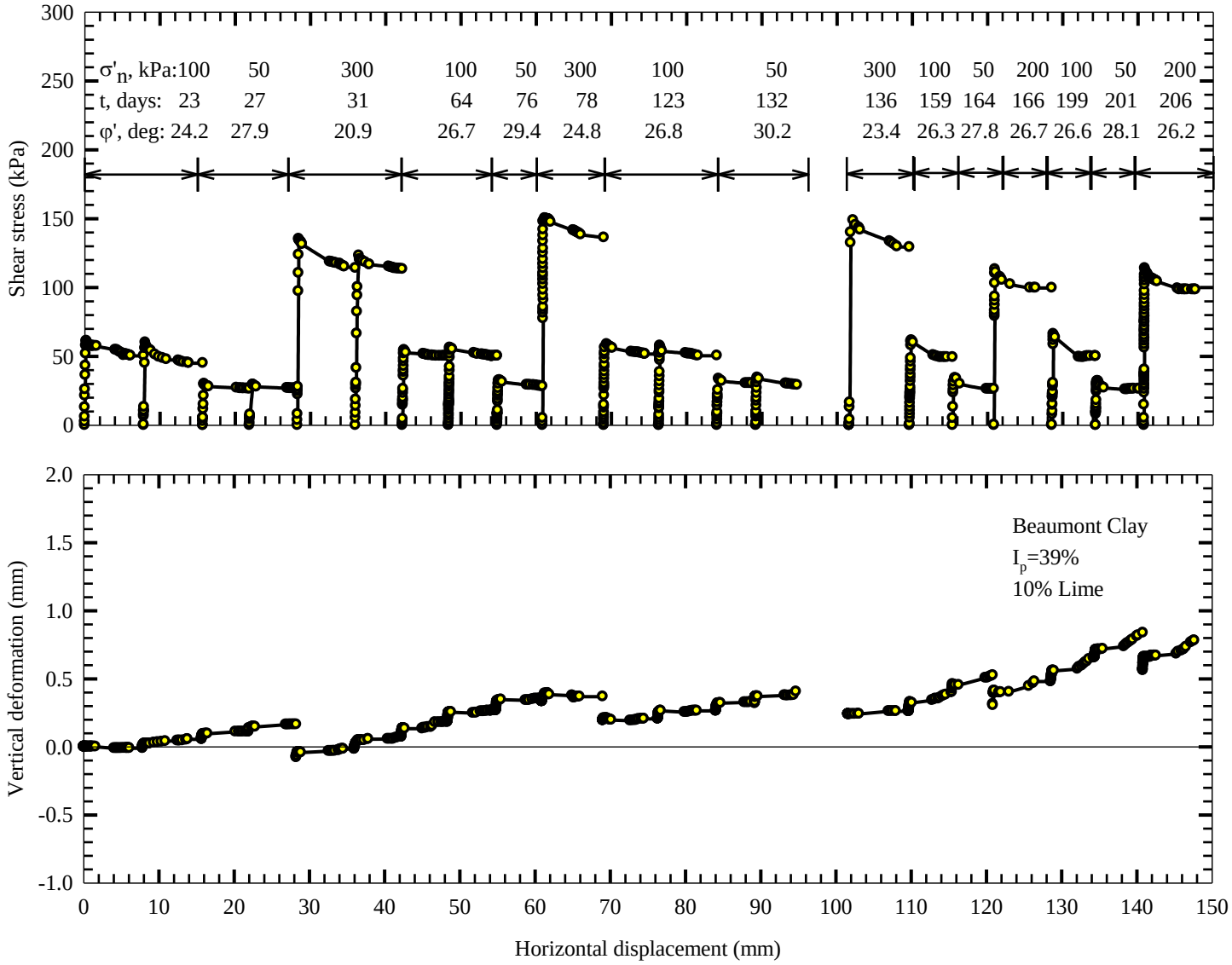

Figure 5.60: Shear stress-shear displacement and vertical displacement-shear displacement curves for Specimen 130 (precut); manually reversed; one forward under low effective normal stress not shown due to rotation of top half

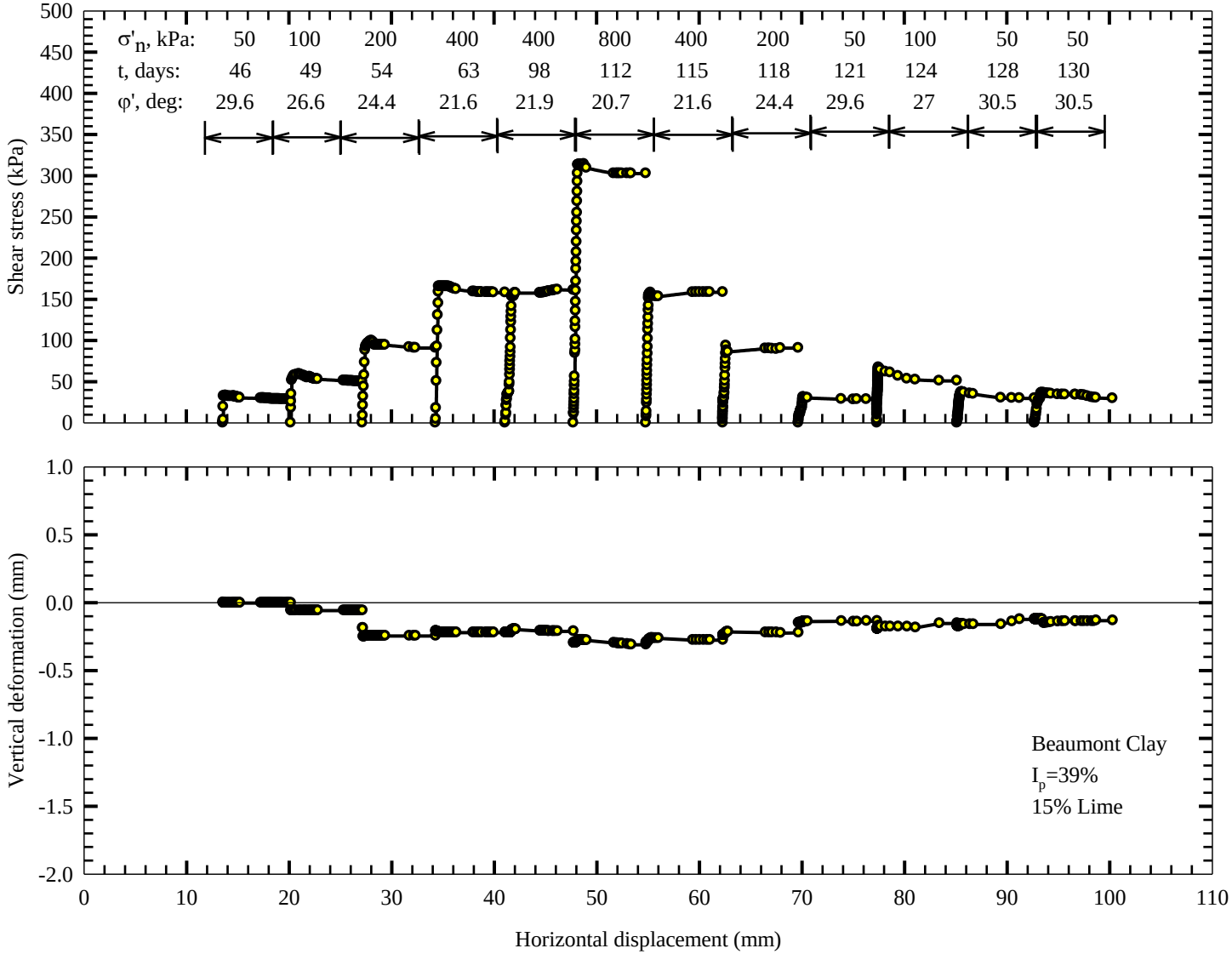

Figure 5.61: Shear stress-shear displacement and vertical displacement-shear displacement curves for Specimen 131(an intact specimen was cut); manually reversed

5.2 RESIDUAL SHEAR STREGTH WITH CURING TIME

The results of the tests on the precut specimens were used to investigate the effect of curing time on the residual strength of treated clays. The test results performed on the precut specimens of Chicago clay show that the secant residual friction angle of Chicago clay increases in the first few days after treatment and remains relatively constant as curing time increases, as shown in Figure 5.62 for 3% lime content. The secant residual friction angle of Lower Brenna clay also increases in a few days after treatment and remains relatively constant as curing time increases. For example, the secant residual friction angle of 7% lime treated Lower Brenna clay reaches its maximum in the first or second week of curing, as shown in Figure 5.63. The secant residual friction angle of 10% lime treated Lower Brenna clay increases gradually with curing time and reaches its maximum in two weeks or earlier, as shown in Figure 5.64. No further increase is observed as curing time increases.

The increase in the secant residual friction angle of Beaumont clay treated with 5%, 7% and 10% lime with time is shown in Figures 5.65-5.67, respectively. The data pertain to curing periods up to 180 days and effective normal stresses ranging from 50 to 300 kPa. The secant residual friction angle increases substantially within the first or second week of curing and remains more or less constant with time. The residual strength is controlled by the degree of aggregation which takes place at early stages of treatment and remains constant, whereas the peak (intact) shear strength is controlled by both aggregation and inter-aggregation bonds, with latter improving with time, as shown in Figures 4.56-4.60.

The increase in the secant residual friction angle of Chicago clay treated with 3% lime, and Lower Brenna and Beaumont clays treated with 7% lime is shown Figure 5.68 as curing time increases. A major increase in the secant residual friction angle takes place during the first week of curing as aggregation occurs inside floccules. As curing time increases, A slight increase in the secant residual friction angle is achieved owing to inter-aggregate bonds which do not contribute to the residual strength.

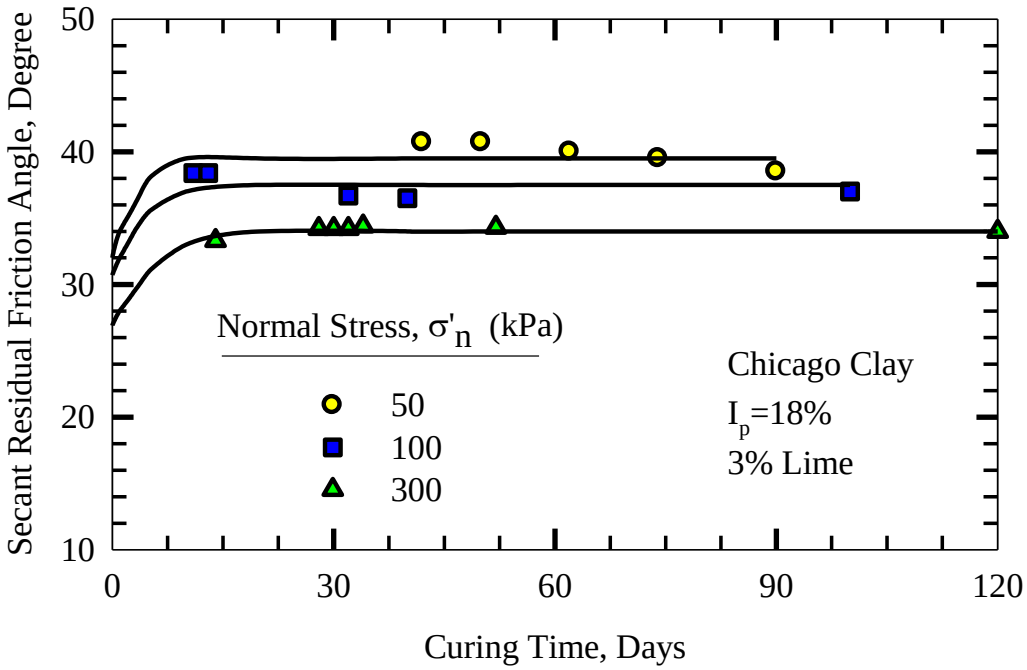

Figure 5.62: Secant residual friction angle plotted against time for 3% lime-Chicago clay

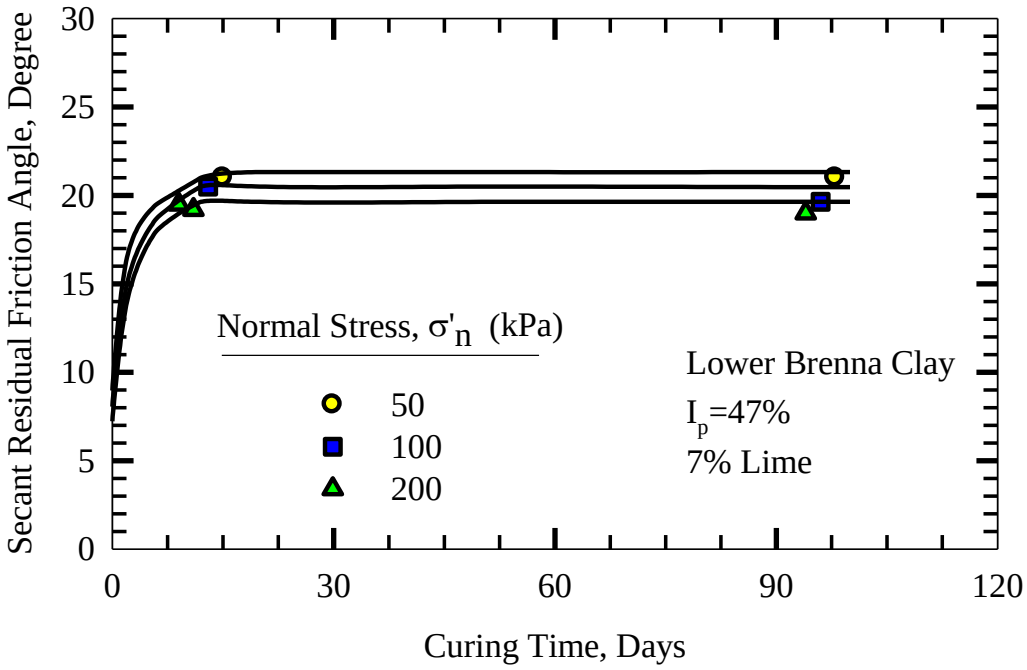

Figure 5.63: Secant residual friction angle plotted against time for 7% lime-Lower Brenna clay

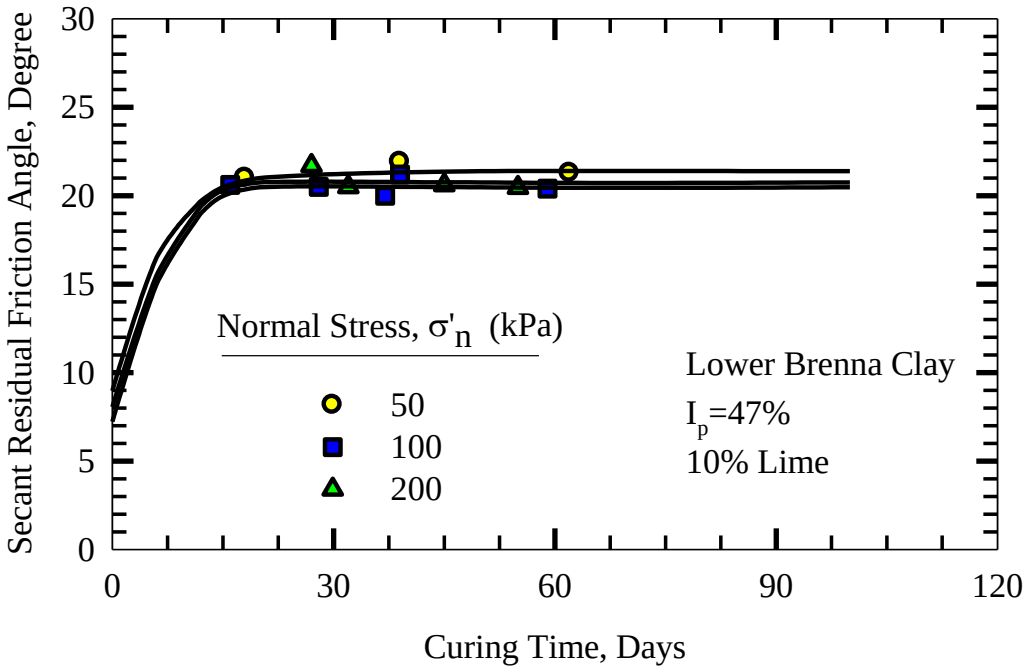

Figure 5.64: Secant residual friction angle plotted against time for 10% lime-Lower Brenna clay

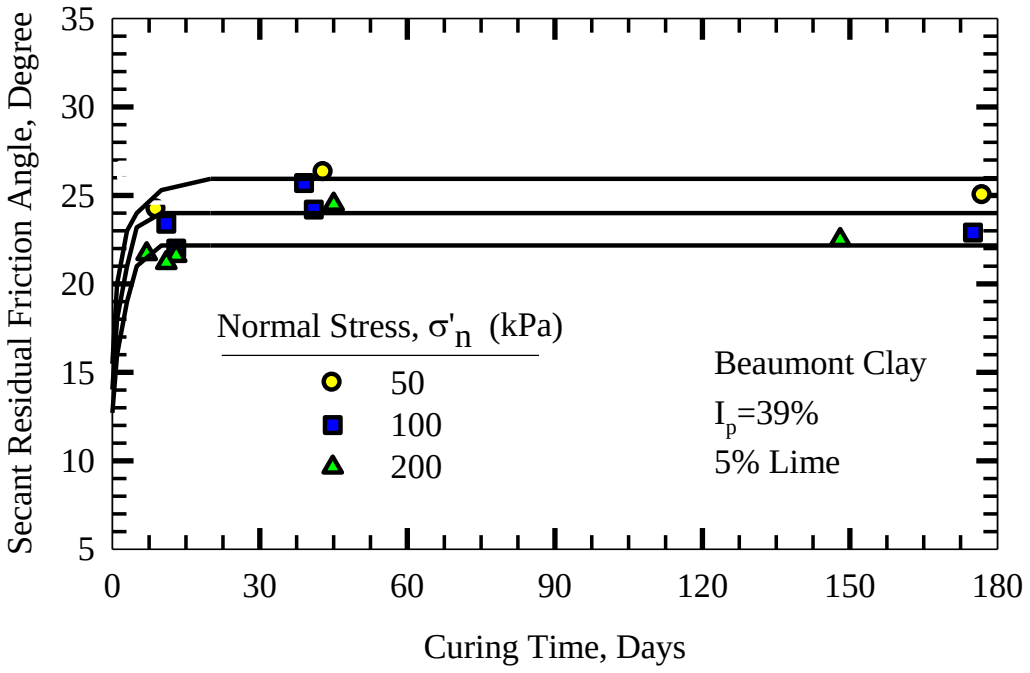

Figure 5.65: Secant residual friction angle plotted against time for 5% lime-Beaumont clay

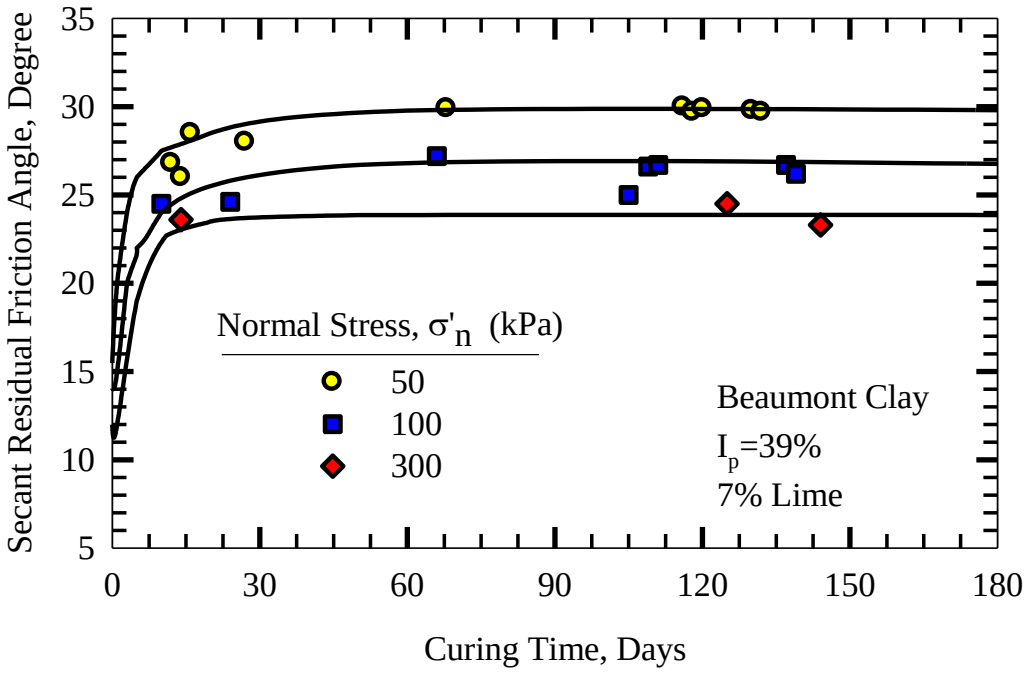

Figure 5.66: Secant residual friction angle plotted against time for 7% lime-Beaumont clay

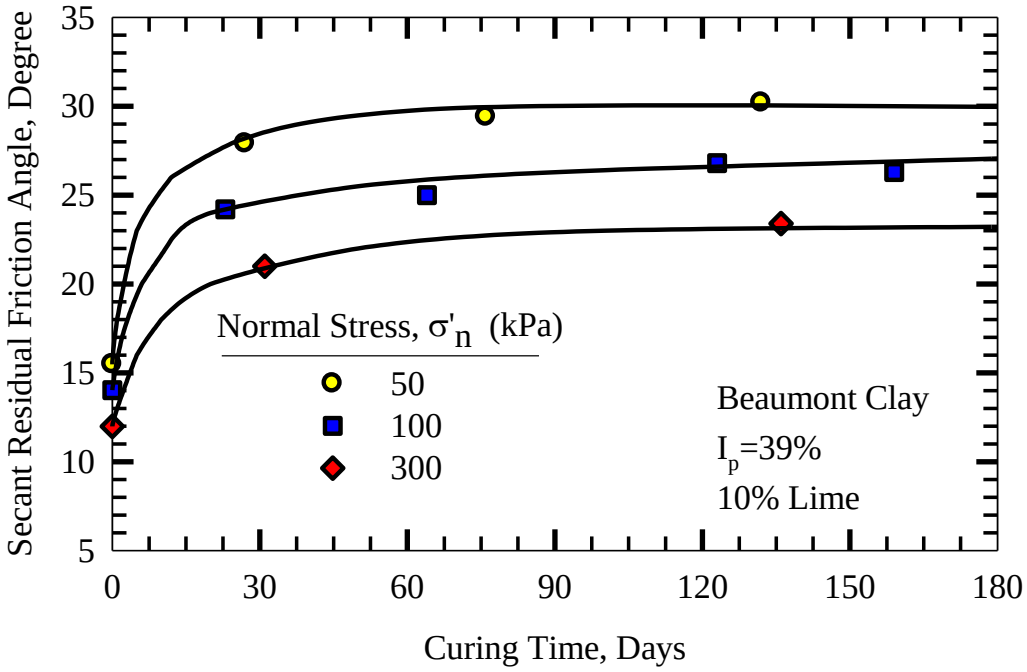

Figure 5.67: Secant residual friction angle plotted against time for 10% lime-Beaumont clay

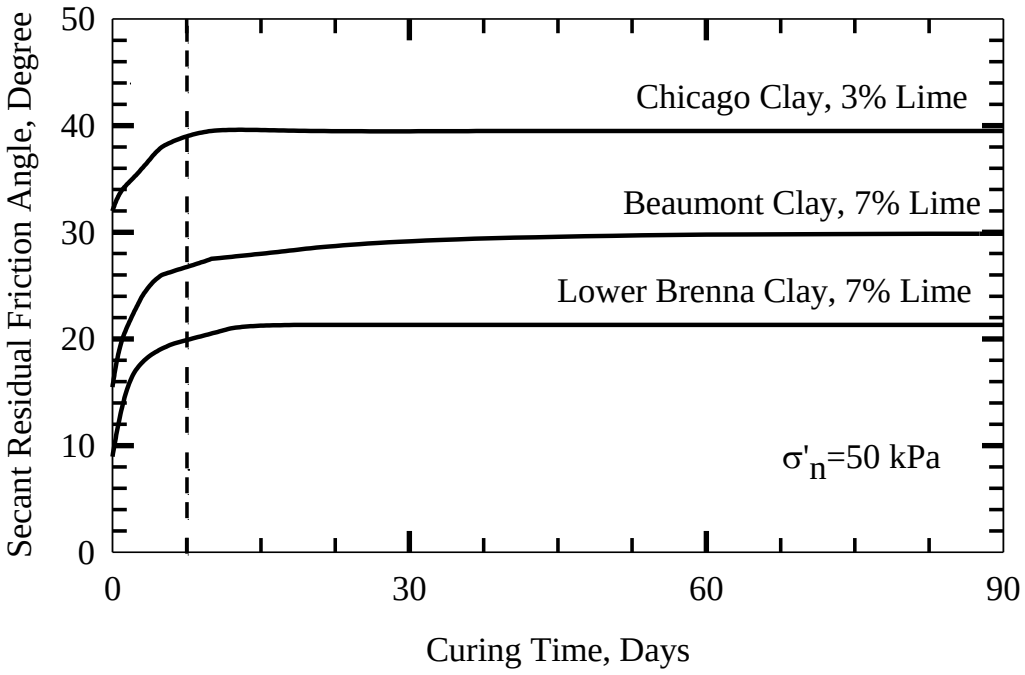

Figure 5.68: Secant residual friction angle plotted against time for various treated clays

5.3 RESIDUAL SHEAR STREGTH ENVELOPES

Residual shear strength envelopes of Chicago clay treated with lime contents in the range of 1-10% are shown in Figures 5.69-5.73. Improvement in the residual friction angle is observed for a lime content as low as 1%.

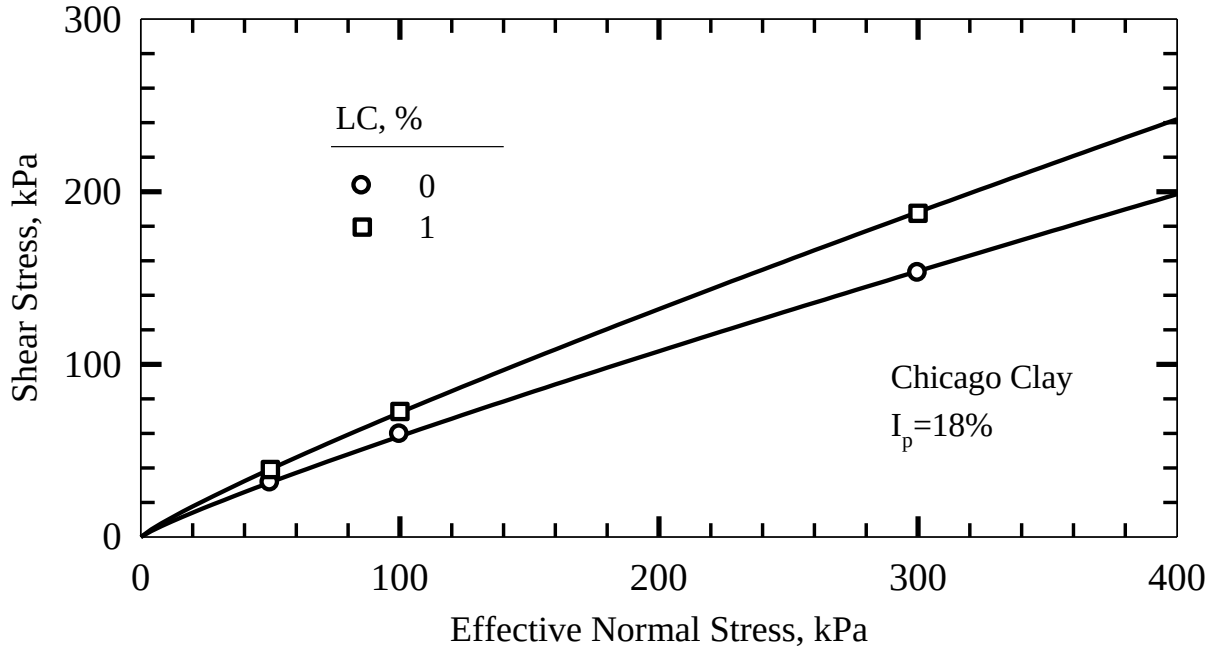

Figure 5.69: Residual shear strength envelopes for Chicago clay tretaed with 1% lime

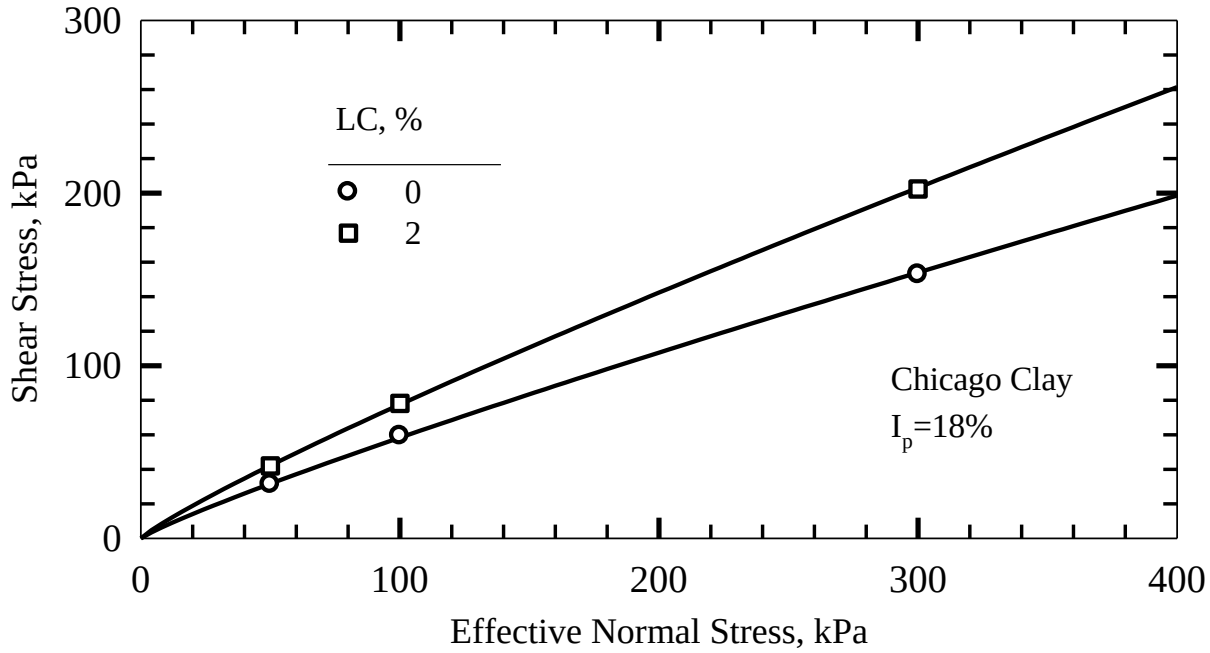

Figure 5.70: Residual shear strength envelopes for Chicago clay tretaed with 2% lime

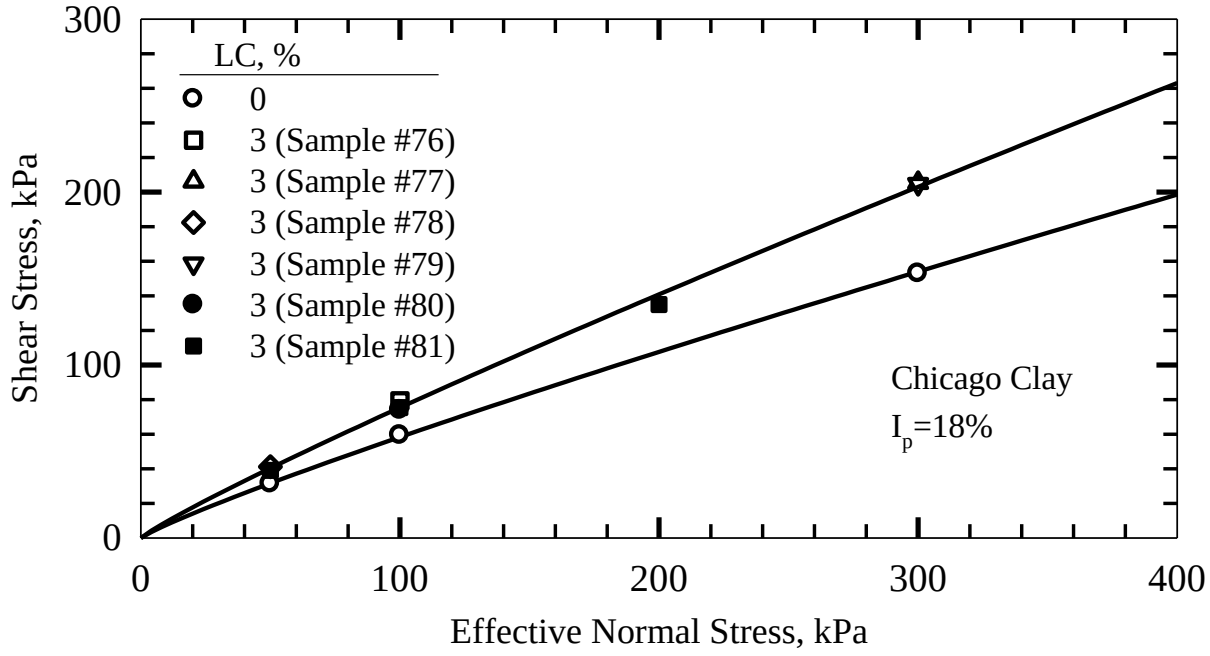

Figure 5.71: Residual shear strength envelopes for Chicago clay tretaed with 3% lime

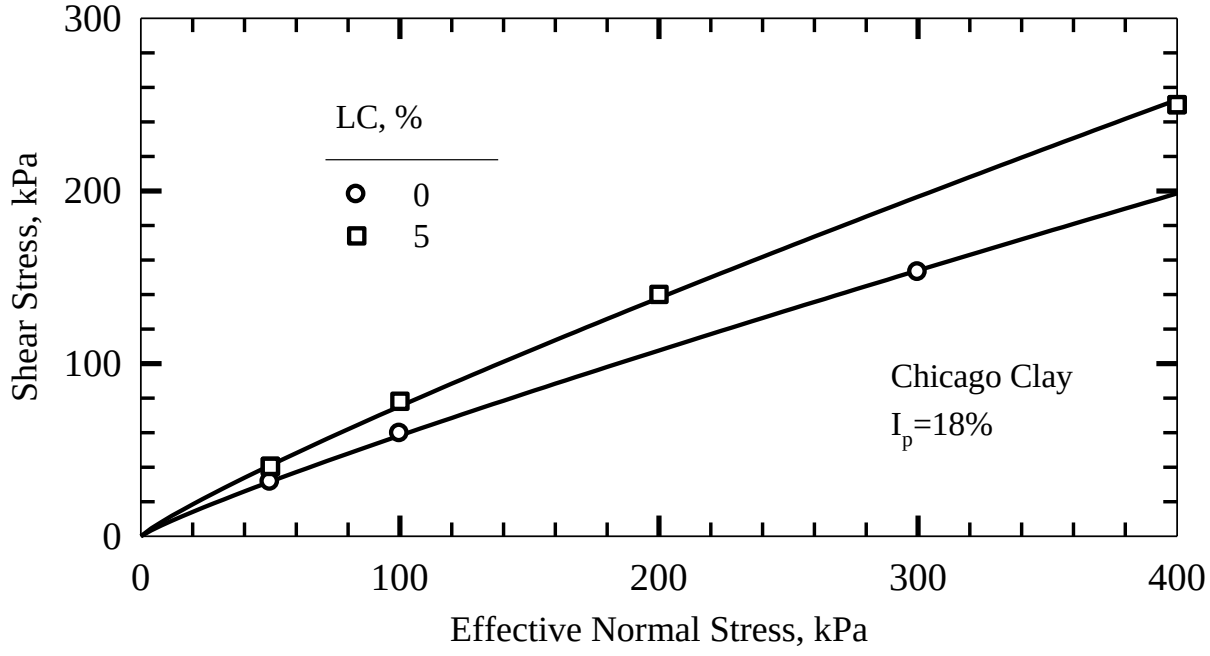

Figure 5.72: Residual shear strength envelopes for Chicago clay tretaed with 5% lime

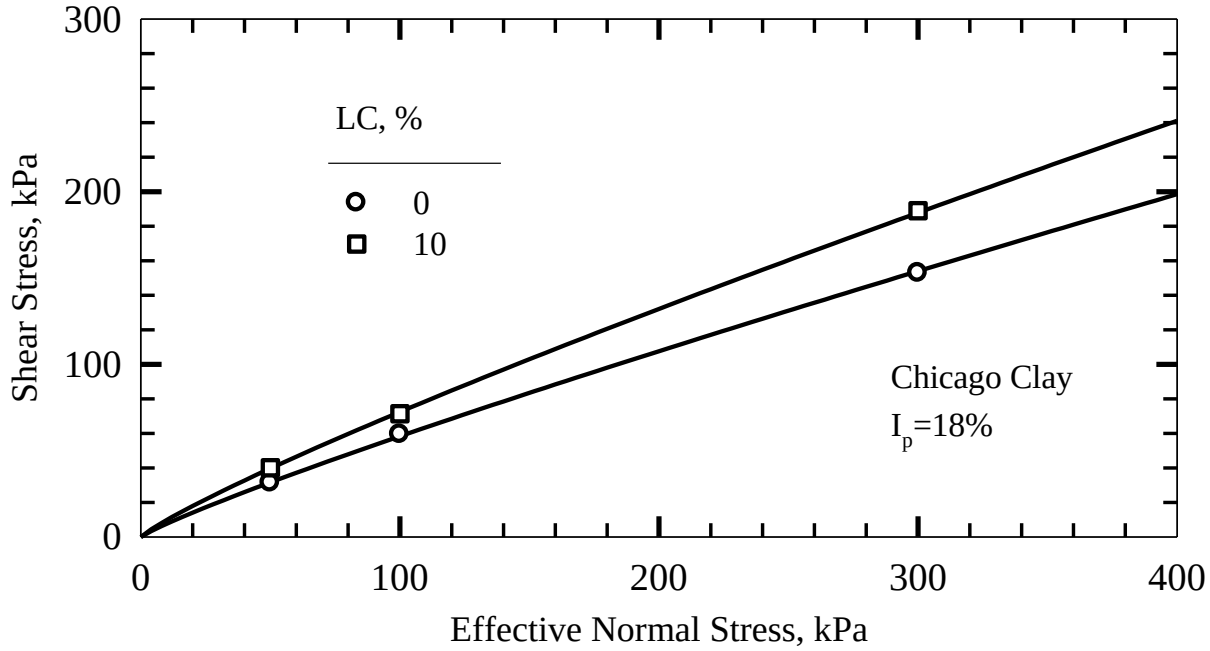

Figure 5.73: Residual shear strength envelopes for Chicago clay tretaed with 10% lime

Residual shear strength envelopes of Lower Brenna clay treated with lime contents in the range of 3-15% are shown in Figures 5.74-5.78. No major improvement in residual strength is observed for the specimen treated with 3% lime. For some of the lime contents (i.e., 5, 7, and 10%), the results of tests on more than one sample are plotted. All the specimens have the same lime contents, but their loading and curing history is different. The details of the properties of each sample is shown in Table 3.6. Despite some scatter, the data are in good agreement, implying a relatively similar secant residual friction angle for all the samples with the same lime content. The scatter is partly due to the data pertaining to short curing periods when the specimens are in the process of gaining strength.

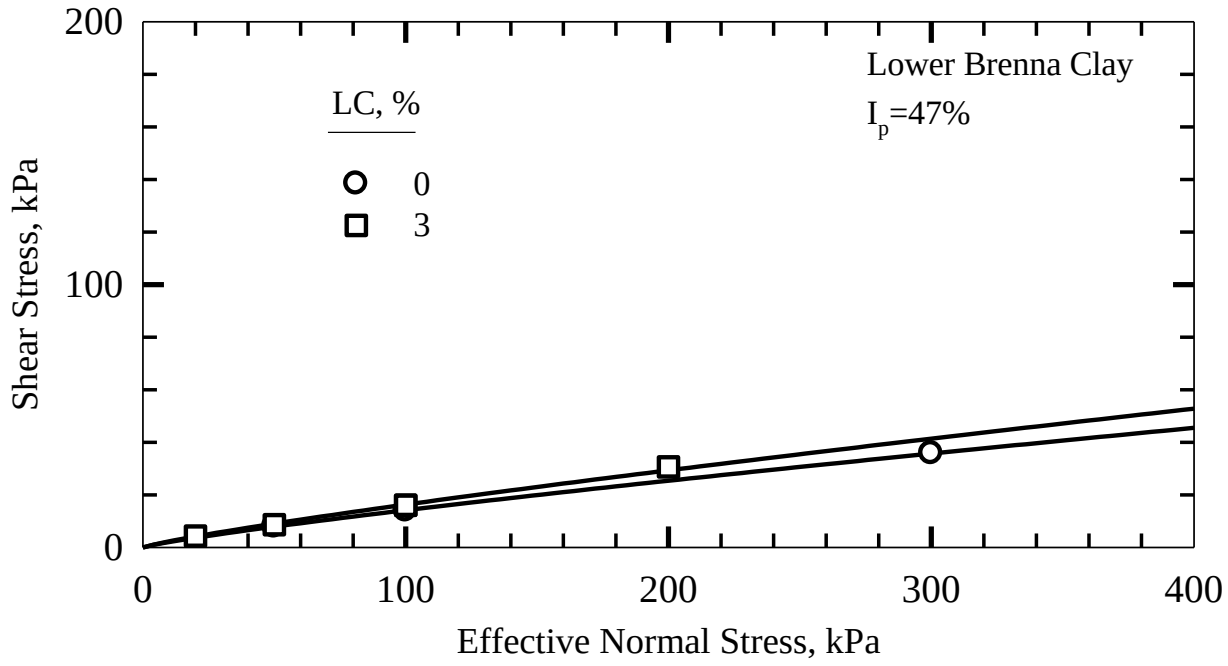

Figure 5.74: Residual shear strength envelopes for Lower Brenna clay tretaed with 3% lime

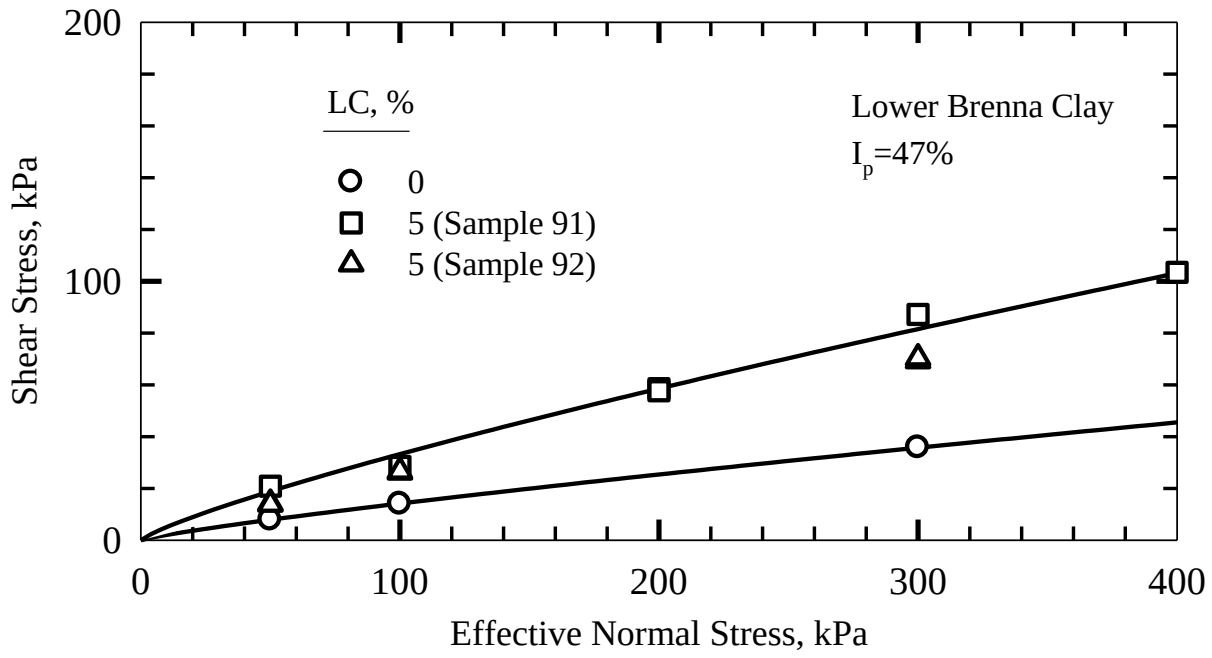

Figure 5.75: Residual shear strength envelopes for Lower Brenna clay tretaed with 5% lime

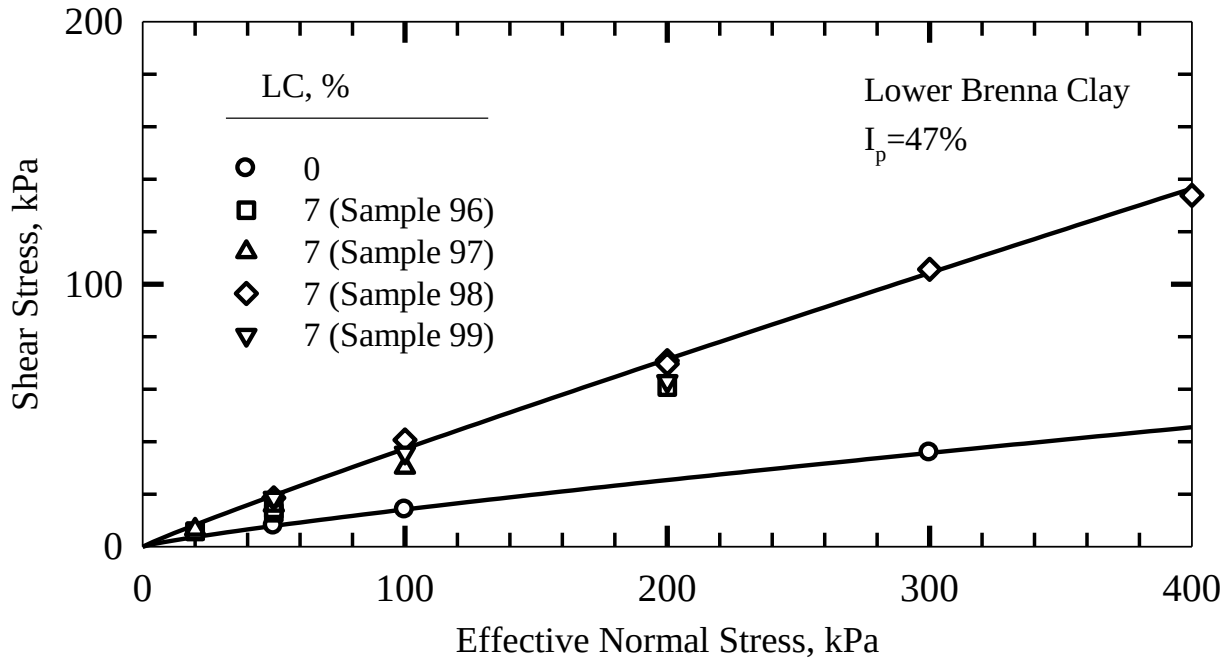

Figure 5.76: Residual shear strength envelopes for Lower Brenna clay tretaed with 7% lime

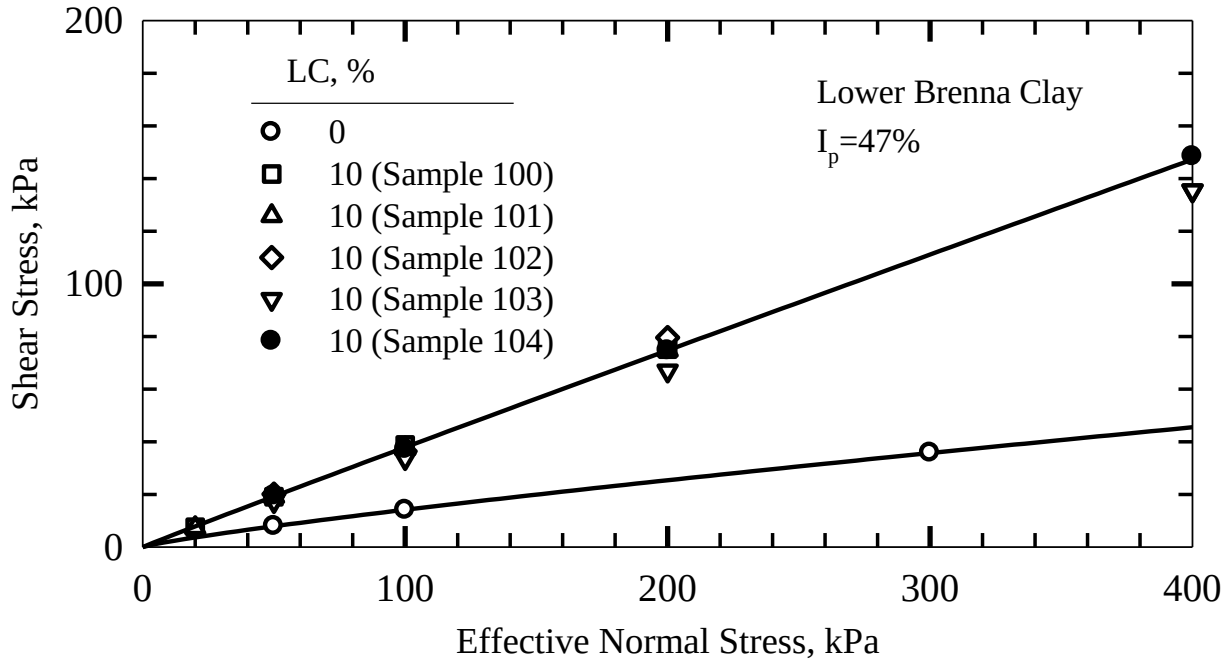

Figure 5.77: Residual shear strength envelopes for Lower Brenna clay tretaed with 10% lime

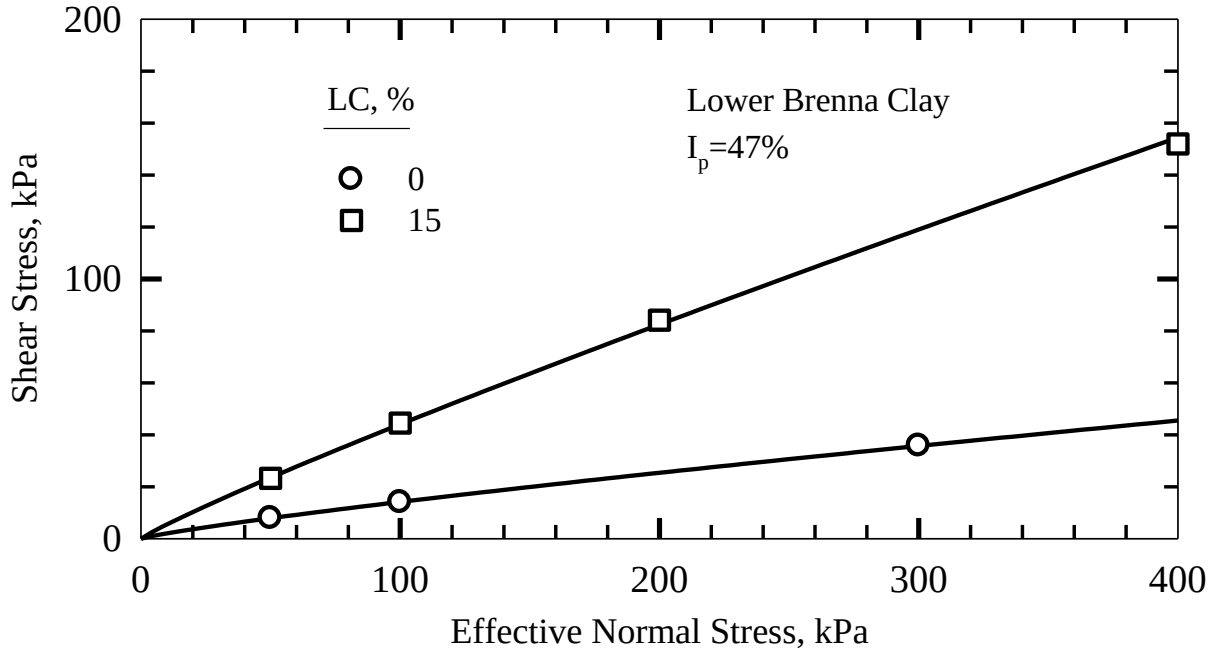

Figure 5.78: Residual shear strength envelopes for Lower Brenna clay tretaed with 15% lime

Residual shear strength envelopes of Beaumont clay treated with lime contents in the range of 1-15% are shown in Figures 5.79-5.84. The details of the properties of each sample is shown in Table 3.7. No major improvement in the residual strength is observed for lime contents of 1-3% while 5% lime content causes a significant increase in the secant residual friction angle. The data for various specimens with 7% or 10% lime contents show minimal scatter. Conversely, the 5% lime content data show the highest scatter. Later in this chapter, secant residual friction angle is plotted against lime content, where a lime content of 5% is found to be in a transition zone. This is the zone that secant residual friction angle continues to increase with lime content before it levels off.

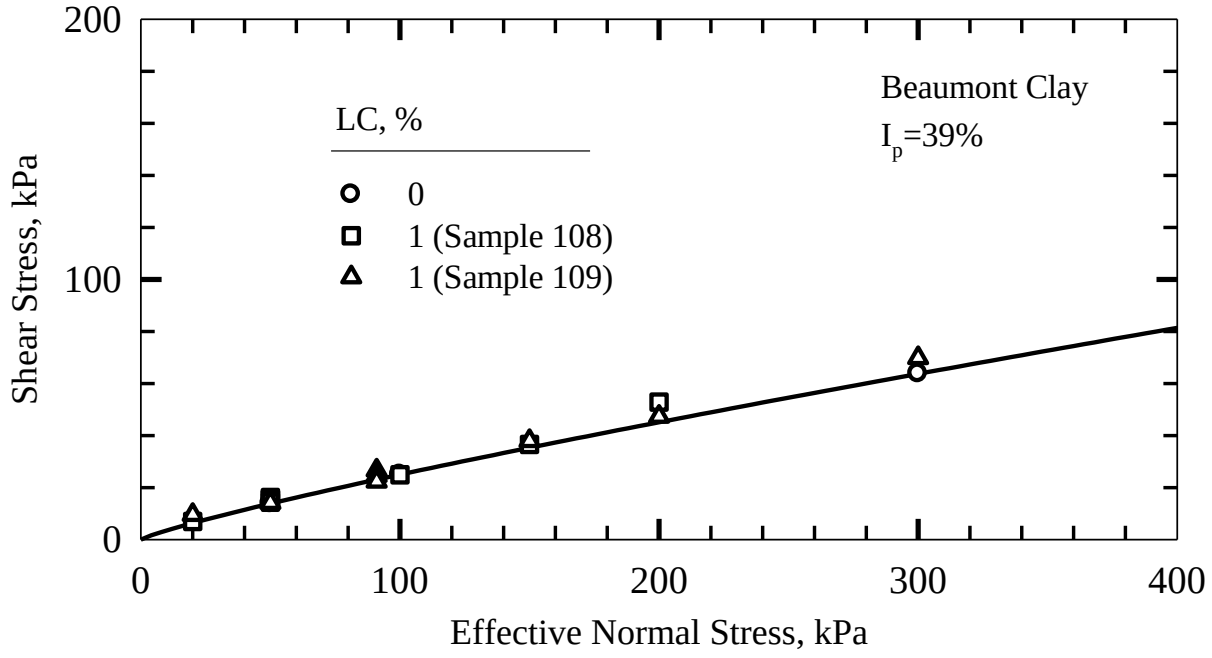

Figure 5.79: Residual shear strength envelopes for Beaumont clay tretaed with 1% lime

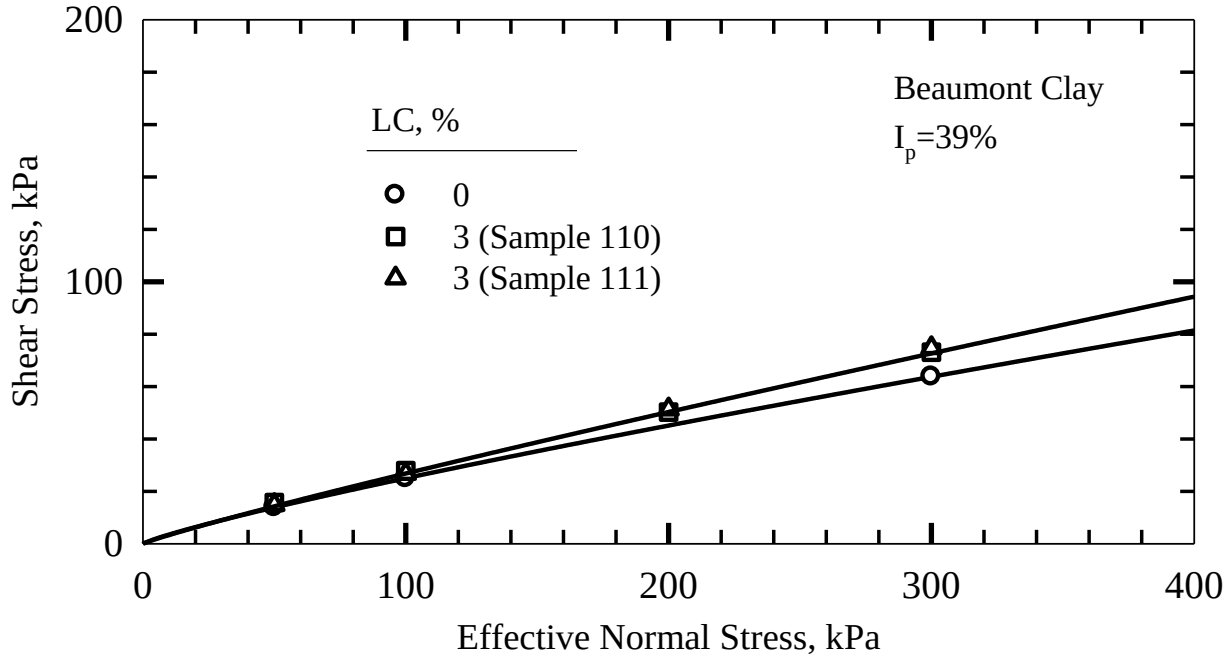

Figure 5.80: Residual shear strength envelopes for Beaumont clay tretaed with 3% lime

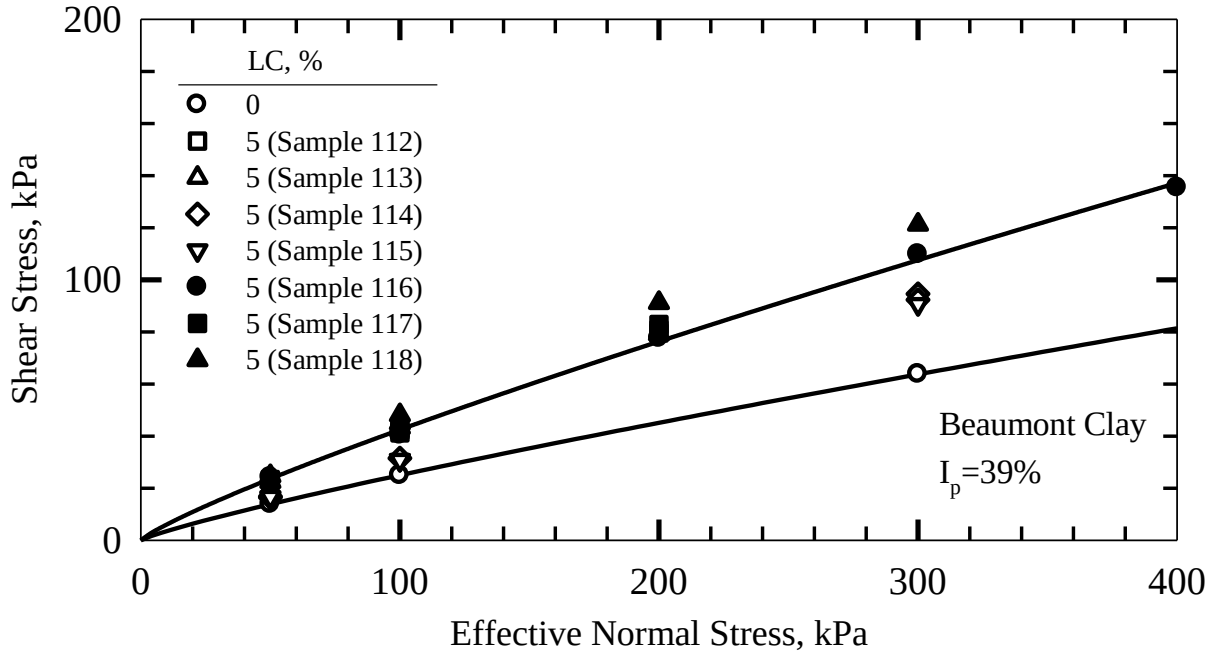

Figure 5.81: Residual shear strength envelopes for Beaumont clay tretaed with 5% lime

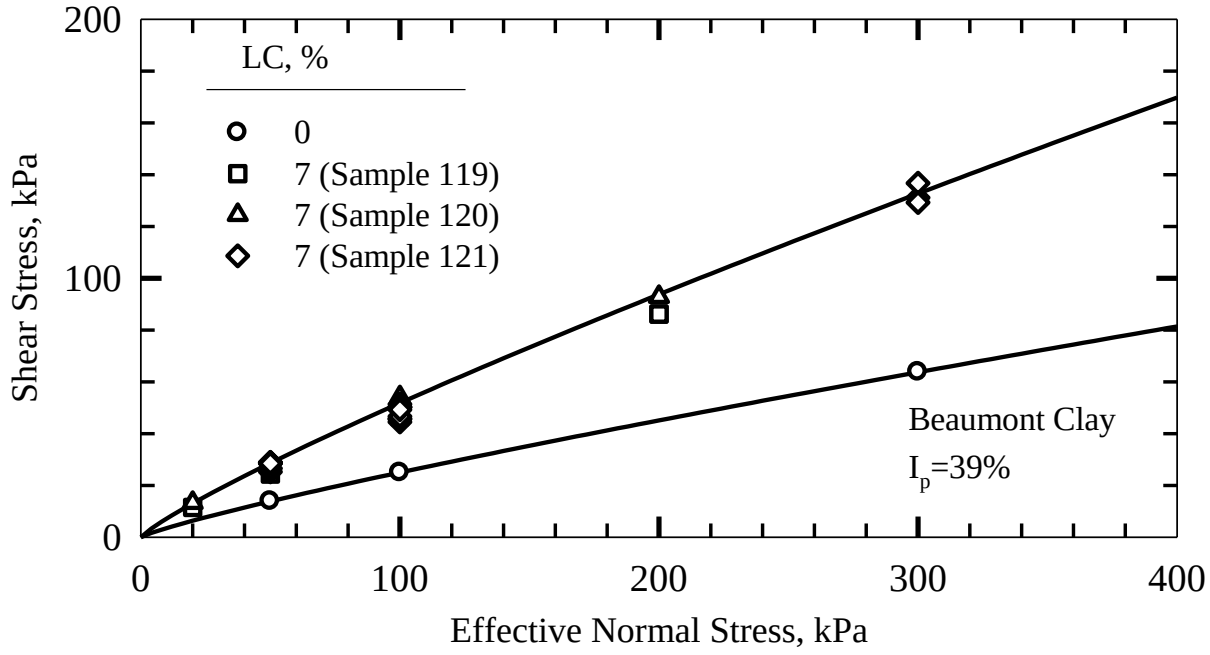

Figure 5.82: Residual shear strength envelopes for Beaumont clay tretaed with 7% lime

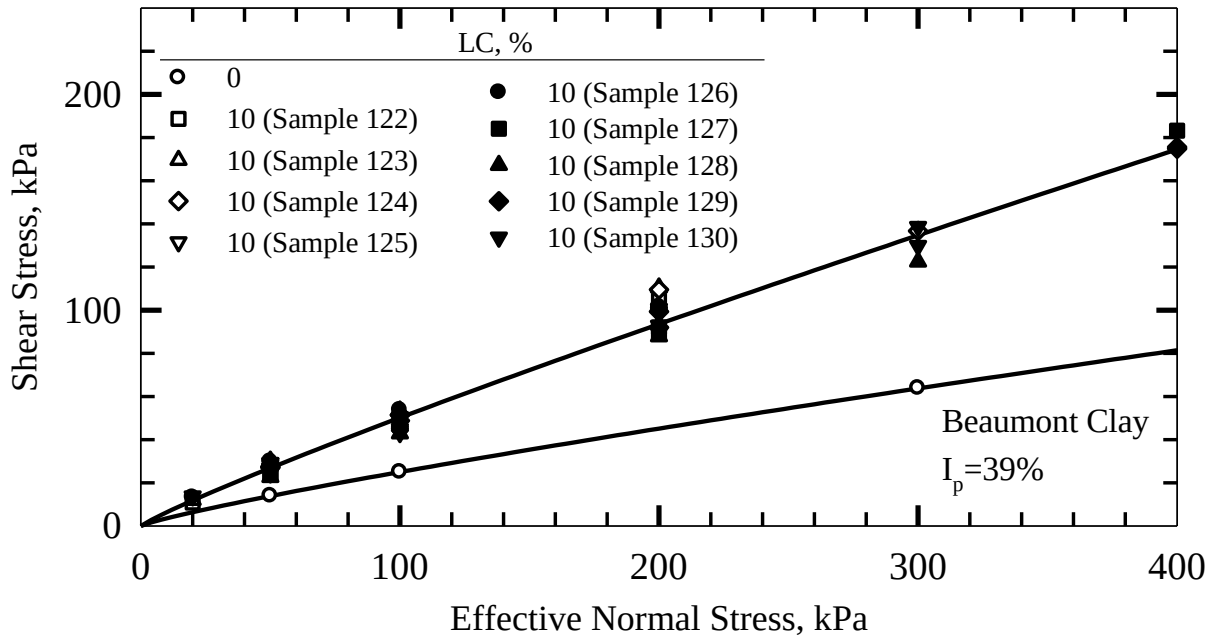

Figure 5.83: Residual shear strength envelopes for Beaumont clay tretaed with 10% lime

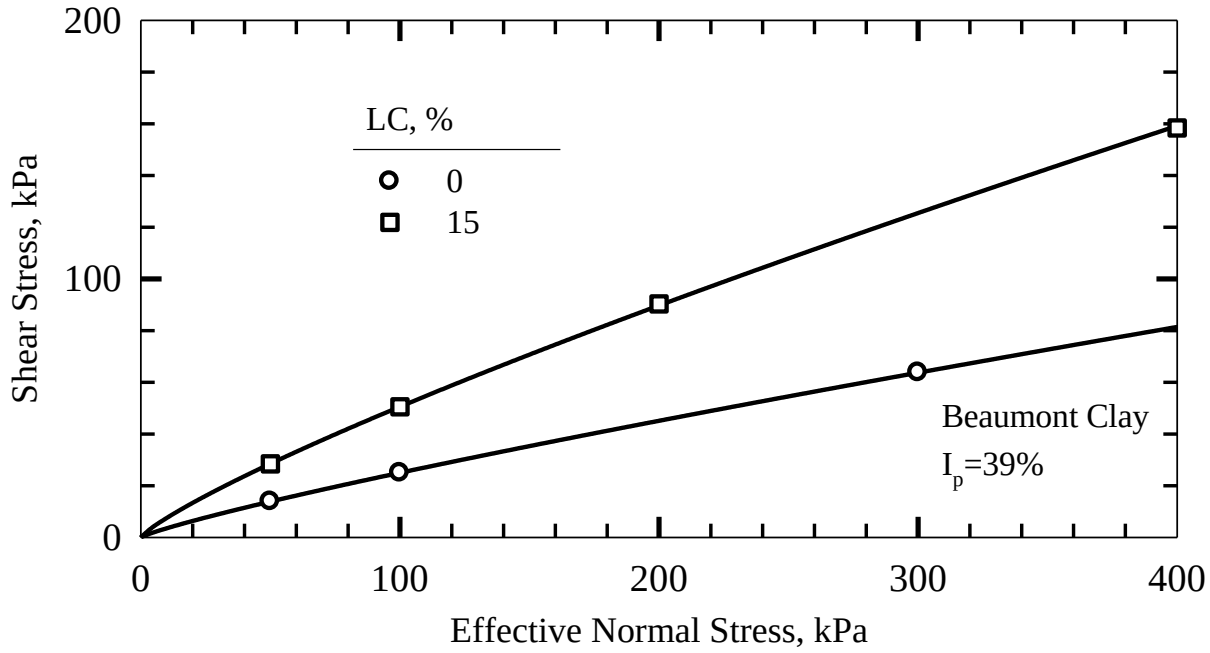

Figure 5.84: Residual shear strength envelopes for Beaumont clay tretaed with 15% lime

5.4 SECANT RESIDUAL FRICTION ANGLE-LIME CONTENT RELATIONSHIP

Figure 5.85 shows the secant residual friction angle of treated Chicago clay with lime contents in the range of 1-10% and effective normal stresses of 50-400 kPa. The secant residual friction angle increases by addition of 1% lime. The maximum improvement in the residual friction angle of Chicago clay is observed at a lime content of 2%. For lime contents higher than 2%, the secant friction angle decreases slightly, but remains higher than that for untreated Chicago clay.

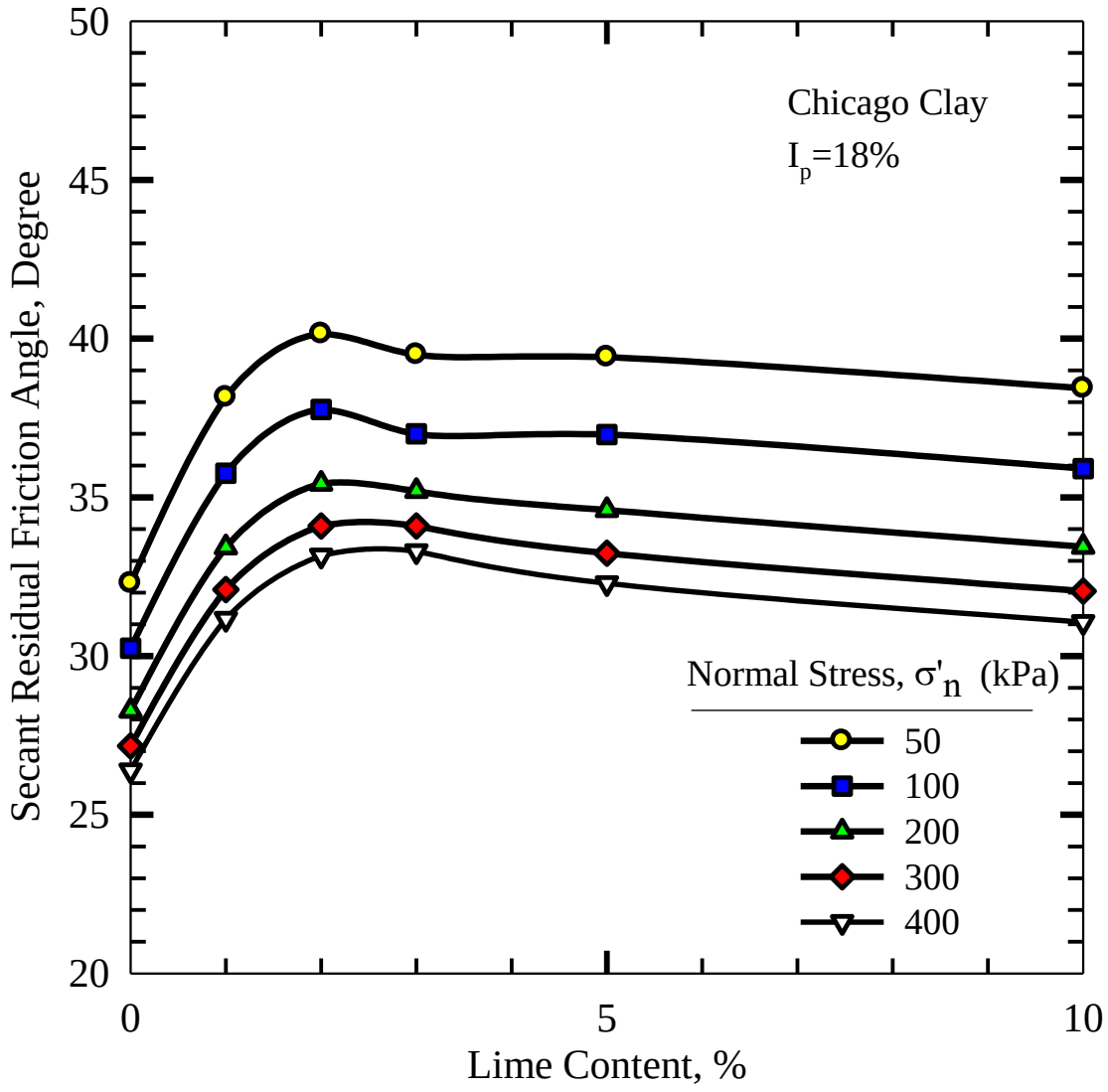

Figure 5.85: Secant residual friction angle plotted against lime content for Chicago clay

Figure 5.86 shows the secant residual friction angle of treated Lower Brenna clay with lime contents in the range of 3-15% and effective normal stresses of 50-400 kPa. The secant residual friction angle of treated Lower Brenna clay shows a very slight improvement for lime contents up to 3%. For lime contents above 3%, the secant residual friction angle increases substantially, suggesting the aggregation of clay particles. The bonds survived at this stage are the intra-cluster bonds. As lime content increases to 7%, the secant residual friction angle continues to increase. For lime contents above 7%, the secant residual friction angle increases but at a decreasing rate.

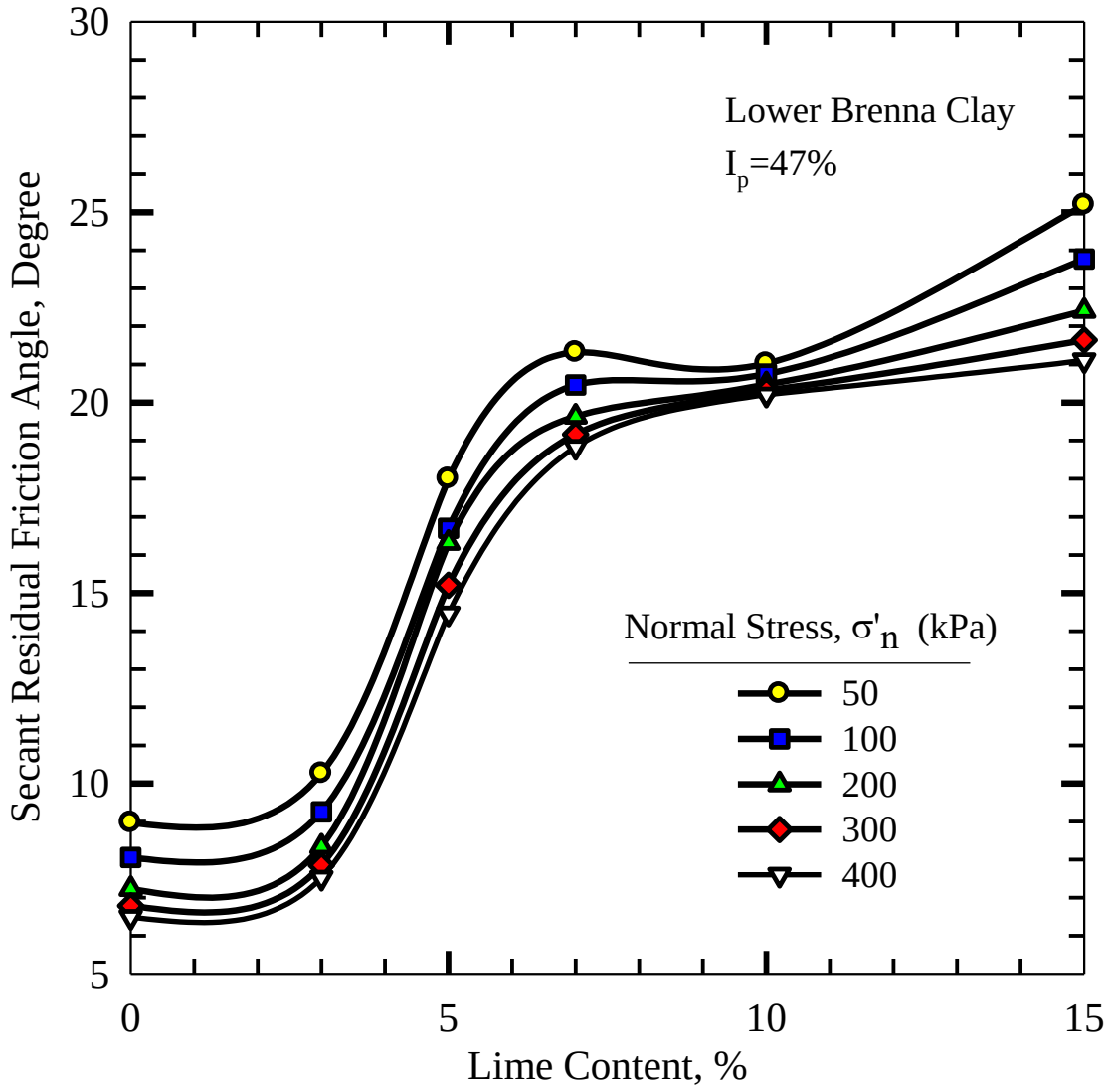

Figure 5.86: Secant residual friction angle plotted against lime content for Lower Brenna clay

Figure 5.87 shows the secant residual friction angle of Beaumont clay treated with lime contents in the range of 1-15%, and effective normal stresses of 50-400 kPa. The secant residual friction angle of Beaumont clay increases more or less as the lime content increases to 3% but a dramatic increase is observed for lime contents between 3 and 5%. A major aggregation, therefore, is seen for a lime content of 5%. As lime content increases to 7%, the secant residual friction angle continues to increase at a lower rate. As the lime content increases above 7%, the secant residual friction angle remains constant or slightly decreases.

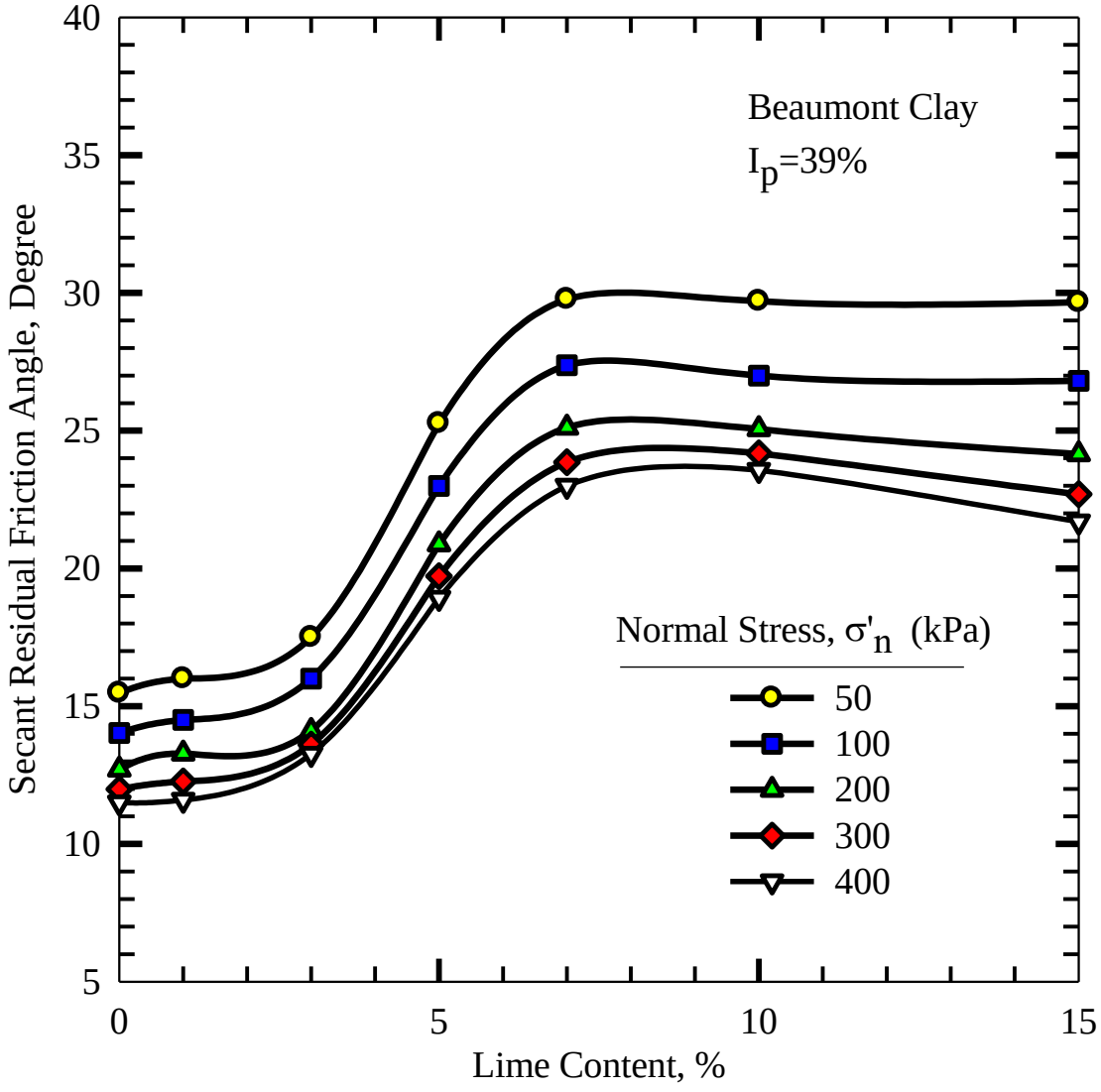

Figure 5.87: Secant residual friction angle plotted against lime content for Beaumont clay

For untreated stiff clays and clay shales, the magnitude of the drop in shear strength from the fully softened condition to the residual condition depends on the degree of plateyness, and thus plasticity of the clay (Mesri and Shahien, 2003). The difference between $[\phi'_{fs}]_s$ and $[\phi'_r]_s$ maximizes at a plasticity index around 50%, approaching zero at very low plasticity where particle reorientation is not a factor and at very high plasticity where predominant particle interaction even for a random fabric is face to face (Mesri and Cepeda-Diaz, 1986).

The secant minimum post-peak friction angle of intact specimens and residual friction angle of precut specimens of 7% lime treated Lower Brenna clay cured for 35 days at an effective normal stress of 400 kPa are 23.2 and 18.8 degrees, respectively, while the secant fully softened and residual friction angles are 21.7 and 6.5 degrees for untreated clay. This shows the dramatic reduction in plasticity of the treated clay. The aggregation caused by lime addition reduces the plateyness, and thus plasticity of clay particles.

For Chicago clay treated with 3% lime and cured for 28 days, the nonlinearity of the residual shear strength envelope, m_r, was calculated 0.90 compared to the nonlinearity of peak shear strength envelope, m_i, of 0.57. For 7% lime treated Lower Brenna clay cured for 35 days, a value of m_r=0.94 was obtained for residual condition. Comparing the m_r value with m_i=0.37 for the intact condition shows the destruction of inter-cluster bonds contributing to a more linear shear strength envelop in residual condition. For Beaumont clay treated with 10% lime and cured for 35 days, the m_r and m_i values were calculated to be 0.90 and 0.56, respectively.

CHAPTER 6

ATTERBERG LIMITS AND PH MEASUREMENTS

6.1 ATTERBERG LIMITS AND CORRESPONDING FRICTION ANGLE

The index properties, i.e., liquid limit and plasticity index, are both measures of the ability of the clay particles to hold water. As the particle size decreases, the particle surface area per unit dry weight increases and liquid limit and plasticity index increase. There is correlation between size and plateyness of common clay mineral particles (Mesri and Cepeda-Diaz 1986; Mesri and Shahien 2003). Plateyness of clay mineral particles increases as size of particles decreases. Therefore, liquid limit or plasticity index can be used as an indication of the plateyness of clay particles.

The plastic limit increases dramatically for all treated clays because large amount of water is enclosed within the flocs and agglomerates. However, only part of the porewater contributes to plasticity. This is similar to diatoms with poriferous particles in soils such as the Mexico clay, and andosols containing allophane in which water is trapped within soil aggregates (Mesri et al., 1975; Terzaghi et al. 1996). The plastic limit of Chicago clay increases from 20 to 31% by adding 3% lime, as shown in Figure 6.1. There is a slight increase to 35% in the plastic limit for a lime content of 5%. It remains more or less in the same range for higher lime contents. The Atterberg limits shown in Figure 6.1 were measured on the direct shear specimens cured under confined condition. The curing period ranges from 3 to 4 weeks. The plasticity index of Chicago clay remains constant and independent of lime content, because the increase in liquid limit was similar to the increase in plastic limit.

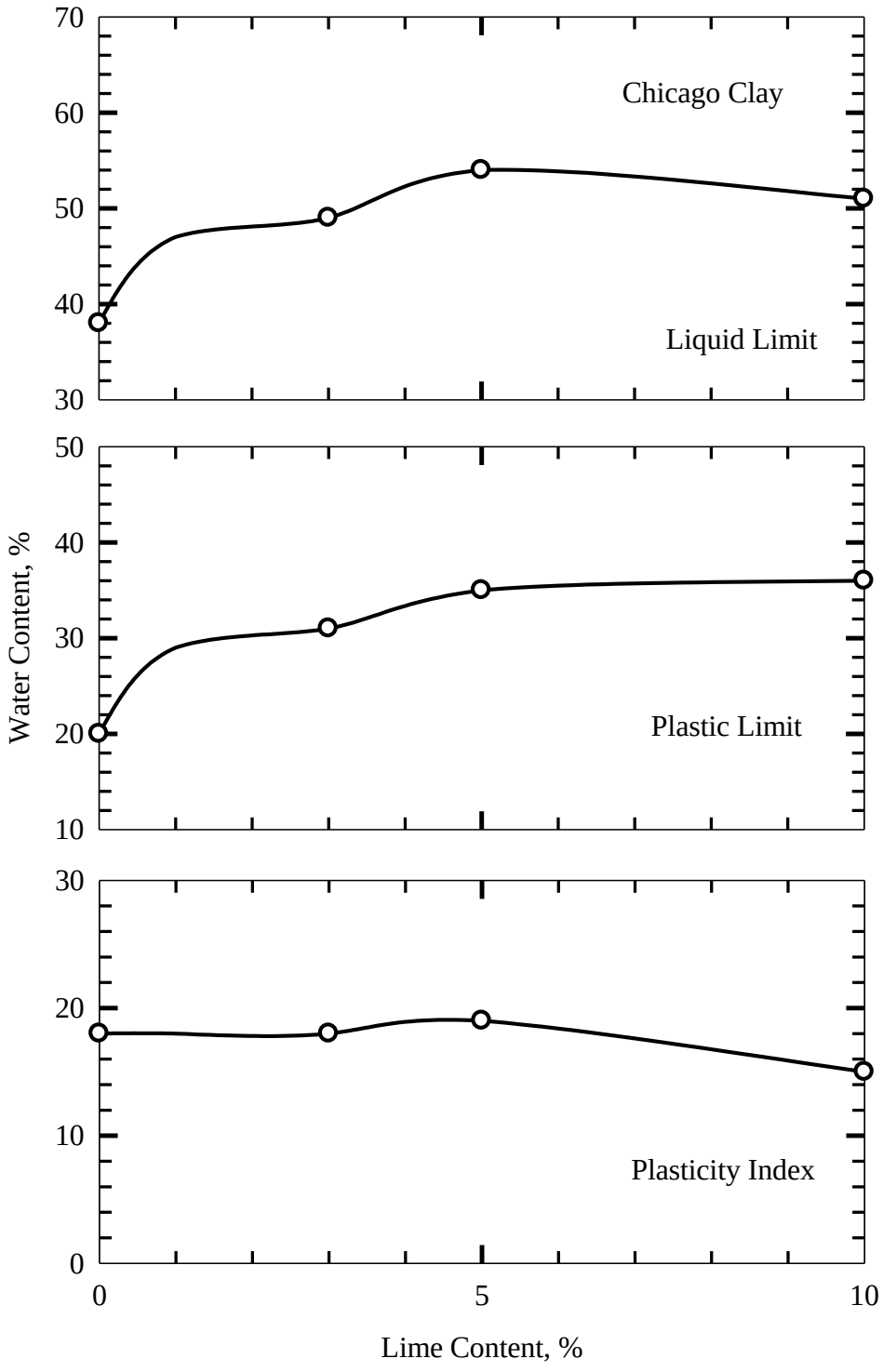

Figure 6.1: Atterberg limits of Chicago clay treated with various lime contents, cured under confined condition for perids in the range of 3-4 weeks

The Atterberg limits of Lower Brenna clay and Beaumont clay with lime contents of 0-10% are shown in Figures 6.2 and 6.3, respectively. The data for Lower Brenna clay pertain to the direct shear specimens cured under confined condition. The curing period of specimens is about 4-7 weeks, except for the 10% lime specimen that was cured for 12 weeks. Similarly, the Atterberg limits of Beaumont clay were measured on the direct shear specimens cured for 7-12 weeks under confined condition. The plastic limit of Lower Brenna and Beaumont clays increased from 40 to 62% and from 28 to 42%, respectively, by adding 3% lime. The plastic limit of the two clays remained relatively constant for lime contents more than 3%.

The change in the liquid limit of treated clays is rather unpredictable. After addition of 3-10% lime, the liquid limit of Chicago clay increased (Figure 6.1), while Lower Brenna (Figure 6.2) and Beaumont (Figure 6.3) clays experienced an overall decrease in the liquid limit for lime contents in the range of 3-10%.

The plasticity index of Chicago clay remained more or less the same after addition of lime (Figure 6.1). The high plasticity clays, i.e. Lower Brenna (Figure 6.2) and Beaumont (Figure 6.3) clays, experienced a significant drop from 47 to 18% and from 34 to 13%, respectively, by adding 3% lime. The plasticity index of Lower Brenna and Beaumont clays remained relatively constant for the lime contents in the range of 3-10%.

Lime treatment reduces the plasticity index particularly by increasing the plastic limit. A lime content of 3% reduced the plasticity substantially immediately after addition of lime to Lower Brenna or Beaumont clays. This is similar to “Lime fixation point” concept of Hilt and Davidson (1960) which is the lime required to increase plastic limit to its maximum. This lime is fixed and lime in excess of this value contributes to an increase in the shear strength.

Figure 6.4 shows the Atterberg limits as a function of time measured for a series of direct shear specimens of Upper Brenna clay with lime content of 6.6%. The increase in the plastic limit is evident. The liquid limit varies from 112 and 130%, compared to 117% for the untreated clay. The increase in the liquid limit is not dramatic. Hence the plasticity index with time remains below that of untreated clay.

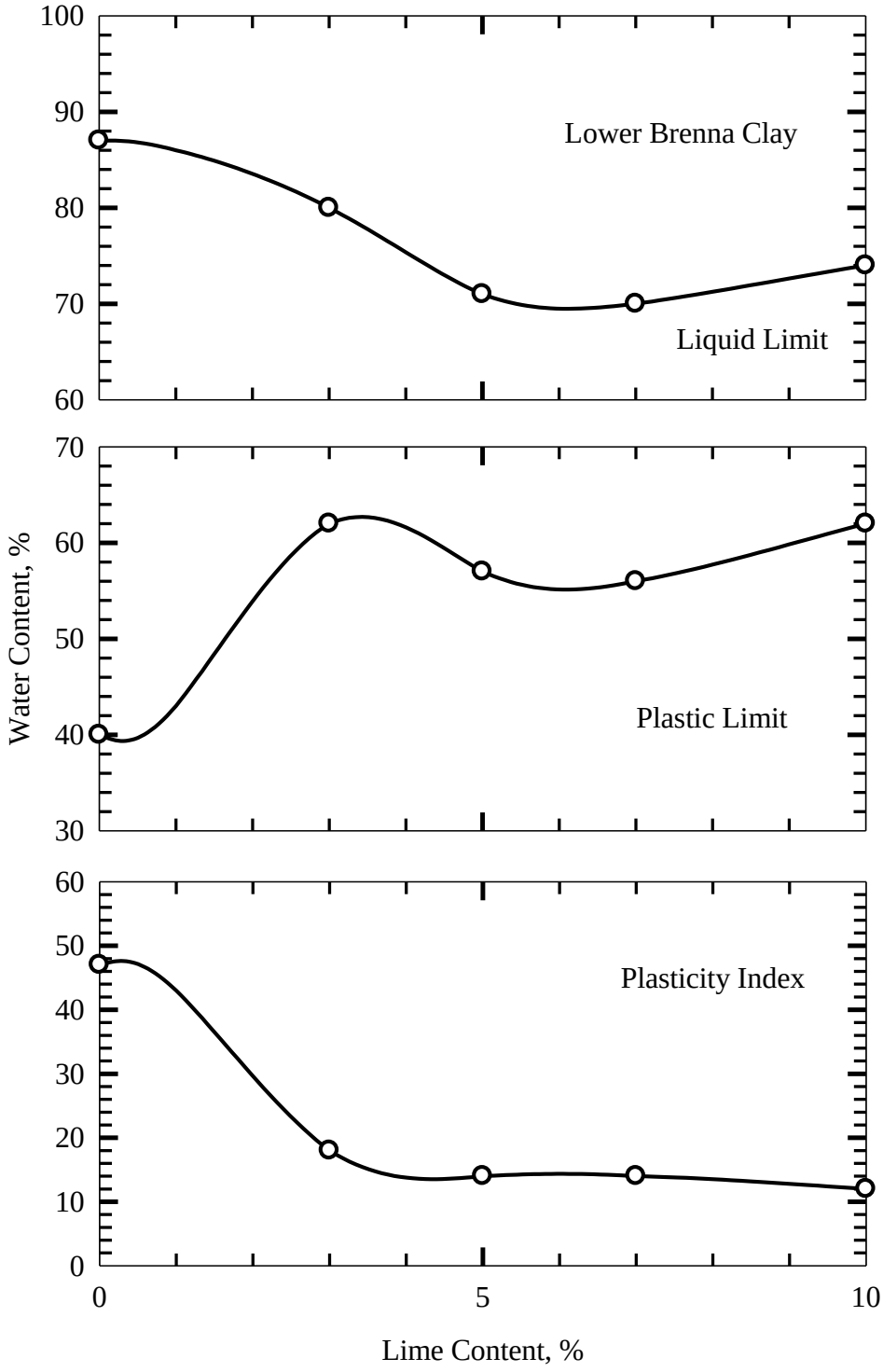

Figure 6.2: Atterberg limits of Lower Brenna clay treated with various lime contents, cured under confined condition for perids in the range of 4-12 weeks

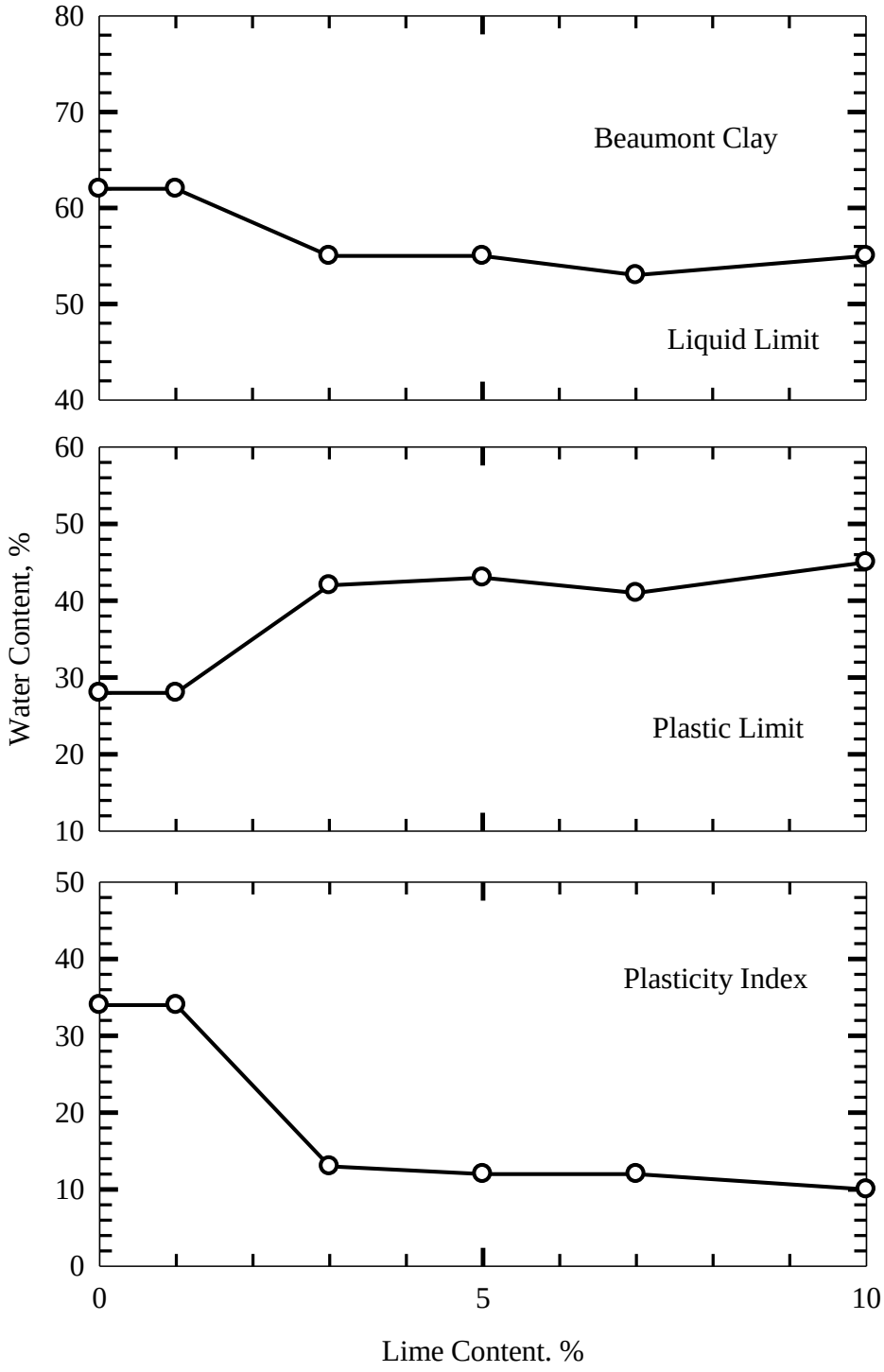

Figure 6.3: Atterberg limits of Beaumont clay treated with various lime contents, cured under confined condition for perids in the range of 7-12 weeks

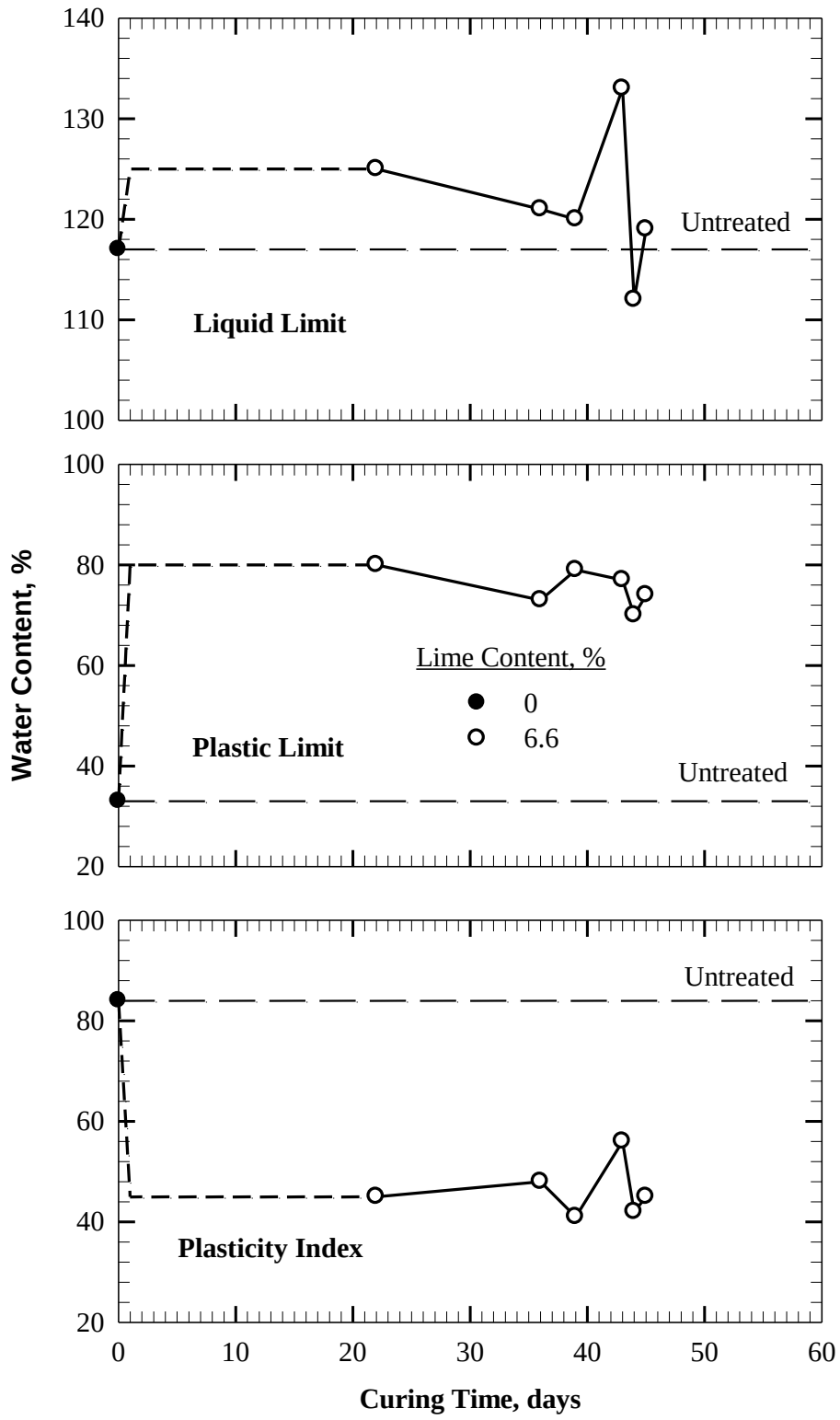

Figure 6.4: Atterberg limits of lime-tretaed Upper Brenna clay cured under confined condition (The dashed line are based on observed data in Figures 6.5 and 6.6)

It is again noted that the Atterberg limits shown on Figures 6.1-6.4 were measured on direct shear samples cured under confining pressures. The direct shear specimens were air-dried, crushed, pulverized and rehydrated to measure Atterberg limits. The results of plasticity index measurements of treated Lower Brenna and Beaumont clay confirms the aggregation of platy-shaped clay particles.

When the curing of lime treated Lower Brenna clay takes place unconfined, liquid limit dramatically increases above the liquid limit of treated clay as curing time prolongs; whereas when curing takes place under confining pressure condition (imposed effective stress such as the σ'_n in direct shear tests), there is a decrease in liquid limit. The plastic and liquid limits of 5% lime-Lower Brenna clay increase from 87 to 105% and 40 to 74%, respectively, after 90 days of unconfined curing (Figure 6.5). The plasticity index of 5% lime treated Lower Brenna clay cured unconfined decreases at early stage of curing; however, it increases as curing prolongs. The plasticity index deceases to 13 immediately after addition of lime but increases to 31% after 90 days and reaches the plasticity index of untreated Lower Brenna clay, i.e., 47%, after 180 days. Although the plastic limit remains constant over time, increase in the liquid limit is so dramatic that it results in an increase in plasticity index.

Brenna clay contains a small amount of sulfate in its composition which promotes ettringite formation. Two reactions are in process when lime is added to Brenna clay, pozzolanic and ettringite reactions. At early stages, cementitious products formed by pozzolanic reactions aggregate the clay particles and thus reduce the plasticity. However, ettringite formation overcomes as curing prolongs under unconfined condition, causing an increase in plasticity of the treated clay.

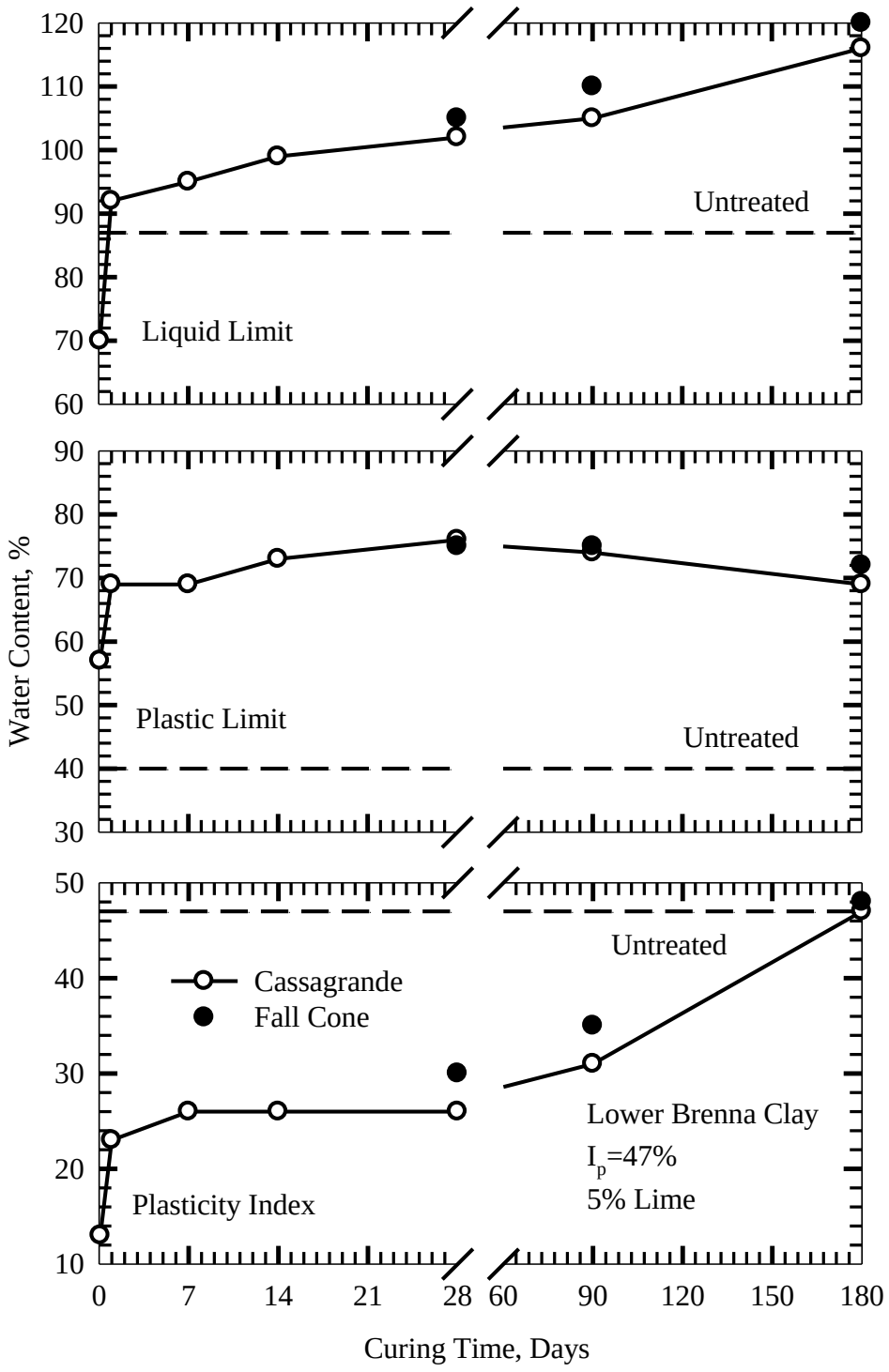

Figure 6.5: Atterberg limits of Lower Brenna clay treated with 5% lime under unconfined condition

The secant residual friction angle at an effective vertical stress of 50 kPa, $[\phi'_r]_s^{50}$, measured for a precut specimen of 5% lime treated Lower Brenna clay cured unconfined for 7 days (Specimen 93, Table 3.6, Figure 5.23) increased from 9.1 degrees for untreated clay to 11.8 degrees after 40 days. The secant residual friction angle, $[\phi'_r]_s^{50}$, measured for another 5% lime treated precut specimen cured unconfined for 120 days (Specimen 94, Table 3.6, Figure 5.24) was 11.5 degrees after 153 days. The secant residual friction angle, $[\phi'_r]_s^{100}$, of a precut specimen from the same batch of 5% lime treated clay after 140 days of curing unconfined (Specimen 95, Table 3.6, Figure 5.25) also showed only a slight increase to 10.2 degrees compared to 8.2 degrees for untreated clay. As the plasticity index of the treated clay approaches that of the untreated clay, its residual friction angle approaches that of the untreated clay, implying the formation of products which do not contribute to the aggregation of clay particles and increase in residual strength of treated Lower Brenna clay.

Similarly, the liquid limit of 10% lime treated Lower Brenna clay cured unconfined increases over time after an initial decrease at early stages of treatment, as shown in Figure 6.6. As the lime content increases from 5 to 10%, more lime becomes available for pozzolanic reactions after some of the lime is used for ettringite formation. An increase in the plastic limit which is a characteristic of treated clays, maintains the plasticity index below that of untreated Lower Brenna clay during the first 180 days of curing. A series of reversal direct shear tests on a 10% lime treated precut specimen cured for 180 days under unconfined condition (Specimen 105, Table 3.6, Figure 5.35) showed an increased secant residual friction angle, $[\phi'_r]_s^{300}$, of 10.2 degrees which is 3.4 degrees greater than that of untreated clay. Other specimens treated with 10% lime but cured under confined condition (Specimens 100-104) exhibited an increased residual friction angle of 18.5-21.5) degrees which is 11.7-14.7 degrees greater than that of untreated clay. The higher residual friction angle measured for the specimens cured confined confirms formation of crystals and aggregation of clay particles in compact arrangement contributing to strength increase. The plasticity index of 10% lime treated Lower Brenna clay cured unconfined increased to that for the untreated clay after 365 days, implying the formation of expanding ettringite with time. Ettringite is a swelling crystal; when Lower Brenna clay specimens are cured confined, ettringite is prevented from taking water, resulting in a more compact structure.

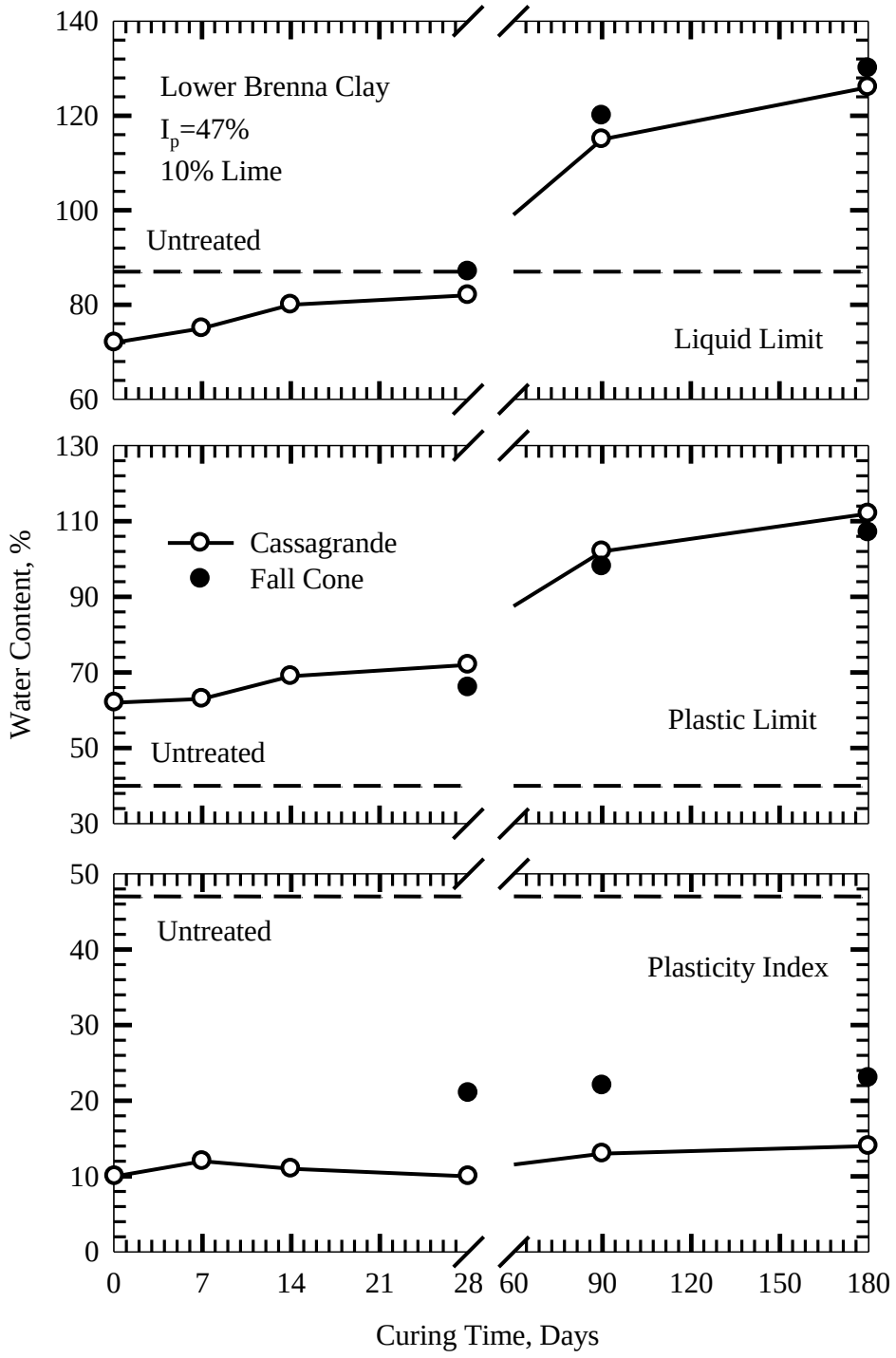

Figure 6.6: Atterberg limits of Lower Brenna clay treated with 10% lime under unconfined condition

Atterberg limits of Chicago clay treated confined and unconfined are different. The changes are, however, less pronounced due to low plasticity of Chicago clay and the fact that ettringite formation is not an issue for Chicago clay. In general, strength improvement in Chicago clay due to lime treatment is not as pronounced as that in clays of higher plasticity. The liquid limit increases from 38% for the untreated Chicago clay to 57% following 5% lime treatment and remains above 61% after 365 days of curing unconfined (Figure 6.7). The plasticity index increases from 18% for the untreated Chicago clay to 25% immediately after addition of 5% lime and increases further to 32% after 365 days of curing. Lower liquid and plastic limits are achieved when Chicago clay is cured confined, as pozzolanic products form and produce aggregation and connect particles to each other under confined condition in compact arrangement. At confined condition, the plasticity index remains more or less close to that of the untreated clay, as shown in Figure 6.1.

A similar behavior was observed for 10% lime treated Chicago clay. The higher Atterberg liquid and plastic limits of treated clay when cured unconfined (Figure 6.8) versus confined (Figure 6.1) is evident. After curing unconfined for 180 days, 10% lime treated Chicago clay shows an increased liquid limit from 38% for untreated clay to 74%. The same sample cured confined showed a liquid limit of 51%. The plasticity index by Cassagrande method of the samples cured unconfined and confined was 22 and 15%, respectively, compared to the plasticity index of 18% for the untreated Chicago clay.

Pozzolanic products form under unconfined condition, but do not contribute much to aggregation, whereas under confining pressure, pozzolanic products form and contribute to aggregation.

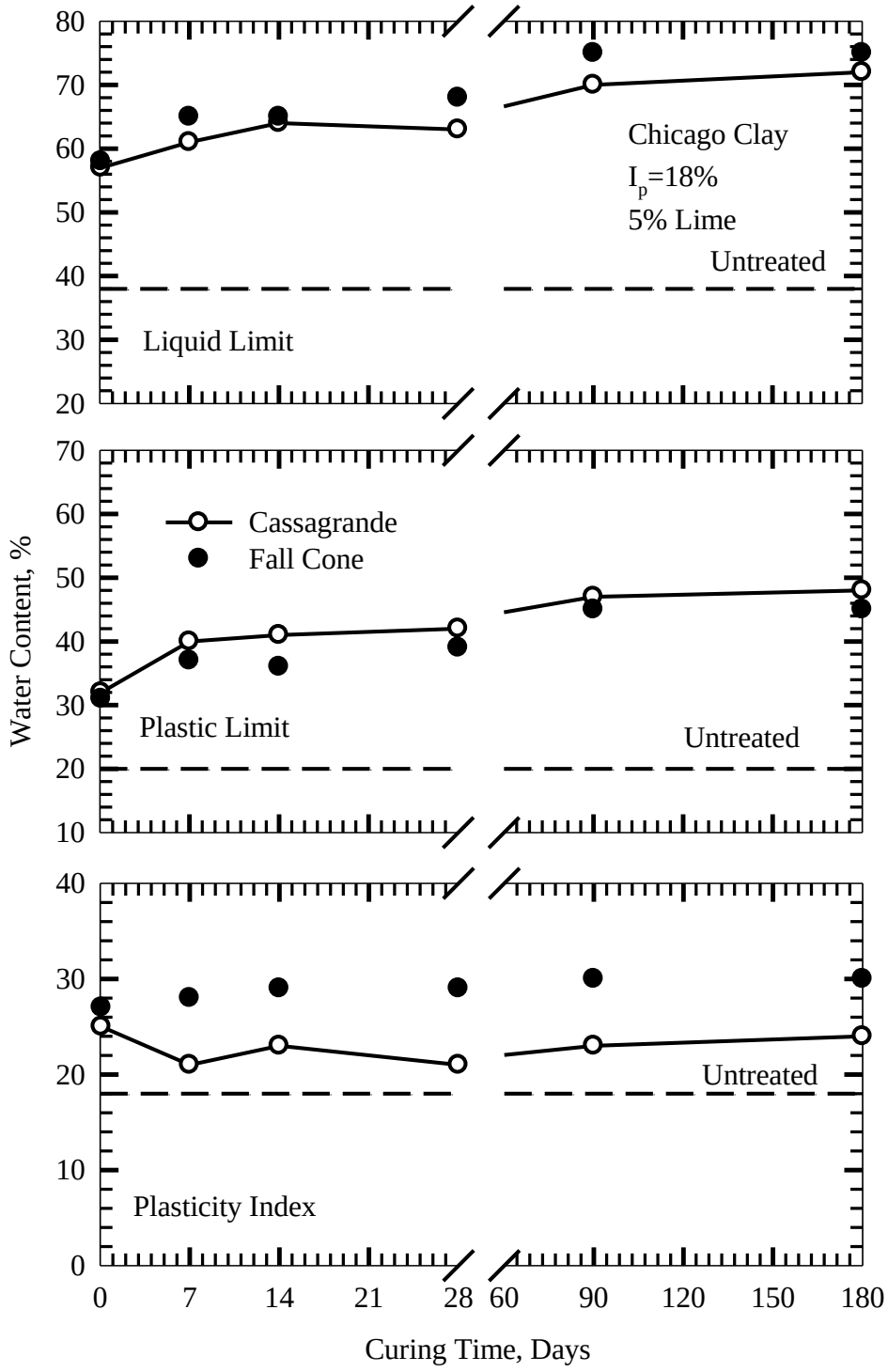

Figure 6.7: Atterberg limits of Chicago clay treated with 5% lime under unconfined condition

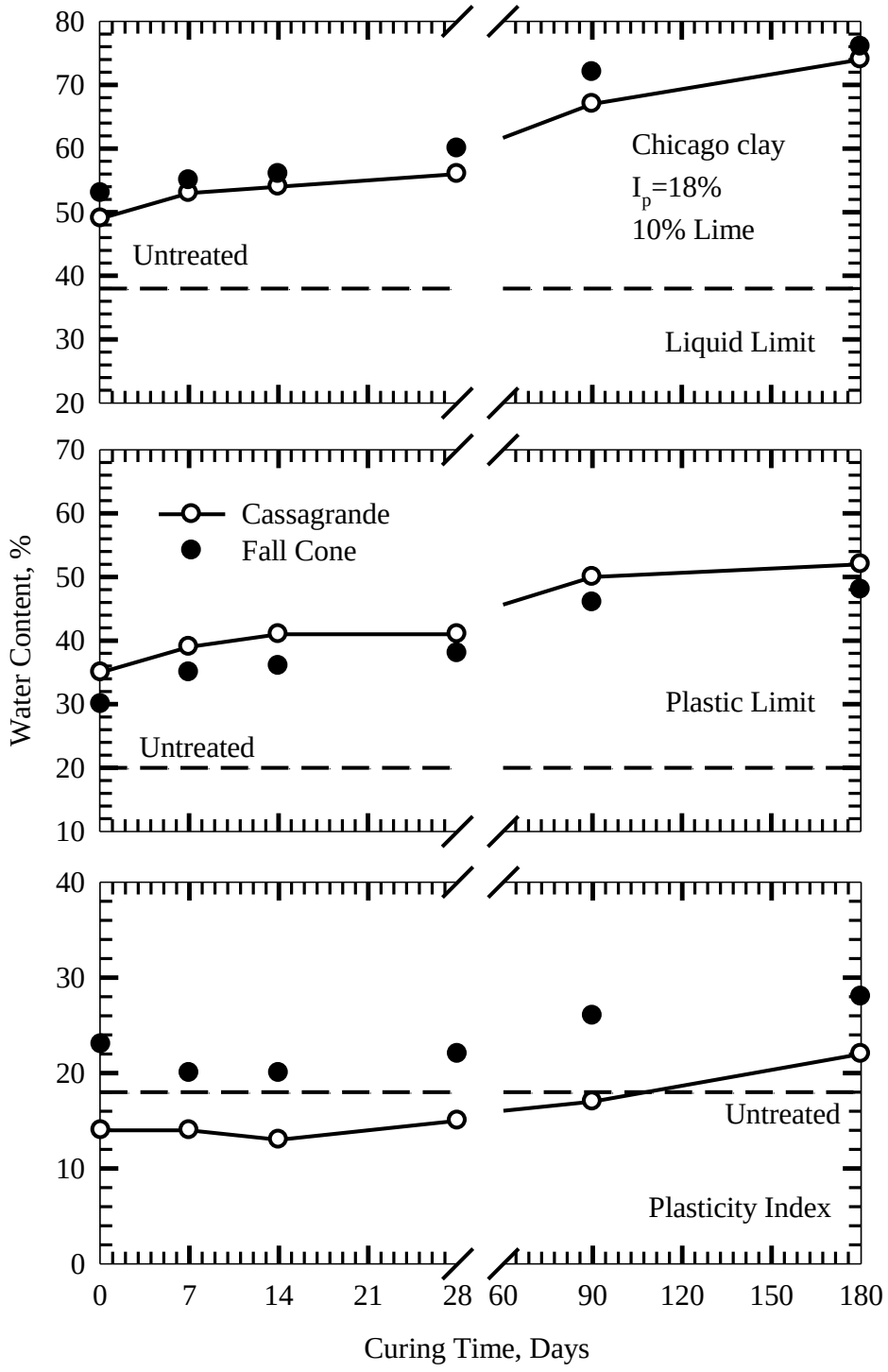

Figure 6.8: Atterberg limits of Chicago clay treated with 10% lime under unconfined condition

The secant residual friction angle at an effective normal stress of 300 kPa, $\left[\phi'_r\right]_s^{300}$, increased from 26.9 degrees for untreated Chicago clay to 29.6 and 32 degrees for 5% lime treated specimens respectively cured unconfined (Specimen 83, Figure 5.13) and confined (Specimen 84, Figure 5.14). Similarly, $\left[\phi'_r\right]_s^{100}$ of 5% lime treated specimen, cured confined, is 6.1 degree higher than that of the same specimen cured unconfined. The low plasticity Chicago clay does not exhibit a great improvement in residual strength upon addition of lime compared to what was observed for high plasticity clays; no major difference in the plasticity index is observed cured under confined or unconfined condition.

Two specimens of 7% lime treated Beaumont clay were cured for 147 days. One specimen was cured under unconfined condition and the other specimen was cured under an effective normal stress of 2,700 kPa (Specimen 121,). The liquid limit of the specimen cured unconfined increased from 62% for untreated Beaumont clay to 80%, and the plastic limit increased from 28% for the untreated clay to 64%. The liquid and plastic limits under confined condition are 47% and 32%, respectively. Both specimens have a comparable plasticity index of 16 and 15% for unconfined and confined curing condition, respectively. The residual friction angle at an effective normal stress of 100 kPa, $\left[\phi'_r\right]_s^{100}$, measured for the specimens cured under confined condition increased from 14.0 degrees for untreated Beaumont clay to 24.8-28.4 degrees for treated specimens (Specimens 119-121) for curing pressures in the range of 50-200 kPa and curing period in the range of 14-144 days.

The secant fully softened and residual friction angles of untreated clays are well correlated with plasticity index and are directly or indirectly related to one or both of the fundamental factors of particle size and plateyness. Mesri and Shahien (2003) correlated $\left[\phi'_{fs}\right]_s$ and $\left[\phi'_r\right]_s$ with the plasticity index, I_p. The plasticity index to some extent encapsulates information on both liquid limit and clay size fraction. For treated clays, both an increase and decrease of the liquid limit has been reported. However, in general, the plasticity index decreases due to a sharp increase in the plastic limit. Although an increase in the friction angle and reduction in the plasticity index of the treated clays is evident, empirical correlations between $\left[\phi'_{fs}\right]_s$ or $\left[\phi'_r\right]_s$ and liquid limit or plasticity index for untreated clays may not be directly applicable to clays or shales that are composed of

clay minerals that are not plate-shaped, such as attapulgite and allophane, or are exceptionally aggregated such as treated clays (Chandler, 1984; Mesri and Cepeda-Diaz, 1986; Terzaghi et al., 1996, Wesley, 2003). For clays composed of plate-shaped particles, ability to hold water is a measure of size and plateyness of particles, and thus an indicator of frictional strength. On the other hand, the ability of treated clays to hold water is not only controlled by the plate-shaped particles. Water held inside the aggregates formed by pozzolanic reactions also contributes to the ability of treated clays to hold water.

There is also no empirical relation between the physical properties and Atterberg limits for clays with halloysite or allophane as the predominant mineral (Wesley, 1973; Terzaghi et al., 1996). The water is held in the pores of clusters or aggregates that are cemented together. Therefore, at the same water content or liquid limit the soils have significantly higher shear strength than soils consisting of the clay minerals with platey particles. In andosols, allophane is the predominant clay mineral, where a major part of pore water is trapped within the soil particles. Therefore, plastic limit is unusually high, and the plasticity index is low. When these soils are air dried, water removal causes the pore cluster to shrink. This process is irreversible, resulting in hard grains with lower liquid limit and plasticity index. Wesley (2003) also pointed out that correlation of residual strength of clays with Atterberg limits are unlikely to be applicable to all soils on a general basis.

6.2 PH MEASUREMENTS

The pH values of Chicago clay with lime contents of 1, 3, 5 and 10% show that a lime content of 1-3% is sufficient to maintain the pH value elevated, as shown in Figures 6.9 and 6.10. This implies that the Chicago clay requires less lime for reaction with its composition. The secant residual friction angle of Chicago clay subjected to an effective normal stress of 100 kPa, Figure 5.85, increases from 30 degrees to 38 degrees by addition of 2% lime, and remains more or less constant for higher lime contents.

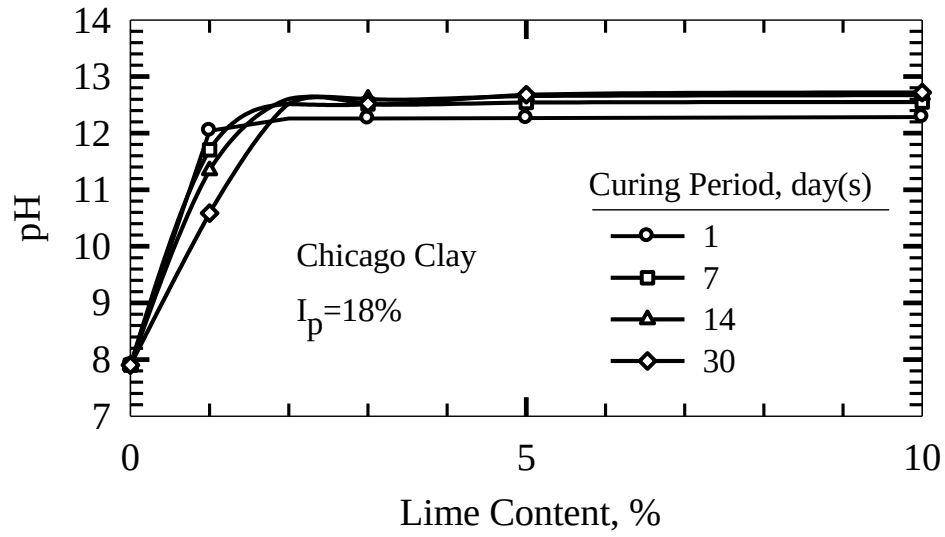

Figure 6.9: pH values of Lime-Chicago clay

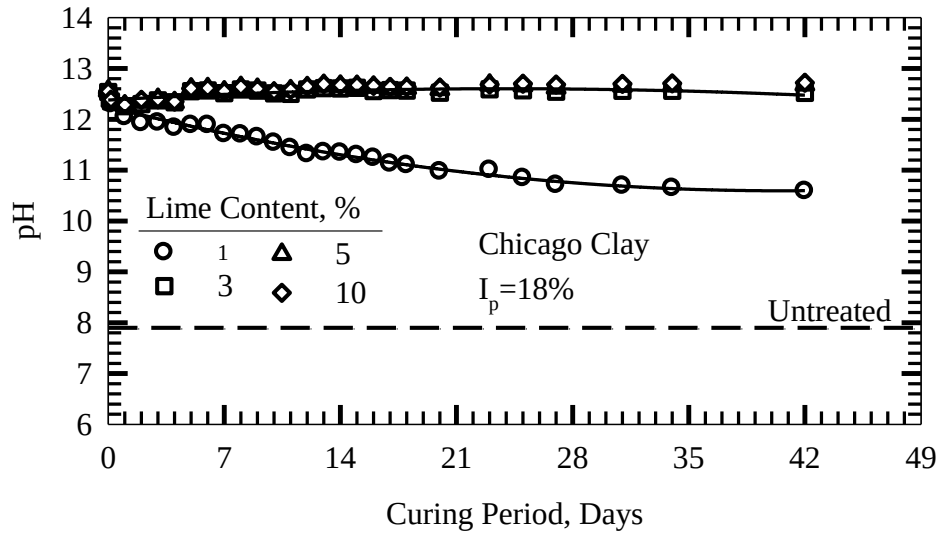

Figure 6.10: pH values of Chicago clay with time

The pH values of treated Lower Brenna clay are plotted with lime content in Figure 6.11. The pH values of Lower Brenna clay treated with 2, 5 and 9% lime are plotted against curing time in Figure 6.12. A lime content of 3% appears to be enough to increase the pH to its maximum value, but 3% lime does not maintain the elevated pH condition. The pH drops one day following addition of lime. Lime contents of equal or higher than 5% maintain the elevated pH over time.

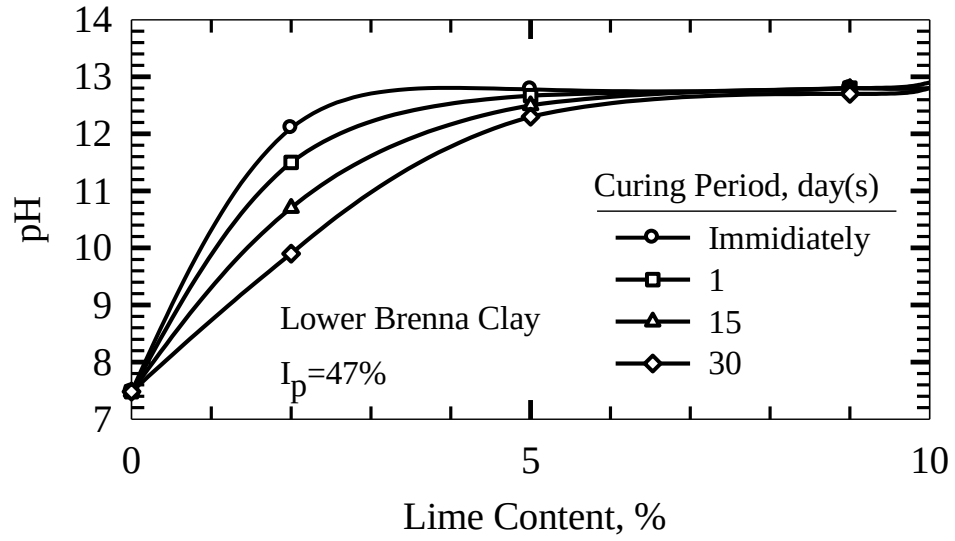

Figure 6.11: pH values of Lime-Lower Brenna clay

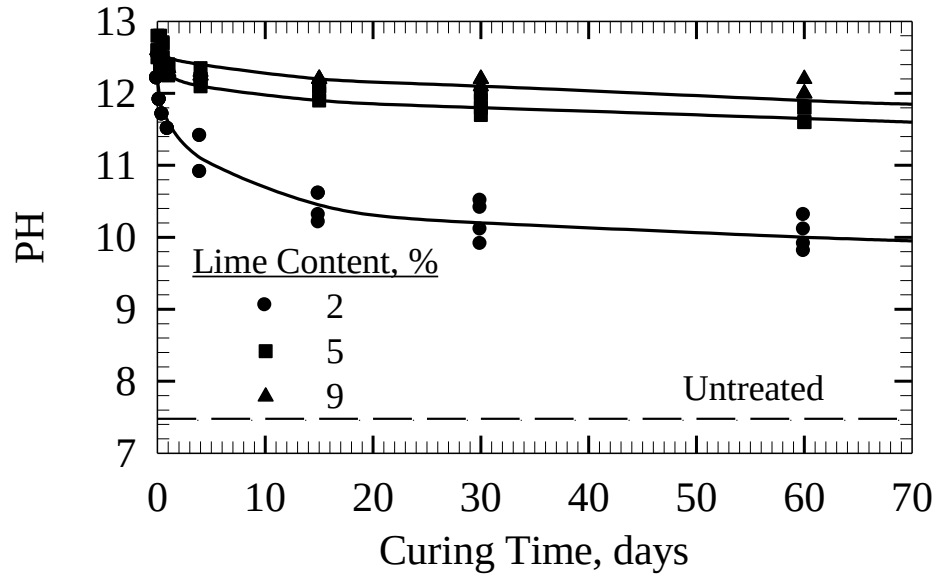

Figure 6.12: pH values of Lime-Lower Brenna clay with time

The pH values of Beaumont clay are plotted against lime content for curing periods of 1, 7, 14 and 30 days in Figure 6.13. A lime content of 3% is sufficient to increase the pH of Beaumont clay above 12.4. However, for lime contents less than 5%, the pH drops rapidly with curing period. Lime contents of more than 5% maintain the pH elevated during the first 130 days of curing, as shown in Figure 6.14. A lime content of less than or equal to 3% is only sufficient to satisfy

adsorption, but the cementitious products are not strong enough to aggregate clay particles as observed in residual strength measurements.

A lime content of 3% is sufficient to increase the pH to its maximum immediately after addition of lime, as shown in Figure 6.13. However, a lime content of less than or equal to 3% is not adequate to maintain pH elevated. Lime contents of equal or higher than 5% maintain the elevated pH over time.

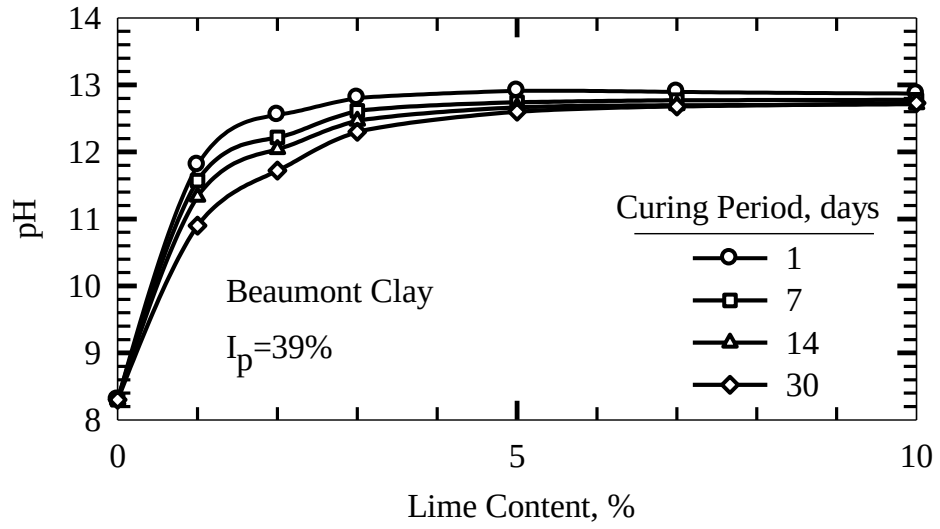

Figure 6.13: pH measurments of Lime-Beaumont clay

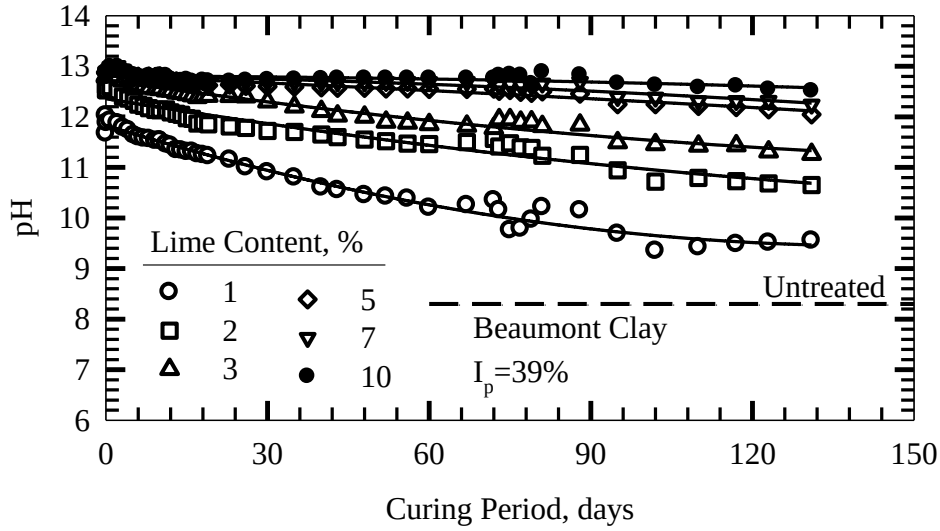

Figure 6.14: pH values of Lime-Beaumont clay with time

Due to low solubility of lime in water, a small amount of lime in excess of adsorbed lime is enough to increase the pH of treated clay to the maximum value. As shown in Figures 6.11-6.13, for lime contents of equal or less than adsorbed lime, pH values decrease with time, implying an ongoing reaction. The increase in the secant peak friction angle of treated clays for lime contents of equal to adsorbed lime suggests that the adsorbed lime is used up in reactions creating bonds among individual clay particles, while no permanent aggregation of clay particles takes place. When lime in access of adsorbed lime is added, aggregation of clay particles occurs through dissolution process.

CHAPTER 7

CLAY-LIME REACTION MANIFEST

7.1 CLAY-LIME REACTION

When dry hydrated lime is thoroughly mixed with a wet soil, lime is consumed, in the absence of carbonation, through two mechanisms: (a) part of the lime particles is adsorbed on soil particles during the mixing process, and (b) part of the remaining lime is dissolved in the soil porewater. The solubility of calcium hydroxide in water is rather small (0.75 g/ℓ). Therefore, the maximum lime content as percent of dry weight of soil that can dissolve in the porewater during the mixing process is quite small and a function of soil water content (less than 0.1% at soil water content of 100%). Dissociation of hydrated lime to $(OH)^-$ and Ca^{2+} leads to a rise in the pH. If enough lime is left, after satisfying the adsorption, soil porewater becomes saturated and pH increases to approximately 12.3 to 12.4. Under the strong alkaline condition, soil mineral particle surfaces become unstable and begin to dissolve in the porewater. Simultaneously, under the elevated pH condition, adsorbed lime particles begin to attack the soil particle surfaces at the points of contact.

Dissolved silica and alumina react with the dissociated calcium hydroxide and form new compounds. As the dissolved hydrated lime is used up in the chemical reactions with silica and alumina, the remaining free lime, if any, dissolves in the porewater and pH is maintained at 12.3-12.4. The dissolution of soil particles and local attack of adsorbed lime on the particle surfaces continue at the initial rate until all free lime is completely consumed. Thereafter, pH begins to decrease as the dissociated calcium hydroxide is used up in the chemical reactions with dissolved silica and alumina. This has been confirmed by pH measurements and chemical analyses conducted by Clare and Cruchley (1957) and Diamond et al. (1964). Dissolution of soil particle surfaces continues at a decreasing rate, becoming insignificant as pH drops to values probably less than around 9 (Eades and Grim, 1960; Eades et al., 1962; Hunter, 1988). The reaction products begin to harden or crystallize as pH decreases. A calcium hydroxide particle is attached to more than one soil particle, connecting them together and producing silt- and sand-sized flocs and

agglomerates (Diamond et al., 1964; Verhasselt, 1990). The Atterberg plastic limit increases, often dramatically, because large amount of water is enclosed within the flocs and agglomerates. In other words, only part of the porewater contributes to plasticity. This is similar to diatoms with poriferous particles in soils such as the Mexico City clay, and andosols containing allophane in which water is trapped within soil aggregates (Mesri et al., 1975; Terzaghi et al., 1996). Both soils display unusually high plastic limits. In summary, total lime content, l_c, is used up through adsorption, l_{ca}, and dissolution, l_{cd}.

As shown in Figure 6.11, a lime content of 3% for Lower Brenna clay is interpreted as the adsorbed lime that is just sufficient to increase the pH above 12.4 immediately after addition of lime but is not adequate to maintain the pH elevated. The secant residual friction angle of Lower Brenna clay does not show a major improvement for a lime content of 3%, whereas there is a significant increase in the secant residual friction angle for a lime content of 5% (Figure 5.86). This is the lime content at which pH remains elevated for a considerable period of time. A maintained elevated pH is required to connect particles together and form stable aggregates. The secant residual friction angle continues to increase for up to a lime contents of 7%, above which it more or less levels off or increases at a lower rate.

Untreated Lower Brenna clay is composed of platy particles, as shown in SEM images in Figure 7.1. Untreated Brenna clay is rich in Si and Al. It also contains Ca as it is a calcium montmorillonite clay. After addition of 3% lime, a light cementation between clay particles take place, Figure 7.2. Few needle-shaped products (ettringite) form by addition of 3% lime as shown in the SEM images. No major stable aggregation occurs at this lime content. As lime content increases to 7%, large aggregates are produced with numerous needle-shaped products filling the voids, as shown in Figure 7.3 for 7% lime Lower Brenna clay cured for 7 weeks. The needle-shaped products are composed of Si, Al, Ca, and S according to the EDS analysis results, Figure 7.3, which confirms the nature of the crystals as ettringite. The SEM images of Lower Brenna clay treated with 7% cured for 17 weeks show cementitious products covering clay aggregates, Figure 7.4. A 10% lime treated specimen cured for 10 weeks were examined by SEM, as shown in Figure 7.5. High degree of cementation and ettringite formation similar to 7% lime treated samples are observed for 10% lime treated clay. All specimens were cured under a confined condition.

A series of Upper Brenna clay specimens were prepared with water contents in the range of 70-180%, treated with 7% lime, and cured for 6 or 12 months under unconfined condition to examine the products forming under such condition. The SEM images of the specimens with 70% water content, cured for 6 months (Figure 7.6) and 1 year (Figure 7.7) show cementitious material in the form of a network of interlacing wires (reticulation) with small pores within the reticulated area and large pores around them. A higher water content of 120% provides enough water to produce needle-shaped ettringite as shown in Figures 7.8 and 7.9. As water content increases to 180%, flexible fiber-shaped products form with open structure in which cementitious products fail to bridge between clay particle and form a packed structure. Figure 7.12 shows the SEM images of a 7% lime treated specimen with 180% water content after shearing. The images reveal a network of fiber-shaped products. Theses fibers do not provide enough interlocking when cured under unconfined condition where particles are not in intimate contact. Hence the needle-shaped crystals and fibers do not contribute to frictional resistance. Alternatively, when cured under confined condition, needle-shaped crystals and fibers form in a compact arrangement and connect particles together, leading to a solid structure.

According to the pH measurements for treated Beaumont clay (Figure 6.13), a minimum lime content of 3% is required to increase the pH above 12.4 immediately after addition of lime. This is the definition of adsorbed lime, l_{ca}. However, the pH of 3% lime-Beaumont clay drops below 12.4 quickly as time passes, as shown in Figures 6.13 and 6.14. A minimum lime content of 5% is required to maintain pH above 12.4 over time. This is the lime content at which a significant increase in the residual friction angle is achieved (Figure 5.87), suggesting that aggregation has taken place. For lower lime contents, e.g. 3%, although there is a significant increase in the peak strength, the residual friction angle experiences a minimal increase. This suggests that lime contents of equal or less than the adsorbed lime, l_{ca}, of 3% do not initiate aggregation of the clay particles. Once the lime content increases to 5%, a major clay particle aggregation takes place by pozzolanic reactions through dissolution. Adsorption process attach clay particle edges and connect particles to each other to produce floccules. Lime in excess of adsorbed lime maintains elevated pH condition and attach particles together by producing pozzolanic reaction products through dissolution. The peak strength is more determined by inter-particle or inter-aggregate bonding.

The SEM images of untreated Beaumont clay are shown in Figure 7.13. Individual platy particles are observed in untreated clay. As shown in SEM images in Figure 7.14 for Beaumont clay treated with 5% lime and cured for 4 weeks, clay particles are coated by cementitious products forming large aggregates. The EDS analysis, Figure 7.14, shows that the products are rich in Si, Ca, and Al, confirming formation of CSH and CASH cementitious products. The lime is enough to produce cementitious reaction products and stable aggregates to increase the residual strength of the clay. As lime content increases to 10%, more cementitious products form to fill the voids, as shown in Figure 7.15. The EDS analysis results, Figure 7.15, show the nature of the reaction products composed of Si, Al, Ca. More cementitious material is observed in 10% lime treated Beaumont clay, resulting in larger aggregates and smaller voids. Both 5% and 10% lime treated samples were cured under a confined condition.

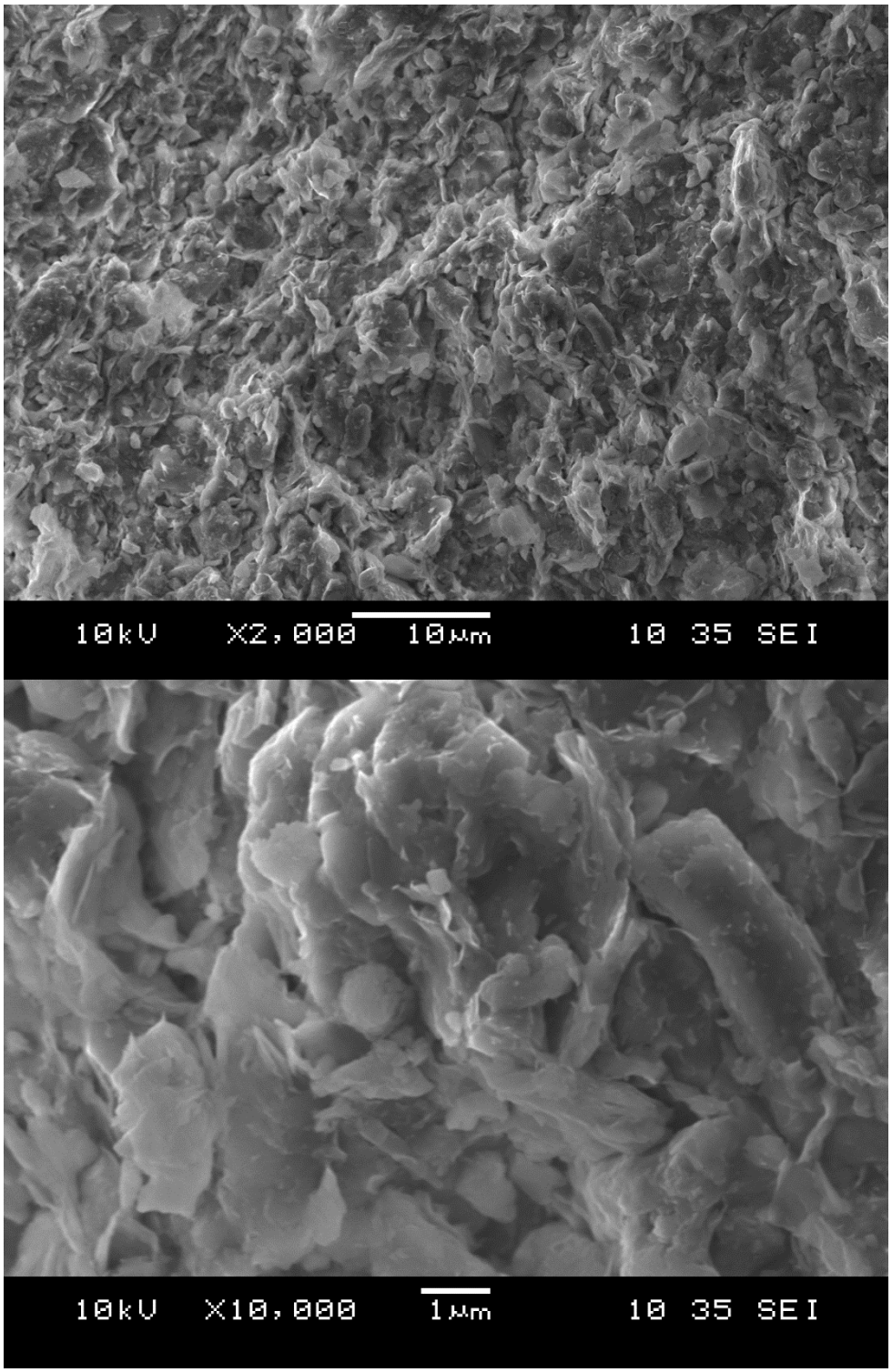

Figure 7.1: SEM image and EDS of untreated Lower Brenna clay

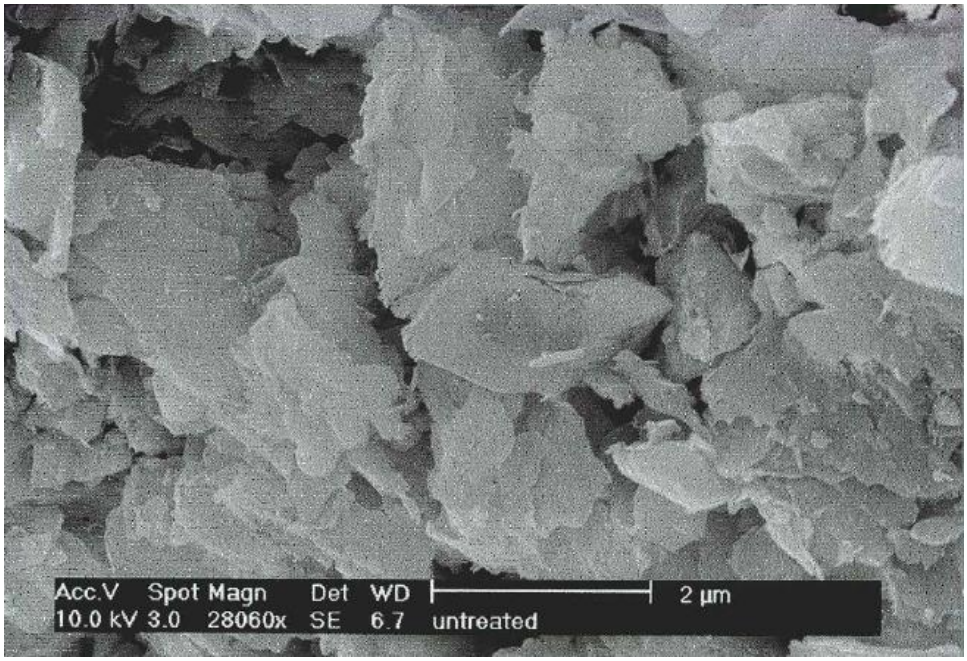

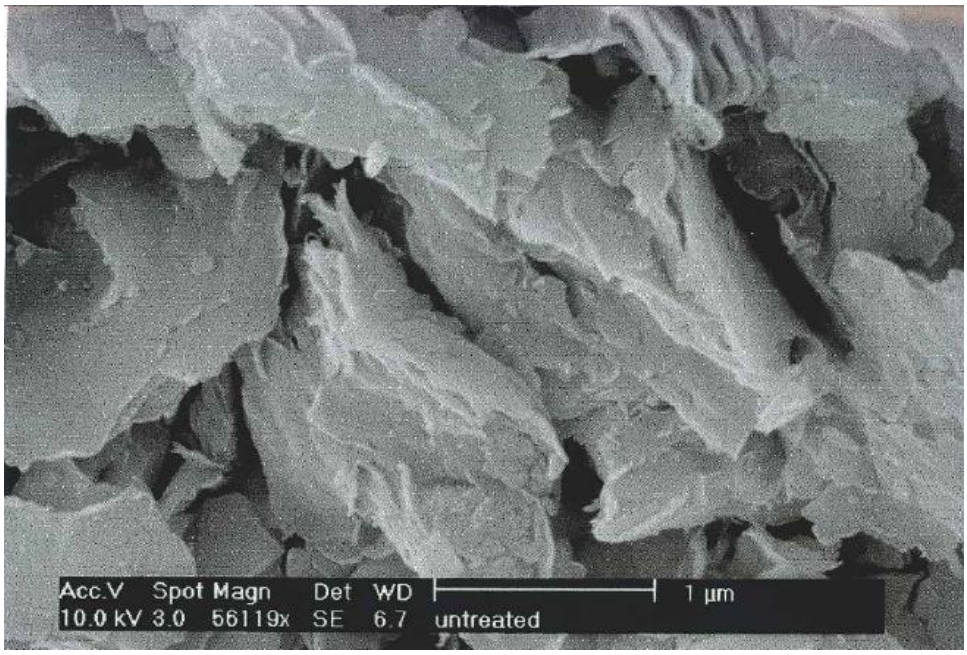

Figure 7.1: (cont'd)

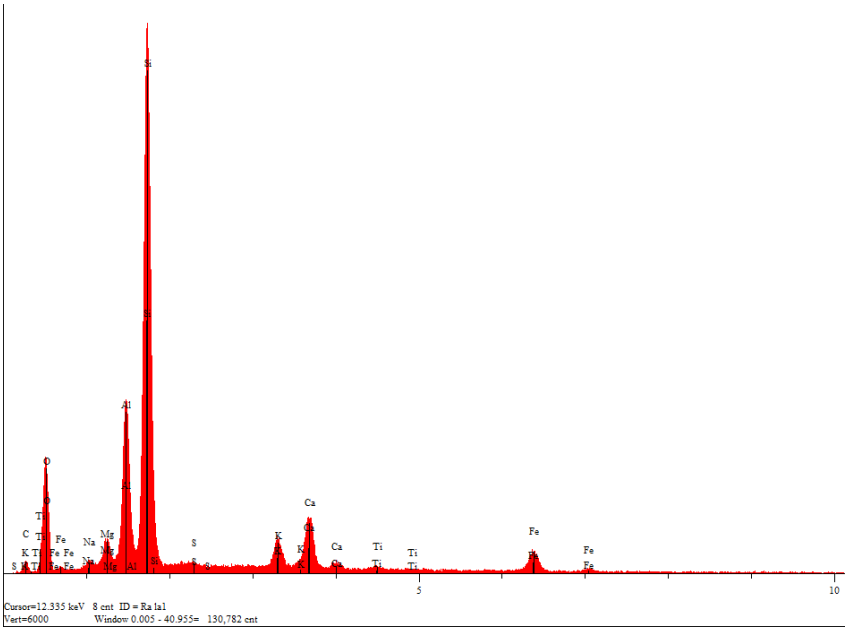

Figure 7.1: (cont'd)

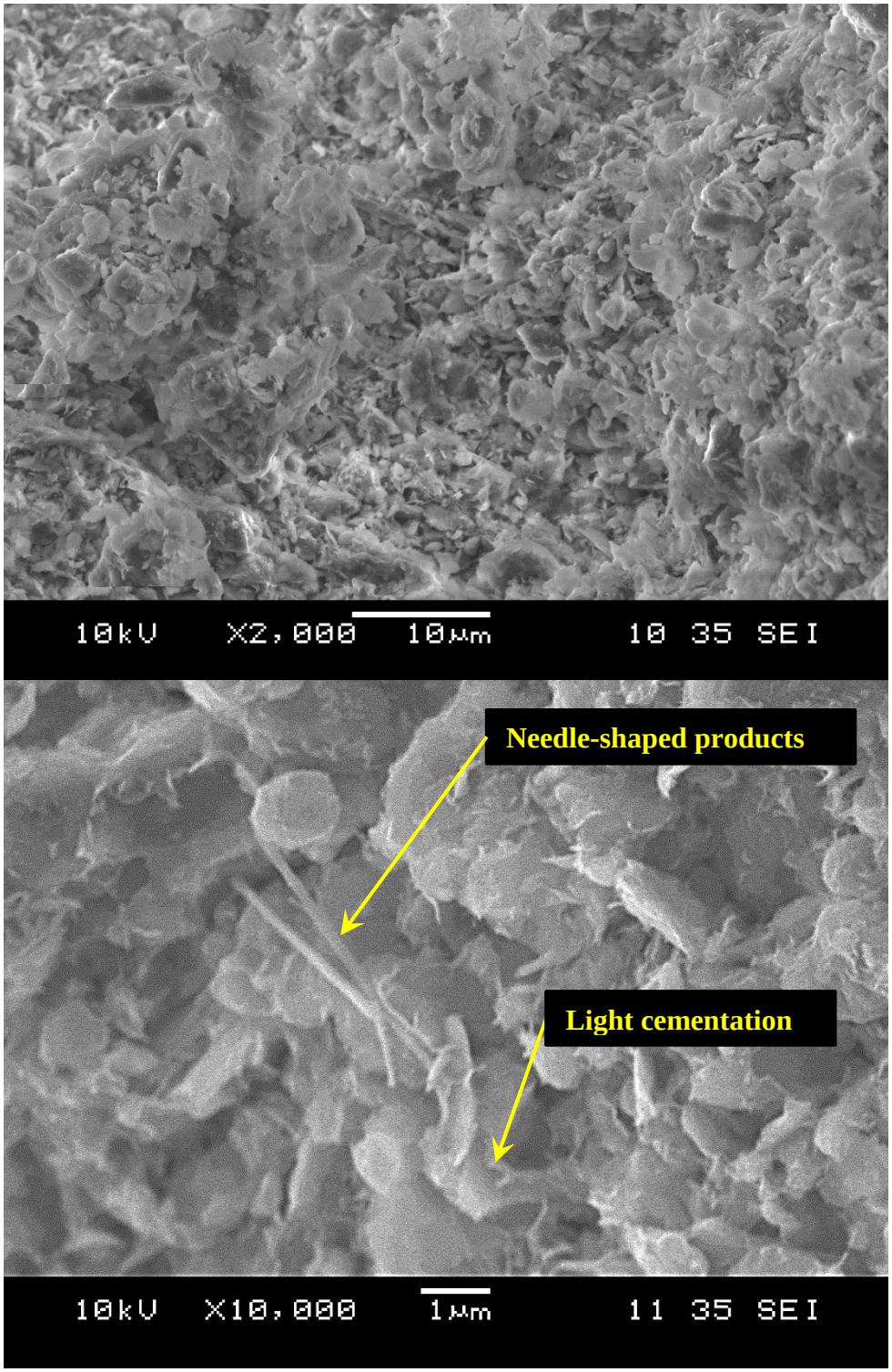

Figure 7.2: SEM image and EDS of Lower Brenna clay treated by 3% lime, cured for 4 weeks under confined condition

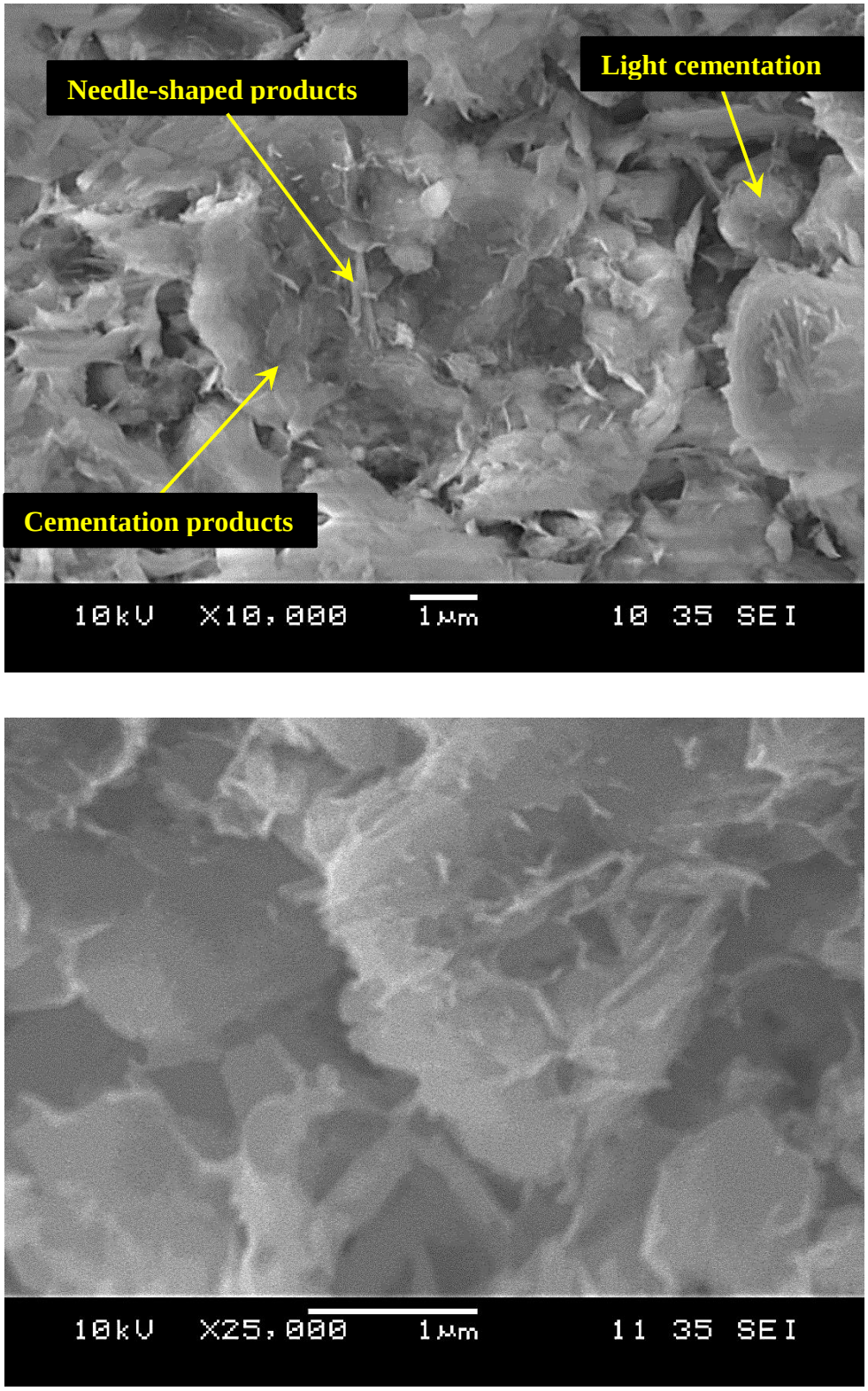

Figure 7.2: (cont'd)

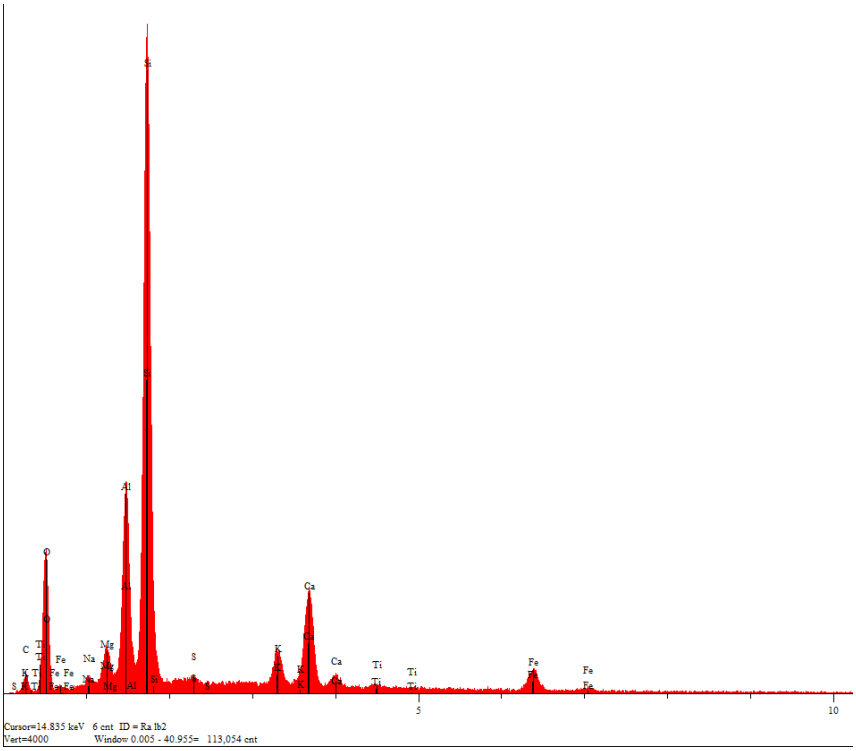

Figure 7.2: (cont'd)

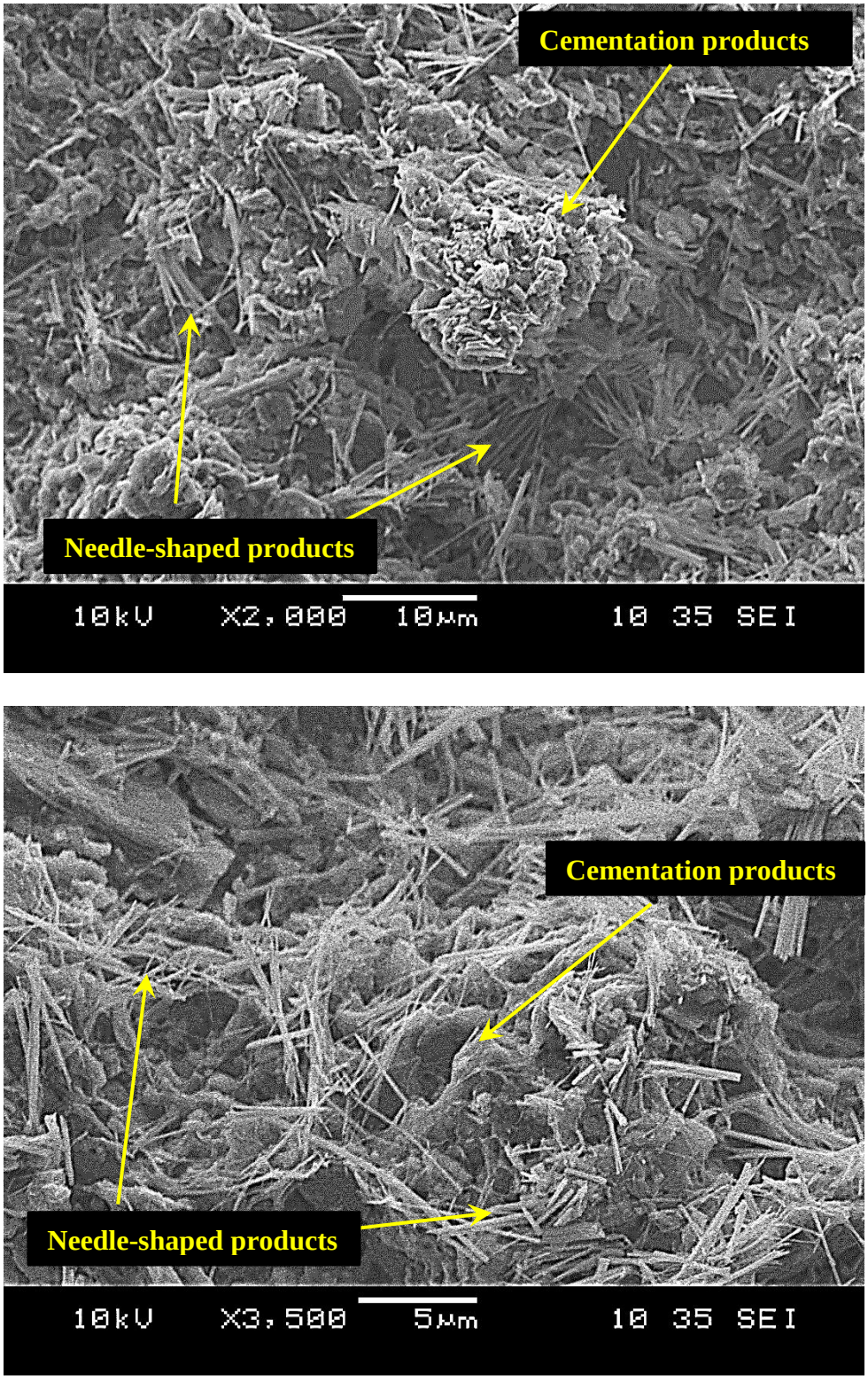

Figure 7.3: SEM image and EDS of Lower Brenna clay treated by 7% lime, cured for 6 weeks under confined condition

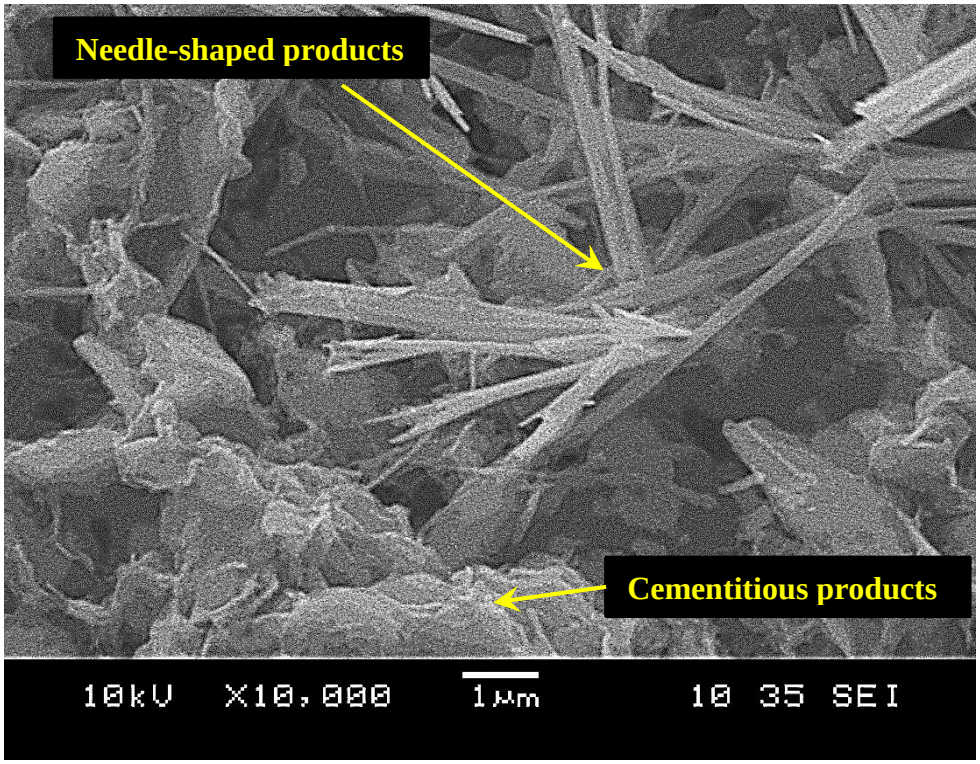

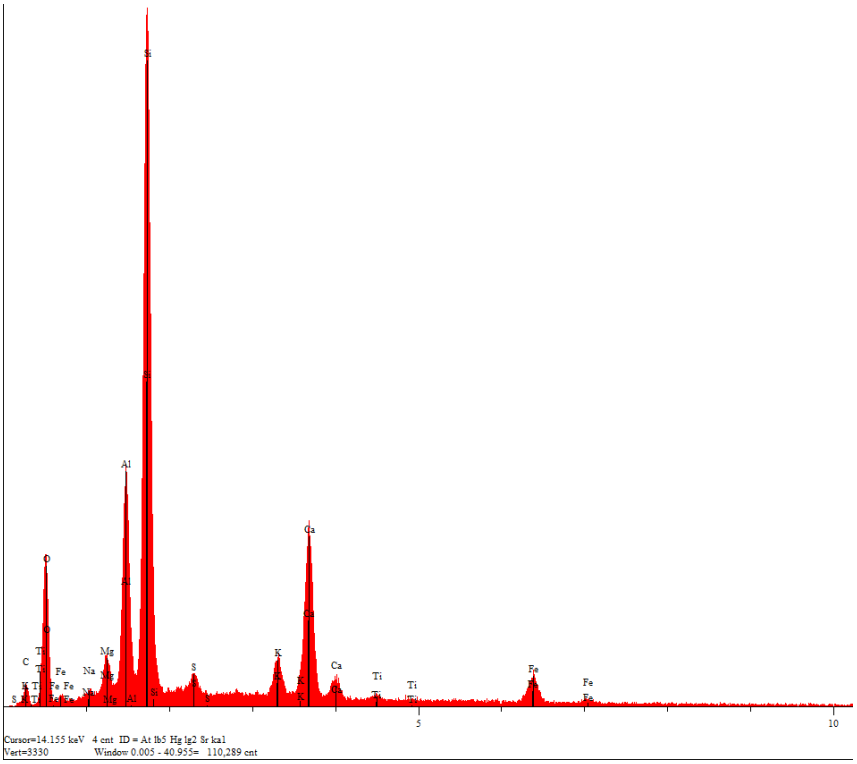

Figure 7.3: (cont'd)

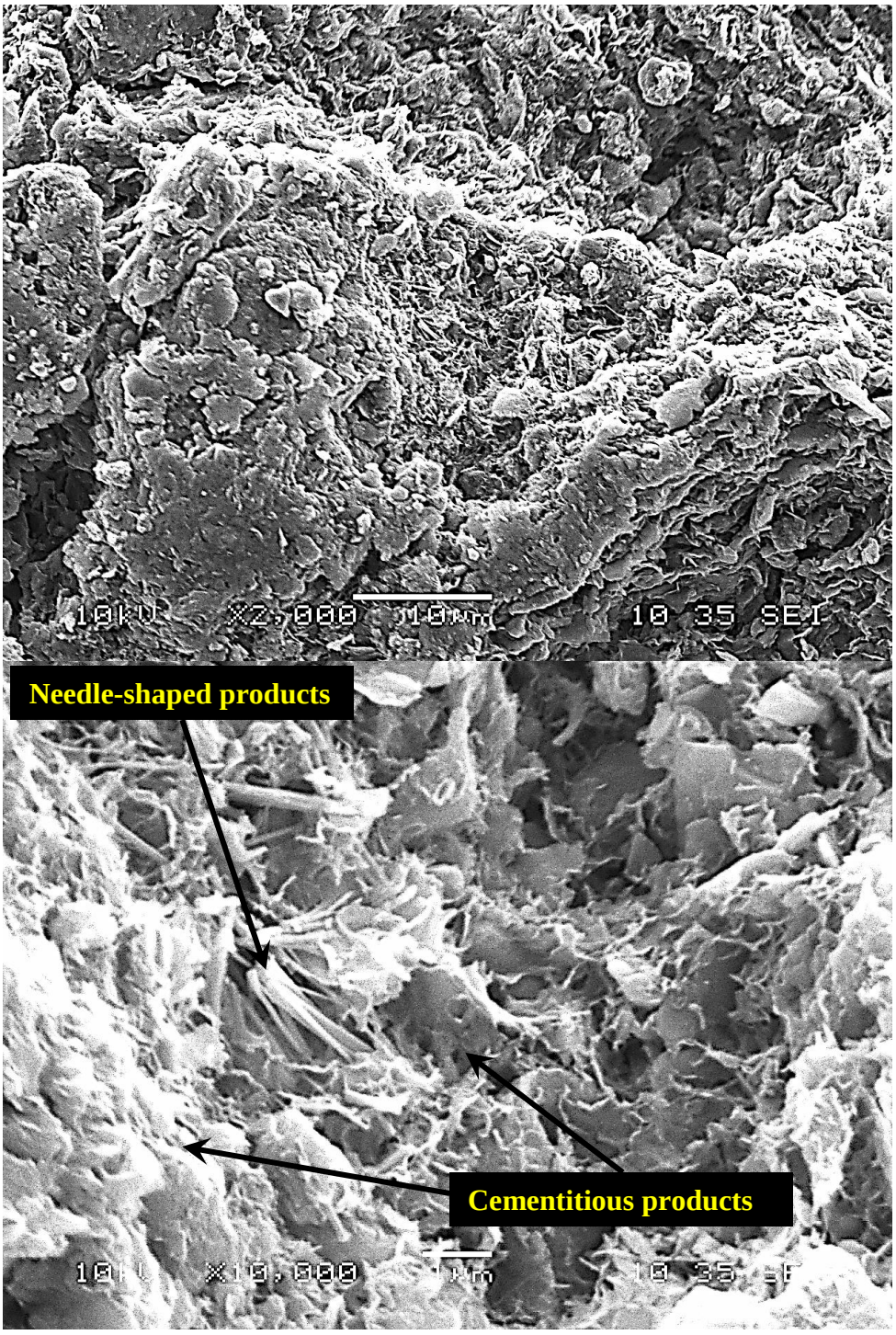

Figure 7.4: SEM image of Lower Brenna clay treated by 7% lime, cured for 12 weeks under confined condition

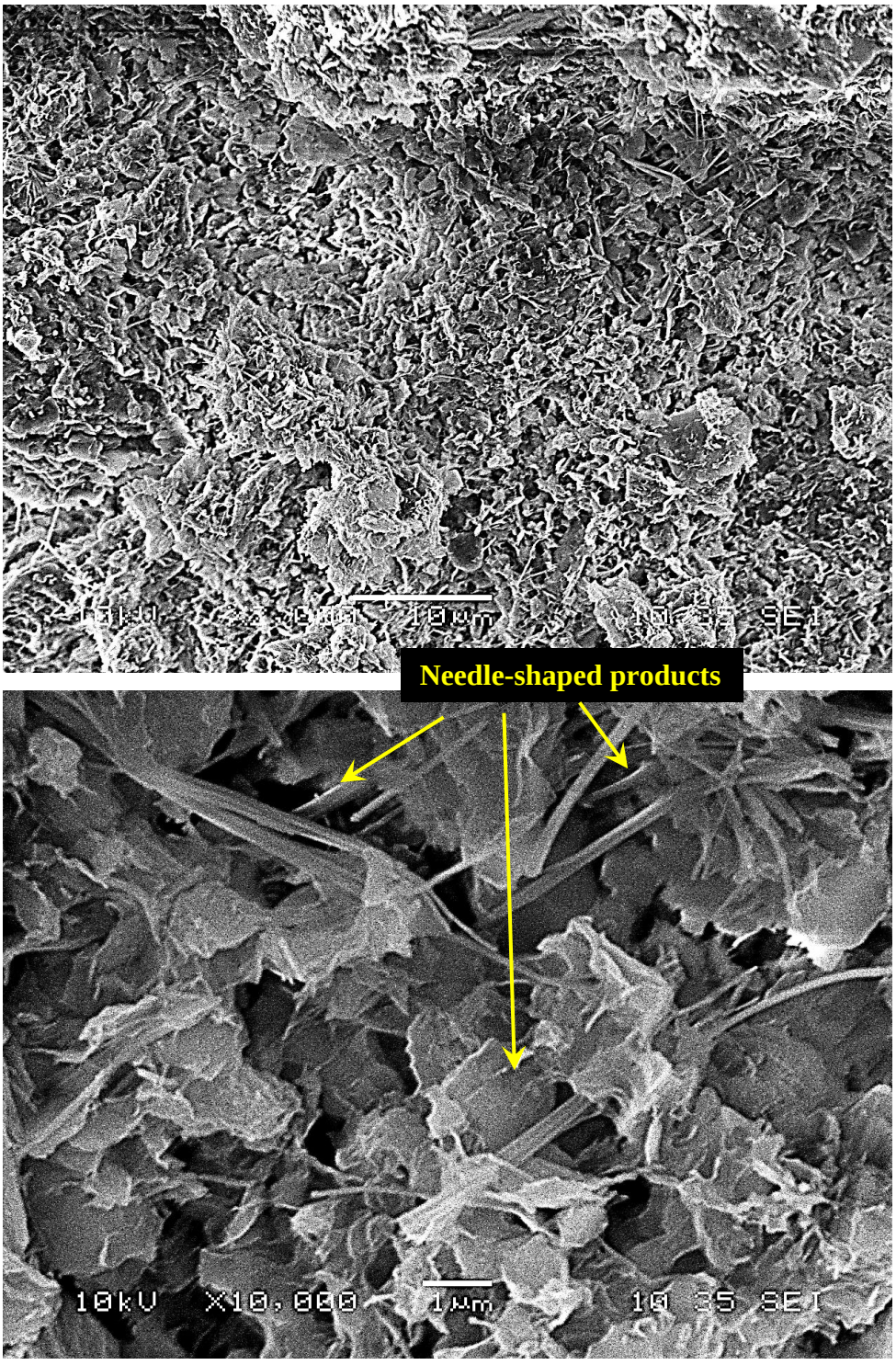

Figure 7.5: SEM image of Lower Brenna clay treated by 10% lime, cured for 7 weeks under confined condition

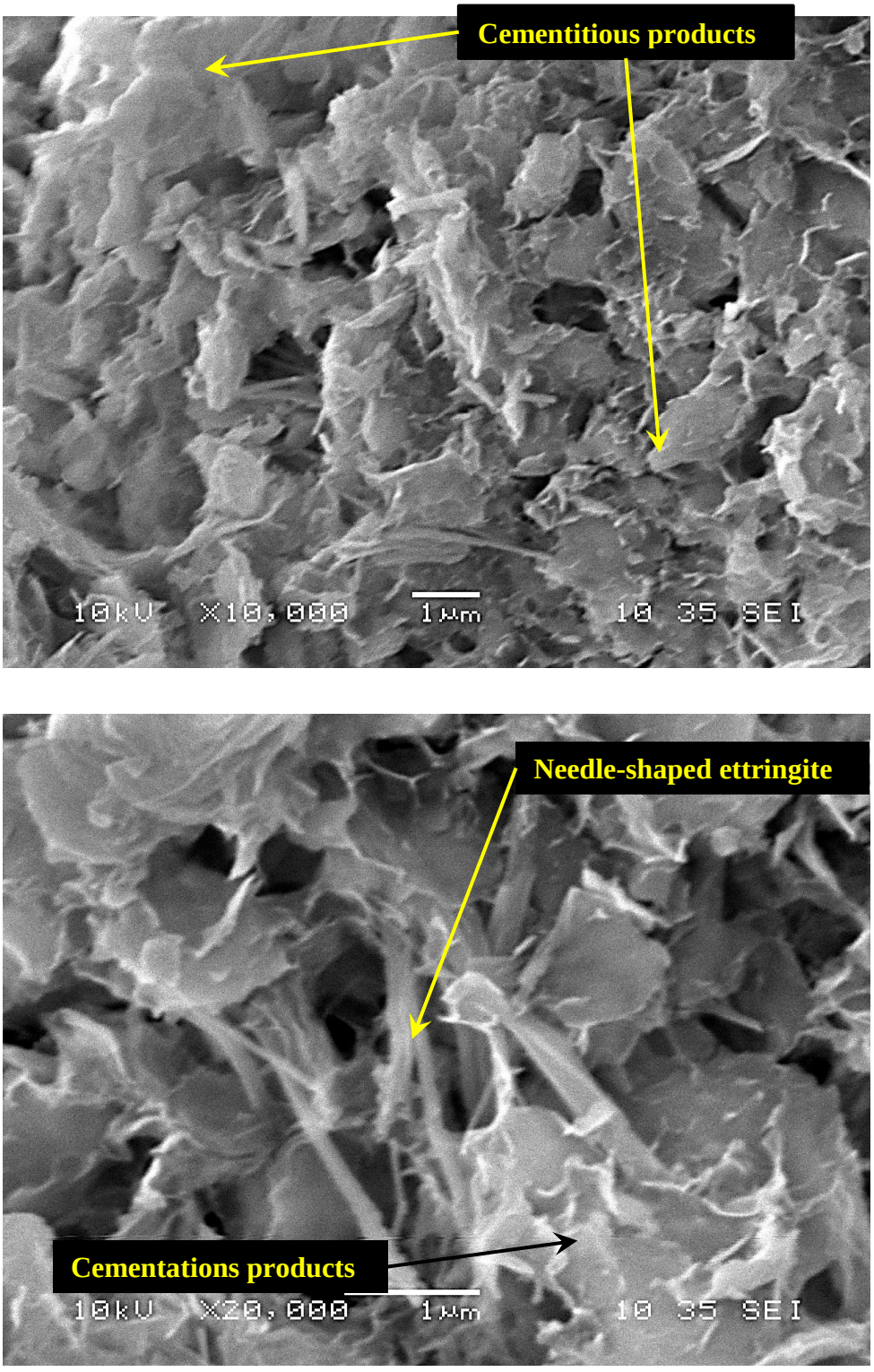

Figure 7.5: (cont'd)

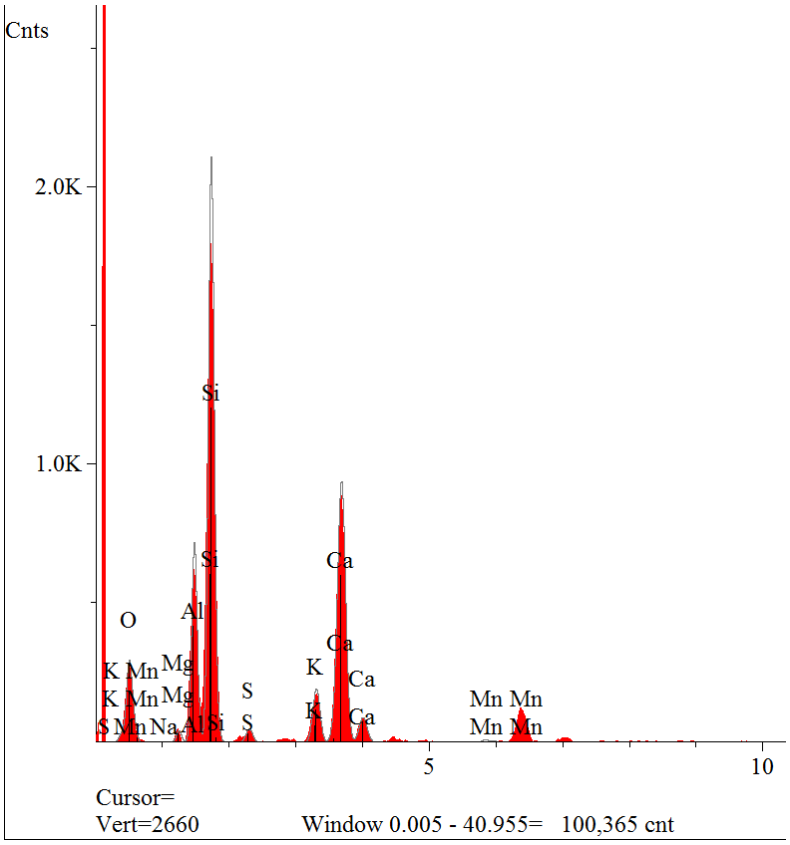

Figure 7.5: (cont'd)

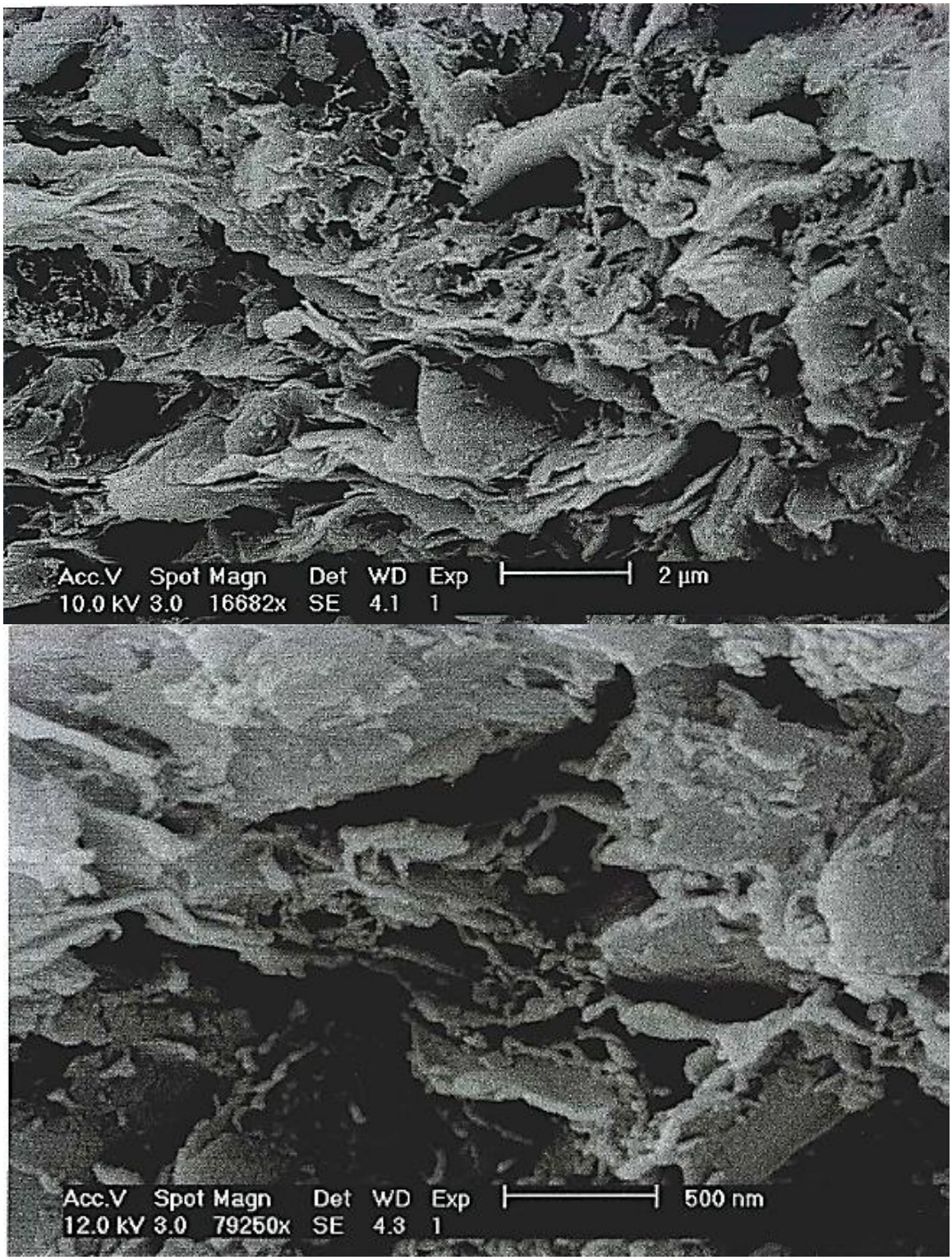

Figure 7.6: SEM image of Upper Brenna clay, 70% water content, treated by 7% lime, and cured for 6 month under unconfined condition

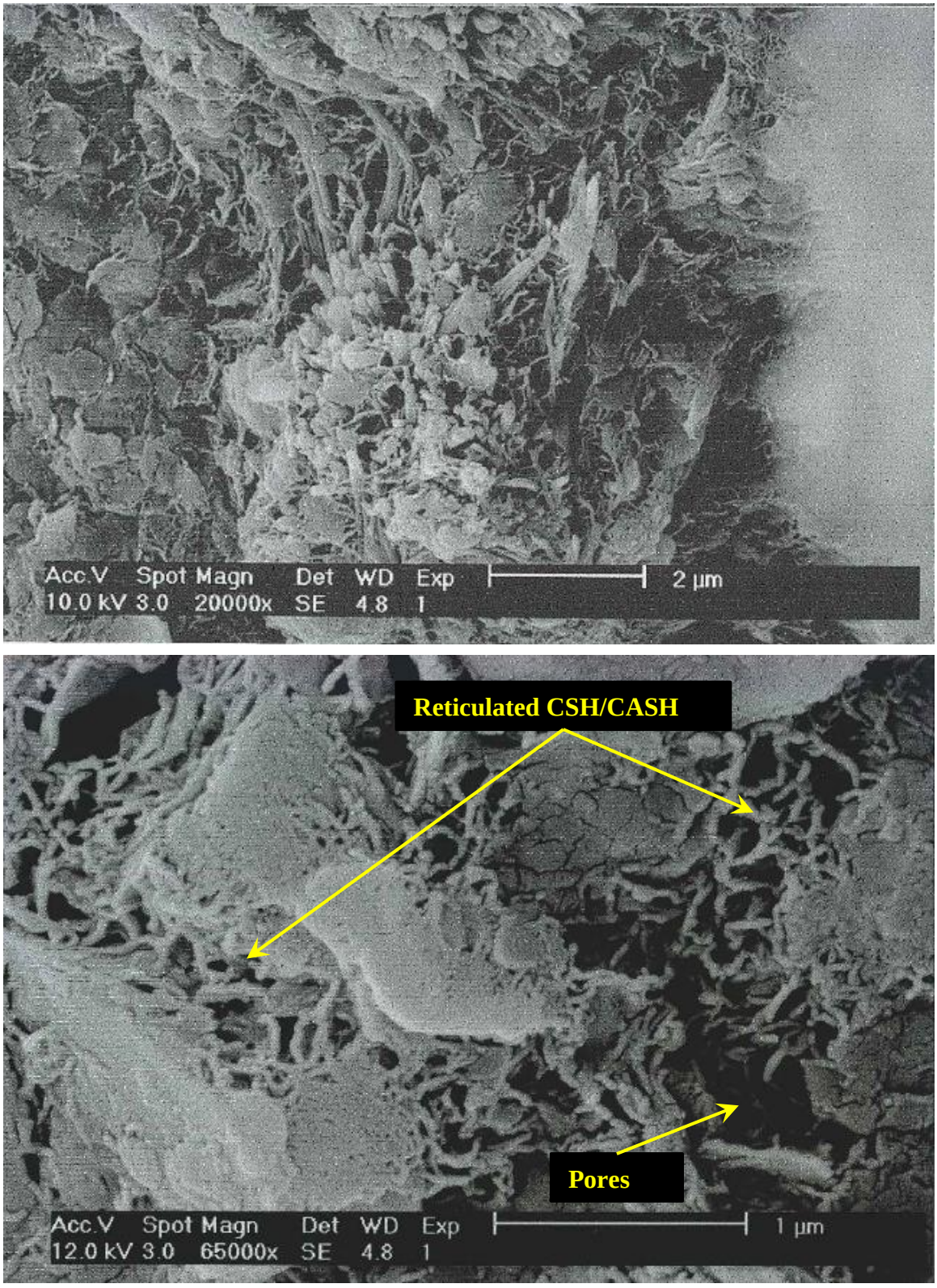

Figure 7.7: SEM image of Upper Brenna clay, 70% water content, treated by 7% lime, and cured for 1 year under unconfined condition

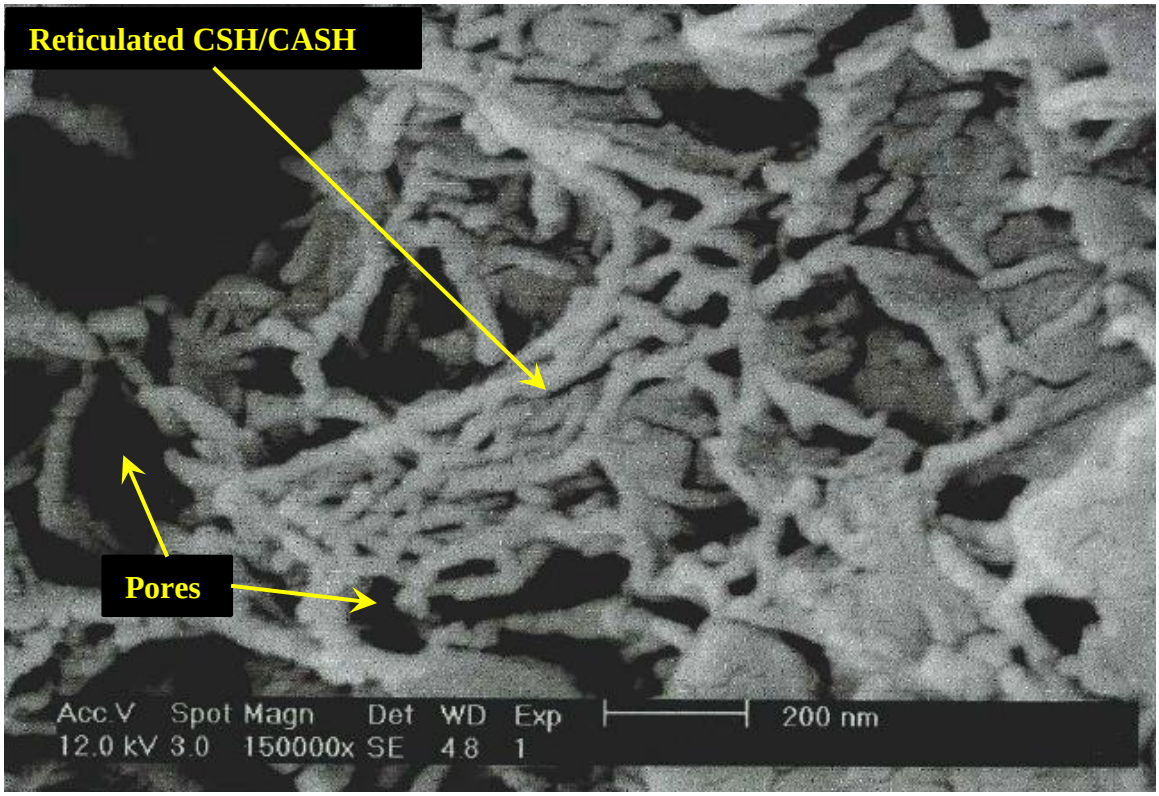

Figure 7.7: (cont'd)

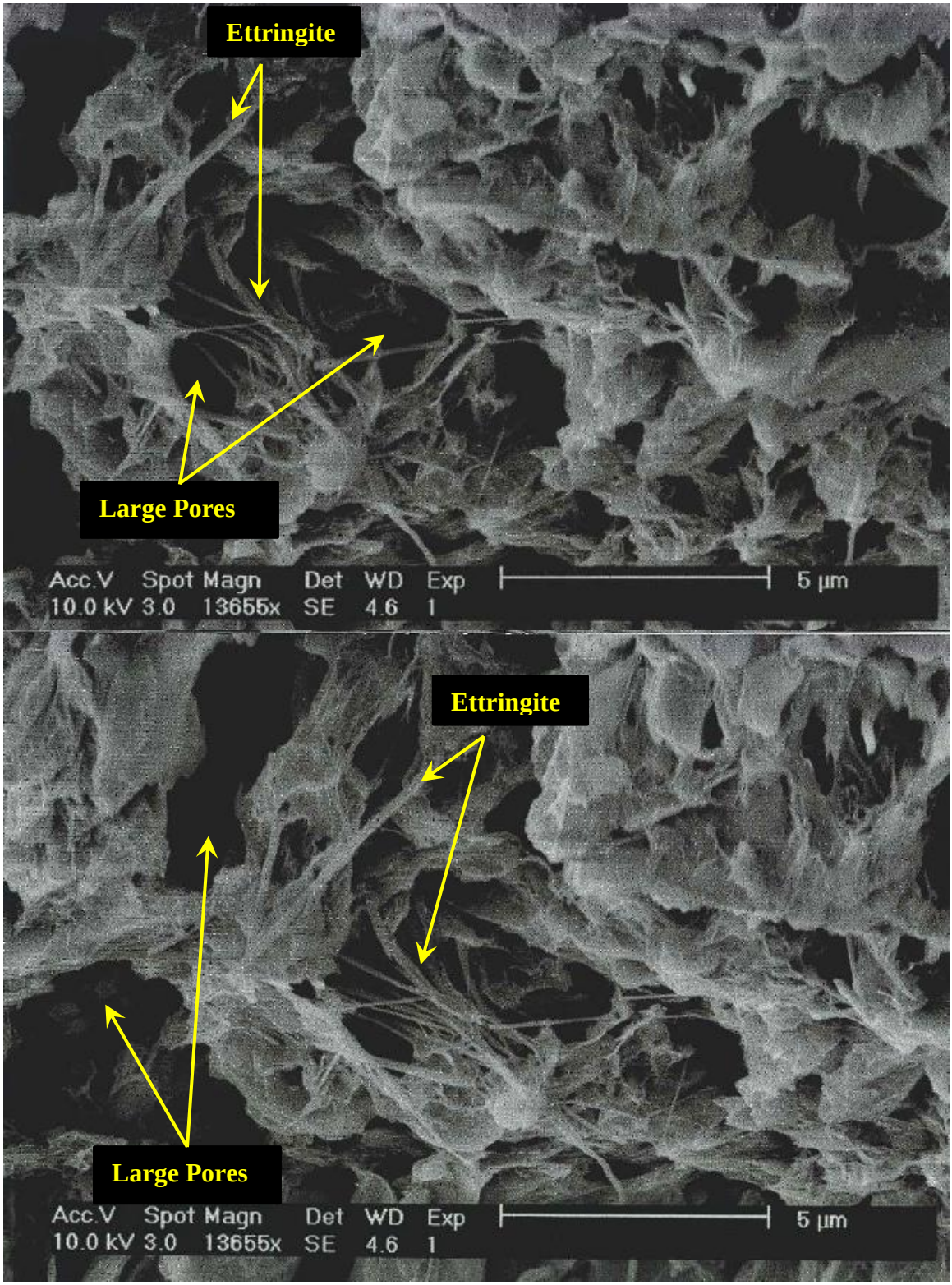

Figure 7.8: SEM image of Upper Brenna clay, 120% water content, treated by 7% lime, and cured for 6 months under unconfined condition

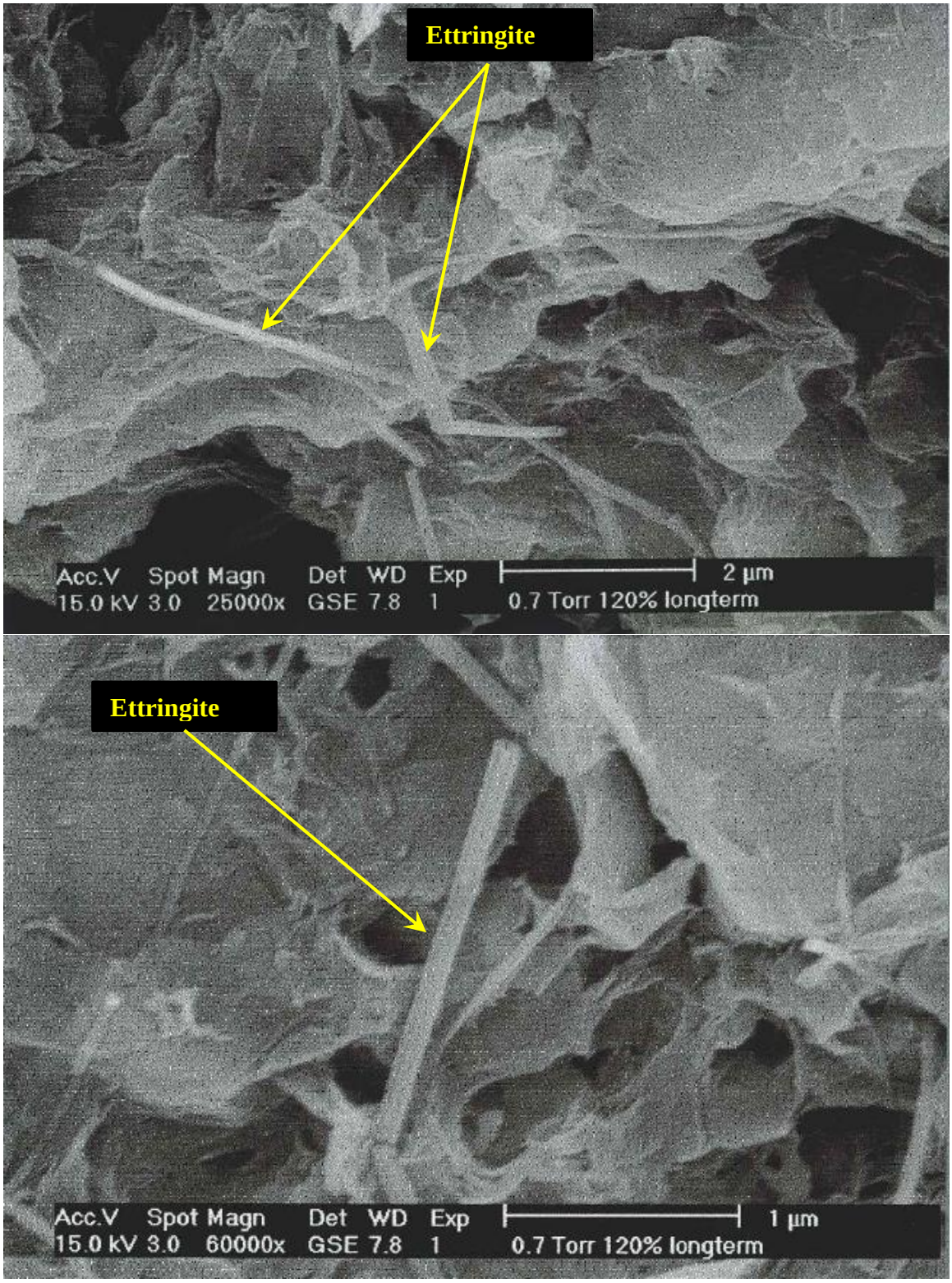

Figure 7.9: SEM image of Upper Brenna clay, 120% water content, treated by 7% lime, and cured for 1 year under unconfined condition

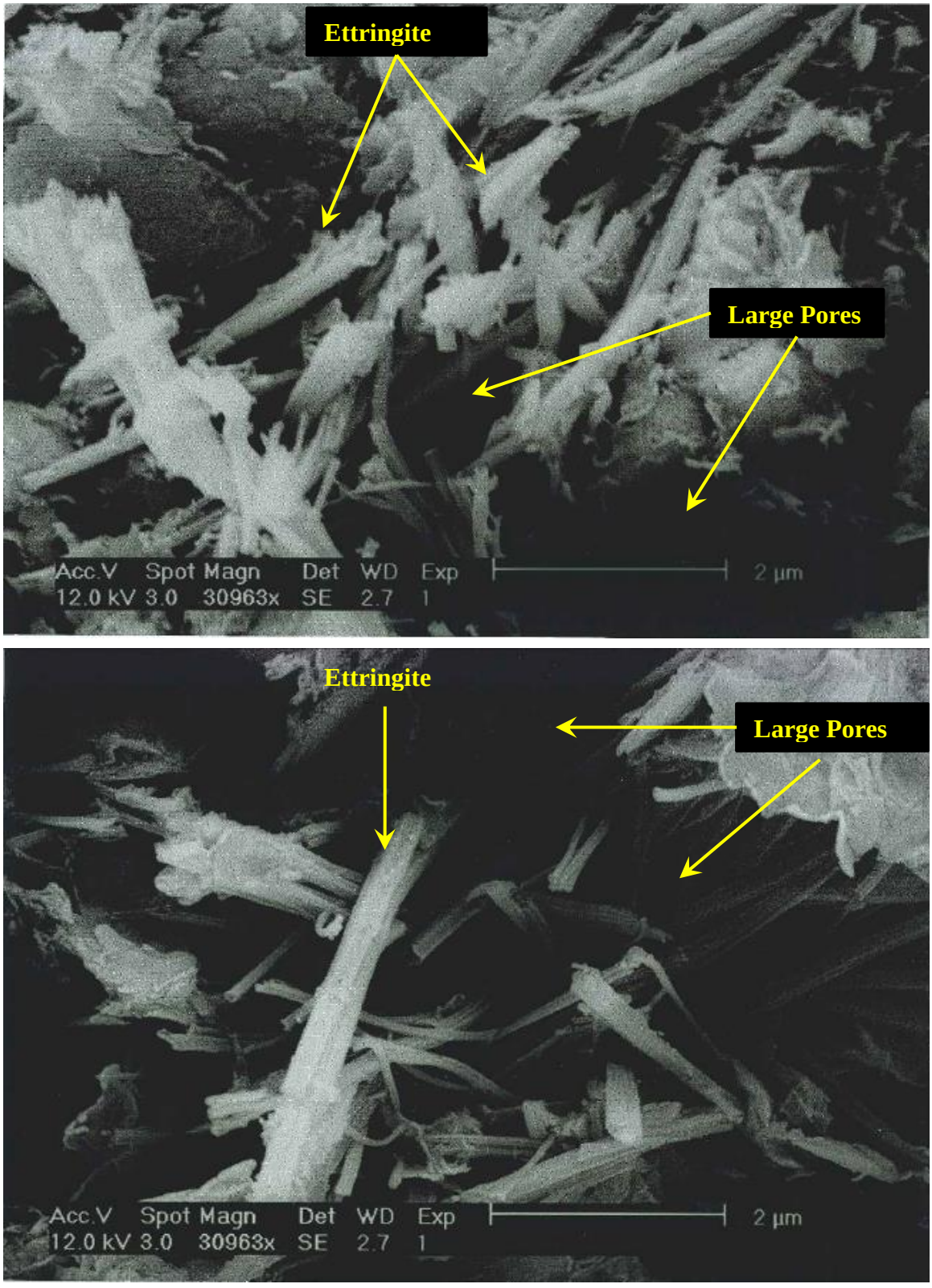

Figure 7.10: SEM image of Upper Brenna clay, 180% water content, treated by 7% lime, and cured for 6 months under unconfined condition

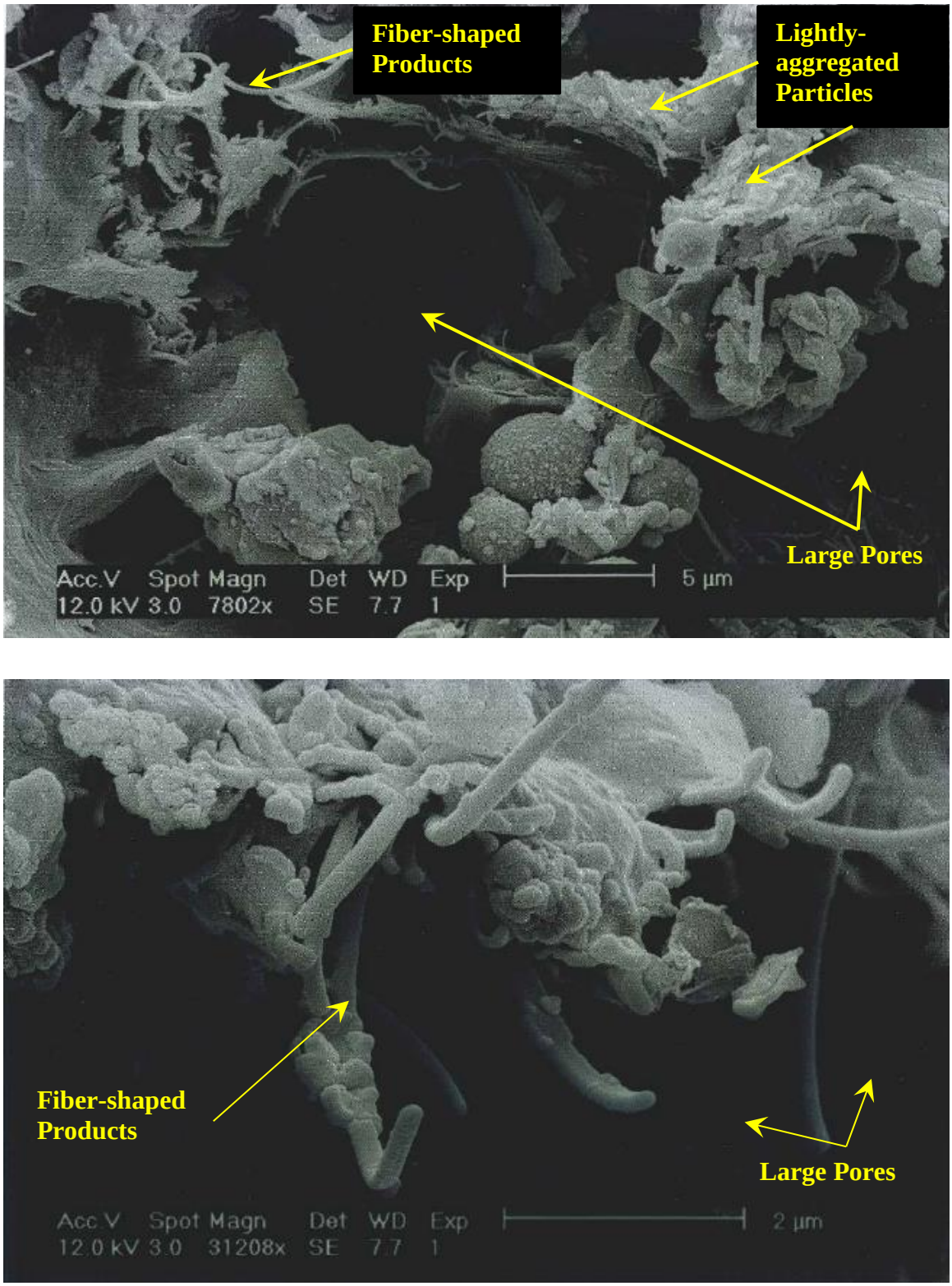

Figure 7.10: (cont'd)

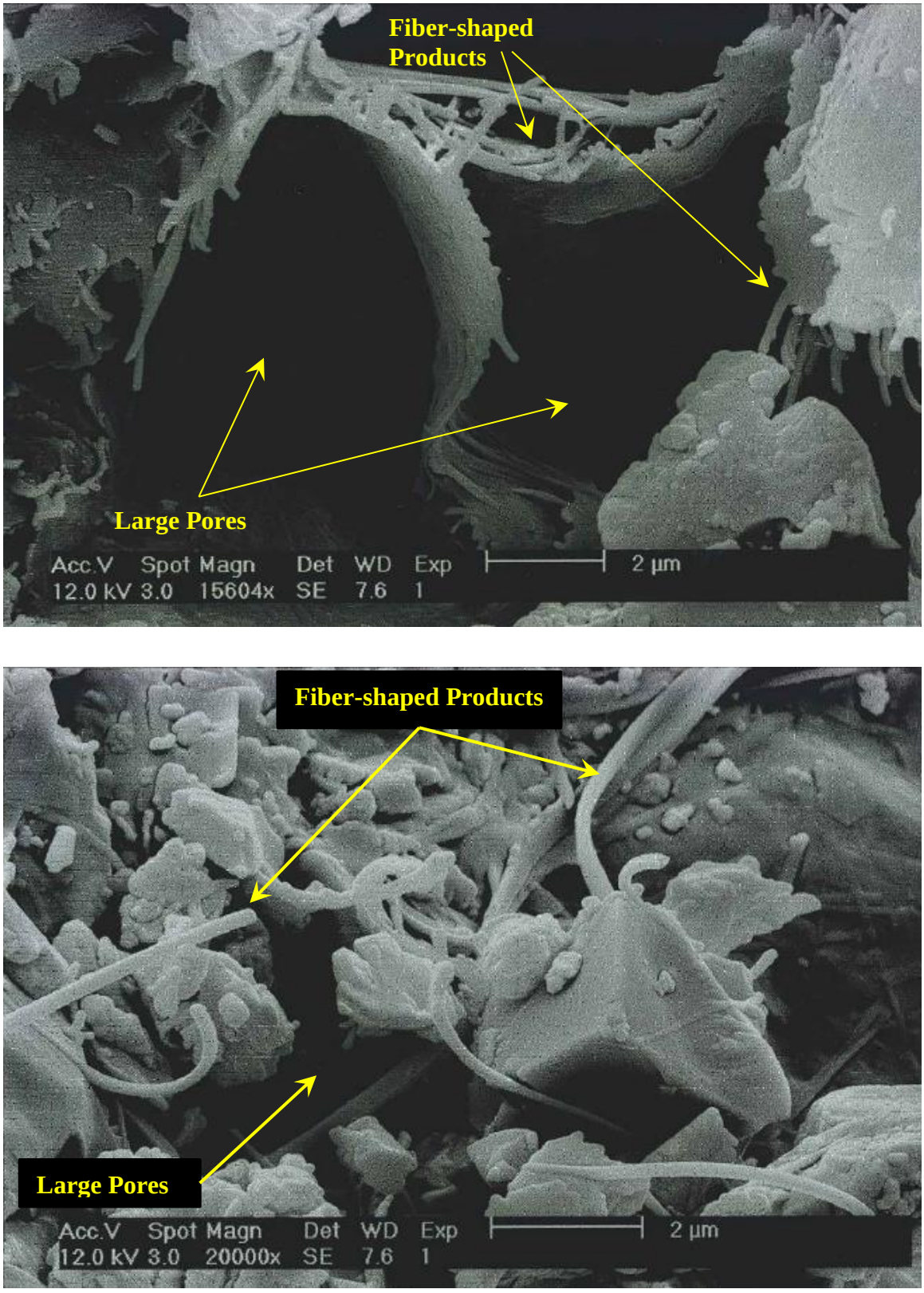

Figure 7.10: (cont'd)

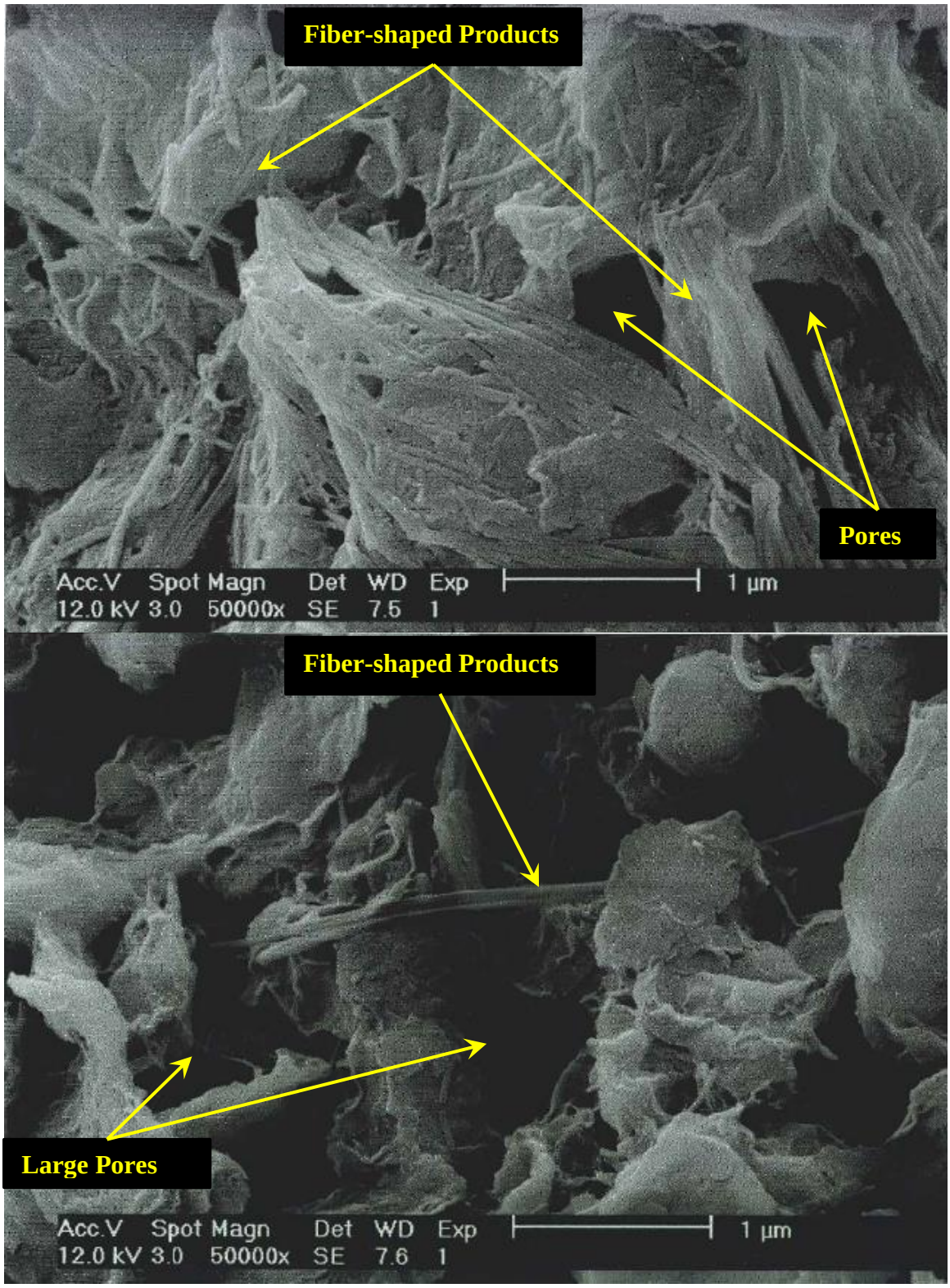

Figure 7.10: (cont'd)

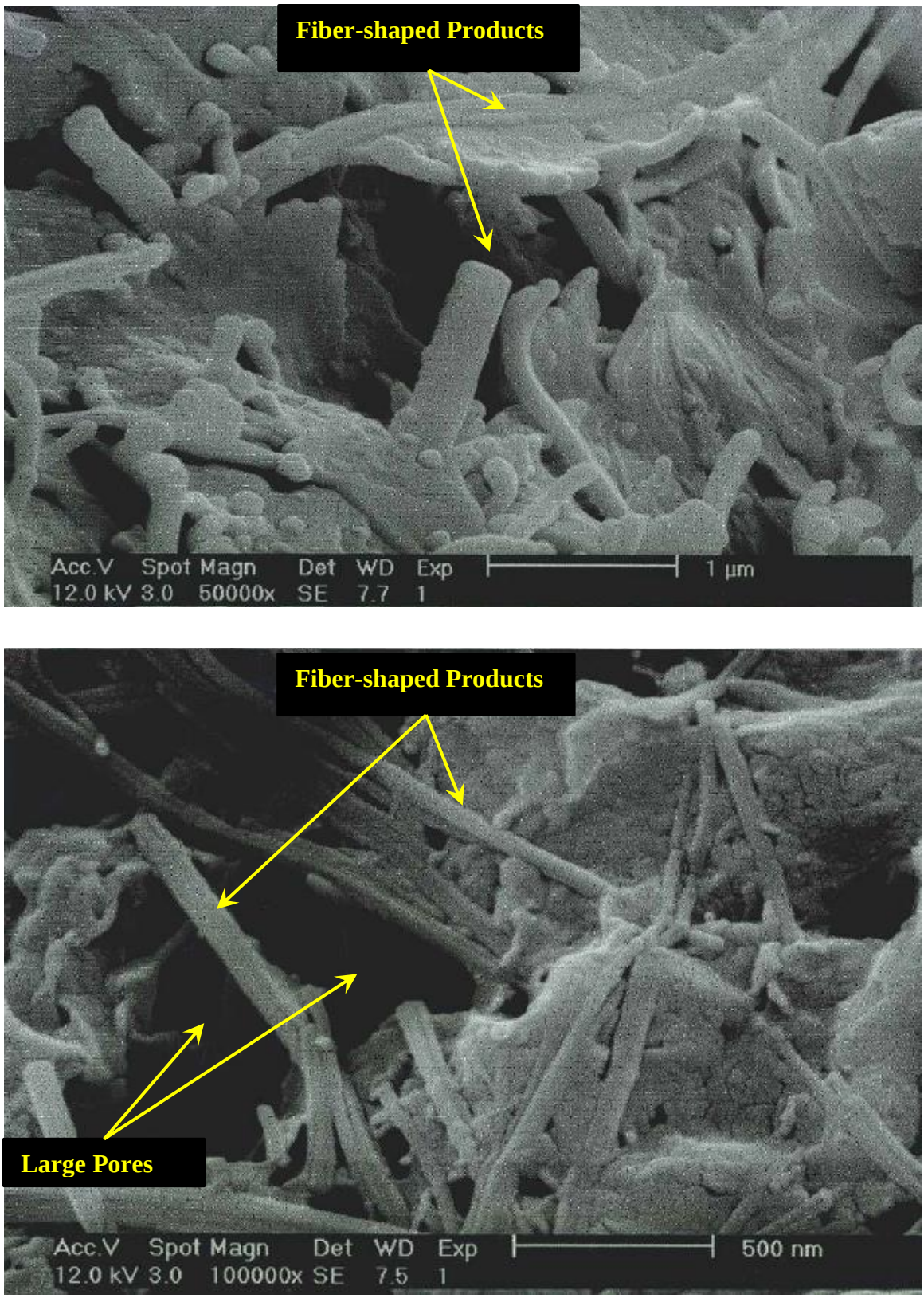

Figure 7.11: SEM image of Upper Brenna clay, 180% water content, treated by 7% lime, and cured for 1 year under unconfined condition

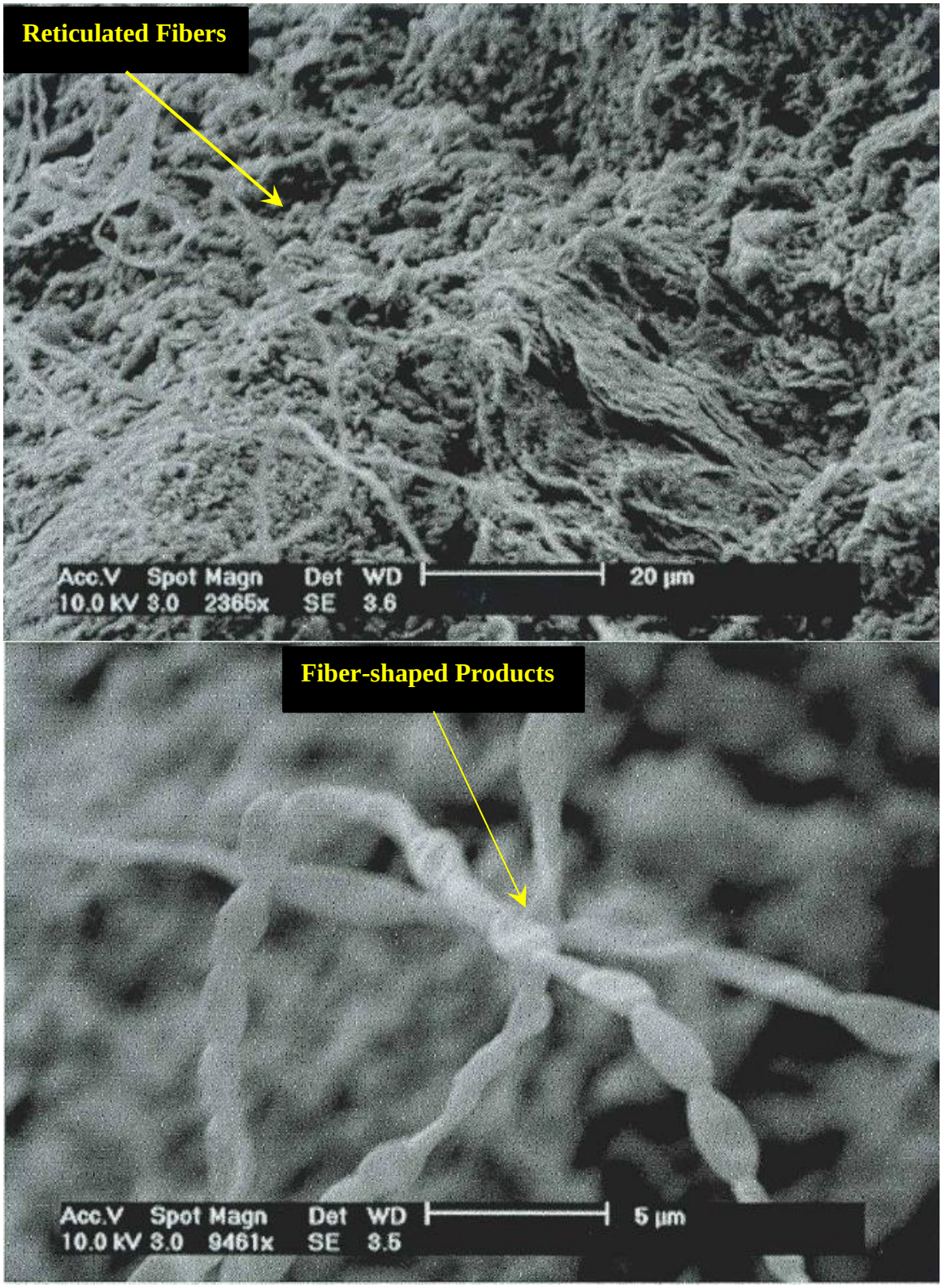

Figure 7.12: SEM image of Upper Brenna clay, 180% water content, treated by 7% lime, cured for 6 months under unconfined condition and sheared for 2 months

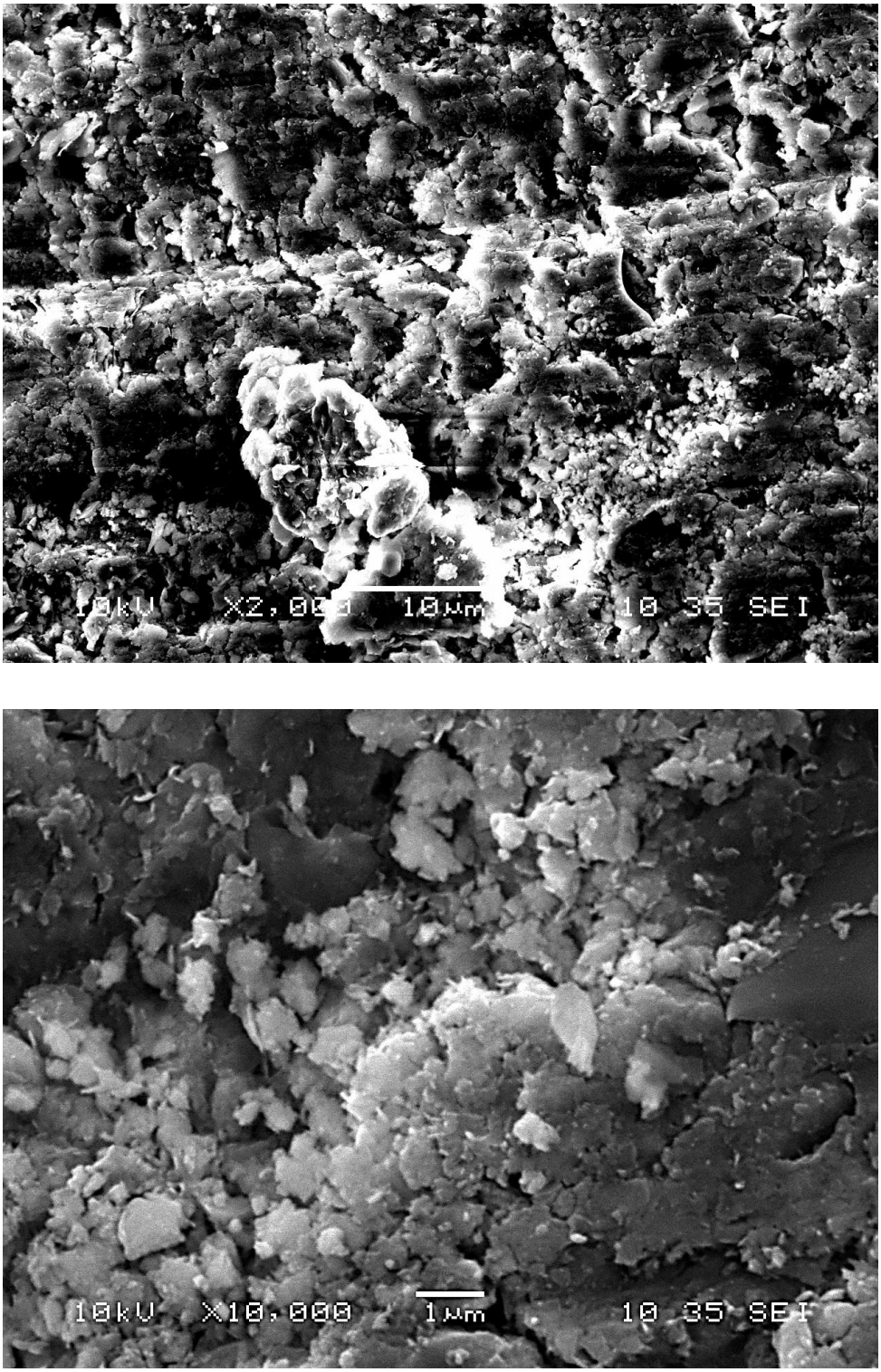

Figure 7.13: SEM image of untreated Beaumont clay

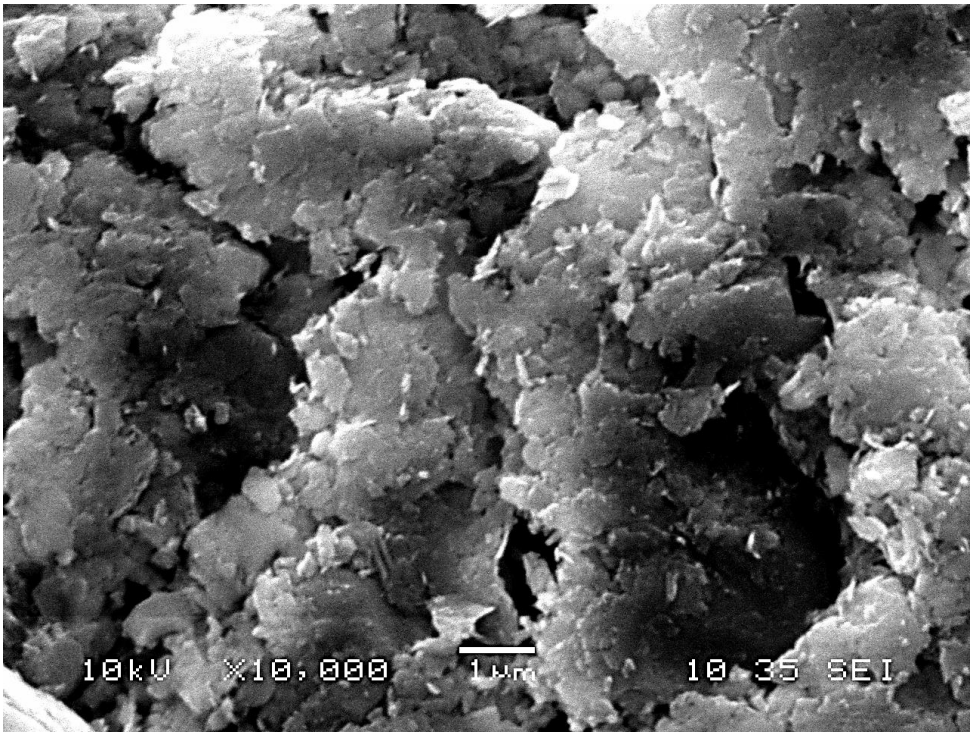

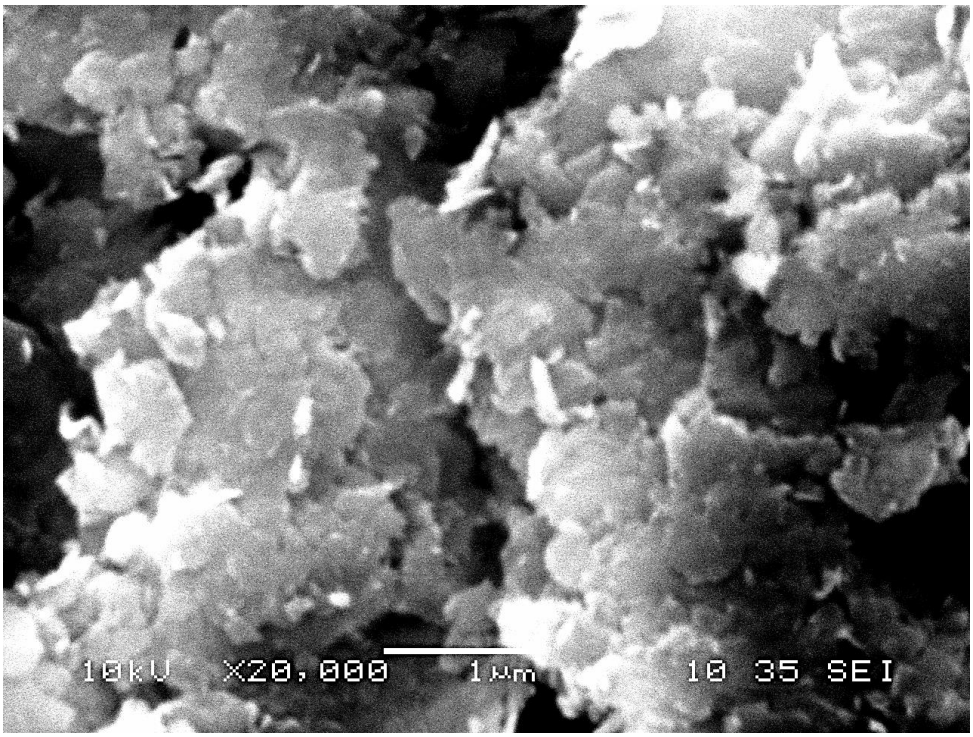

Figure 7.13: (cont'd)

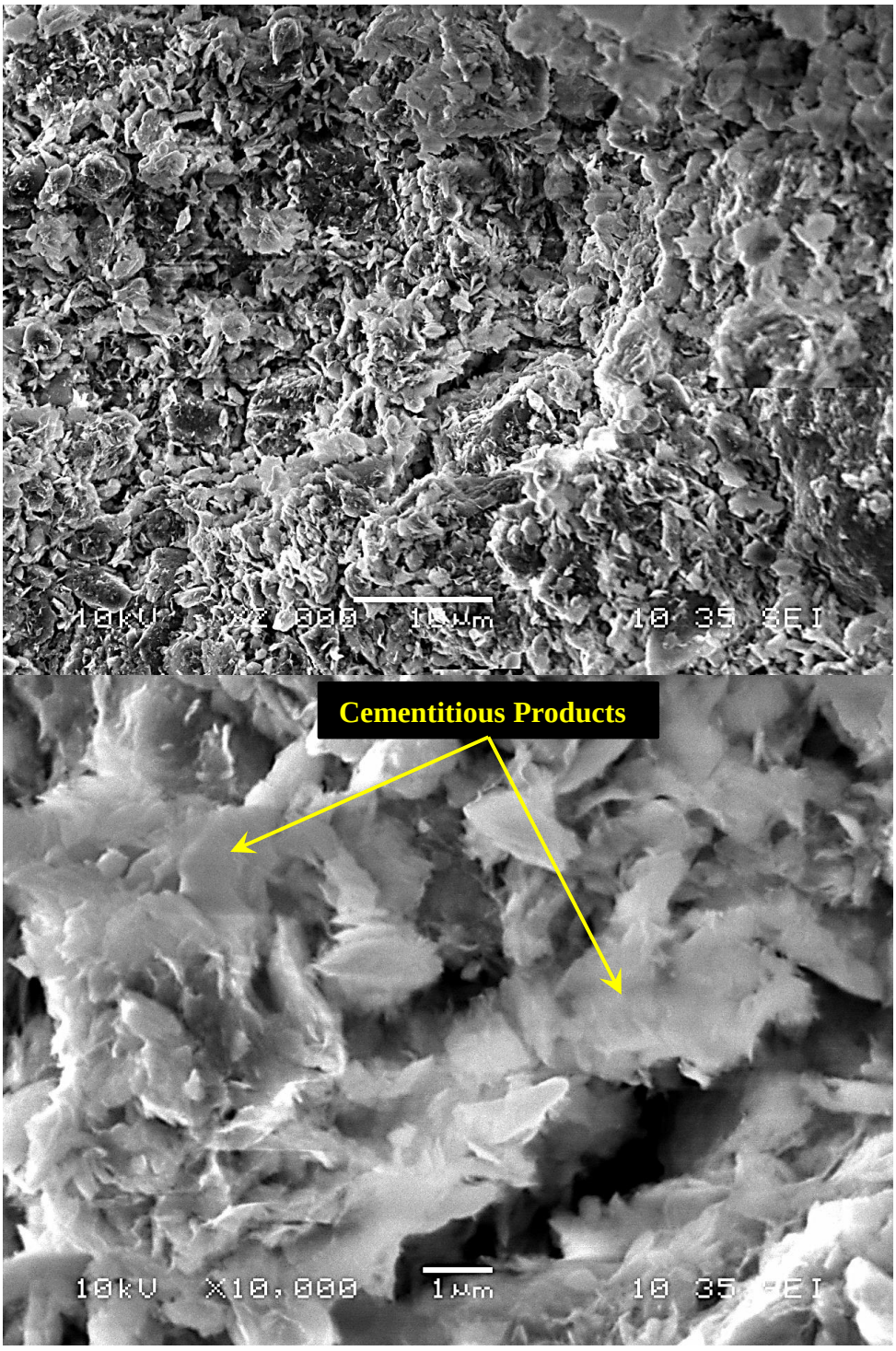

Figure 7.14: SEM image of Beaumont clay treated by 5% lime, cured for 4 weeks under confined condition

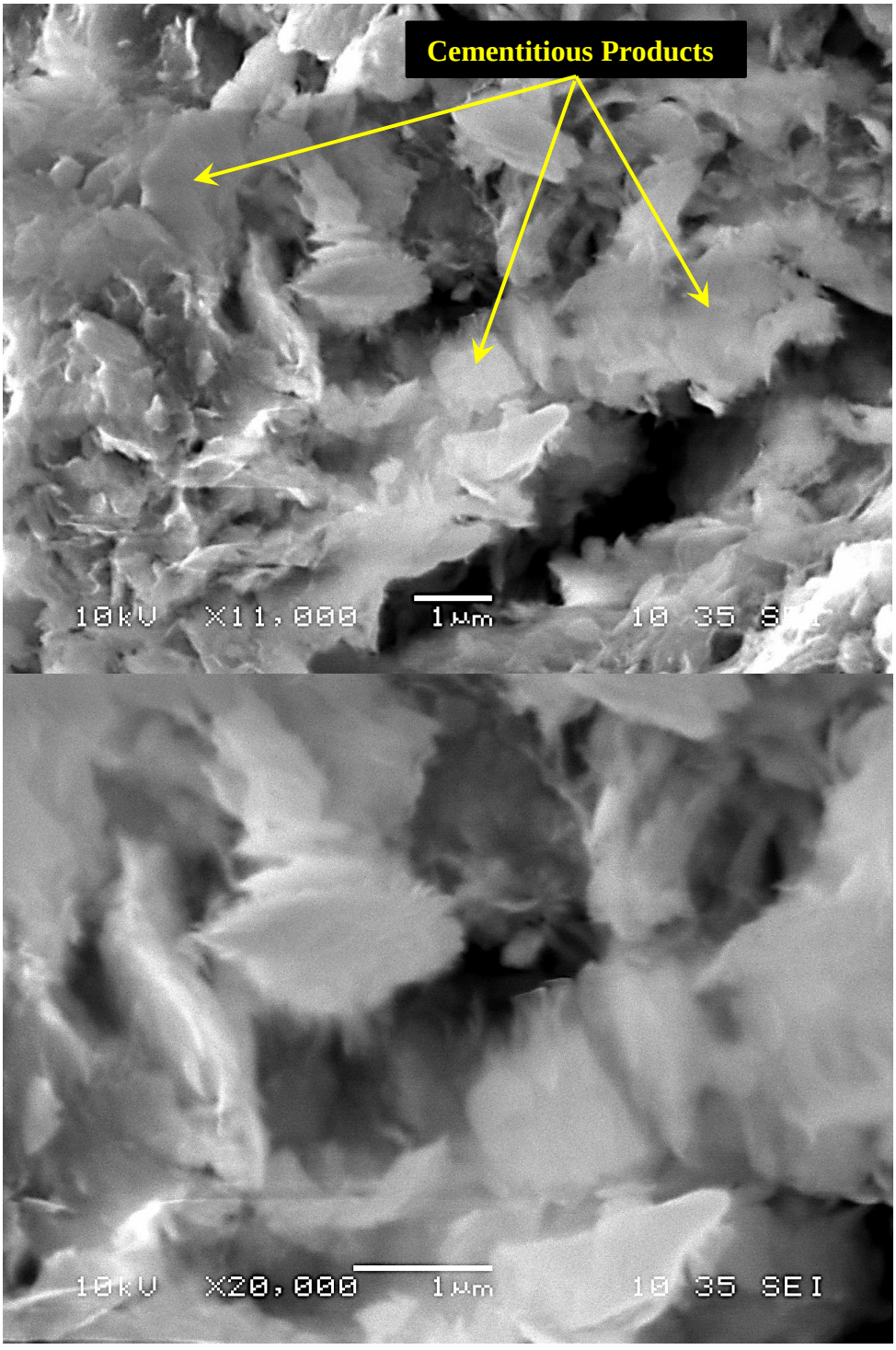

Figure 7.14: (cont'd)

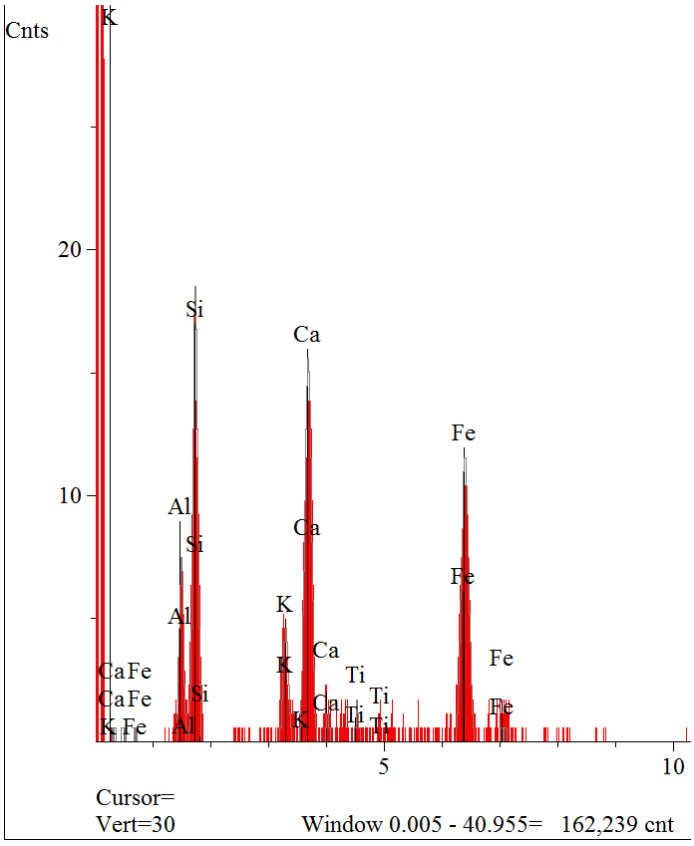

Figure 7.14: (cont'd)

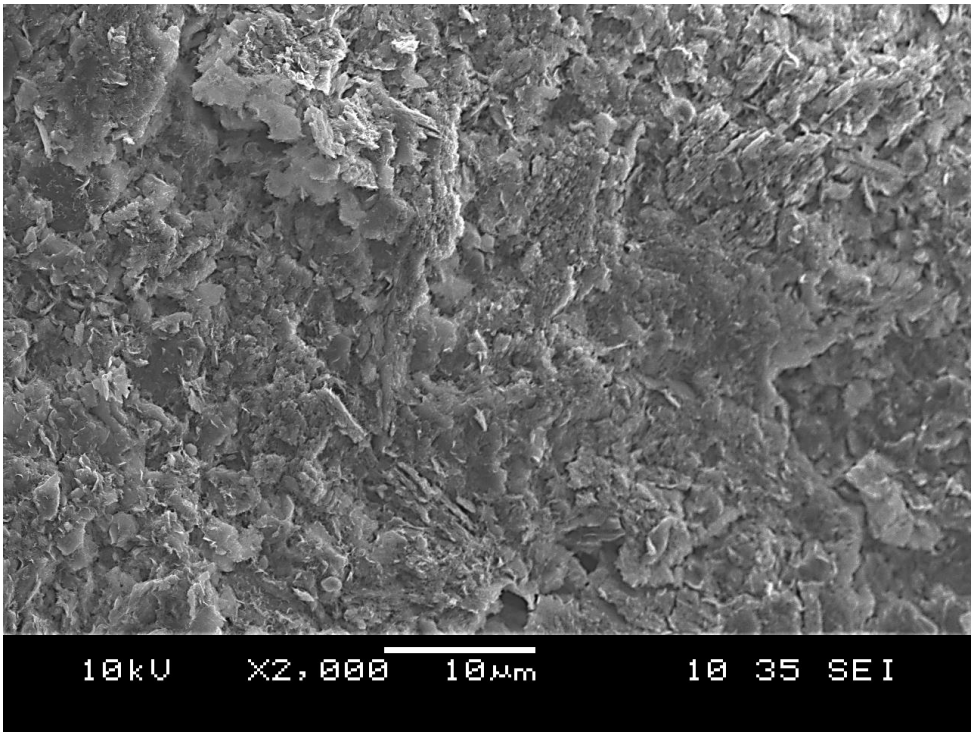

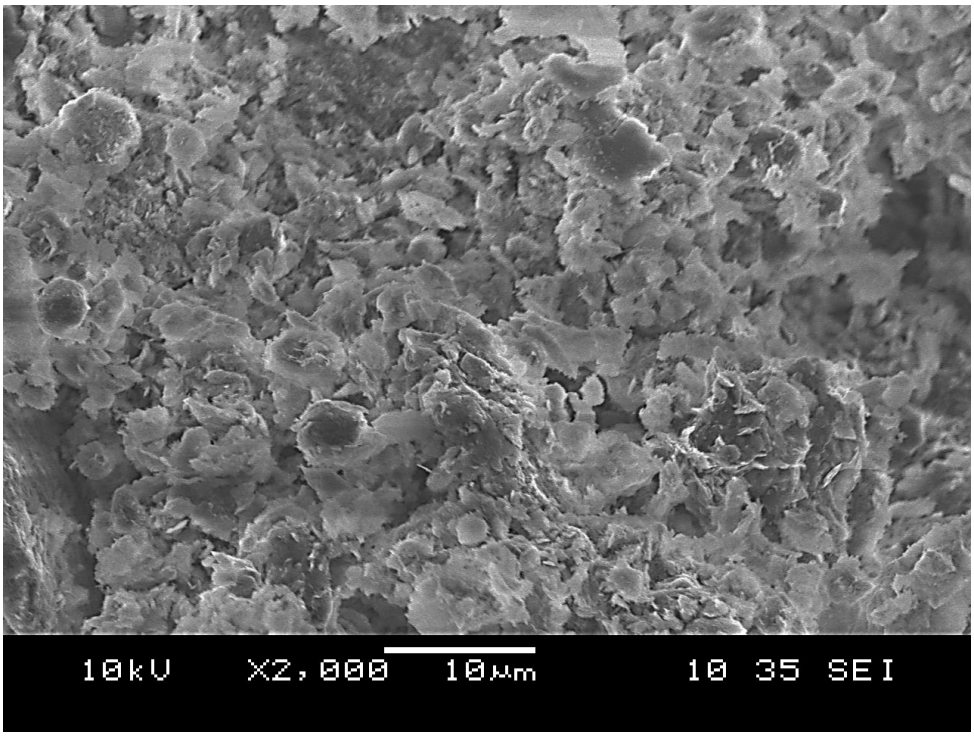

Figure 7.15: SEM image of Beaumont clay treated by 10% lime, cured for 15 weeks under confined condition

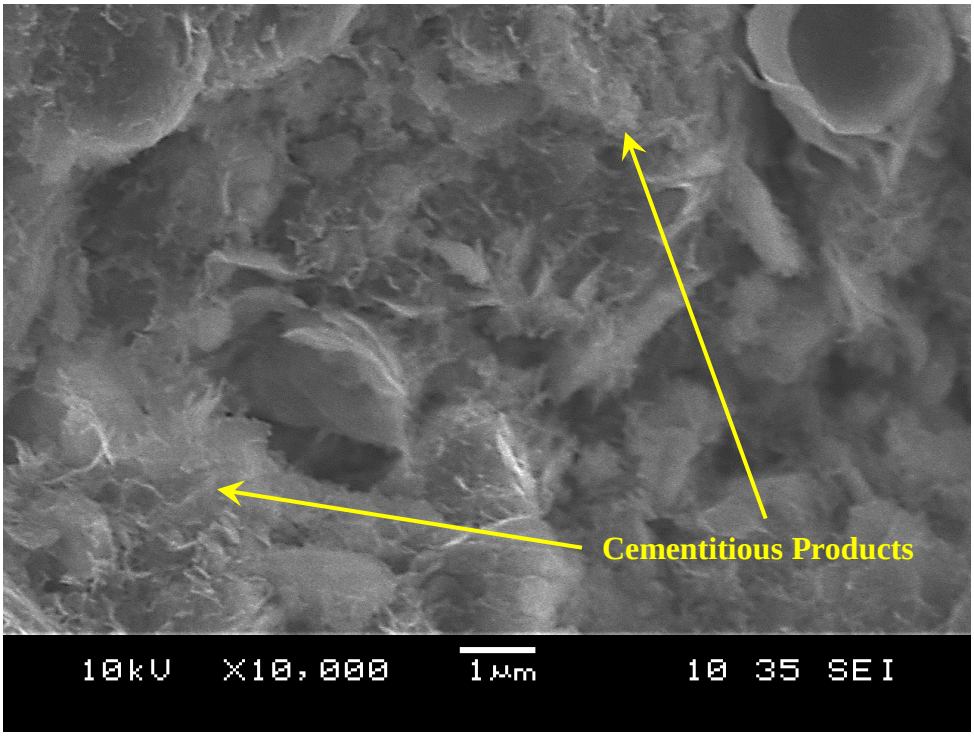

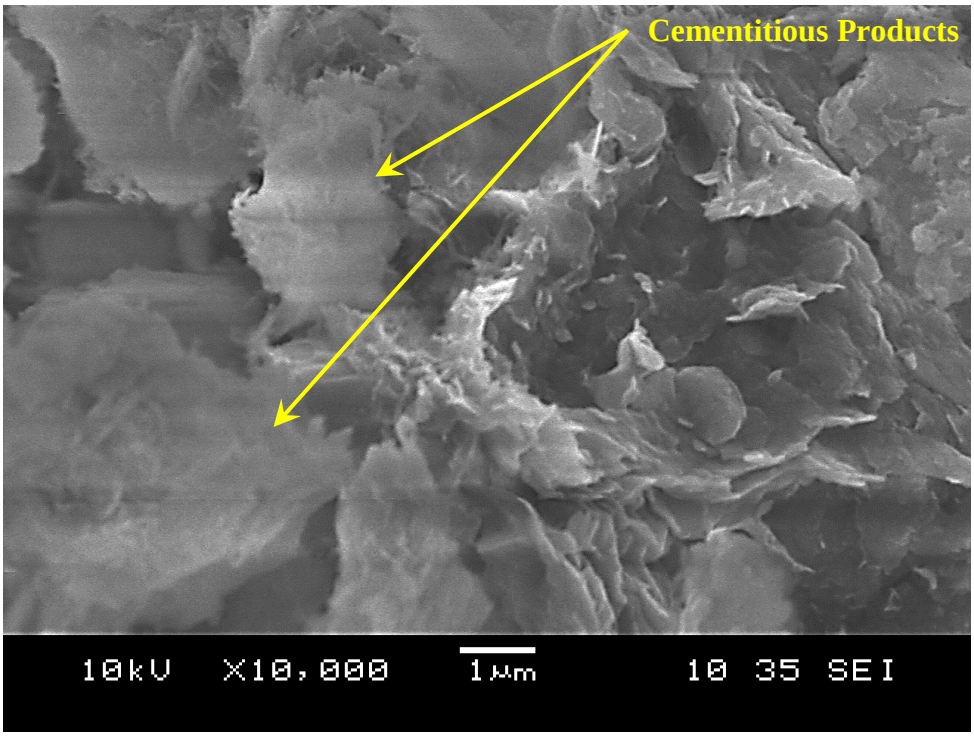

Figure 7.15: (cont'd)

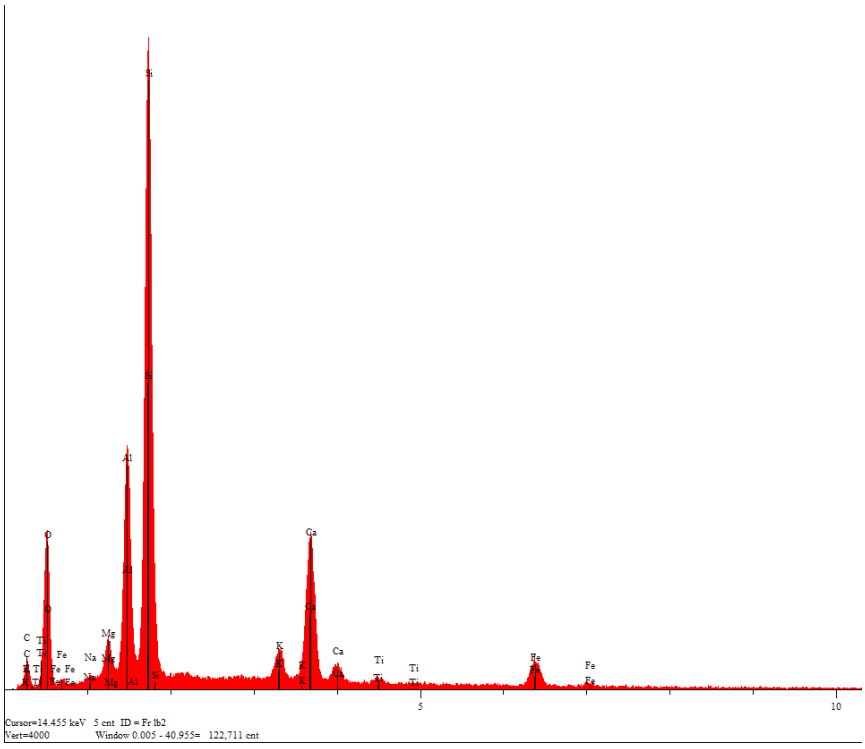

Figure 7.15: (cont'd)

It should be mentioned here that the dramatic increase in plastic limit upon lime treatment is rather unrelated to replacement of original exchangeable cations by the calcium ions or to the increase in concentration of Ca^{2+} in the porewater, as had been proposed by Gallaway and Buchanan (1964) and subsequently accepted by others (e.g. Thompson, 1964), and challenged (e.g., Verhasselt, 1990). This is confirmed by the Atterberg limit data which show that plastic limit of calcium montmorillonite is relatively low in comparison to plastic limit of lime-treated soils, as shown in Figures 6.1-6.3, and in fact plastic limit of calcium montmorillonite is less than that of sodium montmorillonite, and is particularly independent of concentration of calcium ions in the porewater (Mesri and Olson, 1971).

The time-dependent manifestation of adsorbed lime is a gradual chemical reaction of calcium hydroxide with soil particle surfaces. As the reaction products continue to form and later harden or crystallize at the reaction sites of adsorbed lime particles, they improve soil particle connections within the flocs and agglomerates that may mature into porous soil aggregates (Baver,

1956). The comparison of secant peak and residual friction angles shows that the secant residual friction angle increases with time and levels off after a period of time, depending on the lime content. However, the secant peak friction angle continues to increase for a longer time. The increase in the peak strength is attributed to the additional reticulation (inter-aggregate bonding) formed over time. The proposed concept of lime particle adsorption on soil particles is somewhat similar to physical adsorption of calcium hydroxide molecules proposed by Diamond and Kinter (1965). However, considering that a clay-sized hydrated lime particle may contain 10^{11} molecules of $Ca(OH)_2$, a more significant time-dependent chemical reaction of adsorbed lime with soil particle surfaces is expected for adsorbed lime particles than for adsorbed lime molecules. Richardson et al. (1994) have mentioned layers of $Ca(OH)_2$ sandwiched between silicate layers.

The lime content required to fully satisfy adsorption is mainly related to soil particle size and shape and therefore, the mineralogy of soil solids (Goldberg and Klein, 1952; Eades and Grim, 1960) and degree of dispersion or aggregation. As soil particle size decreases and therefore, surface area increases, l_{ca} increases. Lime content consumed through adsorption is probably also related to the soil water content as it influences dispersion of soil particles and facilitates thorough mixing to allow full distribution and intimate contact between lime and soil particles, degree of pulverization of hydrated lime, and the intensity of mixing. Considerable differences were found by Petry and Wohlgemuth (1988) in the strength of a highly active soil depending on the gradation used to make specimens (only on stability of specimens). Assuming that standard approaches are followed to select mixing water content and mixing procedure, the primary factors determining lime requirement for full adsorption, l_{ca}, are mineralogy of soil solids and degree of dispersion of soil particles as determined by degree of pulverization plus interaction with water. For any soil, an increase in l_{ca} can be expected to improve the strength and stiffness of lime-stabilized soil when sufficient lime is available. For a given soil this depends on degree of pulverization, mixing water content, and quality of mixing (Wissa et al., 1971; Petry and Wohlgemuth, 1988). For the specimens prepared in this study, the soil samples were pulverized and passed through Sieve #40 U.S. Standard. Lime was then added and mixed with the clay in dry condition. Water was added and for majority of samples, a water content close to the liquid limit of clay was used to allow for a proper mixing. Lower Brenna and Beaumont clays have higher l_{ca} than Chicago clay. Hence the

effect of lime on shear strength is more pronounced for Lower Brenna and Beaumont clays as compared with Chicago clay.

Because the solubility of calcium hydroxide in water is very small, for typical soil water contents a very small lime content is required to saturate the porewater. For example, approximately 0.07% lime is required to saturate Lower Brenna clay at the liquid limit. However, test results indicate that pH remains below 12.3-12.4 for lime contents far in excess of that required for the saturation of porewater. This behavior suggests that lime adsorption must be satisfied before lime is dissolved in the porewater to increase the pH. Zolkov (1962) considered it as remarkable that in spite of the very small solubility of lime in water, large amount of lime was required "to bring the pH of the soil slurry to 12.6." The pH test proposed by Eades and Grim (1966) is a good indicator of the lime content to fully satisfy lime adsorption, l_{ca}. “Lime fixation point” concept of Hilt and Davidson (1960) is also a measure of l_{ca}. The l_{ca}, determined by measurements is used to indicate optimum modification, however, may be influenced by the mixing water content, degree of dispersion of soil particles, and the intensity of mixing.

A lime content of 3% increases the pH of Beaumont clay to above 12.6 immediately after addition of lime, as shown in Figure 6.13. This is the lime consumed through adsorption and also it is high enough to increase the peak strength to some extent. However, as lime is consumed, there is not enough lime available to maintain the pH elevated. The pH drops below 12.6 rapidly with time. The lime consumed to fully satisfy adsorption is 3% for Lower Brenna clay and approximately 1-2% for Chicago clay.

Some chemical reaction products have a layer structure, with high surface area, and a particle morphology that has been described as thin plates, foils, and rolled up sheets (Diamond et al., 1964); however, sometimes fibers or laths occur which could contribute to particle interlocking (Richardson et al., 1994). On the other hand, adequate but not excessive lime attack may improve morphology of existing soil particles by producing ragged, irregular, frosted or serrated particles and following proper compaction connect soil particles by the new reaction products. These features are expected to improve mechanical behavior of soils. The needle-shaped crystals formed in the treated Lower Brenna clay which are the reaction products of lime, clay particles and a small amount of sulfate in the Lower Brenna clay composition improve the frictional behavior of the

clay once cured under confined condition. They connect particles together producing grains and contribute to interlocking of the particles. A combination of aggregated clay particles and interlocking needle-shaped crystals observed in the SEM images of treated Lower Brenna clay are responsible for increased secant peak and residual friction angles.

In summary, adsorption and dissolution of hydrated lime and associated chemical reactions of lime and soil begin during the mixing of lime and wet soil. Adsorption is completed during the mixing process; however, dissolution continues until all free lime is consumed. The total lime content, l_c, should be large enough to fully satisfy lime adsorption, l_{ca}, and sufficient lime left over to dissolve in porewater, l_{cd}, to maintain the pH at 12.3-12.4 in order to sustain chemical reactions for an adequate period of time. The adequate time for the chemical reactions depends on mineralogy of soil particles, including particle size and shape, and also on the density of lime-treated soil. Chemical reactions through both adsorbed lime and dissolved lime are likely to be more rapid and intense for amorphous or poorly crystalline silicates than for well crystallized silicates.

7.2 FIRCTION ANGLE-LIME CONTENT AND PH RELATIONSHIP

The friction angle-lime content and pH relationship for Chicago clay is shown in Figure 7.16. A lime content of 1% causes the pH of treated Chicago clay to stay elevated, leading to an increase in the secant residual friction angle. However, increases in secant residual friction angle is not significant for Chicago clay.

The friction angle-lime content and pH relationship for Lower Brenna clay is shown in Figure 7.17. At a lime content of 3%, considered as adsorbed lime, pH increases to its maximum value of just above 12.6. A lime content above 3%, leads to permanent aggregation of clay particles and thus an increase in the secant residual friction angle.

The friction angle-lime content and pH relationship for Beaumont clay is shown in Figure 7.18. The pH increases to above 12.4 upon addition of 3% lime; however, it drops rapidly with time. No increase in the residual friction angle is observed up to 3% lime content, implying no significant aggregation. A lime content of 5% is enough to maintain pH elevated over time. Therefore, peak friction angle increases significantly within the first week of curing due to

formation of pozzolanic reaction products. Also, there is a significant increase in the residual friction angle for a lime content of 5%. The lime content above which there is an increase in the secant residual friction angle, is the lime content which fully satisfies lime adsorption, l_{ca} and it is similar to the pH test proposed by Eades and Grim (1966) to increase pH to 12.6.

At a lime content equal to l_{ca}, there is an increase in the secant peak friction angle but no increase in the residual friction angle, suggesting a cemented fabric but no significant aggregation. Lime in excess of l_{ca} causes an increase to both peak and residual friction angles. The pH for lime contents less than l_{ca} drops with time faster than that for lime contents more than l_{ca}. For lime contents below l_{ca}, pH decreases with time as lime is consumed, contributing to an increase in peak strength. For lime contents above l_{ca}, pH remains elevated for a longer period of time, contributing to an increase in both peak and residual strength.

The lime content consumed through dissolution, l_{cd}, should be large enough to maintain the pH at 12.3-12.4 to sustain the pozzolanic reactions for a sufficient period of time. As soil particle size decreases or the water content increases, the lime content consumed through solution is used up rapidly, whereas for coarse particle sizes or at low water contents, l_{cd} is used up gradually (Thompson, 1966; Ingles and Metcalf, 1973).

For both Lower Brenna and Beaumont clays, a lime content above 3% triggers the aggregation of clay particles through dissolution and pozzolanic reactions. A high degree of aggregation is achieved at 5% lime content. For Beaumont clay, no major drop in the pH is observed with time at 7% lime content, indicating that the lime is sufficient to maintain the pH at 12.3-12.4 for a period of time. The lime content required to maintain the pH at its maximum for Lower Brenna clay is 7%, at which the full aggregation of clay particle and floccules is reached. Higher lime contents result in no or minimal increase in the residual strength. Increase in the peak and residual shear strength of Lower Brenna clay for the increase in lime contents above 7% is negligible. As a matter of fact, lime contents of 10% and above show a gradual decrease in both peak and residual shear strengths of Beaumont clay, as probably excessive lime remains uncreative.

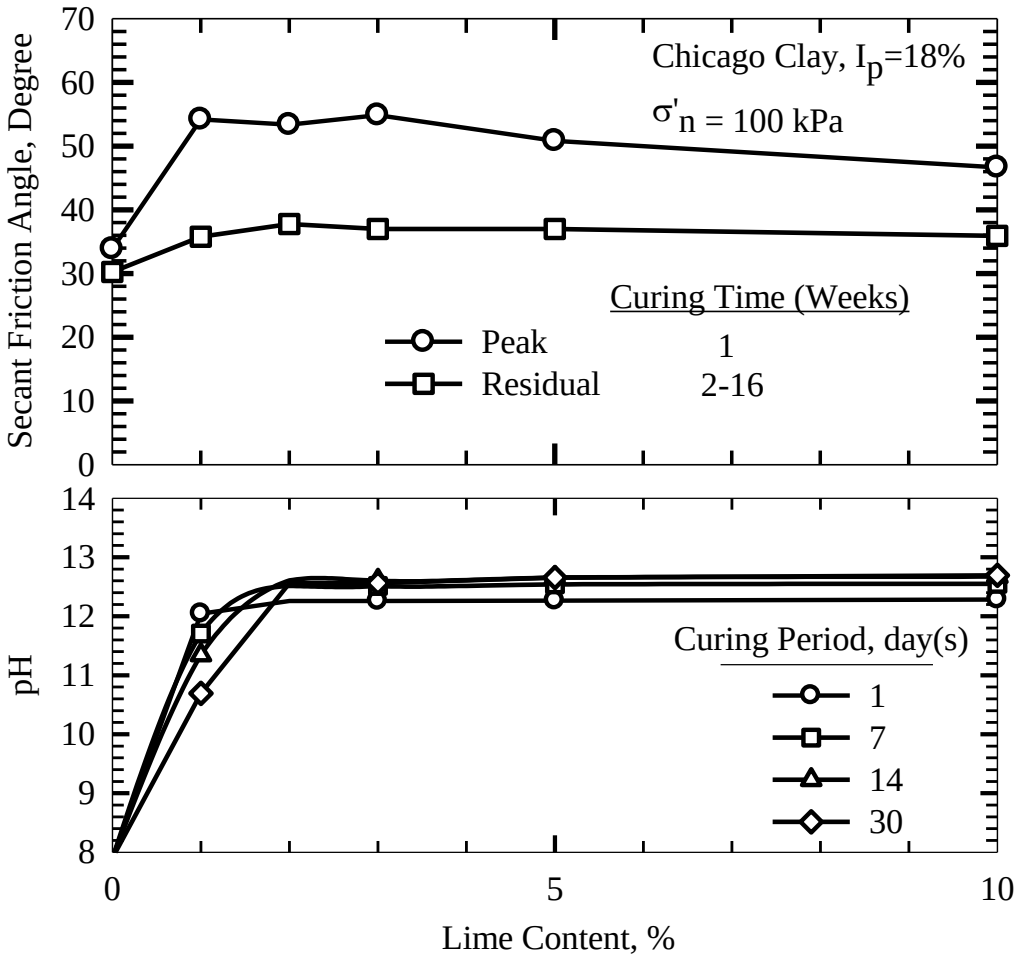

Figure 7.16: Friction angle-lime content and pH relationship for Chicago clay

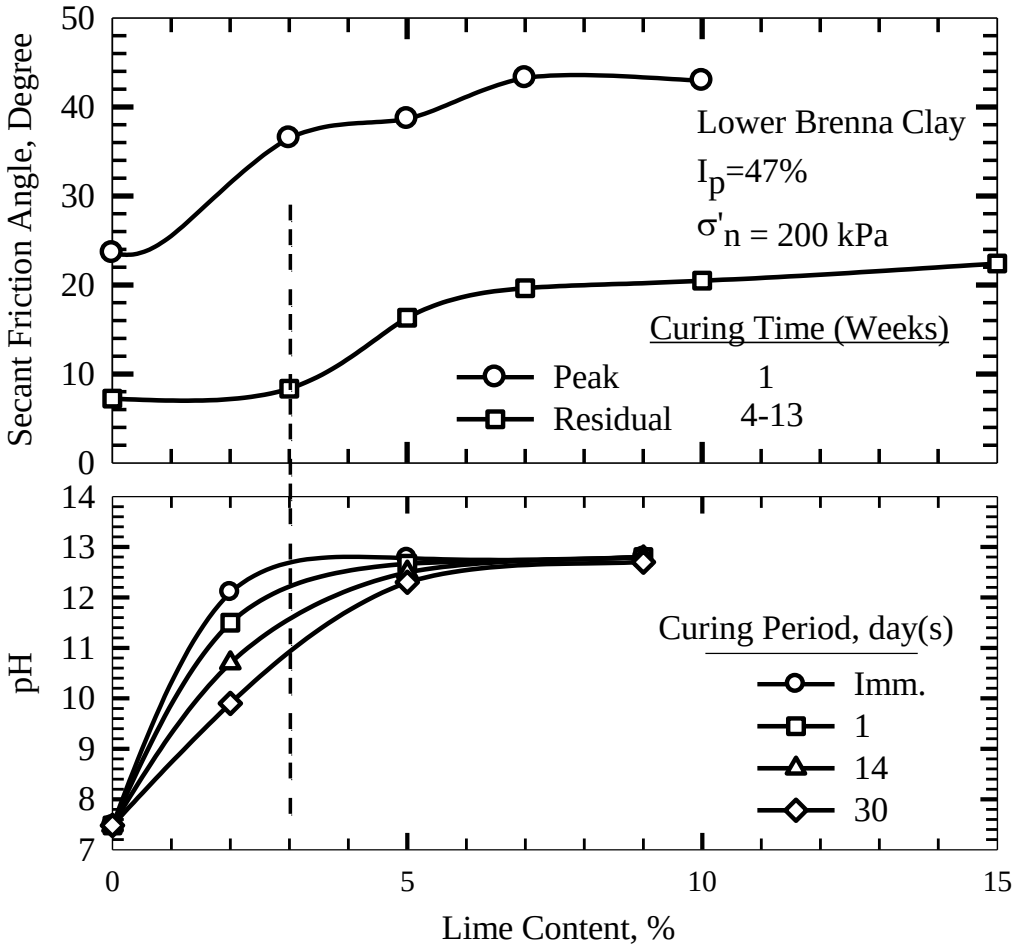

Figure 7.17: Friction angle-lime content and pH relationship for Lower Brenna clay (Imm. = Immidiately)

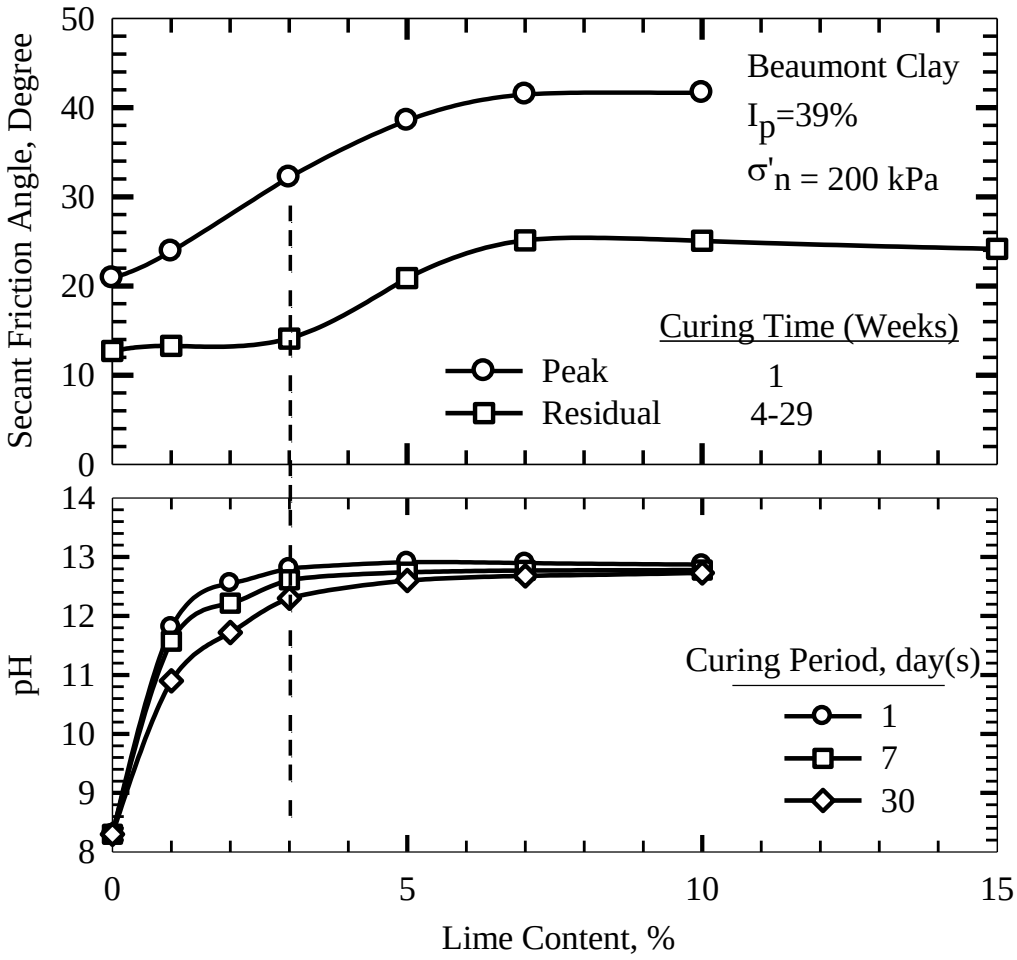

Figure 7.18: Friction angle-lime content and pH relationship for Beaumont clay

As shown in Figures 4.56-4.58 for Lower Brenna clay at lime contents of 5, 7 and 10%, and Figures 4.59 and 4.60 for Beaumont clay at lime contents of 5 and 10%, the secant peak friction angle increases significantly within the first week of lime addition and continues to increase at a lower rate afterwards as the pH decreases. For 7% lime, more cementitious material is formed in the first week, contributing to an increase to the peak and residual shear strengths. As pH decreases, the peak shear strength increases due to crystallization and hardening of the cementitious products.

7.3 FRICTION ANGLE-LIME CONTENT AND ATTERBERG LIMITS RELATIONSHIP

Because some of the reaction products during the stabilization process are amorphous and hydrated, drying of lime-treated soils during stabilization is likely to result in some irreversible dehydration as well as irreversible aggregation. The lower Atterberg liquid limit and plasticity index measured for air dried lime-treated specimens of direct shear tests, cured under confined condition, indicate that the reaction products experience irreversible dehydration, similar to andosols containing allophane.

The plastic limit of Chicago clay (Figure 7.19) increases by addition of lime, but the plasticity index remains unchanged. A lime content of 3% for both Lower Brenna clay (Figure 7.20) and Beaumont clay (Figure 7.21) show a sharp increase in the plastic limit and decrease in the plasticity index. The change in the Atterberg liquid limit upon addition of lime is rather unpredictable. Alternatively, a sharp increase in the plastic limit at a lime content equal to adsorbed lime, l_{ca}, is evident. This is similar to "Lime fixation point" concept of Hilt and Davidson (1960) which is the lime required to increase plastic limit to its maximum. This lime is fixed and causes flocculation of clay particles. Lime in excess of adsorbed lime is required to increase residual shear strength, owing to aggregation of clay particles through dissolution process. The increase in the secant residual friction angle of Lower Brenna clay and Beaumont clay for lime contents above 3% is shown in Figures 7.20 and 7.21, respectively.

The largest decrease in the plasticity index is for high plasticity clays containing montmorillonite such as Upper Brenna, Lower Brenna, and Beaumont clays. The lime improvement in illitic clays such as Chicago clay is less effective. The clays with Kaolinite as the dominant mineral can be expected to have the least improvement by lime addition.

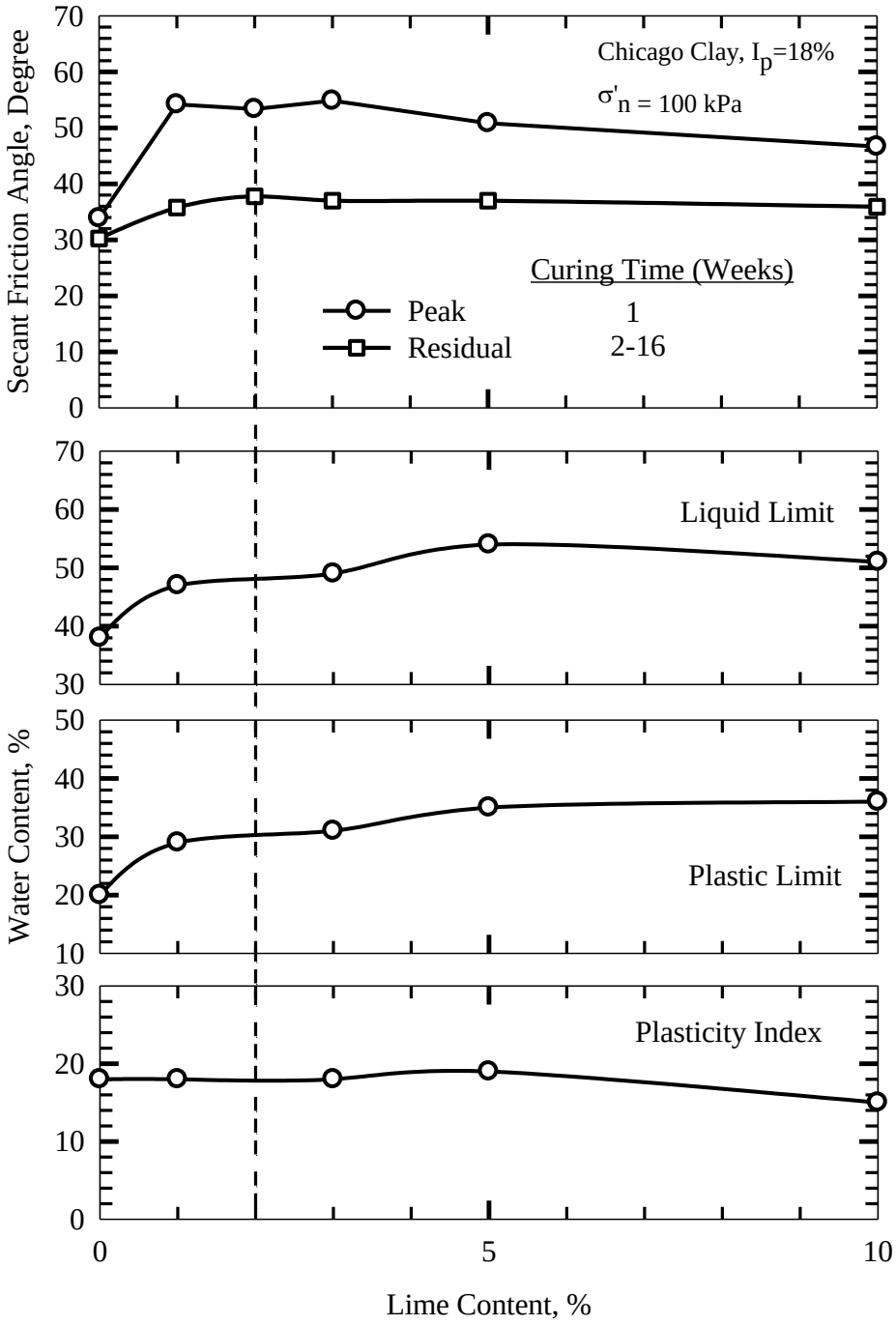

Figure 7.19: Friction angle, Atterberg limits and lime content relationships for Chicago clay

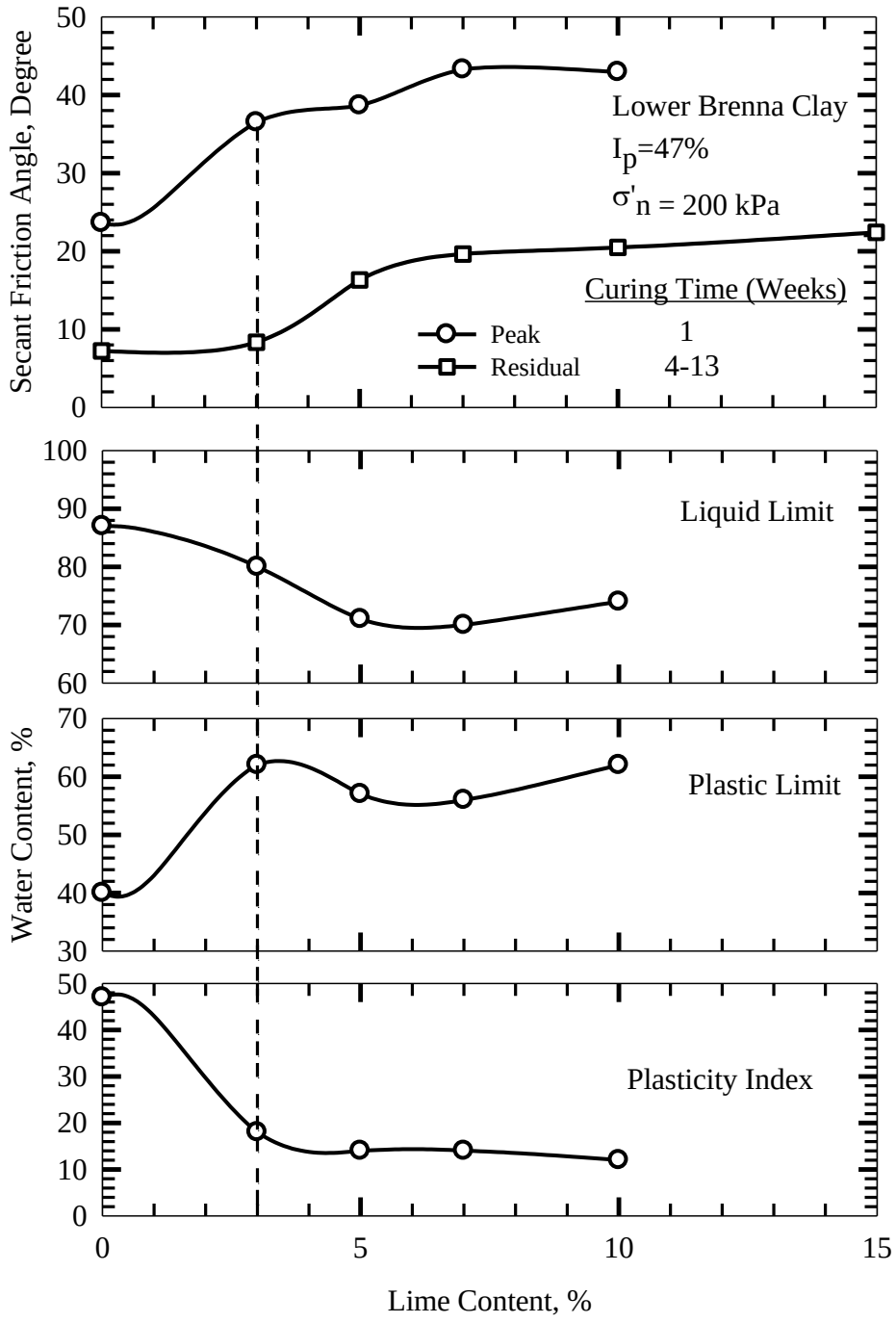

Figure 7.20: Friction angle, Atterberg limits and lime content relationships for Lower Brenna clay

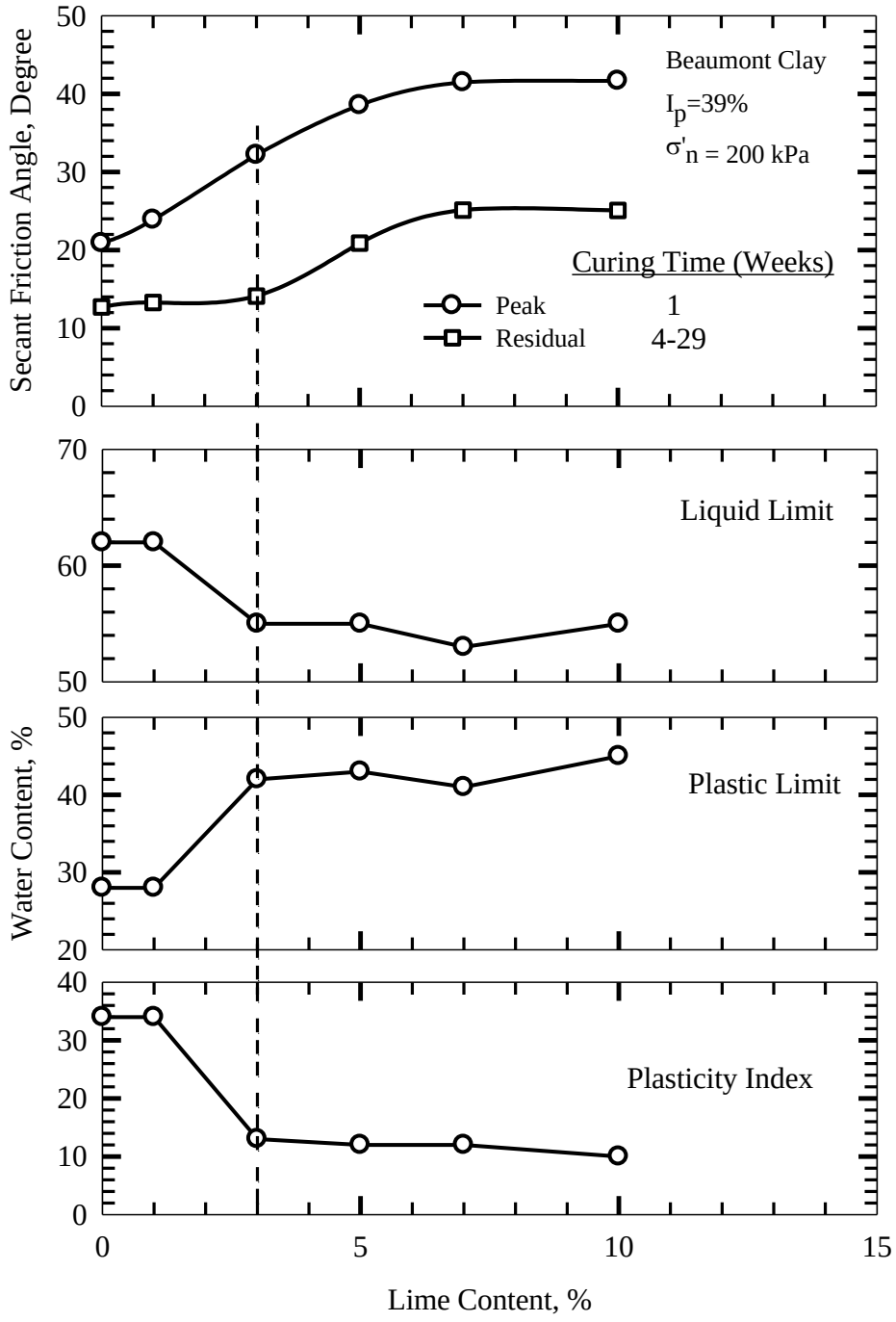

Figure 7.21: Friction angle, Atterberg limits and lime content relationships for Beaumont clay

7.4 INCREASE IN FRICITONAL RESISTANCE OF CLAYS

The pH measurements show that lime dissociation begins immediately after addition of lime and continues over days and months if lime is available in excess of what is required to fully satisfy adsorption. The increased pH of the porewater promotes pozzolanic reactions. The residual friction angles measured for 5, 7 and 10% lime treated clays show that the pozzolanic products form and increase residual strength at early stages of treatment as shown in Figures 5.63 and 5.64 for Lower Brenna clay, and Figures 5.65-5.67 for Beaumont clay. The edges of the clay particles become ragged by lime adsorption. Floccules form immediately following lime treatment, as shown by reduction of plasticity index. Subsequently, aggregation take place inside floccules in the first few days, confirmed by the increase in residual strength. The increase in residual friction angle of treated clay for curing periods more than one week is negligible compared to the increase during the first week of treatment although pH remains high, implying lime is available. For example, $\left[\phi'_r\right]_s^{100}$ increases from 14.0 degrees for untreated Beaumont clay to 23.6 degrees in 5 day and remains around 23-24 degrees in 200 days after addition of 5% lime (Figure 5.65). The pH of 5% lime-Beaumont clay remains elevated above 12.1 in this time period, which means that lime is available for pozzolanic reactions.

The secant peak friction angle at 100 kPa, $\left[\phi'_p\right]_s^{100}$, increases from 23.2 degrees for untreated Beaumont clay to 50.4 degrees in one week after addition of 5% lime. The peak friction angle continues to increase to 63.7 degrees after 35 days of curing. An increased peak friction angle while a constant residual friction angle after one week of curing suggests that the aggregation of clay particles and floccules occur in the first few days after treatment. After the clay particles and floccules are aggregated, more cementitious products are formed by pozzolanic reactions coating and connecting the aggregates and filling the voids between the aggregated floccules as the curing time prolongs. In other words, the additional cementitious materials connect the clay clusters which contribute to the peak strength but not to the residual strength.

Although, for lime-treated clays, there is no direct relationship between residual friction angle and Atterberg limits, at each lime content, there is an increase in plastic limit and a reduction in the plasticity index. The Atterberg limits carried out on the direct shear specimens of Beaumont

clay treated with 5% lime as indirect measures of changes in particle size and shape show flocculation of clay particles. The plasticity index, I_p, decreases from 34% for untreated clay to 12% immediately after addition of 5% lime. The plasticity index remains more or less constant as curing time increase to 62 days.

The secant residual friction angle of Lower Brenna clay at 200 kPa, $\left[\phi'_r\right]_s^{200}$, increases from 7.2 degrees for untreated clay to 19.5 degrees in 9 days after addition of 7% lime (Figure 5.63). The residual friction angle, $\left[\phi'_r\right]_s^{200}$, remains more or less the same after 100 days of curing. The secant peak friction angle at 200 kPa, $\left[\phi'_r\right]_p^{200}$, increases from 23.6 degrees for untreated clay to 43.3 degrees for 7% treated clay cured for 7 days (Figure 4.64). The peak friction angle continues to increase to 50.2 degrees and 60.8 degrees after 14 and 35 days of curing, respectively. The Atterberg limits measured on the direct shear specimens show that in 26 days plasticity index decreases from 47% for untreated clay to 13%. A similar plasticity index of 13% was measured for another direct shear specimen cured for 170 days.

Lower Brenna clay treated with 10% lime shows an improvement in frictional resistance by addition of lime as follows. The secant residual friction angle of Brenna clay at 100 kPa, $\left[\phi'_r\right]_s^{100}$, increases from 8.2 degrees for untreated clay to 20.6 degrees after 16 days and remains in the same range after 59 days of curing (Figure 5.64). The secant peak friction angle, $\left[\phi'_p\right]_s^{100}$, increases from 25.4 degrees for untreated Brenna clay to 52.8 degrees 7 days after addition of 10% lime (Figure 4.64). The peak friction angle continues to increase to 60.0 degrees and 69.2 degrees after 14 and 35 days, respectively. The increase in the frictional resistance is substantial from 2 weeks to 5 weeks. The peak shear strength ratio ($\tau_{p,\,Treated}/\tau_{p,\,Untreated}$) is $\tan 52.8°/\tan 25.4°=2.8$ after 7 days and $\tan 69.2°/\tan 25.4°=5.5$ after 35 days of curing while the residual shear strength remains constant.

The secant residual friction angle of Beaumont clay at 100 kPa, $\left[\phi'_r\right]_s^{100}$, increased from 14.0 degrees to 24.5 degrees in 10 days after addition of 7% lime (Figure 5.66). The secant residual friction angle remained more or less constant afterwards; it increased to 26.7 degrees after 120

days of curing. The secant peak friction angle at 100 kPa, however, increased from 23.2 degrees to 54.2 degrees after 7 days of curing (Figure 4.68). The increase in the secant peak friction angle continued and reached approximately 68 degrees after 35 days of curing. The secant peak friction angle of 7% treated Beaumont clay after 35 days of curing is an interpolation between 63.7 degrees for 5% and 67.8 degrees for 10% lime (Figure 4.70). There are no data available on the Atterberg limits of 7% lime after 1 week. However, the plasticity index was measured immediately after treatment and 50 days after curing. The plasticity index decreased from 34% for untreated clay to 19% immediately after lime was added and to 12% after 50 days. This suggests that the reduction in the plasticity index, measured on direct shear specimens, mostly occurred immediately following treatment due to flocculation of clay particles.

The secant residual friction angle of Beaumont clay at 100 kPa increased from 14.0 degrees for untreated clay to 24.2 degrees for 10% lime after 23 days of curing (Figure 5.60). It reached 26.8 degrees in 123 days and remained constant for longer curing periods up to 200 days. The secant peak friction angle of Beaumont clay increase from 23.2 degrees for untreated clay to 53.5 degrees in 7 days, to 58.9 degrees in 14 days, and to 67.8 degrees in 35 days (Figure 5.71). The secant residual friction angle shows very little increase after 2 weeks while the peak friction angle continues to increase after 2 weeks of curing.

A lime content of 3% satisfies adsorption for Lower Brenna clay, and a further increase in the lime content results in aggregation of clay particles through dissolution process and thus a permanent change in size and shape of clay particles. An increase in the peak friction angle is observed for 3% lime after 1 week. However, this much lime is not enough for permanent aggregation of clay particles by pozzolanic reaction products. The plasticity index examination shows that it decreases from 47% for untreated Lower Brenna clay to 18% by addition of 3% lime. This decrease is a result of flocculation caused by adsorbed lime attacking the clay particles. Further increases of lime content above the adsorption limit is used in pozzolanic reactions to aggregate clay particles. When the lime content increases to 5%, the secant residual friction angle, $\left[\phi'_r\right]_s^{200}$, increases from 7.2 degrees for the untreated clay to 16.3 degrees for the lime treated clay. The secant residual friction angle continues to increase as lime content increases to 15%; however, for lime contents above 7%, the increase in the residual strength is at a lower rate. The most

significant aggregation, and thus improvement in the secant residual friction angle of Lower Brenna clay, occurs between lime contents of 3 and 7%, where $\left[\phi'_r\right]_s^{100}$ increases from 9.3 degrees to 20.5 degrees. Addition of 7% lime to Lower Brenna clay is sufficient for a major aggregation of clay particles through dissolution mechanism. Although lime contents higher than 15% were not used in this study, one may expect lime contents above a specific value to have detrimental effects on residual strength. The excessive lime may remain unreactive and reduce the residual strength.

A lime content of 3% in Beaumont clay is enough to satisfy the adsorption but does not promote pozzolanic reactions to aggregate clay particles permanently. Flocculation takes place immediately after addition of lime through adsorption. When a lime content greater than that consumed through adsorption is added to the clay, permanent aggregation of clay particles occurs by pozzolanic reaction products inside floccules and increases residual strength. The lime in excess of the adsorbed lime consumed in pozzolanic reactions was noted in the secant residual friction angles. From the secant residual friction angle measurements, it is observed that a major aggregation occurs between 3 and 7% lime contents. The residual friction angle, $\left[\phi'_r\right]_s^{100}$, increases from 16.0 degrees to 27.4 degrees when lime content increases from 3 to 7%, implying the change in the nature of the clay particles and reduction in their plateyness. Pozzolanic reactions continue over time, connecting the aggregated floccules and increasing peak strength.

In view of the lime adsorption (or lime fixation capacity), the adsorbed lime increases plastic limit, hence decreases plasticity index, but does not contribute to residual shear strength increase. After adsorption capacity is satisfied, the excess lime through maintaining a high pH level promotes the pozzolanic reactions, producing stable aggregates and improving residual shear strength. There is a substantial increase in the peak shear strength of Beaumont clay by addition of 3% lime, while there is no increase in the residual shear strength. This suggests that small amounts of lime in the range of adsorbed lime may increase the peak strength, yet it may not be enough for permanent aggregation of clay particles. In other words, there is not enough lime to produce individual firm clusters through dissolution to increase the residual strength, rather it creates bonds between individual particles. When a specimen with less than 3% lime is subjected to shearing, it exhibits an increased peak strength as a result of these bonds between clay particles.

When shearing continues to residual condition, these bonds break and soil texture is back to the original texture with the same plateyness of particles because no aggregation has taken place. A lime content at which residual strength begins to increase may be interpreted as the adsorbed lime. The adsorbed lime may contribute to create some bonds between clay particles but does not change the nature of particles.

A similar behavior is observed for Lower Brenna clay. The secant peak friction angle, $\left[\phi'_p\right]_s^{200}$, of Lower Brenna clay increases from 23.6 degrees for untreated clay to 36.5 degrees by addition of 3% lime; however, the residual friction angle, $\left[\phi'_r\right]_s^{200}$, does not exhibit a considerable increase. Therefore, 3% lime improves the peak strength by creating bonds between individual particles, but it is not sufficient to improve size and shape of particles. Once these bonds break by shearing to large strains, a residual strength close to that of untreated clay is obtained, implying that no improvement in size and shape of particles has been achieved.

By examining the residual friction angle as a measure of degree of aggregation, Atterberg limits as indirect measures of particle size and shape, and comparing them with the peak friction angle, it is concluded that when there is enough lime in excess of adsorption capacity, clay floccules become aggregated inside by pozzolanic reaction products in early stages of treatment. Plateyness of clay particles reduces due to lime treatment and aggregated particles increase frictional resistance. As time passes, more cementitious products form between the aggregated floccules, filling the voids and connecting them together. These bonds create a network which contributes to peak strength. When the treated clay is subject to shearing, these bonds are responsible for the peak. These bonds break at small strains leading to a drop in the shear strength from peak to post-peak strength. However, as shearing continues, aggregated clusters become the dominant factor in the shear strength increase.

CHAPTER 8

LIME TREATMENT TO INCREASE THE STABILITY OF SLOPES

In this chapter, the common methods of lime treatment in the field are reviewed. These methods include deep mixing and jet grouting. Two methods to inject lime to the shear zone of a reactivated slope are introduced. The stability of slopes in three case studies are investigated and safety factors before and after addition of lime are calculated to evaluate the treatment.

8.1 INTRODUCING LIME TO SHEAR ZONE OF REACTIVATED LANSLIDES

A uniform mixing with high energy can yield high strength at a given lime content and curing period due to better distribution of lime, particularly in high plasticity clays (Berube and Locat, 1987; Choquette, 1988; Locat et al., 1990). This underlines the effect of in situ mixing on the strength of stabilized soils.

One of the applications of lime treatment is to stabilize reactivated slopes. A number of methods are currently used for landslide remediation including horizontal drains, structural piles, and key trench. In the remediation method introduced herein, the treatment is directly applied to the shear zone; therefore, it is believed to lead to an effective and economical treatment. After the pre-existing slip surface is determined using site investigation including inclinometers and stratigraphy from boring logs, a layout of treatment locations is designed to introduce lime to segments of the shear zone.

Before the proposed methods to introduce lime or cement to the shear zone of reactivated landslide are presented, it should be noted that the challenging part is the possibility of treatment of medium stiff to stiff clays. A number of case studies have been presented where Jet Grouting (JG) method was used to introduce lime or cement to a medium stiff to stiff clay layer (Durgunoglu et al., 2004; Walker, 1997; Shen et al., 2009; Wong and Poh, 2000). In these case studies, a depth

of up to 30 m has been reached using jet grouting equipment. Where a soft clay layer was underlain by medium stiff clay, a penetration in the range of 3-9 m into the medium stiff to stiff clay was achieved. The diameter of JG columns has been in the range of 0.6-1.8 m and the undrained shear strength (s_u) of the untreated clays has been in the range of 14-50 kPa (soft to medium stiff clay). The diameter, integrity and compressive strength of the cement- or lime-treated columns were verified as part of the quality control program. The undrained shear strengths of 3,600-7,300 kPa were measured using unconfined compression tests on the samples cored within the treated zone. A lime/cement content in the range of 5-30% has typically been used to stabilize soils (Ahnberg et al., 1995; Okumura, 1996; Bruce, 2001; Porbaha et al., 2000). It has been reported that the strength properties of treated soil following compaction can be similar to those of soft rock; and that the undrained shear strength of treated soil can be 10-20% of plain concrete (Jo et al., 2011) depending on binder type and content, and curing period (Chew et al. 2004; Kitazume and Terashi 2013).

Prior to the production grouting, a series of trial columns are usually installed to determine the operation parameters such as air pressure, grout pressure, rotational speed, withdrawal rate, etc. The operation parameters can be adjusted based on the strength of clay layers encountered in the field. Wong and Poh (2000) presented a case history where a soft marine clay layer was underlain by a medium stiff to very stiff silty clay layer. A slower rod withdrawal rate of about half of that used for the soft marine clay was used for the stiff layer, with the other operation parameters remaining unchanged.

Double and Triple Fluid methods have been used in stiff clays to increase the extent of treatment (Walker, 1997; Shen et al., 2009; Wong and Poh, 2000). In the Double Fluid method, air shroud around the grout is utilized to produce greater cutting efficiency, as shown in Figure 8.1. In the Triple Fluid method, the cutting medium is a high pressure water jet with an air shroud with a low pressure separate grout nozzle for replacing the cut material, Figure 8.1. In very stiff clay layers, precutting has been employed where water at high pressure was used in the first pass instead of grout and then a second pass was carried out with the conventional Double Fluid method (Walker, 1997).

Wang et al (1999) compared the effects of two methods of jet grouting installation, i.e. Triple Fluid method and Superjet method. These methods were compared using a trial test during the construction of a two-level basement structure in soft marine clay of Singapore. In Superjet method, a lower jet grouting pressure and a higher flow rate were used compared to Triple Fluid method. Results of test columns showed a more uniform shear strength distribution in Superjet columns with an average 14-day strength (s_u) of 300 kPa compared to 198 kPa for Triple Fluid columns. A diameter of up to 4-5 m was possible to achieve in Superjet columns. Superjet was found to have less impact on adjacent buildings than Triple Fluid method because the impact was mainly due to the grout pressure which was less in the case of Superjet columns.

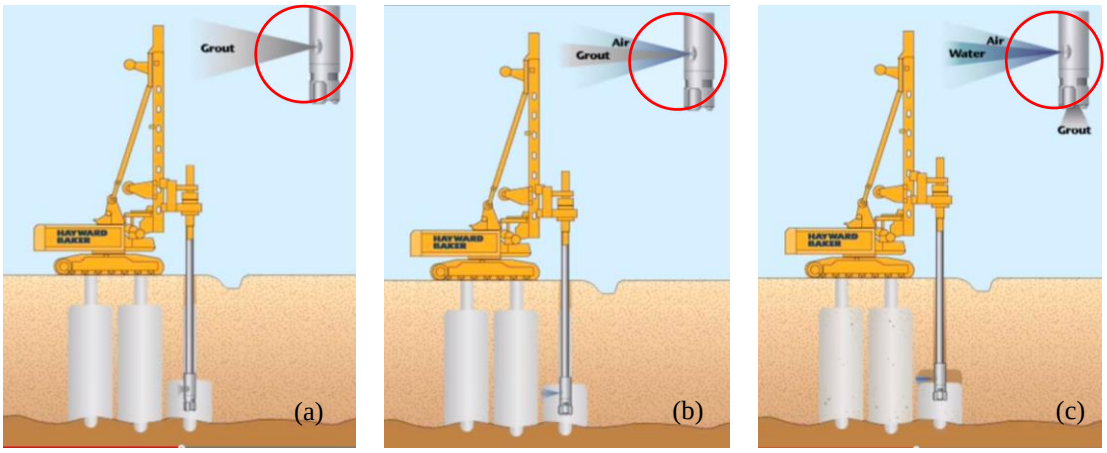

Figure 8.1: Jet Grouting Systems; (a) Single Fluid, (b) Double Fluid, (c) Triple Fluid (Courtesy of Hayward Baker Inc.)

Treatment of marine clays by application of deep lime mixing techniques to improve their behavior has extensively been studied by researchers (Okumura and Terashi, 1975; Rajasekaran, 1994; Narasimha Rao and Rajasekaran, 1992; Narasimha Rao and Rajasekaran, 1996, Rajasekaran et al., 1997a). Deep Soil Mixing (DSM) method has been used in medium to stiff clays (Madhyannapu et al., 2009). The columns were installed in the clays with undrained shear strength (s_u) in the range of 35-150 kPa. The columns with a typical diameter of 0.6 m were installed to a depth of 3-3.6 m. using single shaft augers.

The variables in DSM columns include, column diameter and length, replacement ratio, binder type and binder content (Porbaha et al., 2000). The typical column diameter ranges from

0.5 to 1.75 m. The center-to-center spacing between the columns is typically in the range of 1-1.5 m. The columns are usually 10-30 m long which can increase to 60 m for special applications such as harbor structures (Bruce, 2001).

The replacement ratio, a, defined as the ratio of the treated area to total area is in the range of 10-30% (Bruce, 2001), which can increase to 50% in particular situations such as stabilizing a slide in seismic conditions (Bergado et al., 1996).

The DSM technique has been used to repair the slips in New Zealand. A large number of slips (such as Edwards, Portland, Mountain Road Crawler Lane, Rawence Bluff and Gallies slips) occurred in Northland, New Zealand where a large number of slope instability and creep movement cases were reported due to a combination of problematic soil and high rainfall (Finlan et al., 2004; Terzaghi et al., 2004; Terzaghi et al., 2005). New Zealand's geology generally consists of young and soft soils; hence, road embankments have suffered from settlement and bearing capacity during years (Terzaghi et al., 2005).

The subsurface condition generally consisted of 1-4.5 m of soft clay overlaying 1-1.5 m of stiff silty clay. The stiff clay layer was underlain by weathered siltstone/mudstone. In some cases, there was a pre-existing slip plane within the soft clay. The fully softened friction angle of 20-26 degrees and residual friction angle of as low as 8 degrees were reported for the soil where the slope failures occurred (Terzaghi et al., 2004).

The typical remedial works included the installation of cement-treated columns spaced 2-3 m in a staggered pattern. A twin-hollow-string system, where each string had a diameter of 0.3 m was used in New Zealand for an extensive slip repair program (34 sites). This configuration was able to produce columns as large as 0.5 m x 0.3 m. Where extremely stiff clays were encountered, pre-drilling with small diameter auger and water was required prior to DSM construction (Terzaghi et al., 2004). Figure 8.2 illustrates a typical remedial work using DSM columns in road slip stabilization in Northland, New Zealand.

For example, a total of 60 cement-treated columns were installed in 9 working days at the Edwards slip. Core samples were taken from two columns after 80 days of curing and a minimum undrained shear strength (s_u) of 1,500 kPa was measured.

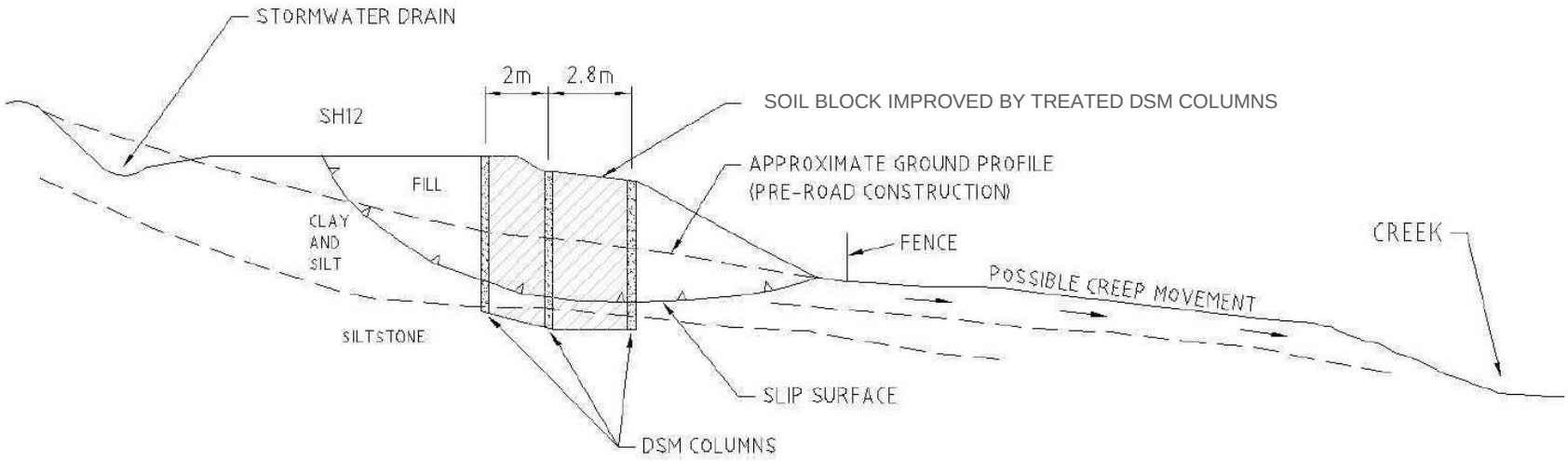

Figure 8.2: DSM columns used in road slip stabilization in Northland, New Zealand (Terzaghi et al., 2004)

The mechanical soil mixing is typically performed using single or multiple augers and mixing paddles. The auger is slowly rotated into the ground, typically at 10-20 rpm, and advanced at 0.5-1.5 meters per minute. As the auger advances, lime or cement slurry is pumped through the hollow stem of the rod feeding out at the tip of the auger. Mixing paddles are arrayed along the shaft above the auger to provide mixing and blending of the slurry and soil. After final destination is reached, the tools are withdrawn which is typically at twice the speed of penetration, 1-3 meters per minute. This method has the ability to create soil mix columns, typically 1.5-2.5 m in diameter, to depths up to 25 m. This method is very economical for mass ground improvement projects (DeepXcav, 2011).

In jet grouting, high-pressure lime or cement slurry at a pressure up to 280 Bar is pumped through horizontal ports in a drill string above the drill bit (Porbaha, 1998; Porbaha et al., 2005). The high velocity and pressure of the lime/cement jets cuts and mixes the soil in-situ (. A different method called DJM (Dry Jet Mixing) is used in high moisture content soils. Compressed air carries lime to the hole where mixing paddles blend the dry stabilizing agent with the soil. Jet mixing is fast and the system of choice to construct cylindrical soil cement elements, 1 m in diameter, to depth of up to 20 m (MDC, 2011). Figure 8.3 shows typical dry deep mixing tools for mechanical mixing and nuzzles next to the blade for injecting lime (Larsson, 2005).

A combination of mechanical mixing and jet mixing has been used for soil improvement in the past (Kitazume and Terashi, 2013). When the mixing tool is rotated into the soil, lime/cement under high pressure discharges via a number of nuzzles placed along the blades.

In order to introduce lime or cement to the shear zone of a reactivated landside, a rotary drilling method can be employed to reach the shear zone and then a retractable mixing tool such as the tools shown in Figure 8.4 (courtesy of Rodrill manufactures and Huanli Industries) can be used to introduce lime/cement to the shear zone and mix it with in-situ soil. By using these belling (underream) tools, it is believed that it would be possible to introduce lime or cement to a significant area of the shear zone during each run. The cost advantages of under-reamed lime/cement columns are due to the reduced diameter in the upper ground that does not need to be treated.

(a) DDM standard
(courtesy of DDM Association)

(b) The Nordic dry mixing "standard" tool according to SGF (2000)
(Larsson & Nilsson, 2005)

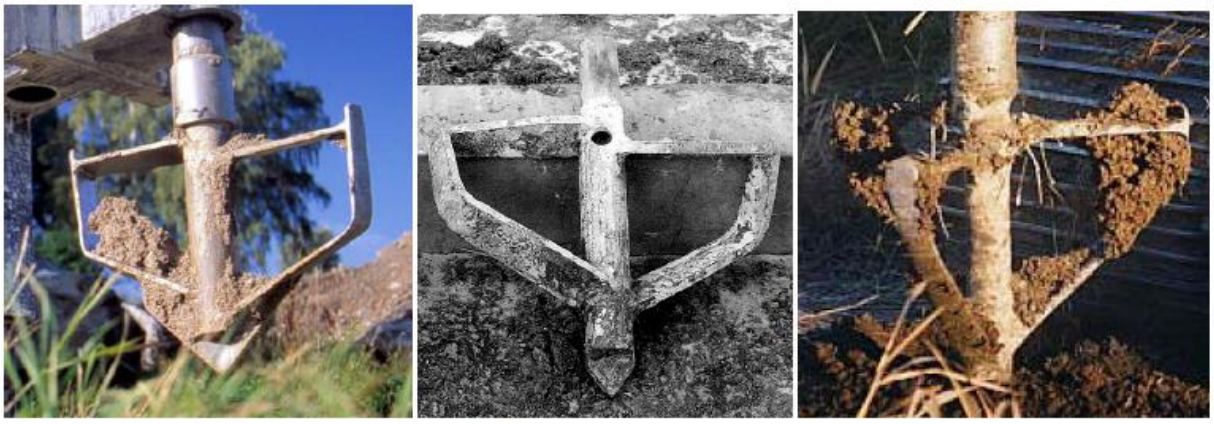

(c) Three versions of the Nordic dry mixing "standard" tool
(courtesy of Hercules Grundläggning and LCM)

(d) Nordic dry mixing "Pinnborr"
(courtesy of LCM)

(e) Modified dry deep mixing (LCTechnology, 2002)

Figure 8.3: Dry Deep Mixing (DDM) Tools (Larsson, 2005)

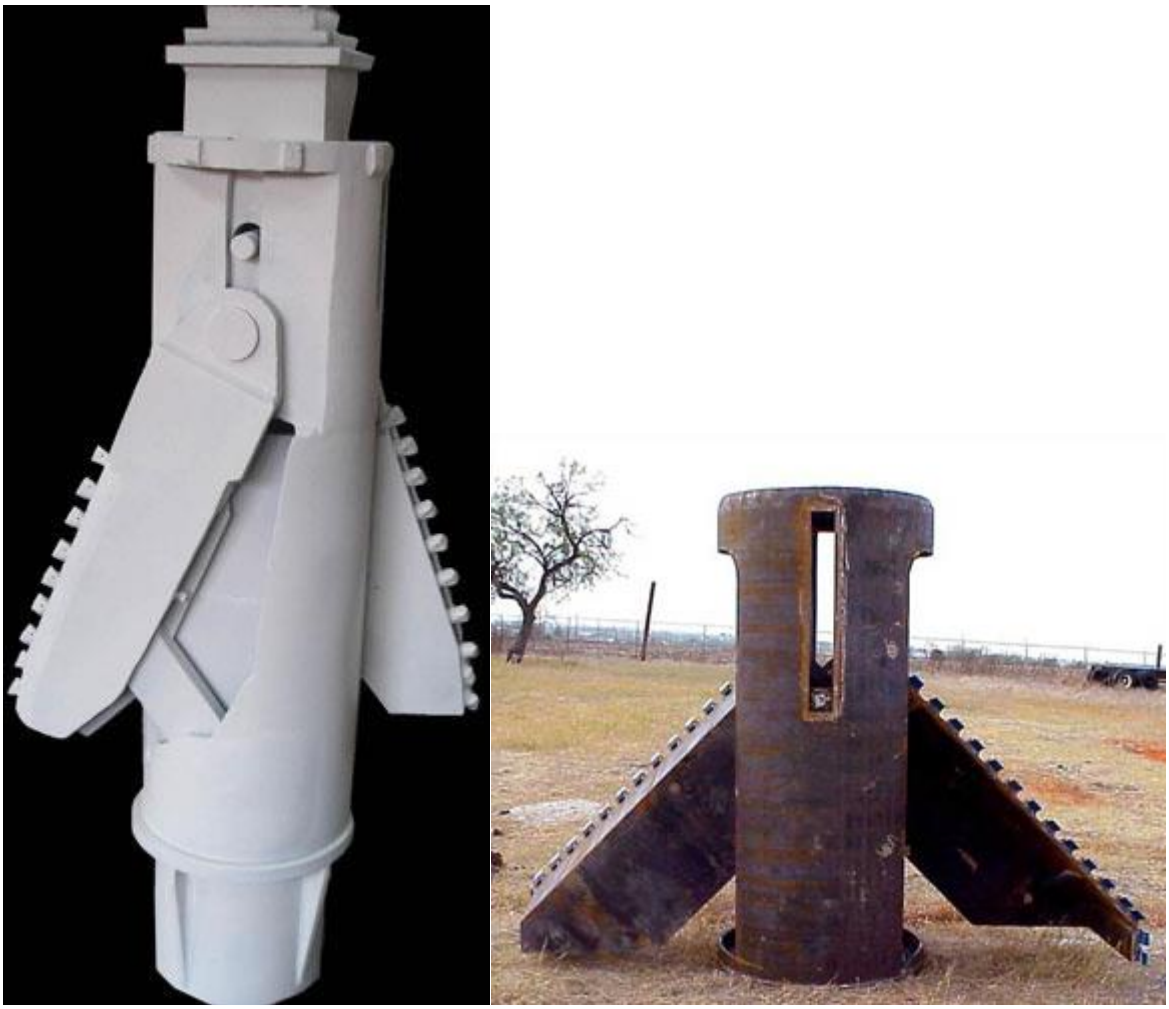

Figure 8.4: Belling tools (Courtesy of Rodrill Manufactures and Huanli Industries)

Figure 8.5 illustrates a retractable mixing tool designed as part of the present study. Because the retracted diameter is small, a lower force is required for pushing it inside the soil. Two pairs of blades are opened and closed through a sliding sleeve. The mixing tool has hinged arms, which can be opened by a downward force on the sleeve when the drill rod remains fixed. The arms can be retracted by applying an upward force to the sleeve.

Locations of the columns need to be marked on site prior to starting work. The retractable mixing tool attached to the drill rod is placed at the predetermined locations; the drilling tool is rotated and advanced to the shear zone. When reaching the depth to be treated (i.e. shear zone of a reactivated landslide), the mixing tool is pushed outward by a downward force on the sleeve. Then, dry lime/cement or slurry, depending on the water content of the clay to be treated, is injected to the area. The lime/cement which has been pressurized in a separate storage tank is pneumatically (dry) or hydraulically (slurry) conveyed into the ground. Lime or cement is injected into the soil from nozzles located on the blades. The tool is rotated to mix lime or cement with the soil.

Figure 8.6 shows the treatment procedure of a reactivated slip surface:

1. Penetrate ground until the specified depth that is the shear zone of a reactivated landslide;
2. Open the mixing tool by pushing the sleeve down while holding the rod in place;
3. Inject dry lime or slurry depending on the water content of the original soil;
4. Rotate the rod to mix the lime with the soil;
5. Retract the mixing tool by pulling the sleeve up while holding the rod in place;
6. Pull the sleeve up till the mixing tool is out of the ground;
7. The treatment procedure is repeated for different locations on the reactivated slip surface in directions parallel and perpendicular to direction of the slide.

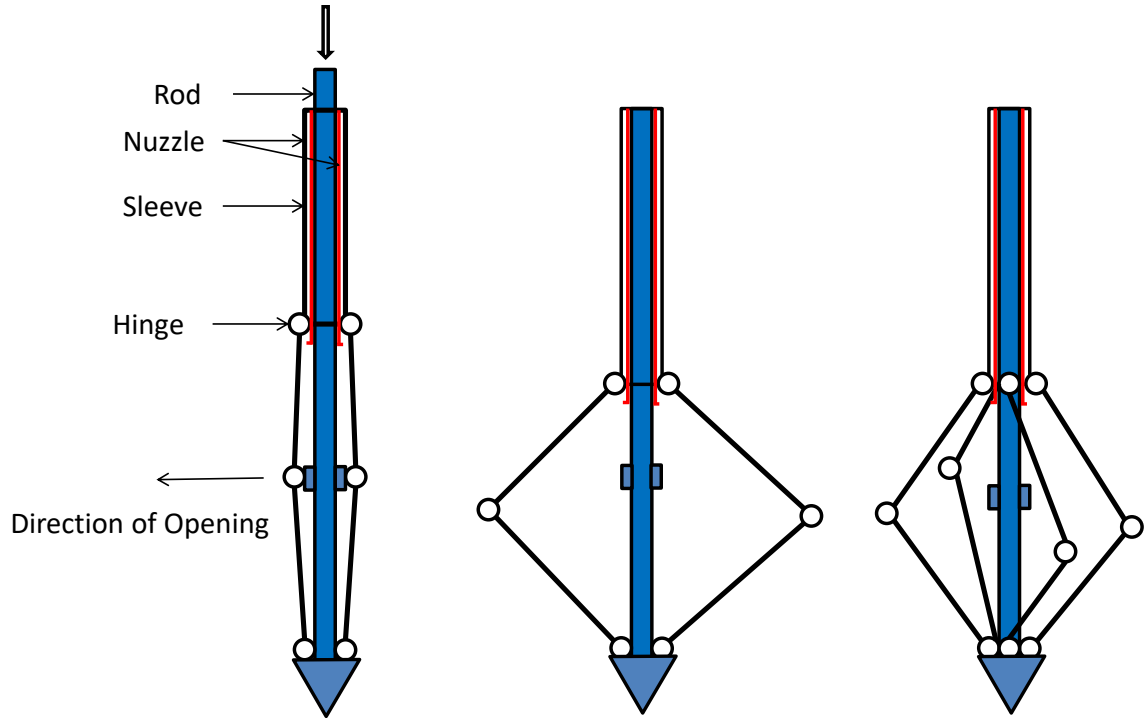

Figure 8.5: A small retractable mixing tool designed to push inside the soil easily

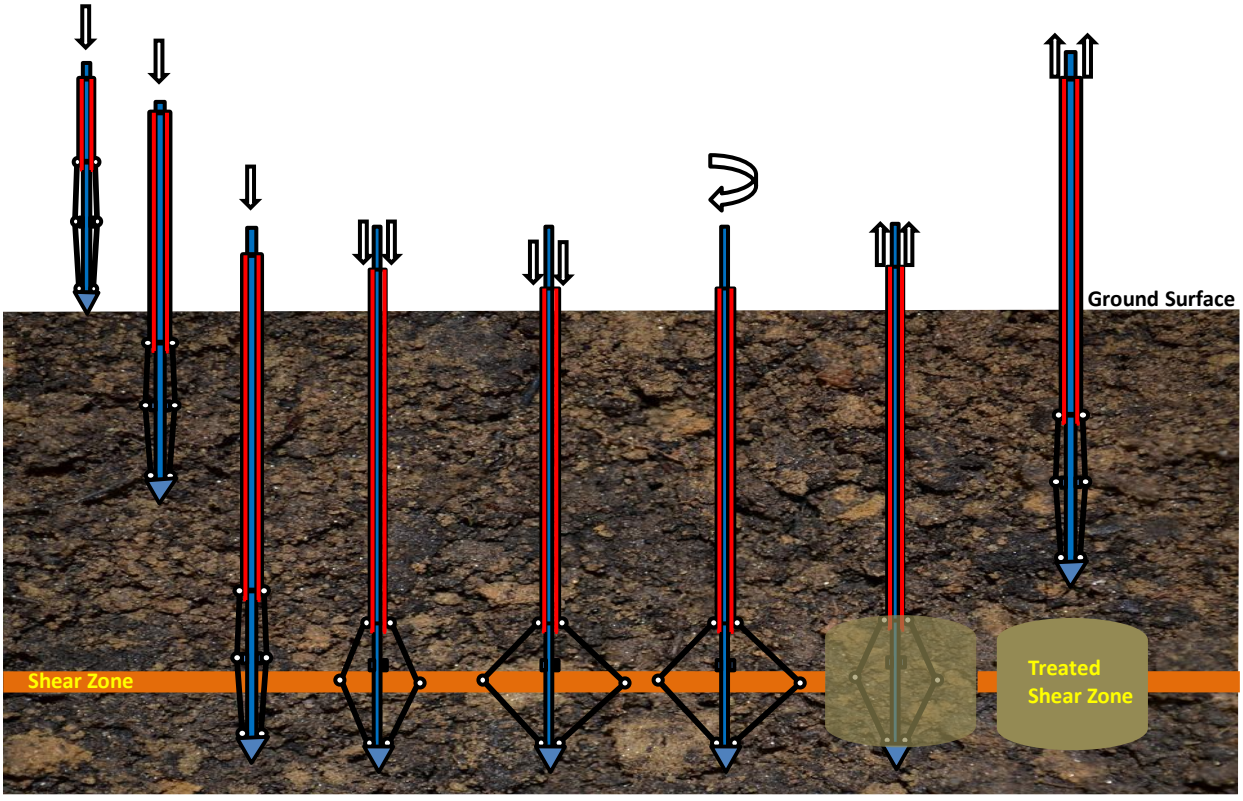

Figure 8.6: Lime treatment of a reactivated slip surface using a retractable mixing tool

Another method which can be used in treatment of reactivated shear surfaces is Horizontal Directional Drilling (HDD). HDD has been extensively used to install cables and pipelines for gas, oil, telecommunications, etc. underneath rivers, railroads, roads and under areas congested with buildings. HDR involves (DTD, 2004):

1. Drilling a pilot bore hole towards a target;

2. Back-reaming the borehole to the drill rig if a larger diameter borehole is needed.

According to Bayer (2007), HDD has been used for slope stabilization purposes in the southern German Keuperbergland (Stuttgard area, Swabian Forest, Mittelfranken and Nuremberg area) due to the unstable ground. HDD system were installed at down slope with a proper safe distance so that the bore is drilled with a rising gradient towards the shear zone in order to allow a free flow of the water from the shear zone once that zone is reached. One of the advantages of HDD was to eliminate the vibrating loads on top of the slope caused by construction of classical vertical well bores. Using HDD system, stabilizing agents can be high-pressure injected through HDD bore head or a jet grouting bore head from the borehole into the shear zone and mixed with the soil. HDD has a very low environmental impact, a predictable and short construction schedule, and very low cost compared to other alternatives. The rig spread requires a minimum 30 m wide by 45 m long space. The longest crossing to date has been about 1.8 km. and borehole diameters of up to 1.2 m have been drilled (H&H Enterprises). A typical HDD rig spread is shown in Figure 8.7 (Courtesy of Suffolk Water Connections Inc).

After the treatment locations are marked on a site, HDD method can be used to bore along the slip surface. Then lime/cement is introduced to the shear zone and mixed with in-situ soil using a mixing tool (i.e. mechanical and jet mixing tool, Figure 8.8) attached to the horizontal driller.

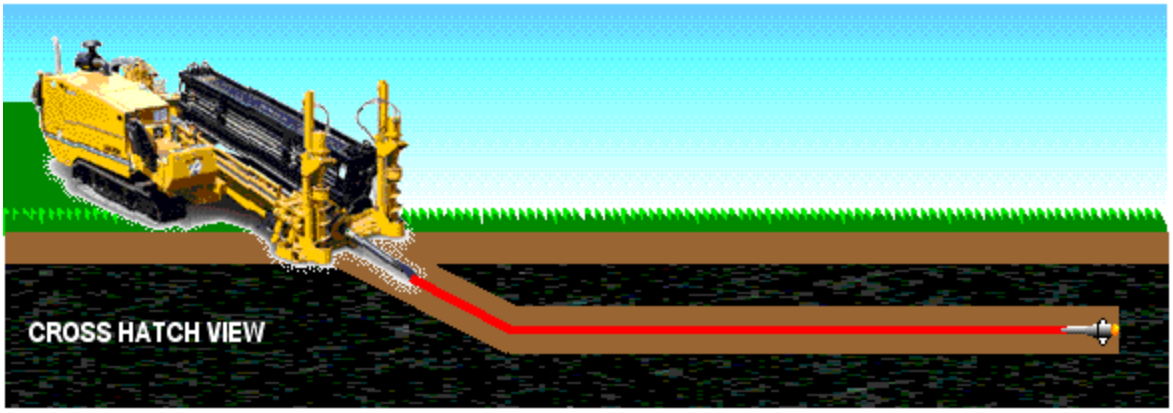

Figure 8.7: HDD Method (Courtesy of Suffolk Water Connections Inc.)

Figure 8.8: Mixing tool with a discontinuous auger and a nuzzle for injecting lime (Larsson, 2005)

It is possible to guide the horizontal driller from the ground surface very accurately with recent technology developed in HDD method (DTD 2004). There is a signal receiver at the ground surface that receives the signal sent form the horizontal driller. This receiver is able to track down the driller under the ground and direct it very accurately. It might be necessary to repeat the treatment procedure vertically if the shear zone is too thick. It is very important to mix lime with soil across the entire thickness of the reactivated slip surface.

Figure 8.9 shows the lime treatment of a reactivated slip surface after a number of lines of treatment along the direction of sliding have been selected:

1. Insert the drill bit into the ground from the top of the slope;
2. Advance the drill bit along the reactivated slip surface towards the toe of the slope using a signal receiver on the ground surface;
3. Add more rods as the drill bit proceeds;
4. Take the drill bit off at the toe of the slope and attach the reamer and mixing tool
5. Start from the toe of the slope and inject dry lime or slurry depending on the water content of the original soil;
6. Rotate the rod to mix lime with soil while pulling back the mixing tool;
7. Withdraw the rods, reamer and mixing tool from the top of the slope;
8. Repeat the procedure for several lines of treatment.

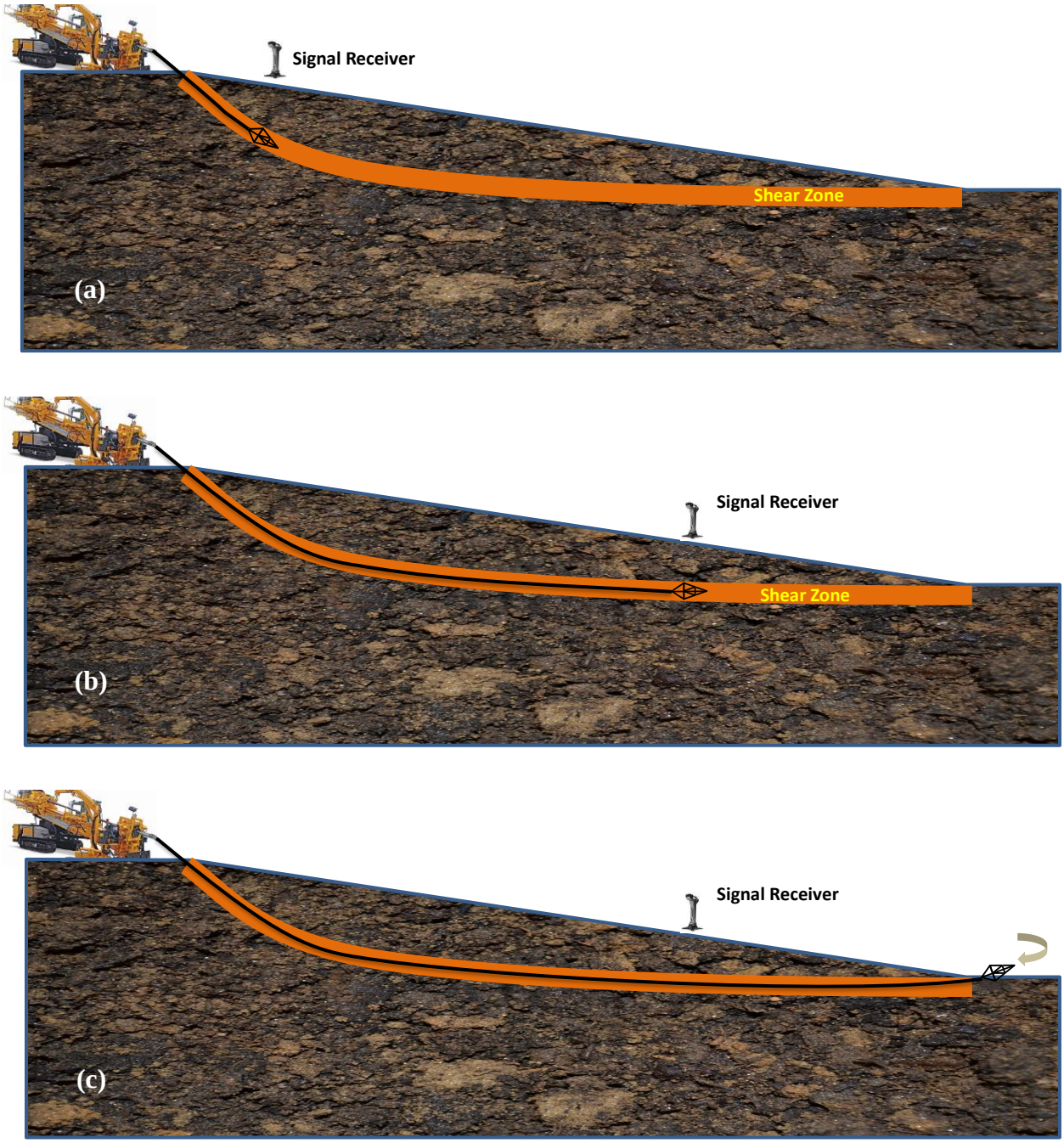

Figure 8.9: Lime treatment of a reactivated slip surface using a combination of Combined Horizontal Directional Drilling (HDD), Mechanical Deep Mixing (MDM) and Jet Mixing (JM)

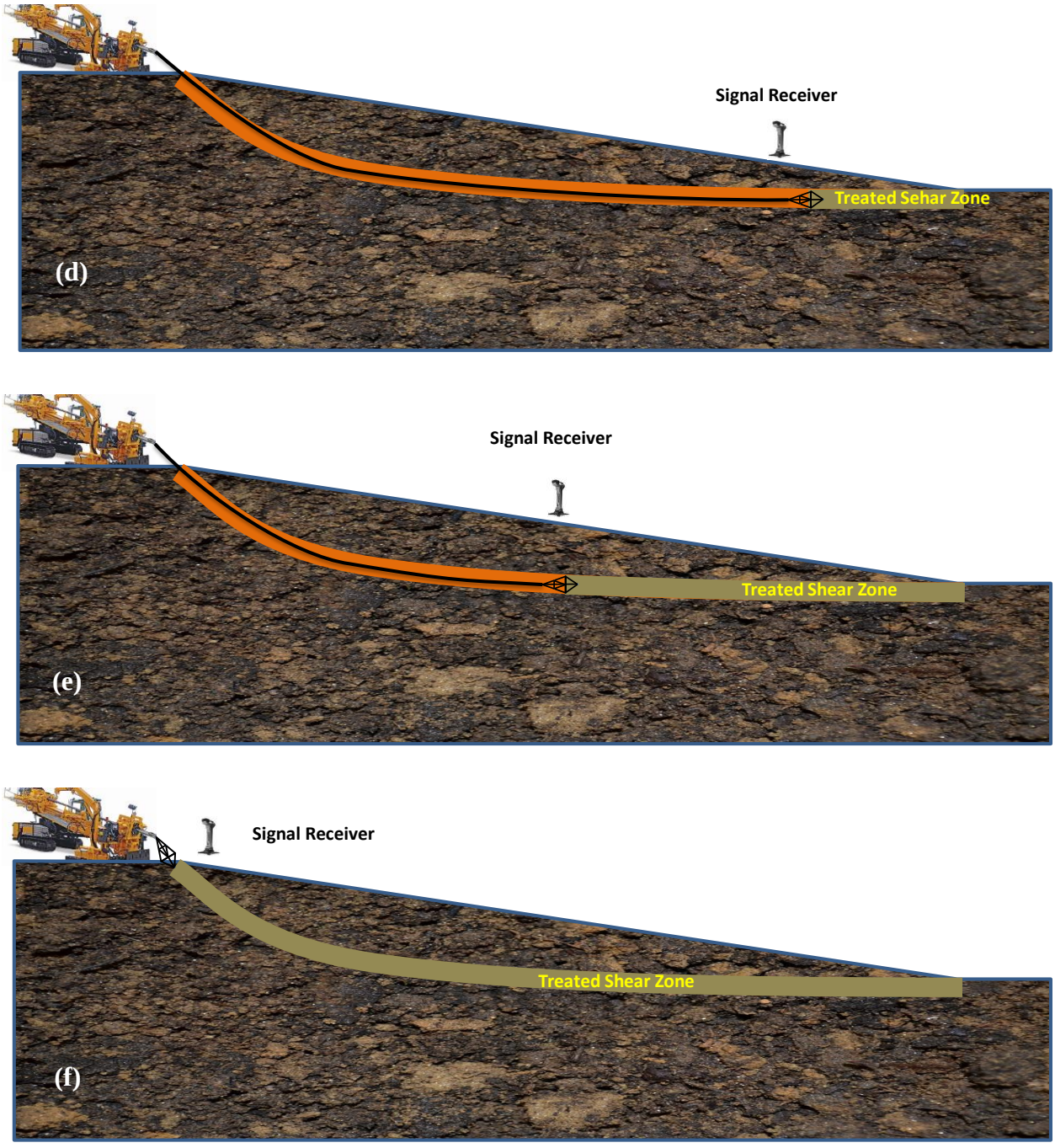

Figure 8.9: (cont'd)

8.2 INFLUENCE OF LIME TREATMENT ON STABILITY OF SLOPES

The shear strength of lime-treated soil determined from the laboratory tests are used to evaluate the stability of Red River slopes in Grand Forks, North Dakota (Mesri and Huvaj, 2004), CUP O'Hare reservoir slopes in Chicago, Illinois, and the slope failures in drainage channels in Harris County, Texas.

The following equation can be used to calculate friction angle for partially lime treated ground in slope stability analysis, as shown in Figures 8.10 and 8.11 for HDD method and lime treated columns, respectively:

$$\tan[\phi'_{PT}]_s^{\sigma'_n} = a.\tan[\phi'_T]_s^{\sigma'_n} + (1\text{-}a).\tan[\phi'_{UT}]_s^{\sigma'_n} \quad (8.1)$$

where,

$[\phi'_{PT}]_s^{\sigma'_n}$ = friction angle of soil following treatment of part of slip surface,

$[\phi'_T]_s^{\sigma'_n}$ = friction angle of the treated soil,

a = Treatment area ratio, i.e. ratio of treated area to total area of slip surface.

$[\phi'_{UT}]_s^{\sigma'_n}$ = friction angle of untreated soil.

Alternatively, the following equation can be used to calculate the factor of safety of a partially treated slope:

$$FS_{PT} = a.FS_T + (1\text{-}a).FS_{UT} \quad (8.2)$$

where,

FS_{PT}: factor of safety of slope following treatment of part of slip surface (with a treatment area ratio a),

FS_T: factor of safety of entirely treated slope, and

FS_{UT}: factor of safety of untreated slope.

Figures 8.10 and 8.11 show typical treatment lines using Horizontal Directional Drilling (HDD) method and lime treated columns using Deep Soil Mixing (DSM) method, respectively. The treatment area ratio, a, is calculated as follows:

For HDD method (Figure 8.10)

- a=w/s, where w=width and s=center-to-center spacing of the treated lines,

For DSM lime treated columns (Figure 8.12)

- $a=\pi d^2/4s_{1.}s_2$ (Rectangular pattern)
- $a=\pi d^2/4s_{1.}s_{2.}\sin\theta$ (Triangular pattern)

where d=diameter of lime treated columns, s_1= center-to-center spacing between lime treated columns in the direction parallel to slope, s_2 = center-to-center spacing between lime treated columns in the direction perpendicular to slope, and θ = angle of arrangement between treated soil columns.

Various patterns of DSM columns can be utilized to introduce lime to the shear zone including square, triangular, ring, group columns, block, etc., as shown in Figure 8.13. A pattern can be selected based on the situation and the ratio of treatment to meet the required safety of factor.

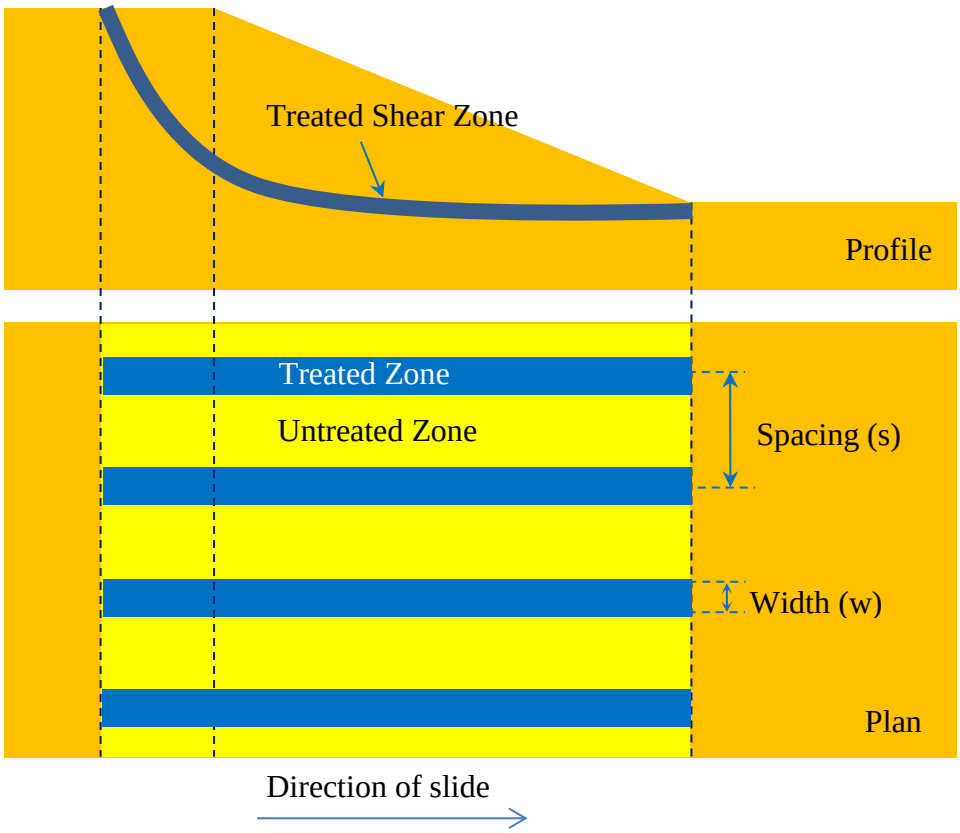

Figure 8.10: Treatment of part of slip surface using Horizontal Directional Drilling (HDD) method (a=0.3)

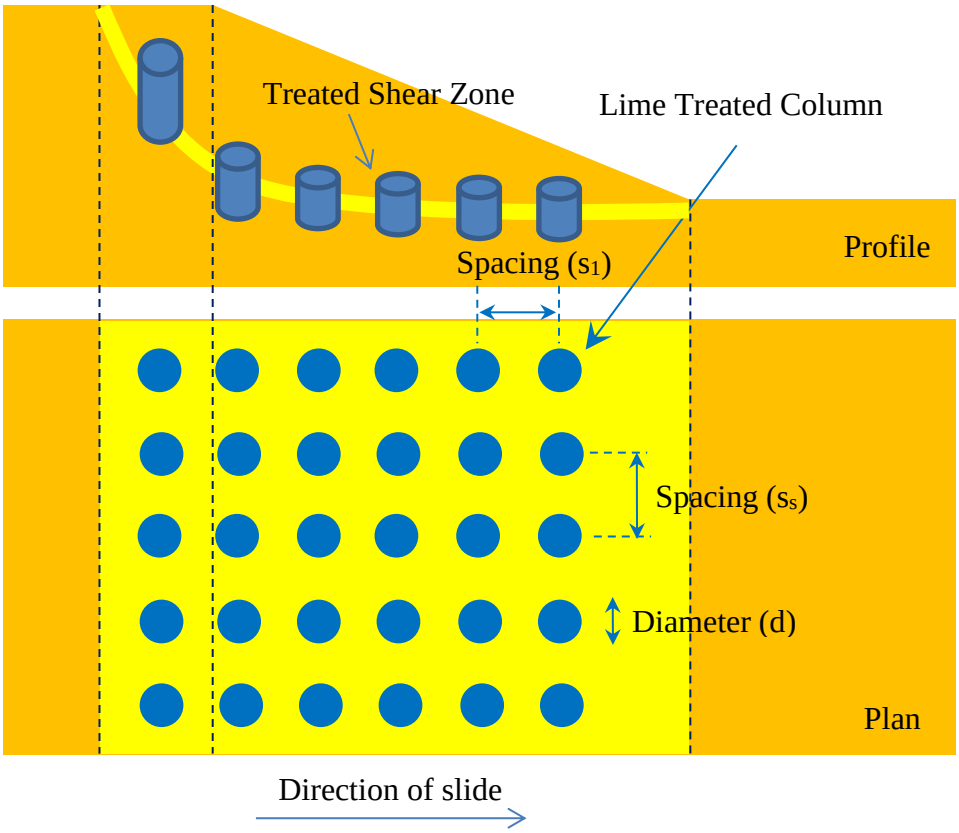

Figure 8.11: Treatment of part of slip surface using Deep Soil Mixing (DSM) method (rectagngular pattern, a=0.25)

Figure 8.12: Treated soil column patterns: (a) rectangular patern; (b) triangular pattern

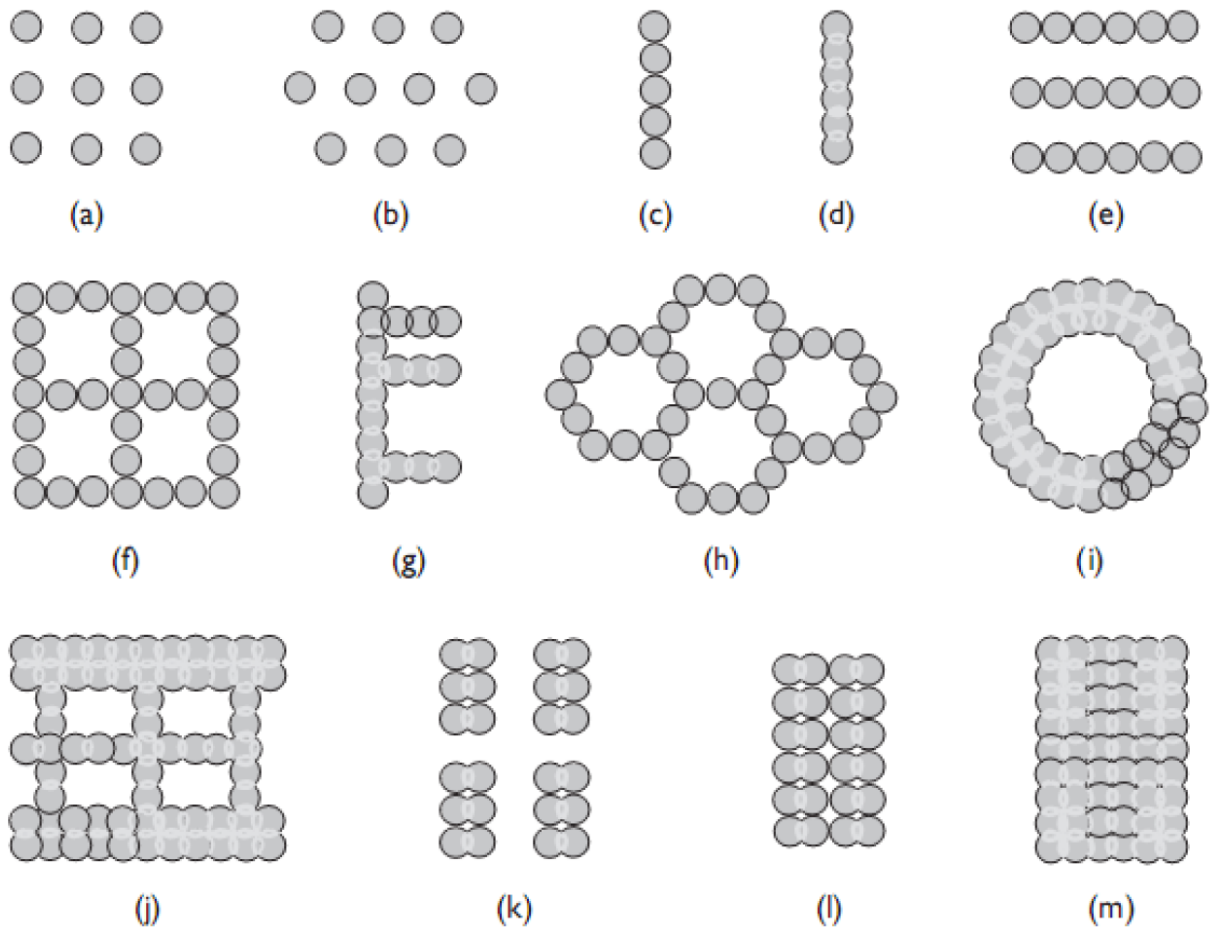

Figure 8.13: DSM column patterns: (a) square; (b) triangular; (c) tangent wall; (d) overlapped wall; (e) tangent walls; (f) tangent grid; (g) overlapped wall with buttresses; (h) tangent cells; (i) ring; (j) lattice; (k) group columns; (l) group columns in-contact; (m) block (Esmaieli et al. 2013)

8.2.1 Red River Slopes

A number of Red River slopes are selected in this section to examine the effect of lime treatment on the safety factor of the slopes. The slopes selected for the analysis are reactivated slides in the sense that the entire slip surface is at residual condition (Mesri and Huvaj, 2004). The Red River separates Grand Forks, North Dakota, from East Grand Forks, Minnesota, as it flows north to Lake Winnipeg in Manitoba, Canada (Figure 8.14). A large number of slope instabilities have been reported due to flooding along Red River. According to Baracos and Graham (1981), all the river banks along the Red River in Winnipeg, Canada, have previously experienced a slide.

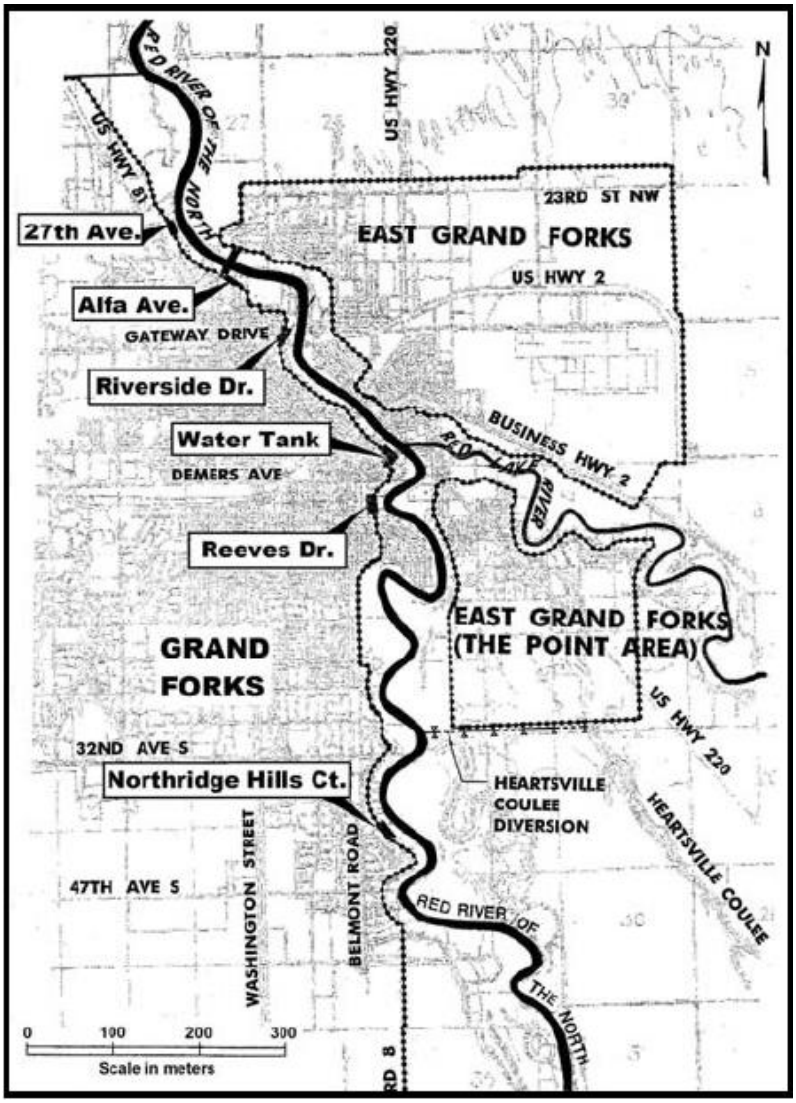

Figure 8.14: Red River area map. The slide locations analyzed in this study are indicated with arrows.

The lowest unit of the slope failure, Falconer Formation, overlying the bedrock, is a medium stiff, low to moderate plasticity, silty and sandy clay till (Arndt, 1977). Falconer Formation underlies the Brenna Formation that is a uniform, soft to firm, dark grey, glacio-lacustrine clay with little or no visible stratification; however, is full of small slickensides (Hill and Rutledge, undated). The highly plastic montmorillonitic Pierre Shale bedrock is the major source of slickensided Brenna Formation (Quigley, 1968; Baracos, 1977), which is divided into two layers, Lower Brenna and Upper Brenna.

The Sherack Formation overlying the Brenna Formation is a laminated, medium stiff, glacio-lacustrine silty clay and clayey silt. This layer underlies soft to medium stiff, fluvial or alluvial silty clay or clayey silt from the Red River flood sediments (USACE, 1998).

The slip surface in the Red River slopes has been located using (Mesri and Huvaj, 2004):

1. Visual site inspection,
2. Boring logs and sampling, and
3. Inclinometers

It has been determined that the base of the slip surface for slopes along the Red River generally lies just above the contact between the Upper and Lower Brenna layers. In the cases where the Upper Brenna has been eroded and replaced with the more competent alluvial/fluvial deposits, the slip surface descends to the base of the Lower Brenna layer, then ascends to the slope (Hill and Rutledge, undated).

Stability of the Red River slopes at different locations before and after lime treatment was evaluated according to the procedure suggested by USACE (2003). The stability analyses were performed using GeoStudio 2016 with the limit equilibrium code Slope/W (GeoSlope International, 2016). The geometry of the slopes and identified shear surface are shown in Figures 8.15-8.19.

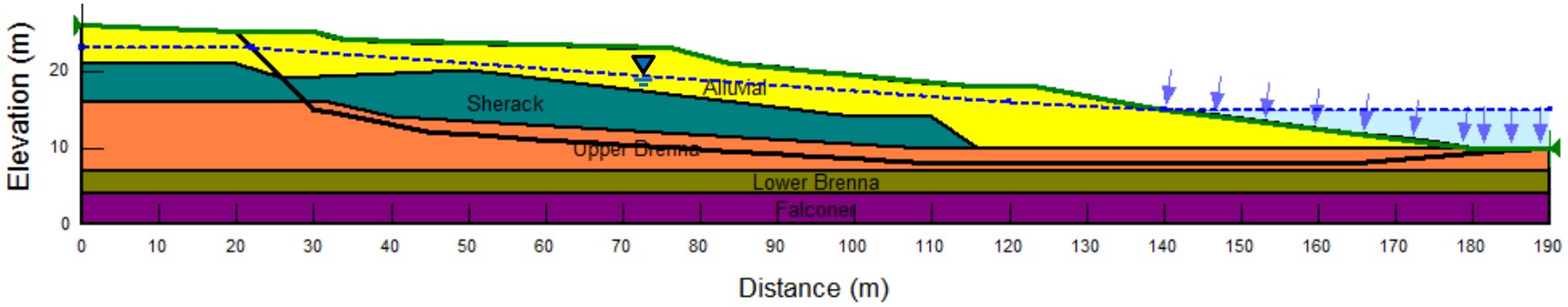

Figure 8.15: 27th Avenue slide

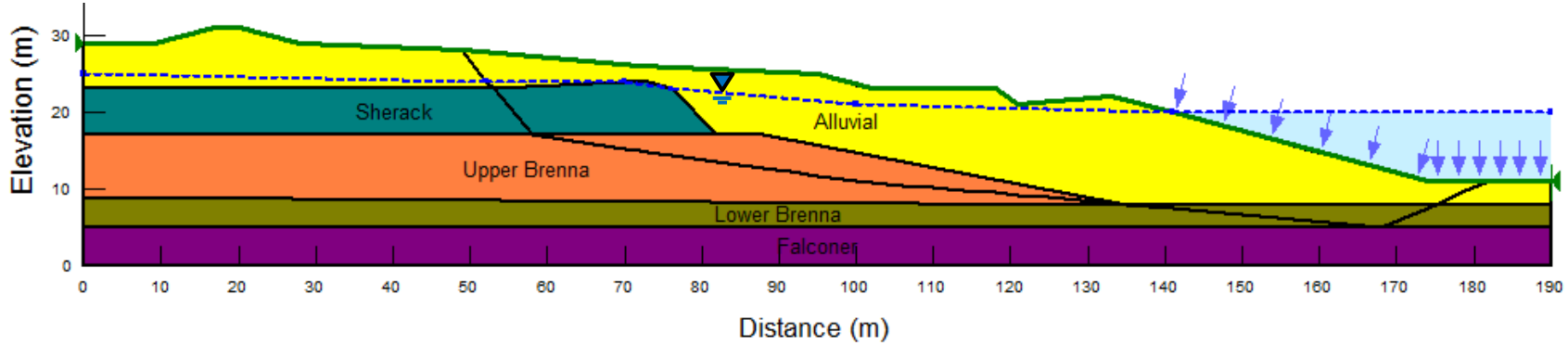

Figure 8.16: Alpha Avenue slide

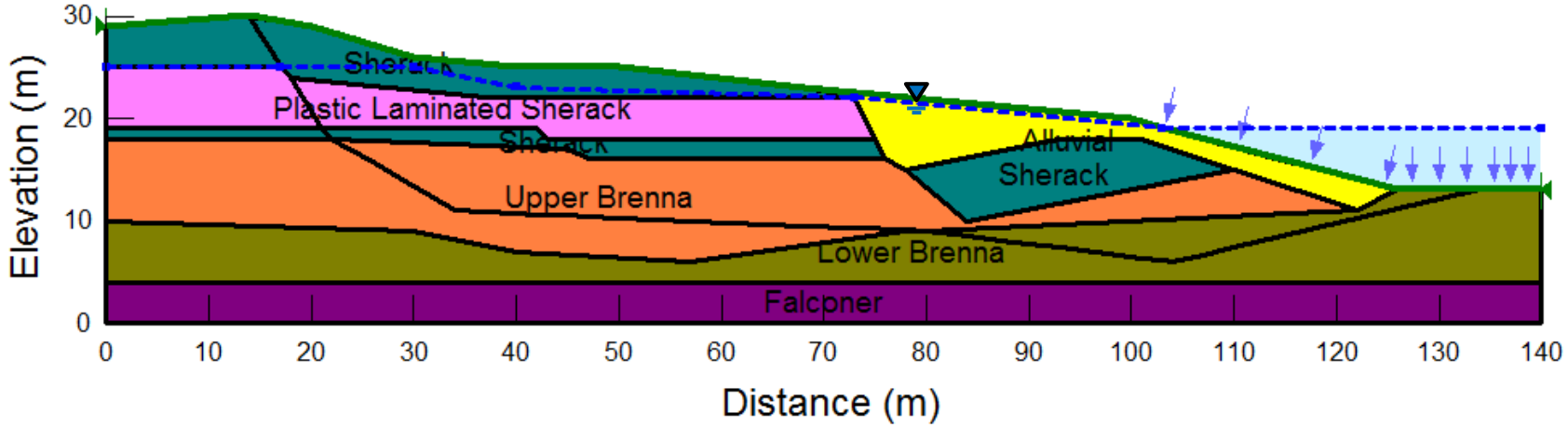

Figure 8.17: Riverside Drive slide

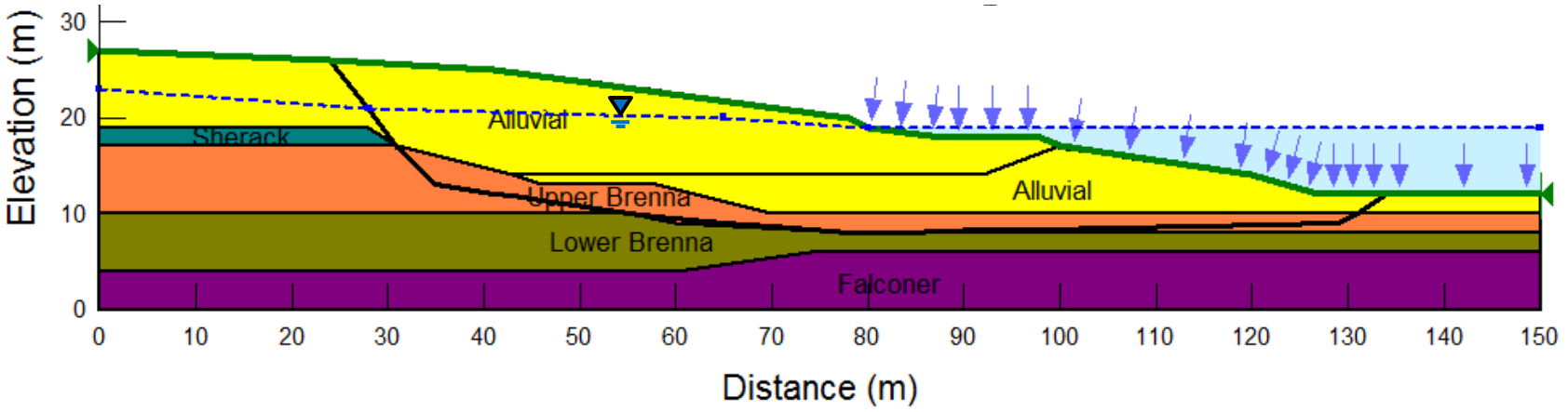

Figure 8.18: Water Tank slide

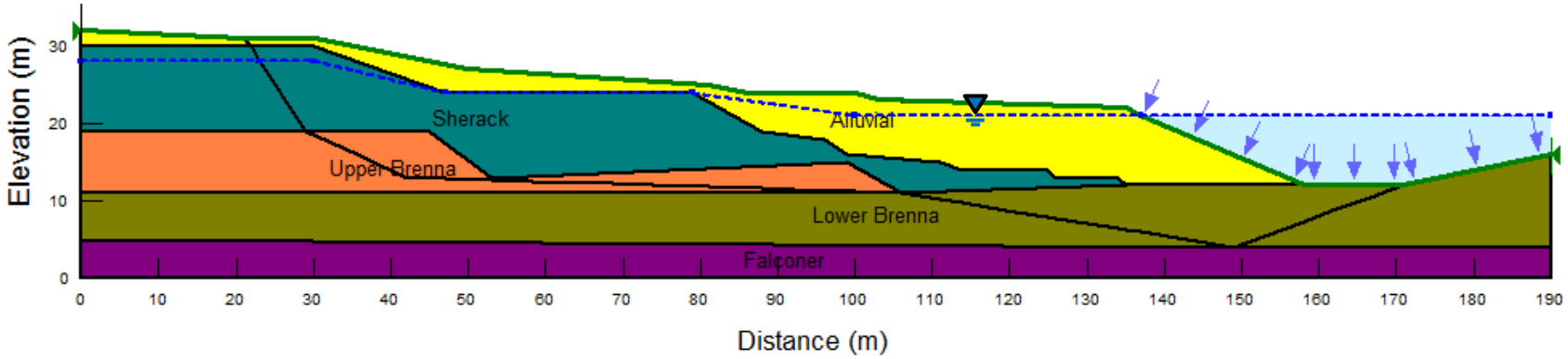

Figure 8.19: Reeves Drive slide

Table 8.1 summarizes the parameters used in the slope stability analyses for Alluvial, Sherack, Plastic Laminated Sherack, and Falconer layers. For soil layers other than Brenna clay, constant values of friction angle were used in the stability analyses (linear relationship between shear strength and effective normal stress). For Brenna clay, the nonlinear shear strength envelopes of untreated and 7% lime-clay obtained from the laboratory tests, as shown in Figure 8.20, were used in the analyses. The stability of the treated slopes was evaluated for the peak shear strength after 1, 2, and 5 weeks of curing. The factor of safety was also calculated for the residual condition after treatment.

Table 8.1: Soil properties from the laboratory tests of USACE (1998)

Soil	γ, kN/m^3	I_p, %	ϕ'_{fs}, Degrees	ϕ'_r, Degrees
Alluvial	17.7	20-45	30	28
Sherack	17.7	20-50	30	27
Plastic Laminated Sherack	16.2	50-65	22	11
Falconer	18.3	15-35	28	28

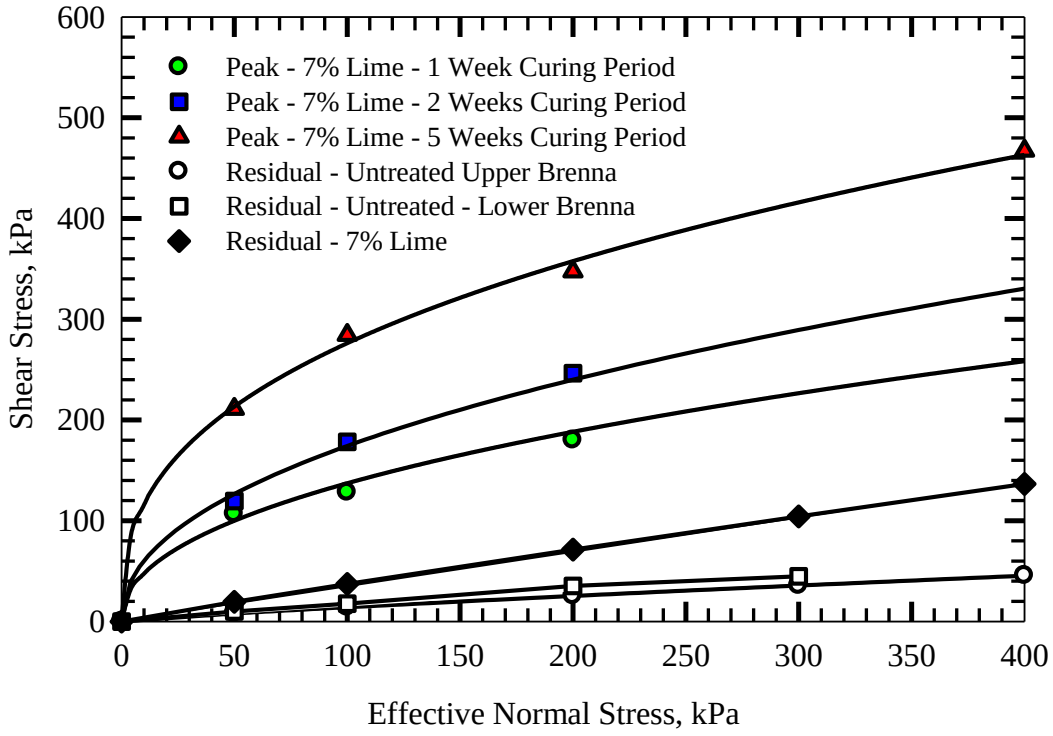

Figure 8.20: Shear strength envelopes of untreated and treated Brenna Clay

The percentage of the slip surface passing through Brenna clay is sown in Table 8.2. The stability analyses of the current condition of the slopes show a marginally stable condition, as the factor of safety of the slopes calculated before treatment imply (Table 8.3).

Table 8.2: Percentage of slip surface passing through Brenna clay in Red River slopes

Slope	Length of slip surface in a clay / total length of slip surface, %	
	Other formations	Brenna formation
27the Avenue	7	93
Alpha Avenue	10	90
Riverside Drive	11	89
Water Tank	10	90
Reeves Drive	8	92

The calculated safety factors shown in Tables 8.3 and 8.4 pertain to the treatment of ten and twenty percent of the slip surface, respectively. The treatment ratio is calculated as:

$$\text{Treatment ratio (a)} = \frac{\text{Treated area}}{\text{Total area of sip surface passing through Brenna clay}}$$

A significant increase in the safety factor is observed after introducing lime to the shear zone for both ten and twenty percent treatment ratios.

Table 8.3: Safety factors of Red River slopes following treatment of ten percent of slip surface (a=0.1) with 7% lime

Slope	Before treatment	After treatment			
		Peak strength Curing time, weeks			Residual strength
		1	2	5	
27the Avenue	1.00	1.93	2.18	2.89	1.24
Alpha Avenue	1.00	1.73	1.93	2.48	1.18
Riverside Drive	1.00	1.70	1.91	2.50	1.12
Water Tank	1.00	1.74	1.96	2.58	1.14
Reeves Drive	1.00	1.62	1.81	2.32	1.12

Table 8.4: Safety factors of Red River slopes following treatment of twenty percent of slip surface (a=0.2) with 7% lime

Slope	Before treatment	After treatment			
		Peak strength Curing time, weeks			Residual strength
		1	2	5	
27the Avenue	1.00	2.77	3.27	4.69	1.40
Alpha Avenue	1.00	2.40	2.80	3.90	1.31
Riverside Drive	1.00	2.39	2.81	4.01	1.24
Water Tank	1.00	2.48	2.92	4.16	1.27
Reeves Drive	1.00	2.25	2.63	3.64	1.24

For the 27th Avenue slide, 7% lime content treatment of ten percent of the slip surface increases computed factor of safety from 1.09 to 1.93, 2.18 and 2.89 after 1, 2 and 5 weeks of curing, respectively, using the peak strength. The safety factor at residual condition increases to 1.24. A twenty percent treatment ratio of the slip surface leads to an increase in the safety factor of the slopes to 2.77, 3.27 and 4.69 after 1, 2 and 5 weeks of curing, respectively. The safety factor at residual condition increases to 1.40 for twenty percent treatment of the slip surface.

For Alpha Avenue slide, the safety factor increases following ten percent treatment of the slip surface from 1.06 to 1.73, 1.93 and 2.48 by using peak strength of 7% lime content for curing periods of 1, 2 and 5 weeks, respectively. The safety factor was calculated 1.18 at the residual condition. For a treatment ratio of twenty percent, the safety factor increases to 2.40, 2.80 and 3.90 for 1, 2 and 5 weeks of curing. The safety factor at residual condition was calculated 1.31 for twenty percent treatment ratio.

The safety factor of Riverside Drive slide increases from 1.00 to 1.70, 1.91 and 2.50 for ten percent treatment of the slip surface using peak strength after 1, 2 and 5 weeks of curing. The residual strength of treated clay increases the safety factor to 1.12 for ten percent treatment ratio. The safety factor of the slope was calculated 2.39, 2.81 and 4.01 after 1, 2 and 5 weeks of curing for twenty percent treatment ratio. The safety factor at residual condition was calculated 1.24 for twenty percent treatment of the slip surface.

For Water Tank slide, lime treatment of ten percent of the slip surface increases the safety factor from 1.00 to 1.74 after 1 week using the peak strength. The safety factor increases to 1.96 after 2 weeks and to 2.58 after 5 weeks of curing. An increased safety factor of 1.14 was obtained for the treated slope at residual condition. For twenty percent treatment of the slip surface, the safety factor increases to 2.48, 2.92 and 4.16 for 1, 2 and 5 weeks of curing. The safety factor at residual condition increases to 1.27 following treatment of twenty percent of the slip surface.

For ten percent treatment of slip surface at Reeves Drive slide, the computed safety factor increases from 1.00 to 1.62, 1.81 and 2.32 for curing periods of 1, 2 and 5 weeks using the peak strength, and to 1.12 at the residual condition. With the treatment ratio increasing to twenty

percent, the safety factor increases to 2.25, 2.63 and 3.64 after 1, 2 and 5 weeks of curing using the peak strength and to 1.24 at the residual condition.

The safety factors of marginally stable slopes at Red River in the range of 1-1.1 increase substantially after treatment of ten percent of the slip surface with 7% lime. The safety factors for peak strength increase to the range of 1.62-1.93 after 1 week, 1.81-2.18 after 2 weeks, and 2.32-2.89 after 5 weeks of curing. The safety factor increases to the range of 1.12-1.24 at residual condition following treatment of ten percent of the slip surface. The safety factors using peak strength increases to the range of 2.25-2.77 after 1 week, 2.63-3.27 after 2 weeks, and 3.64-4.69 after 5 weeks of curing for twenty percent treatment ratio. The safety factor increases to the range of 1.24-1.40 at residual condition following treatment of twenty percent of the slip surface. This level of lime remediation effort is expected to have a significant effect on rate of movement of the slide.

The stability of the slopes was evaluated for 7% lime treatment after 35 days of curing using the post-peak strength. As shear strain increases, shear strength decreases to post-peak strength. The peak, post-peak, and residual shear strength envelopes of 7% lime treated, cured for 35 days, are shown in Figure 8.21 for Brenna clay. The post-peak shear strength envelopes correspond to the shear strains of 5, 10, 20, and 30%.

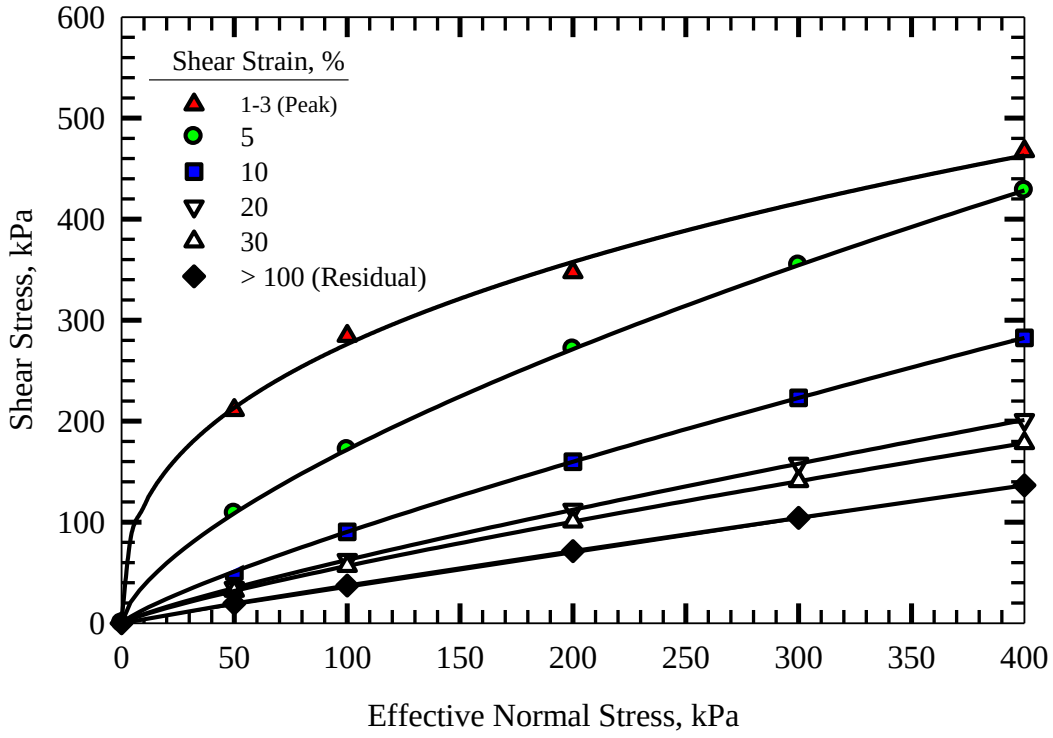

Figure 8.21: Peak, post-peak and residual shear strength envelopes of 7% lime treated Brenna Clay, cured for 35 days

The safety factors computed using the post-peak shear strength for shear strains in the range of 5-30% are summarized in Tables 8.5 and 8.6 for ten and twenty percent treatment ratios, respectively.

Table 8.5: Safety factors of Red River slopes following treatment of ten percent of slip surface (a=0.1) with 7% lime, cured for 35 days using post-peak shear strength

Slope	Shear strain, %			
	5	10	20	30
27the Avenue	2.14	1.59	1.42	1.37
Alpha Avenue	1.91	1.47	1.32	1.29
Riverside Drive	1.86	1.41	1.26	1.23
Water Tank	1.92	1.44	1.28	1.25
Reeves Drive	1.82	1.40	1.26	1.22

Table 8.6: Safety factors of Red River slopes following treatment of twenty percent of slip surface (a=0.2) with 7% lime, cured for 35 days using post-peak shear strength

Slope	Shear strain, %			
	5	10	20	30
27the Avenue	3.20	2.10	1.75	1.66
Alpha Avenue	2.76	1.88	1.58	1.52
Riverside Drive	2.72	1.81	1.52	1.45
Water Tank	2.83	1.88	1.57	1.50
Reeves Drive	2.63	1.80	1.52	1.45

The relation of the safety factor of the Red River slopes with the increase in the shear strain is shown in Figures 8.22-8.26. The safety factor before treatment was calculated for residual strength along the entire slip surface. The safety factor drops significantly when shear strains increases to 10%. For the shear strains greater than 10%, the safety factor decreases at a lower rate. At large strains, the safety factor after lime treatment is still higher than the safety factor prior to lime treatment.

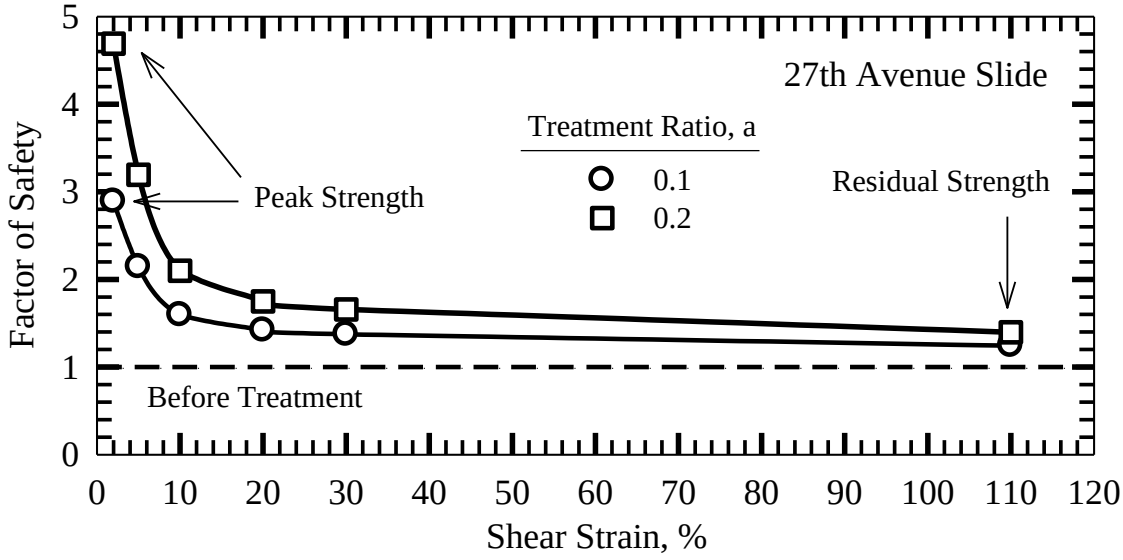

Figure 8.22: Safety factor reduction with shear strain, 27th Avenue slide

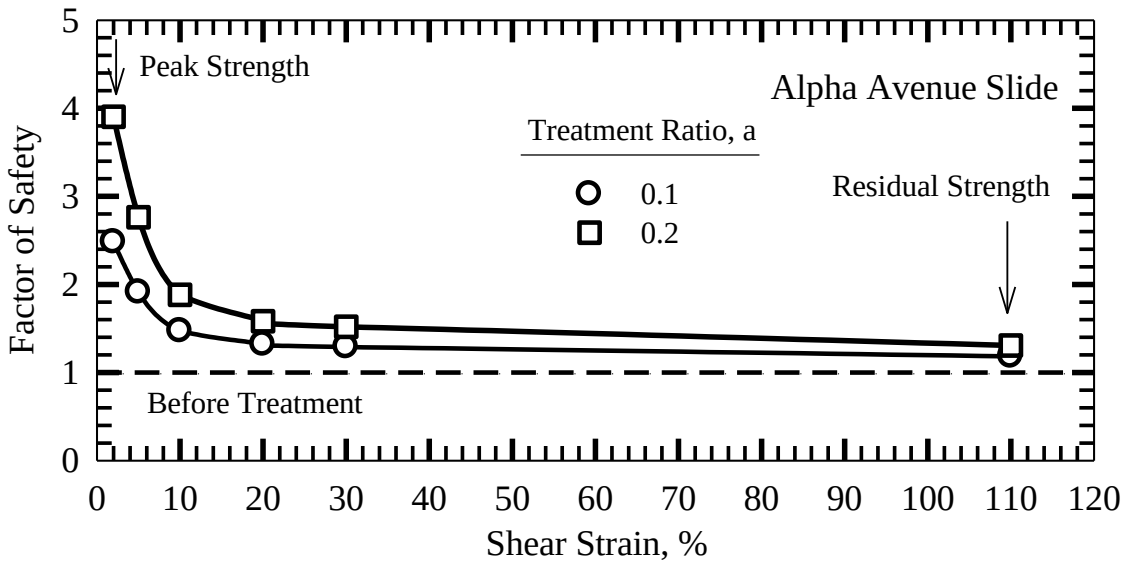

Figure 8.23: Safety factor reduction with shear strain, Alpha Avenue slide

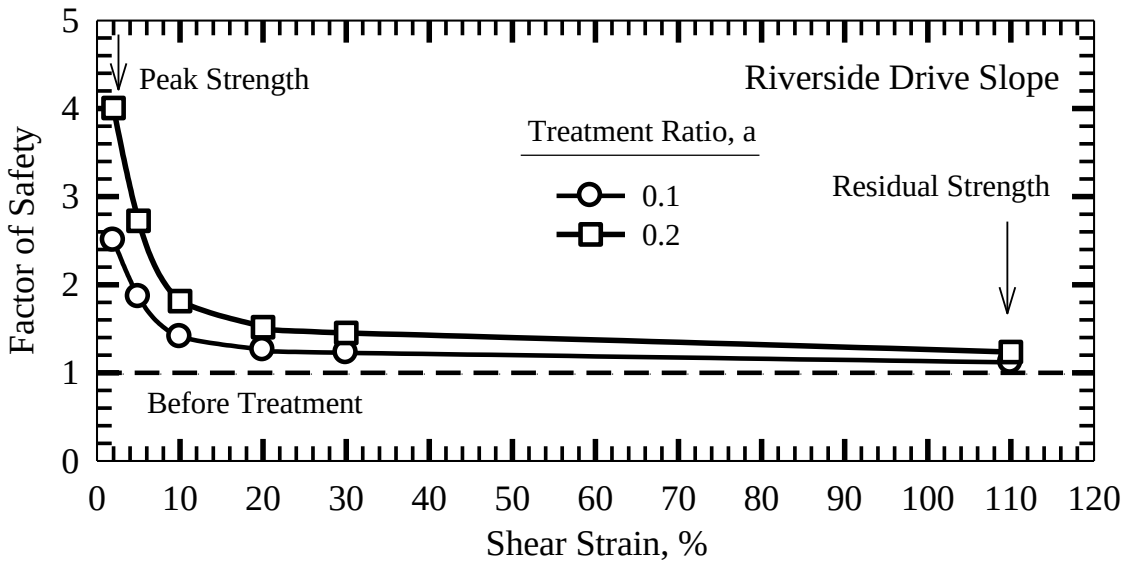

Figure 8.24: Safety factor reduction with shear strain, Riverside slide

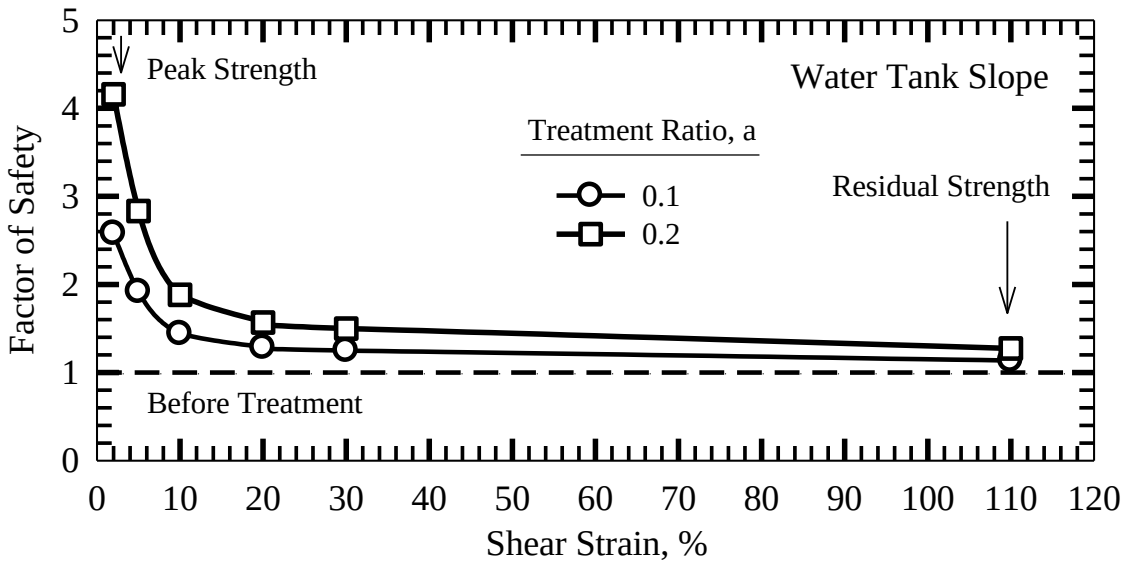

Figure 8.25: Safety factor reduction with shear strain, Water Tank slide

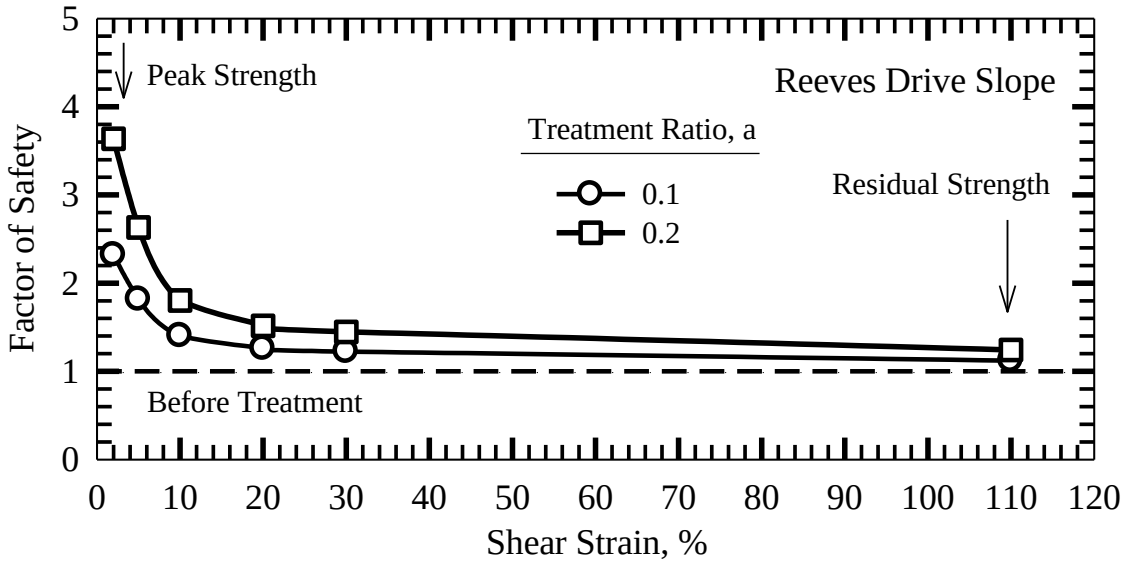

Figure 8.26: Safety factor reduction with shear strain, Reeves Drive slide

8.2.2 CUP O'Hare Reservoir Repair and Rehabilitation

The CUP O'Hare Reservoir is located in Elk Grove Village in northwestern Cook County, Illinois, about two miles northwest of O'Hare International Airport. This facility is one of the three terminal reservoirs of the Tunnel and Reservoir Plan (TARP) system constructed to temporarily store Combined Sewer Overflows (CSO) during storm events, alleviating storm and sanitary sewer backup and flooding in portions of Des Plaines, Mount Prospect and Arlington Heights.

The CUP O'Hare Reservoir was constructed by excavating 80 to 90-ft (24 to 27-m) deep in glacial deposits, including the Chicago clay up to top of bedrock, with general side slopes of 2H:1V and a 15-ft (4.6-m) wide intermediate bench at mid-slope. The height of the slopes varies from 73 ft (22.3 m) at the west to 88 ft (26.8 m) at the east side of the reservoir. The reservoir bottom is approximately 600 ft x 1,000 ft (183 m x 305 m). The reservoir rim elevation is at El. 660 ft (201 m) +/- North American Vertical Datum of 1988 (NAVD 88), the finished elevation of the intermediate bench is at El. 625 ft (191 m)+/-, and the finished elevation of the reservoir bottom varies from El. 587 ft (179 m) +/- at the west to El. 572 ft (174 m) +/- at the east. The design maximum storage water elevation is reported to be at about 23 ft (7 m) below the reservoir rim, El. 637 ft (194 m). The intermediate bench road is paved with RCC. The slopes below the bench road are covered with geotextile sheet drains and a 60-mil (1.5 mm) thick High Density Polyethylene (HDPE) membrane, Figure 8.27. Although the design maximum storage level is above the intermediate bench, only the lower slopes of the reservoir were lined. The sheet drain is connected to a toe drain to minimize the uplift under the geomembrane.

Figure 8.27: Reservoir looking to the northwest corner from the southeast corner

Slope failures below the intermediate bench have been triggered at several locations by high water tables left in the slopes after storage events, Figure 8.28. The sloughs and failures along the lower slopes could be associated with exfiltration of combined sanitary/storm water through the broken liner system or seepage from the pounded water and drainage area around the upper slopes.

Figure 8.28: Note gully under liner at the corner. Heavily vegetated junction between RCC bottom and geomembrane liner.

Figure 8.29 shows the sloughing and severe erosion of slopes above the intermediate bench level. In general, slope areas consist of silty clay with layers of saturated granular material. The instability of the slopes has contributed to the deterioration of the liner and slope drainage system, including the cracking of the RCC along the intermediate bench at El. 625 ft (191 m) +/-. Specifically, the northwestern corner of the reservoir has incurred slope failures causing 2.5 inch-wide cracks in the RCC of the intermediate bench and large ground distortion noted under the HDPE liner, Figures 8.30 and 8.31.

Figure 8.29: Sloughing and severe erosion of slopes above intermediate bench level

Figure 8.30: 1-inch wide crack parallel to slope. Cracks filled with epoxy and vegetation.

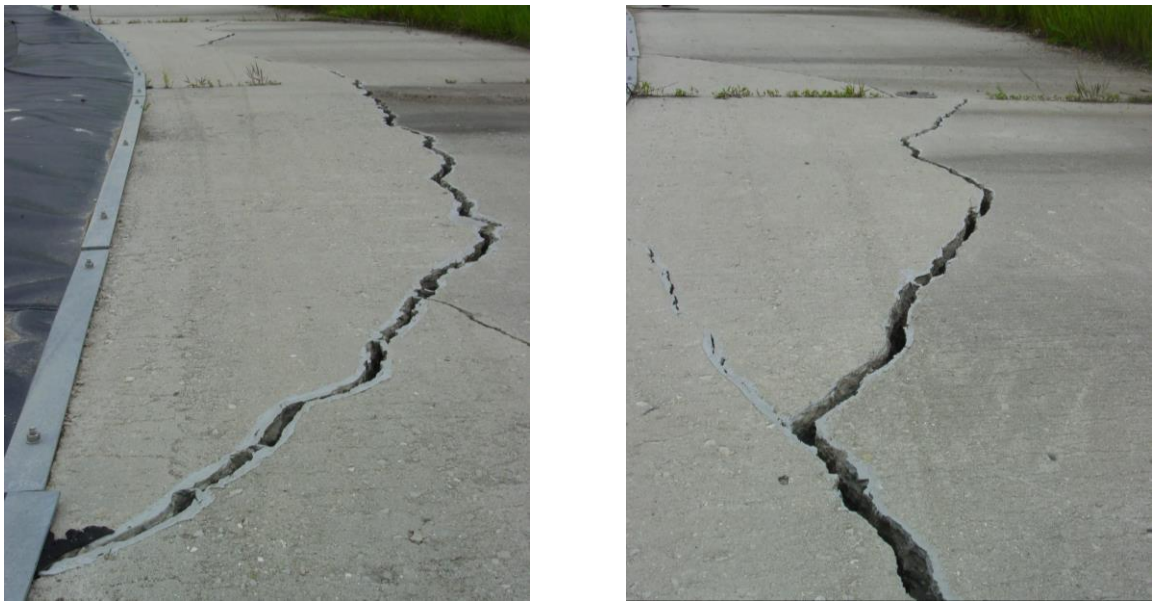

Figure 8.31: Largest crack along the bench. 1- to 2-inch wide crack parallel to slope. This crack has been opening, indicating that the northwest lower slope is of marginal stability.

Slope stability analyses of CUP O'Hare Reservoir were performed at NW cross section to evaluate the current conditions of the reservoir slopes, Figure 8.32. The piezometric water level data collected during dry reservoir periods from the nearest piezometers installed at the reservoir bench and rim were used in the analysis. Transient seepage analyses were performed to estimate the overburden groundwater tables in the reservoir slopes during and after the reservoir dewatering (rapid drawdown). Slope stability analyses were performed for normal (dry reservoir) and rapid drawdown conditions.

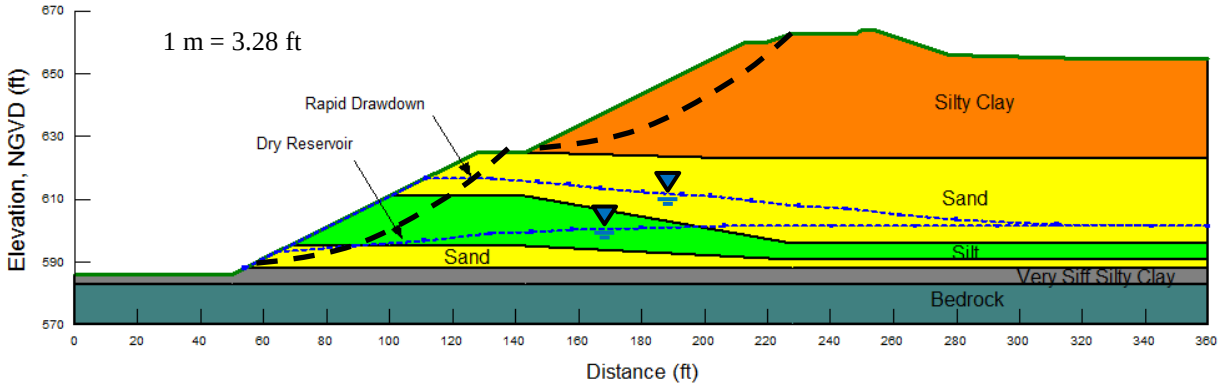

Figure 8.32: Slope stability analysis of CUP O'Hare Reservoir at NW cross section before treatment (curent condition)

Standard Penetration Test (SPT) and laboratory tests performed on the soils were used to estimate the soil parameters for stability analysis. A constant friction angle was used for each of sand, silt and very stiff silty clay, as summarized in Table 8.7.

Table 8.7: Soil properties from the laboratory and in-situ tests

Soil	γ, kN/m^3	ϕ' Degrees	c' kpa
Sand	18.9	33	0
Silt	18.1	30	0
Very Stiff silty clay	22.0	33	10

Lime treatment of Silty Clay (Chicago clay) at upper slopes of the NW corner is proposed for improvement of the upper slopes as well as global stability. In order to increase the stability of the lower slopes at the NW corner, it is proposed to replace 7 ft (2.1 m) of soil perpendicular to the slope with lime treated Chicago clay. Horizontal drains are also suggested to be installed in the slopes to drain the water in case of HDPE liner deficiency.

The curved shear strength envelope of untreated Chicago clay from the laboratory tests was used to evaluate the current condition of the slopes. To assess the stability of the slopes following

lime treatment, the curved peak shear strength envelope of 3% lime treated Chicago clay corresponding to 1 and 4-week curing periods from the laboratory tests were utilized. The shear strength envelopes of untreated and treated Chicago clay used in slope stability analyses are shown in Figure 8.33.

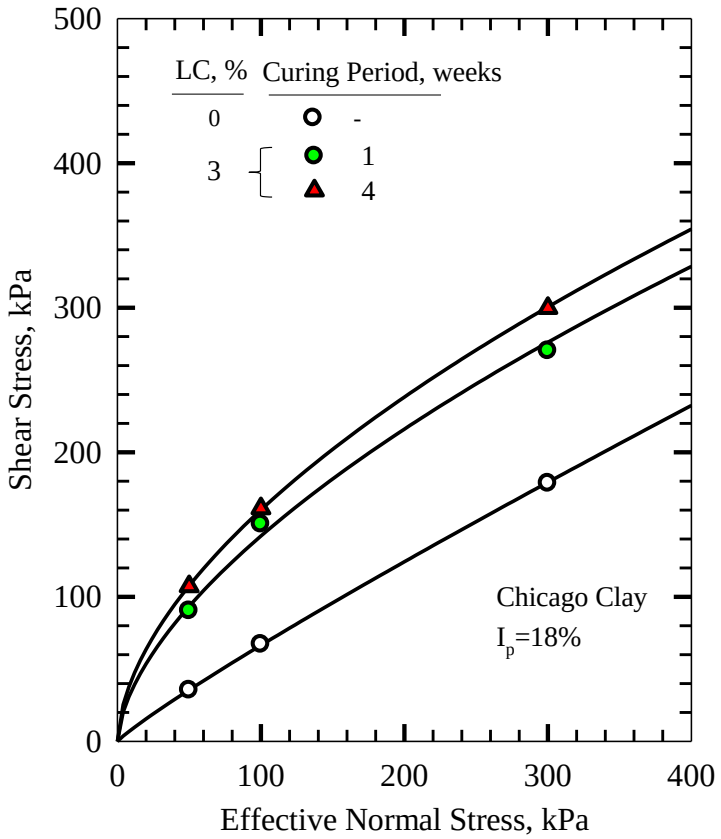

Figure 8.33: Shear strength envelopes of untreated and 3% lime treated Chicago Clay (Peak)

Although horizontal drains as well as drains along the slopes are recommended to be installed to drain the water inside the slopes into the toe drain, the slope stability analysis of slopes in rapid drawdown condition were performed for the worst condition, where the water remains at the surface of the slopes.

The slip surfaces analyzed for the current condition of the lower slope are shown in Figures 8.34 and 8.35 for the rapid drawdown and normal conditions, respectively. The critical surface at the upper slope before treatment is shown in Figure 8.36. The global slip surfaces involving the

current upper and lower slopes are shown in Figures 8.37 and 8.38 for the rapid drawdown and normal conditions, respectively. The computed values of safety factor for the slopes before treatment are listed in Table 8.8. As mentioned earlier, the lower slope has failed in rapid drawdown and upper slope has failed in high water condition. A safety factor of less than 1.00 was calculated for the current condition of the lower slope during rapid drawdown, because the effect of the liner was neglected. There are observed failures and bulged areas under the geomembrane.

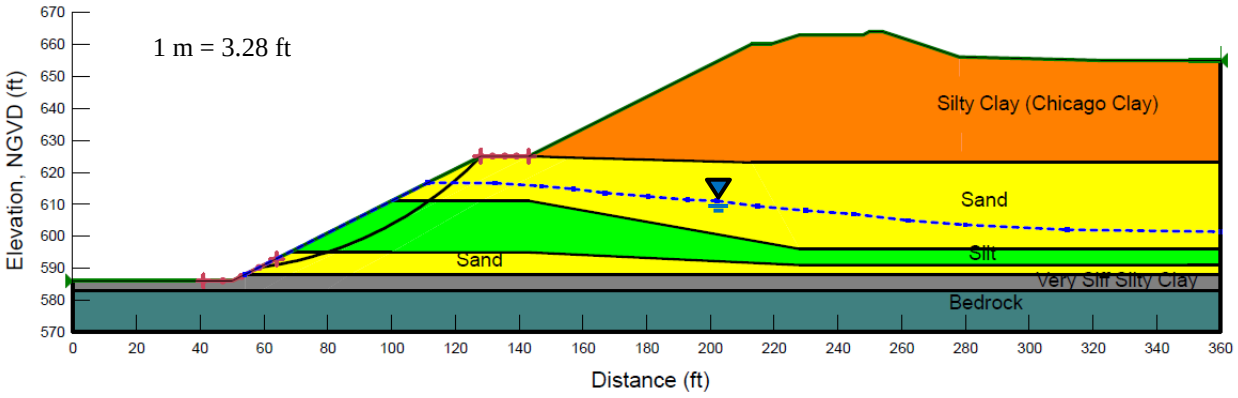

Figure 8.34: Stability analysis of current condition of CUP O'Hare Reservoir, lower slope, rapid drawdown condition

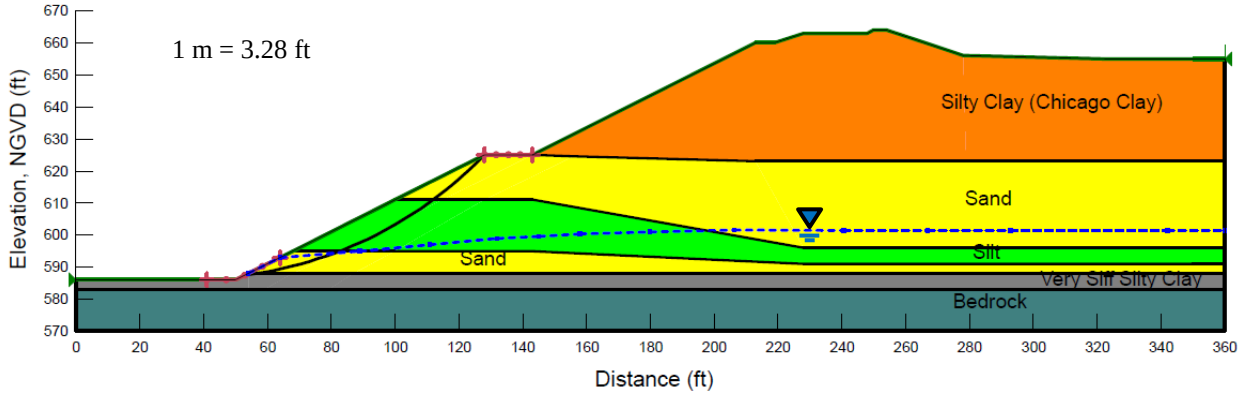

Figure 8.35: Stability analysis of current condition of CUP O'Hare Reservoir, lower slope, Normal condition

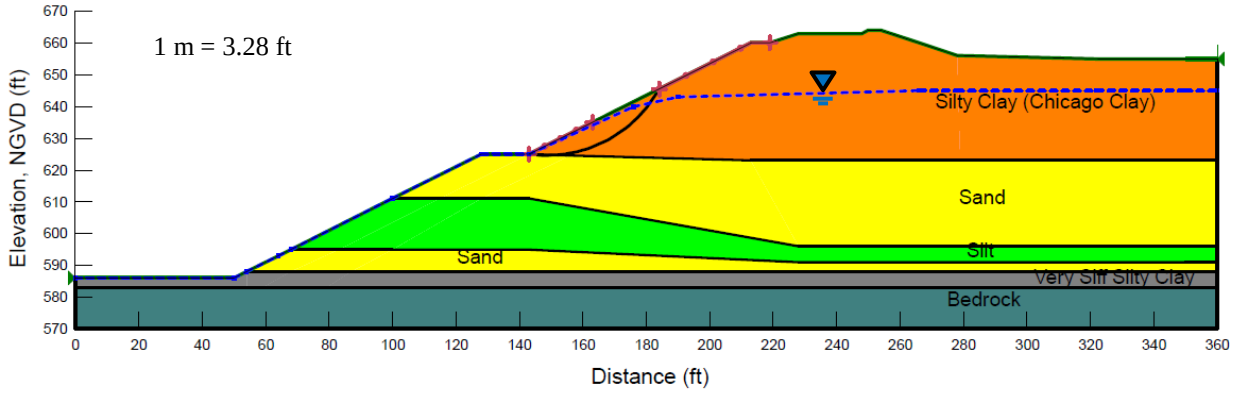

Figure 8.36: Stability analysis of current condition of CUP O'Hare Reservoir, upper slope

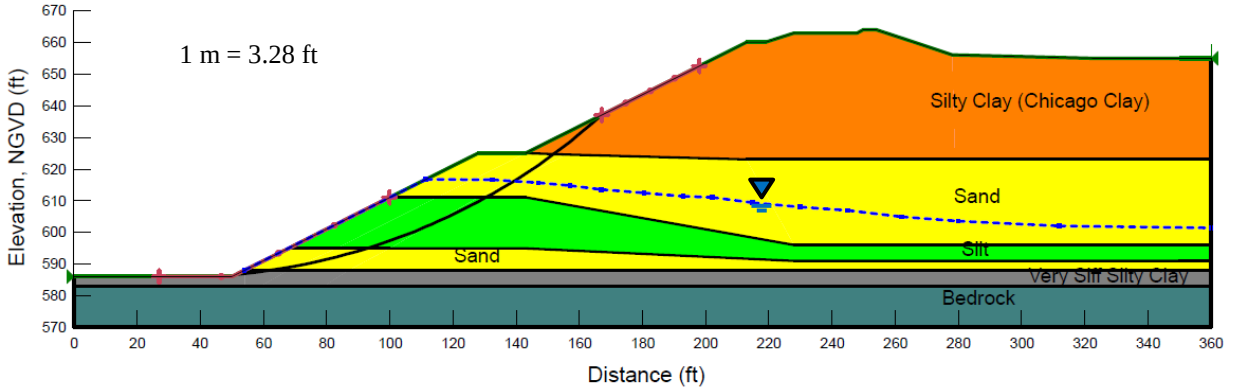

Figure 8.37: Stability analysis of current condition of CUP O'Hare Reservoir, global slip surface, rapid drawdown condition

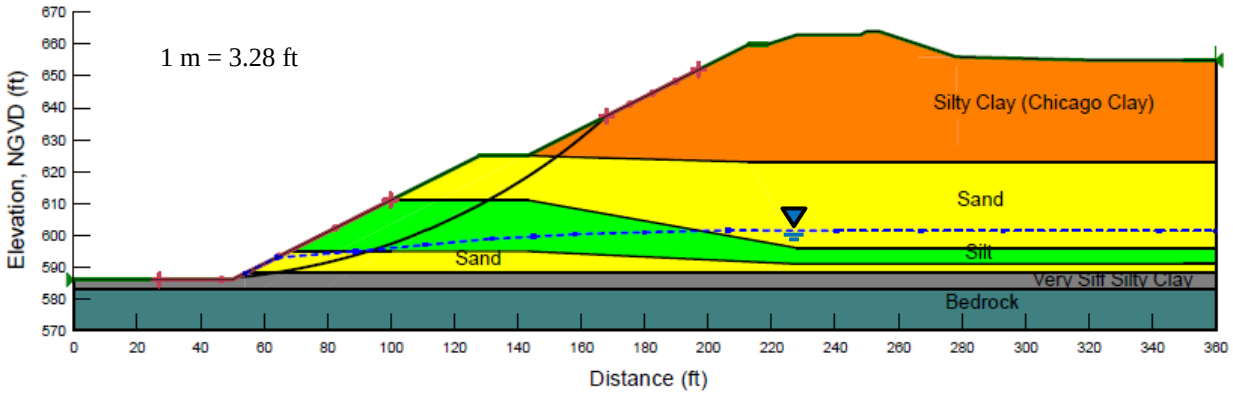

Figure 8.38: Stability analysis of current condition of CUP O'Hare Reservoir, global slip surface, normal condition

The safety factors calculated following treatment of lower and upper slopes with 3% lime for curing periods of 1 and 4 weeks are shown in Table 8.8. It is recommended that 7 ft (2.1 m) of soil on the lower slope, measured perpendicular to the slope, be excavated and replaced with Chicago clay mixed with 3% lime. The 3% lime-clay mix is to be compacted on the lower slope. The upper slopes can be treated with lime-treated columns. The values of calculated factor of safety in Table 8.8 correspond to a 100% lime treatment of the Chicago clay on the lower slope and a 30% lime treatment of the wedge in front of the upper slope. The in-situ soil on the lower slope, i.e. sand and silt, is excavated and lime treated Chicago clay is placed and recompacted. The wedge in front of the upper slope is improved by lime-treated columns.

The values of safety factor in Table 8.8 show that it is possible to improve the stability of CUP O'Hare slopes for both normal and rapid drawdown conditions through lime treatment. The critical slip surfaces following treatment of the slopes with 3% lime are illustrated in Figures 8.39-8.48.

Table 8.8: Safety factors of CUP O'Hare slope for current condition and following 3% lime treatment of Chicago clay

Slope	Condition	Before treatment	After treatment	
			Curing time, weeks	
			1	4
Lower Bench	Rapid drawdown	0.52	1.15	1.22
	Normal	1.21	1.66	1.75
Upper Bench	High water	1.01	1.22	1.25
Global	Rapid drawdown	0.89	1.22	1.29
	Normal	1.46	1.80	1.89

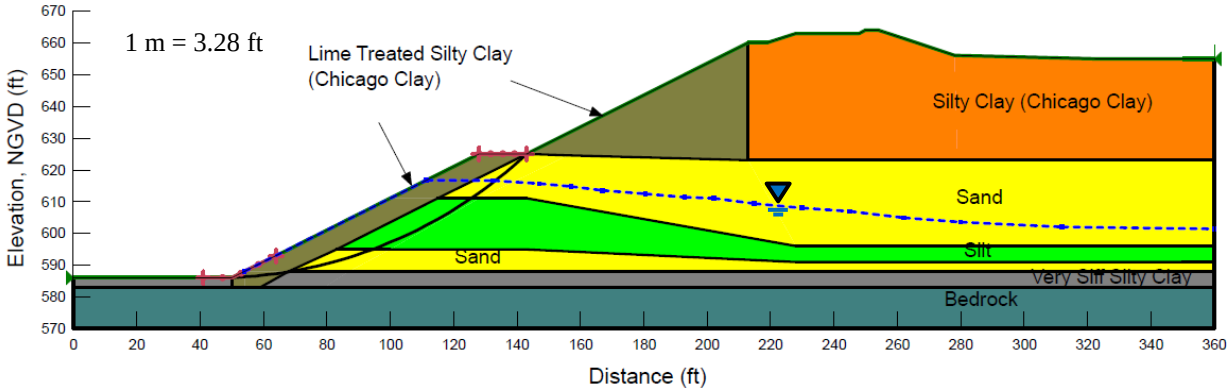

Figure 8.39: Stability analysis of of CUP O'Hare Reservoir slope treated with 3% lime, cured for 1 week; lower slope subjected to rapid drawdown condition

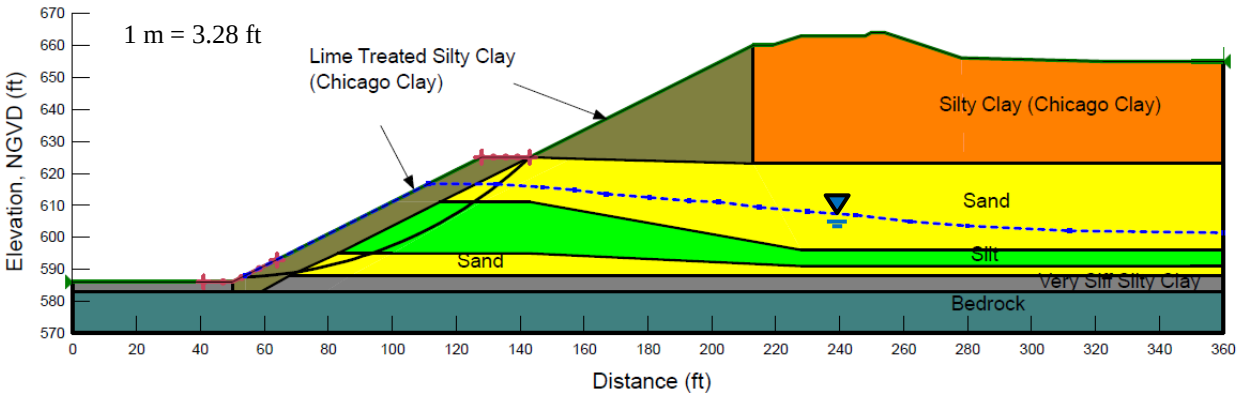

Figure 8.40: Stability analysis of of CUP O'Hare Reservoir slope treated with 3% lime, cured for 4 weeks; lower slope subjected to rapid drawdown condition

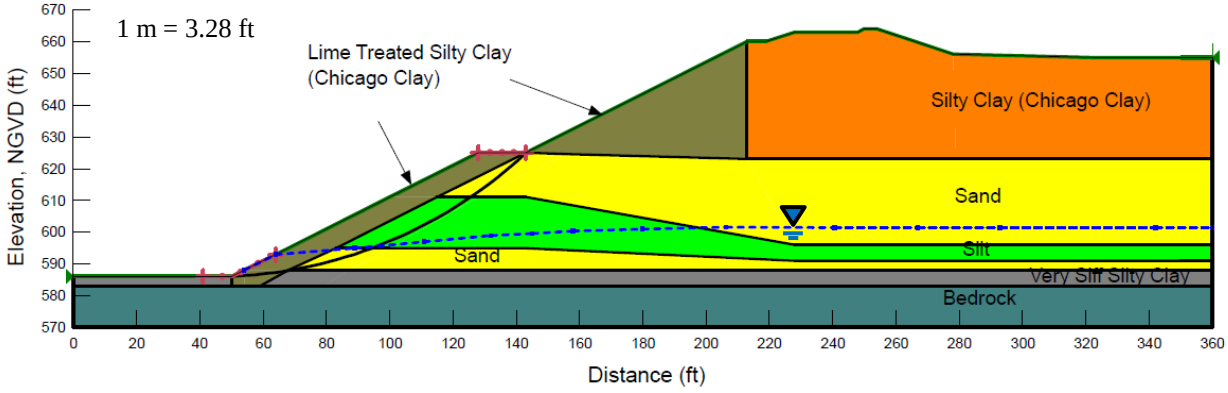

Figure 8.41: Stability analysis of of CUP O'Hare Reservoir slope treated with 3% lime, cured for 1 week; lower slope, normal condition

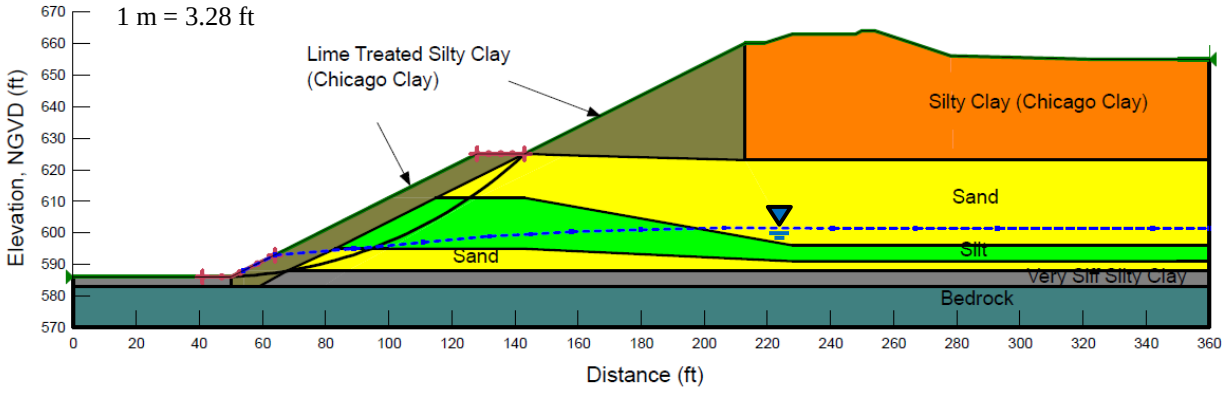

Figure 8.42: Stability analysis of of CUP O'Hare Reservoir slope treated with 3% lime, cured for 4 weeks; lower slope, normal condition

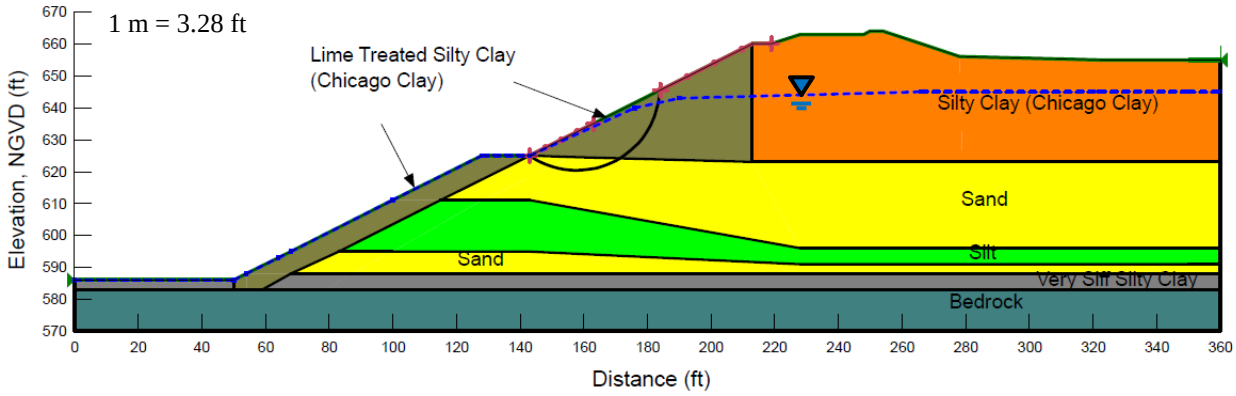

Figure 8.43: Stability analysis of of CUP O'Hare Reservoir slope treated with 3% lime, cured for 1 week; upper slope, high water condition

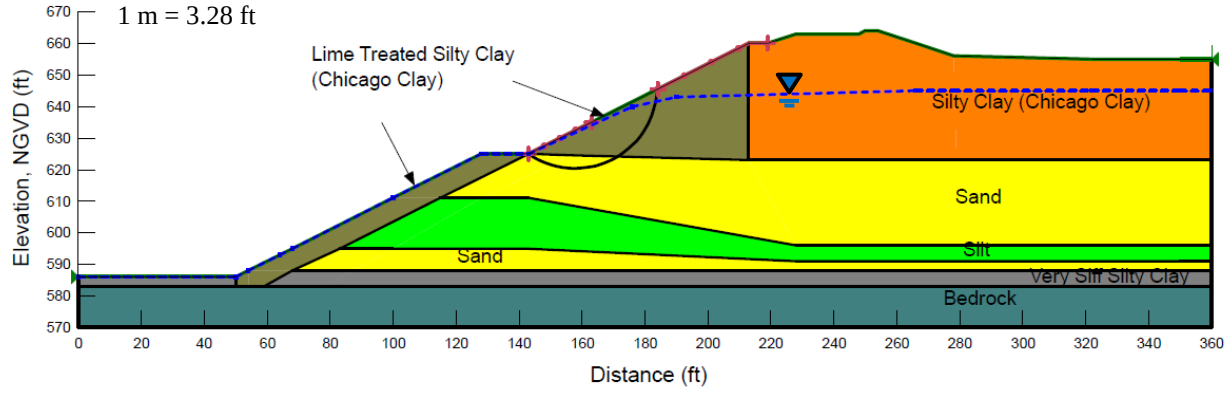

Figure 8.44: Stability analysis of of CUP O'Hare Reservoir slope treated with 3% lime, cured for 4 weeks; upper slope, high water condition

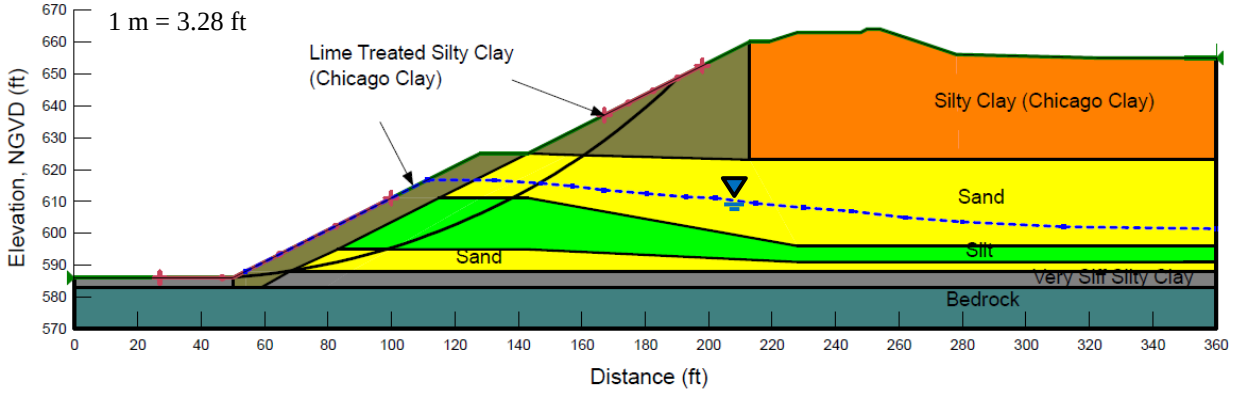

Figure 8.45: Stability analysis of of CUP O'Hare Reservoir slope treated with 3% lime, cured for 1 week; global slip surface subjected to rapid drawdown condition

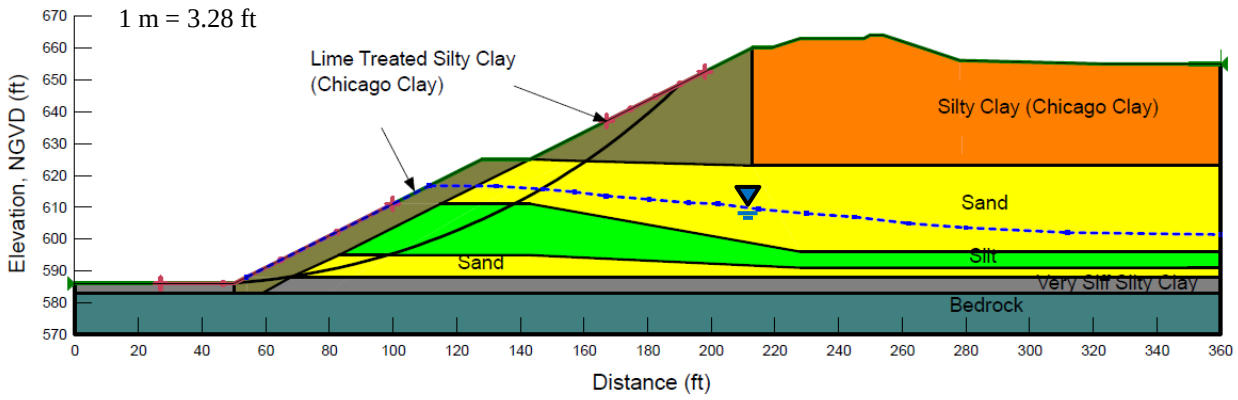

Figure 8.46: Stability analysis of of CUP O'Hare Reservoir slope treated with 3% lime, cured for 4 weeks; global slip surface subjected to rapid drawdown condition

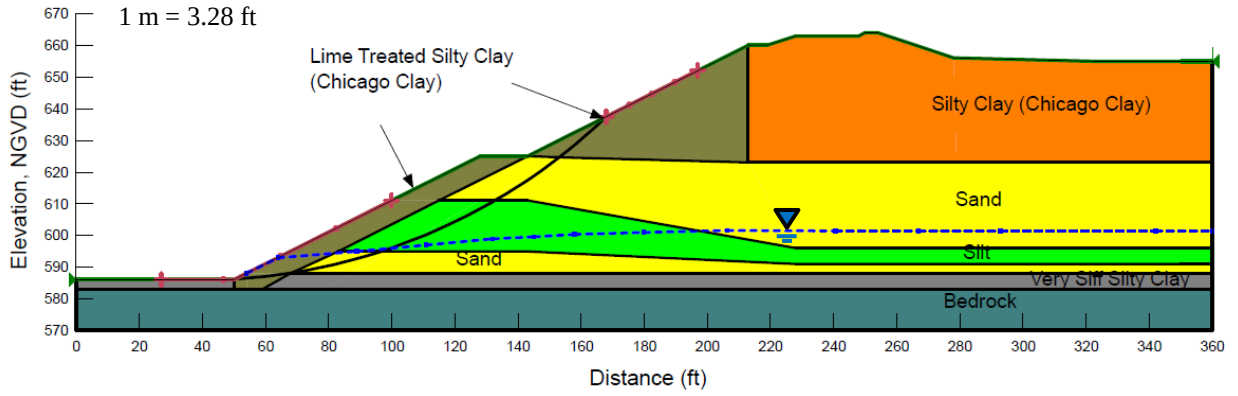

Figure 8.47: Stability analysis of of CUP O'Hare Reservoir slope treated with 3% lime, cured for 1 week; global slip surface, normal condition

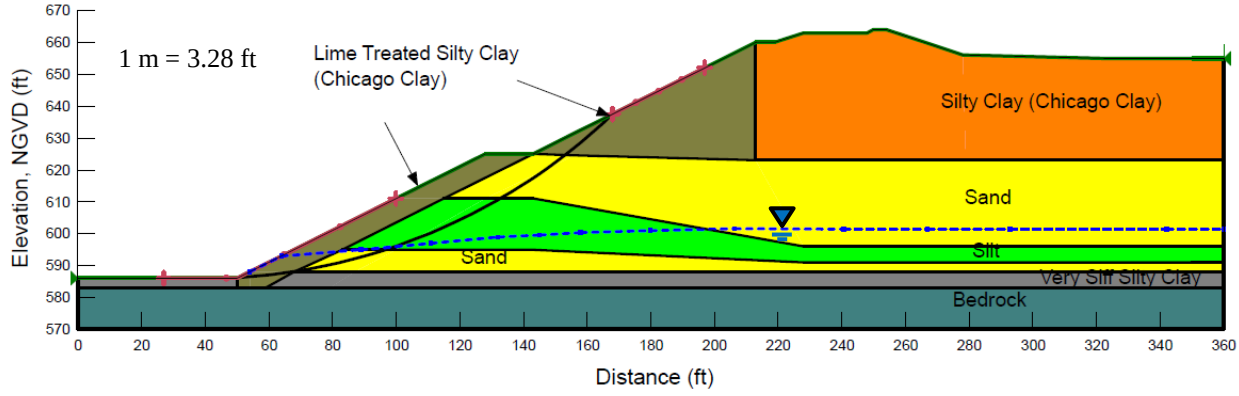

Figure 8.48: Stability analysis of of CUP O'Hare Reservoir slope treated with 3% lime, cured for 4 weeks; global slip surface, normal condition

8.2.3 Channel and Detention Basin Slope Stability in Harris County Flood Control District (HCFCD)

There are 22 major watersheds in Harris County draining into Galveston Bay, as shown in Figure 8.49 (HCFCD, 2015). Harris County's population is 4.5 million; the drainage and flood control infrastructure of Harris County include more than 1,500 channels with a total length of approximately 2,500 miles. The HCFCD spends $7-8M each year to maintain channel slopes.

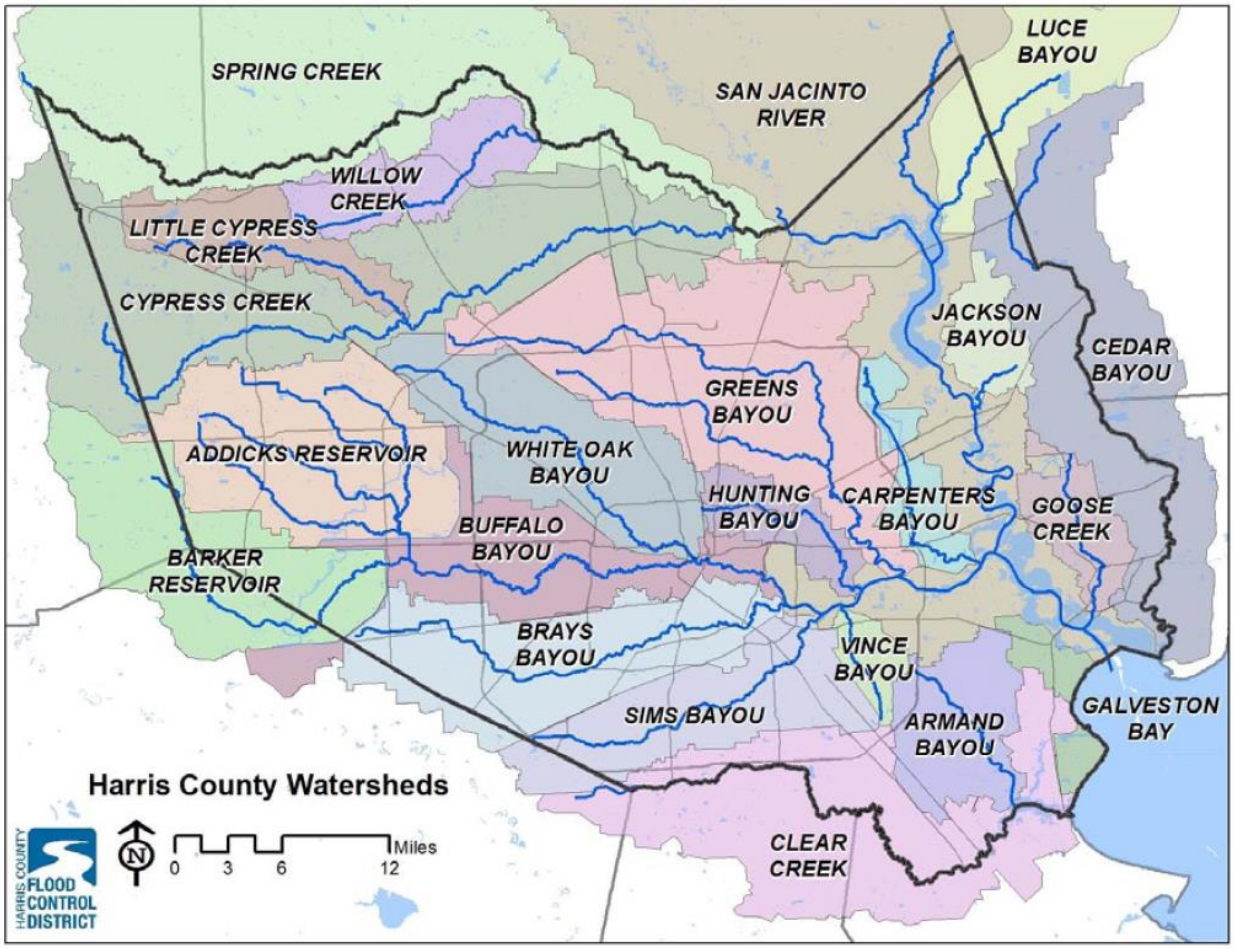

Figure 8.49: Harris County watersheds (HCFCD, 2015)

Failures observed in the slopes of Harris County Flood Control District include shallow rotational, deep rotational, shallow slough and block slip surfaces, as shown in Figure 8.50. Examples of deep and shallow rotational failures in the field are shown in Figures 8.51 and 8.52, respectively.

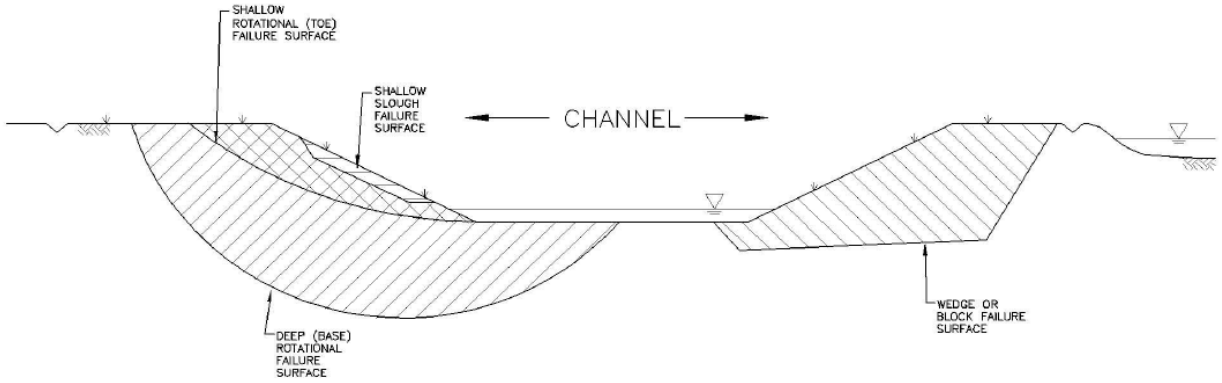

Figure 8.50: Types of HCFCD slope failures (Langston, 2005)

Figure 8.51: Deep failue of HCFCD slopes (Langston, 2005)

Figure 8.52: Shallow failue of HCFCD slopes (Langston, 2005)

Tension cracks formed parallel to the top of high steep bank due to wetting and drying of clays and erosion of toe of the slope, lead to bank failure, as shown in Figures 8.53 and 8.54 for Buffalo Bayou. These failures cause the slopes to become steeper. At some locations, when slope becomes steep due to toe erosion, a large block of soil becomes unstable and falls into the stream (HCFCD, 2015).

Sudden and intense storm events cause water to rise quickly, saturating the clays. When water level in the streams drops, the slope often fails in rapid drawdown. The streams with their flow controlled by reservoir (detention basin) operations, such as Buffalo Bayou, are prone to instability due to frequent rapid drawdown events. Water leakage from the pools and irrigation systems at the top of slopes also contribute to saturation of the clay and lead to slope failure.

Figure 8.53: Slope failure in Buffalo Bayou (HCFCD, 2015)

Figure 8.54: Streambank failure in Buffalo Bayou (HCFCD, 2015)

One of the main sources of slope instability in HCFCD is the Beaumont clay. The current conditions of slope failures at Greens Bayou, Berry Bayou, and Carpenters Bayou were analyzed and effect of lime treatment on stability of the slopes was investigated. Three channel slope failures at Greens Bayou of HCFCD (i.e. Middle slope, North slope and South slope) were analyzed. The existing shear strength (before treatment) was back-calculated for the slope failures, representing the shear strength mobilized in the field. Subsurface conditions, as well as the location of the slip surface were defined by means of borings, deep trenches, and sampling for laboratory testing. For example, 35-foot deep borings, 10-foot deep trenches, and sampling for laboratory testing were utilized to explore the subsurface conditions at Berry Bayou.

The current condition of failed slopes was examined, including slope history, subsurface condition, slope geometry, groundwater condition, and observed slip surface. For the slope geometries commonly encountered in channels and basins of HCFCD and for the FCD clays with overconsolidation ratios in the range of 4 to 6, short term stability is not expected to be a factor.

The clays involved in the slope failures in HCFCD include lean and fat clays with plasticity index, I_p, of 28% and 46%, respectively. The mobilized strength along the slip surface in the lean Clay in Greens Bayou (Figures 8.55-8.57) is assumed to be equal to the untreated fully softened strength. The back-calculated mobilized shear strength for a relatively deep slip surface in the fat clay, with maximum effective normal stress of 52 to 72 kPa, is near the untreated residual shear strength, $\tan[\phi'(mob)]_s / \tan[\phi'_r]_s$=0.945-1.310. For Berry Bayou failure (Figure 8.58) and Carpenter failure (Figure 8.59), the entire slip surface was determined to be at the fully softened condition (untreated). The slopes have failed and it was assumed that the failure took place during a rapid drawdown of channel or basin water level from a fully submerged flood water condition.

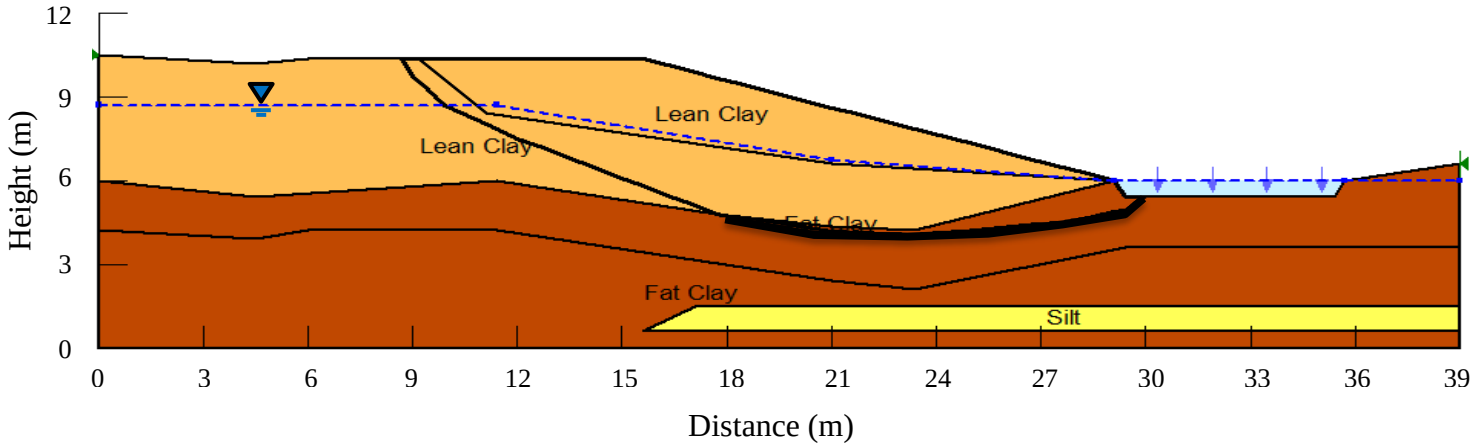

Figure 8.55: Greens Bayou, Middle slope failure

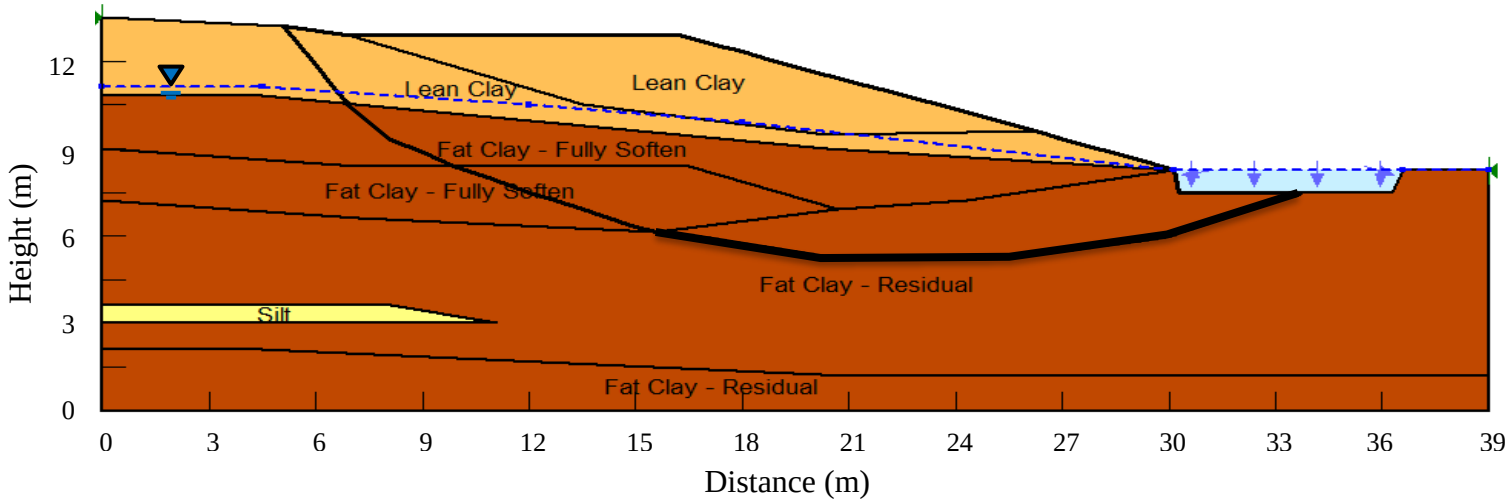

Figure 8.56: Greens Bayou, North slope failure

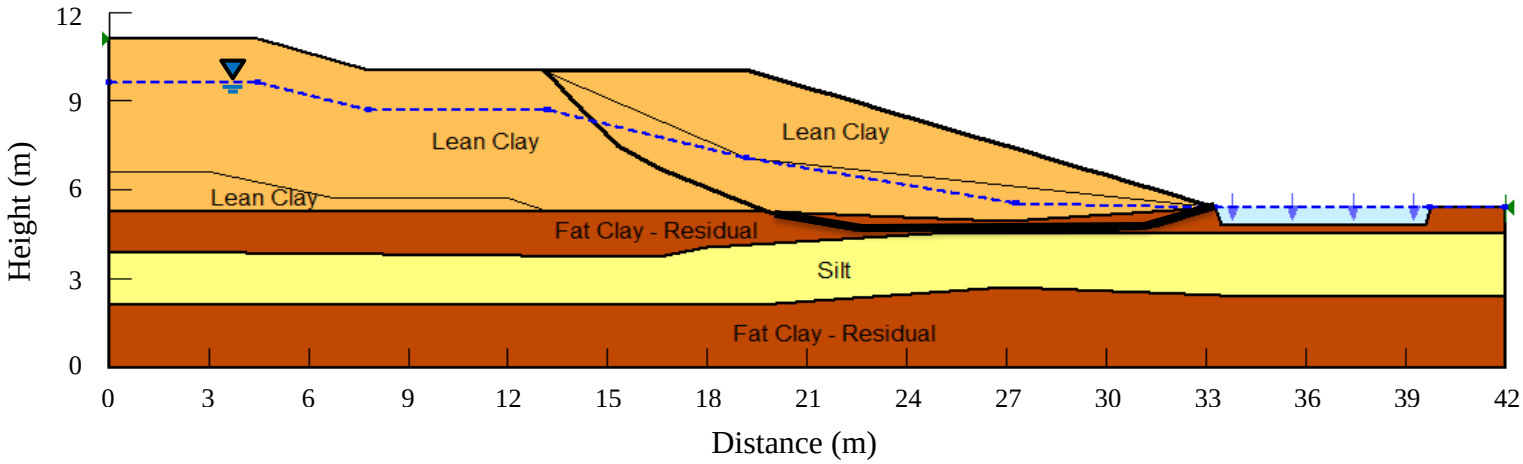

Figure 8.57: Greens Bayou, south Slope

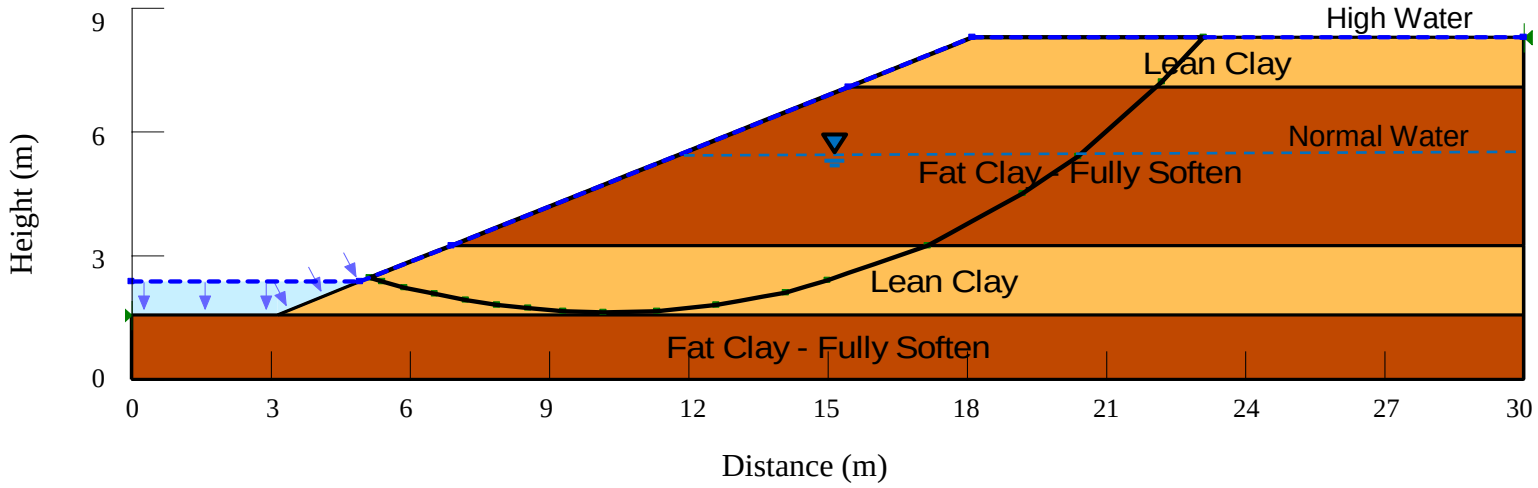

Figure 8.58: Berry Bayou failure

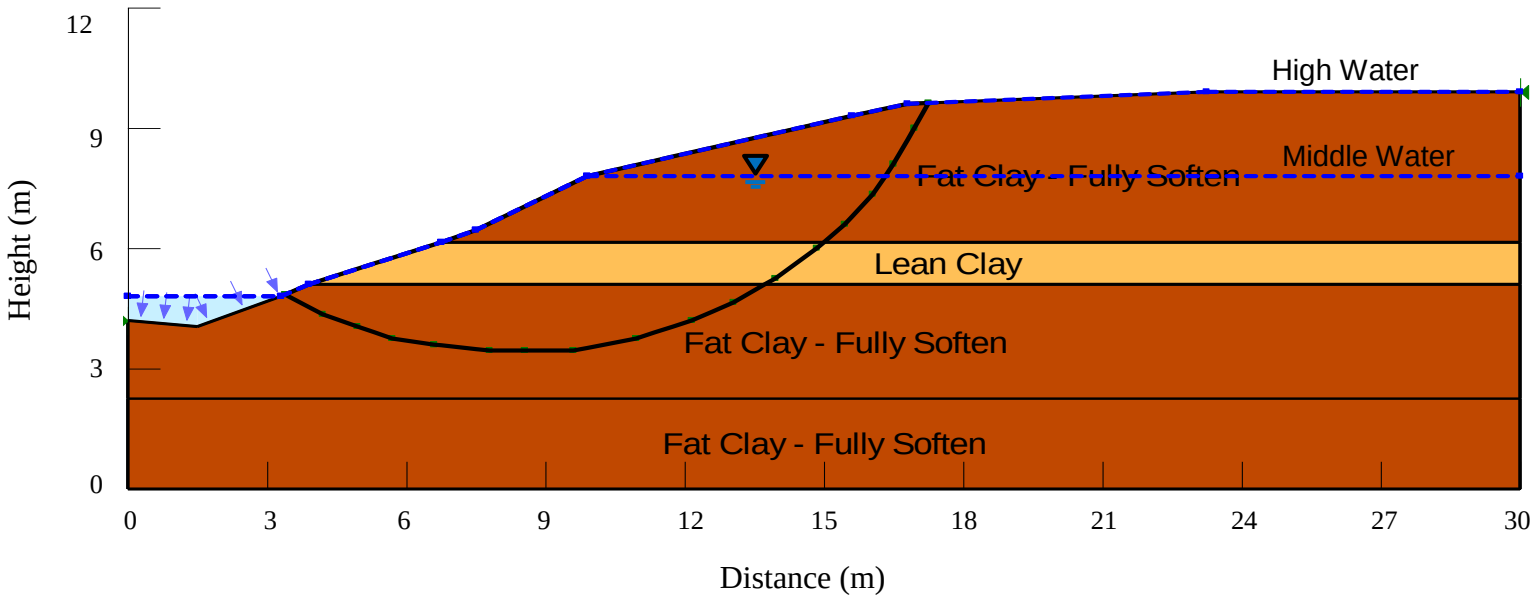

Figure 8.59: Carpenters Bayou failure

The current condition of slope failures were analyzed using the untreated secant fully softened and secant residual friction angles shown in Figure 8.60, which correspond to plasticity indices of 28 and 46 for lean and fat clays, respectively (from empirical correlations in Mesri and Shahien, 2003). The bold line on Figures 8.56-8.60 shows the segment of the shear surface which is in residual condition.

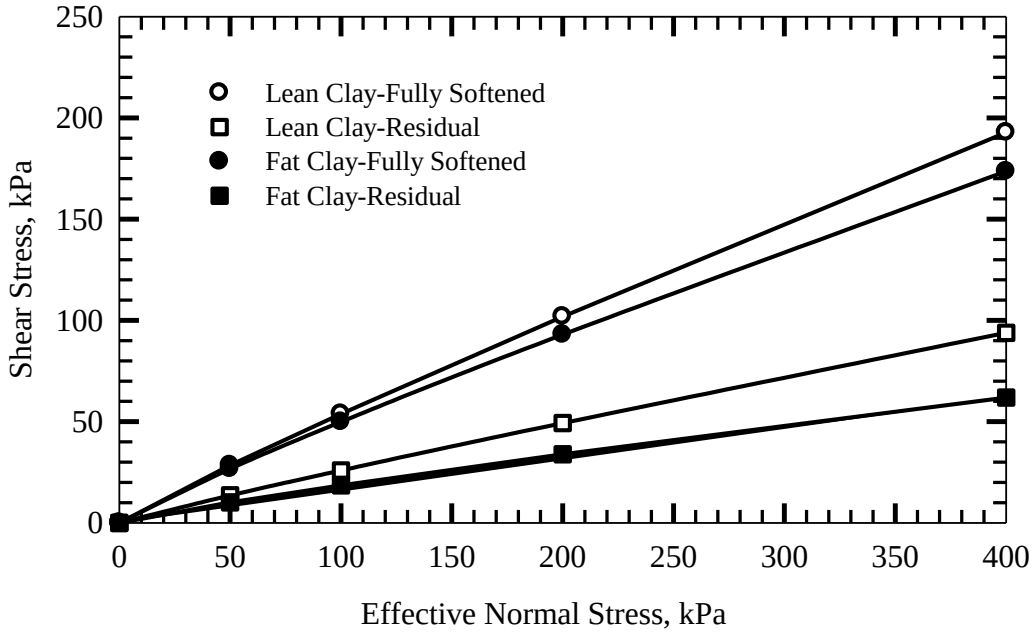

Figure 8.60: Shear strength envelopes of lean and fat clays

Table 8.9 shows the percentage of the slip surface passing through lean and fat clays. The treatment is only considered for the fat clay and no treatment was considered in the slip surface passing through lean clay. The treatment ratio is calculated as:

$$\text{Treatment ratio (a)} = \frac{\text{Treated area}}{\text{Total area of sip surface passing through fat clay}}$$

Therefore, the percentage of the slip surface passing through fat clay is a factor of significance in the stability of the slopes following lime treatment. Among the Harris County slopes analyzed herein, Barry Bayou slope has the least length percentage passing through fat clay, i.e. 31%.

Table 8.9: Percentage of slip surface passing through lean and fat clays in Harris County slopes

Slope	Length of slip surface in a clay / total length of slip surface, %	
	Lean	Fat
Greens Bayou, Middle slope	47	53
Greens Bayou, North slope	10	90
Greens Bayou, South slope	38	62
Berry Bayou	69	31
Carpenters Bayou	10	90

A lime content of 7% provides the highest improvement in the peak shear strength of Beaumont clay, as shown in Figure 4.68. Because there are more test data available for 10% than 7% lime treated Beaumont clay, shear strength envelopes have been determined more accurately for various curing periods. The shear strength of 7% and 10% lime treated Beaumont clay are reasonably in the same range. Hence the peak shear strength envelopes of fat (Beaumont) clay for a lime content of 10% and curing periods of 7, 14 and 35 day , as shown in Figure 8.61, are used in lieu of those for a lime content of 7% to analyze the slopes following treatment.

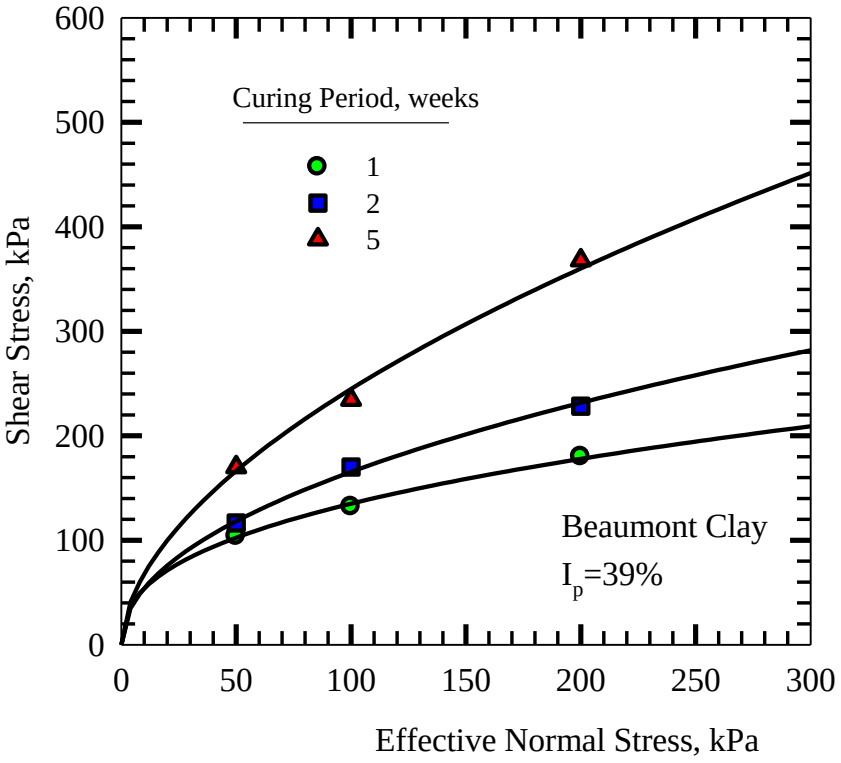

Figure 8.61: Peak shear strength envelopes of 10% (in lieu of 7%) lime treated Beaumont clay

The current factor of safety of Harris County slopes for rapid drawdown and long-term conditions are shown in Table 8.10. The slopes have failed in rapid drawdown condition following high water. The safety factor of the slopes was calculated following lime treatment of ten percent (a=0.1) and twenty percent (a=0.2) of the slip surface passing through fat clay, as shown in Tables 8.10 and 8.11, respectively. The HDD method shown in Figure 8.9 can be employed for treatment of the slopes.

Because significant part of the slip surface at Berry Bayou passes through lean clay (i.e. 69%), a higher treatment ratio of fifty percent (a=0.5) was also considered for this slope, as shown in Table 8.12.

The safety factor of the slopes was calculated for the peak and post-peak shear strengths of treated fat clay. A significant increase in the safety factor is observed following lime treatment. The safety factor increases with curing time. In addition, the Greens Bayou slopes were analyzed for the residual condition in fat clay following lime treatment, as shown in Tables 8.10 and 8.11 for treatment ratios of ten and twenty percent, respectively.

For the Middle slope at Greens Bayou, 7% lime treatment of ten percent of the slip surface passing through fat clay increased the factor of safety from 1.00 to 1.36 in rapid drawdown condition and from 1.21 to 1.63 in normal condition after one week of curing using the peak strength. The safety factors increase to 1.40 and 1.61 in rapid drawdown condition and to 1.69 and 1.94 in normal condition after 2 and 5 weeks of curing, respectively. For ten percent treatment ratio, the safety factor is in the range of 1.36-1.61 in rapid drawdown and 1.63-1.94 in normal conditions. For twenty percent treatment ratio, the safety factor increases to the range of 1.71-2.23 and 2.05-2.66 in rapid drawdown and normal conditions, respectively. The safety factor of the Middle slope was calculated 1.04 for rapid drawdown and 1.29 for normal conditions using treated residual strength following ten percent treatment. The safety factors increase to 1.08 and 1.37 for rapid drawdown and normal condition, respectively, as treatment ratio increases to twenty percent.

Table 8.10: Safety factors of Green Bayou slopes following treatment of ten percent of slip surface (a=0.1) with 7% lime

Slope	Water condition	Before treatment	After treatment			
			Peak strength Curing time, weeks			Residual strength
			1	2	5	
Greens Bayou Middle slope	High water	1.00	1.36	1.40	1.61	1.04
	Normal water	1.21	1.63	1.69	1.94	1.29
Greens Bayou North slope	High water	1.00	1.53	1.60	1.93	1.06
	Normal water	1.23	1.82	1.93	2.33	1.32
Greens Bayou South slope	High water	1.00	1.42	1.46	1.70	1.04
	Normal water	1.27	1.80	1.88	2.19	1.38
Berry Bayou	High water	1.00	1.07	1.07	1.09	-
	Normal water	1.30	1.42	1.44	1.50	-
Carpenters Bayou	High water	1.00	1.43	1.48	1.73	-
	Normal water	1.25	1.72	1.77	2.05	-

Table 8.11: Safety factors of Harris County slopes following treatment of twenty percent of slip surface (a=0.2) with 7% lime

Slope	Water condition	Before treatment	After treatment			
			Peak strength Curing time, weeks			Residual strength
			1	2	5	
Greens Bayou Middle slope	High water	1.00	1.71	1.81	2.23	1.08
	Normal water	1.21	2.05	2.17	2.66	1.37
Greens Bayou North slope	High water	1.00	2.05	2.21	2.86	1.12
	Normal water	1.23	2.42	2.64	3.43	1.41
Greens Bayou South slope	High water	1.00	1.84	1.93	2.40	1.08
	Normal water	1.27	2.32	2.48	3.10	1.48
Berry Bayou	High water	1.00	1.13	1.13	1.19	-
	Normal water	1.30	1.54	1.58	1.70	-
Carpenters Bayou	High water	1.00	1.86	1.95	2.46	-
	Normal water	1.25	2.18	2.29	2.86	-

Table 8.12: Safety factors of Berry Bayou slope, Harris County following treatment of fifty percent of slip surface (a=0.5) with 7% lime

Slope	Water condition	Before treatment	After treatment			
			Peak strength Curing time, weeks			Residual strength
			1	2	5	
Berry Bayou	High water	1.00	1.33	1.33	1.47	-
	Normal water	1.30	1.91	1.99	2.30	-

For the North slope at Greens Bayou, the safety factor increases from 1.00 to 1.53 for rapid drawdown and from 1.23 to 1.82 for normal condition following ten percent treatment using the peak strength after one week of curing. For ten percent treatment, the safety factor of the treated slope in rapid drawdown increases to 1.60 and 1.93 as curing time increases to 2 and 5 weeks, respectively. These safety factors are 2.21 and 2.86 for twenty percent treatment. The safety factors of the treated slope in residual condition are 1.06 and 1.12 in rapid drawdown condition for ten and twenty percent treatment ratios, respectively. The safety factors in normal condition are 1.32 for ten percent and 1.41 for twenty percent treatment ratios using residual strength.

For the South slope at Green Bayou, ten percent treatment ratio causes the safety factor to increase from 1.00 to 1.42 and from 1.27 to 1.80 after one week of curing using the peak strength. The safety factor increases to 1.70 and 2.19 for rapid drawdown and normal conditions, respectively, as curing time increases to 5 weeks. For twenty percent treatment ratio, safety factors increase to 2.40 for rapid drawdown and 3.10 for normal condition after 5 weeks of curing. The safety factors of the treated slope are 1.38 and 1.48 at residual condition for normal condition following ten and twenty percent treatment ratios, respectively.

The safety factor of the Berry Bayou slope was calculated for lime treatment of ten, twenty and fifty percent of the slip surface passing through fat clay. Only 31 percent of the slip surface passes through fat clay in Berry Bayou slope. Rapid drawdown and normal conditions were analyzed to evaluate the current condition of the slope. Safety factors of 1.00 and 1.30 were calculated for rapid drawdown and normal conditions, respectively. The back-calculated shear strength mobilized along the slip surface was determined to be at the untreated fully softened condition for both lean and fat clays. Lime treatment increases the safety factor for rapid drawdown condition after 5 weeks of curing from 1.00 to 1.09, 1.19 and 1.47 for 10, 20 and 50% treatment ratios, respectively. At normal condition, the safety factor increase from 1.30 to 1.50, 1.70 and 2.30 for 10, 20 and 50% of treatment ratios, respectively. For fifty percent treatment, the safety factor in normal condition increases from 1.91 to 2.30 as the curing time increases from 1 to 5 weeks.

The safety factor of the Carpenters Bayou slope was calculated for lime treatment ratios of ten and twenty percent in rapid drawdown and normal conditions. The back-calculated shear

strength mobilized along the slip surface in both lean and fat clays was determined to be at fully softened condition for the untreated slope. Safety factors of 1.00 in rapid drawdown and 1.25 in normal condition calculated for the untreated slope increase to 1.43 and 1.72, respectively, following ten percent treatment after 1 week of curing. These safety factors were calculated 1.86 and 2.18, respectively, for twenty percent treatment. As curing time increases from 1 to 5 weeks, the safety factor of twenty percent lime treated slopes increase to 2.46 and 2.86 for rapid drawdown and normal conditions, respectively.

The safety factors of the slopes were also calculated for the post-peak shear strength conditions, as shown in Figure 8.62 for shear strains in the range of 5-30%. The safety factors calculated for the post-peak shear strength are shown in Tables 8.13 and 8.14. In addition to ten and twenty percent treatment ratios, the safety factor of treated Berry Bayou slope was calculated for fifty percent treatment ratio, as shown in Table 8.15, because only 31% of the total length of the slip surface passes through fat clay.

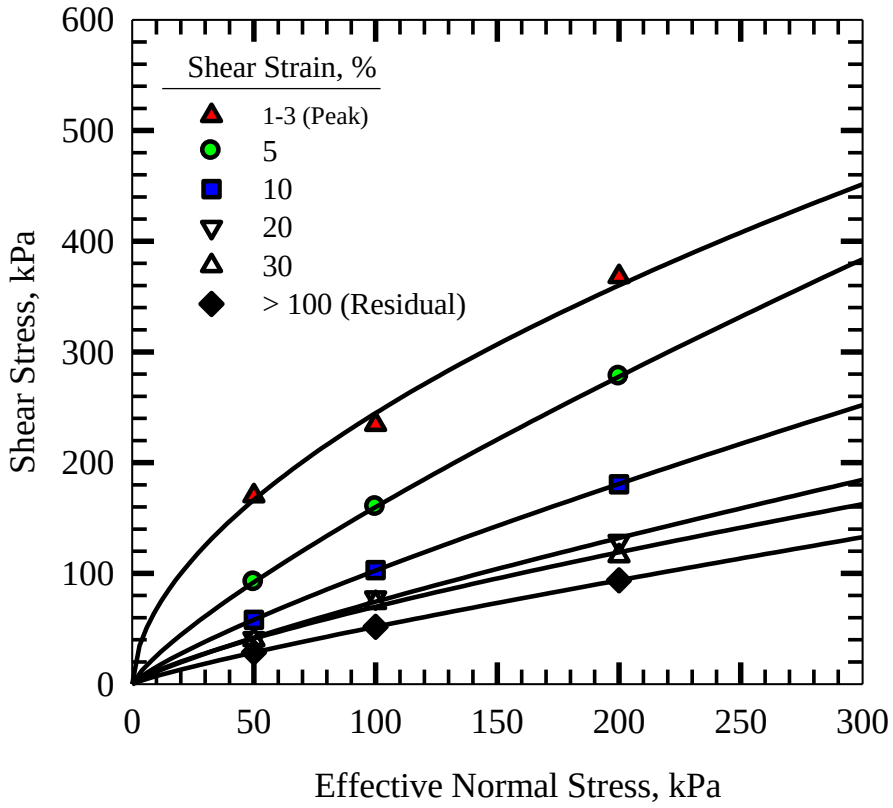

Figure 8.62: Peak, post-peak and residual shear strength envelopes of 10% (in lieu of 7%) lime treated Beaumont clay, cured for 35 days

Table 8.13: Safety factors of Harris County slopes following treatment of ten percent of slip surface (a=0.1) with 7% lime, cured for 35 days using post-peak shear strength

Slope	Water condition	Shear strain, %			
		5	10	20	30
Greens Bayou Middle slope	High water	1.26	1.14	1.08	1.08
	Normal water	1.56	1.42	1.35	1.35
Greens Bayou North slope	High water	1.41	1.22	1.13	1.13
	Normal water	1.78	1.53	1.42	1.41
Greens Bayou South slope	High water	1.28	1.15	1.09	1.09
	Normal water	1.72	1.54	1.45	1.44
Berry Bayou	High water	1.03	1.01	1.00	1.00
	Normal water	1.39	1.34	1.32	1.32
Carpenters Bayou	High water	1.27	1.14	1.07	1.07
	Normal water	1.55	1.40	1.32	1.33

Table 8.14: Safety factors of Harris County slopes following treatment of twenty percent of slip surface (a=0.2) with 7% lime, cured for 35 days using post-peak shear strength

Slope	Water condition	Shear strain, %			
		5	10	20	30
Greens Bayou Middle slope	High water	1.52	1.28	1.17	1.17
	Normal water	1.92	1.62	1.49	1.48
Greens Bayou North slope	High water	1.83	1.45	1.27	1.26
	Normal water	2.32	1.84	1.61	1.59
Greens Bayou South slope	High water	1.57	1.31	1.18	1.19
	Normal water	2.17	1.80	1.63	1.62
Berry Bayou	High water	1.05	1.02	1.00	1.00
	Normal water	1.47	1.38	1.34	1.34
Carpenters Bayou	High water	1.55	1.27	1.14	1.15
	Normal water	1.85	1.54	1.40	1.40

Table 8.15: Safety factors of Berry Bayou slope, Harris County following treatment of fifty percent of slip surface (a=0.5) with 7% lime, cured for 35 days using post-peak shear strength

Slope	Water condition	Shear strain, %			
		5	10	20	30
Berry Bayou	High water	1.13	1.05	1.01	1.01
	Normal water	1.74	1.51	1.40	1.40

The relation of the safety factor of the HCFCD slopes with the increase in the shear strain is shown in Figures 8.63-8.67. The safety factor for current condition of slopes at Green Bayou (Figures 8.63-8.65) was calculated assuming fully softened shear strength for lean clay and residual shear strength for fat clay. The safety factor before treatment was calculated for fully softened strength along the entire slip surface for Berry Bayou (Figure 8.66) and Carpenters Bayou slopes (Figure 8.67).

Two treatment ratios of ten and twenty percent were considered for each slope. For Berry Bayou slope, where a major part of the slip surface passes through lean clay, an additional treatment ratio of fifty percent was also analyzed. No treatment was considered for lean clay in the analyses.

The safety factor drops significantly when shear strain increases to 10%. For the shear strains larger than 10%, the safety factor decreases at a lower rate. At large strains, the safety factor after lime treatment is still more than that prior to lime treatment. For Berry Bayou and Carpenters Bayou, the safety factor at 30% strains (minimum post-peak strength) is slightly higher than that before treatment. The reason is that the minimum post-peak strength of treated clay is slightly higher than that of the fully softened shear strength of untreated clays, as observed in laboratory tests. However, the residual shear strength of treated clay is significantly higher than the residual strength of untreated clay.

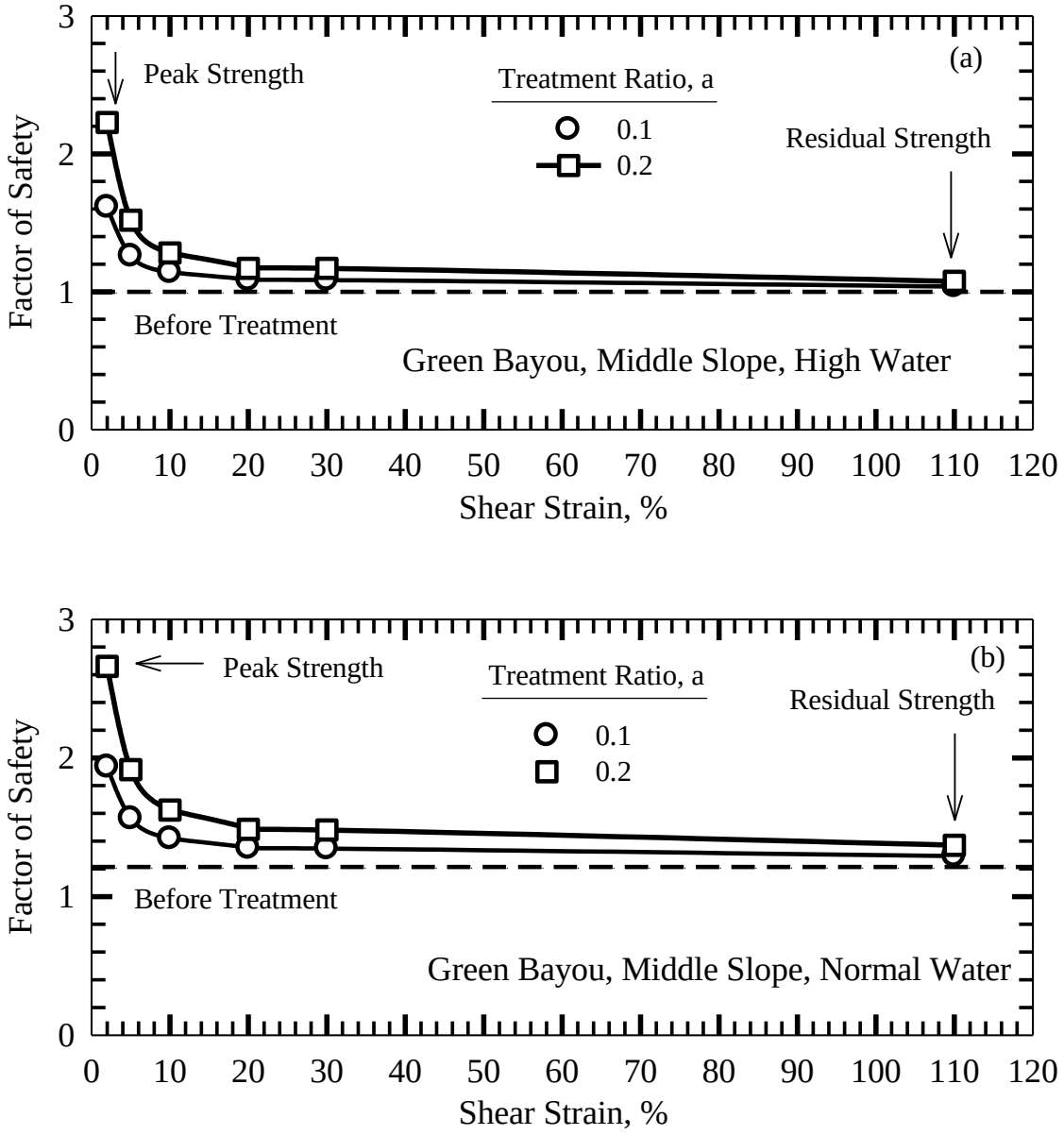

Figure 8.63: Safety factor reduction with shear strain, Greens Bayou, Middle slope for: (a) high water; (b) normal water

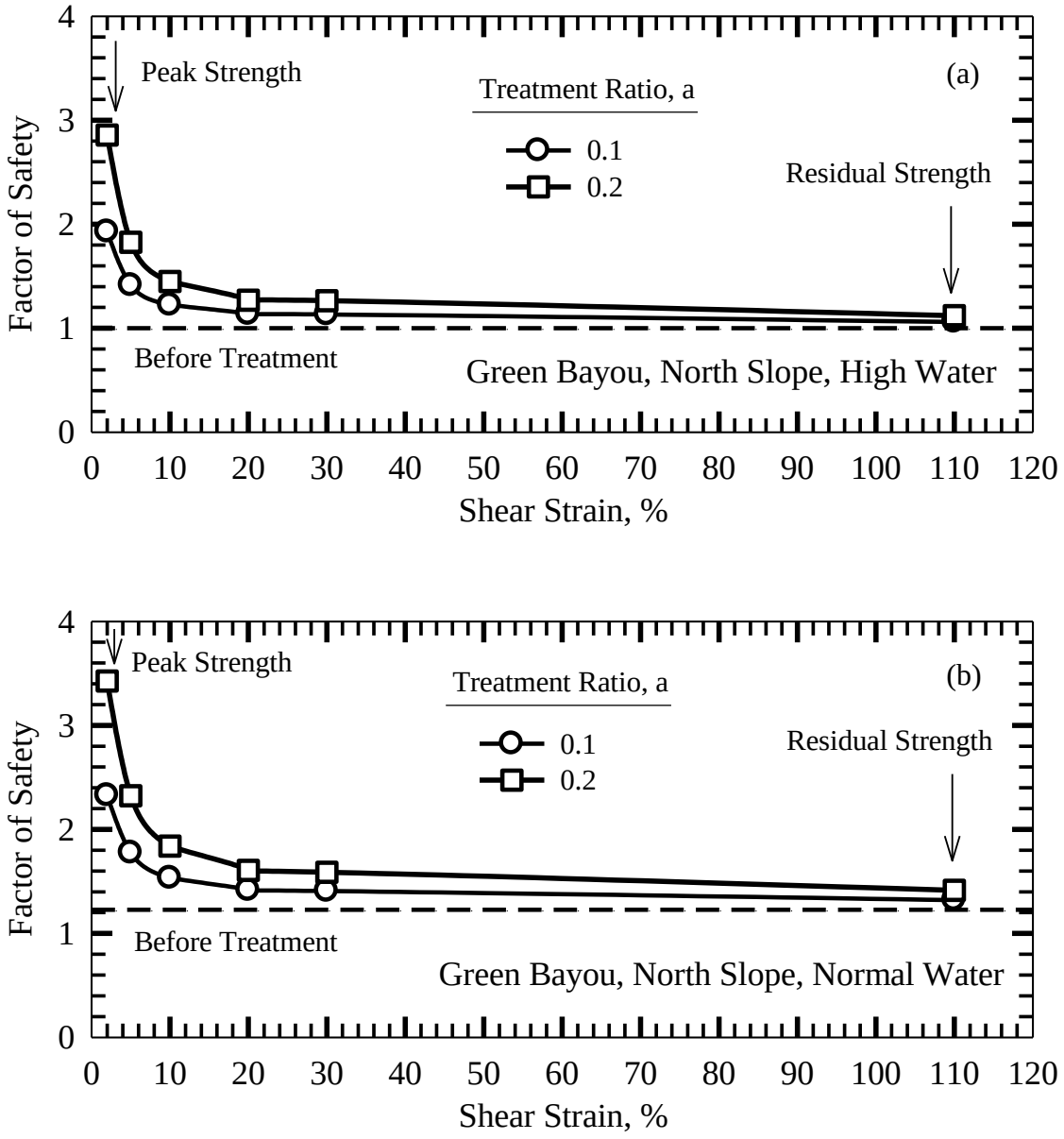

Figure 8.64: Safety factor reduction with shear strain, Greens Bayou, North slope for : (a) high water; (b) normal water

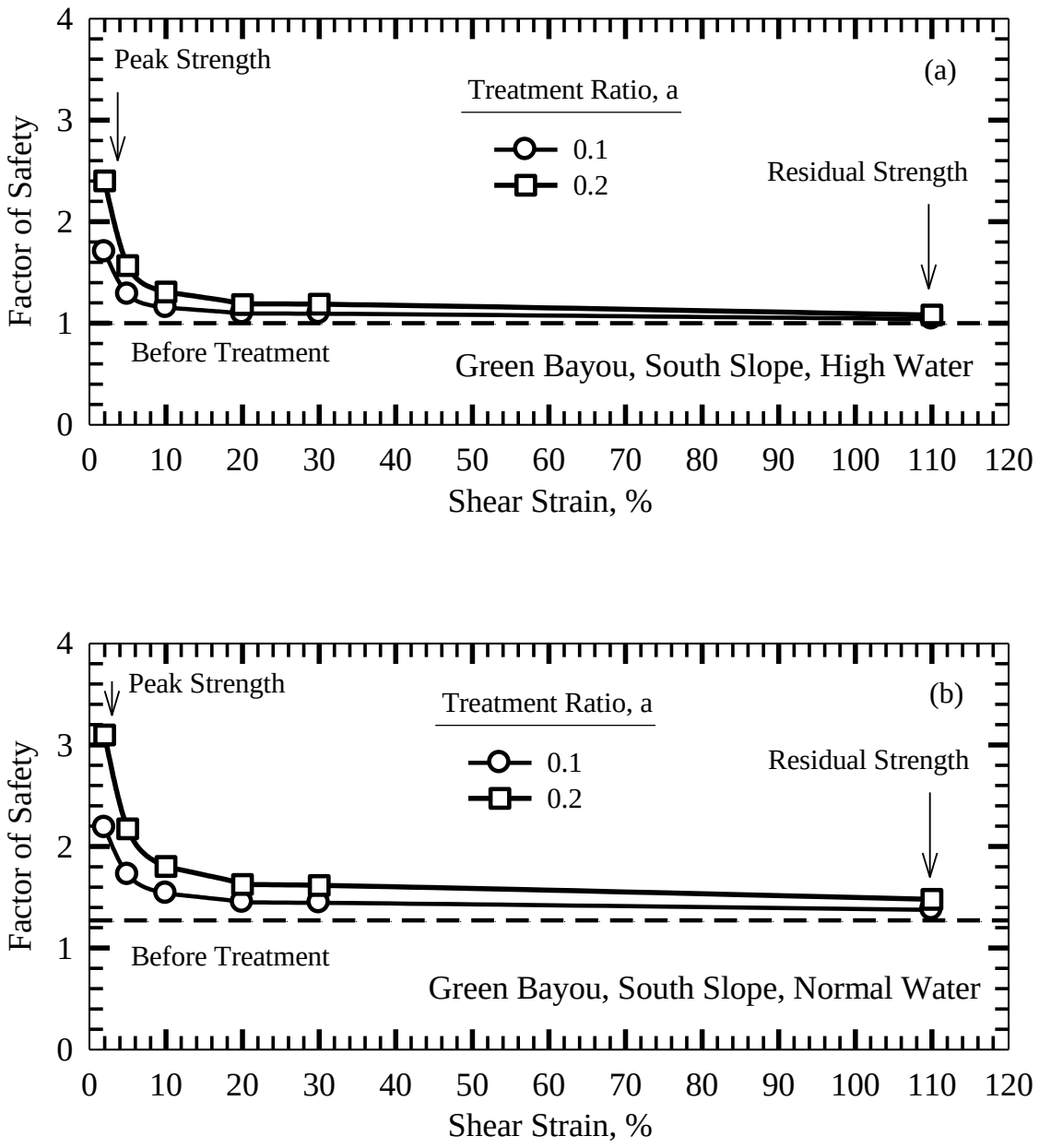

Figure 8.65: Safety factor reduction with shear strain, Greens Bayou, South slope for: (a) high water; (b) normal water

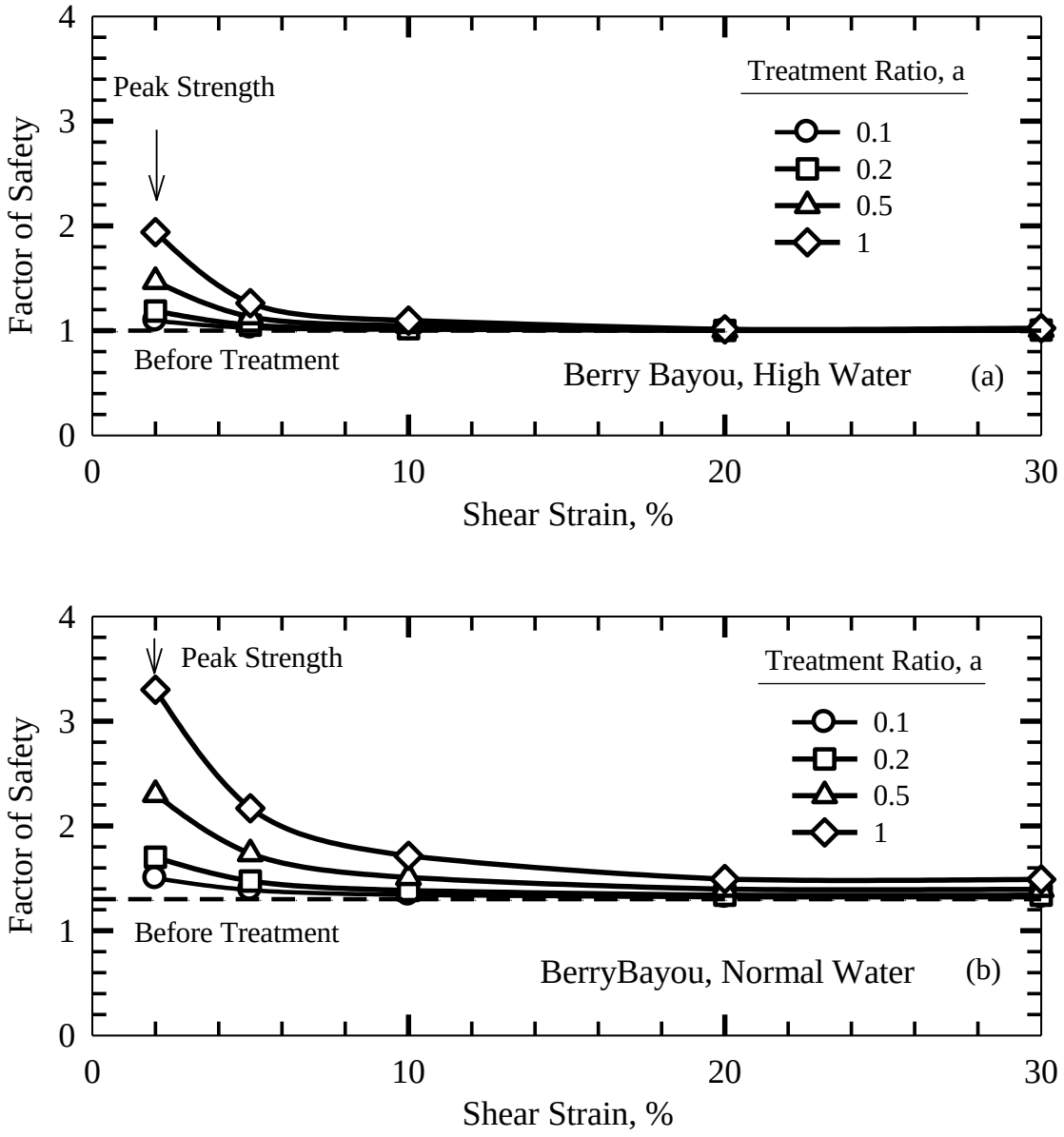

Figure 8.66: Safety factor reduction with shear strain, Berry Bayou slope for: (a) high water; (b) normal water

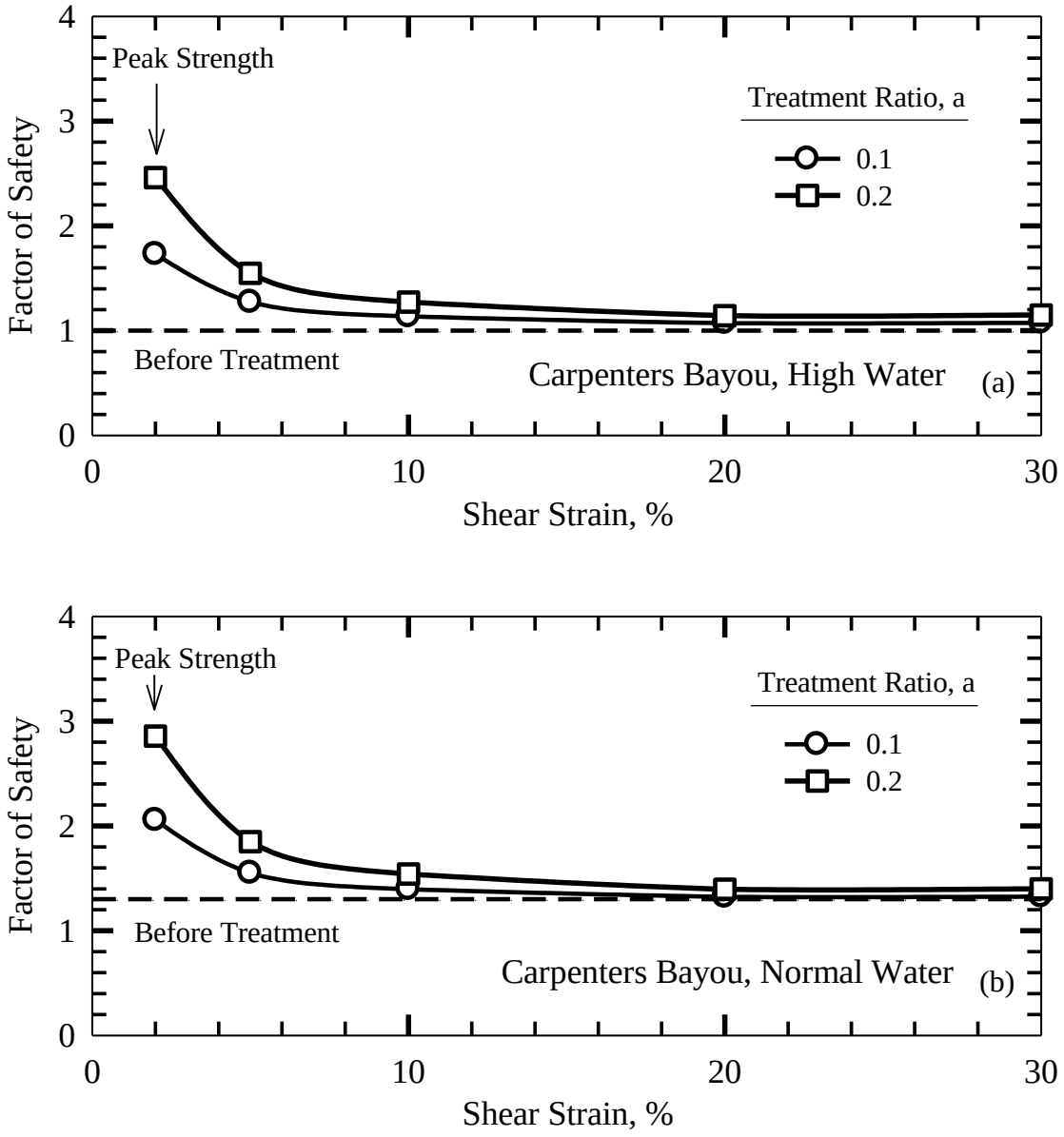

Figure 8.67: Safety factor reduction with shear strain, Carpenter slope for: (a) high water; (b) normal water

CHAPTER 9

SUMMARY AND CONCLUSION

There are similarities between reaction of clay with lime and that with cement. Understanding clay-lime reactions would help in comprehending pozzolanic reactions occurring when cement or other additives are added to clay. Three clays with different characteristics were utilized in this study to investigate the products formed in lime-stabilized clays. The studied clays include low plasticity Chicago clay, and high plasticity Brenna and Beaumont clays. Brenna and Beaumont clays both consist of significant amount of calcium montmorillonite. Brenna clay contains small amount of sulfate in its composition.

The objective of lime treatment in this study was to improve long-term stability of first-time or reactivated landslides in stiff clays and shales, hence permanent changes in the size and shape of clay particles is a requirement. Clay-lime reactions producing less platy and aggregated clay particles begin and continue with time under the highly alkaline pH environment. In this study, measurements of pH as an indicator of chemical environment, SEM images as a direct measure of particle size, shape and arrangement, Atterberg plastic limit and liquid limit as indirect measures of changes in particle size and shape, and secant friction angles, were examined to understand possible mechanisms of lime-soil reactions. The effects of water content, lime content, curing period and curing stress on peak, post-peak and residual strength were explored.

Adsorption and dissolution of hydrated lime and associated chemical reactions of lime and soil begin during the mixing of lime and wet soil. Adsorption is completed during the mixing process; however, dissolution continues until all free lime is consumed. The total lime content, l_c, should be large enough to fully satisfy lime adsorption, l_{ca}, and sufficient lime left over to dissolve in porewater, l_{cd}, to maintain the pH at 12.3-12.4 in order to sustain chemical reactions for an adequate period of time.

Secant friction angle

The peak (intact) strength envelope of lime-treated clays displays a pronounced curvature due to a decrease in dilatant response of cemented soil structure as effective normal stress increases. Cementitious bonds formed within and in between clay floccules and lower tendency of treated clays to dilate at high effective normal stresses are responsible for high degree of nonlinearity of the shear strength envelope.

A major increase in the secant peak friction angle of lime-treated clays occurred in the first week of treatment, particularly at low effective normal stresses. The increase in the peak strength continued after the first week of treatment, though with a reduced rate. The significant improvement in the peak strength during the first week of curing is due to the formation of cementitious bonding products under the elevated pH condition. As time passes, these products harden and increase the peak strength.

As shearing displacement continues beyond the peak strength, inter-cluster bonds begin to break, causing partial breakdown of bonds among aggregates. The partial disaggregation is caused by the breakage of bonds between clusters and floccules. However, intra-cluster bonds and aggregation within the floccules survive the shearing. As shearing continues to larger strains, the secant friction angle decreases and approaches that of untreated clay, suggesting that the slip plane passes through clay particles, or the aggregated particles entirely disaggregate within the shear zone. As shearing continues, more bonds break, resulting in a decrease in nonlinearity of the shear strength envelope. If shearing continues along the shear plane to even larger strains, the shearing resistance decreases to the residual strength. The secant residual friction angle of lime-treated clay increased within the first few days of treatment and remained relatively constant as curing time increased. The residual strength is controlled by aggregation which takes place at early stages of treatment and remains constant, whereas the peak (intact) shear strength is controlled by both aggregation and inter-aggregate bonds, with latter improving with time.

Despite some scatter, the secant residual friction angle of lime-treated clays is independent of curing history (i.e. curing stress, curing time at each confining stress), and only depends on lime content and effective confining pressure. No major improvement in residual strength was observed for Lower Brenna and Beaumont clays treated with 3% lime while the residual strength of Chicago

clay increased for a lime content as low as 1%. For lime contents above 3%, the secant residual friction angle of Lower Brenna clay increases substantially, suggesting the aggregation of clay particles. The bonds survived at this stage are the intra-cluster bonds. As lime content increased to 7%, the secant residual friction angle continued to increase. For lime contents above 7%, the secant residual friction angle increased but at a decreasing rate. Likewise, a major aggregation occurred for Beaumont clay treated with 5% lime content. As lime content increased to 7%, the secant residual friction angle continued to increase at a lower rate. As the lime content increased above 7%, the secant residual friction angle remained constant or slightly decreased.

Atterberg Limits

Plastic limit increased dramatically for all treated clays because large amount of water is enclosed within the flocs and agglomerates; however, only part of the porewater contributing to plasticity. The change in the liquid limit of treated clays is rather unpredictable. After addition of lime, the liquid limit of Chicago clay increased, while Lower Brenna and Beaumont clays exhibited a decrease in their liquid limit. The plasticity index of Chicago clay remained more or less the same after addition of lime. The high plasticity clays, i.e. Lower Brenna and Beaumont clays, experienced a significant drop by addition of 3% lime. The plasticity index of Lower Brenna and Beaumont clays remained relatively constant for the lime contents equal or more than 3%. The reduction in the plasticity index occurred immediately after addition of lime content equal or more than 3%. This is considered to be the adsorbed lime which is required to increase plastic limit to its maximum. This lime is fixed and lime in excess of this value contributes to an increase in the shear strength.

When the curing of lime treated Lower Brenna clay took place unconfined, liquid limit dramatically increased above the liquid limit of treated clay as curing time increased; whereas when curing took place under confining pressure condition (imposed effective stress such as the σ'_n in direct shear tests), there was a decrease in liquid limit.

Brenna clay contains a small amount of sulfate in its composition which promotes ettringite formation. Two reactions are in process when lime is added to Brenna clay, pozzolanic and ettringite reactions. At early stages, cementitious products formed by pozzolanic reactions aggregate the clay particles and thus reduce the plasticity. However, ettringite formation

overcomes cementation as curing prolongs under unconfined condition, causing an increase in plasticity of the treated clay.

Introducing lime to shear zone in the field

Two methods were proposed to introduce lime or cement to the potential shear zone of first-time slides or shear zone of reactivated slopes to enhance the stability and impede the movement of slopes. A retractable mixing tool was designed to target and effectively treat a shear zone. The mixing tool is extended when reaching the treatment depth and it is retracted after mixing process is complete. The second proposed method is to use horizontal directional drilling technique. This method is employed to mix lime or cement with soil along a shear zone. The drill bit is pushed into the shear zone from top to toe of slope and soil is treated while the mixing tool is pulled back.

Lime treatment effect on stability of slopes

The stability of Red River slopes in Grand Forks, North Dakota, CUP O'Hare reservoir slopes in Chicago, Illinois, and the slope failures in drainage channels in Harris County, Texas, was evaluated before and after lime treatment using the shear strength envelopes determined from the laboratory tests. Five slides along Red River (i.e. 27th Avenue, Alpha Avenue, Riverside Drive, Water Tank, Reeves Drive) were analyzed. The factors of safety calculated for the slopes before treatment showed that they were marginally stable with the factors of safety in the range of 1-1.1. The factors of safety increase significantly subsequent to treatment of ten percent of the slip surface with 7% lime. The safety factors for peak strength increased to 1.62-1.93 after 1 week, 1.81-2.18 after 2 weeks, and 2.32-2.89 after 5 weeks of curing. The safety factor increases to 1.12-1.24 for residual condition following treatment of ten percent of the slip surface. The safety factors using peak strength increase to 2.25-2.77 after 1 week, 2.63-3.27 after 2 weeks, and 3.64-4.69 after 5 weeks of curing for twenty percent treatment ratio. The safety factor increases to 1.24-1.40 for residual condition following treatment of twenty percent of the slip surface. This level of lime remediation effort is expected to have a significant effect on rate of movement of the slide.

The analysis of the lower and upper slopes of CUP O'Hare following treatment with 3% lime showed a major increase in the stability of the slopes. It was recommended that 7 ft (2.1 m)

of soil on the lower slope be replaced with 3% lime-treated Chicago clay. Additionally, lime treatment of thirty percent of the upper slope was proposed. The factor of safety of the lower slopes increased from 0.52 (rapid drawdown)-1.21 (normal) to 1.15-1.61 after 1 week and to 1.22-1.75 after 4 weeks following treatment using peak strength envelopes. The factor of safety of the upper slopes increased from 1.01 to 1.22 after 1 week and to 1.25 after 4 weeks. The analysis of global stability of the slopes showed an increase in the factors of safety from 0.89 to 1.22 and 1.29 for 1- and 4-week curing periods, respectively. For Chicago clay, there is only a slight increase in the factors of safety after 1 week.

Three slope failures in Harris County Flood Control District were analyzed, including Greens Bayou, Berry Bayou, and Carpenters Bayou, and the effect of lime treatment on stability of the slopes were investigated. Three channel slope failures at Greens Bayou (i.e. Middle slope, North slope and South slope) were analyzed. For the Middle slope at Greens Bayou, 7% lime treatment of ten percent of the slip surface passing through fat clay increased the factor of safety from 1.00 (high water)-1.21 (normal water) to 1.36-1.63 after 1 week and to 1.61-1.94 after 5 weeks of curing using peak strength envelopes. Following treatment of ten percent of the North slope at Greens Bayou, the safety factor increased from 1.00 (high water)-1.23 (normal water) to 1.53-1.82 after 1 week and to 1.93-2.33 after 5 weeks using peak strength envelopes. For the South slope at Green Bayou, ten percent treatment ratio caused the safety factor to increase from 1.00 (high water)-1.27 (normal water) to 1.42-1.80 after 1 week and to 1.70-2.19 after 5 weeks of curing using peak strength envelopes. A twenty percent treatment ratio increased the safety factor of the Berry Bayou slope from 1.00 (high water)-1.30 (normal water) to 1.13-1.54 after 1 week and to 1.19- 1.70 after 5 weeks of curing using peak shear strength. Following treatment of ten percent of the slip surface of the Carpenters Bayou slope, the factors of safety increased from 1.00 (high water)-1.25 (normal water) to 1.43-1.72 after 1 week and to 1.73-2.05 after 5 weeks of curing using peak strength. Also. the factor of safety of the lime-treated slopes was calculated as a function of shear strain. The factor of safety dropped significantly when shear strain increased to 10%. For the shear strains larger than 10%, the safety factor decreased at a lower rate. At large strains, the safety factor after lime treatment was still more than that prior to lime treatment.

The safety factor of the Middle slope was calculated 1.04 for rapid drawdown and 1.29 for normal conditions using treated residual strength following ten percent treatment. The safety

factors increase to 1.08 and 1.37 for rapid drawdown and normal condition, respectively, as treatment ratio increases to twenty percent. For the North slope at Greens Bayou, The safety factors of the treated slope in residual condition are 1.06 and 1.12 in rapid drawdown condition for ten and twenty percent treatment ratios, respectively. The safety factors in normal condition are 1.32 for ten percent and 1.41 for twenty percent treatment ratios using residual strength. For the South slope at Green Bayou, the safety factors of the treated slope are 1.38 and 1.48 at residual condition for normal condition following ten and twenty percent treatment ratios, respectively.

REFERENCES

Ahnberg H. 2007. On yield stresses and the influence of curing stresses on stress paths and strength measured in triaxial testing of stabilized soils. Canadian Geotechnical Journal, 44(1), 54-66.

Ahnberg H. 1996. Stress dependent parameters of cement stabilized soil. Grouting and Deep Mixing, Proceedings of IS-Tokyo, 2nd International Conference on Ground Improvement Geosystems, 387-392.

Ahnberg H., Johansson S.E., Pihl H. and Carlsson T., 2003. Stabilising effects of different binders in some Swedish soils. Ground Improvement, 7(1), 9-23.

Ahnberg H., Ljungkrantz C. and Holmqvist L. 1995. Deep stabilization of different types of soft soils, Proceedings of the 11th ECSMFE, 7, 7.167-7.172.

Al-Khashab M.N. and Al-Hayalee, M.T. 2008a. Stabilization of Expansive Clayey Soil Modified by Lime with an Emulsified Asphalt Addition. Engg. and Tech. Jour., 26(10).

Al-Khashab M.N., and Al-Hayalee, M.T. 2008b. Treatment of Expansive Clayey Soil with Crushed Limestone. Engg. and Tech. Jour., 26(3), 376-387.

Al-Layla M.T. 1970. Study of Certain Geotechnical Properties of Beaumont Clay. Dissertation presented to Texas A & M University, College Station, Texas in partial fulfillment of the requirements for the degree of Doctor of Philosophy.

Arndt B.M. 1977. Stratigraphy of offshore sediment Lake Agassiz-North Dakota, Report of Investigation No. 60. North Dakota Geological Survey.

Azman M., Amin M., Bakar I. and Hyde A.F.L. 1995. Effect of initial consolidation on the undrained shear response of cement treated soil. In Balasubramaniam A.S. et al. (eds.), Development in Deep foundations and ground improvement schemes, Bangkok.

Balasubramaniam A.S., Bergado D.T., Buensuceso B.R. and Yang W.C. 1989. Strength and deformation characteristics of lime treated soft clays. Geotechnical Engineering (AIT), 20, 49-65.

Banks S.J., Chan D.H., Lee K.H. and Lam K.C. 2001. Triaxial Testing of Kaolin-Cement Mixture: Laboratory Program and Preliminary Results. 3rd International Conference on Soft Soil Engineering, Hong Kong, PRC, 545-550.

Baracos A. 1977. Compositional and structural anisotropy of Winnipeg soils – a study based on scanning electron microscopy and X-ray diffraction analysis. Can. Geotech. .J, 14(1), 125-143.

Baracos A. and Graham J. 1981. Landslide problems in Winnipeg. Canadian Geotechnical J. 18, 390-401.

Baver L.D. 1956. Soil Physics, 3rd edition. John Wiley & Sons, London.

Bayer H.J. 2007. HDD Practice Handbook. Vulkan-Verlag GmbH.

Bell F.G. 1993. Engineering treatment of soils. Spon, London, 1-302.

Bell F.G. 1996. Lime stabilization of clay minerals and soils. Engineering Geology 42, 223-237.

Bergado D.T., Anderson L.R., Miura N. and Balasubramaniam A.S.1996. Soft Ground Improvement in Lowland and Other Environments. ASCE Press, New York, U.S.A.

Berube M.A. and locat J . 1987. Stabilisation a la chaux des argiles sensibles: ro1e de la nature du sol. Ministere des Transports du Quebec, Final Report GGL-87-03.

Bishop A.W. 1967. Progressive failure - with special reference to the mechanism causing it. Proceedings of Geotechnical Conference., Oslo, 2, 142-150.

Bishop A.W. 1971. Shear strength parameters for undisturbed and remolded soil specimens. Proceedings of the Roscoe Memorial Symposium, Cambridge University. Edited by R.G. Parry; G.T. Foulis and Co. Ltd. Oxfordshire, 3-58.

Bishop A.W., Green G.E., Garga V.K., Andresen A. and Brown J.D. 1971. A new ring shear apparatus and its application to the measurement of residual strength. Geotechnique, 21(4), 273-328.

Bjerrum L. 1967. Progressive failure in slopes in overconsolidated plastic clay and clay shales. Terzaghi Lecture. J. of the Soil Mech. and Found. Div., ASCE, 93(5), 3-49.

Bressani L.A. 1990. Experimental properties of bonded soils. Ph.D. thesis, University of London.

Broms, B.B. 1986. Stabilization of soft clay with lime and cement columns in Southeast Asia. Applied Research Project RP10/83, Nanyang Technical Institute, Singapore.

Bruce D.A. 2001. Practitioner's guide to the deep mixing method. Proceedings of the Institution of Civil Engineers - Ground Improvement, 5(3), 95-100.

Burkart B., Goss G. and Kern J. 1999. The Role of gypsum in production of sulfate-induced deformation of lime-stabilized soils. Journal of Environmental and Engineering Geoscience, 5(2), 173-187.

Burland J.B. 1990. On the compressibility and shear strength of natural clays. Geotechnique, 29(3), 329-378.

CDIT 2000. The deep mixing method: principles, design and construction, Coastal Development Institute of Technology. The Netherlands.

CDM 1994. Publication of Cement Deep Mixing Association of Japan, Tokyo, 1-194. (in Japanese)

Chandler R J. 1984. Recent European experience of landslides in overconsolidated clays and soft rocks. Proceedings of 4th International Symposium on Landslides, Canadian Geotechnical Society, Richmond, BC, Canada, 1, 61-81.

Chew S.H., Lee F.H. and Lee Y. 1997. Jet Grouting in Singapore Marine Clay. Proceedings of the 3rd Asian Young Geotechnical Engineering Conference, Singapore: 231–238.

Chew S.H., Kamruzzaman A.H. and Lee F.H. 2004. Physicochemical and engineering behavior of cement treated clays. Journal of geotechnical and geoenvironmental engineering 130, 696-706.

Chin K.G. 2006. Constitutive behavior of cement treated marine clay". Ph.D. thesis, National University of Singapore, Singapore.

Chiu C. F., Zhu W. and Zhang C.L. 2008. Yielding and shear behavior of cement treated dredged materials. Engineering Geology, 103, 1-12.

Choquette M. 1988. La stabilisation a la chaux des sols argileux du Quebec. Ph.D. thesis, Department of Geology, Universite Laval, Quebec, Que.

Choquette M., Berube M. and Locat J. 1987. Mineralogical and microtextural changes associated with lime stabilization of marine clays from eastern Canada. Appl Clay Sci 2, 215–232.

Clare K.E. and Cruchley A.E. 1957. Laboratory experiments in the stabilization of clays with hydrated lime. Géotechnique 7 (2), 97-111.

Clough G.W., Rad N.S., Bachus R.C. and Sitar N. 1981. Cemented sands under static loading. J. Geotech. Eng. Div., Am. Soc. Civ. Eng., 107, 799–817.

Collepardi M. 2003. A state-of-the-art review on delayed ettringite attack on concrete. Cement and Concrete Composites, 25(4-5), 401-407.

Coop M.R. and Atkinson J.H. 1993. The mechanics of cemented carbonate sands. Géotechnique, 43(1), 53-67.

Cordon W.A. 1962. Resistance of soil cement exposed to sulfates. Highway Research Board Bulletin 309, Washington, DC.

Cotecchia F. and Chandler R.J. 2000. A general framework for the mechanical behavior of clays. Géotechnique 50(4), 431-447.

Crammond N.J. 1985. Thaumasite in failed cement motors and renders from exposed brickwork. Cem. Concr. Res., 15(6), 1039-1050.

Crammond N.J. 2003. The thaumasite form of sulfate attack in the UK. Cement and Concrete Composites, 25(8), 809-818.

Croft J., 1964. The pozzolanic reactivities of some New South Wales flyashes and their application to soil stabilization. Proceeding of 2nd Australian Road Research Board (ARRB) Conference, Melbourne.

Cuccovillo T. and Coop M.R. 1997. Yielding and pre-failure deformation of structured sands. Géotechnique, 47(3), 491-508.

Dam T.K.L., Yamane N., Hanzawa H. and Porbaha A. 1997. Evaluation of progressive failure potential of natural clay deposit. In Deformation and progressive failure in geomechanics, Asaoka A., Adachi, T. and Oka F. (Eds.) . Elsevier.

Delage P. and Lefebvre G. 1984. Study of the structure of a sensitive Champlain clay and of its evolution during consolidation. Revue Canadienne de Géotechnique 21, 21-35.

Dermatas D. 1995. Ettringite-induced swelling in soils: State-of-theart. Appl. Mech. Rev., 48(10), 659-673.

Dermatas D., Chrysochoou M., Moon D.H., Pardali S., Christodoulatos C., Lazarte C. A., Pendleton C.H., Bonaparte R., Briggs R., Myers M., French C., Morris J. and Kaouris M. 2005. Mineralogical Characterization of Chromite Ore Processing Residue (COPR) at Dundalk Marine Terminal Area 1800, Proc. of the 8th Battelle In-situ and On-site Bioremediation International Symposium, Baltimore, Maryland, June 6-9.

Desrues J., Chambon R., Mokni M. and Mazerolle F. 1996. Void ratio evolution inside shear bands in triaxial sand specimens studied by computer tomography, Geotechnique, 46(3), 529–546.

DeepXcav 2011. User's Manual. Deep Excavation LLC (www.deepexcavation.com).

D'Elia B., Picarelli L., Leroueil S. and Vaunat J. 1998. Geotechnical characterisation of slope movements in structurally complex clay soils and stiff jointed clays. Italian Geotechnical Journal, Anno XXXII, 3, 5-32.

Diamond S. and Kinter E.B. 1965. Mechanisms of soil-lime stabilization: an interpretive review. Highway Research Record 92, 83-102.

Diamond A., White J.L. and Dolch W.L. 1964. Transformation of clay minerals by calcium hydroxide attack. In: Bradley, W.F.(Ed.), Proc. 12th Int. Conf. Clays and Clay Minerals. Pergamon Press, New York, 359-379.

Directed Technologies Drilling (DTD) 2004. Horizontal Environmental Well Handbook.

Du Y.J., Jiang N.J., Liu S.Y., Jin F., Singh D.N., and Puppala A.J. 2014. Engineering properties and microstructural characteristics of cement-stabilized zinc-contaminated kaolin. Canadian Geotechnical Journal, 51(3), 289-302.

Durgunoglu H.T., Chinchelli M., Ikiz S., Emrem C., Hurley T. and Catalbas F. 2004. Soil improvement with jet-grout columns: a case study from the 1999 Kocaeli earthquake. Proceedings of Fifth International Conference on Case Histories in Geotechnical Engineering, New York.

Eades J.L. and Grim R.E. 1960. Reaction of hydrate lime with pure clay minerals in soil stabilization. Highway Research Record 262, 51-63.

Eades J.L., Nichols F.P. and Grim R.E. 1962. Formation of new minerals with lime stabilization as proven by field experiments in Virginia. Highway Research Board 335, 31-39.

Eades J.L. and Grim R.E. 1966. A quick test to determine lime requirements for soil stabilization. Highway Research Record 139, 61-72.

Endo M. 1976. Recent development in dredged material stabilization and deep chemical mixing in Japan. Soils and Site Improvement. University of California, Berkeley, lifelong learning seminar.

Finlan S., Quickfall G. and Terzaghi S. 2004. Innovation in slip and settlement remedials: the soil mixing option. 9th Australia New Zealand conference on geomechanics, 405-411.

Gallaway B.M. and Buchanan S.J. 1964. Lime stabilization of clay soils. Proceedings of the Australian Road Research Board, 2, 1169-1203.

Georgiannou V.N. and Burland J.B. 2001. A laboratory study of post-rupture strength. Geotechnique 51 (8), 665-675.

GeoSlope International, 2016. GeoStudio Software Package, Calgary, Alberta, Canada. (www.geo-slope.com)

Goldberg I. and Klein A. 1952. Some effects of treating expansive clays with calcium hydroxide. ASTM Special Publication 142, Symp. on Exchange Phenomenon in Soils, 112-128.

Grim R.E. 1968. Clay Mineralogy, McGraw-Hill, New York, N. Y.

Harris P., Harvey O., Jackson L., DePugh M., and Puppala A. 2014. Killing the Ettringite Reaction in Sulfate-Bearing Soils. Transportation Research Record: Journal of the Transportation Research Board, (2462), 109-116.

Hausmann M.R. 1990. Engineering principles of ground modification. McGraw Hill, New York.

HCFCD. 2015. Streambank stabilization handbook. A guide for Harris County landowners. Version 2.

Herbert B., Little D., Nair S. and Markley C. 2009. Site-specific risk assessment of sulfate induced heave in lime-stabilized clay soils. In Contemporary Topics in Ground Modification, Problem Soils, and Geo-Support, 558-565.

Herzog A. and Mitchell J.K. 1963. Reactions accompanying stabilization of clay with cement. Highway Research Board Record, 36, 146-171.

Hill H. and Rutledge P.C. undated, circa 1960. Earth movements in Red River Valley of the North. Unpublished paper presented at an ASCE meeting.

Hilt G.H. and Davidson D.T. 1960. Lime fixation in clayey soils. Highway Research Board 262, 20-32.

Horpibulsuk S., Miura N. and Bergado D.T. 2004. Undrained Shear Behavior of Cement Admixed Clay at High Water Content. Journal of Geotechnical and Geoenvironmental Engineering, ASCE, 130(10), 1096-1105.

Huat B.B.K., Maail S. and Mohamed T.A. 2005. Effect of Chemical Admixtures on the Engineering Properties of Tropical Peat Soils. American Journal of Applied Sciences, 2(7), 1113-1120.

Hunter D. 1988. Lime-induced heave in sulphate-bearing clay soils. J. Geotech. Engrg. 114(2), 150-167.

Ingles O.G. and Metcalf J.B. 1973. Soil stabilization Principles and Practice, 1st edition. John Wiley & Sons, New York, 374 p.

Ingles O.H. 1987. Soil stabilization, chapter 38. In: Bell, F.G. (Ed.), Ground Engineer's Reference Book. Butterworths, London, 38/1-38/26.

Irassar E.F., Di Maio A., and Bati O.R. 1996. Sulfate attack on concrete with mineral admixtures. Cement and Concrete Research, 26(1), 113-123.

Jardine R.J. 1992. Some observations on the kinematic nature of soil stiffness. Soils and foundations, 32(2), 111-124.

Jardine R.J., St John H.D., Hight D.W. and Potts D.M. 1991. Some practical applications of a non-linear ground model. Proc. 10th ECSMFE, Florence, 1, 223-228.

Jefferis S.A. 2011. Discussion of “Addressing sulfate-induced heave in lime treated soils” by by Little D.N., Nair S. and Herbert B. 2010. Journal of Geotechnical and Geoenvironmental Engineering, 137(8), 813-814.

Jo A.N., Hafez M. and Norbaya S. 2011. Study of bearing capacity of lime–cement columns with pulverized fuel ash for soil stabilization using laboratory model. Electronic Journal of Geotechnical Engineering, 16, 1595-1605.

Kamon M. and Nontananandh S. 1991. Combining industrial wastes with lime for soil stabilization. Journal of geotechnical engineering, ASCE 117(1), 1-17.

Kamruzzaman A. H. M. 1998. Chemical stabilization of Bangkok Clay–Addition of salts and other additives. MEng thesis, GE-97-15, Asian Institute of Technology, Thailand.

Kamruzzaman A.H.M. 2002. Physico-chemical and engineering behavior of cement treated Singapore marine clay. PhD Thesis, Department of Civil Engineering, National University of Singapore.

Kamruzzaman A.H., Chew S.H. and Lee, F.H. 2009. Structuration and Destructuration Behavior of Cement-Treated Singapore Marine Clay. Journal of geotechnical and geoenvironmental engineering 135, 573-589.

Kasama K., Ochiai H. and Yasufuku N. 2000. On the stress–strain behaviour of lightly cemented clay based on an extended critical state concept. Soils Found., 40(5), 37-47.

Kawamura M. and Diamond S. 1975. Stabilization of clay soils against erosion loss. Clay and Clay Minerals. 23, 443-451.

Kawamura M., Torii K. and Hasaba S. 1986. Reaction process and microstructure in compacted fly ashes and fly ash-chemical additive mixtures. 8th International Congress on the Chemistry of Cement, 92-97.

Kawasaki H. 1988. Properties of sediment of New Creeks in the lower Chikugo river basin. Bull. Kyushu Natl Agric. Exp. Station 25, 77-92.

Kawasaki T., Niina A., Saitoh S., Suzuki Y. and Honjo Y. 1981. Deep mixing method using cement hardening agent. Proceedings of the 10th international conference on soil mechanics and foundation engineering, 3, 721-724.

Kinuthia J.M., Wild S. and Jones G.I. 1999. Effects of monovalent and divalent metal sulphates on consistency and compaction of lime-stabilized kaolinite. Applied Clay Science, 14(1-3), 27-45.

Kitazume M. and Terashi M. 2013. The Deep Mixing Method. CRC Press/Balkema, Teylor & Francis Group, London, UK.

Kohler S., Heinz D. and Urbonas L. 2006. Effect of ettringite on thaumasite formation. Cem. Concr. Res., 36(4), 697-706.

Kozan G.R. 1960. Soil stabilization: Investigation of a chemically modified cement as a stabilizing material. U.S. Army Engineer Waterways Experiment Station, Technical Report 3-455, Report 3.

Ladd C.L., Moh Z.C. and Lambe, T.W. 1960. Recent soil-lime research at the Massachusetts Institute of Technology," Bulletin No. 262, Highway Research Board, Washington, D. C., 64-85.

Lade P.V. and Overton D.D. 1989. Cementation effects in frictional materials. Journal of Geotech. Engerg. Div., ASCE, 115(10), 1373-1387.

Lambe T.W., Michaels A.S. and Moh Z.C. 1960. Improvement of soil-cement with alkali metal compounds. Highway Research Board Bulletin 241, 67-103.

Langston R. 2005. Slope stability in Harris County. Presentation to Foundation Performance Association.

Larsson S. 2005. State of Practice Report – Execution, monitoring and quality control. International Conference on Deep Mixing - Recent Advances and Best Practice, Stockholm, Sweden.

Lasledj A. and Al-Mukhtar M. 2008. Effect of hydrated lime on the engineering behavior and the microstructure of highly expansive clay. 12th International Conference of International Association for Computer Methods and Advances in Geomechanics (IACMAG), Goa, India. 3590-3598.

Lea, F.M. 1956. The chemistry of cement and concrete. Edward Arnod (Publishers) Ltd., London.

Lee K.H. and Lee S. 2002. Mechanical properties of weakly bonded cement stabilized kaolin. KSCE Journal of Civil Engineering, 6 (4), 389-398.

Lefebvre G. 1981. Strength and slope stability in Canadian soft clay deposits. Canadian Geotechnical Journal, 18(3), 420-442.

Leroueil S., and Hight D.W. 2003. Behavior and properties of natural soils and soft rocks. Characterization and engineering properties of natural soils, 1, 29-254.

Le Roux A. 1969. Traitement des sols argileux par la chaux. Bulletin de Liaison des Laboratoires des Ponts et Chaussees, 40, 59-95.

Le Roux A. and Toubeau Ph. 1987. Mise en evidence du seuil de nocivite et du mecanisme d'action des sulfures au cours d'un traitement a la chaux. 9th South East Asian Geotechnical Conference, Bangkok.

Little D.N. 1999. Evaluation of structural properties of lime stabilized soils and aggregates, Volume 1: Summary of findings. National Lime Association.

Little D.N. 1995. Handbook for stabilization of pavement subgrades and base courses with lime. Kendall/Hunt, Iowa.

Little D.N. 2006. Evaluation of the sulfate threshold for ettringite formation in soils from Frisco, Texas. Rep. Prepared for CTL-Thompson, Inc. in support of Subgrade and Pavement Study: Existing Distressed Streets Investigation and Methods for Street Rehabilitation, Report No. DA6399, CTL/Thompson, Denver.

Little D. N. and Graves R.E. 1995. Guidelines for use of lime in sulfate bearing soils. Chemical Lime Co., Fort Worth, Tex.

Little D.N., Herbert B. and Kunagalli S.N. 2005. Ettringite formation in lime-treated soils: Establishing thermodynamic foundations for engineering practice. Transp. Res. Rec., 1936, 51-59.

Little D.N., Nair S. and Herbert B. 2010. Addressing sulfate-induced heave in lime treated soils. Journal of Geotechnical and Geoenvironmental Engineering, 136(1), 110-118.

Little D.N., Thompson M.R., Terrell R.L., Epps J.A. and Bahrenberg E.J. 1982. Soil Stabilization for roadways and airfields. Engineering and Services Laboratory, Air Force Engineering and Services Center, Tyndall Air Force Base, Florida 32403.

Littleton 1995. Some observations on the presence of sulphates in lime stabilized clay soils. Buxton Lime Industries Ltd.

Locat J., André B.M. and Choquette M. 1990. Laboratory investigations on the lime stabilization of sensitive clays: shear strength development. Canadian Geotechnical Journal, 27, 294-304.

Locat J., Lefebvre G. and Ballivy G. 1984. Mineralogy, chemistry, and physical properties interrelationships of some sensitive clays from Eastern Canada. Canadian Geotechnical Journal, 21, 530-540.

Locat J., Tremblay H. and Lerouil S. 1996. Mechanical and hydraulic behavior of a soft inorganic clay treated with lime. Canadian Geotechnical Journal, 33 (4), 654-669.

Madhyannapu R.S., Puppala A.J., Bhadriraju V. and Nazarian S. 2009. Deep Soil Mixing (DSM) treatment of expansive soils. ASCE, US-China Workshop on Ground Improvement Technologies, 130-139.

Maher L.J. and O'Neill M.W. 1983. Geotechnical characterization of dessicated clay. J. Geotech. Engrg., ASCE, 109(1), 56-71.

Malandraki V. and Toll D.G. 1996. The definition of yield for bonded materials. Geotechnical and Geological Engineering, 14(1), 67-82.

McCallister L.D. and Tidwell L. 1997. Double lime treatment to minimize sulfate lime induced heave in expansive clays. Draft Tech. Rep., U.S. Army Engineers, Waterways Experiment Station, Vicksburg, Miss.

MDC 2011. Soil Mixing Systems. Malcolm Drilling Company.

Mehra S.R., Chadda L.R. and Kapur R.N. 1955. Role of detrimental salts in soil stabilization with and without cement, I. The effect of sodium sulfate. Indian Concrete Journal 29, 336-337.

Mehta P.K. 1973. Mechanism of expansion associated with ettringite formation. Cement and Concrete Research, 3(1), 1-6.

Mehta P.K. 1983. Mechanism of sulphate attack on Portland cement concrete-another look. Cement Concrete Res. 13, 401-406.

Mesri G., and Abdel-Ghaffar M.E.M. 1993. Cohesion intercept in effective stress-stability analysis. Journal of Geotechnical Engineering, 119(8), 1229-1249.

Mesri G. and Cepeda-Diaz A.F. 1986. Residual shear strength of clays and shales. Géotechnique 36(2), 269-274.

Mesri G. and Huvaj N. 2004. Residual shear strength mobilized in Red River slope failures. Proc. 9th Int. Symp. on Landslides, Brazil, 925-931.

Mesri G. and Huvaj-Sarihan N. 2012. Residual shear strength measured by laboratory tests and mobilized in landslides. J. Geotech. and Geoenviron. Engrg. 138(5), 585-593.

Mesri G. and Olson R.E. 1971. Mechanism controlling the permeability of clays. Clays and Clay Minerals, 19, 151-158.

Mesri G., Rokhsar A. and Bohor B.F. 1975. Composition and compressibility of typical samples of Mexico City clay. Géotechnique 25(3), 527-554.

Mesri G. and Shahien M. 2003. Residual shear strength mobilized in first-time slope failures. J. Geotech. and Geoenviron. Engrg. 129(1), 12-31.

Mitchell J.K. 1976. Fundamentals of Soil Behavior, John Wiley and Sons, New York.

Mitchell J.K. 1986a. Practical problems from surprising soil behavior. J. Geotech. Eng., ASCE, 112, 259-289.

Mitchell J.K. 1986b. Delayed failure of lime-stabilized pavement bases. J. Geot. Eng. 112, 274-279.

Mitchell J.K. and Dermatos D. 1990. Clay-soil heave caused by lime-sulphate reactions. ASTM Symposium on Innovations and Uses of Lime, San-Francisco.

Mitchell J.K. and Dermatas D. 1992. Clay soil heave caused by lime-sulfate reactions. Innovations and uses of lime. ASTM STP, 1135, 41-64.

Miura N., Horpibulsuk S. and Nagaraj T.S. 2001. Engineering behavior of cement stabilized clay at highwater content. Soils Found. 41(5), 33-45.

Moon H.M., Dermatas D., Wazne M., Sanchez A.M., Chrysochoou M. and Grubb, D.G. 2007. Swelling related to ettringite crystal formation in chromite ore processing residue. Environ. Geochem. Health, 29(4), 289-294.

Moore A.E. and Taylor H.F.W. 1970. Crystal structure of ettringite. Acta Crystallogr., Sect. B: Strcut. Sci., 26, 386-393.

Morgenstern N.R. 1977. Slopes and excavations. State of the Art Report, Proceedings of 9th International Conference on Soil Mechanics and Foundation Engineering, 2, 567–581.

Muhunthan B. and Sariosseiri F. 2008. Interpretation of geotechnical properties of cement treated soils. WSDOT Report No. WA-RD 715.1.

Nagaraj, T.S., Miura, N., Yaligar P., Yamadera, A. 1996. Predicting strength development by cement admixture based on water content. Proceedings of the IS-Tokyo 96, 2nd International Conference on Ground Improvement Geosystems, Grouting and Deep mixing, Tokyo, 1, 431-436.

Nagaraj T.S., Miura N., Yamadera A. and Yaligar P. 1997. Strength assessment of the cement admixtures soft clays-Parametric study. Proc., Int. Conf. on Ground Improvement Techniques, 379–386. Singapore: CI-Premier.

Narasimha Rao S. and Rajasekaran G. 1992. Behavior of lime piles in a soft marine clay International Conference on Deep Foundation Practice incorporating Piletalk ‘92, Singapore, 185-192.

Narasimha Rao S. and Rajasekaran G. 1996. Reaction products formed in lime-stabilized marine clays. Journal of Geotechnial Engineering, 122, 329-336.

Okumura T. 1996. Deep mixing method of Japan. Proceedings of the 2nd International Conference on Ground Improvement Geosystem, Tokyo, 2, 879-888.

Okumura T. and Terashi M. 1975 Deep-lime-mixing method of stabilization for marine clays. Proceedings of the 5th Asian Regional Conference on Soil Mechanics and Foundation Engineering. 1, 1, 69-75.

Ouhadi V.R. and Yong R.N. 2008. Ettringite formation and behavior in clayey soils. Appl. Clay Sci., 42, 258-265.

Perret P. 1977. Contribution a l'etude de la stabilisation des sols fins par la chaux: etude globale du phenomkne et applications. Doctoral thesis, Institut national des sciences appliquees, Rennes, France.

Petry T.M. 1994. Studies of factors causing and influencing localized heave of lime treated clay soils (sulfate induced heave). Technical Rep. Prepared for U.S. Army Corps of Engineers, Waterways Experiment Station, Vicksburg, Miss.

Petry T.M. and Little D.N. 1992. Update on sulfate-induced heave in treated clays: Problematic sulfate levels. Transp. Res. Rec., 1362, 51-55.

Petry T.M. and Wohlgemuth S.K. 1988. Effects of pulverization on the strength and durability of highly active clay soils stabilized with lime and portland cement. Transportation Research Record, 1190, 38-45.

Porbaha A. 1998. State of the art in deep mixing technology: part I. Basic concepts and overview. Proceedings of the Institution of Civil Engineers-Ground Improvement, 2(2), 81-92.

Porbaha A., Shibuya S. and Kishida T. 2000. State of the art in deep mixing technology. Part III: Geomaterial characterization. Proceedings of the ICE-Ground Improvement 4, 91-110.

Porbaha A., Weatherby D., Macnab A., Lambrechts J., Burke G., Yang D. and Puppala A.J. 2005. Regional report: North American practice of deep mixing technology. International Conference on Deep Mixing - Best Practice and Recent Advances: R47–R73, Swedish Deep Stabilization Centre, Stockholm, Sweden.

Puppala A.J., Viyanant C., Kruzik A.P. and Perrin L. 2002. Evaluation of a modified soluble sulfate determination method for fine grained cohesive soils. Geotech. Test. J., 25(1), 85-94.

Quigley R.M. 1968. Soil mineralogy, Winnipeg swelling clays. Can.Geotech. J., 5 (2), 120-122.

Quigley R.M. 1980. Geology, mineralogy, and geochemistry of Canadian soft soils: a geotechnical perspective. Canadian Geotechnical Journal, 17, 261-285.

Quigley R. and Di Nardo L. 1982. Soil-cement and soil-lime stabilization of weathered surface clays of outhwestern Ontario. Ontario Ministry of Transportation and Communication, Research Report RR-232,121.

Raja A. 1990. Influence of sulphates on consolidation and swelling behaviour of lime treated calcium bentonite. M.Tech Thesis, Indian Institute of Technology, Madras, India.

Rajasekaran G. 2005. Sulphate attack and ettringite formation in the lime and cement stabilized marine clays. Ocean Engineering, 32(8-9), 1133-1159.

Rajasekaran G. 1994. Physico-chemical behavior of lime treated marine clay. Ph.D. Thesis, Indian Institute of Technology, Madras, India.

Rajasekaran G., Murali K. and Srinivasaraghavan, R. 1997a. Fabric and mineralogical studies on lime treated marine clays. Ocean Engng, 24(3), 227-234.

Rajasekaran G., Murali K., Srinivasaraghavan R., 1997b. Effect of chlorides and sulphates on lime treated marine clays. Soils Foundations, 37, 105-115.

Rajasekaran G. and Narasimha Rao S. 1998. X-ray diffraction and microstructural studies of lime-marine clay reaction products. Geotechnical Engineering. 29. 1-27.

Rajasekaran G and Narasimha Rao S. 2000. Strength characteristics of lime-treated marine clay. Proceedings of the institution of Civil Engineers-Ground Improvement, 4(3), 127-136.

Rajasekaran G and Narasimha Rao S. 2005. Sulphate attack in lime-treated marine clay. Marine Georesources and Geotechnology, 23, 93-116.

Richardson I.G., Brough A.R., Groves G.W. and Dobson C.M. 1994. The characterization of hardened alkali-activated blast-furnace slag pastes and the nature of the calcium silicate hydrate (C-S-H) phase. Cement Concrete Res. 24(5), 813-829.

Rollings R.S., Pete Burkes J. and Rollings M.P. 1999. Sulphate attack on cement stabilized sand. Journal of Geotechnical and Geoenvironmental Engineering, ASCE 125, 364-372.

Rotta G.V., Consoli N.C., Prietto P.D.M., Coop M.R., and Graham J. 2003. Isotropic yielding in an artificially cemented soil cured under stress. Geotechnique, 53(5), 493-501.

Saitoh S., Suzuki, Y. and Shirai K. 1985. Hardening of soil improved by deep mixing method. Proceedings of 11th International Conference on Soil Mechanics and Foundation Engineering, San Francisco.

Sellards G.H., Adkins W.S and Plummer F.B. 1932. The geology of Texas. University of Texas Press.

Schaefer V.R., Abramson L.W., Drumheller,J.C. and Sharp, K. D. 1997). Ground improvement, ground reinforcement and ground treatment: Developments 1987-1997. ASCE. Special Publications, GSP, 69.

Shen Z.J. 1993. An elasto-plastic damage model for cemented clays. Chinese Journal of Geotechnical Engineering, 15(3), 21-28.

Shen Z.J. 1996. Mathematics model of soil structure - soil mechanic core problems in 21st century. Chinese Jounal of Geotechnical Engineering, 18,1,95-97.

Shen S.L., Lue C.Y., Xiao X.C and Wang J.L. 2009. Improvement efficiency of RJP method in Shanghai soft deposit. ASCE, US-China Workshop on Ground Improvement Technologies, 170-178.

Sherwood P.T. 1962. The effect of sulphates on cement and lime stabilized soils. Roads and Road Construction, 40, 34-40.

Sherwood P.T. 1982. Effect of sulphates on cement and lime treated soils, HRB Bull.,353, 98-107.

Sherwood P.T. 1993. Soil stabilization with cement and lime.

Sivapullaiah P.V., Sridharan A. and Bhaskar Raju K.V. 2000a. Role of Amount and Type of Clay in the Lime Stabilisation of Soils. Proceedings of the ICE - Ground Improv., 4(1), 37-45.

Sivapullaiah P.V., Sridharan, A, and Ramesh, H.N. 2000b. Strength behaviour of lime-treated soils in the presence of sulphate. Canadian Geotechnical Journal, 37(6), 1358-1367.

Sivapullaiah P.V., Sridharan A., and Ramesh H.N. 2006. Effect of sulphate on the shear strength of lime-treated soils kaolinitic soil. Proceedings of the ICE - Ground Improv.,10(1), 23-30.

Skempton, A.W. 1964. Long Term Stability of Clay Slopes.Geotechnique, 14(2), 77-101.

Skempton A.W. 1985. Residual strength of clays in landslides, folded strata and the laboratory. Geotechnique, 35, 3-18.

Smith P.R., Jardine R.J. and Hight D.W. 1992. The yielding of Bothkennar clay. Géotechnique, 42(2), 257-274.

Snedker E.A. 1996. M40-Lime stabilization experiences, Lime Stabilization. The Institution of Engineers,142–158.

Sridhran A., Sivapullaiah P.V. and Ramesh H.N. 1995. Consolidation behavior of lime treated sulphatic soils. Proc. Int. Symp. Compression Consolidation Clayey Soils, Hiroshima, Japan I, 183-188.

Stanley B., Chowdhury B. and Haque A. (2012). A preliminary study of strength behaviour of lime-slag treated pyrite bearing soft Coode Island Silt. Australian Geomechanics, 47(2), 17-23.

Tasong W.A., Wild S. and Tilley R.J.D. 1999. Mechanism by which ground granulated blast furnace slag prevents sulfate attack of lime-stabilized kaolinite. Cement and Concrete Research, 29(7), 975-982.

Tatsuoka F. and Kobayashi A. 1983. Triaxial Strength Characteristics of Cement-Treated Clay. Proc. 8th ECSMFE, Helsinki: 8(1), 421-426.

Taylor D.W. 1948. Fundamentals of Soils Mechanics. New York: John Wiley & Son.

Taylor H.F.W., Famy C. and Scrivener K.L. 2001. Review Delayed Ettringite Formation. Cement and Concrete Research, 31, 683-693.

Terzaghi S., Okada W., Houghton, L.G. and Quickfall G. 2005. Deep soil mixing in new Zealand – An update. International conference on deep mixing best practice and recent advances.

Terzaghi S., Okada W. and Houghton L. 2004. Deep soil mixing in New Zealand - Role in slope stabilization. Amélioration des sols en place, Paris.

Terzaghi K., Peck R.B. and Mesri G. 1996. Soil Mechanics in Engineering Practice, 3rd edition. John Wiley & Sons, New York, 549 p.

Thompson M.R. 1964. The Significance of Soil Properties in Lime-Soil Stabilization. Civil Engineering Studies, Highway Engineering Series 13, Illinois Cooperative Highway Research Program Series 23. Department of Civil Engineering, University of Illinois, Urbana, IL.

Thompson M.R. 1966. Lime Reactivity of Illinois Soils. Journal of the Soil Mechanics and Foundation Division, American Society of Civil Engineers, 92(5), 67-92.

Tillard-Ngan D., Desrues J., Raynaud S. and Mazerolle F. 1993. Strain localization in Beaucaire marl. Proc, Int. Symp. On Hard Soils and Soft Rocks, Athens, 2, 1679-1686.

Tsatsos N. and Dermatas D. 1998. Correlation between mineralogy and swelling of lime-treated contaminated soil mixes. Proceeding of 3rd International Congress on Environmental Geotechnics, Portugal, 2, 473–478.

Uddin K., Balasubramaniam A.S. and Bergado D.T. 1997. Engineering behavior of cement-treated Bangkok soft clay. Geotechnical Engineering. 28(1), 89–119.

USACE 2003. Engineering and Design – Slope Stability. EM 1110-2-1902.

USACE. 1998. Local Flood Reduction Project Red River of the North, General Revaluation Report and Environmental Impact Assessment, Supplementary Documentation, Appendix B - Geotechnical Appendices. U.S. Army Corps of Engineers St. Paul District.

Vaughan P.R. 1988. Characterizing the mechanical properties of the in-situ residual soil. Proc. 2nd Int. Conf. Geomechanics Tropical Soils, Singapore 2, 469-487.

Verhasselt A. 1990. Lime-cement stabilization of wet cohesive soils. Proc. 6th Int. Symp. on Concrete Roads, Madrid, 67-76.

Vichan S., Rachan R. and Horpibulsuk S. 2013. Strength and microstructure development in Bangkok clay stabilized with calcium carbide residue and biomass ash. Science Asia, 39, 186-193.

Viggiani G., Rampello S., and Georgiannou V.N. 1993. Experimental analysis of localisation phenomena in triaxial tests on stiff clays. Proc. Int. Symp. on Hard Soils–Soft Rocks, Athens, 1, 849-856.

Walker A.D. 1997. An example of the use of jet grouting to permit tunneling in chemically weathered limestone. 6th Multidisciplinary Conference on Sink Holes and the Engineering & Environmental Impacts of Karst, Springfield, Missouri.

Wang J.G., Oh B., Lim S.W. and Kumar G.S. 1999. Effect of different jet-grouting installation on neighboring structures. Field Measurments in Geomechanics, Balkema, Rotterdam, 511-516.

Wesley L.D. 1973. Some basic engineering properties of halloysite and allophane clays in Java, Indonesia. Geotechnique, 23(4), 471-494.

Wesley L.D. 2003. Residual strength of clays and correlations using Atterberg limits. Geotechnique, 53(7), 669-672.

Wild S., Kinuthia J.M., Jones G.I. and Higgins D.D. 1999. Suppression of swelling associated with ettringite formation in lime stabilized bearing clay soils by partial substitution of lime with ground granulated blastfurnace slag. Eng. Geol. 51, 257-277.

Wissa A.E.Z., Ladd C.C. and Lambe T.W. 1965. Effective stress strength parameters of stabilized soils. Proceedings of the VI Internationl Conference of Soil Mechanics and Foundation Engineering, Montreal, 412-416.

Wissa A.EZ., McGillivray R.T. and Paniagua J.G. 1971. The effects of mixing conditions, method of compaction, and curing conditions on the effective stress-strength behavior of a stabilized soil. Research Report No. R71-34, Soils Publication No. 287, Department of Civil Engineering, Massachusetts Institute of Technology, Cambridge, MA.

Wong I.H. and Poh T.Y. 2000. Effects of jet grouting on adjacent ground and structures. Journal of geotechnical and Geoenvironmental Engineering, 126(3), 247-256.

Xiao H.W. 2009. Yielding and failure of cement treated soil. Ph.D. thesis. National University of Singapore.

Yin J.H. and Lai C.K. 1998. Strength and stiffness of Hong Kong marine deposits mixed with cement. Geotechnical Engineering, 29(1), 29-44.

Yu Y., Pu J. and Ugai K. 1997. Study of mechanical properties of soil-cement mixture for a cutoff wall. Soils and foundations, 37(4), 93-103.

Zolkov E. 1962. Influence of chlorides and hydroxides of calcium and sodium on consistency limits of fat clay. Highway Research Record 309, 109-115.